



THE UNIVERSITY *of* EDINBURGH

This thesis has been submitted in fulfilment of the requirements for a postgraduate degree (e.g. PhD, MPhil, DClinPsychol) at the University of Edinburgh. Please note the following terms and conditions of use:

This work is protected by copyright and other intellectual property rights, which are retained by the thesis author, unless otherwise stated.

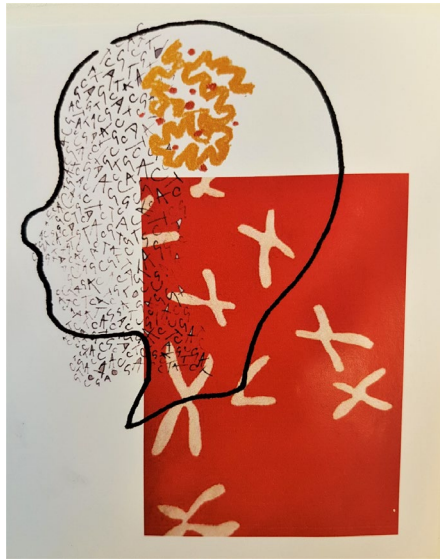
A copy can be downloaded for personal non-commercial research or study, without prior permission or charge.

This thesis cannot be reproduced or quoted extensively from without first obtaining permission in writing from the author.

The content must not be changed in any way or sold commercially in any format or medium without the formal permission of the author.

When referring to this work, full bibliographic details including the author, title, awarding institution and date of the thesis must be given.

The Role of the
Swain-Langley and McCoy Polymorphisms in
Complement Receptor 1
in Cerebral Malaria



Dr Olivia Swann

A thesis submitted in partial fulfilment for the degree of

Doctor of Philosophy

University of Edinburgh

September 2018

(Image credit: Claudia Carreras, Vivian Chen, Katie Forrest-Smith and Rebecca Raper)

I. Abstract

Malaria has been a major driving force in the evolution of the human genome. In sub-Saharan African populations, two neighbouring polymorphisms in the Complement Receptor 1 (CR1) gene, named Swain-Langley (*S/2*) and McCoy (*McC^b*), occur at high frequencies, consistent with selection by malaria. This thesis investigates the association between these two polymorphisms and severe malaria. Previous studies into this area have produced conflicting findings.

Using a large case-control study of severe malaria in Kenyan children and statistical models adjusted for confounders, I found that the *S/2* polymorphism was associated with markedly reduced odds of cerebral malaria and death, while the *McC^b* polymorphism was associated with increased odds of cerebral malaria. I also identified an interaction between *S/2* and α^+ thalassaemia, with the protective association of *S/2* greatest in children with normal α -globin.

Following these epidemiological findings, I explored potential biological hypotheses which might explain them. The first approach examined whether the *S/2* and *McC^b* polymorphisms affected how CR1 forms clusters on erythrocyte membranes, a process which is key in the binding and transfer of immune complexes from erythrocytes to macrophages. Using erythrocytes from Kenyan children, I performed immunofluorescence assays (IFAs) with confocal microscopy to quantify CR1 cluster number and volume. I found no association between the *S/2* and *McC^b* polymorphisms and either the number or volume of CR1 clusters formed.

The second approach investigated whether the cerebral malaria-specific associations seen with *S/2* and *McC^b* might be due to expression of CR1 by human brain endothelial cells (HBEC). The immortalised cell line HBEC-5i was investigated for expression of CR1 using IFA, flow cytometry, western blotting, functional C3b degradation assays, mass spectrometry, immunoprecipitation and siRNA knockdown experiments. A pool of α -CR1 monoclonal antibodies recognised an intracellular antigen in permeabilised HBEC-5i cells which was a similar molecular weight to CR1 on western blotting. However, when the α -CR1 monoclonal

antibodies were tested individually, only E11 recognised an HBEC-5i antigen. Further investigative approaches did not support the presence of CR1 on HBEC-5i cells, instead suggesting that E11 was not specific for CR1 and was instead recognising a protein in the Golgi apparatus.

The final approach was to examine whether the *S12* and *McC^b* polymorphisms might influence the binding of the complement components mannose binding lectin, C1q and L-ficolin to the LHR-D region of CR1. I aimed to generate recombinant proteins of the LHR-D region which included the polymorphisms. Site-directed mutagenesis of the region was successful and subcloning and expression of the mutant amplicons will be performed at a later date.

In summary, I have identified opposing associations between the *S12* and *McC^b* polymorphisms and cerebral malaria, which do not appear to be due to differences in CR1 clustering or expression of CR1 by human brain endothelial cells. My investigation into whether the polymorphisms might influence complement component binding is ongoing.

II. Lay Summary

Malaria kills over half a million children in sub-Saharan Africa every year. Mosquitoes infected with malaria parasites spread them to humans when they bite. Once inside a human, the parasites infect the red blood cells. In severe cases, these red blood cells can stick to the walls of small blood vessels supplying the brain and hinder the flow of oxygen, causing a coma. This is called cerebral malaria and can be fatal.

Small changes (called polymorphisms) in certain human genes can protect against malaria. Over time, polymorphisms that protect people living in Africa from dying from malaria have been passed down through generations. Finding new polymorphisms that protect against malaria help scientists understand how severe malaria happens and eventually develop new drugs and vaccines against the disease. Some studies have found that polymorphisms in a gene called complement receptor 1 (CR1) may be protective against malaria, although others have disagreed. I set out to investigate this further in this thesis.

Firstly, I analysed genetic and health information on more than 5,500 children in Kenya to see if the severity of malaria differed depending on whether they had a CR1 polymorphism. I found that children with one of these CR1 polymorphisms were a third less likely to get cerebral malaria and half as likely to die as children without the polymorphism. I also found that the CR1 polymorphism was only protective against severe malaria when the child does not have another malaria-protective polymorphism called α -thalassemia. In children with α -thalassemia, the CR1 polymorphism does not make a difference.

I then tried to work out how this polymorphism might protect against cerebral malaria and death. I looked at whether it might affect how CR1 molecules on red blood cells bunch up or “cluster” when they bind foreign particles, e.g. bits of microorganisms (which is one of the key jobs of CR1). I used blood samples from Kenyan children with and without the polymorphism and looked at the CR1 clusters which formed on them. I found that the mutation made no difference to the

number or the size of CR1 clusters, making this unlikely to be involved in the how the polymorphism protects against cerebral malaria.

After this, I wondered if brain blood vessel cells might have CR1 on their surface. If this was the case it could explain why the polymorphism protected only against malaria in the brain and not elsewhere. I used human brain blood vessel cells that had been modified so that they could survive in a laboratory and employed many different scientific techniques to try and detect CR1 on these cells. However, I could not find any evidence that there was CR1 on the surface of brain blood vessels, making this unlikely to be how the polymorphism protects against cerebral malaria.

Finally, I decided to make some protein that contained the polymorphism myself so I could study it more closely and see how it might influence other parts of the immune system. I did this by taking a section of CR1 DNA (the genetic recipe which tells the body how to make CR1) and putting it into a bacteria, which I then used as a tiny factory to make more CR1 DNA. I used enzymes (biological molecules that carry out chemical reactions) to make the polymorphism in the CR1 DNA. My next project will be to use the bacteria to make CR1 with and without the polymorphism, so that I can see if it affects how CR1 interacts with other parts of the immune system.

In summary, I have shown that Kenyan children with a polymorphism in CR1 are protected against cerebral malaria and death and that this doesn't appear to be due to the polymorphism making CR1 cluster differently or due to brain blood vessels having CR1 on their surfaces. I am in the process of making CR1 proteins with and without the polymorphism in order to study them further and work out what the effect might be. If I can do that, further down the line, this may lead to a new drug or vaccine against cerebral malaria.

III. Declaration

I declare that the content of this thesis is my own work and that all contributions and collaborations have been explicitly acknowledged in the text. No material presented in this thesis has been submitted to any other university or for any other degree.

Dr Olivia Swann

July 2018

IV. Dedication

This thesis is dedicated to my dear friend Caz, who taught me
that life is brief and beautiful
and that we are all stronger than we think we are.

(Caroline Lane 1981-2017)

V. Acknowledgements

Science is so much more than experiments. This thesis has been supported and shaped by a number of extraordinary people to whom I would like to extend my deep thanks:

To Prof Alex Rowe for your exceptional supervision and guidance. Your patience and trust in my work has allowed me to develop into an autonomous and confident scientist. You are a true advocate for high quality, open and honest science. I hope one day to pass on your values and attitudes to another generation of researchers.

To my Rowe lab group members, past and present: Ahmed, Ash, Gabbi, Yvonne, Yonxy, Jennifer, Hussein, Fiona and Flo. You have all taught me so much in so many ways. We may be small, but we are mighty.

To Prof Tom Williams for your encouragement, big thinking and refreshing irreverence.

To the Williams' lab group and laboratory staff in Kilifi: Sophie, Alex, Metrine, Emily and Mike. Thank you for your warm welcome, patience and Tuskers. And you're right, there should be more dancing during experiments.

To Herbert Opi for your enormous smile, optimism and infectious love of science. I feel very lucky to follow in your research footsteps.

To the Matthews' group for allowing me to regularly delve into your knowledge, expertise and reagents!

To Martin Waterfall for imparting the joys of flow cytometry.

To Prof John Iredale for "taking a punt" on me and giving a fellowship to a paediatrician who had never held a pipette.

To the Wellcome Trust for funding a progressive PhD programme which gave me the space to explore many possible projects until I found the one that I loved.

To the ECAT directors, students and post-docs. Your calm support and experience in navigating the tricky road of clinical-academia has given me the confidence to persist and see how far I can go.

To the inimitable Jo Ness for helping me clear the administrative hurdles and minimise the chaos.

To my fabulous parents, Mike and Franny, for your unflagging support, despite never quite understanding what on earth I'm talking about.

To my unflappable brother Henry for always knowing exactly the right words.

To my dear Floss for keeping me sane when you had so much going on yourself.

To my hilarious sons, Callan and Finn. You bring so much joy and remind me on a daily basis what is most important. You remain the most successful experiment of my PhD; $n=2$, both excellent. Please never stop asking questions.

And lastly, to my husband and best friend, Ewen. Thank you for making me apply in the first place, for firmly believing in me, even when I didn't, and for slowly helping me shake off my imposter syndrome. I am constantly inspired by your energy, your inquisitiveness and your profound sense of the ridiculous. Here's to many more years discussing of statistics while we brush our teeth.

VI. Abbreviations

°C	Degrees Celsius
ANOVA	Analysis of variance
AP	Alternative pathway
BBB	Blood-brain barrier
BCS	Blantyre coma score
bp	Base pairs
BSA	Bovine serum albumin
CI	Confidence interval
cyfu	Child years of follow up
DC	Domain cassette
DNA	Deoxyribonucleic acid
CCP	Complement control protein
CR1	Complement receptor 1
sCR1	Soluble CR1
CP	Classical pathway
cDNA	Complementary DNA
Da	Daltons
DAPI	4,6-diamidino-2-phenylindole
DBL	Duffy-like binding domain
dH ₂ O	Distilled water
DMEM	Dulbecco's Modified Eagle's Medium/Nutrient Mixture F-12 Ham
DNA	Deoxyribonucleic acid
dNTP	Deoxyribonucleotide triphosphate
EPCR	Endothelial Protein C Receptor
FACS	Fluorescent activated cell sorting
G6PD	Glucose-6-phosphate dehydrogenase
HBEC	Human brain endothelial cells
HI-FBS	Heat-inactivated foetal bovine serum
IC	Immune complex
ICAM-1	Intercellular adhesion molecule 1
IE	Infected erythrocyte
IFA	Immunofluorescence assay
IFN	Interferon
IL	Interleukin
IPTG	Isopropyl β -D-1-thiogalactopyranoside

IRR	Incidence rate ratio
IQR	Inter-quartile range
KHDSS	Kilifi Health and Demographic Surveillance System
LB	Luria-Bertani
LD	Linkage disequilibrium
LHR	Long homologous region
LP	Lectin pathway
LRTI	Lower respiratory tract infection
mAb	Monoclonal antibody
MAC	Membrane attack complex
MAKI	Malaria acute kidney injury
<i>McC</i>	McCoy polymorphism
OR	Odds ratio
PBS	Phosphate-buffered saline
PBMC	Peripheral blood mononuclear cell
PCR	Polymerase chain reaction
PfEMP1	<i>Plasmodium falciparum</i> erythrocyte membrane protein one
PfRh	<i>Plasmodium falciparum</i> reticulocyte homologue
PMN	Polymorphonuclear cell (neutrophils, eosinophils and basophils)
RBC	Red blood cell
RD	Respiratory distress
RFLP	Restriction fragment length polymorphism
rpm	Revolutions per minute
siRNA	Short interfering ribonucleic acid
<i>Sl</i>	Swain Langley polymorphism
SNP	Single nucleotide polymorphism
SDS-PAGE	Sodium dodecyl sulfate-polyacrylamide gel electrophoresis
SEM	Standard error of mean
SMA	Severe malaria anaemia
TNF	Tumor necrosis factor
URTI	Upper respiratory tract infection
UM	Uncomplicated malaria
WHO	World Health Organisation

Contents

1	Introduction	1-1
1.1	The genetic arms race between man and malaria.....	1-1
1.2	General background	1-2
1.2.1	Global prevalence of malaria	1-2
1.2.2	The life cycle of <i>Plasmodium falciparum</i>	1-3
1.2.3	Clinical sub-phenotypes of malaria.....	1-5
1.2.4	<i>P. falciparum</i> virulence factors	1-10
1.2.5	Cerebral malaria pathogenesis	1-14
1.2.6	Models of cerebral malaria	1-16
1.3	Host genetic resistance against malaria.....	1-18
1.3.1	Sickle cell trait	1-19
1.3.2	α^+ thalassaemia	1-20
1.3.3	Polymorphisms associated with protection against cerebral malaria.....	1-20
1.4	The complement system	1-22
1.4.1	Complement activation and function	1-22
1.4.2	Complement regulation	1-23
1.4.3	Exploitation by microorganisms.....	1-25
1.5	Complement and malaria	1-25
1.5.1	Complement and cerebral malaria	1-26
1.6	Complement receptor one (CR1)	1-28
1.6.1	Expression and structure	1-28
1.6.2	CR1 Function	1-29
1.6.3	CR1 size polymorphism	1-30

1.6.4	CR1 copy number polymorphism.....	1-32
1.6.5	CR1 as a therapy.....	1-32
1.7	CR1 and malaria.....	1-33
1.7.1	CR1 and rosetting.....	1-33
1.7.2	CR1 and erythrocyte invasion	1-34
1.7.3	CR1 copy number and malaria.....	1-35
1.8	The Knops blood group polymorphisms in CR1	1-37
1.8.1	Molecular basis of the polymorphism	1-37
1.8.2	Global prevalence of the <i>S/</i> and <i>McC</i> polymorphisms	1-37
1.8.3	Epidemiological studies of the <i>S/</i> and <i>McC</i> polymorphisms relationship with malaria in Africa	1-40
1.9	Aims and hypotheses of this thesis.....	1-46
2	Are the Swain Langley and McCoy polymorphisms in CR1 associated with severe malaria?.....	2-47
2.1	Declaration	2-47
2.2	Abstract	2-48
2.3	Additional introduction to this manuscript.....	2-48
2.4	Introduction.....	2-49
2.5	Materials and methods	2-50
2.5.1	Datasets studied.....	2-50
2.5.2	The Kenyan study area.....	2-51
2.5.3	The Kenyan case-control study.....	2-51
2.5.4	Sample processing and quality control for the Kenyan case-control study	2-53
2.5.5	The Kenyan longitudinal cohort study	2-53

2.5.6	The Malian case-control study.....	2-54
2.5.7	Ex vivo rosetting.....	2-54
2.5.8	Laboratory procedures.....	2-55
2.5.9	Statistical analysis	2-55
2.5.10	Ethical statement	2-57
2.6	Results	2-58
2.6.1	The <i>SI2/SI2</i> genotype is associated with protection against cerebral malaria and death in the Kenyan case-control study	2-58
2.6.2	The <i>McC^b</i> allele is associated with increased susceptibility to cerebral malaria and death in the Kenyan case-control study	2-68
2.6.3	Analysis of haplotypic effects and genotype combinations	2-68
2.6.4	The <i>SI2/SI2</i> genotype was associated with protection against uncomplicated malaria in the Kenyan longitudinal cohort study.....	2-70
2.6.5	The <i>McC^b</i> allele was associated with protection from common non-malarial childhood diseases in the Kenyan longitudinal cohort study.	2-75
2.6.6	The <i>SI2</i> allele was associated with reduced ex vivo rosette frequency in <i>P. falciparum</i> clinical isolates from Mali.	2-76
2.7	Supplementary information and results	2-80
2.7.1	Statistical model fitting and bootstrapping for the Kenyan case-control study	2-80
2.7.2	Comparison between this study and Rockett et al.....	2-85
2.7.3	Exploration of alternative haplotype and combined genotype models..	2-87
2.7.4	Exploration of the negative epistasis between sickle trait and α^+ thalassaemia.....	2-88
2.7.5	Statistical model fitting for the longitudinal cohort study	2-92

2.8	Discussion	2-96
2.9	Additional discussion to this manuscript	2-99
2.9.1	Potential functions of the <i>SI</i> and <i>McC</i> polymorphisms.....	2-99
2.9.2	Association of the <i>SI</i> and <i>McC</i> polymorphisms with other diseases in Africa	2-102
2.10	Directions of investigation.....	2-103
3	Do the Swain Langley and McCoy polymorphisms influence how CR1 clusters on the erythrocyte membrane?.....	3-104
3.1	Declaration	3-104
3.2	Abstract	3-105
3.3	Additional introduction to this manuscript.....	3-105
3.4	Introduction.....	3-107
3.5	Aims	3-111
3.6	Methods	3-111
3.6.1	Study Population and Ethical Approval.....	3-111
3.6.2	Donor selection and genotyping.....	3-111
3.6.3	Sample collection and processing.....	3-112
3.6.4	CR1 copy number determination.....	3-112
3.6.5	Immunofluorescent staining of CR1 clusters.....	3-114
3.6.6	Confocal microscopy	3-116
3.6.7	Image Analysis.....	3-116
3.6.8	Statistical analyses	3-120
3.7	Results	3-121
3.7.1	Increased CR1 copy number in individuals with the <i>McC^b/McC^b</i> genotype.	3-123

3.7.2	Increased CR1 cluster number in individuals with the <i>McC^b/McC^b</i> genotype.	3-126
3.7.3	No evidence of an association between Knops genotype and CR1 cluster number after adjustment for CR1 copy number.	3-131
3.7.4	No evidence of an association between Knops genotype and erythrocyte CR1 cluster volume after adjustment for CR1 copy number. ...	3-133
3.8	Discussion	3-135
3.9	Additional discussion to this manuscript	3-139
4	Do human brain endothelial cells express CR1?	4-141
4.1	Abstract	4-141
4.2	Introduction.....	4-142
4.2.1	The blood-brain barrier.....	4-142
4.2.2	Complement and the endothelium.....	4-143
4.2.3	CR1 expression on endothelial cells.....	4-145
4.3	Aims	4-148
4.4	Methods	4-148
4.4.1	Antibodies used.....	4-148
4.4.2	Human Brain Endothelial cell line (HBEC-5i).....	4-153
4.4.3	HBEC-5i culture media	4-154
4.4.4	HBEC-5i thawing.....	4-154
4.4.5	General HBEC-5i culture and passage.....	4-155
4.4.6	HBEC-5i freezing.....	4-155
4.4.7	CHO cell culture.....	4-156
4.4.8	Mycoplasma surveillance.....	4-156
4.4.9	Preparation of cell lysates.....	4-157

4.4.10	Immunofluorescence assays	4-158
4.4.11	Flow cytometry	4-160
4.4.12	Sodium dodecyl sulfate polyacrylamide gel electrophoresis (SDS-PAGE)	4-161
4.4.13	Western blotting	4-162
4.4.14	C3b degradation assay	4-163
4.4.15	Transfection of HBEC-5i with CR1 siRNA.....	4-166
4.4.16	Immunoprecipitation	4-167
4.4.17	Mass Spectrometry	4-168
4.5	Results	4-170
4.5.1	HBEC-5i cell line expresses expected cellular markers.....	4-170
4.5.2	α -CR1 monoclonal antibodies recognise an epitope on HBEC-5i...	4-173
4.5.3	HBEC-5i together with factor I can cleave C3b to C3dg, but this is not inhibited by the α -CR1 monoclonal antibody 3D9.....	4-182
4.5.4	Mass spectrometry of HBEC-5i lysate fails to detect CR1.....	4-186
4.5.5	E11 is the only α -CR1 monoclonal antibody to recognise an HBEC-5i antigen	4-191
4.5.6	CR1 siRNA knockdown does not alter E11 staining of HBEC-5i	4-200
4.5.7	Immunoprecipitation of HBEC-5i lysate fails to produce CR1	4-203
4.5.8	Intracellular HBEC-5i antigen recognised by E11 α -CR1 monoclonal antibody colocalises to the Golgi apparatus.....	4-205
4.6	Discussion	4-210
4.6.1	Summary and interpretation of results	4-210
4.6.2	E11 and the Golgi apparatus.....	4-214
4.6.3	Findings in context	4-217

5	Do the <i>SI</i> and <i>McC</i> polymorphisms affect the binding of complement components to CR1?	5-218
5.1	Abstract	5-218
5.2	Introduction.....	5-219
5.2.1	Function of the LHR-D region and relevance to malaria.....	5-219
5.2.2	Previous investigations into <i>SI/McC</i> polymorphisms and complement function	5-223
5.2.3	Choice of protein expression system and CR1 glycosylation.....	5-224
5.3	Aim.....	5-226
5.4	Methods	5-226
5.4.1	Overview of cloning strategy	5-226
5.4.2	Primer sequences.....	5-226
5.4.3	PCR amplification of CR1 CCP 22-30	5-227
5.4.4	Adding 3' adenine overhangs.....	5-229
5.4.5	Agarose gels	5-229
5.4.6	Gel fragment isolation and purification.....	5-230
5.4.7	Preparation of growth media.....	5-232
5.4.8	Ligation into the pCRII cloning vector	5-232
5.4.9	Transformation into <i>E. coli</i>	5-233
5.4.10	Colony PCR	5-234
5.4.11	Miniprep.....	5-235
5.4.12	Diagnostic restriction digestion	5-235
5.4.13	Sequencing.....	5-236
5.4.14	Glycerol stocks	5-236
5.4.15	Site-directed mutagenesis	5-237

5.4.16	Expression plasmid.....	5-239
5.4.17	Maxi prep	5-240
5.4.18	Adding restriction sites to mutant inserts	5-241
5.4.19	Double digestion	5-242
5.4.20	Ligation into expression vector	5-243
5.5	Results	5-245
5.5.1	Creation of the pCRII plasmid with CCP 22-30 insert.....	5-245
5.5.2	Sequencing of the inserts.....	5-247
5.5.3	Creation of <i>SI2</i> and <i>McC^b</i> mutations.....	5-251
5.5.4	Creation of the double mutant <i>SI2/McC^b</i>	5-256
5.5.5	Sub-cloning of the CCP 22-30 mutants into the expression plasmid.....	5-259
5.6	Discussion	5-264
5.6.1	Generation of Knops blood group mutant inserts.....	5-264
5.6.2	Inability to ligate mutant inserts into digested expression vector .	5-264
5.6.3	Troubleshooting for future experiments	5-265
5.6.4	The Thr1885Ile substitution	5-265
5.6.5	Future intended experiments	5-266
6	General Discussion and Conclusion	6-267
6.1	Summary of findings.....	6-267
6.2	Limitations of these findings	6-268
6.2.1	Limitations of genetic association study.....	6-268
6.2.2	Limitations of laboratory-based studies	6-270
6.3	Questions remaining and future work	6-272

6.3.1	What are the functional effects of the <i>SI</i> and <i>McC</i> polymorphisms?	6-272
6.3.2	Why are the <i>SI</i> and <i>McC</i> associations specific to cerebral malaria?	6-273
6.3.3	What is the underlying mechanism of the <i>SI</i> / α +thalassaemia interaction?	6-275
6.4	Conclusion	6-278
7	References.....	7-279
8	Appendices.....	8-327
8.1	Mass spectrometry data.....	8-327
8.2	University of Edinburgh regulations: Including Publications in Postgraduate Research Theses.....	8-328
8.3	Open Access Licence for Chapter 2	8-330
8.4	Open Access Licence for Chapter 3	8-331
8.5	Publications arising from this thesis.....	8-332
8.6	Presentations arising from this thesis	8-332
8.7	Grants arising from this thesis.....	8-334
8.8	Public engagement projects arising from this thesis	8-334

List of Figures

Figure 1-1. Global burden of malaria cases and deaths from 2013.....	1-2
Figure 1-2. Life-cycle and developmental stages of <i>P. falciparum</i>	1-3
Figure 1-3. Intra-erythrocytic blood stages of <i>P. falciparum</i>	1-4
Figure 1-4. Severity of malaria varies with age in an area of moderate transmission.	1-7
Figure 1-5. Adhesion mechanisms of <i>P. falciparum</i> -infected erythrocytes to endothelial cells, platelets and other erythrocytes.	1-11
Figure 1-6. Approximate distributions of malaria, HbS and α^+ thalassemia in sub- Saharan Africa.	1-19
Figure 1-7. Overview of the pathways of complement activation.	1-24
Figure 1-8. Diagram of the most common Complement Receptor 1 size variant (CR1*1).....	1-29
Figure 1-9. Overview of the functions of CR1.	1-31
Figure 1-10. Global distribution of the CR1 Knops SI and McC alleles.....	1-39
Figure 2-1. Patient inclusion flow chart for the Kenyan case-control study.	2-52
Figure 2-2. The SI2 and McC ^b alleles have opposing associations with cerebral malaria (CM) and death.	2-64
Figure 2-3. The protective association of SI2 with cerebral malaria and death is only evident in children with normal α -globin.	2-66
Figure 2-4. Parasite densities by SI and Mc genotypes.....	2-67
Figure 2-5. Patient inclusion flow chart for Mali case-control study.....	2-77
Figure 2-6. The SI2 allele is associated with reduced ex vivo rosette frequency of <i>P.</i> <i>falciparum</i> clinical isolates.	2-79
Figure 3-1. Schematic representation of the most common CR1 size variant (CR1*1).	3-108
Figure 3-2. Immunofluorescence staining and flow cytometry to determine CR1 copy number.	3-113
Figure 3-3. Immunofluorescent staining of erythrocyte CR1 clusters and image analysis.	3-115

Figure 3-4. Determining the optimal number of erythrocytes to image.....	3-118
Figure 3-5. CR1 cluster number and volume for three samples taken over consecutive days from one donor.	3-119
Figure 3-6. The McC ^b genotype is associated with CR1 copy number and cluster number.....	3-124
Figure 3-7. Preliminary exploration of the association of donor variables and erythrocyte CR1 copy number (mean number of CR1 molecules per cell).	3-125
Figure 3-8. Box plot to illustrate within individual variation in number of CR1 clusters per cell.	3-127
Figure 3-9. Box plot to illustrate within individual variation in median cluster volume per cell.....	3-128
Figure 3-10. Preliminary exploration of the association of donor variables and mean erythrocyte cluster volume.....	3-129
Figure 3-11. Positive correlation between CR1 copy number, cluster number and cluster volume.....	3-130
Figure 4-1. Example of a neurovascular unit in a rat brain.....	4-143
Figure 4-2. Epitopes of α -CR1 mouse monoclonal antibodies used in this chapter.....	4-150
Figure 4-3. PCR programme for mycoplasma surveillance.....	4-157
Figure 4-4. Representation of western blot transfer stack.....	4-162
Figure 4-5. The C3 degradation pathway.....	4-164
Figure 4-6. HBEC-5i can take up Dil-Ac-LDL.	4-170
Figure 4-7. HBEC-5i form tight junctions and express intercellular adhesion molecule 1 (ICAM-1).	4-171
Figure 4-8. HBEC-5i contain intracellular von Willebrand factor (vWF) and do not express α -smooth muscle actin (α -SMA).....	4-172
Figure 4-9. Extended pool of α -CR1 monoclonal antibodies recognises an antigen on the surface of HBEC-5i cells.	4-174
Figure 4-10. Staining of HBEC-5i by extended pool of α -CR1 antibodies is increased under hypoxic conditions.....	4-175

Figure 4-11. α -CR1 monoclonal pool detects intracellular pool of antigen in permeabilised HBEC-5i.....	4-176
Figure 4-12. α -CR1 monoclonal pool stains dividing HBEC-5i.....	4-176
Figure 4-13. Example of gating strategy used for HBEC-5i flow cytometry experiments.	4-178
Figure 4-14. Staining of HBEC-5i by an α -CR1 antibody pool is increased with permeabilisation and heat treatment but decreased by treatment with trypsin.....	4-179
Figure 4-15. Western blot of HBEC-5i lysate reveals a band of the same molecular weight as CR1.	4-181
Figure 4-16. HBEC-5i can breakdown C3b to C3dg with factor I, but this is not inhibited by the α -CR1 monoclonal antibody 3D9.....	4-183
Figure 4-17. Polyclonal α -vWF antibody is unable to inhibit the breakdown of C3b \rightarrow C3dg by HBEC-5i.....	4-185
Figure 4-18. Western blot of HBEC-5i and CR1-CHO lysates illustrating gel slices sent for mass spectrometry	4-187
Figure 4-19. Peptides matching the CR1 amino acid sequence identified in the positive control by mass spectrometry.....	4-189
Figure 4-20. CR1 peptide fragments can be identified in CR1-CHO sample but not in HBEC-5i.....	4-190
Figure 4-21. Only E11 recognises an antigen on HBEC-5i when staining is performed with individual α -CR1 monoclonal antibodies.	4-192
Figure 4-22. A pool of isotype control antibodies increases background staining of HBEC-5i compared to a single isotype control antibody.	4-193
Figure 4-23. Only E11 recognises an antigen in HBEC-5i lysates when western blotting is performed with individual α -CR1 monoclonal antibodies.....	4-195
Figure 4-24. Only E11 recognises an antigen in HBEC-5i lysates when western blotting is performed with individual α -CR1 monoclonal antibodies.....	4-196
Figure 4-25. Rabbit α -CR1 antibodies do not recognise antigens of a similar molecular weight to CR1 in HBEC-5i lysate.....	4-197

Figure 4-26. E11 does not recognise HBEC-5i antigen after heat treatment.	4-199
Figure 4-27. CR1 siRNA knockdown of HBEC-5i does not alter E11 staining (lower magnification).	4-201
Figure 4-28. CR1 siRNA knockdown of HBEC-5i does not alter E11 staining (higher magnification).	4-202
Figure 4-29. E11 can immunoprecipitate CR1 from CR1-CHO lysate but not from HBEC-5i lysate.	4-204
Figure 4-30. E11 staining of HBEC-5i cells colocalises with staining for the Golgi marker RCAS (part 1).	4-206
Figure 4-31. E11 staining of HBEC-5i cells colocalises with staining for the Golgi marker RCAS (part 2).	4-207
Figure 4-32. Isotype controls for colocalisation experiment.	4-208
Figure 4-33. Small area of homology between CR1 and two Golgi-specific proteins sequences.	4-210
Figure 5-1. Putative binding site for MBL on CR1.	5-220
Figure 5-2. Glycosylation sites in CR1.	5-225
Figure 5-3: PCR programme for amplification of CCP 22-30 from CR1 cDNA.	5-229
Figure 5-4. Isolation of agarose gel band to minimise exposure of sample to UV light.	5-231
Figure 5-5: Cartoon of TA cloning.	5-233
Figure 5-6. PCR programme for screening of colonies.	5-235
Figure 5-7: PCR programme for site-directed mutagenesis	5-238
Figure 5-8: Original expression plasmid pcDNA3.1 (-) CCP 22-30 His.	5-240
Figure 5-9: PCR programme to add AgeI and PstI restriction sites to mutant inserts ..	5-241
Figure 5-10: Amplified region of CR1 cDNA.	5-245
Figure 5-11: Amplification and cloning of CCP 22-30 fragment.	5-246
Figure 5-12: EcoRI restriction digestion of miniprep eluates.	5-247
Figure 5-13: Spacing and direction of primers for sequencing of the insert.	5-247
Figure 5-14: Sanger sequencing of CCP 22-30 insert (Clone 1).	5-248

Figure 5-15. Site-directed mutagenesis PCR products for SI2 and McC ^b mutants	5-252
Figure 5-16. Preliminary sequencing of SI2 mutation site-directed mutagenesis.....	
.....	5-253
Figure 5-17. Preliminary sequencing of McC ^b mutation site-directed mutagenesis.....	
.....	5-254
Figure 5-18. Full sequencing of SI2 and McC ^b mutant constructs.	5-255
Figure 5-19. PCR product of McC ^b mutant on background of SI2 shows a band of expected size (~6 kb).....	5-256
Figure 5-20. Preliminary sequencing of McC ^b mutation on back of SI2.	5-257
Figure 5-21. Full sequencing of the McC ^b mutation on back of SI2.	5-258
Figure 5-22. Pasi restriction site in CCP 22-30 insert.	5-259
Figure 5-23. Mutant inserts after amplification using AGEI_PRIMER and PASI_PRIMER.....	5-260
Figure 5-24. Expression vector pcDNA 3.1 (-) CCP 22-30 His before and after digestion with Pasi.	5-261
Figure 5-25. Double digest of expression vector with Pasi and AgeI.....	5-262
Figure 5-26. Diagnostic restriction digest of final mutant constructs using BamHI-HF and HindIII-HF.	5-263
Figure 5-27. New cloning strategy using BsmBI restriction sites on the cloning and expression plasmids.	5-265

List of Tables

Table 1-1. Antigens of the Knops blood group system.....	1-38
Table 1-2. Summary of epidemiological investigations of the SI and McC polymorphisms relationship with malaria in Africa.....	1-44
Table 2-1. General characteristics for the Kenyan case-control study.....	2-58
Table 2-2. Characteristics for the Kenyan case-control study by SI genotype.....	2-59
Table 2-3. Characteristics for the Kenyan case-control study by McC genotype...	2-60
Table 2-4. Hardy Weinberg equilibrium calculations for controls in the Kenyan case-control study.	2-61
Table 2-5. Unadjusted odds ratios for clinical outcomes for the Kenyan case-control study.....	2-62
Table 2-6. Adjusted Odds Ratios (aOR) for severe malaria by SI ² (recessive) and McC ^b (additive) genotype in Kenya.....	2-63
Table 2-7. SI and McC combined genotypes and adjusted odds ratios for cerebral malaria in the Kenyan case-control study.....	2-69
Table 2-8. SI and McC combined genotypes and adjusted odds ratio for death in the Kenyan case-control study.	2-69
Table 2-9. General characteristics of the Kenyan longitudinal cohort study population by SI and McC genotypes.....	2-71
Table 2-10. Incidence of common childhood diseases by SI genotypes in the Kenyan cohort study.	2-72
Table 2-11. Incidence of common childhood diseases by McC genotypes in the Kenyan cohort study.	2-72
Table 2-12. Unadjusted Incidence Rate Ratios (IRR) for uncomplicated malaria and non-malarial diseases in the Kenyan longitudinal cohort study by SI and McC genotype.	2-73
Table 2-13. Adjusted Incidence Rate Ratios (aIRR) for uncomplicated malaria and non-malarial diseases in Kenya by SI and McC genotype.....	2-74
Table 2-14. Incidence of uncomplicated malaria by SI genotype and α^+ thalassaemia status in the Kenyan longitudinal cohort study.....	2-75

Table 2-15. General characteristics for cases and controls in the Mali case-control study.....	2-77
Table 2-16. Table of Characteristics for the Malian case-control study by SI and McC genotype.	2-78
Table 2-17. Adjusted Odds Ratios for different genetic models for the SI polymorphism in the Kenyan case-control study.	2-82
Table 2-18. Adjusted Odds Ratios for different genetic models for the McC polymorphism in the Kenyan case-control study.	2-83
Table 2-19. Reanalysis of Kenyan case-control study including children who lived outside of the KHDSS study area.	2-86
Table 2-20. Investigation of the sickle trait/ α^+ thalassaemia negative epistatic interaction and the SI2/ α^+ thalassaemia interaction by clinical outcome in the Kenyan case-control study.	2-89
Table 2-21. Reanalysis of the Kenyan case-control study excluding all children with one or more sickle cell alleles does not alter findings.	2-90
Table 2-22. Raw data for the combined sickle trait, α^+ thalassaemia and SI genotype by clinical outcome in the Kenyan case-control study.	2-91
Table 2-23. Correlations between the sickle cell, α^+ thalassaemia, SI2 and McC ^b variants in the Kenyan case-control study.	2-92
Table 2-24. Adjusted Incidence Rate Ratios for SI disease associations in the longitudinal cohort study by genetic models of inheritance.	2-94
Table 2-25. Adjusted incidence rate ratios for McC disease associations in the longitudinal cohort study by genetic models of inheritance.	2-95
Table 3-1. Characteristics of individuals studied.	3-122
Table 3-2. Effect of donor variables on cluster number from mixed effects Poisson regression.....	3-132
Table 3-3. Effect of donor variables on cluster volume from mixed effects linear regression.....	3-134
Table 4-1. Summary of published data investigating CR1 expression by human endothelial cells.	4-147

Table 4-2. Summary of α -CR1 antibodies used in this chapter.	4-149
Table 4-3. Primary antibodies used for HBEC-5i experiments.....	4-151
Table 4-4. Secondary antibodies used for HBEC-5i experiments.	4-152
Table 4-5. CR1 peptides detected in the CR1-CHO positive control by mass spectrometry.....	4-188
Table 4-6. Golgi proteins identified by mass spectrometry of HBEC-5i lysate	4-209
Table 5-1: Primer sequences.....	5-227
Table 5-2: Comparison of published amino acids at the site of interest.....	5-250
Table 5-3 Mutations and their respective nucleotide, amino acid and charge....	5-251

“What is wanted is not the wish to believe,
but the will to find out,
which is the exact opposite.”

Bertrand Russell, *Free Thought and Official Propaganda*, 1922

1 Introduction

1.1 The genetic arms race between man and malaria

The greasy fingerprints of malaria run through the length of the human genome. For tens of thousands of years, each species has been attempting to outwit the other through the mutation, shuffling and repurposing of their genes, both with the ultimate goal of survival. Many of these genetic changes are not without cost. It is a sign of the magnitude of the threat from malaria that potentially fatal genetic mutations such as sickle cell have become firmly established in some populations as the payoff – protection against death from malaria – is so great. In return, the parasite expends huge amounts of energy in evading and subverting the human immune system. It is over 70 years since Haldane first suggested that the high frequency of β -thalassaemia in an Italian population was due to selection by malaria (Haldane, 1949) and we are still unearthing new human genetic polymorphisms that protect against the disease. More recently, we have begun to consider how individual human polymorphisms tessellate and interact to shape an individual's susceptibility to malaria.

This thesis explores two polymorphisms in the complement receptor 1 (CR1) gene whose role may have been inappropriately discounted in the genetic skirmish against malaria. These polymorphisms may yet provide a valuable window into alternative ways to protect against or treat malaria, if, as is so often the case, nature has got there first.

1.2 General background

1.2.1 Global prevalence of malaria

The World Health Organisation (WHO) estimated a global burden of 216 million cases of malaria including 445,000 deaths worldwide in 2016 (WHO, 2017). Ninety percent of these cases occurred in sub-Saharan Africa, with the majority of deaths occurring in children under five years. The decline in malaria seen between 2010 and 2014 has stalled, acting as a stark warning against complacency. The lack of an effective vaccine and the persistent threat of resistance to antimalarial drugs and insecticides ensure it is still a major challenge (Ashley et al., 2014; Sokhna et al., 2013). The global distribution of malaria is detailed in Figure 1-1.

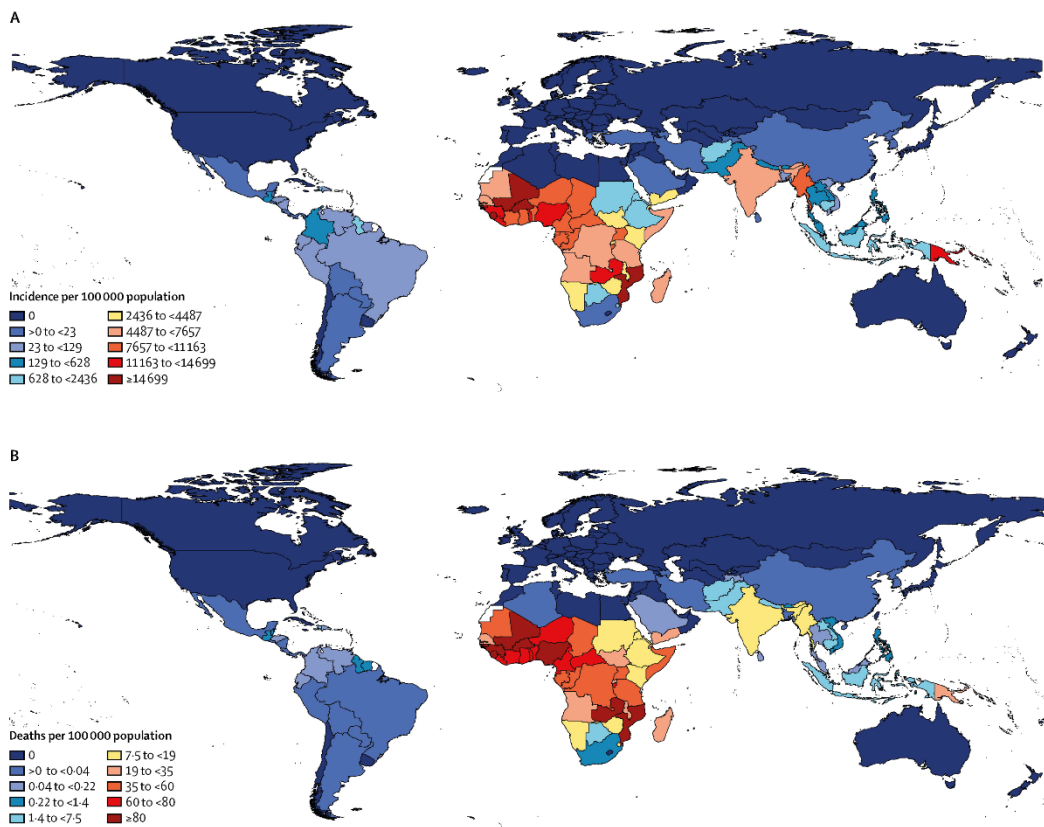


Figure 1-1. Global burden of malaria cases and deaths from 2013. Age-standardised malaria incidence (top panel) and death (bottom panel) rates in 2013. Image taken directly from (Murray et al., 2014).

1.2.2 The life cycle of *Plasmodium falciparum*

Malaria is due to infection by *Plasmodium* parasites, of the phylum Apicomplexa. Five *Plasmodium* species can cause malaria in humans. *Plasmodium falciparum* is responsible for 99% of cases of malaria in Africa and the majority of global mortality (WHO, 2017) and is thought to have originated from the zoonotic transfer of *P. praefalciparum* from gorillas to humans approximately 10,000 years ago (Liu et al., 2010). This thesis investigates genetic polymorphisms found almost exclusively in African populations and focuses entirely on *P. falciparum*.

P. falciparum is transmitted when a human is bitten by an infected female *Anopheles* mosquito, which acts as the obligate host for parasite sexual development. Sporozoites are injected via the mosquito's salivary glands during a blood meal. This initial injection usually contains less than 100 sporozoites, which travel through the circulation to invade hepatocytes (reviewed in (Prudêncio et al., 2006)). Invasion is followed by intense mitosis and merozoites (exoerythrocytic forms of the parasite) are packaged into merozoites (Sturm et al., 2006). The parasite induces liver cell death and release of the merozoites into the circulation approximately six days after the mosquito bite.

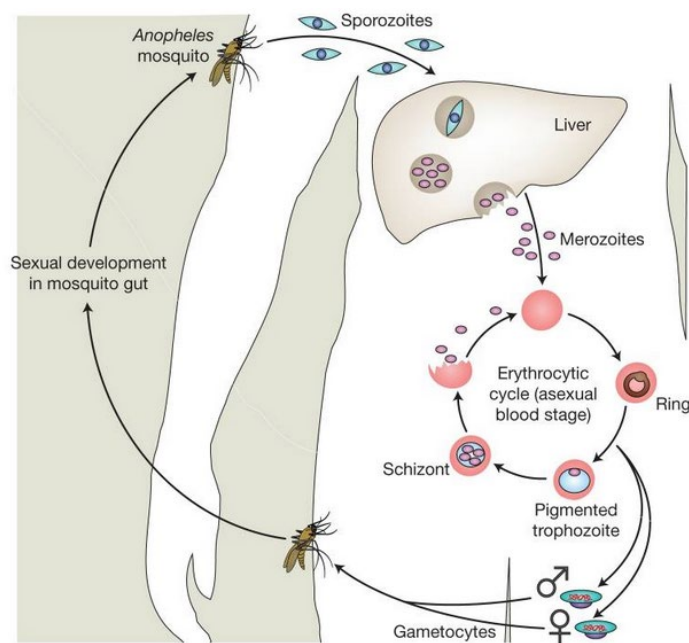


Figure 1-2. Life-cycle and developmental stages of *P. falciparum*.
Image taken directly from (Rowe et al., 2009).

Once in the blood, merozoites invade erythrocytes via a complex process involving multiple receptor-ligand interactions (reviewed in (Cowman et al., 2012)). These interactions include complement receptor 1 (CR1) on the erythrocyte and the parasite adhesin *P. falciparum* reticulocyte-binding homologue 4 (PfRh4, see section 1.7.2)

The merozoite develops from ring stage to a mature pigmented trophozoite and finally to a schizont (Figure 1-3). During this process, the infected erythrocyte (IE) undergoes modification by the parasite including the digestion of haemoglobin to haem (toxic to the parasite) and then to haemozoin (non-toxic, reviewed in (Egan, 2002)). As the parasite matures, the erythrocyte becomes increasingly rigid (Suwanarusk et al., 2004) and multiple parasite proteins are exported to the surface of its membrane. Each schizont gives rise to 8-36 daughter merozoites on rupture and the invasion process begins again (Garg et al., 2015). This cycle repeats every 48 hours, with merozoites free in the circulation for only a matter of seconds.

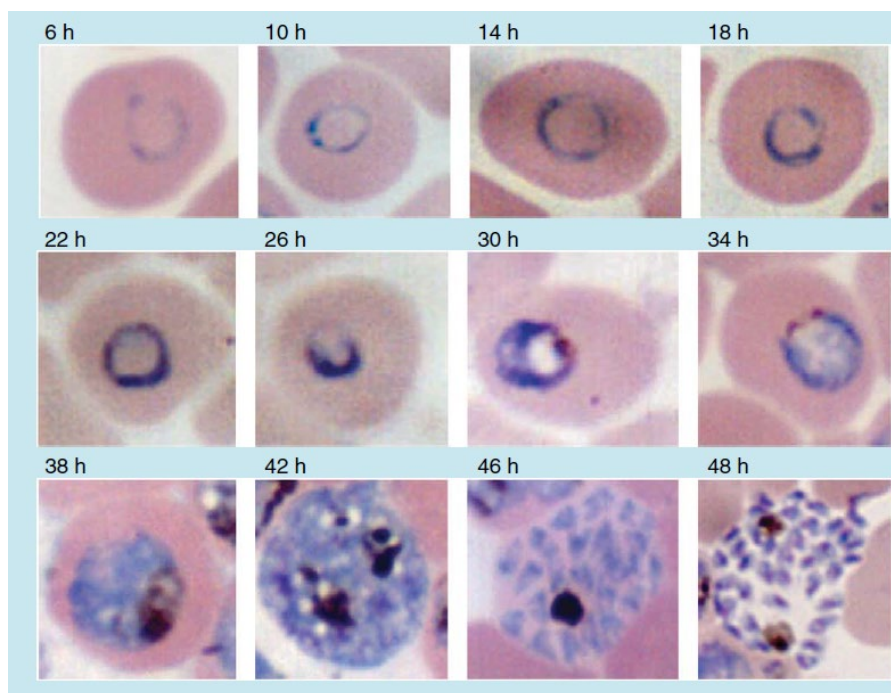


Figure 1-3. Intra-erythrocytic blood stages of *P. falciparum*.
Ring stage (6-22 hours), trophozoite stage (22-38 hours) and schizont stage (38-48 hours).
Merozoites can be seen at 48 hours prior to erythrocyte rupture and new invasion.
(Figure taken directly from (Radfar et al., 2009).

Not all merozoites follow this cycle, with some committing to differentiate into male or female gametocytes after invading an erythrocyte (Silvestrini et al., 2000). These forms are responsible for the transmission of the parasite from the human host to a new insect host. The male and female gametocytes are ingested during a mosquito blood meal and form a zygote in the insect's midgut. The zygote forms an ookinete which infiltrates the midgut wall to form an oocyst, in turn producing thousands of sporozoites (reviewed in (Kuehn and Pradel, 2010)). The oocyst bursts releasing the sporozoites which migrate to the mosquito's salivary gland, allowing the cycle to begin again.

1.2.3 Clinical sub-phenotypes of malaria

Infection with *P. falciparum* can result in a wide range of clinical symptoms ranging from asymptomatic parasitaemia to severe malaria. While diagnosis previously relied on detection by microscopy, antigen-based rapid diagnostic tests (RDTs) are now the standard of care in many settings, with an estimated 312 million RDTs carried out globally in 2017 (WHO, 2017).

1.2.3.1 Uncomplicated malaria

Although repeated infection with malaria results in acquired natural immunity, sterile immunity does not occur (reviewed in (Doolan et al., 2009; Hviid, 2005)). As such, some individuals are parasitaemic with no symptoms of the disease (asymptomatic malaria). In susceptible individuals, symptoms of uncomplicated malaria (UM) include fever and vomiting with rigors, headaches, malaise, muscle and joint pains and diarrhoea. Children can also present with a cough or difficulty breathing. Fevers coincide with schizont rupture and the release of merozoites from IEs, occurring every 48 hours (Golgi, 1886). However, the cluster of symptoms is often non-specific. First-line treatment for UM varies with local resistance, but involves three days of artemisinin-based combination therapy, which combines an artemisinin derivative (artemether, artesunate or dihydroartemesinin) with a longer-acting antimalarial with a different mechanism of action (lumefantrine, amodiaquine, mefloquine, piperaquine or sulfa-doxine-pyrimethamine) (World Health Organization and Global Malaria Programme, 2015).

1.2.3.2 Severe malaria

Patterns of severe malaria vary with transmission intensity. In areas of stable, high transmission (e.g. sub-Saharan Africa), infants and young children are most at risk of severe disease (Carneiro et al., 2010; Snow et al., 1997)). However, in areas of unstable or low transmission (e.g. South East Asia), older children and adults are more likely to be affected (Dondorp et al., 2008a). In sub-Saharan Africa, the median age of patients with severe malaria is inversely proportional to transmission intensity, i.e. infants and young children suffering most in areas of high transmission (Modiano et al., 1998; Snow et al., 1994). In populations with year-round high transmission, the commonest manifestation of severe malaria is severe malarial anaemia (very young children), whereas in areas of lower or seasonal transmission, the picture is more of cerebral malaria (older children) (Modiano et al., 1998; Snow et al., 1994). While WHO collects data on UM cases and deaths, the burden of severe disease is harder to ascertain. However, the WHO estimates that *“1-3% of uncomplicated cases were assumed to have moved to the severe stage”* (WHO, 2017).

In areas of continual exposure, natural immunity to malaria increases with age. Immunity against severe disease is acquired rapidly, followed by immunity against mild malaria and finally, most malaria infections in adulthood are asymptomatic (Figure 1-4, (Marsh and Kinyanjui, 2006; White et al., 2014)). A prospective study of 882 Tanzanian children revealed that most cases of severe malaria occurred after having one or more episodes of UM, rather than during their first infection (Gonçalves et al., 2014). In addition, although 102 children developed severe malaria over the study period, only 15 of these had a second episode. Examining the parasite densities of study participants revealed that this naturally acquired resistance to severe disease was not due to controlling parasite density.

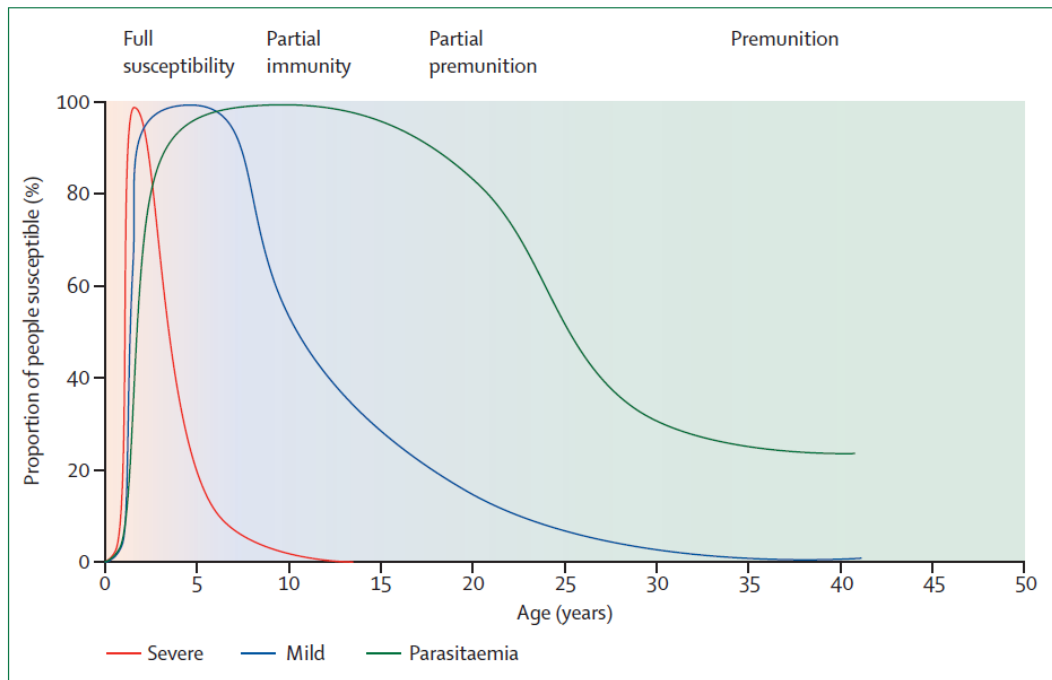


Figure 1-4. Severity of malaria varies with age in an area of moderate transmission. Repeated exposure results in development of protection against severe malaria, followed by mild malaria and finally some protection against asymptomatic malaria. (Image taken directly from (White et al., 2014), which is modified from (Marsh and Kinyanjui, 2006)).

In sub-Saharan Africa, severe malaria is predominantly a disease of children, with the most common symptoms being impaired consciousness, seizures, respiratory difficulties, severe anaemia and jaundice with laboratory findings including hypoglycaemia, high lactate and metabolic acidosis (Marsh et al., 1995; WHO, 2014). In particular, the presence of impaired consciousness or respiratory distress was found to predict 84% of deaths in Kenyan children admitted to hospital with malaria (Marsh et al., 1995). These symptoms are classically categorised into the (sometimes overlapping) syndromes of cerebral malaria (CM), severe malarial anaemia (SMA) and respiratory distress (RD, outlined below). Severe malaria can be difficult to diagnose as the symptoms and laboratory findings are similar to other severe infections.

1.2.3.3 Cerebral malaria

Cerebral malaria (CM) is diagnosed when a patient is in an unrousable coma (Blantyre coma score ≤ 2) in association with *P. falciparum* parasitaemia and after the exclusion of other causes of coma (including prolonged seizure activity, hypoglycaemia and meningitis) (World Health Organization and Global Malaria Programme, 2015). However, even when this definition was strictly applied, an autopsy series of Malawian children diagnosed with “cerebral malaria” found that 7 of the 31 children had actually died of other causes (Taylor et al., 2004). This misclassification was improved by an additional retinal examination which identifies retinal features that mirror the infected microvasculature in the brain. These include retinal whitening, retinal haemorrhages, vessel changes and papilloedema (reviewed in (Beare et al., 2006)). The mortality rate of CM in Africa varies from 15-30% (Marsh et al., 1995; Molyneux et al., 1989; Oluwayemi et al., 2013; Walker et al., 1992; Waller et al., 1995), with 9-14% of survivors suffering from neurological sequelae (Molyneux et al., 1989; Oluwayemi et al., 2013). Current therapy for CM is sub-optimal, relying on the same anti-malarial medications as for UM together with supportive treatment and high quality nursing care (WHO, 2014).

Intravenous artesunate has been the standard of care in severe malaria (World Health Organization and Global Malaria Programme, 2015) since an open-label randomised controlled trial across nine African countries comparing parenteral artesunate and quinine. Artesunate was associated with reduced mortality (OR 0.75, 95% CI 0.63-0.90) (Dondorp et al., 2010). However, even in the arm receiving intravenous artesunate under trial conditions, CM mortality was still 18%.

1.2.3.4 Severe malarial anaemia

In children, severe malarial anaemia (SMA) is diagnosed as a haemoglobin of ≤ 5 g/dL with a parasitaemia of $>10,000/\mu\text{L}$ (World Health Organization and Global Malaria Programme, 2015). SMA is more common in younger children and in areas of stable malaria transmission (Snow et al., 1997). SMA has a mortality rate of 4-16% when occurring alone which rises when presenting in combination with other syndromes (Marsh et al., 1995; Slutsker et al., 1994). SMA is multifactorial and

involves the destruction not only of deformed IEs by the spleen, but also uninfected bystander cells (Abdalla, 1988; Waitumbi et al., 2004) as well as dysregulation of erythropoiesis (Abugri et al., 2014; Dörmer et al., 1983). Nutritional status and intestinal parasites are also likely to be important in predisposition to SMA (Calis et al., 2008). In addition to anti-malarial treatment, SMA requires the transfusion of virus-screened fresh whole blood, which is often in short supply (World Health Organization and Global Malaria Programme, 2015).

1.2.3.5 Respiratory distress

In African children, respiratory distress is the manifestation of metabolic acidosis and represents the attempt to compensate for this through expellation of carbon dioxide. Metabolic acidosis is primarily due to the accumulation of lactic acid and 3-hydroxybutyric acid (Sasi et al., 2007) and is strongly associated with increased mortality (Dondorp et al., 2010; Marsh et al., 1995). In some cases, respiratory distress can be due to concomitant pneumonia or cardiac failure due to severe anaemia (World Health Organization and Global Malaria Programme, 2015). Specific treatment is difficult, with the role of intravascular fluid replacement particularly unclear after a large study of febrile African children admitted to hospital with impaired tissue perfusion found that giving fluid boluses actually increased mortality when compared to maintenance fluids (Maitland et al., 2011).

1.2.3.6 Malaria acute kidney injury

Another severe life-threatening complication is malaria acute kidney injury (MAKI) clinically manifesting as oliguria, encephalopathy, cardiac dysrhythmias and acidosis (WHO, 2014). MAKI has also been associated with increased risk of neurodisability in African children and biomarkers of renal injury (cystatin C, blood urea nitrogen and urinary chitinase-3-like 1) also correlate with mortality (Conroy et al., 2016, 2018; von Seidlein et al., 2012).

MAKI is particularly common in adults in low malaria transmission areas of Asia and historically was not commonly reported in paediatric populations in sub-Saharan Africa (reviewed in (Mishra and Das, 2008)). A retrospective study from Nigeria

reported that MAKI only accounted for 3% of all paediatric severe malaria (Okpere et al., 2017). However, the prevalence of MAKI may be under-reported as children may not suffer overt clinical signs or they may be overshadowed by the more clinically evident symptoms of cerebral malaria. Indeed, one Gambian study found that 25% of children with cerebral malaria also had evidence of renal impairment (Weber et al., 1999). Another recent study examining the renal function of 180 Ugandan children with severe malaria found 46% met the diagnostic criteria for MAKI (Conroy et al., 2016).

The pathogenesis of MAKI is incompletely understood. Unlike CM, MAKI does not appear to be due to cytoadherence or sequestration of infected parasites (MacPherson et al., 1985; Nguansangiam et al., 2007). Instead, the pathological process may include malarial immune complex deposition in the glomerular capillaries, pro-inflammatory cytokines, reactive oxygen intermediates together with intravascular haemolysis, hypovolaemia and hypoxia (reviewed in (Mishra and Das, 2008)). More recently, both haem and haemopexin have been implicated in the pathogenesis of AKI, possibly through the triggering of endothelial dysfunction and subsequent impairment of renal perfusion (Elphinstone et al., 2016).

1.2.4 *P. falciparum* virulence factors

The *P. falciparum* parasite has an extensive repertoire of virulence factors which result in cytoadherence and immune evasion. A hallmark of *P. falciparum* infection is the absence of mature parasite stages from the peripheral circulation. This is due to their adhesion to the endothelium of capillary venules, resulting in sequestration in multiple organs including the brain, heart, lung and gut (Milner et al., 2015) in order to avoid destruction by the liver and spleen (Mebius and Kraal, 2005). Pigmented trophozoites use three adhesion mechanisms; rosetting (adhesion to uninfected erythrocytes), cytoadherence to endothelial cells and platelet-mediated clumping (Figure 1-5 and reviewed in (Rowe et al., 2009)). IEs can assume one or more of these phenotypes at a time (Adams et al., 2014; Claessens et al., 2012).

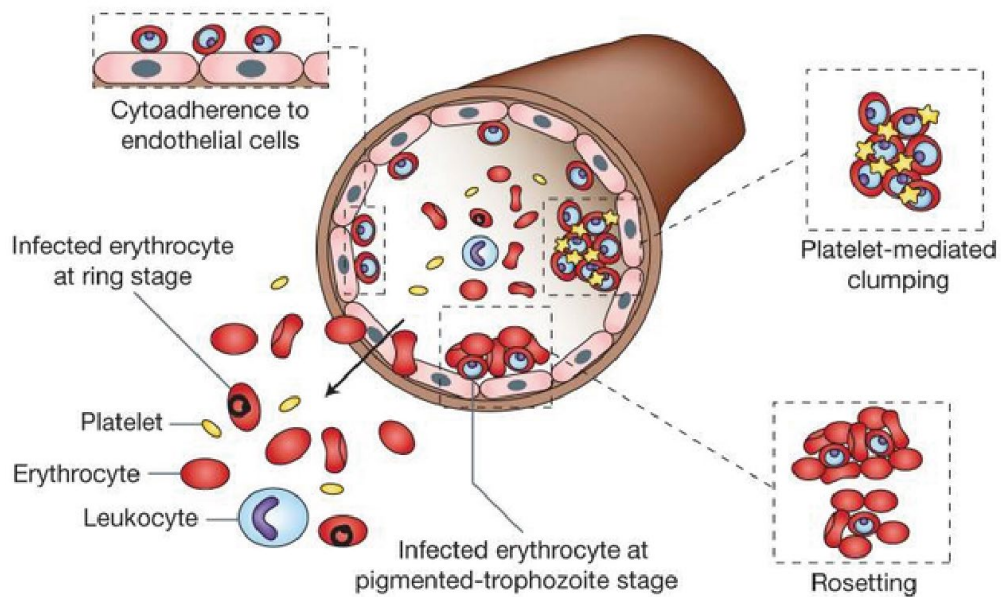


Figure 1-5. Adhesion mechanisms of *P. falciparum*-infected erythrocytes to endothelial cells, platelets and other erythrocytes.

Image taken directly from (Rowe et al., 2009).

Sequestration of parasitized erythrocytes may lead to obstruction of the microvasculature (Dondorp et al., 2004, 2008b), with the downstream effects of acidosis, hypoglycaemia and inflammatory mediator release (reviewed in (Planche and Krishna, 2006; Schofield, 2007)).

1.2.4.1 *P. falciparum* variant surface antigens

In order to evade the immune system, *P. falciparum* expresses hundreds of variant surface antigens (Miller et al., 2002; Scherf et al., 2008). Many variant antigens also mediate adhesion to host cells. The *P. falciparum* genome contains multi-gene families which include *var* genes (Baruch et al., 1995; Smith et al., 1995; Su et al., 1995), the repetitive interspersed family (*rif*) (Cheng et al., 1998; Fernandez et al., 1999; Kyes et al., 1999) and subtelomeric variant open reading frame (*stevor*) (Kaviratne et al., 2002).

Parasite adhesion is predominantly mediated by *P. falciparum* erythrocyte membrane protein 1 (PfEMP1), a transmembrane protein expressed on the surface of IEs. Each parasite genome contains approximately 60 *var* genes, each encoding variants of PfEMP1 (Baruch et al., 1995; Smith et al., 1995; Su et al., 1995). One

PfEMP1 variant is expressed at any given time, and the parasite can switch *var* gene transcription with each erythrocytic cycle to avoid immune system recognition (Chen et al., 1998; Roberts et al., 1992). These *var* genes are classified into Group A, B, C and E, with Group A and B/A being associated with severe malaria and showing a non-CD36 binding phenotype, whereas Group B, C and B/C are associated with non-severe disease and CD36 binding (Avril et al., 2013; Claessens et al., 2012; Jensen et al., 2004; Kyriacou et al., 2006).

PfEMP1 ligands include endothelial receptors (e.g. CD36, intracellular adhesion molecule 1 (ICAM-1), chondroitin sulfate A and endothelial protein C receptor (EPCR)), receptors on the erythrocyte surface (e.g. blood group antigens A and B, heparan sulfate and complement receptor 1 (CR1)) and serum components (including IgM, reviewed in (Bull and Abdi, 2016; Rowe et al., 2009)).

1.2.4.2 Cytoadherence to endothelial cells

The cytoadherence of IEs to endothelial cells is of particular interest in CM, where sequestration is implicated both in direct obstruction of the cerebral microvasculature and associated inflammation and coagulopathic changes (see also section 1.2.5) (Dondorp et al., 2004, 2008b; van der Heyde et al., 2006; Milner et al., 2008). The endothelial binding receptors for PfEMP1 in CM are still to be fully elucidated. Some parasite strains can bind to ICAM-1 expressed on endothelial cells (Berendt et al., 1989) which may be upregulated by TNF stimulation in CM (Wassmer et al., 2011).

A recently described *P. falciparum* binding receptor in brain endothelium is endothelial protein C receptor (EPCR) (Turner et al., 2013). EPCR binds specific adhesion domains (domain cassettes or DC) of PfEMP1; DC 8 and DC 13 (Lau et al., 2015; Turner et al., 2013) which are associated with cerebral and severe malaria and also bind to human brain endothelial cells (HBECs) (Bertin et al., 2013; Lavstsen et al., 2012). There is also evidence that IEs use a combination of ICAM and EPCR to bind to HBECs (Avril et al., 2016). These findings were predominantly based on PfEMP1 recombinant protein experiments. However, recent work using parasite

lines expressing the same PfEMP1 variants as previously reported found they bound to HBEC and expressed DC 13, but did not bind to EPCR, questioning the biological relevance of EPCR in parasite sequestration in CM (Azasi et al., 2018).

1.2.4.3 Rosetting

A rosette is formed when an IE binds to two or more uninfected erythrocytes, a process which occurs spontaneously at various rates in field isolates (Udomsangpetch et al., 1989). Together with cytoadherence to endothelial cells, rosetting is a key mechanism in the obstruction of the microvasculature (reviewed in (Wahlgren et al., 2017)). In studies of African children, all sub-phenotypes of severe malaria have been associated with high rates of rosetting and larger rosettes when compared to cases of UM (Dumbo et al., 2009; Kun et al., 1998; Rowe et al., 1995, 2002a, 2007; Treutiger et al., 1992). However, the association does not extend to south east Asia (Angkasekwina et al., 1998; Ho et al., 1991), implying geographical differences in pathogenesis.

PfEMP1 mediates rosetting (Rowe et al., 1997), with *P. falciparum* field isolates showing a strong association between rosetting frequency and Group A *var* gene transcription (Bull et al., 2005; Kyriacou et al., 2006; Warimwe et al., 2012). The best characterised rosetting receptor is complement receptor 1 (CR1), which is discussed in detail in section 1.7.1. In addition to erythrocyte receptors, serum components play a role, with decreased rosette frequency seen when parasites are cultured in serum-free media (Somner et al., 2000). Some rosetting parasites bind non-immune IgM, a property associated with increased severity of disease (Ghumra et al., 2008; Rowe et al., 2002a). IgM binding appears to reinforce rosettes by cross-linking PfEMP1 molecules (Stevenson et al., 2015a). α 2-macroglobulin has also been reported as a serum rosetting factor, with the ability to cross-link PfEMP1, working synergistically with IgM in the development of rosettes (Stevenson et al., 2015b).

1.2.4.4 Platelet-mediated clumping

The auto-agglutination of IEs into clumps is mediated by platelets (Pain et al., 2001). In addition to contributing to microvascular obstruction, platelet clumping may

function as a bridge between IEs and activated endothelium (Wassmer et al., 2004). Platelet clumping has not been as extensively studied as rosetting and there is conflicting evidence as to the role it plays in the development of severe malaria in Africa (Arman et al., 2007; Mayor et al., 2011; Pain et al., 2001; Wassmer et al., 2008).

1.2.5 Cerebral malaria pathogenesis

Despite decades of research, the pathogenesis of CM remains incompletely understood. Sequestration of mature *P. falciparum* IEs is one of the hallmarks of CM, with multiple autopsy studies reporting a higher level of parasite sequestration in the brain than in other organs (MacPherson et al., 1985; Milner et al., 2014; Pongponratn et al., 1991, 2003). Sequestration is associated with mechanical obstruction of the blood flow and impaired tissue perfusion and localised hypoxia (Dondorp et al., 2008b), with both infected and uninfected erythrocytes becoming less deformable (Dondorp et al., 1997). Importantly, a recent paper has reported that neurovascular sequestration of IEs can be directly observed at the bedside as orange discolouration of the retinal vessels on indirect ophthalmoscopy of Malawian children with CM (Barrera et al., 2018). Monocytes containing malaria pigment and fibrin–platelet thrombi have also been reported to sequester in the brain of African children with CM, particularly in those with HIV co-infection (Dorovini-Zis et al., 2011; Hochman et al., 2015).

A series of detailed autopsy studies in Malawian children with CM defined two discrete phenotypes, those with sequestration alone (CM1) and those with additional intravascular and perivascular pathology (CM2), including ring haemorrhages and extra-erythrocytic pigment (Dorovini-Zis et al., 2011; Milner et al., 2014). These changes were associated with permeability of the blood-brain barrier (BBB) in African children, with evidence of fibrinogen extravasation associated with ring haemorrhages (Dorovini-Zis et al., 2011). This is in contrast to a large study of Thai adults with CM which found the BBB to be intact and CSF opening pressures to be lower in cases of fatal CM than in CM survivors (Warrell et al., 1986). However, a magnetic resonance imaging (MRI)-based investigation of 168

Malawian children with CM found that 84% of children who died with CM had evidence of severe brain swelling on admission, compared to 27% of CM-survivors, suggesting increased brain volume with raised intracranial pressure may influence CM outcome (Seydel et al., 2015). Following this, a detailed MRI study of CM in India (5 adults, 6 children) showed results consistent with vasogenic oedema in all patients, with 5 also showing venous congestion, which was considered to be due to the sequestration of IEs in the cerebral microvasculature (Mohanty et al., 2017). A recent Zambian MRI study of children with CM using a stronger magnetic field further supported this hypothesis that the cerebral oedema was vasogenic rather than cytotoxic in nature and that results were consistent with parasite sequestration, local inflammation and vascular congestion (Potchen et al., 2018).

Other studies suggest activation and dysfunction of the cerebral microvascular endothelium are key in CM, occurring through a combination of direct interaction with IEs and the effect of pro-inflammatory cytokines (reviewed in (Medana and Turner, 2006)). The rupturing of schizonts releases parasite toxins into the bloodstream, with the subsequent activation of monocytes and neutrophils and cytokine secretion (reviewed in (Gazzinelli and Denkers, 2006)). Pro-inflammatory cytokines IL-1 β , IL-6 and IL-8 are raised in malaria-infected individuals and correlate with disease severity (Day et al., 1999; Lyke et al., 2004). Patients with CM have increased levels of both TNF- α and soluble TNF- α receptors, with high levels of the cytokine correlating with increased mortality (Kwiatkowski et al., 1990; Molyneux et al., 1993). TNF- α activates endothelial cells resulting in upregulation of surface receptors including ICAM-1, whilst stimulation of HBEC in vitro with TNF increases cytoadherence of parasitized erythrocytes (Wassmer et al., 2005). In addition, microvascular endothelial cells from the subcutaneous tissue of Malawian children with CM or UM showed differential reactivity to stimulation with TNF- α , with cells from CM patients showing higher ICAM-1 upregulation, IL-6 production and microparticle shedding (Wassmer et al., 2011). A pro-coagulant state is also seen in CM, with localised coagulopathy characterised by fibrin deposits reported in the brains of African children with CM (Dorovini-Zis et al., 2011).

1.2.6 Models of cerebral malaria

In disentangling the pathology of any disease, a suitable model is necessary.

1.2.6.1 Human model

Historically, CM has been studied in humans using autopsies. By their nature, autopsy studies provide a static view of the disease end-point, with the disease process itself needing to be inferred. Access to patients who have died is limited and cultural and ethical issues pertaining to post-mortem studies must not be underestimated, particularly regarding children in resource-poor settings (Lewis et al., 2018; Lishimpi et al., 2001). Autopsy studies also compare brains with CM against those from patients who died from other causes, rather than against healthy individuals. The brains of survivors are, by definition, unavailable for comparison.

There a number of complementary methods to investigate CM during life. These approaches include ocular fundoscopy, which has described a unique malaria retinopathy, increasing specificity in CM diagnosis (reviewed in (Beare et al., 2006)). In addition, neuroimaging enables sequential visualisation throughout the disease process and during follow up of CM survivors. Computed tomography (CT) has been crucial in establishing the increase in brain volume seen in CM (Mohanty et al., 2011; Newton et al., 1994; Patankar et al., 2002) and the technology is more widely available than magnetic resonance imaging (MRI). However, the detail afforded by MRI together with the ability to perform functional MRI (fMRI) scans makes this modality the current neuroimaging of choice (Loareesuwan et al., 2009; Mohanty et al., 2014) However, the availability of MRI scanners in malaria-endemic areas has limited this approach to a few key research centres.

Microcirculatory studies provide another dynamic route of investigation, with orthogonal polarization spectral imaging used to examine accessible areas of microcirculation during severe malaria as a proxy for the disease process in the brain (Dondorp et al., 2008b; Hanson et al., 2012, 2015). However, heterogeneity of endothelial cells means findings may not be extrapolatable to the brain (Aird, 2012).

1.2.6.2 Murine models

While the use of mouse models has been indispensable in the investigation of many diseases, their place in CM is a subject of heated debate. As *P. falciparum* does not infect mice, alternative rodent parasites are required, including *P. chabaudi*, *P. berghei* and *P. yoelii*. In particular, the *P. berghei* ANKA infection in CBA or CB57BL/6 mice is a commonly used model with mice genetically resistant or susceptible to CM (reviewed in (Lou et al., 2001)). However, this model results in markedly different histopathological features to human CM. The major difference is in sequestration of IEs in the cerebral microvasculature, which is a hallmark of post-mortem studies of human CM (e.g. (Barrera et al., 2018; Dorovini-Zis et al., 2011; Seydel et al., 2006; Turner et al., 1994) but not consistently reported in murine CM studies, which are instead associated with the accumulation of leucocytes in the brain vessels and varying levels of IEs in multiple organs (Cabrales et al., 2010; Franke-Fayard et al., 2005; Riley et al., 2010). Indeed, these differences have led one researcher to quip: “(...) one cannot have cerebral malaria without cerebral sequestration (unless, of course, you are a mouse)...” (Milner, 2010). Some researchers consider the processes in murine CM to be so different from human CM that the “(...) pathological and therapeutic interpretations derived from it were largely irrelevant for the understanding and treatment of HCM (human CM) (Craig et al., 2012).” Findings from murine CM studies must be interpreted with caution.

1.2.6.3 In vitro models

A number of endothelial cell lines have been used in the investigation of CM. Human umbilical vein endothelial cells (HUVECs) are primary cells which can easily be obtained at birth. HUVECs have historically been used in studies of malaria pathogenesis (Nash et al., 1992; Udeinya et al., 1981) but have significant limitations. In addition to their variability between donors, HUVECS are macrovascular cells, and are not the usual target for IE sequestration. Primary human brain endothelial cells (HBEC) circumvent one of these issues and have been used widely in the study of CM (e.g. (Adams et al., 2014; Avril et al., 2012, 2016; Claessens et al., 2012)), however genetic and environmental differences between

donors may again influence findings and their reproducibility (reviewed in (Bouis et al., 2001). In addition, both primary cell lines are limited by the length of time they can be cultured and the potential for contamination with unwanted cells from the donor.

Immortalised human brain endothelial cell lines, which include the HBEC-5i (Dorovini-Zis et al., 1991; Wassmer et al., 2006) and hCMEC/D3 lines (Weksler et al., 2013), provide a reproducible cerebral microvascular environment which can be cultured with parasitized erythrocytes. Although many additions can be made to this approach, for example co-culturing with peripheral blood mononuclear cells (PBMCs) (Khaw et al., 2013), or platelets (Wassmer et al., 2006), the approach is inherently limited by the absence of the immune system. In addition, the immortalisation process may result in unanticipated changes to the properties of these cells (Urich et al., 2012) and as such, findings require replication in primary HBEC experiments.

It is evident that no perfect model of CM exists, however immortalised HBEC-based models may provide the clearest starting point for investigating cellular level hypotheses in CM.

1.3 Host genetic resistance against malaria

Host genetic factors play a large role in an individual's susceptibility to severe malaria with one Kenyan study estimating 25% of the variation in malaria hospitalisation rates was attributable to genetic factors (Mackinnon et al., 2005). Of particular interest are erythrocyte polymorphisms. Two of the most widely reported polymorphisms in sub-Saharan Africa are sickle cell trait and α^+ thalassaemia, whose geographical distributions closely mirror the incidence of malaria (Figure 1-6) (Flint et al., 1998; Piel et al., 2010).

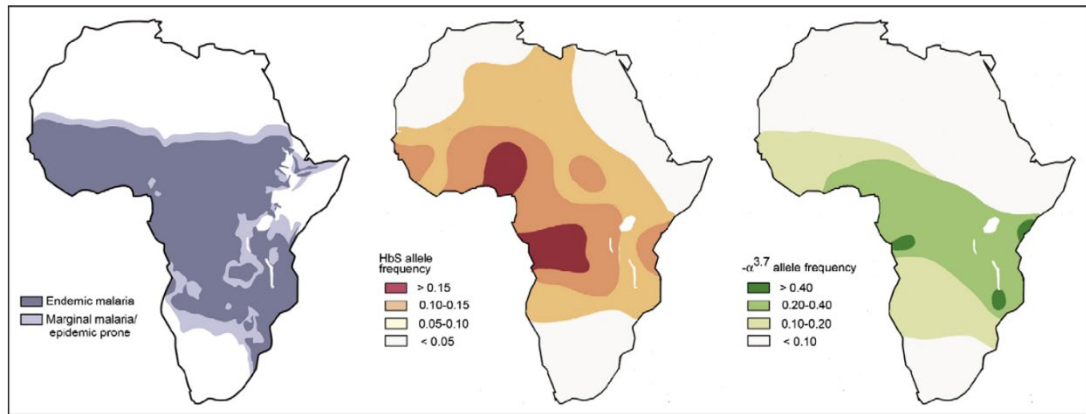


Figure 1-6. Approximate distributions of malaria, HbS and α^+ thalassemia in sub-Saharan Africa. Deletions of the $-\alpha^{3.7}$ type are the most common cause of α^+ thalassemia in Africa. Image taken directly from (Wellems and Fairhurst, 2005)

1.3.1 Sickle cell trait

The sickle cell polymorphism was the first point mutation to be associated with malaria over 50 years ago (Allison, 1964). The polymorphism comprises a glutamic acid to valine substitution in the β -globin gene on chromosome 11, resulting in the unstable haemoglobin variant HbS (Serjeant and Serjeant, 2001). The heterozygous form (HbAS, sickle cell trait) is clinically silent, but confers a high degree of protection against all forms of severe and UM (Taylor et al., 2012; Williams et al., 2005a). The strength of association is staggering, with results from a recent large multi-centre study into severe malaria across 12 locations in Africa, Asia and Oceania reporting that HbAS was associated with reduced odds of all severe malaria (OR 0.14, $p = 1.6 \times 10^{-225}$), CM (OR 0.11, $p = 4.7 \times 10^{-88}$) and SMA (OR 0.11, $p = 9.3 \times 10^{-65}$) (Rockett et al., 2014). Sickle cell represents a classic example of a balanced mutation, with protection against malaria for heterozygotes, whilst homozygotes (HbSS) suffer from severe sickle cell disease, which is fatal without modern medical input. The protective mechanisms of HbAS have not been confirmed but may involve the early removal of IEs (Ayi et al., 2004), lower levels of rosetting (Carlson et al., 1994; Udomsangpetch et al., 1993), decreased cytoadherence and a reduction in the display of PfEMP1 on the surface of IEs (Cholera et al., 2008).

1.3.2 α^+ thalassaemia

α^+ thalassaemia arises from a deletion in the α -globin gene on chromosome 16, resulting in inadequate synthesis of α -globin (reviewed in (Weatherall and Clegg, 2001). The most common polymorphism responsible for α^+ thalassaemia in African populations is the 3.7-kb α -globin deletion. (Flint et al., 1998). Both heterozygous ($-\alpha, \alpha\alpha$) and homozygous ($-\alpha, -\alpha$) forms have been reported to protect against severe malaria (Taylor et al., 2012; Williams et al., 2005b). A meta-analysis examining the relationship between α^+ thalassaemia and severe malaria reported an odds ratio of 0.63 (95% CI 0.48-0.83) for homozygotes and 0.83 (95% CI 0.74-0.92) for heterozygotes (Taylor et al., 2012). In contrast, the polymorphism did not influence parasite density or protect against UM (Taylor et al., 2012; Williams et al., 1996, 2005b).

The protective mechanisms for α^+ thalassaemia may include the formation of smaller, weaker rosettes (Carlson et al., 1994), reduced cytoadherence (Butthep et al., 2006; Krause et al., 2012) and the spreading of haemoglobin across a higher number of smaller erythrocytes (Fowkes et al., 2008). Protection offered by α^+ thalassaemia may not be limited to malaria, with a report from Papua New Guinea associating the polymorphism with protection against severe non-malaria disease such as respiratory infections, gastroenteritis and meningitis (Allen et al., 1997).

1.3.3 Polymorphisms associated with protection against cerebral malaria

1.3.3.1 Southeast Asian ovalocytosis

Southeast Asian ovalocytosis (SAO) causes erythrocytes to be ovoid instead of biconcave discs and is caused by a deletion mutation in the erythrocyte membrane protein band 3 (SLC4A1 Δ 27), with heterozygosity specifically associated with protection against CM in Papua New Guinea (Allen et al., 1999; Genton et al., 1995). Not a single individual with SAO was found to suffer from CM across these two studies. *P. falciparum* infected SAO erythrocytes showed a marked increase in

binding to the endothelial receptor CD36 under flow conditions (Cortés et al., 2005). As CD36 is only sparsely expressed on brain endothelial cells (Turner et al., 1994), CD36 on endothelium out-with the brain may act as a decoy increasing sequestration outside of the cerebral microvasculature. Indeed, a clinical trial of exchange transfusions from donors with SAO has recently been suggested as a treatment for CM (Jajosky et al., 2017).

1.3.3.2 HbC

Another example of a red blood cell polymorphism with reported CM-specific protection is the structural variant of haemoglobin, HbC (May et al., 2007). Although the heterozygous state (HbAC) had been previously associated with protection against other forms of severe malaria in other smaller studies (Agarwal et al., 2000; Mockenhaupt et al., 2004), this larger study by May et al. carefully stratified patients by clinical outcome to identify the association of HbAC with a reduced OR of CM (0.64, 95% CI 0.45-0.91, $p=0.03$). This specificity may be due to the finding that *P. falciparum* infected HbAC erythrocytes express ~30% less PfEMP1 on their membranes, potentially altering their ability to bind to cerebral endothelium (Fairhurst et al., 2005).

1.3.3.3 Glucose-6-phosphate dehydrogenase (G6PD) deficiency

An alternate model for protection against CM can be seen in the X-linked condition glucose-6-phosphate dehydrogenase (G6PD) deficiency. Recently, evidence has been building that increasing levels of G6PD deficiency are associated with decreased odds of CM but increased risk of severe malaria anaemia (Clarke et al., 2017; Rockett et al., 2014; Uyoga et al., 2015). A working hypothesis for this CM-specificity is lacking at present, with evidence suggesting more global effects of the polymorphism on early phagocytosis of ring-stage infected G6PD erythrocytes (Cappadoro et al., 1998) and inhibition of *P. falciparum* growth inside G6PD erythrocytes (Roth et al., 1983), neither of which are specific to CM.

1.4 The complement system

1.4.1 Complement activation and function

The complement system is a network of almost 60 fluid-phase and membrane-bound proteins (Elvington et al., 2016). Complement activation produces three main effectors: the anaphylatoxins C3a and C5a, which result in leucocyte activation and recruitment, the opsonins C3b, iC3b, and C3d, which bind to and identify target cells and immune complexes (ICs) for removal by phagocytes and the terminal membrane attack complex (MAC, C5b-9) which causes direct cell lysis (reviewed in (Noris and Remuzzi, 2013)). Complement activation is triggered by danger signals via three major pathways; the classical (CP), alternative (AP) and lectin pathways (LP), which all lead to the production of a C3 convertase.

In the CP, the initiator molecule C1q binds to antigen-antibody complexes containing IgG or IgM or to other molecules including C-reactive protein and apoptotic/necrotic cells (Nauta et al., 2003), with sequential activation of C1r and C1s. Activated C1s then cleaves C4 (to C4a and C4b) and C2 (to C2a and C2b). C4bC2a, a C3 convertase, is then formed (reviewed in (Orsini et al., 2014)).

The LP produces the same C3 convertase, but via a different mechanism. Mannose binding lectin (MBL, structurally and functionally similar to C1q), collectins or ficolins act as the initiator molecules by recognising carbohydrate patterns including N-acetylglucosamine or mannose (reviewed in (Garred et al., 2016)), providing specificity for altered endogenous and exogenous surfaces (reviewed in (Takahashi and Ezekowitz, 2005)). This binding activates MBL-associated serine proteases (MASP-1, MASP-2 and MASP-3), cleaving C4 and C2 to form the C3 convertase C4b2a in a manner reminiscent of the classical pathway (Ehrnthaller et al., 2011; Vorup-Jensen et al., 2000). Regardless of whether the C3 convertase C4b2a has originated from the LP or CP, it is then able to cleave C3 to C3a and C3b. C3b subsequently complexes with C4b2a to form C4b2a3b, a C5 convertase.

Activation of the AP is slightly different and is due to the slow, spontaneous hydrolysis of C3 in the circulation to form C3(H₂O), known as “tick-over.” C3(H₂O)

binds factor B which is cleaved by factor D to form C3(H₂O)b, which is the C3 convertase of the AP, cleaving C3 into C3a and C3b. This C3b has three fates; amplification of the pathway by creating more C3 convertase (C3bBb), binding to an existing molecule of C3bBb to form the C3bBb3b complex (which is a C5 convertase), or inactivation by factor I and a cofactor.

Both C5 convertases (C4b2a3b and C3bBb3b) cleave C5 to C5a (anaphylotoxin) and C5b, which interacts with C6, C7, C8 and C9 to form C5b-9, the membrane attack complex (MAC), which is inserted into the target cell membrane, creating a pore which leads to cell lysis (reviewed in (Morgan, 1999)). In addition to the MAC, complement activation produces the opsonins C3b, iC3b, and C3d and C3a and C5a fragments. The latter are potent anaphylatoxins with roles in leucocyte chemotaxis, adhesion and up-regulation of vascular adhesion molecules on the endothelium (Albrecht et al., 2004; Hugli, 1981). Thrombin, plasmin and factors IXa, Xa, and XIa can also cleave C3 and C5 (Amara et al., 2010). A simplified overview of these pathways and their downstream effects is shown in Figure 1-7.

1.4.2 Complement regulation

The destructive abilities of complement are powerful but fairly non-specific and excessive complement activation on self tissue can have severe effects. To counter this, a number of complement regulators help to restrict inappropriate activation and amplification. Two functions are key; inactivation of C3b (and C4b) and acceleration of the decay of the C3 and C5 convertase complexes. Factor I is necessary for the inactivation of C3b and C4b, but requires the presence of a cofactor. Five complement regulators perform the tasks of decay acceleration and/or cofactor activity; the membrane-bound regulators complement receptor 1 (CR1), membrane cofactor protein (MCP) and decay accelerating factor (DAF), and the soluble regulators factor H (FH) and C4 binding protein (C4BP). These homologues belong to the regulators of complement activation (RCA) family which are made up of complement control protein (CCP) modules (reviewed in (Kirkidze and Barlow, 2001)). The regulatory protein CR1 is discussed in detail in section 1.6 and its points of regulation in the complement cascade are shown in Figure 1-7.

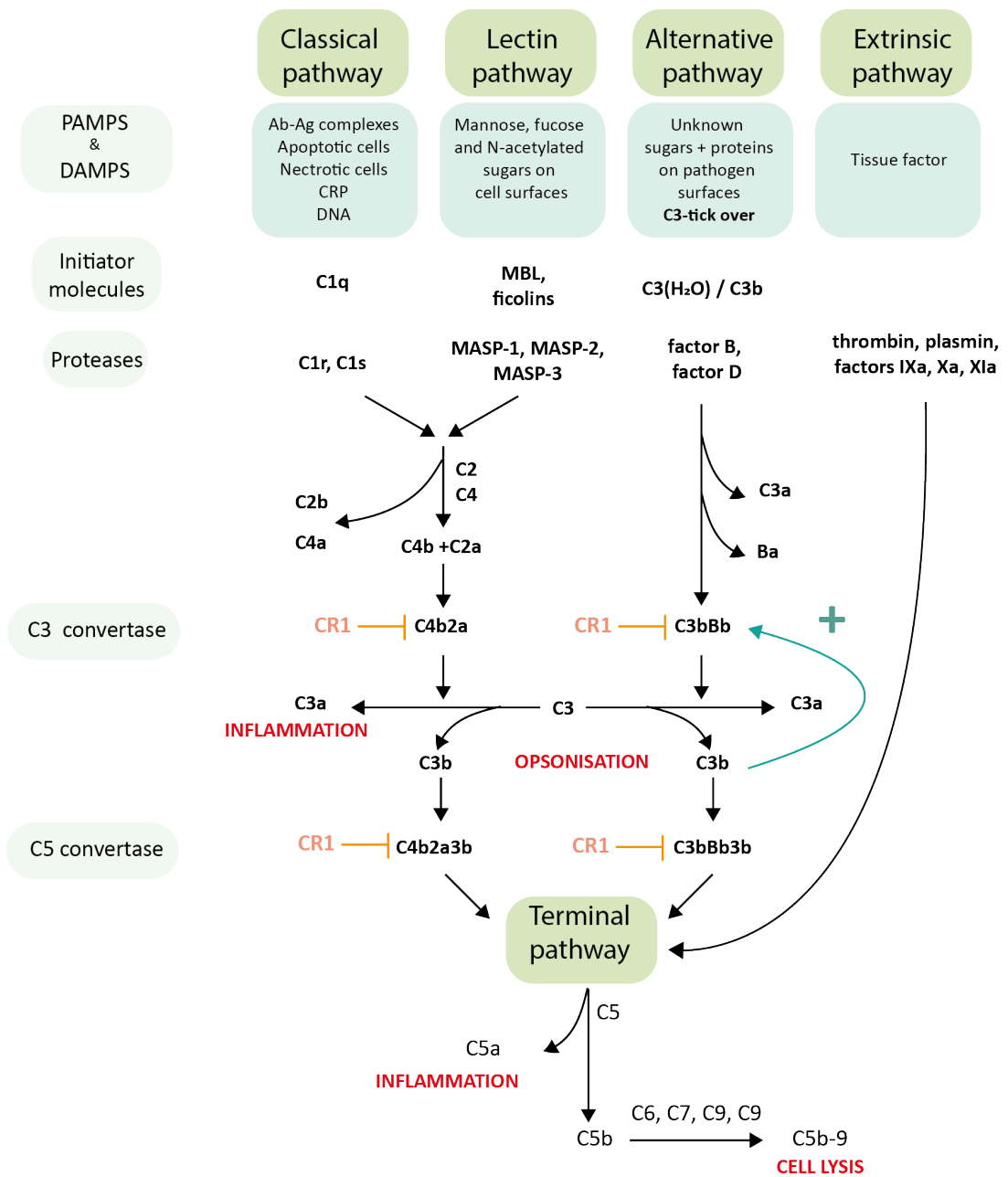


Figure 1-7. Overview of the pathways of complement activation.

See text for details.

Points marked **CR1** indicate where complement receptor 1 acts to inhibit complement activation.

In addition, CR1 acts as a cofactor with factor I to bind and degrade C3b.

Image adapted from (Orsini et al., 2014).

1.4.3 Exploitation by microorganisms

Subversion of the host immune system is a common strategy used by pathogens and the wide variety of complement receptors and regulatory proteins provides fertile ground for such subterfuge. Immune evasion includes the acquisition or mimicking of complement regulators, for example the expression of a factor H-binding protein by strains of *Neisseria meningitidis* (Biagini et al., 2016; Schneider et al., 2009). Another approach is to degrade complement proteins, e.g. *Pseudomonas aeruginosa* which produces elastase to break down C3 (Schmidtchen et al., 2003).

Other pathogens voluntarily activate the cascade, allowing themselves to be opsonised, interact with complement receptors and gain entry to the host cells (reviewed in (Lambris et al., 2008)). Many pathogens use CR1 as an invasion receptor, including *Mycobacteria tuberculosis* and *M. leprae* into monocytes and macrophages (Schlesinger and Horwitz, 1990; Schlesinger et al., 1990), *Legionella pneumophila* into monocytes (Payne and Horwitz, 1987) and *Leishmania spp.* into macrophages (Da Silva et al., 1989).

1.5 Complement and malaria

An association between malaria and complement activation was first described 100 years ago, when it was noted that erythrocytes from an infected individual were able to activate complement in vitro (Thomson, 1918). Evidence of complement activation has been consistently reported in malaria, with depletion of complement components C3, C4 and C1q (Ade-Serrano et al., 1981; Greenwood and Brueton, 1974; Neva et al., 1974; Phanuphak et al., 1985; Srichaikul et al., 1975) and an increase in the level of soluble MAC (sC5b-9) (Berg et al., 2015; Roestenberg et al., 2007). Complement activation correlates with severity of disease with level of activation associated with increased production of IL-6, IL-8, monocyte chemoattractant protein 1 and macrophage inflammatory protein 1 β (Berg et al., 2015; Nyakoe et al., 2009). Parasite components have been reported to activate complement, including merozoites (Korir et al., 2014), the digestive vacuole (Dasari et al., 2012, 2014), haemozoin and haematin (Berg et al., 2015; Pawluczko et al., 2007).

Infection with *P. falciparum* is associated with all three pathways of complement activation. Elevated levels of C1rs-C1inh were found in experimental human *P. falciparum* infection (Roestenberg et al., 2007), together with an increased clearance of radiolabelled C1q in natural *P. falciparum* infections (Srichaikul et al., 1975), implicating CP involvement. An increased level of C3bBb has also been reported in malarial infection (Roestenberg et al., 2007; Wenisch et al., 1997), suggesting concurrent AP involvement. The LP has also been linked with malaria, with three studies reporting MBL's ability to recognise malarial antigens (Garred et al., 2003; Klabunde et al., 2002; Korir et al., 2014). Complement activation was investigated using a case-control study of Kenyan children with UM or SMA and a functional complement activity ELISA (Nyakoe et al., 2009). The authors reported 100% consumption of the LP, 90% consumption of the CP and 63% consumption of the AP in children with SMA. Over half of the children with SMA had no measurable activity across all three complement pathways, suggesting complete consumption.

1.5.1 Complement and cerebral malaria

Of particular interest to this thesis is the role of complement in the development of CM. Complement activation was originally suspected when adult CM patients were found to be hypocomplementaemic with higher levels of the complement activation product C3d than patients with UM (9 CM cases, 23 UM cases) (Adam et al., 1981). Other reports of complement activation in severe malaria have included small numbers of CM cases alongside other severe phenotypes (Helegbe et al., 2007; Phanuphak et al., 1985; Srichaikul et al., 1975), or give no details on CM cases (Nyakoe et al., 2009). One such report included 23 adult Thai patients with severe malaria of whom 18 were diagnosed with CM (Wenisch et al., 1997). This study reported a marked increase in the complement activation products MAC, C4d (C4b degradation product) and Bb (product of factor B cleavage by factor D) in cases compared to healthy controls, indicating CP and AP activation in a group of (predominantly) CM cases. A small study of Ugandan children (n = 64) also reported significantly higher in C5a levels in children with CM than UM (Kim et al., 2014).

Direct histopathological investigation of complement activation in CM is distinctly lacking. Staining for complement components or receptors was not included in the major autopsy studies of Malawian children with CM (Dorovini-Zis et al., 2011; Hochman et al., 2015; Milner et al., 2014). The first direct histopathological evidence of complement activation in the brains of patients with CM was reported from an autopsy series of eight Malawian children with CM, which showed high levels of intravascular α -C5b-9 staining (membrane attack complex, MAC) in association with sequestered IEs (Brown et al., 2001). A more recent study investigating complement deposition on erythrocytes in *P. falciparum* infection also presented brief data on complement deposition on the brain of seven Thai adults with CM (Dasari et al., 2014). Brain paraffin sections were stained with α -C3d and α -C5b-9, with cortical capillaries staining for both complement components. The MAC may have a modulatory role in CM as administration of MAC to endothelial cells has been reported to upregulate expression of ICAM-1 (Kilgore et al., 1995), a receptor involved in the parasite sequestration (discussed in section 1.2.4).

A causal role for complement activation in the pathogenesis of malaria has been difficult to establish. As with much of the data on CM pathogenesis, the role of complement in the disease has been examined in greater detail in mouse rather than human studies. The role of complement in murine CM has been well reviewed (Biryukov and Stoute, 2014; Schmidt et al., 2015). In brief, the data suggests a large role for C5a, with susceptibility to murine CM correlating to the ability to produce functional C5a or C5a receptors and treatment of mice with CM with C5a-blocking antibody providing partial resistance (Kim et al., 2014; Patel et al., 2008). Others have questioned this need for C5a and suggested a role for MAC, with the finding of C9 deposits in the brains of mice with CM and treatment with an α -C9 antibody reducing mortality (Ramos et al., 2011). Whilst murine data are important, it should be recalled how different murine CM (with a strong role for inflammation) is from human CM (with a strong role for sequestration, section 1.2.6). It appears the role of complement in human CM is unclear, not because studies are conflicting, but because they are so scarce.

1.6 Complement receptor one (CR1)

1.6.1 Expression and structure

Complement receptor 1 (CR1, also known as CD35) is a large transmembrane glycoprotein and a key regulator of complement activation. CR1 is expressed on the membrane of most peripheral blood cells including erythrocytes, monocytes, neutrophils and B lymphocytes but is absent from platelets, natural killer cells and most T cells (Fearon, 1980; Tedder et al., 1983). Although leucocytes express up to 100 times more CR1 than erythrocytes, the absolute number of erythrocytes means that they account for >85% of CR1 in the peripheral blood (reviewed by (Moulds, 2010)). CR1 is also expressed by follicular dendritic cells (Reynes et al., 1985), retinal pigment epithelial cells (Fett et al., 2012) and glomerular podocytes (Fischer et al., 1986). Soluble CR1 (sCR1) is found in the circulation from cleavage of CR1 on the surface of leucocytes (Danielsson et al., 1994) and urinary CR1 from cleavage of glomerular CR1 (Pascual et al., 1994a).

CR1 is encoded by the *CR1* gene at the 1q32 locus, spans approximately 133 kb and comprises 39 exons (Vik and Wong, 1993). The *CR1* gene is part of the regulation of complement activation (RCA) cluster of genes, with RCA proteins sharing structural similarity and consisting of repeating blocks of 60-70 amino acids referred to as complement control proteins (CCP) or short consensus repeats (SCR) (reviewed in (Hourcade et al., 1989)). The ectodomain of the most common form of CR1 (CR1*1, see section 1.6.3) comprises 30 CCPs, with the first 28 grouped into four long homologous repeats A-D (LHRs A-D) each consisting of seven CCPs (Klickstein et al., 1987). Significant homology is seen between CCPs occupying the same position across LHRs. The last two CCPs (29 and 30) are not part of the LHRs and are followed by a transmembrane domain and a cytoplasmic tail. The structure of CR1*1 is shown in Figure 1-8.

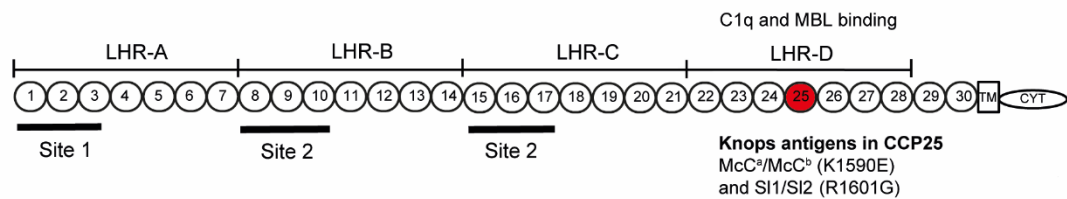


*Figure 1-8. Diagram of the most common Complement Receptor 1 size variant (CR1*1). The ectodomain of CR1 is composed of 30 Complement Control Protein (CCP) domains which are organized into four “Long Homologous Repeats” (LHR). The single nucleotide polymorphisms determining the SI and McC antigens of the Knops blood group system are found in CCP 25 in LHR-D (red). Various functions have been mapped to different regions of CR1, including Site 1 (decay accelerating activity for C3 convertases; binding of the complement components C3b and C4b and the *P. falciparum* invasion ligand PfrH4), and Site 2 (cofactor activity for factor I; binding of C3b and C4b and *P. falciparum* rosetting). LHR-D is thought to bind C1q and Mannose Binding Lectin (MBL), but the specific binding sites have not been mapped. TM, transmembrane region; CYT, cytoplasmic tail. Image and legend taken directly from (Opi, Swann et al, 2018).*

1.6.2 CR1 Function

The two major functions of CR1 are regulation of complement activation and immune adherence. Specific complement regulatory functions have been mapped to the first three CCPs of LHRs A, B and C; LHR-A contains CCPs 1-3 which comprise site 1 while CCPs 8-10 and 15-17 in LHRs B and C respectively comprise two (almost identical) copies of site 2 (Figure 1-8). Site 1 binds C4b (strongly) and C3b (weakly) (Kalli et al., 1991; Klickstein et al., 1988; Krych et al., 1991). Site 1 is also the predominant location for decay accelerating activity (enhancing the breakdown) for the C3 convertases (C4b2a and C3bBb) and C5 convertases (C4b2a3b and C3Bb3b), thus regulating both the classical and alternative pathways (Iida and Nussenzweig, 1981; Krych-Goldberg et al., 1999).

Site 2 binds both C3b and C4b efficiently and also cooperates with site 1 to enhance binding of these ligands (Klickstein et al., 1988; Tetteh-Quarcoo et al., 2012; Tham et al., 2011). Site 2 is also the major site for cofactor activity in the cleavage of C3b to iC3b in conjunction with factor I and subsequently the cleavage of iC3b to C3dg and C3c (described in section 4.4.14.1) (Medof et al., 1982; Ross et al., 1982). iC3b and C3dg are ligands for CR2 on B cells, providing an immunostimulatory role and a

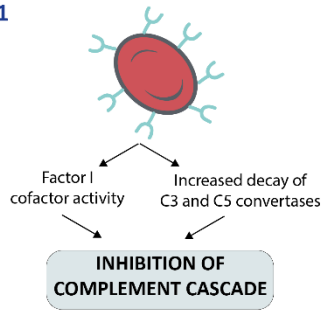
bridge between innate and adaptive immune responses (Dempsey et al., 1996; Hannan, 2016; Weis et al., 1984). The function of the LHR-D region is less clear, with potential binding sites for C1q, mannose binding lectin and ficolins (Ghiran et al., 2000; Jacquet et al., 2013; Klickstein et al., 1997), discussed in section 5.2.1.

CR1 on erythrocytes is also responsible for immune adherence, the binding of C3b- and C4b-opsonised matter (primarily antigen-antibody ICs but also bacteria and viruses). ICs are shuttled to CR1 on resident macrophages in the liver and spleen and phagocytosed (Emlen et al., 1992; Schifferli and Taylor, 1989). CR1 is dispersed on the resting erythrocyte membrane but forms clusters on binding a ligand (Chevalier and Kazatchkine, 1989; Ghiran et al., 2008; Paccaud et al., 1988, 1990). The functions of CR1 are outlined in Figure 1-9.

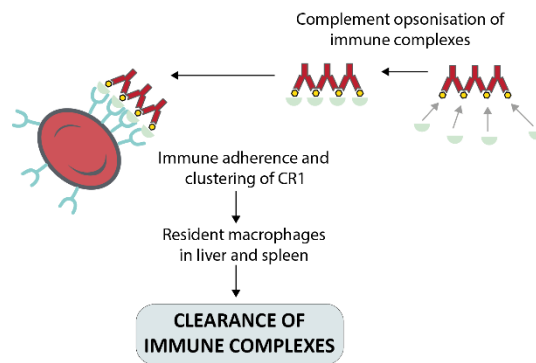
1.6.3 CR1 size polymorphism

CR1 exhibits an unusual size polymorphism, with four allelic variants whose molecule weights increase in 30 kDa increments under reducing conditions; CR1*3 (190 kDa), CR1*1 (220 kDa), CR1*2 (250 kDa) and CR1*4 (280 kDa) (reviewed in (Krych-Goldberg and Atkinson, 2001). The CR1*1 variant is the most common and contains four LHRs (A-D). The 30 kDa size difference between these variants corresponds to the deletion or duplication of a LHR, with CR1*2 containing an extra LHR between LHR-A and LHR-B and CR1*3 lacking LHR-B (Wong and Farrell, 1991; Wong et al., 1989). CR1*4 is anticipated to have 6 LHRs, although this has yet to be confirmed (Birmingham and Hebert, 2001). The frequencies of the variants are not well characterised, but CR1*1 has been reported to occur at a frequency of 86% in Caucasians, 75-78% in African Americans and 96-98% in Asians studied, whereas CR1*2 occurred at 13%, 20- 21% and 1-2% respectively and CR1*3 and CR1*4 being very rare (Dykman et al., 1984; Van Dyne et al., 1987).

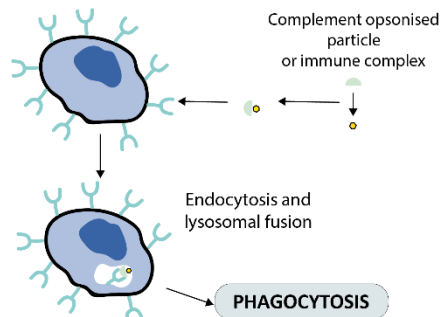
Erythrocyte CR1



CR1 Clustering



Phagocyte CR1







-  CR1
-  Antibody
-  Complement protein
-  Antigen

Figure 1-9. Overview of the functions of CR1.
Adapted from (Khara and Das, 2009)

1.6.4 CR1 copy number polymorphism

In addition to the size polymorphism, the level of CR1 on erythrocytes, known as the CR1 copy number, is also under genetic control. In healthy individuals, the CR1 copy number on erythrocytes has been reported to vary from 50-1200 molecules per cell (Cockburn et al., 2004; Wilson et al., 1986). In Caucasian and Asian populations, CR1 copy number correlates with a *HindIII* restriction fragment length polymorphism (RFLP) in intron 27 of the *CR1* gene (Herrera et al., 1998; Wilson et al., 1986). The polymorphism results in two co-dominant alleles, the H allele (high expression) and the L alleles (low expression). Homozygotes for the L allele typically have CR1 copy numbers of <200, while homozygotes for the H allele have 3-10 times this amount (Wilson et al., 1986). A number of other candidate polymorphisms have been identified in exons 19, 22 and 33 of the *CR1* gene, which are in linkage disequilibrium with the *HindIII* RFLP (Herrera et al., 1998; Xiang et al., 1999). However, in African populations, the *HindIII* RFLP does not correlate with low CR1 copy number and the mechanism controlling copy number in this setting remains to be elucidated (Herrera et al., 1998; Rowe et al., 2002b).

1.6.5 CR1 as a therapy

Considering the strong complement regulatory effects of CR1, there has been particular interest in developing recombinant soluble CR1 (sCR1) as a therapy. Therapeutic sCR1 was originally developed as TP10 by the pharmaceutical company Avant and has been trialled for ischaemia-reperfusion in cardiopulmonary bypass surgery with some success (Keshavjee et al., 2005; Lazar et al., 2007). In addition, pre-clinical studies have investigated a role for sCR1 in the treatment of conditions as diverse as spinal cord injury (Li et al., 2010), arthritis (Goodfellow et al., 2000) and myasthenia gravis (Piddlesden et al., 1996). The therapeutic possibilities of sCR1 have been limited by the size of the molecule. As such, some work has focused on the recombinant fragment APT070, which represents the first three CCPs of CR1 together with a lipopeptide that tethers it to the surface of the cell to be protected (reviewed in (Smith, 2002)).

1.7 CR1 and malaria

1.7.1 CR1 and rosetting

Complement receptor 1 (CR1) is the best characterised of the rosetting receptors. The original report found that erythrocytes with CR1 copy numbers of <100 showed reduced rosetting frequency with *P. falciparum* laboratory strains, with soluble CR1 (sCR1) inhibiting rosette formation (Rowe et al., 1997). CR1 deficient erythrocytes also showed reduced or absent binding to the DBL1 α domain of PfEMP1 from the R29 strain when expressed on COS-7 cells. The same group used recombinant CR1 deletion mutants and α -CR1 antibodies to map the region required for rosetting to site 2 in LHR B (CCPs 8-10) and LHR C (CCPs 15-17) (Rowe et al., 2000) (Figure 1-8). Further investigation revealed that only the J3B11 antibody was able to reverse rosetting. The predicted binding sites for J3B11 are CCPs 3, 10 and 17 (Nickells et al., 1998), suggesting CCPs 10 and 17 are critical for rosetting. In addition to laboratory strains, J3B11 was also found to reverse rosetting in clinical *P. falciparum* isolates from Kenya (13 out of 14) and Malawi (5 out of 10), suggesting the role of CR1 in rosetting may vary with geographical location.

From the parasite perspective, the site of CR1 binding in DBL α has been further refined using deletion constructs of DBL α from laboratory strain R29 expressed on COS-7 cells (Mayor et al., 2005). The authors compared the binding of erythrocytes with normal or low CR1 copy numbers to the constructs to isolate the CR1 binding residues to cysteines C5 to C12 in the central region of DBL α . However, it should be noted that there is currently no direct evidence for the binding of PfEMP1 to CR1. Indeed one study using both recombinant short CR1 proteins and sCR1 was unable to detect any binding between these proteins and immobilized recombinant versions DBL α from R29 using surface plasmon resonance (although data for this assertion was not presented) (Tetteh-Quarcoo et al., 2012). While this may be due to the use of recombinant protein fragments, it also raises the possibility of an intermediate molecule in the binding of CR1 and PfEMP1.

1.7.2 CR1 and erythrocyte invasion

CR1 has been identified as a receptor for the sialic acid-independent invasion of *P. falciparum* into erythrocytes, providing an alternative invasion pathway to glycophorins (Spadafora et al., 2010; Tham et al., 2010). Two separate groups reported this finding almost simultaneously. Spadafora et al. used neuraminidase-treated enterocytes (i.e. devoid of sialic acid and hence the glycoprotein invasion receptors) and found erythrocyte invasion by laboratory strains could be inhibited by incubation with sCR1 and α -CR1 antibodies. Similar results were seen for three clinical isolates in this study and eight others in a separate investigation (all from Kenya), with invasion proportional to the level of erythrocyte CR1 expression (Awandare et al., 2011; Spadafora et al., 2010; Tham et al., 2010).

Tham et al. extended these findings to show that the parasite adhesin *P. falciparum* reticulocyte-binding homologue 4 (PfRh4) was responsible for direct binding to CR1. Investigations using recombinant CR1 fragments revealed the PfRH4 binding site to be in site 1 of CR1 (CCPs 1-3, see Figure 1-8 (Tham et al., 2011)). Truncation and deletion constructs of LHR-A revealed the binding site for PfRh4 to be CCP 1 (Park et al., 2013) and a α -PfRh4 monoclonal antibody capable of inhibiting erythrocyte invasion has been identified, suggesting therapeutic possibilities (Lim et al., 2015).

The clinical importance of CR1 as an invasion receptor for *P. falciparum* is unclear as it is rarely employed without prior neuraminidase treatment of erythrocytes (Awandare et al., 2011; Mensah-Brown et al., 2015; Spadafora et al., 2010; Tham et al., 2010). A study of children in Papua New Guinea reported that antibodies against PfRh4 were associated with protection against symptomatic malaria and high-density parasitaemia, although the CR1 invasion pathway was not directly examined (Reiling et al., 2012). Other studies do not support a clinically important role for CR1 as an invasion receptor, with reports from Brazil and Papua New Guinea finding no association between CR1 level and parasite density (Lin et al., 2010; Soares et al., 2008). It has been suggested that a hierarchy of invasion receptors exists, with CR1-invasion only becoming clinically important if other receptors have been rendered unavailable by antibodies or polymorphisms (Baum et al., 2005).

1.7.3 CR1 copy number and malaria

1.7.3.1 *Theories of association*

The association between CR1 copy number and malaria has been much investigated but remains unclear. This is partly because the optimal amount of CR1 on erythrocytes may differ depending on the outcome required in terms of minimising rosetting, reducing C3b deposition on erythrocytes or clearing immune complexes (ICs). For example, CM has been associated with high levels of ICs containing IgG and IgE and their deposition has also been reported in brain microvasculature (Maeno et al., 2000; Mibei et al., 2008). High CR1 expression on erythrocytes may allow increased binding and clearance of these ICs (Cosio et al., 1990; Madi et al., 1991; Schifferli et al., 1989). However, high CR1 might also increase the risk of rosetting (Rowe et al., 1997). Conversely, whilst low CR1 copy number may reduce rosetting, it might render low-CR1 erythrocytes susceptible to C3b deposition, increasing the risk of SMA (Odhiambo et al., 2008; Stoute et al., 2003; Waitumbi et al., 2000). Alternatively, erythrocytes with high CR1 levels might carry more ICs, interacting with PBMCs and endothelial cells to increase inflammatory mediator release (Beynon et al., 1994; Chou et al., 1985).

1.7.3.2 *CR1 copy number and malaria – Studies from Asia and Papua New Guinea*

Most studies examining the relationship between CR1 expression and severe malaria come from Asia and Papua New Guinea (PNG); three from eastern India (Panda et al., 2012; Rout et al., 2011; Sinha et al., 2009), two from Thailand (Nagayasu et al., 2001; Teeranaipong et al., 2008) and one from PNG (Cockburn et al., 2004). Two of the case-control studies from eastern India reported high CR1 copy number SNPs were associated with increased odds of CM (Panda et al., 2012; Rout et al., 2011), whilst the third did not break down severe malaria cases by sub-phenotype (Sinha et al., 2009). In contrast, one Thai study reported a high CR1 copy number SNP was associated with an decrease in odds of CM in an endemic area (Teeranaipong et al., 2008), contradicting the Indian studies. The study from PNG tells a different story, with a low CR1 copy number SNP being associated with protection against SMA (Cockburn et al., 2004).

These disparities may be due to differences in methodology, parasite strains or other host malaria-susceptibility genes. It is also possible that the association between disease severity and CR1 copy number could be influenced by the local transmission intensity of *P. falciparum*. For example, severe malaria in Asia affecting adults is more commonly a picture of multiorgan failure and metabolic acidosis (Dondorp et al., 2008a; White, 1987) than severe malaria in PNG affecting children, which is predominantly characterised by CM and SMA (Allen et al., 1996).

1.7.3.3 CR1 copy number and malaria – Studies from Africa

The genetic determinant of CR1 copy number has yet to be established in African populations (Herrera et al., 1998; Rowe et al., 2002b; Xiang et al., 1999). As such, it is unsurprising that a Gambian study based on *HindIII* genotyping (rather than direct quantification of CR1 copy number on erythrocytes) found no association with severe malaria (Bellamy et al., 1998). A collection of studies has focused on the relationship between CR1 copy number and severe malaria in Western Kenya. The level of CR1 varied with age, with the lowest levels of CR1 seen between 6 and 24 months (Odhiambo et al., 2008; Waitumbi et al., 2004). The same group reported that low CR1 copy number was associated with lower IC binding, higher circulating levels of ICs and increased C3b deposition on erythrocytes and subsequent phagocytosis in children with SMA than children with UM or asymptomatic malaria (Odhiambo et al., 2008; Owuor et al., 2008; Stoute et al., 2003) (Waitumbi et al., 2000). In further studies, the same group reported that high CR1 erythrocytes which had been pre-saturated with ICs stimulated higher levels of TNF- α production from macrophages than low CR1 erythrocytes (although this was not statistically significant) (Odera et al., 2011). The authors suggested that IC-laden high CR1 erythrocytes in the sluggish blood flow of CM might stimulate microglial cells (resident macrophages) to produce inflammatory cytokines.

If any conclusion can be drawn as to the relationship between CR1 copy number and severe malaria, it is that it is complex, may differ with geographic region and is incompletely understood.

1.8 The Knops blood group polymorphisms in CR1

1.8.1 Molecular basis of the polymorphism

The third CR1 polymorphism is the Knops blood group and is independent of both copy number and size polymorphisms. The Knops blood group system comprises nine antigens; three antithetical pairs (Kn^a/Kn^b , McC^a/McC^b , $SI1/SI2$), one conformational epitope ($SI3$) and two single antigens (Yk^a and $KCAM+$, summarised in Table 1-1). All polymorphisms are found in exon 29 (corresponding to CCP 25 in the CR1 molecule) (Moulds et al., 1991, 2001, 2002, 2005) except for the York antigen (Yk^a) which is located in exon 26 (corresponding to the linker between CCP 22-23) (Veldhuisen et al., 2011). This thesis will focus on the antithetical antigen pairs McCoy (McC^a/McC^b) and Swain-Langley ($SI1/SI2$).

1.8.2 Global prevalence of the *SI* and *McC* polymorphisms

The global distributions of *SI2* and *McC^b* alleles are striking. The alleles are almost absent in Caucasian populations (Covas et al., 2007; Moulds et al., 2004) yet occurring at high frequencies in populations of African origin (Figure 1-10). In African populations, frequency of the *SI2* allele ranges from 0.32 in Malawi to 0.80 in The Gambia (Fitness et al., 2004a; Zimmerman et al., 2003). The *McC^b* allele is less prevalent than *SI2*, but ranges from a frequency of 0.24 in Mali to 0.38 in The Gambia (Noumsi et al., 2011; Zimmerman et al., 2003). The distribution of *SI2* and *McC^b* in populations of African origin has been hypothesised to be due to selection pressure by *P. falciparum* (Moulds et al., 2000). Interestingly, the *SI2* and *McC^b* polymorphisms appear absent from malaria-endemic Asian populations (Gandhi et al., 2009; Teeranaipong et al., 2008), either suggesting that the selection pressure may not be *P. falciparum*, or that these populations have evolved diverging protective mechanisms.

ISBT reference number	Antithetical antigen	Antigen symbol	Exon	Nucleotide change	Amino acid change	Phenotype	SNP
KN1	KN2	Kn ^a	29	4681A	Val1561	Kn(a+b-)	rs41274768
KN2	KN1	Kn ^b	29	4681G	Met1561	Kn(b+a-)	
KN3	KN6	McC ^a	29	4768A	Lys1590	McC(a+b-)	rs17047660
KN6	KN3	McC ^b	29	4768G	Glu1590	McC(a-b+)	
KN4	KN7	SI1	29	4801A	Arg1601	SI(1,-2)	rs17047661
KN7	KN4	SI2	29	4801G	Gly1601	SI(-1, 2)	
KN5	-	Yk ^a	26	4223C>T	Thr1408Met	Yk(+)	rs3737002
KN8	-	SI3	29	4801A /4828A>T	Arg1601/Ser1610 [†]	SI(1,-2,3)	rs4844609
KN9	-	KCAM	29	4843A>G	Ile1615Val	KCAM(+)	rs6691117

Table 1-1. Antigens of the Knops blood group system.

Nucleotide positions given in reference to NCBI accession number NM_000573.3 (https://www.ncbi.nlm.nih.gov/nuccore/NM_000573.3). [†] Arg1601 is also required for KN8 (SI3) expression. The SI and McC polymorphisms are highlighted in blue ISBT = International Society of Blood Transfusion. Information collated from (Moulds et al., 1991, 2001, 2002, 2004, 2005; Veldhuisen et al., 2011)

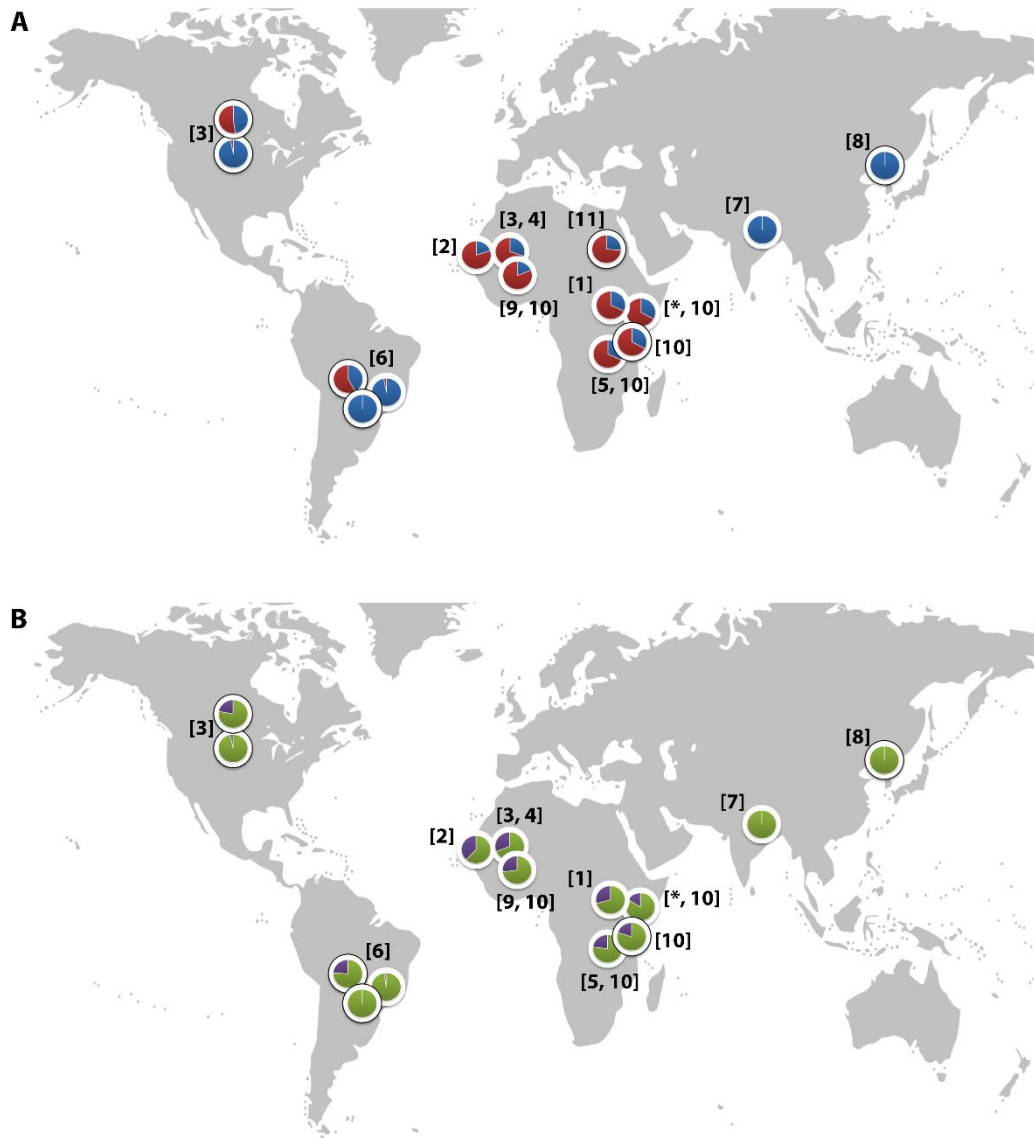


Figure 1-10. Global distribution of the CR1 Knops SI and McC alleles.

A) Shows the global frequencies of the SI alleles. SI1 is represented in blue and SI2 in red.

B) Shows the global frequencies of the McC alleles. McC^C is represented in green and McC^b in purple. The two samples in North and South America showing high frequencies of SI2 and McC^b alleles are both derived from populations with African heritage. Numbers in parentheses indicate the studies from which the SI and McC allele frequencies were derived. [1] Thathy et al., 2005; [2] Zimmermann et al., 2003; [3] Moulds et al., 2004; [4] Noumsi et al., 2011; [5] Fitness et al., 2004; [6] Covas et al., 2007; [7] Gandhi et al., 2009; [8] Yoon et al., 2013; [9] Hansson et al., 2013; [10] Kariuki et al., 2013; [11] Eid et al., 2010.

(Image and legend taken directly from (Opi, Swann et al, 2018)).

1.8.3 Epidemiological studies of the *SI* and *McC* polymorphisms relationship with malaria in Africa

The ten studies examining this relationship are summarised in Table 1-2.

1.8.3.1 *Studies reporting an association between SI / McC and severe malaria*

Thathy et al. performed a matched case-control study Western Kenya with SMA cases recruited from the malaria holoendemic region of Kisumu and CM cases from Kisii, an area in the highlands with seasonal malaria transmission (Thathy et al., 2005). Controls were cases of UM matched for ethnicity, age, sex and location of residence with analysis by conditional logistic regression. The study reported the *SI2/SI2* genotype was associated with reduced odds of CM but not SMA. The study also examined the *SI* and *McC* polymorphisms together, which makes biological sense in terms of proximity (33 bp apart). Surprisingly, this found the genotype *SI2/SI2 McC^a/McC^b* to be associated with reduced odds of CM.

A large multi-centre study by the MalariaGen group comprised a consortia of case-control studies across 12 global sites (Rockett et al., 2014). The study was extremely powerful, with 11890 cases of severe malaria and 17441 controls. Genotyping was performed centrally for 55 malaria candidate SNPs, including *SI* and *McC*. However, there was marked heterogeneity across the study sites, including controls used (varying from cord-blood samples to matched or unmatched community controls with or without minor infections), malaria transmission patterns and disparity in sample number from each site (e.g. 2801 from The Gambia and 114 from Nigeria). To account for heterogeneity, the authors included a Bayesian approach in their detailed statistical analysis (which also adjusted for ethnicity and HbS). The authors noted: “(...) it is undoubtedly also the case that authentic genetic associations might be missed by multi-centre studies if the effect is weak and there is heterogeneity of effect across different study sites.” Considering these points, *McC^b* was associated with increased odds of CM on pooled analysis of all sites, a finding which appears to contradict that of Thathy et al.

Another study reported an association between *McC^b* and seizures in severe malaria and was a sub-analysis of data from four of the MalariaGen African sites (Malawi, Kenya, Ghana and Tanzania) (Kariuki et al., 2013). The *McC^b/McC^b* genotype was associated with increased odds of prolonged and repetitive malaria-associated seizures (MAS). Much of this signal was driven by data from the Kenyan component of the study, reinforcing the problems with heterogeneity in multi-centre studies. Together with Rockett et al., the increased odds of CM and MAS with *McC^b* appear to suggest a selection pressure other than malaria for this polymorphism.

Two small case control studies also reported associations between *SI/McC* and severe malaria (Eid et al., 2010; Tettey et al., 2015). Neither study was clear in the recruitment of their participants, making it difficult to assess potential sources of bias. Such small studies are also vulnerable to sparse data bias (i.e. leading to a considerable upward bias in ORs when there are few study participants at key combinations of the outcome and exposure (Greenland et al., 2016)). For example, Tettey et al. report that *McC^b/McC^b* was associated with protection against severe malaria, but this statement was based on only eight controls and a single case of SMA and CM (Tettey et al., 2015). As such, the contribution of these studies to the body of evidence is limited.

1.8.3.2 Studies reporting no association between SI/McC and severe malaria

Other studies have reported no association between *SI* or *McC* and severe malaria. The first of these was by performed in The Gambia using a matched case-control study with controls selected from outpatients with “mild illnesses” (predominantly non-malarial infections) (Zimmerman et al., 2003). This choice of controls is potentially problematic it has been reported that Knops blood group polymorphisms may be associated with infectious disease other than malaria (Fitness et al., 2004a; Noumsi et al., 2011). As such, if *SI* and *McC* had a broader effect on complement (rather than a malaria-specific effect), the inclusion of controls with other infections may obscure an association. This study reports that the “(...) *SI2/McC^b allele* (...)” was not associated with severe malaria, but data is not shown.

A larger study from The Gambia also reported no association between *SI/McC* and severe malaria (Jallow et al., 2009). This study had well-defined inclusion criteria and used newborn controls. This study was primarily a genome wide association study (GWAS) using the Affymetrix 500K array. Neither *SI* nor *McC* were as identified using this approach. Twelve malaria candidate SNPs (including *SI*) were then directly genotyped and their association with severe malaria examined and *SI* was not significantly associated with severe malaria.

Two other case control studies from Tanzania and Mali have also reported no association between *SI/McC* and severe malaria (Manjurano et al., 2012; Toure et al., 2012). The studies shared many similarities; both were matched case-control studies of a similar size with community controls matched for age, sex and location. Both studies included data on children with UM who were used either as additional controls or additional cases in different analyses, which may have potentially influenced findings.

A final small study from Ghana reported no association between *SI/McC* polymorphisms individually or in combination (Hansson et al., 2013). The controls for this study were poorly defined, being community controls from healthy children “(...) with or without detectable *P. falciparum* in a thick blood smear (...)” In addition, the number of controls differs throughout the paper (275 controls used in some analyses and 448 in others) without explanation. The authors also allude to differences in ethnicity between cases and controls, but do not account for this. Finally, an analysis using eight Knops haplotypes was undertaken, reducing the power to detect statistically significant associations in an already small study.

Study (date)	Location	Design	Controls (n)	Cases (n)	Genotyping	Analysis	Confounders considered	Combined <i>SI</i> / <i>McC</i> genotype?	Findings (aOR (95% CI))
Zimmerman et al. (2003)	The Gambia (Banjul)	Matched case-control study	MID (390)	Total cases (463)* CM (331) SMA (152) Died (98)	PCR-LDR	χ^2 and Fisher's exact test. Unclear if regression used	Age Location	Alluded to, but data not shown	No signif associations reported for <i>SI</i> or <i>McC</i> or genotype combinations
Thathy et al. (2005)	Western Kenya (Kisumu and Kisii)	Matched case-control study	UM (230)	SMA (137) CM (93)	RFLP-PCR	Conditional logistic regression	Ethnicity Age Sex Location	Yes	<i>SI</i> 2/2 assoc with ↓ CM 0.17 (0.04 - 0.72), p= 0.02 <i>SI</i> 2/2 <i>McC</i>^{a/b} assoc ↓ CM 0.18 (0.04 - 0.77), p = 0.02
Jallow et al. (2009)	The Gambia (Kombos region)	Unmatched case-control study	NC (1500)	Total cases* (1060) CM (82%) SMA (30%) RD (11 %)	"Direct genotyping"	"p-value refers to results from the trend test"	Ethnicity	No	No signif associations reported for <i>SI</i> <i>McC</i> not examined
Eid et al. (2010)	Sudan (Sinnar)	Case-control study. Methods obscure	"Healthy Nilo-Saharan speaking individuals" (60)	Inpatients with malaria (52)	Sequenom® iPLEX Mass-Array platform	Logistic regression	Ethnicity	No	<i>SI</i>2 assoc with ↓ inpatient malaria 0.10 (0.03-0.43) (no p value given)
Manjurano et al. (2012)	Tanzania (Muheza)	Matched case-control	CC (480)	Total cases* (507) UM (247) CM (99)	Sequenom® iPLEX Mass-Array platform	Logistic regression	Ethnicity Age Sex	No	No signif associations reported for <i>SI</i> or <i>McC</i>
Toure et al. (2012)	Mali (Bamako)	Matched case-control	CC (393)	Total cases* (541) UM (83) SMA (304) CM (350)	Sequenom® iPLEX Mass-Array platform	Logistic regression	Ethnicity Age Location HbS	No	No signif associations reported for <i>SI</i> or <i>McC</i>

Study (date)	Location	Design	Controls (n)	Cases (n)	Genotyping	Analysis	Confounders considered	Combined <i>SI/McC</i> genotype?	Findings (aOR (95% CI))
Hansson et al. (2013)	Southern Ghana (Accra)	Unmatched case-control study	CC (275)	UM (89) SMA (57) CM (121)	PCR-LDR	Logistic regression	Age Sex	Yes part of 8 haplotypes	No signif associations reported for <i>SI</i> or <i>McC</i> or genotype combinations
Kariuki et al. (2013)	Across 4 African sites ^{&}	Sub-analysis of 4 case-control studies	Severe malaria without seizures (2377)	Malaria-associated seizures (MAS) (2095)	Sequenom® iPLEX Mass-Array platform	Logistic regression	Ethnicity Age Sex Adverse perinatal effects	No	<i>McC^b/McC^b</i> assoc with ↑ prolonged MAS 2.56 (1.41 – 4.67), p = 0.002 <i>McC^b/McC^b</i> assoc with ↑ repetitive MAS 1.97 (1.22-3.22), p = 0.005 No signif assoc reported for <i>SI</i>
Rockett et al. (2014)	Across 12 global sites [§]	Consortia of case-control studies	Various (see text) (17441)	SMA (2196) CM (3345) SMA+CM (742) Other (5607)	Sequenom® iPLEX Mass-Array platform	Logistic regression and Bayesian analysis	Ethnicity Sex HbS	No	<i>McC^b</i> assoc with ↑ CM (additive model) 1.09 (1.02-1.17), p = 0.008 No signif assoc reported for <i>SI</i>
Tettey et al. (2015)	Southern Ghana (Accra)	Unmatched case-control study	UM (50)	SMA (50) CM (50)	RFLP-PCR	Logistic regression	Age Sex	No	<i>McC^{a/b}</i> assoc with ↑ severe malaria 2.31 (1.03-5.20), p = 0.043 <i>McC^{b/b}</i> assoc with ↓ severe malaria 0.12 (0.02-0.64), p = 0.013

Table 1-2. Summary of epidemiological investigations of the *SI* and *McC* polymorphisms relationship with malaria in Africa.

* Overlapping syndromes. [§] Global sites = Burkina Faso, Cameroon, The Gambia, Ghana, Kenya, Malawi, Mali, Nigeria, Tanzania, Vietnam and Papua New Guinea
[&] African sites = Malawi (Blantyre), Kenya (Kilifi), Ghana (Kumasi) and Tanzania (Muheza). UM = uncomplicated malaria. MID = mild infectious disease (outpatients).
CC = community controls, either healthy or with asymptomatic parasitaemia. NC = neonatal controls. SMA = Severe malarial anaemia. CM = Cerebral malaria.
RD = Respiratory distress. RFLP-PCR = Restriction fragment length polymorphism-polymerase chain reaction.
PCR-LDR = Post-polymerase chain reaction multiplexed ligation detection reaction.

1.8.3.3 A comment on the disparity of findings

It is clear there is no consensus on whether *SI/Mc* are associated with severe malaria in Africa. In addition to the methodological differences discussed above, there are many other potential explanations for the variation in findings. The multiple study settings cover a range of malaria transmission intensities. For example, even without information on transmission rates, this is hinted at by examining the mean age of CM patients in different studies; e.g. 2.4 years in Thathy et al (western Kenya, seasonal transmission) compared to 4.4 years in Tettey et al. (Accra, Ghana, low-stable transmission (National Malaria Control Programme et al., 2013)). In addition, differing parasite strains or environmental factors could influence associations. Host genetic factors might also interact with *SI* and *McC*. Only three studies considered the effect of other malaria-resistance polymorphisms in their analyses and this was limited to HbS (Manjurano et al., 2012; Rockett et al., 2014; Toure et al., 2012). It is also plausible, given the proximity of the two SNPs, that an association between *SI* and *McC* and severe malaria is only apparent when both SNPs are included in the same model, an approach only taken by three studies (Hansson et al., 2013; Thathy et al., 2005; Zimmerman et al., 2003). It must also be remembered that *SI* and *McC* may not be causative SNPs, but instead might be tagging an unknown mutation that is in linkage disequilibrium with a causative SNP in, for example, Kenyan populations but not in Gambian populations.

A final point to consider is that these ten studies are not all truly independent; four use the same data and could be considered sub-analyses of Rockett et al. (Jallow et al., 2009; Kariuki et al., 2013; Manjurano et al., 2012; Toure et al., 2012). As such, whilst MalariaGen is a large consortium of well-designed and carried out studies, all genotyping has been centrally performed, with the potential for multiple studies being affected if there are any unidentified errors in this.

1.9 Aims and hypotheses of this thesis

1. **Chapter 2** investigates the hypothesis that the *SI* and *McC* polymorphisms are associated with severe malaria in Kilifi, Kenya. Specifically, I hypothesised that the association between CM and *SI2* observed in western Kenya might also be observed in eastern Kenya. Investigation was undertaken using a large, well defined case-control study analysed using mixed effect logistic regression analysis.

2. **Chapter 3** investigates the hypothesis that the *SI* and *McC* polymorphisms influence how CR1 molecules cluster on the surface of an erythrocyte. Specifically, I hypothesised that the *SI* or *McC* polymorphisms might alter the volume or number of CR1 clusters on an erythrocyte, therefore influencing the binding and transfer of immune complexes during infection with malaria. Field samples from Kilifi, Kenya were used and investigation undertaken using an immunofluorescence assay analysed using confocal microscopy and specialised imaging software.

3. **Chapter 4** investigates the hypothesis that human brain endothelial cells can express functional CR1. Specifically, I hypothesised that the protective association against CM seen with the *SI2* polymorphism was due to direct expression of the CR1 protein on endothelial cells, potentially influencing parasite cytoadherence, immune complex deposition or complement activation. Investigation used immortalised human brain endothelial cells, α -CR1 antibody based assays, siRNA knock-down, functional complement assays and mass spectrometry.

4. **Chapter 5** investigates the hypothesis that the *SI* or *McC* polymorphisms directly influence binding of C1q, mannose binding lectin or L-ficolin to the LHR-D region of CR1. Site-directed mutagenesis was performed to introduce the *SI2* and *McC^b* mutations into a plasmid containing the LHR-D region with the aim of generating recombinant proteins and testing their binding to various complement components.

Please note that as these chapters each use distinct methodological approaches with little overlap, the relevant methods section is found at the beginning of each chapter, rather than in a separate methods chapter.

2 Are the Swain Langley and McCoy polymorphisms in CR1 associated with severe malaria?

The body of this chapter is reproduced from the manuscript “*Two complement receptor one alleles have opposing associations with cerebral malaria and interact with α -thalassaemia*” published in eLife on 25.04.18 on which I am joint first author (Opi, Swann et al, 2018). In accordance with the University of Edinburgh guidelines for inclusion of publications in a thesis (Appendix 8.2), the publication is presented with an additional introduction and discussion. Abstract, introduction, methods, results, discussion, figures, tables and legends are taken directly from the publication. The manuscript has been re-formatted to correspond to thesis style. Supplementary information has been placed in-line where possible. A PDF of the manuscript can be found at <https://www.elifesciences.org/articles/31579> and corresponding open access licence in Appendix 8.3.

2.1 Declaration

I was responsible for the data curation, investigation and statistical analyses of the Kenyan and Malian case-control studies which constitute the majority of this manuscript. Writing of the manuscript was undertaken by myself with assistance from Herbert Opi. The final draft of the manuscript was edited by Alex Rowe and approved by all collaborators. Herbert Opi was responsible for the statistical analysis of the Kenyan cohort study. Ewen Harrison provided advice on statistical methods. Gavin Band provided advice on haplotype analysis and linkage disequilibrium. Dominic Kwiatkowski and Kirk Rockett oversaw *SI*, *McC*, HbS and ABO blood group genotyping and Sophie Ugoya and Alex Macharia performed the α -thalassaemia genotyping for the Kenyan studies. Thomas Williams designed and oversaw recruitment of the Kenyan case-control and cohort studies. Carlyne Ndila was responsible for data curation. For the Malian case-control study, *SI* and *McC* genotyping was performed by Joann Moulds and ABO serotyping and ex vivo rosetting assays were performed by Alex Rowe and Ahmed Raza.

2.2 Abstract

Malaria has been a major driving force in the evolution of the human genome. In sub-Saharan African populations, two neighbouring polymorphisms in the Complement Receptor One (*CR1*) gene, named *S/2* and *McC^b*, occur at high frequencies, consistent with selection by malaria. Previous studies have been inconclusive. Using a large case-control study of severe malaria in Kenyan children and statistical models adjusted for confounders, we estimate the relationship between *S/2* and *McC^b* and malaria phenotypes, and find they have opposing associations. The *S/2* polymorphism is associated with markedly reduced odds of cerebral malaria and death, while the *McC^b* polymorphism is associated with increased odds of cerebral malaria. We also identify an apparent interaction between *S/2* and α^+ thalassaemia, with the protective association of *S/2* greatest in children with normal α -globin. The complex relationship between these three polymorphisms may explain previous conflicting findings, highlighting the importance of considering genetic interactions in disease-association studies.

2.3 Additional introduction to this manuscript

The distribution of *S/2* and *McC^b* in populations of African origin has been hypothesised to be due to selection pressure by *P. falciparum* (Moulds et al., 2000). However, the evidence is conflicting and varying in quality and has been reviewed in depth in section 1.8.3. This chapter sought to examine this hypothesis in a large Kenyan case-control study of severe malaria, with detailed analyses which included the two polymorphisms in a single model and considered the possibility of interactions with other known malaria-resistance genes.

2.4 Introduction

Complement Receptor One (CR1) plays a key role in the control of complement activation and the immune clearance of C3b/C4b coated immune complexes (Krych-Goldberg and Atkinson, 2001). CR1 is expressed on a range of cells including red blood cells (RBCs), leucocytes and glomerular podocytes (Krych-Goldberg and Atkinson, 2001). A number of CR1 polymorphisms have been described, including four molecular weight variants and variation in the number of CR1 molecules expressed on the surface of RBCs (reviewed by (Krych-Goldberg et al., 2002; Schmidt et al., 2015)). Missense substitutions of CR1 form the basis of the Knops blood group system of antigens, that includes the antithetical antigen pairs of Swain-Langley 1 and 2 (SI1 and SI2) and McCoy a and b (McCa and McCb) (Moulds, 2010). The non-synonymous single nucleotide polymorphisms (SNPs) A4828G (rs17047661) and A4795G (rs17047660) within exon 29 of the *CR1* gene give rise to the *SI1/SI2* and *McC^a/McC^b* alleles, encoding R1601G and K1590E respectively (Moulds et al., 2001) (Figure 1-8).

CR1 has been implicated in the pathogenesis of multiple diseases, with epidemiological and in vitro data suggesting a role in malaria (reviewed in (Schmidt et al., 2015)). The *SI2* and *McC^b* alleles occur at high frequencies only in populations of African origin (Figure 1-10) (Covas et al., 2007; Eid et al., 2010; Fitness et al., 2004a; Gandhi et al., 2009; Hansson et al., 2013; Kariuki et al., 2013; Moulds et al., 2004; Noumsi et al., 2011; Thathy et al., 2005; Yoon et al., 2013; Zimmerman et al., 2003), which, given the historical prevalence of the malaria-causing parasite *Plasmodium falciparum* in sub-Saharan Africa, might suggest a possible survival advantage against malaria (Rowe et al., 1997, 2000). CR1 is a receptor for the invasion of RBCs by *P. falciparum* merozoites (Spadafora et al., 2010; Tham et al., 2010) and for the formation of clusters of *P. falciparum*-infected erythrocytes (IEs) and uninfected RBCs, known as rosettes (Rowe et al., 1997). The rosetting phenotype is associated with severe malaria in sub-Saharan Africa (Doumbo et al., 2009), with pathological effects likely due to the obstruction of microcirculatory

blood flow (Kaul et al., 1991). RBCs from donors with the high frequency African CR1 Knops mutations bind poorly to the parasite ligand *P. falciparum* erythrocyte membrane protein-1 (PfEMP1) that mediates rosetting by IEs, potentially protecting against severe malaria by reducing rosetting (Rowe et al., 1997). Nevertheless, epidemiological data supporting this possibility are contradictory, with some studies showing an association between *SI* and *McC* genotypes and severe malaria (Kariuki et al., 2013; Tettey et al., 2015; Thathy et al., 2005) and others finding none (Hansson et al., 2013; Jallow et al., 2009; Manjurano et al., 2012; Rockett et al., 2014; Toure et al., 2012; Zimmerman et al., 2003). Some previous studies have not considered *SI* and *McC* genotypes together in the same statistical model, despite their physical adjacency in the CR1 molecule, nor taken into account potential interactions with other malaria resistance genes. Given the important biological role of CR1 in malaria host-parasite interactions, we aimed to clarify the relationship between the *SI* and *McC* alleles and severe malaria in a case-control study of Kenyan children. These investigations were supplemented with a separate longitudinal cohort study of Kenyan children, examining the associations of these alleles with UM and other common childhood illnesses. Finally, we also investigated the influence of these alleles on the formation of *P. falciparum* rosettes, as a potential functional explanation for these results through ex vivo laboratory studies.

2.5 Materials and methods

2.5.1 Datasets studied

This study uses data from a Kenyan case-control study of severe malaria, with samples collected between 2001 and 2010, a Kenyan longitudinal cohort study, with samples collected between 1998 and 2001 and a Malian case-control study performed between July 2000 and December 2001. Historic datasets (i.e. >10 years old) are widely used in genetic epidemiological studies of malaria due to the logistical challenges of sample collection in malaria endemic countries and the changing epidemiological patterns of disease.

2.5.2 The Kenyan study area

All epidemiological and clinical studies in Kenya were carried out in the area defined by the Kilifi Health and Demographic Surveillance System (KHDSS), with Kilifi County Hospital (KCH) serving as the primary point of care (Scott et al., 2012). Malaria transmission is seasonal in this region following the long and short rains. An Entomological Inoculation Rate (EIR) of up to 50 infective bites per person per year was measured in the late 1990s (Mbogo et al., 2003), but transmission has since declined (O’Meara et al., 2008).

2.5.3 The Kenyan case-control study

Between January 2001 and January 2008, children aged <14 years who were admitted to KCH with severe malaria were recruited as cases, as described previously (Rockett et al., 2014), except that children who were resident outside the KHDSS were excluded (Figure 2-1). Severe malaria was defined as the presence of blood-film positive *P. falciparum* infection complicated by one or more of the following features: cerebral malaria (CM) (a Blantyre coma score (BCS) of <3) n=943; severe malarial anaemia (SMA) (haemoglobin concentration of <5g/dl) n=483; respiratory distress (RD) (abnormally deep breathing) n=522 or “other severe malaria” (no CM, SMA or RD but other features including prostration (BCS 3 or 4), hypoglycaemia and hyperparasitaemia) n=318. Controls (n=3829) consisted of children 3-12 months of age who were born consecutively within the KHDSS study area between August 2006 and September 2010 and were recruited to an ongoing genetic cohort study (Williams et al., 2009). As such, controls were representative of the general population in terms of ethnicity and residence but not of age. The use of controls who are considerably younger than cases differs from the classical structure of a case-control study. However, this method (using cord blood or infant samples as controls) has been widely used in African genetic association studies (e.g. (Band et al., 2013; Busby et al., 2016; Clarke et al., 2017)), and is the most logistically feasible way of collecting sufficiently large numbers of control samples in many sub-Saharan African settings.

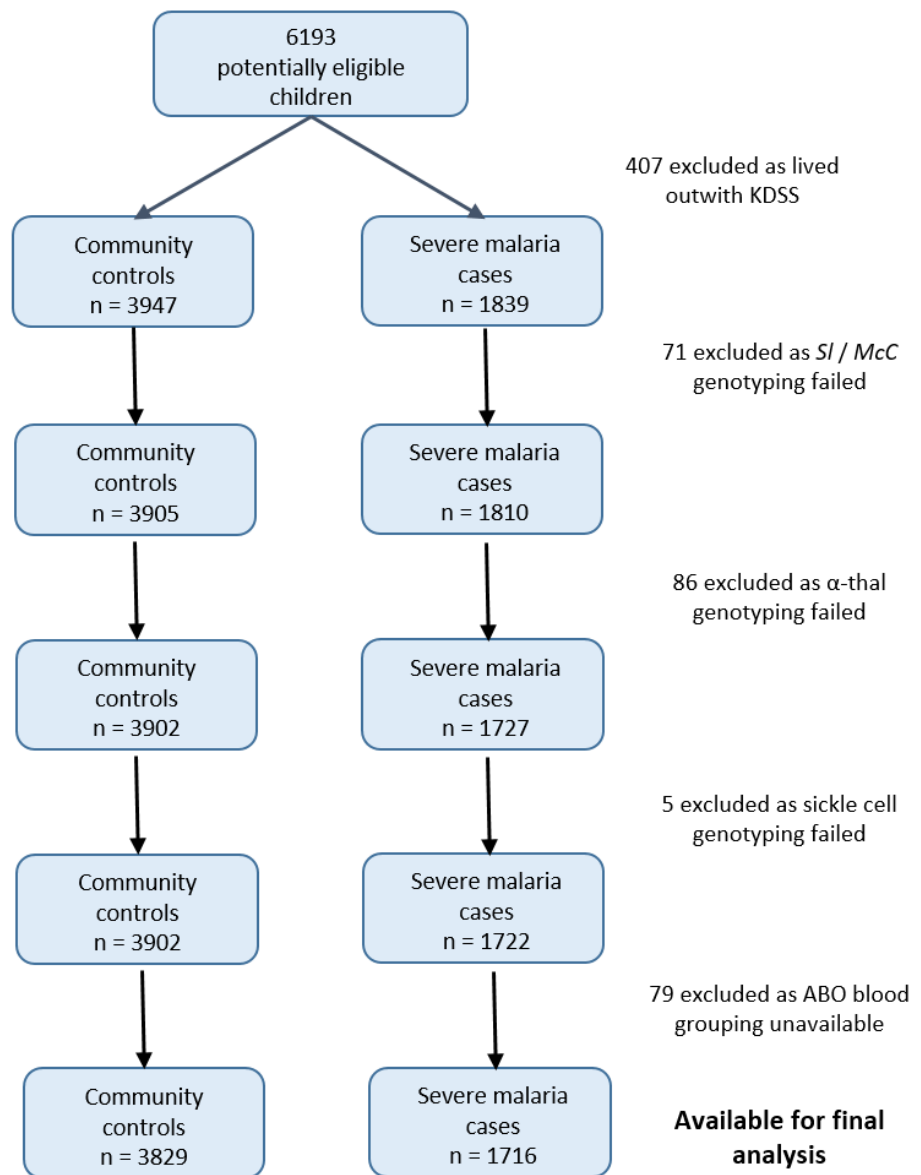


Figure 2-1. Patient inclusion flow chart for the Kenyan case-control study.

2.5.4 Sample processing and quality control for the Kenyan case-control study

The *SI* and *McC* polymorphisms were originally typed as part of a larger study by Rockett et al. (Rockett et al., 2014), which included case-control data from 12 global sites. In Kenya, 0.5ml blood samples were collected into ethylenediaminetetraacetic acid (EDTA) tubes and DNA extracted using Qiagen DNeasy blood kits (Qiagen, Crawley, UK). DNA was stored at -20°C and shipped frozen to Oxford. Sample processing is described in detail in the supplementary methods of Rockett et al. (Rockett et al., 2014). Briefly, samples underwent a whole-genome amplification step using Primer-Extension Pre-Amplification. Genotyping was performed using SEQUENOM® iPLEX® Gold with 384 samples processed per chip. Samples were typed for 73 SNPs; 55 of these SNPs were chosen on the basis of a known association with severe malaria, 3 SNPs were used to confirm gender and the remaining 15 SNPs to aid quality control. Samples were excluded if they did not have clinical data for gender or if genotypic gender of the sample did not match clinical gender. Samples were included if they were successfully genotyped for more than 90% of 65 “analysis” SNPs.

2.5.5 The Kenyan longitudinal cohort study

This study has been described in detail previously (Nyakeriga et al., 2004). Briefly, this study was established with the aim of investigating the immuno-epidemiology of uncomplicated clinical malaria and other common childhood diseases in the northern part of the KHDSS study area, approximately 15km from KCH (Williams et al., 2005a). The study was carried out between August 1998 and August 2001 involving children aged 0-10 years recruited either at the start of the study or at birth when born into study households during the study period. They were actively followed up on a once-weekly basis for both malaria and non-malaria related clinical events. In addition, on presentation with illnesses, cohort members were referred to a dedicated outpatient clinic for more detailed diagnostic tests. The cohort was monitored for the prevalence of asymptomatic *P. falciparum* infection

through four cross-sectional surveys carried out in March, July and October 2000 and June 2001. Exclusion criteria included migration from the study area for more than 2 months, the withdrawal of consent and death. Uncomplicated clinical malaria was defined as fever (axillary temperature of $>37.5^{\circ}\text{C}$) in association with a *P. falciparum* positive slide at any density. The most common non-malaria related clinical events reported during the study period included upper respiratory tract infections (URTIs), lower respiratory tract infections (LRTIs), gastroenteritis, helminth infections and skin infections, as defined in detail previously (Williams et al., 2005a). Malaria negative fever was defined as an axillary temperature of $>37.5^{\circ}\text{C}$ in association with a slide negative for *P. falciparum*. This analysis includes 208 children aged <10 years for whom full *Sl*, *McC*, sickle cell genotype, α^+ thalassaemia genotype and ABO blood group data were available.

2.5.6 The Malian case-control study

This study has been described in detail previously (Lyke et al., 2003). Briefly, between July 2000 and December 2001, children ranging from 1 month–14 years of age were recruited into a case-control study in the Bandiagara region in East Central Mali, an area of intense and seasonal *P. falciparum* malaria infection. In order to address the specific question of whether the *Sl2/Sl2* genotype is associated with protection against cerebral malaria in Mali, only the subset of children suffering strictly-defined cerebral malaria (a BCS of <3 , with other obvious causes of coma excluded, $n=34$) or UM ($n=184$, symptomatic children with *P. falciparum* parasitaemia and an axillary temperature $\geq 37.5^{\circ}\text{C}$, in the absence of other clear cause of fever), and for whom *Sl* and *McC* genotyping was available were analysed.

2.5.7 Ex vivo rosetting

The rosette frequency (percentage of mature IEs forming rosettes with two or more uninfected erythrocytes) of *P. falciparum* isolates from patients recruited into the Mali case-control study was determined by microscopy after short term culture (24–48 hours), as described in detail previously (Dumbo et al., 2009). Of the 209 isolates studied previously, 167 were successfully genotyped for the *Sl* and *McC*

alleles and are analysed here. The rosetting assays were performed before we genotyped the study participants, excluding observer bias. The rosette frequency of parasites from hosts with differing *Sl* and *McC* genotypes were compared by a Kruskal-Wallis test with Dunn's multiple comparisons (Prism v6.0, Graphpad Inc, San Diego, California).

2.5.8 Laboratory procedures

DNA was extracted either from fresh or frozen whole blood by proprietary methods using either the semi-automated ABI PRISM® 6100 Nucleic acid prep station (Applied Biosystems, Foster City, CA, USA) or using QIAamp DNA Blood Mini Kits (Qiagen, West Sussex, United Kingdom). SNPs giving rise to the *Sl* and *McC* alleles were genotyped using either the SEQUENOM iPLEX® Gold multiplex system (Agena Biosciences, Hamburg, Germany) (Kenyan study) (Rockett et al., 2014) or by an established PCR-RFLP method as described previously (Malian study) (Moulds et al., 2004). Genotyping for sickle cell trait (HbAS) and the common African α^+ thalassaemia variant caused by a 3.7kb deletion in the *HBA* gene were performed by PCR as described in detail elsewhere (Chong et al., 2000; Waterfall and Cobb, 2001).

2.5.9 Statistical analysis

The effects of the *Sl* and *McC* alleles were examined in genotypic, dominant, recessive and additive models of inheritance, with the best fitting model selected based on Akaike information criterion (AIC). Analyses for the Kilifi case-control study were performed in R (R Foundation for Statistical Computing, Vienna, Austria) (R Development Core Team, 2010) using the “ggplot2”, “lme4”, and “HardyWeinberg” packages (Bates et al., 2013; Graffelman and Camarena, 2008; Wickham, 2009), while analyses for the longitudinal study were performed in Stata v11.2 (StataCorp, Texas, USA). In both studies, a p value of <0.05 was considered statistically significant. Graphs were generated using R or Prism v6.0 (Graphpad Inc, San Diego, California).

For the Kenyan case-control study, *Sl* and *McC* genotype were included together in a statistical model to examine their associations with malaria susceptibility. Odds Ratios (ORs) and 95% Confidence Intervals (CI) were generated using mixed effect logistic regression analysis both with and without adjustment for ethnicity and location of residence as random effects, and sickle cell genotype, α^+ thalassaemia genotype, and ABO blood group (O or non-O) as fixed effects (variables which have been associated with malaria susceptibility in multiple previous studies on this population) (Atkinson et al., 2014; Fry et al., 2008; Malaria Genomic Epidemiology Network, 2015; Penman et al., 2009; Rockett et al., 2014; Rowe et al., 2007; Williams et al., 2005b, 2005a). The ethnicity variable was compressed from 28 categories to four; Giriama (n=2728), Chonyi (n=1800), Kauma (n=588) and other (n=429). Binary parameterization of the α^+ thalassaemia variable was used, i.e. comparing those children with no α^+ thalassaemia alleles against those with one or more α^+ thalassaemia alleles. This division was chosen in accordance with a previous report showing that both heterozygous and homozygous α^+ thalassaemia genotypes are associated with protection against severe malaria and death in the Kilifi area (Williams et al., 2005b). 2000 bootstrapped iterations were run to give 95% CIs and p values.

For the Kenyan longitudinal cohort study, Incidence Rate Ratios (IRRs) and 95% CIs were generated using a random effects Poisson regression model that took into account within-person clustering. Data were examined with and without adjustment for confounding by *McC* genotype (for *Sl* analyses), *Sl* genotype (for *McC* analyses) sickle cell genotype, α^+ thalassaemia genotype, ABO blood group, ethnic group, season (defined as 3 monthly blocks), and age in months as a continuous variable.

For the Malian case-control study, ORs and 95% CIs were computed using mixed effect logistic regression analysis with adjustment for location of residence as a random effect and age, ABO blood group (O or non-O) and ethnicity (Dogon or non-Dogon) as fixed effects. α^+ thalassaemia genotyping was not available for the Malian

study and sickle cell trait is extremely uncommon in this population, therefore neither variable was included in the model. 2000 bootstrapped iterations were run to give adjusted ORs.

Corrections for multiple comparisons were not performed, instead all adjusted odds ratios, confidence intervals and p values have been clearly reported. This approach has been repeatedly advocated, particularly when dealing with biological data (Fiedler et al., 2012; Nakagawa, 2004; Perneger, 1998; Rothman, 1990, 2014). A detailed description of the statistical model fitting for the Kenyan studies is given in section 2.7.1.

2.5.10 Ethical statement

Human subjects: This work involved analysing blood samples from patients with malaria and from healthy controls. Written informed consent was obtained from the parents or legal guardians of all participants. The studies received ethical approval from the Kenya Medical Research Institute National Ethical Review Committee (case control study: SCC1192; cohort study: SCC3149), the University of Bamako/Mali Faculty of Medicine, Pharmacy and Dentistry Institutional Review Board (which, at the time the study was accepted did not give out approval numbers) and the University of Maryland (approval number #0899139).

2.6 Results

2.6.1 The *S12/S12* genotype is associated with protection against cerebral malaria and death in the Kenyan case-control study

Data were obtained from 5545 children enrolled in a case-control study of severe malaria (Figure 2-1). The general characteristics of the cases and controls are shown in Table 2-1, and the characteristics of the dataset by *SI* and *McC* genotype are shown in Table 2-2 and Table 2-3. The *S12* and *McC^b* allele frequencies (0.68 and 0.16 respectively) were comparable to other African populations (Figure 1-10). There was no significant deviation from Hardy-Weinberg equilibrium for the *SI* or *McC* genotypes among controls (Table 2-4).

	Controls n = 3829	All severe malaria cases n = 1716	p value
Gender			
Males	1931 (50.4 %)	862 (50.2 %)	0.915
Females	1898 (49.6 %)	854 (49.8 %)	
Ethnicity			
Giriama	1775 (46.4 %)	953 (55.5 %)	<0.001
Chonyi	1365 (35.6 %)	435 (25.4 %)	
Kauma	440 (11.5 %)	148 (8.6 %)	
Others	249 (6.5 %)	180 (10.5 %)	
Age in months*			
Median (IQR)	6 (5-8)	28 (15-43)	<0.001

Table 2-1. General characteristics for the Kenyan case-control study. Comparisons performed using Pearson's χ^2 test except *Kruskal Wallis test.

		<i>SI1/SI1</i>	%	<i>SI1/SI2</i>	%	<i>SI2/SI2</i>	%	p value
Clinical status	Control	378	9.9	1730	45.2	1721	44.9	
	All severe cases	177	10.3	801	46.7	738	43.0	0.403
	CM	95	10.1	457	48.5	391	41.5	0.144
	Severe no CM	71	10.5	297	44.1	306	45.4	0.804
	SMA	53	11.0	230	47.6	200	41.4	0.319
	SMA no CM	27	12.1	100	44.8	96	43.0	0.541
	RD	54	10.3	245	46.9	223	42.7	0.630
	RD no CM	24	12.5	80	41.7	88	45.8	0.407
	Died	25	13.9	80	44.4	75	41.7	0.203
	Died with CM	16	12.2	59	45.0	56	42.7	0.659
	Died no CM	8	19.0	18	42.9	16	38.1	0.148 [#]
	Died with SMA	9	16.1	24	42.9	23	41.1	0.304
	Died with RD	10	13.7	34	46.6	29	39.7	0.467
	Gender	M	270	9.7	1287	46.1	1236	44.3
F		285	10.4	1244	45.2	1223	44.4	0.637
Ethnicity	Giriama	235	8.6	1223	44.8	1270	46.6	
	Chonyi	204	11.3	832	46.2	764	42.4	
	Kauma	68	11.6	279	47.4	241	41.0	
	Other	48	11.2	197	45.9	184	42.9	0.007
Sickle	Hb AA	489	10.0	2234	45.8	2158	44.2	
	Hb AS	60	9.6	282	45.3	280	45.0	
	Hb SS	6	14.3	15	35.7	21	50.0	0.660 [#]
α^+thalassaemia	$\alpha \alpha$	189	9.5	912	45.8	890	44.7	
	$\alpha -\alpha$	279	10.3	1244	45.8	1196	44.0	
	$-\alpha -\alpha$	87	10.4	375	44.9	373	44.7	0.892
Blood group	O	287	9.8	1328	45.5	1302	44.6	
	Non-O	268	10.2	1203	45.8	1157	44.0	0.855
Median age	Months		IQR		IQR		IQR	
		8	5-18	8	5-13	8	5-12	0.636

Table 2-2. Characteristics for the Kenyan case-control study by *SI* genotype. CM, cerebral malaria; SMA, severe malarial anaemia; RD, respiratory distress; IQR, interquartile range. Significance testing for each clinical status uses control as the reference group. Age: Kruskal Wallis test. #: Fisher's exact test. All other analyses: Pearson's χ^2 .

		<i>McC^a/McC^a</i>		<i>McC^a/McC^b</i>		<i>McC^b/McC^b</i>		p value
			%		%		%	
Clinical status	Control	2700	70.5	1040	27.2	89	2.3	
	All severe cases	1182	68.9	484	28.2	50	2.9	0.278
	CM	633	67.1	284	30.1	26	2.8	0.122
	Severe no CM	479	71.1	175	26.0	20	3.0	0.520
	SMA	346	71.6	128	26.5	9	1.9	0.761
	SMA no CM	162	72.6	56	25.1	5	2.2	0.791
	RD	355	68.0	153	29.3	14	2.7	0.488
	RD no CM	132	68.8	54	28.1	6	3.1	0.626 [#]
	Died	119	66.1	53	29.4	8	4.4	0.128 [#]
	Died with CM	83	63.4	44	33.6	4	3.1	0.184 [#]
	Died no CM	31	73.8	9	21.4	2	4.8	0.304 [#]
	Died with SMA	38	67.9	14	25.0	4	7.1	0.088 [#]
	Died with RD	51	69.9	21	28.8	1	1.4	0.934 [#]
Gender	M	1928	69.0	802	28.7	63	2.3	
	F	1954	71.0	722	26.2	76	2.8	0.071
Ethnicity	Giriama	1881	69.0	777	28.5	70	2.6	
	Chonyi	1307	72.6	462	25.7	31	1.7	
	Kauma	410	69.7	160	27.2	18	3.1	
	Other	284	66.2	125	29.1	20	4.7	0.003
Sickle	Hb AA	3404	69.7	1348	27.6	129	2.6	
	Hb AS	444	71.4	168	27.0	10	1.6	
	Hb SS	34	81.0	8	19.0	0	0.0	0.311 [#]
α*thalassaemia	$\alpha\alpha$	1398	70.2	551	27.7	42	2.1	
	$\alpha-\alpha$	1898	69.8	739	27.2	82	3.0	
	$-\alpha-\alpha$	586	70.2	234	28.0	15	1.8	0.200
Blood group	O	2042	70.0	799	27.4	76	2.6	
	Non-O	1840	70.0	725	27.6	63	2.4	0.879
Median age	Months	8	IQR 5-12	8	IQR 5-14	8	IQR 5-18.5	0.441

Table 2-3. Characteristics for the Kenyan case-control study by *McC* genotype. CM, cerebral malaria; SMA, severe malarial anaemia; RD, respiratory distress; IQR, interquartile range. Significance testing for each clinical status uses control as the reference group. Age: Kruskal Wallis test. #: Fisher's exact test. All other analyses: Pearson's χ^2 .

<i>SI1/SI1</i>	<i>SI1/SI2</i>	<i>SI2/SI2</i>	χ^2	p value
378	1730	1721	3.43	0.064*

<i>McC^a/McC^a</i>	<i>McC^a/McC^b</i>	<i>McC^b/McC^b</i>	χ^2	p value
2700	1040	89	0.81	0.369

*Table 2-4. Hardy Weinberg equilibrium calculations for controls in the Kenyan case-control study. *Although SI and McC were found to be in Hardy Weinberg Equilibrium (HWE), SI was of borderline statistical significance. HWE calculations for SI were stratified by ethnicity and found to deviate from HWE for the Giriama ethnicity ($\chi^2 = 5.12$, $p = 0.024$), but not for the other ethnic groups. Ethnicity was subsequently included as a variable in all analyses performed. To further investigate whether a genotyping error could be responsible for the borderline significant deviation from HWE for SI in the Kenyan population, a subset of samples ($n = 2344$) were genotyped using a second platform (Illumina HumanOmni2.5-4) as previously described (Malaria Genomic Epidemiology Network, 2015). The concordancy rates between the two methods were 98.3 % (2304/2344 samples) for SI and 98.8 % (2317/2344) for McC.*

Using a simple logistic regression model containing only *SI* and *McC* genotypes (referred to as the unadjusted analysis below), we found a non-significant association between the *SI2* allele and severe malaria overall, with the *SI2/SI2* genotype being associated with an OR for severe malaria of 0.90 (95% CI 0.79-1.01; $p=0.07$) (Table 2-5). We attempted to refine this signal by fitting a more complete model to the data, including the potential confounding factors of ethnicity, location, sickle cell trait, ABO blood group and α^+ thalassaemia genotype, as well as considering possible first order interactions between terms (referred to as the full adjusted analysis below, Table 2-6 and Figure 2-2).

Clinical Outcome	<i>SI2/SI2</i>		<i>McC^b</i>	
	Unadjusted OR (95% CI)	p value	Unadjusted OR (95% CI)	p value
All severe malaria (n=1716)	0.90 (0.79 – 1.01)	0.071	1.17 (1.00 – 1.25)	0.056
CM (n=943)	0.82 (0.71 – 0.95)	0.010	1.21 (1.05 – 1.39)	0.008
Severe without CM (n=674)	1.09 (0.86 – 1.21)	0.829	1.00 (0.84 – 1.18)	0.985
Died (n=180)	0.80 (0.58 – 1.09)	0.164	1.34 (1.00 – 1.77)	0.046
Died with CM (n=131)	0.82 (0.57 – 1.19)	0.306	1.39 (0.99 - 1.92)	0.052
Died without CM (n=42)	0.74 (0.38 – 1.41)	0.373	1.05 (0.54 – 1.91)	0.881
SMA(n=483)	0.87 (0.71 – 1.06)	0.177	0.98 (0.80 – 1.18)	0.800
SMA without CM (n=223)	0.94 (0.71 – 1.25)	0.693	0.93 (0.70 – 1.23)	0.620
Died with SMA (n=56)	0.77 (0.43 – 1.24)	0.327	1.40 (0.83 – 2.27)	0.192
RD ^s (n=522)	0.88 (0.72 – 1.06)	0.181	1.16 (0.96 – 1.38)	0.129
RD without CM (n=192)	1.01 (0.74 – 1.37)	0.955	1.10 (0.82 – 1.45)	0.529
Died with RD (n=73)	0.80 (0.48 – 1.29)	0.363	1.05 (0.64 – 1.66)	0.834

Table 2-5. Unadjusted odds ratios for clinical outcomes for the Kenyan case-control study. Model includes only SI2/SI2 in recessive form (i.e. vs SI1/SI1 and SI1/SI2) and McC^b in additive form (i.e. impact of each additional McC^b allele). The data are not adjusted for the potential confounders ethnic group, location, sickle cell trait, ABO blood group or α^+ thalassaemia genotype. Confidence intervals by Wald. The 95% CIs and p values are not bootstrapped. OR = odds ratio; CI = confidence interval; CM = cerebral malaria; SMA = severe malarial anaemia; RD, respiratory distress. 34/56 cases who died with SMA also had CM. 56/73 cases who died with RD also had CM.

Clinical Outcome	SI2		McC ^b	
	aORs (95% CI) ^{&}	p value	aORs (95% CI)	p value
All severe malaria [§] (n=1716)	0.78 (0.64-0.95)	0.011	1.10 (0.97-1.25)	0.108
CM [#] (n=943)	0.67 (0.52-0.87)*	0.006	1.19 (1.02-1.38)	0.025
Severe without CM (n=674)	1.00 (0.76-1.30)	0.994	0.98 (0.82-1.17)	0.811
Died (n=180) [§]	0.50 (0.30-0.80)*	0.002	1.31 (0.95-1.72)	0.086
Died with CM (n=131)	0.44 (0.23-0.78)*	0.007	1.34 (0.94-1.88)	0.104
Died without CM (n=42)	0.73 (0.18-2.30)	0.636	1.00 (0.48-1.94)	0.940
SMA [†] (n=483)	0.76 (0.55-1.05)	0.099	0.96 (0.78-1.17)	0.688
SMA without CM (n=223)	0.82 (0.51-1.26)	0.366	0.91 (0.67-1.20)	0.553
Died with SMA [‡] (n=56)	0.65 (0.21-1.67)	0.374	1.35 (0.77-2.20)	0.229
RD [§] (n=522)	0.81 (0.59-1.10)	0.181	1.12 (0.92-1.35)	0.225
RD without CM (n=192)	1.06 (0.66-1.68)	0.805	1.07 (0.80-1.43)	0.615
Died with RD [¶] (n=73)	0.39 (0.14-0.88)*	0.027	1.01 (0.59-1.61)	0.948

Table 2-6. Adjusted Odds Ratios (aOR) for severe malaria by SI2 (recessive) and McC^b (additive) genotype in Kenya.

[&]Adjusted Odds Ratios (aOR) and 95% Confidence Intervals (CI) are presented for the SI2 genotype in the recessive form (i.e. SI2/SI2 vs all other SI genotypes) and McC^b genotype in the additive form (i.e. change in aOR with each additional McC^b allele). SI and McC genotype were included together in a statistical model to examine their associations with malaria susceptibility. aORs displayed are adjusted for ethnicity, location of residence, sickle cell genotype, α^+ thalassaemia genotype and ABO blood group. An interaction term between SI genotype and α^+ thalassaemia was included in the model. Model outputs following 2000 bootstrapped iterations are shown.

[§]99 children (7 of whom died) were severe malaria cases whose CM status was not recorded, hence these children are included in the numbers for "All severe malaria" and "Died" but not in "with CM" or "without CM" categories.

*Models that showed significant evidence of interaction between SI2 and α^+ thalassaemia.

[#]CM, cerebral malaria (*P. falciparum* infection with a Blantyre coma score of <3)

[†]SMA, severe malarial anaemia (*P. falciparum* infection with Hb < 5 g/dl)

[‡]34/56 cases who died with SMA also had CM.

[§]RD, respiratory distress (*P. falciparum* infection with abnormally deep breathing)

[¶] 56/73 cases who died with RD also had CM.

Adjusted Odds Ratios for *Sl* and *McC* genotypes

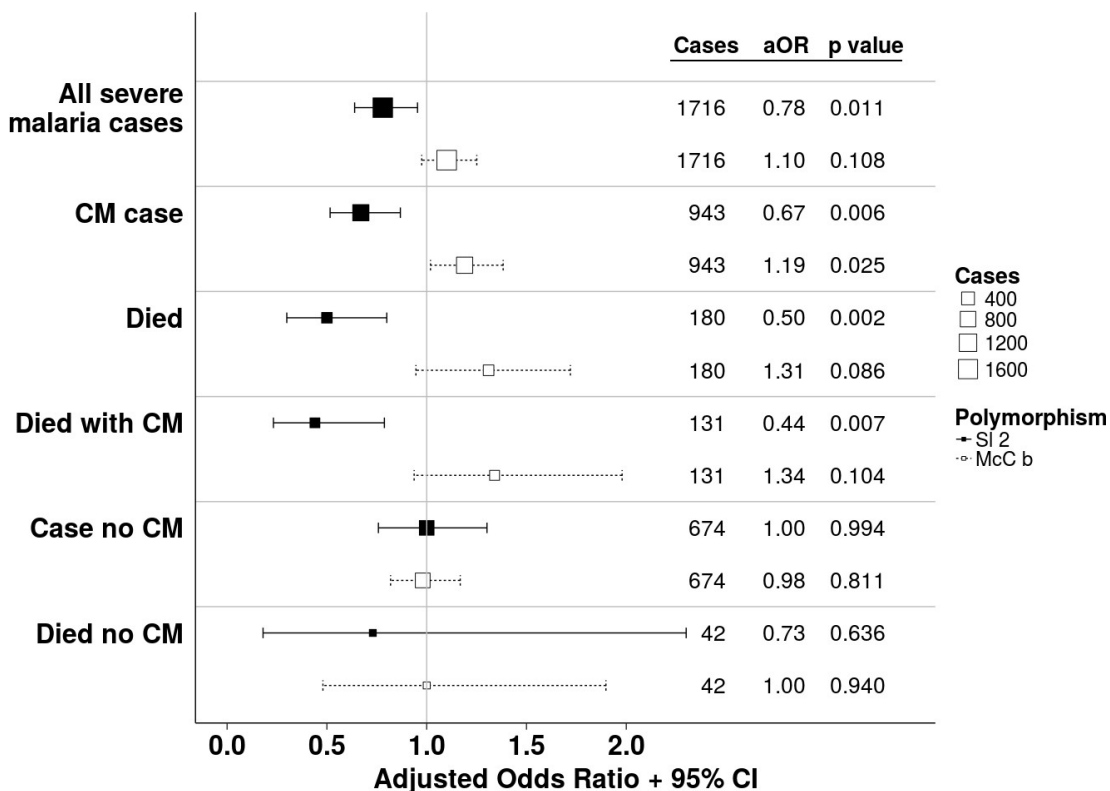


Figure 2-2. The *Sl*² and *McC*^b alleles have opposing associations with cerebral malaria (CM) and death.

Forest plot showing the associations between *Sl* and *McC* polymorphisms and severe malaria in Kilifi, Kenya. Filled boxes: adjusted Odds Ratios (aOR) for the *Sl*² genotype in the recessive form (i.e. *Sl*²/*Sl*² vs all other *Sl* genotypes). Open boxes: *McC*^b in the additive form (i.e. change in odds ratio with each additional *McC*^b allele).

Sl and *McC* genotype were included together in a statistical model to examine their associations with malaria susceptibility. aORs displayed are adjusted for ethnicity, location of residence, sickle cell genotype, α^+ thalassaemia genotype and ABO blood group.

An interaction term between *Sl* genotype and α^+ thalassaemia is included in the model.

Model outputs following 2000 bootstrapped iterations are shown.

A significant protective association was observed for *S12* in the recessive form (adjusted Odds Ratio (aOR) 0.78; 95% CI 0.64-0.95; $p=0.011$), which was most marked for cerebral malaria (aOR 0.67; 0.52-0.87; $p=0.006$, Figure 2-2 and Table 2-6). The *S12/S12* genotype was also associated with significant protection against death from severe malaria (aOR 0.50; 0.30-0.80; $p=0.002$), and death among children admitted with a specific diagnosis of cerebral malaria in the full adjusted analysis (aOR 0.44; 0.23-0.78; $p=0.007$, Figure 2-2 and Table 2-6). Unexpectedly, we observed a significant interaction between *S12* and α^+ thalassaemia genotype, such that the protective associations of *S12* were only seen in individuals of normal α -globin genotype (Figure 2-3). We found no evidence for an association between *S12* and any other clinical form of severe malaria (Table 2-6), or with *P. falciparum* parasite density (Figure 2-4).

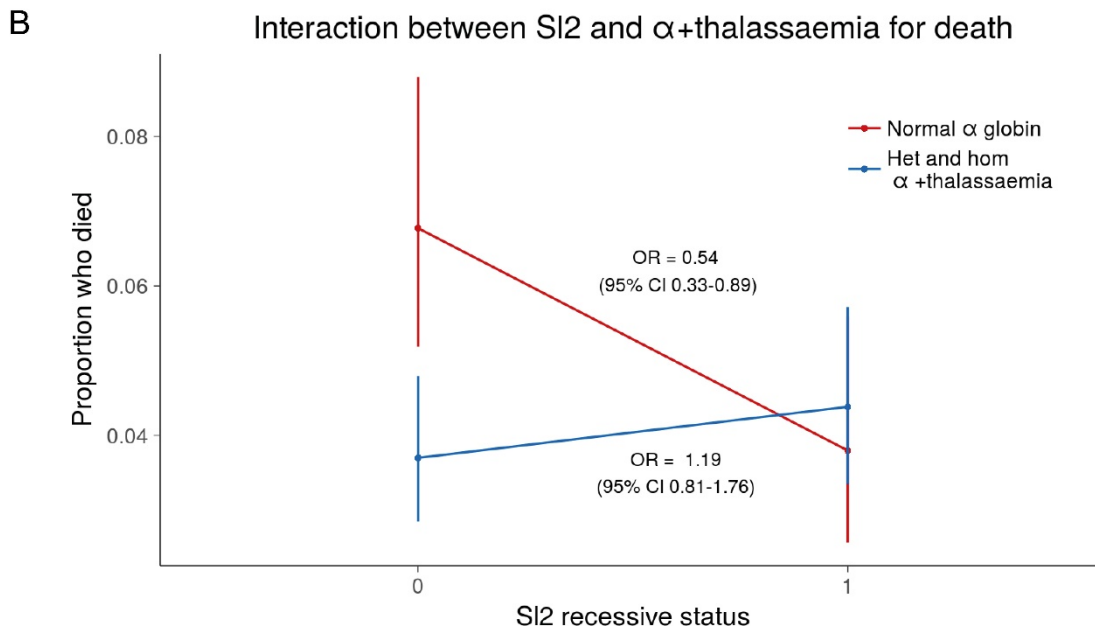
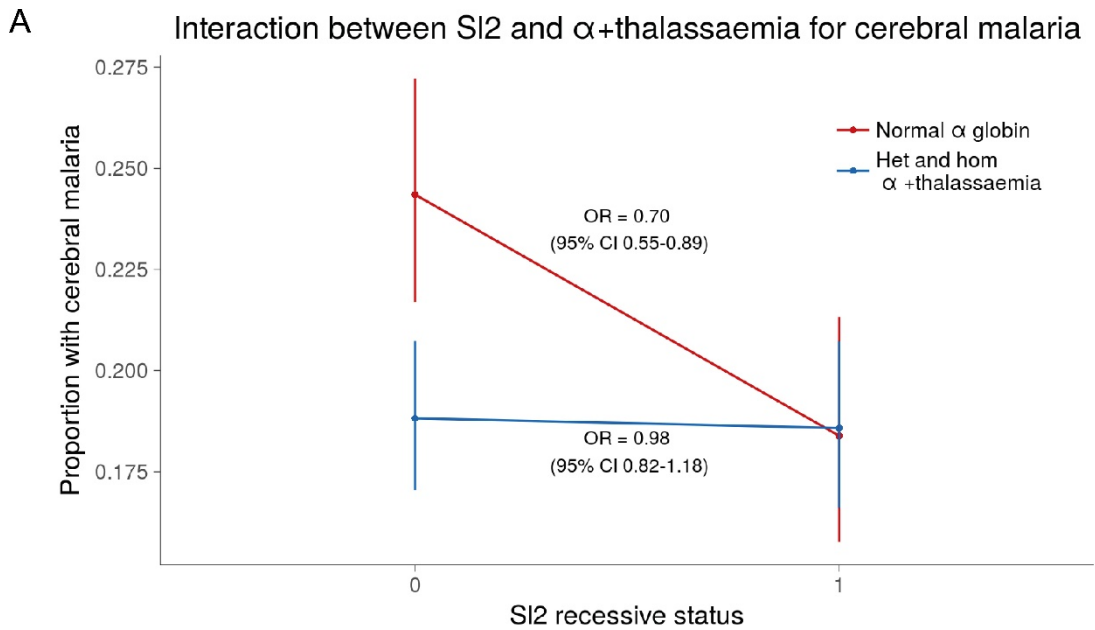


Figure 2-3. The protective association of S12 with cerebral malaria and death is only evident in children with normal α -globin.

Interaction plots showing the interaction between S1 (recessive) and α^+ thalassaemia for the proportion of children suffering (A) cerebral malaria and (B) death. For α^+ thalassaemia status, 0=wild type α -globin; 1= heterozygote or homozygote for α^+ thalassaemia. For S1 (recessive) status, 0= S11/S11 or S11/S12 genotype; 1= S12/S12 genotype.

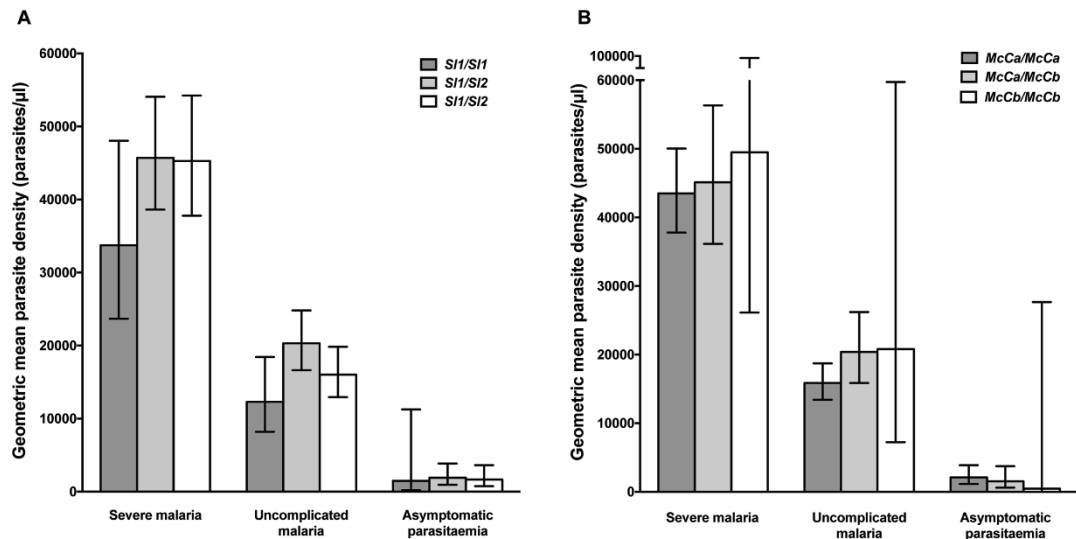


Figure 2-4. Parasite densities by SI and Mc genotypes.

Geometric mean parasite densities in the Kenyan case-control study (severe malaria) and longitudinal disease cohort study (uncomplicated malaria and asymptomatic parasitaemia) by A) SI genotypes and B) McC genotypes. The data on severe malaria includes 1695 children: (SI1/SI1 (175), SI1/SI2 (793), SI2/SI2 (727) and McC^a/McC^a (1167), McC^a/McC^b (478) and McC^b/McC^b (50). The data on uncomplicated malaria includes 162 children: (SI1/SI1 (16), SI1/SI2 (75), SI2/SI2 (71) contributing 124, 488 and 461 episodes respectively and McC^a/McC^a (107), McC^a/McC^b (49) and McC^b/McC^b (6) contributing 699, 349 and 25 episodes respectively. The data on asymptomatic parasitaemia includes 57 children: (SI1/SI1 (5), SI1/SI2 (26), SI2/SI2 (26) contributing 6, 35 and 35 episodes respectively and McC^a/McC^a (34), McC^a/McC^b (20) and McC^b/McC^b (3) contributing 47, 25 and 4 episodes respectively.

Differences in parasite densities by genotype were tested by linear regression analysis with adjustment for HbAS, age as a continuous variable and ABO blood group in the severe malaria cases, HbAS and season (defined into 3-monthly blocks) in the uncomplicated malaria samples and HbAS and ABO blood group in the asymptomatic parasitaemia samples. Data were adjusted for within-person-clustering of events in the uncomplicated malaria and asymptomatic parasitaemia studies.

Bars represent 95% confidence intervals.

2.6.2 The *McC^b* allele is associated with increased susceptibility to cerebral malaria and death in the Kenyan case-control study

The unadjusted analysis showed a borderline significant association between *McC^b* and increased susceptibility to severe malaria overall (OR 1.17; 1.00-1.25; $p=0.056$, Table 2-5), and significant associations with increased risk of cerebral malaria (OR 1.21; 1.05-1.39; $p=0.008$) and death (OR 1.34; 1.00-1.77; $p=0.046$, Table 2-5). Similar associations were seen in the full adjusted analysis, although this only reached statistical significance for cerebral malaria (aOR 1.19; 1.10-1.38; $p=0.025$ (additive model), Figure 2-2 and Table 2-6). We found no association between *McC^b* and any other clinical form of severe malaria (Table 2-5 and Table 2-6) or with *P. falciparum* parasite density (Figure 2-4).

2.6.3 Analysis of haplotypic effects and genotype combinations

We considered whether the observed results for *SI* and *McC* could be consistent with the effect of a single haplotype spanning *SI* and *McC*, or with the effect of a specific genotype combination. *SI* and *McC* are 33bp apart and are in linkage disequilibrium, with only three of four possible haplotypes observed in our data. We therefore reanalysed the data under a haplotype model in which the per-individual count of each of the three observed haplotypes was included as a predictor along with the potential confounding factors, as well as under a genotypic model in which the count of each of the six possible *SI/McC* genotype combinations was included as a predictor (detailed in 2.7). These analyses suggest an additive protective association with the *SI2/McC^a* haplotype (aOR=0.85; 0.75-0.96; $P=0.007$), with broadly consistent results observed for analysis of genotype combinations (Table 2-7 and Table 2-8). Thus, the opposing effects of *SI2* and *McC^b* observed above could plausibly result from the protective association of a single haplotype at the locus, although this is difficult to distinguish from the individuals SNPs acting independently and additively based on the statistical evidence alone.

Genotype	Number of controls/ CM cases	aOR	95% CI	p value
<i>SI1/SI1-McC^a/McC^a</i>	378/95	Ref	Ref	Ref
<i>SI1/SI2-McC^a/McC^a</i>	1330/322	0.89	0.59 - 1.41	0.622
<i>SI1/SI2-McC^a/McC^b</i>	400/135	1.15	0.69 - 1.92	0.606
<i>SI2/SI2-McC^a/McC^a</i>	992/216	0.70	0.44 – 1.11	0.123
<i>SI2/SI2-McC^a/McC^b</i>	640/149	0.57	0.33 – 0.96	0.031
<i>SI2/SI2-McC^b/McC^b</i>	89/26	1.12	0.38 – 2.76	0.749

Table 2-7. *SI* and *McC* combined genotypes and adjusted odds ratios for cerebral malaria in the Kenyan case-control study.

Genotype	Number survived/ died	aOR	95% CI	p value
<i>SI1/SI1-McC^a/McC^a</i>	378/25	Ref	Ref	Ref
<i>SI1/SI2-McC^a/McC^a</i>	1330/57	0.73	0.35 – 1.77	0.383
<i>SI1/SI2-McC^a/McC^b</i>	400/23	1.04	0.43 – 2.72	0.946
<i>SI2/SI2-McC^a/McC^a</i>	992/37	0.44	0.19 – 1.10	0.080
<i>SI2/SI2-McC^a/McC^b</i>	640/30	0.34	0.13 – 0.92	0.034
<i>SI2/SI2-McC^b/McC^b</i>	89/8	1.17	0.00 – 6.09	0.530

Table 2-8. *SI* and *McC* combined genotypes and adjusted odds ratio for death in the Kenyan case-control study.

For both Table 2-7 and Table 2-8: aOR: adjusted Odds Ratio. aORs were adjusted for ethnicity, location of residence, sickle cell genotype, α^+ thalassaemia genotype and ABO blood group. An interaction term between the combined *SI/McC* genotype and α^+ thalassaemia was included in the models. Model outputs following 2000 bootstrapped iterations are displayed.

2.6.4 The *S12/S12* genotype was associated with protection against uncomplicated malaria in the Kenyan longitudinal cohort study.

We next examined the association between *S12* and *McC^b* alleles and uncomplicated malaria in a longitudinal prospective study of 208 Kenyan children. General characteristics of the cohort study population by *Sl* and *McC* genotypes are shown in Table 2-9. The number of episodes, incidence and unadjusted Incidence Rate Ratios for the diseases studied in the longitudinal cohort are shown in Table 2-10, Table 2-11 and Table 2-12.

After adjusting for variables known to influence malaria susceptibility, the *S12* allele was associated with a >50% reduction in the incidence of uncomplicated malaria (additive model) Table 2-13. Once again, a significant interaction was seen with α^+ thalassaemia, such that the protective association of *S12* was only demonstrated in children of normal α -globin genotype (Table 2-14). We found no significant association between the *McC^b* allele and uncomplicated malaria (Table 2-13).

Characteristics	<i>SI1/SI1</i>	%	<i>SI1/SI2</i>	%	<i>SI2/SI2</i>	%	<i>p</i> value	<i>McC^a/</i> <i>McC^a</i>	%	<i>McC^a/</i> <i>McC^b</i>	%	<i>McC^b/</i> <i>McC^b</i>	%	<i>p</i> value
Sample size	22	10.6	94	45.2	92	44.2		137	65.9	63	30.2	8	3.9	
Mean age in months (95% CI)	18 (14-44)		32 (13-43)		23 (8-48)		0.609	25 (11-45)		31 (13-49)		12 (5-21)		0.112
Gender														
Males	13	10.8	56	46.7	51	42.5		82	68.3	33	27.5	5	4.2	
Females	9	10.2	38	43.2	41	46.6	0.844	55	62.5	30	34.1	3	3.4	0.594
Ethnic group														
Giriama	19	10.8	80	45.5	77	43.8		113	64.2	55	31.3	8	4.6	
Chonyi	2	10.0	10	50.0	8	40.0		15	75.0	5	25.0	0	0.0	
Others	1	8.3	4	33.3	7	58.3	0.907	9	75.0	3	25.0	0	0.0	0.877
Sickle														
AA	17	9.3	85	46.7	80	44.0		122	67.0	52	28.6	8	4.4	
AS	5	19.2	9	34.6	12	46.2	0.224	15	57.7	11	42.3	0	0.0	0.228
α^+thalassaemia														
Normal ($\alpha\alpha/\alpha\alpha$)	7	10.5	33	49.3	27	40.3		45	67.2	18	26.9	4	6.0	
Heterozygote ($-\alpha/\alpha\alpha$)	9	8.7	48	46.2	47	45.2		67	64.4	34	32.7	3	2.9	
Homozygote ($-\alpha/-\alpha$)	6	16.2	13	35.1	18	48.7	0.546	25	67.6	11	29.7	1	2.7	0.823
ABO blood group														
O	11	9.4	56	47.9	50	42.7		81	69.2	30	25.6	6	5.1	
Non O	11	12.1	38	41.8	42	46.1	0.628	56	61.5	33	36.3	2	2.2	0.189

Table 2-9. General characteristics of the Kenyan longitudinal cohort study population by *SI* and *McC* genotypes. All comparisons performed using Fisher's exact test. Age = Kruskal Wallis test.

Clinical Outcomes	SI1/SI1		SI1/SI2		SI2/SI2	
	No. of episodes	Incidence	No. of episodes	Incidence	No. of episodes	Incidence
All non-malaria clinic visits	285	5.77	1052	4.92	1020	5.40
Uncomplicated malaria	124	2.51	493	2.31	461	2.44
LRTI [†]	46	0.93	180	0.84	172	0.91
URTI [¶]	111	2.25	394	1.84	403	2.13
Gastroenteritis	64	1.30	158	0.74	145	0.77
Skin infection	37	0.75	196	0.92	176	0.93
Helminth infection	7	0.14	52	0.24	44	0.23
Malaria negative fever	104	2.11	301	1.41	233	1.23

Table 2-10. Incidence of common childhood diseases by SI genotypes in the Kenyan cohort study. Incidence = number of episodes per child-year of follow up. Data were collected from 22 SI1/SI1, 94 SI1/SI2 and 92 SI2/SI2 individuals during 49.4, 213.8 and 188.8 cyfu (child-years of follow-up) respectively.

Clinical Outcomes	McC ^a /McC ^a		McC ^a /McC ^b		McC ^b /McC ^b	
	No. of episodes	Incidence	No. of episodes	Incidence	No. of episodes	Incidence
All non-malaria clinic visits	1595	5.42	685	4.78	77	5.38
Uncomplicated malaria	699	2.37	354	2.47	25	1.75
LRTI [†]	273	0.93	117	0.82	8	0.56
URTI [¶]	624	2.12	246	1.72	38	2.66
Gastroenteritis	252	0.86	101	0.71	14	0.98
Skin infection	261	0.89	141	0.98	7	0.49
Helminth infection	74	0.25	28	0.20	1	0.07
Malaria negative fever	423	1.43	192	1.34	23	1.61

Table 2-11. Incidence of common childhood diseases by McC genotypes in the Kenyan cohort study. Incidence = number of episodes per child-year of follow up. Data were collected from 137 McC^a/McC^a, 63 McC^a/McC^b and 8 McC^b/McC^b individuals during 294.5, 143.2 and 14.3 cyfu respectively. [†]LRTI: Lower Respiratory Tract Infection; [¶]URTI: Upper Respiratory Tract Infection.

Clinical Outcomes	SI2		McC ^b	
	IRRs [§] (95% CI)	p value	IRRs (95% CI)	p value
Uncomplicated malaria	0.95 (0.76-1.18)	0.638 ⁴	0.72 (0.32-1.63)	0.254 ¹
All non-malaria clinical visits	1.03 (0.87-1.22)	0.711 ¹	0.91 (0.79-1.06)	0.242 ⁴
LRTI [†]	1.02 (0.74-1.41)	0.902 ¹	0.54 (0.21-1.43)	0.217 ¹
URTI [¶]	1.08 (0.88-1.33)	0.472 ¹	0.81 (0.65-1.02)	0.077 ³
Gastroenteritis	0.56 (0.34-0.95)	0.031²	0.87 (0.60-1.26)	0.462 ²
Skin infection	1.24 (0.73-2.12)	0.430 ²	0.47 (0.17-1.29)	0.142 ¹
Helminth infection	1.63 (0.69-3.86)	0.265 ²	0.72 (0.46-1.12)	0.147 ⁴
Malaria negative fever	0.70 (0.49-1.02)	0.060 ²	0.91 (0.70-1.19)	0.486 ³

Table 2-12. Unadjusted Incidence Rate Ratios (IRR) for uncomplicated malaria and non-malarial diseases in the Kenyan longitudinal cohort study by SI and McC genotype. Data were collected from 22 SI1/SI1, 94 SI1/SI2 and 92 SI2/SI2 individuals during 49.4, 213.8 and 188.8 cyfu (child-years of follow-up) respectively and 137 McC^a/McC^a, 63 McC^a/McC^b and 8 McC^b/McC^b individuals during 294.5, 143.2 and 14.3 cyfu respectively. SI2 and McC^b alleles were tested separately in univariate analyses for their association with the disease outcomes of interest using logistic regression in the ¹recessive, ²dominant, ³heterozygous and ⁴additive models. The best fitting models as examined using the Akaike information criterion (AIC) were used in the final analysis that accounted for within-person clustering of events. [§]IRRs: (unadjusted) Incidence Rate Ratios; [†]LRTI: Lower Respiratory Tract Infection; [¶]URTI: Upper Respiratory Tract Infection.

Clinical Outcomes	SI2		McC ^b	
	aIRRs [§] (95% CI)	p value	aIRRs (95% CI)	p value
Uncomplicated malaria	0.49 (0.34-0.72)*	<0.001 ⁴	1.24 (0.90-1.70)	0.184 ¹
All non-malaria clinical visits	1.13 (0.96-1.32)	0.140 ¹	0.76 (0.61-0.96)*	0.020 ⁴
LRTI [†]	1.09 (0.81-1.47)	0.561 ¹	0.39 (0.16-0.96)	0.040 ¹
URTI [¶]	1.21 (0.98-1.50)	0.073 ¹	0.79 (0.63-0.99)	0.047 ³
Gastroenteritis	0.66 (0.43-1.03)	0.066 ²	0.55 (0.31-0.97)*	0.038 ²
Skin infection	1.33 (0.79-2.26)	0.285 ²	0.42 (0.16-1.13)	0.086 ¹
Helminth infection	1.98 (0.83-4.71)	0.122 ²	0.68 (0.43-1.07)	0.094 ⁴
Malaria negative fever	0.83 (0.58-1.18)	0.293 ²	1.03 (0.80-1.33)	0.828 ³

Table 2-13. Adjusted Incidence Rate Ratios (aIRR) for uncomplicated malaria and non-malarial diseases in Kenya by SI and McC genotype.

Data were collected from 22 SI1/SI1, 94 SI1/SI2 and 92 SI2/SI2 individuals during 49.4, 213.8 and 188.8 cyfu (child-years of follow-up) respectively and 137 McC^a/McC^a, 63 McC^a/McC^b and 8 McC^b/McC^b individuals during 294.5, 143.2 and 14.3 cyfu respectively. Both SI2 and McC^b alleles were tested for their association with the disease outcomes of interest using Poisson regression in the ¹recessive, ²dominant, ³heterozygous and ⁴additive models. The best fitting models as examined using the Akaike information criterion (AIC) were used in the final analysis that included adjustment for McC genotype (for SI analyses), SI genotype (for McC analyses) α +thalassaemia and sickle cell genotype, ABO blood group, season (divided into 3 monthly blocks), ethnicity, age as a continuous variable and within-person clustering of events.

[§]aIRRs: adjusted Incidence Rate Ratios

*Models that showed significant evidence of interaction between either SI2 or McC^b and α +thalassaemia.

[†]LRTI: Lower Respiratory Tract Infection

[¶]URTI: Upper Respiratory Tract Infection

	<i>SI1/SI1</i>		<i>SI1/SI2</i>		<i>SI2/SI2</i>	
	No of episodes	Incidence	No of episodes	Incidence	No of episodes	Incidence
All samples	124	2.51	493	2.31	461	2.44
Normal α globin	73	4.18	238	2.87	77	1.64
Heterozygous α^+ thalassaemia	32	1.58	209	1.92	302	2.88
Homozygous α^+ thalassaemia	19	1.63	46	2.09	82	2.20

Table 2-14. Incidence of uncomplicated malaria by *SI* genotype and α^+ thalassaemia status in the Kenyan longitudinal cohort study.

Incidence = number of episodes per child-year of follow up (cyfu). Data were collected from 22 *SI1/SI1*, 94 *SI1/SI2* and 92 *SI2/SI2* individuals during 49.4, 213.8 and 188.8 child-years of follow-up respectively.

2.6.5 The *McC^b* allele was associated with protection from common non-malarial childhood diseases in the Kenyan longitudinal cohort study.

The data shown above are incompatible with malaria being the selective pressure for *McC^b* in the Kenyan population, and suggest that other life-threatening childhood diseases may have been responsible for selection of *McC^b*. We therefore used the same longitudinal cohort study to investigate whether the *McC^b* and *SI2* alleles influence the risk of other childhood diseases. *McC^b* was associated with borderline significant protection against several common infectious diseases including LRTIs, URTIs and gastroenteritis (Table 2-13). *SI2* was associated with a borderline reduced incidence of gastroenteritis (Table 2-13). The association of *McC^b* with gastroenteritis was predominantly seen in children of normal α -globin genotype, echoing the interaction seen with *SI2* and malaria.

2.6.6 The *SI2* allele was associated with reduced ex vivo rosette frequency in *P. falciparum* clinical isolates from Mali.

A previous in vitro study based on a culture-adapted *P. falciparum* parasite line suggested that RBC from *SI2* genotype donors had a reduced ability to form rosettes, providing a possible mechanism for protection against severe malaria (Rowe et al., 1997). *P. falciparum* clinical isolates were not available from the Kenyan case-control study to investigate this potential mechanism in that population. However, the association of *SI* and *McC* genotypes with ex vivo *P. falciparum* rosette frequency could be examined using 167 parasite isolates from a case-control study of children with clinical malaria in Mali (Dumbo et al., 2009).

To determine if the Mali case-control study was a suitable source of samples to examine the effect of Knops genotype on *P. falciparum* rosetting, we examined whether there was any evidence to suggest that the association of the *SI2/SI2* genotype with cerebral malaria also occurred in Mali. To do this, we examined the cerebral malaria cases (n=34) and uncomplicated malaria controls (n=184) from the Malian case-control study Figure 2-5. General characteristics of the cases and controls are shown in Table 2-15 and Table 2-16. α^+ thalassaemia genotype data were not available for the Mali samples.

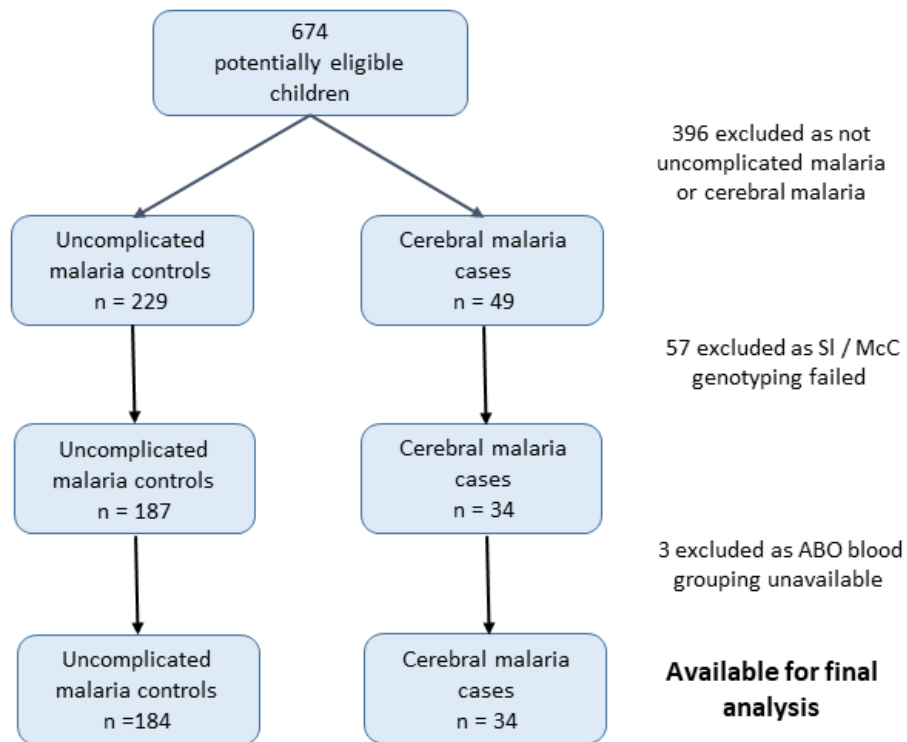


Figure 2-5. Patient inclusion flow chart for Mali case-control study.

	Controls (Uncomplicated malaria)	Cases (Cerebral malaria)	<i>p</i> value
	n = 184	n = 34	
Gender			
Males	90 (49 %)	17 (50 %)	0.920
Females	94 (51 %)	17 (50 %)	
Ethnicity			
Dogon	161 (87.5 %)	30 (88 %)	1
Non-Dogon	23 (12.5 %)	4 (12 %)	
Age in months*	36.5 (19-56)	28 (16-41)	0.026
Median (IQR)			

Table 2-15. General characteristics for cases and controls in the Mali case-control study. Comparisons performed using Pearson's χ^2 test except *Kruskal Wallis test

		SI1/		SI1		SI2/		p		McC ^a /		McC ^a /		McC ^b /		p	
		SI1	%	/SI2	%	SI2	%			McC ^a	%	McC ^b	%	McC ^b	%		
Clinical status	UM	19	10.3	78	42.4	87	47.3			103	56.0	61	33.2	20	10.9		
	CM	5	14.7	19	55.9	10	29.4	0.135 [#]		16	47.1	15	44.1	3	8.8	0.478 [#]	
Gender	M	11	10.3	48	44.9	48	44.9			57	53.3	41	38.3	9	8.4		
	F	13	11.7	49	44.1	49	44.1	0.945		62	55.9	35	31.5	14	12.6	0.430	
Ethnicity	Dogon	21	11.0	88	46.1	82	42.9			108	56.5	66	34.6	17	8.9		
	Non-Dogon	3	11.1	9	33.3	15	55.6	0.448 [#]		11	40.7	10	37.0	6	22.2	0.078	
Blood group	O	13	10.0	63	48.5	54	41.5			68	52.3	49	37.7	13	10.0		
	Non-O	11	12.5	34	38.6	43	48.9	0.355		51	58.0	27	30.7	10	11.4	0.566	
Median age	Months (IQR)	32 (20-57.5)		31 (18-52)		30 (17-55)		0.927		30 (17-53)		31 (18-55)		51 (29-65)		0.229	

Table 2-16. Table of Characteristics for the Malian case-control study by SI and McC genotype.

UM = uncomplicated malaria. CM, cerebral malaria. IQR, interquartile range. Significance testing uses uncomplicated malaria as the reference group. Age: Kruskal Wallis test. #: Fisher's exact test. All other analyses: Pearson's χ^2 .

Analysis of this small case-control study suggested a protective association between the *SI2/SI2* genotype and cerebral malaria (aOR 0.35, 95% CI 0.12-0.89, $p=0.024$) and the *SI2/SI2-McC^a/McC^a* genotype combination was associated with protection against cerebral malaria (aOR 0.14, 95% CI 0.02-0.84, $p=0.031$). As such, we considered samples from this population to be appropriate for testing rosetting as a potential mechanism of action. The median rosette frequency (percentage of infected erythrocytes that form rosettes) was significantly lower in *P. falciparum* isolates from malaria patients with one or more *SI2* alleles than in isolates from *SI1/SI1* donors (Figure 2-6), whereas *McC* genotype had no significant associations with *P. falciparum* rosette frequency (Figure 2-6).

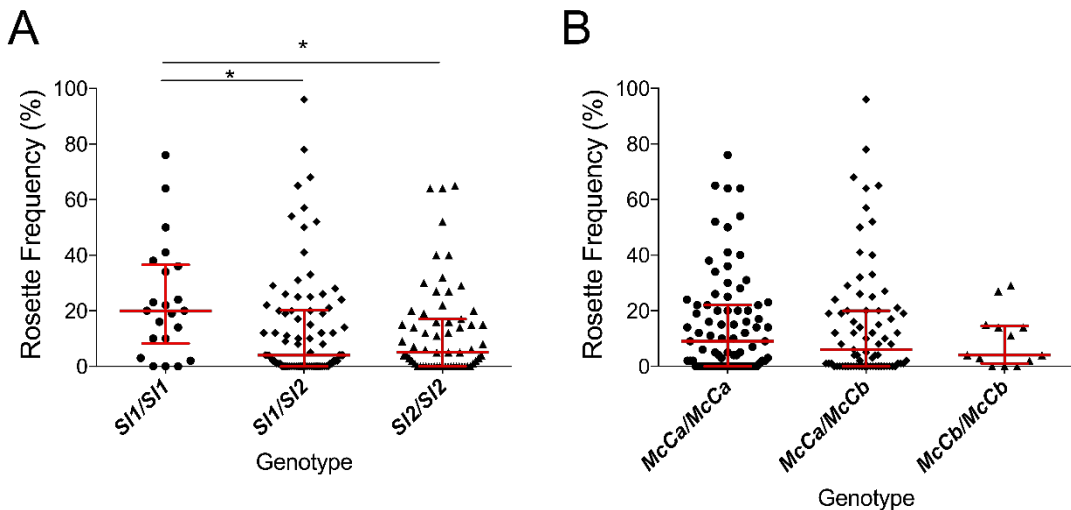


Figure 2-6. The *SI2* allele is associated with reduced *ex vivo* rosette frequency of *P. falciparum* clinical isolates.

Parasite isolates were collected from 167 malaria patients in Mali and matured in culture for 12-24 hours before assessment of rosette frequency (percentage of infected erythrocytes forming rosettes with two or more uninfected erythrocytes). Red bars show the median rosette frequency and interquartile range (IQR) for each genotype. (A) Rosetting by patient *SI* genotype. *SI1/SI1* (n=22, median 20.0, IQR 8.3-36.5), *SI1/SI2* (n=82, median 4.0, IQR 0-20.3), *SI2/SI2* (n=63, median 5.0, IQR 0-17.0); * $p<0.05$, Kruskal Wallis with Dunn's multiple comparison test; (B) Rosetting by *McC* genotype. *McC^a/McC^a* (n=81, median 9.0, IQR 0-22.0), *McC^a/McC^b* (n=73, median 6.0, IQR 0-20.0), *McC^b/McC^b* (n=13, median 4.0, IQR 1-14.5); not significant, Kruskal Wallis with Dunn's multiple comparison test.

2.7 Supplementary information and results

2.7.1 Statistical model fitting and bootstrapping for the Kenyan case-control study

Analyses for the Kilifi case-control study were performed in R (R Foundation for Statistical Computing, Vienna, Austria) (R Development Core Team, 2010) using the “ggplot2”, “lme4”, and “HardyWeinberg” packages (Bates et al., 2013; Graffelman and Camarena, 2008; Wickham, 2009). The dataset was restricted to children who were resident in the Kilifi Health and Demographic Surveillance System (KHDSS) (Scott et al., 2012) and had full genotyping data for *SI*, *McC* α^+ thalassaemia, sickle cell and ABO blood group. This resulted in 1716 cases and 3829 controls (Figure 2-1). The ethnicity variable was compressed from 28 categories to four; Giriama (n=2728), Chonyi (n=1800), Kauma (n=588) and other (n=429). Binary parameterization of the α^+ thalassaemia variable was used, i.e. comparing those children with no α^+ thalassaemia alleles against those with one or more α^+ thalassaemia alleles. This division was chosen in accordance with a previous report showing that both heterozygous and homozygous α^+ thalassaemia genotypes are associated with protection against severe malaria and death in the Kilifi area (Williams et al., 2005b).

A simple unadjusted logistic regression analysis containing only the *SI* and *McC* genotypes suggested potential associations with severe malaria (Table 2-5). We attempted to refine this signal by fitting a more complete model to the data using mixed effect logistic regression analysis. The full adjusted analysis was constructed as follows:

1. Variables associated with malaria susceptibility in multiple previous studies in this population (Atkinson et al., 2014; Fry et al., 2008; Malaria Genomic Epidemiology Network, 2015; Penman et al., 2009; Rockett et al., 2014; Rowe et al., 2007; Williams et al., 2005b, 2005a) were included to give a “base model”. These variables were sickle cell genotype (as a binary variable, sickle trait vs no sickle trait),

α^+ thalassaemia genotype (as a binary variable, one or more α^+ thalassaemia alleles vs no α^+ thalassaemia alleles) and ABO blood group (as a binary variable, group O vs non-group O).

2. Both *Sf* and *McC* genotype were added in the simplest form (additive).

3. All possible models for *Sf* were then examined (genotypic, dominant, recessive, heterozygous and additive models of inheritance, Table 2-17). Model selection was performed using a criterion-based approach by minimizing the Akaike information criterion (AIC) and discrimination (i.e. how well a model separates individuals with and without the outcome of interest) was determined using the c-statistic (area under the receiver operator curve). The recessive model had the best overall fit for *Sf* across clinical outcomes.

4. The process of examining all genetic models of inheritance was then repeated for *McC* (Table 2-18), with *Sf* as recessive included in each model. The additive model had the best overall fit for *McC* across clinical outcomes.

5. All first order interactions were explored. The interaction with the greatest effect on the AIC was included in the final model. This resulted in an interaction term between *Sf* and α^+ thalassaemia being incorporated into the model.

6. Finally, ethnicity and location of residence were incorporated as random effects in order to accommodate population structures which did not require quantification for this study.

	SI2 genotypic (SI1/SI1 = ref)					
	SI2 recessive	SI2 additive	SI2 heterozygous	SI2 dominant	SI1/SI2	SI2/SI2
Case (n=1716)						
aOR	0.77	0.82	1.18	0.79	0.88	0.69
95% CI	0.63-0.95	0.70-0.96	0.96-1.44	0.56-1.11	0.61-1.25	0.48-0.99
p value	0.015	0.012	0.110	0.172	0.460	0.046
All CM (n=943)						
aOR	0.66	0.74	1.35	0.76	0.90	0.61
95% CI	0.51-0.86	0.61-0.90	1.05-1.73	0.50-1.16	0.58-1.39	0.39-0.95
p value	0.002	0.002	0.018	0.205	0.640	0.030
All SMA * (n=483)						
aOR	0.77	0.77	1.06	0.61	0.66	0.54
95% CI	0.56-1.05	0.60-0.97	0.78-1.45	0.38-0.98	0.40-1.08	0.33-0.91
p value	0.101	0.027	0.702	0.040	0.099	0.020
All RD # (n= 522)						
aOR	0.81	0.82	1.10	0.73	0.78	0.66
95% CI	0.59-1.10	0.65-1.04	0.81-1.49	0.44-1.20	0.47-1.32	0.39-1.12
p value	0.175	0.103	0.545	0.211	0.358	0.122
All Deaths (n=180)						
aOR	0.50	0.59	1.53	0.54	0.72	0.38
95% CI	0.30-0.83	0.41-0.84	0.96-2.45	0.27-1.10	0.35-1.50	0.17-0.82
p value	0.007	0.004	0.076	0.090	0.378	0.015

Table 2-17. Adjusted Odds Ratios for different genetic models for the SI polymorphism in the Kenyan case-control study. The "base model" is kept the same throughout (ethnicity and location of residence as random effects; sickle cell genotype, α -thalassaemia genotype and ABO blood group as fixed effects. An interaction term for SI * α -thalassaemia is included). The McC^b allele was kept in the additive form for all analyses.

CM = cerebral malaria; SMA = severe malarial anaemia; RD = respiratory distress.

*199 SMA cases also had CM. # 324 RD cases also had CM. CIs by Wald.

	McC ^b recessive	McC ^b additive	McC ^b heterozygous	McC ^b dominant	McC ^b genotypic (McC ^a / McC ^a = ref)	
					McC ^a / McC ^b	McC ^b / McC ^b
Case (n=1716)						
aOR	1.26	1.10	1.07	1.10	1.09	1.31
95% CI	0.86-1.85	0.98-1.25	0.93-1.23	0.96-1.26	0.94-1.25	0.89-1.92
p value	0.231	0.112	0.338	0.170	0.253	0.176
All CM (n=943)						
aOR	1.19	1.19	1.19	1.22	1.21	1.29
95% CI	0.74-1.92	1.02-1.38	1.01-1.42	1.03-1.44	1.02-1.44	0.79-2.08
p value	0.477	0.024	0.039	0.023	0.029	0.306
All SMA (n=483)						
aOR	0.83	0.96	0.99	0.97	0.98	0.82
95% CI	0.40-1.70	0.78-1.18	0.79-1.24	0.77-1.21	0.78-1.23	0.40-1.70
p value	0.611	0.690	0.913	0.782	0.859	0.598
All RD # (n= 522)						
aOR	1.17	1.12	1.12	1.14	1.13	1.23
95% CI	0.64-2.14	0.93-1.36	0.90-1.39	0.92-1.41	0.91-1.40	0.67-2.26
p value	0.604	0.219	0.300	0.230	0.263	0.498
All Death (n=180)						
aOR	2.11	1.32	1.15	1.28	1.21	2.28
95% CI	0.97-4.56	0.99-1.76	0.82-1.61	0.92-1.78	0.86-1.70	1.04-5.01
p value	0.058	0.060	0.424	0.147	0.275	0.039

Table 2-18. Adjusted Odds Ratios for different genetic models for the McC polymorphism in the Kenyan case-control study. The "base model" is kept the same throughout (ethnicity and location of residence as random effects; sickle cell genotype, α^+ thalassaemia genotype and ABO blood group as fixed effects. An interaction term for Sl * α^+ thalassaemia is included). The Sl2 allele was kept in the recessive form for all analyses.

CM = cerebral malaria; SMA = severe malarial anaemia; RD = respiratory distress.

* 199 SMA cases also had CM. # 324 RD cases also had CM. CIs by Wald.

The final model incorporated ethnicity and location of residence as random effects, and as fixed effects had *Sl*2 in the recessive form (i.e. binary variable, *Sl*2/*Sl*2 vs *Sl*1/*Sl*1 or *Sl*1/*Sl*2); presence of at least one α^+ thalassaemia allele vs no α^+ thalassaemia alleles (binary variable); an interaction term between the *Sl* and α^+ thalassaemia variables; *McC*^b in the additive form (i.e. impact of each additional *McC*^b allele); presence/absence of sickle cell trait as a binary variable; O/non-O blood group as a binary variable.

The code used for the final model was:

```
fit = glmer (outcome ~ (1|ethnicity) + (1|location) +  
Sl_recessive*thalassaemia_allele + Mc + sickle_trait + non_O, data=data, family=  
binomial)
```

Bootstrapping was performed using the “bootMer” function in package “lme4” in R. 2000 iterations were run of each model to calculate 95% confidence intervals and p values. If models did not converge over these 2000 iterations they were inspected for singularities (i.e. a level of one of the variables having a value of 0, for example 0 cases living in the town of Gede). If no singularities were identified, the bootstrapping was rerun using the optimiser “bobyqa” with 10⁵ evaluations.

Corrections for multiple comparisons were not performed in this study, instead all adjusted odds ratios, confidence intervals and p values have been clearly reported. This approach has been repeatedly advocated, particularly when dealing with biological data (Fiedler et al., 2012; Nakagawa, 2004; Perneger, 1998; Rothman, 1990, 2014). The stringency of multiple comparisons increases the risk of type II error, potentially discarding important findings. No single study can be considered conclusive and novel results will always require replication.

2.7.2 Comparison between this study and Rockett et al.

The *SI* and *McC* polymorphisms were originally typed as part of a larger study by Rockett et al. (Rockett et al., 2014), which included case-control data from 12 global sites. The Kenyan samples studied by Rockett et al. originally comprised 2741 cases of severe malaria and 4183 controls. After the quality control of both phenotypic and genotypic data described above, 2268 cases and 3949 controls were analysed by Rockett et al. which were the starting point for our study. Children living outside the KHDSS were excluded, because this allowed us to use “location” as a random effect in the final statistical model, which greatly improved model fit. Children with missing genotypes (*SI*, *McC*, sickle cell, α^+ thalassaemia or ABO blood group) were also excluded (Figure 2-1). After applying these exclusion criteria, 1,716 severe malaria cases and 3829 community controls were available for analysis.

Hence, the number of severe malaria cases differs between our study and Rockett et al. due to differing exclusion criteria. The inclusion of the severe malaria cases who lived outside the KHDSS into our statistical models did not alter the findings of our analysis (Table 2-19). In both our study and that by Rockett et al., the control samples were identical and all came from within the KHDSS. Our study has 120 fewer controls than Rockett et al. due to missing genotypes, because we only used controls for whom full *SI*, *McC*, sickle cell genotype, α^+ thalassaemia genotype and ABO blood group data were available. Our analytical methods differed from Rockett et al., in that we included both *SI* and *McC* in the same statistical model and adjusted for confounders, whereas Rockett et al. examined each SNP independently.

Clinical Outcome	SI2		McCb	
	aOR (95% CI)	p value	aOR (95% CI)	p value
All severe malaria (n= 2100)	0.84 (0.70 - 1.01)	0.069	1.07 (0.96 - 1.19)	0.232
CM (n=1162)	0.72 (0.57 – 0.90)	0.004	1.18 (1.03 – 1.34)	0.016
Severe without CM (n=805)	1.05 (0.82 – 1.35)	0.672	0.967 (0.83 – 1.13)	0.678
Died (n= 241)	0.69 (0.45 – 1.05)	0.083	1.16 (0.90 – 1.49)	0.261
SMA (n= 629)	0.95 (0.72 – 1.24)	0.693	0.92 (0.77 – 1.09)	0.335
RD (n= 653)	0.87 (0.66 – 1.15)	0.333	1.16 (0.98 – 1.36)	0.086

Table 2-19. Reanalysis of Kenyan case-control study including children who lived outside of the KHDSS study area.

Analysis of the dataset including the 386 children who lived outside of the KHDSS study area (407 children lived outside the KHDSS but only 386 had full data on sickle cell, α^+ thalassaemia, SI, McCb and ABO genotype, thus available for inclusion in this analysis). These children were all severe malaria cases and were previously excluded from the main analysis as they did not have location-specific controls.

Adjusted Odds Ratios (aOR) and 95% Confidence Intervals (CI) are presented for the SI2 genotype in the recessive form (i.e. SI2/SI2 vs all other SI genotypes) and McCb genotype in the additive form (i.e. change in aOR with each additional McCb allele). aORs displayed are adjusted for ethnicity, sickle cell genotype, α^+ thalassaemia genotype and ABO blood group. An interaction term between SI genotype and α^+ thalassaemia was included in the model. Confidence intervals by Wald. The 95% CIs and p values are not bootstrapped.

In contrast to the main results table in the manuscript, location of residence could not be used in this model as the newly included cases had no location-specific controls. Removal of the location variable resulted in deterioration of the model fits.

CM = cerebral malaria; SMA = severe malarial anaemia; RD = respiratory distress

2.7.3 Exploration of alternative haplotype and combined genotype models

As one of the four possible *Sl/Mc* haplotype combinations was not seen (*Sl1/McC^b*), the *Sl2* and *McC^b* alleles are likely to be in complete linkage disequilibrium in this population sample (i.e. $D' = 1$, no recombination between these two markers). This situation makes it difficult to distinguish statistically between a model where *Sl* and *McC* act independently and additively or a haplotype model. We considered the possibility that a haplotype model could provide an alternative explanation for our findings, with a separate true protective mutation being positively tagged by the *Sl2* allele and negatively tagged by the *McC^b* allele. Specifically, for each sample we computed the count of each of the three possible *Sl/Mc* haplotypes (assuming only three haplotypes are segregating as above). We then re-fit the logistic regression model for cerebral malaria using haplotype counts as predictors, in addition to potential confounders included in the full adjusted analysis described above. This model estimates a non-zero protective effect of the *Sl2/McC^a* haplotype (additive OR = 0.85; 0.75-0.96; $P=0.007$), but did not fit as well as the full adjusted analysis described above (AIC = 4268.5, versus 4266.8 for the full analysis).

As both *Sl* and *Mc* have sufficient structural effects to alter Knops blood group phenotype, it would appear reasonable to examine their function further before looking for other nearby mutations. In addition, no other strong effects near CR1 have been identified by GWAS studies that could explain the association. However, a haplotype model cannot be excluded as a possibility on the basis of our current data.

2.7.4 Exploration of the negative epistasis between sickle trait and α^+ thalassaemia

Previous studies have described a negative epistatic interaction between sickle trait and α^+ thalassaemia, reporting that α^+ thalassaemia homozygotes who also carry the sickle trait are not protected from severe malaria (Williams et al., 2005c). We wanted to ensure that an unrecognised relationship between sickle cell trait and *SI* genotype did not account for the interaction between α^+ thalassaemia and *SI* that we report in the current study.

Analysis of our current dataset confirmed the existence of negative epistasis between sickle trait and α^+ thalassaemia in this population (Table 2-20). However, of interest, this negative epistatic interaction was only seen in the severe malaria cases without cerebral malaria, whereas the α^+ thalassaemia/*SI* interaction was specific to cerebral malaria cases (Table 2-20). Therefore, the two interactions appear to be mutually exclusive.

The final adjusted analysis was also re-run on a restricted dataset which excluded the 664 children with sickle cell trait or sickle cell disease. The results of this analysis remained unchanged and the α^+ thalassaemia/*SI* interaction persisted without any influence of sickle trait (Table 2-21).

Sickle cell trait did not show a statistical interaction with either *SI* or *McC* genotype. The sickle cell polymorphism is far less common in the KHDSS population than the α^+ thalassaemia polymorphism (~12% of children have one or more sickle cell alleles, compared to ~64% with one or more α^+ thalassaemia alleles). As such, even in a study as large as this one, the power to detect statistically significant interactions between all three of sickle, α^+ thalassaemia and *SI* genotypes is greatly reduced. However, we found no evidence of a three way interaction between these alleles. The raw data for the combined genotypes comprising sickle trait, α^+ thalassaemia and *SI* for each clinical outcome is presented in Table 2-22. Correlations between sickle cell, α^+ thalassaemia, *SI* and *McC* are presented in Table 2-23.

	Sickle trait*		α^+ thalassaemia*		α^+ thalassaemia/sickle trait interaction*	
	aOR (95% CI)	p value	aOR (95% CI)	p value	Interaction effect (95% CI)	p value
All severe malaria (n=1716)	0.11 (0.07-0.16)	<0.001	0.73 (0.61-0.88)	<0.001	3.16 (1.50-6.68)	0.003
CM (n= 943)	0.12 (0.08-0.20)	<0.001	0.67 (0.53-0.84)	<0.001	1.79 (0.57-5.59)	0.316
SMA (n=483)	0.06 (0.03-0.15)	<0.001	0.60 (0.44-0.83)	0.002	3.82 (0.71-20.59)	0.119
Severe without CM (n=674)	0.10 (0.05-0.18)	<0.001	0.81 (0.63-1.04)	0.102	5.54 (2.04-15.03)	0.001

	SI2#		α^+ thalassaemia#		α^+ thalassaemia/ SI2 interaction#	
	aOR (95% CI)	p value	aOR (95% CI)	p value	Interaction effect (95% CI)	p value
All severe malaria (n=1716)	0.77 (0.63-0.94)	0.010	0.73 (0.62-0.86)	<0.001	1.25 (0.97 – 1.60)	0.086
CM (n= 943)	0.68 (0.53-0.87)	0.002	0.73 (0.60-0.89)	0.002	1.41 (1.03 – 1.93)	0.031
SMA (n=483)	0.75 (0.55-1.02)	0.064	0.67 (0.52-0.87)	0.003	1.20 (0.80-1.80)	0.369
Severe without CM (n=674)	0.98 (0.75-1.28)	0.879	0.73 (0.57-0.92)	0.007	0.98 (0.70-1.39)	0.924

Table 2-20. Investigation of the sickle trait/ α^+ thalassaemia negative epistatic interaction and the SI2/ α^+ thalassaemia interaction by clinical outcome in the Kenyan case-control study.

Coefficients and p values are for the sickle trait/ α^+ thalassaemia interaction and the SI2/ α^+ thalassaemia interaction by clinical outcome in two separate models (denoted by * or #). The sickle trait/ α^+ thalassaemia interaction (examined in the * model) was only significant for cases without cerebral malaria, whereas the SI2/ α^+ thalassaemia interaction (examined in the # model) was only significant for cases with cerebral malaria. Both models include ethnicity and location as random effects with additional variables described in the * or # paragraphs below (NB, Mcc^b and ABO are not included in these models). 260/483 cases of SMA also had CM.

* This model included the α^+ thalassaemia variable in recessive form (i.e. α^+ thalassaemia homozygotes vs both α^+ thalassaemia heterozygotes and those without α^+ thalassaemia alleles), sickle cell trait (i.e. sickle cell trait vs both sickle cell homozygotes and those without sickle cell alleles) and an interaction term between these two variables (Williams et al., 2005c).

This model included the SI2 variable in the recessive form (i.e. SI2/SI2 genotype vs both SI1/SI1 and SI1/SI2 genotypes) and the α^+ thalassaemia variable in the dominant form (i.e. one or more α^+ thalassaemia alleles vs no α^+ thalassaemia alleles). This is the novel interaction identified.

The logistic regression interaction effect is interpreted as a ratio of odds ratios. For example, there is a significant association between α^+ thalassaemia homozygosity and sickle cell trait for severe malaria. The association between α^+ thalassaemia homozygosity and severe malaria for those WITHOUT sickle cell trait is aOR=0.73. The association between α^+ thalassaemia homozygosity and severe malaria for those WITH sickle cell trait is aOR=0.73 * 3.16 = 2.31. Confidence intervals by Wald. The 95% CIs and p values are not bootstrapped

Clinical Outcome	<i>SI2</i>		<i>McC^b</i>	
	aOR (95% CI)	<i>p</i> value	aOR (95% CI)	<i>p</i> value
All severe malaria (n= 1665)	0.75 (0.61 - 0.93)	0.009	1.10 (0.97 - 1.24)	0.154
CM (n=913)	0.65 (0.50 - 0.84)	0.001	1.18 (1.01 - 1.37)	0.035
Severe without CM (n= 654)	0.98 (0.74 - 1.29)	0.867	0.97 (0.81 - 1.16)	0.728
Died (n= 170)	0.41 (0.24 - 0.71)	0.001	1.33 (0.99 - 1.79)	0.061
SMA (n=469)	0.74 (0.54-1.02)	0.069	0.95 (0.78- 1.17)	0.658
RD (n= 409)	0.78 (0.57 - 1.07)	0.126	1.12 (0.92 - 1.35)	0.247

Table 2-21. Reanalysis of the Kenyan case-control study excluding all children with one or more sickle cell alleles does not alter findings.

Kilifi case-control dataset restricted to children without sickle cell trait or sickle cell disease (664 children excluded from analysis).

*Adjusted Odds Ratios (aOR) and 95% Confidence Intervals (CI) are presented for the SI2 genotype in the recessive form (i.e. SI2/SI2 vs all other SI genotypes) and McC^b genotype in the additive form (i.e. change in aOR with each additional McC^b allele). aORs displayed are adjusted for ethnicity, location of residence, α^+ thalassaemia genotype and ABO blood group. An interaction term between SI genotype and α^+ thalassaemia was included in the model. Confidence intervals by Wald. The 95% CIs and *p* values are not bootstrapped.*

CM = cerebral malaria; SMA = severe malarial anaemia; RD, respiratory distress.

Sickle Trait	α^+ thalassaemia	SI2	Controls	All severe cases	All cases Proportion (%)	CM cases	CM Proportion (%)	SMA cases	SMA Proportion (%)	Case no CM	Case no CM Proportion (%)
0	0	0	103	68	39.77	35	25.36	27	20.77	29	21.97
0	0	1	495	325	39.63	186	27.31	94	15.96	120	19.51
0	0	2	504	275	35.30	133	20.88	81	13.85	131	20.63
0	1	0	161	85	34.55	51	24.06	24	12.97	28	14.81
0	1	1	740	356	32.48	205	21.69	107	12.63	131	15.04
0	1	2	714	363	33.70	207	22.48	95	11.74	132	15.60
0	2	0	56	22	28.21	7	11.11	2	3.45	14	20.00
0	2	1	232	101	30.33	55	19.16	26	10.08	39	14.39
0	2	2	243	80	24.77	42	14.74	20	7.60	32	11.64
1	0	0	17	1	5.56	1	5.56	0	0.00	0	0.00
1	0	1	87	5	5.43	4	4.40	0	0.00	1	1.14
1	0	2	104	7	6.31	4	3.70	1	0.95	3	2.80
1	1	0	32	1	3.03	1	3.03	0	0.00	0	0.00
1	1	1	139	9	6.08	6	4.14	2	1.42	2	1.42
1	1	2	113	6	5.04	2	1.74	2	1.74	4	3.42
1	2	0	9	0	0.00	0	0.00	0	0.00	0	0.00
1	2	1	37	5	11.90	1	2.63	1	2.63	4	9.76
1	2	2	43	7	14.00	3	6.52	1	2.27	4	8.51

Table 2-22. Raw data for the combined sickle trait, α^+ thalassaemia and SI genotype by clinical outcome in the Kenyan case-control study. Raw data for each clinical outcome presented by sickle trait status (0 = no sickle trait, 1 = sickle trait), α^+ thalassaemia genotype (0, 1, 2 = number of α^+ thalassaemia alleles) and SI2 genotype (0, 1, 2 = number of SI2 alleles). Proportion for each clinical outcome calculated using number of cases/ (number of cases + number of controls).

	Sickle	α^+ thalassaemia	<i>SI2</i>	<i>McC^b</i>
Sickle		0.011	0.006	-0.025
α^+ thalassaemia	0.011		-0.007	0.002
<i>SI2</i>	0.006	-0.007		0.301
<i>McC^b</i>	-0.025	0.002	0.301	

Table 2-23. Correlations between the sickle cell, α^+ thalassaemia, *SI2* and *McC^b* variants in the Kenyan case-control study.

Each variant was coded as 0/1/2 copies of the allele. Shaded area = not applicable.

2.7.5 Statistical model fitting for the longitudinal cohort study

Associations between *SI* and *McC* and mild malaria and other non-malarial related diseases in the longitudinal cohort study were tested in Stata v11.2 (StataCorp, Texas, USA) using a random effects Poisson regression analysis that accounted for within-person clustering of events. This analysis was restricted to children under 10 years old living in the Ngerenya area in the northern part of the KHDSS study area. The analysis was carried out on the 208 children from the cohort with full genotype, ethnic group, season and age data. The model selection process first involved univariate analyses testing for disease associations for *SI* and *McC* independently without potential confounders in genotypic, dominant, recessive, heterozygous and additive models of inheritance. Models were compared using the Akaike information criterion (AIC) for fitness, with the model displaying the minimum AIC values for each respective genotype and outcome of interest chosen as the best fitting model. The unadjusted Incident Rate Ratios and best fitting models are shown in Table 2-12. For each disease outcome, the association with *SI* genotype was then adjusted for confounding by *McC* (best genetic model chosen from the univariate analysis) and for explanatory variables previously associated with outcomes of interest: sickle cell genotype, α^+ thalassaemia genotype, ABO blood group genotype, ethnic group, season (defined as 3 monthly blocks) and age in months as a continuous variable. AIC values were compared to identify the best fitting genetic model (Table 2-24). The same process was carried out for the association of *McC* genotype with each disease outcome, with adjustment for *SI* genotype and the other explanatory variables (Table 2-25). For consistency of

reporting here, the same explanatory variables are included in the statistical models for all disease outcomes in the data presented. Optimized model-fitting for each outcome by removing explanatory variables that did not improve model fit, did not make any material difference to the results shown here.

Finally, we tested for interactions between either *S/I* and *McC* and α^+ thalassaemia (represented as normal, heterozygous and homozygous genotypes) using the likelihood ratio test with a p value of <0.05 indicating statistically significant evidence for interaction, and the appropriate interaction term included in the final model.

		SI2 genotypic (SI1/SI1 = ref)					
		SI2 recessive	SI2 additive	SI2 heterozygous	SI2 dominant	SI1/SI2	SI2/SI2
Uncomplicated malaria	aIRR (95% CI)	0.44 (0.26-0.74)*	0.49 (0.34-0.72)*	0.95 (0.71-1.28)	0.35 (0.16-0.74)*	0.43 (0.20-0.93)*	0.23 (0.10-0.52)*
	p value	0.002	<0.001	0.735	0.006	0.031	<0.001
All non-malaria clinic visits	aIRR (95% CI)	1.13 (0.96-1.32)	1.07 (0.95-1.20)	0.90 (0.77-1.04)	1.00 (0.78-1.27)	0.95 (0.73-1.22)	1.07 (0.82-1.40)
	p value	0.140	0.271	0.148	0.965	0.667	0.602
LRTI[†]	aIRR (95% CI)	1.09 (0.81-1.47)	1.06 (0.85-1.32)	0.93 (0.69-1.24)	1.03 (0.64-1.65)	0.98 (0.60-1.61)	1.08 (0.65-1.77)
	p value	0.561	0.629	0.608	0.918	0.938	0.777
URTI[¶]	aIRR (95% CI)	1.21 (0.98-1.50)	1.12 (0.96-1.32)	0.84 (0.68-1.03)	1.03 (0.74-1.45)	0.94 (0.66-1.33)	1.15 (0.81-1.64)
	p value	0.073	0.148	0.098	0.844	0.732	0.431
Gastroenteritis	aIRR (95% CI)	0.94 (0.69-1.28)	0.87 (0.69-1.09)	0.89 (0.66-1.18)	0.66 (0.43-1.03)	0.66 (0.42-1.04)	0.67 (0.41-1.08)
	p value	0.694	0.214	0.406	0.066	0.072	0.100
Skin infection	aIRR (95% CI)	1.07 (0.78-1.48)	1.11 (0.87-1.42)	1.03 (0.75-1.42)	1.33 (0.79-2.26)	1.32 (0.76-2.29)	1.35 (0.77-2.36)
	p value	0.668	0.410	0.836	0.285	0.324	0.291
Helminth infection	aIRR (95% CI)	1.15 (0.71-1.86)	1.25 (0.86-1.81)	1.10 (0.69-1.76)	1.98 (0.83-4.71)	1.95 (0.80-4.73)	2.04 (0.82-5.07)
	p value	0.577	0.234	0.676	0.122	0.141	0.127
Malaria-negative fever	aIRR (95% CI)	0.91 (0.72-1.15)	0.91 (0.77-1.08)	1.01 (0.81-1.27)	0.84 (0.60-1.18)	0.87 (0.61-1.24)	0.81 (0.56-1.17)
	p value	0.419	0.274	0.910	0.314	0.424	0.257

Table 2-24. Adjusted Incidence Rate Ratios for SI disease associations in the longitudinal cohort study by genetic models of inheritance. Data were collected from 22 SI1/SI1, 94 SI1/SI2 and 92 SI2/SI2 individuals during 49.4, 213.8 and 188.8 cyfu (child-years of follow-up) respectively. SI2 was tested for association with the disease outcomes of interest in the recessive, additive, heterozygous, dominant, and genotypic models. Adjusted incidence rate ratios and 95% confidence intervals (CIs) were generated using Poisson regression analysis, with adjustment for McC, α^+ thalassaemia and sickle cell genotypes, ABO blood group, season (divided into 3 monthly blocks), ethnicity, age as a continuous variable and within-person clustering of events. ^aaIRRs: adjusted Incidence Rate Ratios. *Models that showed evidence of significant interaction between SI and α^+ thalassaemia. [†]LRTI: Lower Respiratory Tract Infection. [¶]URTI: Upper Respiratory Tract Infection.

		McC ^b genotypic (McC ^a / McC ^a = ref)					
		McC ^b					
		McC ^b recessive	McC ^b additive	heterozygous	McC ^b dominant	McC ^a / McC ^b	McC ^b / McC ^b
Uncomplicated malaria	aIRR (95% CI)	1.01 (0.44-2.34)	1.18 (0.90-1.56)	1.24 (0.90-1.70)	1.24 (0.90-1.69)	1.25 (0.91-1.72)	1.12 (0.48-2.60)
	p value	0.977	0.239	0.185	0.184	0.177	0.798
All non-malaria clinic visits	aIRR (95% CI)	0.75 (0.50-1.13)	0.76 (0.61-0.96)	0.95 (0.80-1.12)	0.76 (0.57-0.99)	0.93 (0.79-1.10)	0.73 (0.48-1.10)
	p value	0.163	0.020	0.548	0.047	0.405	0.130
LRTI[†]	aIRR (95% CI)	0.39 (0.16-0.96)	0.87 (0.65-1.15)	1.07 (0.77-1.50)	0.94 (0.68-1.30)	1.02 (0.73-1.42)	0.39 (0.16-0.97)
	p value	0.040	0.314	0.678	0.713	0.913	0.043
URTI[‡]	aIRR (95% CI)	1.08 (0.63-1.87)	0.87 (0.72-1.05)	0.79 (0.63-0.99)	0.81 (0.65-1.01)	0.79 (0.63-0.99)	0.99 (0.57-1.72)
	p value	0.772	0.148	0.047	0.068	0.049	0.975
Gastroenteritis	aIRR (95% CI)	0.78 (0.38-1.62)	0.65 (0.42-1.01)*	0.58 (0.31-1.07)*	0.55 (0.31-0.97)	1.02 (0.73-1.42)	0.78 (0.38-1.64)
	p value	0.501	0.053	0.083	0.038	0.906	0.516
Skin infection	aIRR (95% CI)	0.42 (0.16-1.13)	1.01 (0.75-1.35)	1.25 (0.89-1.76)	1.12 (0.80-1.56)	1.21 (0.86-1.70)	0.45 (0.17-1.21)
	p value	0.086	0.974	0.202	0.520	0.281	0.114
Helminth infection	aIRR (95% CI)	0.34 (0.04-2.70)	0.68 (0.43-1.07)	0.73 (0.44-1.22)	0.68 (0.41-1.12)	0.71 (0.43-1.18)	0.31 (0.04-2.45)
	p value	0.308	0.094	0.232	0.125	0.189	0.266
Malaria-negative fever	aIRR (95% CI)	0.95 (0.52-1.73)	1.01 (0.82-1.25)	1.03 (0.80-1.33)	1.02 (0.80-1.32)	1.03 (0.80-1.33)	0.96 (0.52-1.77)
	p value	0.870	0.926	0.802	0.858	0.822	0.904

Table 2-25. Adjusted incidence rate ratios for McC disease associations in the longitudinal cohort study by genetic models of inheritance. Data were collected from 137 McC^a/McC^a, 63 McC^a/McC^b and 8 McC^b/McC^b individuals during 294.5, 143.2 and 14.3 cyfu (child-years of follow-up) respectively. McC^b was tested for association with the disease outcomes of interest in the recessive, additive, heterozygous, dominant, and genotypic models. Adjusted incidence rate ratios and 95% confidence intervals (CIs) were generated using Poisson regression analysis, with adjustment for SI, α^+ thalassaemia and sickle cell genotypes, ABO blood group, season (divided into 3 monthly blocks), ethnicity, age as a continuous variable and within-person clustering of events. [§]aIRRs: adjusted Incidence Rate Ratios. [†]LRTI: Lower Respiratory Tract Infection. [‡]URTI: Upper Respiratory Tract Infection.

2.8 Discussion

The data presented here provide epidemiological evidence supporting a role for CR1 in the pathogenesis of cerebral malaria. Two neighbouring CR1 polymorphisms belonging to the Knops blood group system of antigens had opposing associations on risk of cerebral malaria. The *S12/S12* genotype was associated with protection against cerebral malaria and death, while the *McC^b* allele was associated with increased susceptibility (Figure 2-2 and Table 2-6). The *S12* allele was also associated with significant protection against uncomplicated malaria, whereas the *McC^b* allele was associated with borderline protection against several common infections in Kenyan children (Table 2-13). The protective association of *S12* against cerebral malaria, death and uncomplicated malaria was influenced by α^+ thalassaemia, being most evident in children of normal α -globin genotype.

The protective association between *S12* and cerebral malaria was first reported in a small case-control study from western Kenya (Thathy et al., 2005), but has remained controversial, especially as most prior studies have been underpowered. Hence, our study is the first adequately powered independent sample set that replicates the protective association between *S12* and cerebral malaria. Other studies found no consistent significant associations between *S1* genotypes and severe malaria (Hansson et al., 2013; Jallow et al., 2009; Manjurano et al., 2012; Rockett et al., 2014; Toure et al., 2012; Zimmerman et al., 2003), including a recent multi-centre candidate gene study that included the sample set analysed here (Rockett et al., 2014). A weak association between *McC^b* and an increased odds ratio for cerebral malaria was shown in the multi-centre study (Rockett et al., 2014).

The complex interactions between *S12*, *McC^b* and α^+ thalassaemia revealed by our study provide possible reasons for the previous inconsistent findings. Although *S12* was associated with protection against cerebral malaria in our study, *McC^b* and α^+ thalassaemia both counteracted this effect. The protective association of *S12* was observed most clearly when both *McC^b* and α^+ thalassaemia genotypes were included in the statistical model, something that has not been considered in

previous studies. It is possible that some of the other discrepant genetic associations with severe malaria (Rockett et al., 2014) might result from interactions between multiple loci that vary across populations and may not be revealed by standard analyses. Biologically, it makes sense to account for *McC* genotype when investigating associations with *Sf2* and vice versa, as the two polymorphisms encode changes only 11 amino acids apart in the CR1 molecule (Figure 1-8). The possibility that the observed association might be due to a haplotype rather than independent effects of *Sf* and *McC* cannot be discounted.

The interaction we describe here between *Sf2* and α^+ thalassaemia is reminiscent of the epistatic interactions that have been observed between α^+ thalassaemia and other malaria-protective polymorphisms including sickle cell trait (HbAS) (Williams et al., 2005c) and haptoglobin (Atkinson et al., 2014). It is possible, therefore, that α^+ thalassaemia has a broad effect on multiple malaria-protective polymorphisms, influencing their restricted global frequencies (Penman et al., 2009), and contributing to the discrepant outcomes of previous association studies. Recent large genetic association studies on malaria do not include data on α^+ thalassaemia, because the causal deletions are not typed on automated platforms (Rockett et al., 2014), instead requiring manual genotyping using labour-intensive PCR-based methods (Chong et al., 2000). Replication of the *Sf2*/ α^+ thalassaemia interaction will be required, and we suggest that α^+ thalassaemia genotype should be included as an important confounding variable in future malaria epidemiological studies and that efforts should continue to discover the mechanism of protection afforded by α^+ thalassaemia, which remains controversial (Carlson et al., 1994; Fowkes et al., 2008; Krause et al., 2012; Opi et al., 2014, 2016).

We examined one possible biological mechanism by which the *Sf2* allele might influence cerebral malaria by studying *P. falciparum* rosetting, a parasite virulence factor associated with severe malaria in African children (Dumbo et al., 2009). Previous in vitro experiments showed that CR1 is a receptor for *P. falciparum* rosetting on uninfected RBCs, and that RBCs serologically typed as negative for the

SI1 antigen (likely to be from donors with *SI1/SI2* or *SI2/SI2* genotypes) (Moulds et al., 2001) show reduced binding to the parasite rosetting ligand PfEMP1 (Rowe et al., 1997). In this study, we found a significantly lower median rosette frequency in *P. falciparum* parasite isolates from Malian patients with *SI2* genotypes compared to *SI1/SI1* controls (Figure 2-6). Therefore, similar to HbC (Fairhurst et al., 2005), blood group O (Rowe et al., 2007) and RBC CR1 deficiency (Cockburn et al., 2004), it is possible that reduced rosetting and subsequent reduced microvascular obstruction (Kaul et al., 1991) may in part explain the protective association of *SI2* against cerebral malaria. However, given the protective association of *SI2* with uncomplicated malaria, and the possible associations of *SI2* and *McC^b* with other common childhood infections, it seems likely that the Knops polymorphisms may be associated with broader effects, for example on the complement regulatory functions of CR1. Previously, we have shown that neither cofactor activity for the breakdown of C3b and C4b nor binding to C1q are influenced by the *SI2* and *McC^b* mutations (Tetteh-Quarcoo et al., 2012). In addition, we can find no association between Knops genotype and CR1 clustering on erythrocytes (Paccaud et al., 1988; Swann et al., 2017). However, other potential effects such as altered immune complex binding and processing or activation of the complement lectin pathway via mannose-binding lectin (Ghiran et al., 2000) have not yet been investigated.

Our studies have several limitations: *McC^b* homozygotes are relatively infrequent in Kenya, which limited our power to detect associations with *McC^b* in the homozygous state. Our longitudinal cohort study generated several values of borderline statistical significance for the *McC^b* allele which are inconclusive. Studies with larger sample sizes will be needed to examine the specific associations of *McC^b* on assorted childhood diseases. Another limitation is that our functional (Mali) and epidemiological (Kenya) studies were conducted in different populations. The mechanisms of rosetting and associations with malaria severity are thought to be similar across sub-Saharan Africa (Rowe et al., 2009), suggesting that data collected in either location are likely to be comparable. Furthermore, our examination of a small set of cerebral malaria cases and controls from Mali suggests a protective

association between *SI2/SI2* genotype and cerebral malaria also occurs in this setting. Ideally, future epidemiological and functional studies of specific polymorphisms on malaria should be conducted within a single population, although this remains logistically challenging.

In conclusion, we show that two high frequency CR1 polymorphisms have opposing associations with cerebral malaria and death in Kenyan children. While the *SI2* allele may have reached high frequency in African populations by conferring a protective advantage against cerebral malaria, our data suggest that *McC^b* arose due to a survival advantage afforded against other non-malarial infections (Fitness et al., 2004a; Noumsi et al., 2011). *SI2* may in part protect against cerebral malaria by reducing rosetting, but additional effects seem likely. Further work is needed to examine both the epidemiological effects of the Knops polymorphisms on diverse childhood diseases, and the biological effects of the *SI2* and *McC^b* polymorphisms on CR1 function. Future epidemiological studies should account for the effect of α^+ thalassaemia on the associations between *SI2* and *McC^b* on malaria and other infectious diseases.

2.9 Additional discussion to this manuscript

2.9.1 Potential functions of the *SI* and *McC* polymorphisms

This study provides epidemiological evidence of an association between the *SI* and *McC* polymorphisms and the outcomes of CM and death with malaria. Although these non-synonymous SNPs are sufficient to alter blood group, their function remains undefined. Only a few studies have investigated their potential function using erythrocytes from individuals with the genotypes of interest (Opi, 2013; Rowe et al., 1997) or recombinant proteins (Tetteh-Quarcoo et al., 2012).

2.9.1.1 *SI/McC and rosetting in P. falciparum infection*

The *SI2* polymorphism has previously been associated with rosetting, with erythrocytes of the *SI* -1,2 phenotype (i.e. likely *SI1/2* or *SI2/2* genotypes) showing lower binding to COS-7 cells expressing the DBL1- α portion of PfEMP1 of the R29 rosetting parasite strain (Rowe et al., 1997), suggesting this might translate into reduced rosetting *in vivo*. A smaller unpublished study examined the rosetting frequency of erythrocytes collected from 55 children in Kilifi, Kenya using the R29 strain but found no association with the *SI* or *McC* polymorphisms (Opi, 2013). However, these experiments were performed using aliquots of frozen erythrocytes which had undergone long-term storage, a factor that may affect complement control proteins (Chen et al., 2007; Cockburn et al., 2002; Pascual et al., 1993). Experiments also used pooled serum from UK donors, which may have influenced findings.

Another study produced short recombinant proteins of CR1 CCP 15-25, with mutations corresponding to the *SI1/McC^a*, *SI1/McC^b*, *SI2/McC^a* and *SI2/McC^b* haplotypes (Tetteh-Quarcoo et al., 2012). These fragments spanned CCP 15-17 which is integral for rosetting (Rowe et al., 2000). Many functions of the proteins were investigated (see below), including their ability to disrupt rosettes in the R29 strain, but no differences were seen between the four recombinant proteins.

2.9.1.2 *SI/McC and erythrocyte invasion, PfEMP1 expression and cytoadherence in P. falciparum infection.*

As outlined in section 1.7.2, CR1 acts a sialic acid-independent invasion receptor for *P. falciparum* into uninfected erythrocytes (Spadafora et al., 2010; Tham et al., 2010). The CCP 15-25 recombinant proteins containing *SI* and *McC* mutations previously described were examined for their ability to inhibit erythrocyte invasion by *P. falciparum* the laboratory strain 3D7 and no differences were found between the variants (Tetteh-Quarcoo et al., 2012). This is perhaps unsurprising as the CCPs mapped for erythrocyte invasion (CCP 1-3 region, likely CCP 1 (Park et al., 2013; Tham et al., 2011)) were not included in these short recombinant proteins.

Unpublished experiments examining invasion of the 3D7 strain into erythrocytes from Kenyan children with various *SI/McC* genotypes also found no association between the two (Opi, 2013). This same set of studies found *SI/McC* genotypes did not influence PfEMP1 display (a characteristic that may be involved in reduced cytoadherence in HbS and α -thalassaemia (Cholera et al., 2008; Krause et al., 2012)) on the surface of IEs. Nor did the polymorphisms appear to affect binding to endothelial cytoadherence receptors CD36 or ICAM. However, it should be noted that these experiments used recombinant CD36 and ICAM receptors spotted on plastic dishes and may not be representative of cytoadherence *in vivo*.

2.9.1.3 *SI/McC and erythrocyte CR1 expression level*

Another hypothesis that has been explored is whether the *SI/McC* polymorphisms might influence CR1 expression level on erythrocytes (copy number). Whilst the *HindIII* polymorphism is associated with CR1 copy number in Caucasian and Asian populations, no correlation is seen in Africans (Rowe et al., 2002b). A large study from Kilifi, Kenya determined the erythrocyte CR1 copy numbers of 3535 children aged 0-13 years and related this to *SI/McC* genotypes (Opi et al., 2016). Both *SI2* and *McC^b* were positively associated with CR1 copy number, with the combined genotype *SI2/SI2 McC^b/McC^b* having the highest level of CR1. However, although statistically significant, the absolute differences seen in CR1 copy number with different genotypes was comparatively small (lowest group mean 250 CR1 copies per cell, highest group mean 347 CR1 copies). As such, the association of *SI/McC* with CR1 copy number may not be functionally significant as this would necessitate a very narrow window of effect if this was the mechanism of action of these SNPs.

2.9.1.4 *SI/McC and complement function*

The effect of the *SI* and *McC* polymorphisms on complement function has only been explicitly examined by one study (Tetteh-Quarcoo et al., 2012). Using the recombinant proteins described above, the authors reported no difference between any of the four recombinant proteins in their ability to bind C1q, C3b and C4b and act as cofactors (with factor I) for the breakdown of C3b and C4b. In addition, the

authors examined whether the *SI2* and *McC^b* polymorphisms might influence the structure of CR1, allowing a “*bent-back architecture that would facilitate co-operation between key functional modules and the Knops blood group antigens.*” However, no such structural differences were identified. It should be noted that this study was limited by the fact that the proteins were expressed in *Pichia pastoris* yeast and then enzymatically de-glycosylated. Correct glycosylation of CR1 appears to be key to its function (discussed in detail in section 5.6) and as such, it is hard to conclude a lack of effect of the *SI* and *McC* polymorphisms when this study specifically used de-glycosylated proteins.

2.9.2 Association of the *SI* and *McC* polymorphisms with other diseases in Africa

Another interesting finding from this chapter was the association of *McC^b* with protection against infectious diseases other than malaria in the Kenyan cohort study. Three other studies have reported links between the *SI/McC* polymorphisms and other infectious diseases. Two studies were conducted in parallel by the same team, with one study focusing on leprosy (*Mycobacterium leprae*) and the other on culture-positive tuberculosis (*Mycobacterium tuberculosis*) (Fitness et al., 2004a, 2004b). Both studies were based in Karonga (northern Malawi) with controls matched by age, sex and location of residence. As both complement-opsonised *M. tuberculosis* and *M. leprae* use CR1 to gain entry into macrophages (Hirsch et al., 1994; Schlesinger et al., 1990), five CR1 polymorphisms (including *SI* and *McC*) were investigated as possible susceptibility mutations, typed by RFLP-PCR. The group reported that the *McC^b/McC^b* genotype was associated with reduced odds of leprosy (aOR 0.3, 95% CI 0.1–0.8, $p=0.02$), but found no significant association for *SI* (Fitness et al., 2004a). Neither *McC* nor *SI* were found to be associated with tuberculosis in Malawi (Fitness et al., 2004b).

A later study re-examined the association between the Knops blood group polymorphisms and culture-positive tuberculosis in Bamako, Mali (Noumsi et al., 2011). The *McC^a/McC^b* and *SI1/SI2* genotypes were associated with reduced odds of

tuberculosis (aOR 0.42, 95% CI 0.22-0.81, $p = 0.007$ and aOR 0.50, 95% CI 0.28-0.90, $p = 0.02$ respectively) whilst the *S12/S12* genotype was associated with increased odd of tuberculosis (aOR 1.73, 95% CI 0.99-3.04, $p=0.05$).

If associations for the *S1* and *McC* polymorphisms are not limited to severe malaria, it may suggest that the SNPs (or a mutation in linkage disequilibrium with them) have broader effects on complement activity. It is possible that one SNP (e.g. *S12* based on Kenyan study data) might be associated with protection against severe malaria whilst simultaneously increasing the odds of other infectious diseases. This may have led to the selection of a second SNP (*McC^b*), to abrogate the effect of *S12*.

2.10 Directions of investigation

The findings of this chapter suggest a strong protective association between the *S12* polymorphism and both CM and death. Conversely, *McC^b* was associated with increased odds of CM, but protection against gastroenteritis, URTI and LRTI. Ex vivo rosetting assays indicated that the protection associated with *S12* may be related to reduced rosetting of IEs. It was clear that further investigation was required to ascertain the functions of these two polymorphisms. In light of the associations seen with *McC^b* and other infectious disease, it was decided not to limit further investigation to *P. falciparum*-based assays. Instead, three broader hypotheses were considered that were pertinent to the pathogenesis of CM, but had wider implications for other infectious disease. The hypotheses pursued were:

- *S12* and *McC^b* may alter how CR1 clusters on the erythrocyte surface
- CR1 may be expressed by human brain endothelial cells
- *S12* and *McC^b* may influence binding of the complement components MBL, C1q or L-ficolin to the LHR-D region of CR1.

The next three chapters explore these hypotheses.

3 Do the Swain Langley and McCoy polymorphisms influence how CR1 clusters on the erythrocyte membrane?

Please note – this main body of this chapter is reproduced from the manuscript “*No Evidence that Knops Blood Group Polymorphisms Affect Complement Receptor 1 Clustering on Erythrocytes*” published in Scientific Reports (Swann et al., 2017). In accordance with the University of Edinburgh guidelines for inclusion of publications in a thesis (Appendix 8.2), the publication is presented in this chapter with an additional introduction and discussion. Abstract, introduction, methods, results, discussion, figures tables and legends are taken directly from the publication itself. For this chapter, the manuscript and accompanying references have been re-formatted to correspond to the style used in this thesis. Supplementary information has been placed in-line for clarity. A PDF of the manuscript is available at <https://doi.org/10.1038/s41598-017-17664-9>, with the corresponding open access licence in Appendix 8.4.

3.1 Declaration

CR1 copy number determination was performed by Emily Nyatichi. *SI*, *McC*, HbS and ABO blood group and α -thalassaemia genotyping had been previously performed by Dominic Kwiatkowski, Kirk Rockett, Sophie Ugoya and Alex Macharia for a separate study. Advice on statistical analysis was provided by Ewen Harrison. Thomas Williams designed and oversaw recruitment of the Immunology Cohort Study in Kilifi, which provided the blood samples for this chapter. All other experiments, analyses and the writing of the manuscript were undertaken by myself. The final draft of the manuscript was edited by Alex Rowe and approved by all collaborators.

3.2 Abstract

Clustering of Complement Receptor 1 (CR1) in the erythrocyte membrane is important for immune-complex transfer and clearance. CR1 contains the Knops blood group antigens, including the antithetical pairs Swain-Langley 1 and 2 (SI1 and SI2) and McCoy a and b (McC^a and McC^b), whose functional effects are unknown. We tested the hypothesis that the *SI* and *McC* polymorphisms might influence CR1 clustering on erythrocyte membranes. Blood samples from 125 healthy Kenyan children were analysed by immunofluorescence and confocal microscopy to determine CR1 cluster number and volume. In agreement with previous reports, CR1 cluster number and volume were positively associated with CR1 copy number (mean number of CR1 molecules per erythrocyte). Individuals with the *McC^b/McC^b* genotype had more clusters per cell than *McC^a/McC^a* individuals. However, this association was lost when the strong effect of CR1 copy number was included in the model. No association was observed between *SI* genotype, sickle cell genotype, α -thalassaemia genotype, gender or age and CR1 cluster number or volume. Therefore, after correction for CR1 copy number, the *SI* and *McC* polymorphisms did not influence erythrocyte CR1 clustering, and the effects of the Knops polymorphisms on CR1 function remains unknown.

3.3 Additional introduction to this manuscript

The analyses presented in Chapter 2 outlined a protective association between the *SI2/SI2* genotype and both cerebral malaria and death while suggesting the *McC^b* might increase the odds of cerebral malaria. Following this finding, a number of hypotheses presented themselves as discussed in section 2.10. A key property of CR1 molecules on the erythrocyte surface is their ability to form clusters on binding to a ligand (Chevalier and Kazatchkine, 1989; Ghiran et al., 2008; Paccaud et al., 1988). Humans and other higher primates are unique in using this process for immune clearance (the binding and transport of opsonised immune complexes from erythrocytes to hepatic/splenic macrophages for phagocytosis of this cargo) (Emlen

et al., 1992; Schifferli and Taylor, 1989), whereas, in non-primate mammals, this process is performed by alternative receptors on platelets and unstimulated neutrophils (Henson, 1969; Taylor et al., 1985).

I chose to examine whether the *SI* and *McC* genotypes affected CR1 clustering as this provided a simple starting point to investigate a number of potential biological processes all relevant to cerebral malaria. These included:

- Immune complex transfer (children with cerebral malaria may have higher levels of circulating immune complexes than in other forms of malaria (Mibei et al., 2008)).
- Rosetting (clustering of CR1 molecules could influence the binding avidity to PfEMP1, influencing size or strength of rosettes formed).
- Deformability of erythrocytes (clustering of CR1 increases deformability of the erythrocyte (Glodek et al., 2010) which might be important in maintaining cerebral blood flow in microvasculature partially obstructed by sequestered IEs).
- Invasion of *P. falciparum* into the erythrocyte (CR1 “capping” of the merozoite reported (Biryukov et al., 2016) which might be influenced by the size or number of CR1 clusters formed).

In light of these possibilities, if the *SI* or *McC* genotypes influence CR1 clustering, they could in turn affect a number of key processes in cerebral malaria, making CR1 clustering a useful starting point for investigation. Indeed, the possibility that the *SI2* polymorphism might affect CR1 clustering was raised 16 years ago but never investigated (Krych-Goldberg et al., 2002).

In this chapter, CR1 clusters were imaged using confocal microscopy in preference to conventional fluorescence microscopy. Traditional fluorescence microscopy images the whole sample simultaneously, using the objective lens of the microscope to render parts of interest brighter and clearer. However, the fluorescent signal from the rest of the sample remains, producing “noise” and blurring the image. In contrast, fluorescence confocal microscopy uses a laser (at a

wavelength to excite the desired fluorophore) which passes through a pinhole aperture to eliminate scattered light (Nwaneshiudu et al., 2012). The beam is focused to a point within the sample and the emitted light is reflected via a dichroic mirror onto a separate photo detector. As a result, confocal microscopy both eliminates light coming from out of focus sections of the sample and permits the collection of serial optical sections which can be recombined into a 3D image. Confocal imaging was thus chosen for this study to maximise image quality and reduce background light that might otherwise jeopardise the identification of very small clusters.

3.4 Introduction

Complement receptor 1 (CR1) is a polymorphic transmembrane glycoprotein expressed in humans on erythrocytes, most leucocytes and glomerular podocytes (Fearon, 1985). It is encoded by the *CR1* gene at the 1q32 locus, spanning approximately 133 kb and consisting of 39 exons (Vik and Wong, 1993). Four size polymorphisms of CR1 have been identified, the most common form being CR1*1 (Dykman et al., 1985). This classical form has a molecular weight of 220 kDa under non-reducing conditions, with an ectodomain comprising 30 short consensus repeats (SCRs), the first 28 of which are arranged into four long homologous repeats (LHRs) A-D (Figure 3-1) (Wong, 1990). Insertion or deletion of LHRs accounts for the variation seen in the molecule size (Wong, 1990). Variation also occurs in erythrocyte CR1 copy number, with the mean number of CR1 molecules per cell varying between individuals from 50 to 1200 (Moulds et al., 1992). A *HindIII* restriction fragment length polymorphism in intron 27 of the *CR1* gene correlates with high (H allele) or low (L allele) CR1 expression on erythrocytes (Wilson et al., 1986). However, this polymorphism is not associated with CR1 copy number in African populations (Herrera et al., 1998; Rowe et al., 2002b).

CR1 is a key regulator of complement cascade activation, namely through accelerating the decay of C3 and C5 convertases thus reducing production of anaphylotoxins C3a and C5a (Iida and Nussenzweig, 1981), and acting as a cofactor

with factor I to inactivate C3b and C4b to iC3b and iC4b (Medof and Nussenzweig, 1984). These functions map to specific sites within the CR1 molecule, with site 1 (SCRs 1-3 in LHR-A) displaying high decay accelerating activity (Krych-Goldberg et al., 1999) and binding C4b (Klickstein et al., 1988; Krych et al., 1991), and site 2 (SCRs 8-10 in LHR B and SCRs 15-17 in LHR C) being responsible for cofactor activity with factor I and the binding of C3b and C4b (Figure 3-1) (Klickstein et al., 1988; Krych et al., 1991).

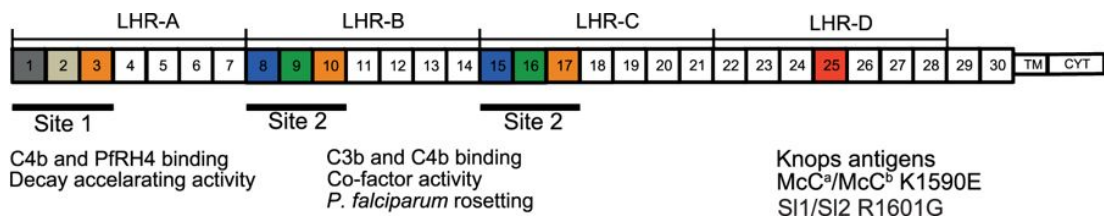


Figure 3-1. Schematic representation of the most common CR1 size variant (CR1*1). Adapted from (Schmidt et al., 2015). The extracellular domain of CR1 is composed of 30 Complement Control Protein (CCP) domains organized into four “Long Homologous Repeats” (LHR). Two major functional sites are found within the CR1 molecule. Site 1 is located in LHR-A (CCP 1-3) and is a binding site for C3b, C4b and the *P. falciparum* invasion ligand PfrH4, and has decay accelerating activity. Site 2 is located in LHR-B (CCP 8-10) and LHR-C (CCP 15-17), and binds C3b and C4b, and interacts with *P. falciparum* infected erythrocytes to form rosettes. In addition, site 2 has factor I-cofactor activity. SNPs determining the SI and McC polymorphisms are localized in LHR-D (CCP 25, shown in red). CCP regions within Sites 1 and 2 that share high sequence identity (between 1 to 3 amino acid changes) are represented with identical shading. TM, transmembrane region; CYT, cytoplasmic tail.

The function of the LHR-D region of CR1 is unclear, but may include binding sites for C1q (Klickstein et al., 1997) and Mannose Binding Lectin (MBL) (Ghiran et al., 2000). SCR 25 in LHR-D also contains the Knops blood group antigens, which include the Swain-Langley (antithetical pairs SI1 and SI2) and McCoy (McC^a and McC^b) antigens (Figure 3-1) (Moulds et al., 2001). The SI2 allele results from a single nucleotide polymorphism (SNP) (rs17047661), encoding an amino acid change from arginine to glycine (R1601G), while the McC^b allele results from a SNP 33 base pairs away (rs17047660), encoding an amino acid change from lysine to glutamic acid (K1590E,

Figure 3-1) (Moulds et al., 2001). The functional effects of the *SI2* and *McC^b* polymorphisms remain unknown. Recent work investigating short recombinant proteins bearing the SI and McC antigens found no difference between the variant forms in their affinities for immobilised C3b, C4b or C1q, nor in their co-factor activity for cleavage of C3b and C4b in conjunction with factor I (Tetteh-Quarcoop et al., 2012).

A marked geographical difference is seen in the frequency of *SI2* and *McC^b* alleles, with the alleles being common in African populations and rare in Caucasians (Moulds, 2010). This has led to the suggestion that these polymorphisms arose due to selection pressure from malaria (Rowe et al., 1997), however, studies to date have been conflicting. An observational study from Western Kenya reported an association between the *SI2/SI2* genotype and a reduced odds ratio of cerebral malaria (OR 0.17, $p = 0.02$) when compared to the *SI1/SI1* genotype (Thathy et al., 2005). Recently, analysis of a large case-control study from Kilifi (eastern Kenya) identified an association between the *SI2/SI2* genotype and protection against cerebral malaria and death from malaria, but conversely found addition of the *McC^b* allele to be associated with increased odds of cerebral malaria (Opi, Swann et al., 2018). However, studies from The Gambia and Ghana did not find significant associations between the polymorphisms and severe malaria (Hansson et al., 2013; Zimmerman et al., 2003).

In addition to complement regulation, CR1 on erythrocytes is responsible for immune adherence, the binding and transfer of opsonised immune complexes (ICs) from the circulation to resident macrophages in the liver and spleen for phagocytosis (Emlen et al., 1992; Schifferli and Taylor, 1989). The clustering of CR1 in the erythrocyte membrane is thought to play a key role in its immune adherence function. On the resting erythrocyte membrane, CR1 is widely dispersed in small clusters, which coalesce into larger clusters when cross-linked by ligands or antibodies (Chevalier and Kazatchkine, 1989; Ghiran et al., 2008; Glodek et al., 2010; Lapin et al., 2012; Melhorn et al., 2013; Paccaud et al., 1988, 1990). CR1 has

also been demonstrated to co-immunoprecipitate with Fas-associated binding protein 1 (FAP-1) in the cytoskeleton fraction, which acts as a scaffolding protein for cross-linked CR1 and cluster formation (Ghiran et al., 2008). It has been hypothesized that CR1 clustering after cross-linking by ligands could prevent ingestion of the erythrocyte during IC transfer to macrophages by concentrating opsonic stimuli in a few areas of the membrane (Ghiran et al., 2008). Ligation of CR1 has also been demonstrated to increase erythrocyte deformability, which could allow IC-laden erythrocytes to traverse the hepatic and splenic capillaries and transfer their cargo to the resident macrophages more easily (Glodek et al., 2010).

The number of CR1 clusters per erythrocyte increases with CR1 copy number (Cosio et al., 1990; Paccaud et al., 1988; Taylor et al., 1991), although CR1 copy number alone does not completely explain inter-individual variation in clustering, implying involvement of other factors (Cosio et al., 1990). The possibility that the *S/2* polymorphism might affect CR1 clustering has been raised (Krych-Goldberg et al., 2002), but never investigated. If the Knops blood group is indeed associated with malaria, there are a number of mechanistic possibilities that could include a role for variation in CR1 clustering. If the *S/2* or *Mcc^b* polymorphisms influenced the size or number of CR1 clusters formed, this might influence the process of invasion of *P. falciparum* into the erythrocyte via CR1 “capping” of the merozoite (Biryukov et al., 2016). Alternatively, CR1 clustering could be important in the pathogenesis of cerebral malaria. Children with cerebral malaria may have higher circulating levels of immune complexes (ICs) than children with other malaria disease syndromes (Mibei et al., 2008). ICs deposited on the endothelial surface can activate complement and stimulate the release of local pro-inflammatory mediators (Jancar and Sánchez Crespo, 2005). ICs can also cross-link Fc-receptors on monocyte and macrophages, stimulating production of tumour necrosis factor (Debets et al., 1988), a cytokine whose relationship with cerebral malaria has been previously reported (Kwiatkowski et al., 1990). As avidity of IC binding to erythrocytes depends on CR1 clustering, clearance of ICs could potentially vary with different CR1 clustering patterns.

3.5 Aims

We therefore set up a study using blood samples from healthy children in Kilifi, Kenya to examine the hypothesis that the *SI2* and *McC^b* polymorphisms might influence erythrocyte CR1 clustering.

3.6 Methods

3.6.1 Study Population and Ethical Approval

The Immunology Cohort Study in Kilifi, Kenya comprises 1041 children resident in the Junju or Ngerenya regions of the Kilifi Demographic Surveillance System (KDSS) (Scott et al., 2012; Williams et al., 2005a). The Kilifi district borders the Indian Ocean and the local economy depends on subsistence farming (Scott et al., 2012). It is a malaria endemic area with seasonal transmission after the long (April-June) and short (October-November) rainy seasons, although recently malaria transmission has fallen in the area (O'Meara et al., 2008). Ethical approval for this study was obtained from the KEMRI Ethical Review Committee and all methods were performed in accordance with the relevant guidelines and regulations. Following informed consent from a parent or guardian, blood samples were obtained by venepuncture between 2nd and 30th April 2013 (inclusive).

3.6.2 Donor selection and genotyping

Donors had previously been genotyped for *SI* and *McC* polymorphisms using the SEQUENOM iPLEX® Gold platform (Fry et al., 2008), for sickle cell (HbS) and α^+ thalassaemia genotype ($-\alpha 3.7$ deletion) by PCR (Chong et al., 2000; Waterfall and Cobb, 2001) and typed for ABO blood group by standard haemagglutination methods (Rowe et al., 2007). Our investigation was limited to the *SI* and *McC* homozygote genotypes, 1a (*SI1/SI1 McC^a/McC^a*), 2a (*SI2/SI2 McC^a/McC^a*) and 2b (*SI2/SI2 McC^b/McC^b*). The 1b genotype does not occur because the *McC^b* polymorphism is only found on the background of the *SI2* variant (Moulds, 2010; Moulds et al., 2001). 148 children in the cohort with 1a, 2a or 2b genotypes, and with complete data on α^+ thalassaemia and sickle cell status (both reported to

influence CR1 copy number (Cockburn et al., 2004; Opi et al., 2016; Otenio et al., 2013)) were eligible for inclusion. Nine children did not attend for venepuncture, 12 were excluded because they were positive for *P. falciparum* on thick blood smear, and two were accidentally discarded, giving 125 samples for analysis (29 with genotype 1a, 88 with genotype 2a and eight with genotype 2b).

3.6.3 Sample collection and processing

4.4 mls of venous blood was collected into a lithium heparin tube, centrifuged at 400g for 10 minutes and plasma removed. The sample was then made up to 5 mls with R2 medium (500 ml RPMI (catalogue number R0883, Sigma-Aldrich, Missouri, USA) with final concentration of 0.02M HEPES (4-(2-hydroxyethyl)-piperazine-ethanesulfonic acid, Gibco, New York, USA), 0.1mM L-glutamine (Gibco, New York, USA), 1% vol/vol Penicillin–Streptomycin Solution Hybri-Max (Sigma-Aldrich, Missouri, USA) and 2% pooled human AB serum). The cell suspension was layered onto 3ml of Lymphoprep (PROGEN Biotechnik, Heidelberg, Germany) and centrifuged at 1000g for 20 minutes at 20°C. The white cell layer was removed and the resulting erythrocytes washed twice in R2 medium without serum by centrifugation at 400g for 5 minutes. They were then adjusted to 4% haematocrit by adding R2 medium without serum. The clustering assay was subsequently performed on these unfixed cells. As storage of blood samples can affect CR1 copy number and function (Chen et al., 2007; Cockburn et al., 2002; Pascual et al., 1993), all clustering assays were performed within eight hours of venepuncture.

3.6.4 CR1 copy number determination.

An aliquot of washed erythrocytes from above was fixed in 5% formaldehyde (Sigma-Aldrich, Missouri, USA) on the day of venepuncture and CR1 copy number was determined within 8 weeks as previously described in detail (Cockburn et al., 2002). Briefly, this method uses flow cytometry to quantify CR1 copy number on fixed erythrocytes using a standard curve derived from donors with known CR1 copy numbers that have been fixed at the same time as the samples. Erythrocytes were stained with 0.5 µg/ml J3D3 anti-CR1 monoclonal antibody (GTX44217,

GeneTex, California, USA), followed by 5 $\mu\text{g}/\text{ml}$ of Alexa Fluor 488-conjugated goat anti-mouse IgG (A-11001, ThermoFisher Scientific, Paisley, UK) and the mean fluorescence intensity determined on a FC500 flow cytometer (Beckman-Coulter Inc.). Examples of the gating strategy and staining of low, intermediate and high CR1 standard donors are shown in Figure 3-2.

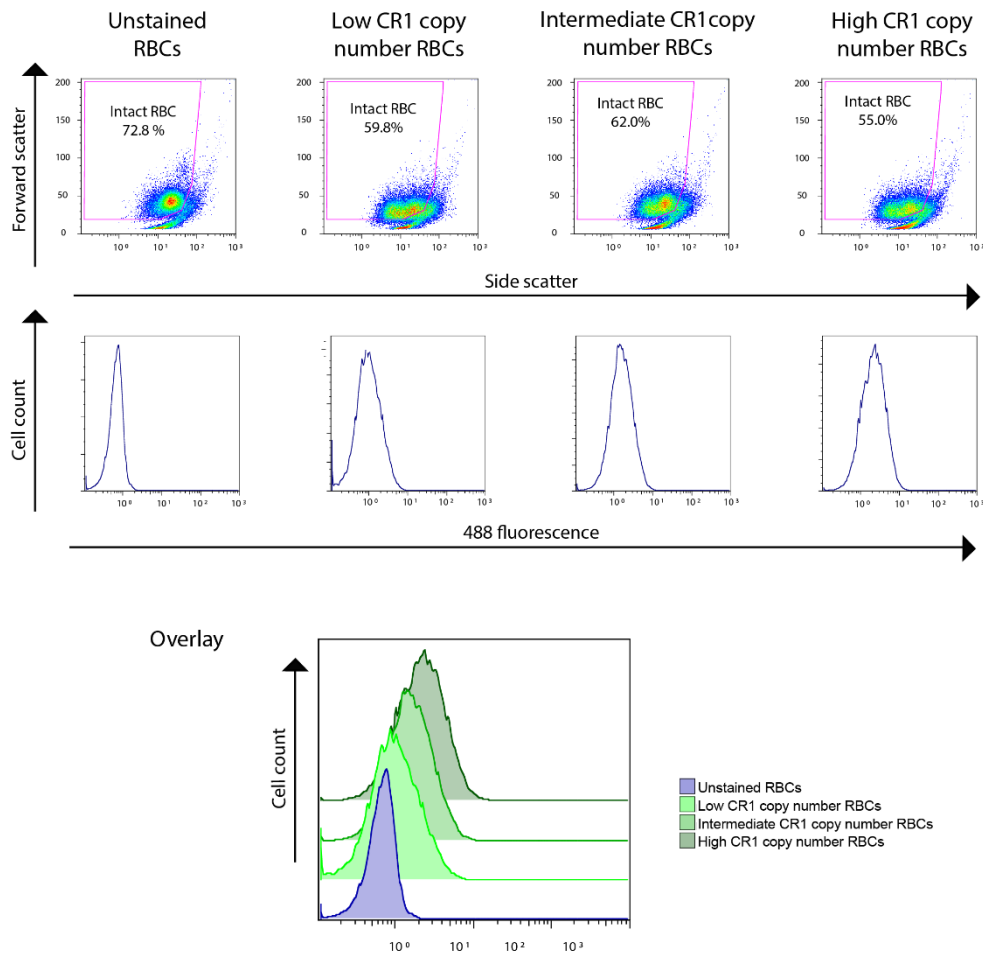


Figure 3-2. Immunofluorescence staining and flow cytometry to determine CR1 copy number. Representative flow cytometry analyses comparing unstained red blood cells (RBCs) with RBCs from individuals with low, intermediate and high CR1 copy numbers. Dot plots (top row) show forward scatter against side scatter with a gating strategy to include only intact cells. Histograms (middle row) show Alexa Fluor488 fluorescence from J3D3 (α -CR1) antibody staining for all intact RBCs in each sample. Increasing fluorescence is seen with higher CR1 copy number. The overlay (bottom row) displays the comparative Alexa Fluor488 fluorescence of intact RBCs from the four donors.

3.6.5 Immunofluorescent staining of CR1 clusters

The IgG1 mouse anti-CR1 monoclonal antibody J3D3 was used to stain CR1 clusters, as it does not recognise epitopes in the LHR-D region (Nickells et al., 1998), so was considered unlikely to influence any effect the *S*/ or *McC* polymorphisms might have on clustering. Two aliquots from each sample of washed, unfixed erythrocytes at 4% haematocrit in PBS/1% BSA were incubated with 5 µg/ml of either J3D3 or IgG1 mouse anti-human isotype control (MCA928, AbD Serotec, Kidlington, UK) to give a final sample volume of 50 µl. Samples were incubated at 4°C for one hour (resuspended every ten mins) and washed three times in 1 ml cold PBS (Oxoid, Basingstoke, UK). 50 µl of 4 µg/ml Alexa Fluor 488-conjugated goat anti-mouse secondary antibody was added and the sample was incubated at 4°C in the dark for one hour (resuspended every ten mins) and subsequently washed three times in 1 ml cold PBS. The sample was resuspended at 30-40% haematocrit, smeared on a glass slide, air-dried, mounted under a 22mm x 22mm glass coverslip with 10 µl of DABCO-glycerol (2.5 mg 1, 4-Diazabicyclo[2.2.2]octane (Sigma-Aldrich, Poole, UK), 0.5 ml glycerol and 0.5 ml PBS) and sealed with nail varnish. All steps to this point were undertaken at the KEMRI-Wellcome Trust Research Unit, Kilifi and the resultant slides were shipped to Edinburgh for confocal microscopy.

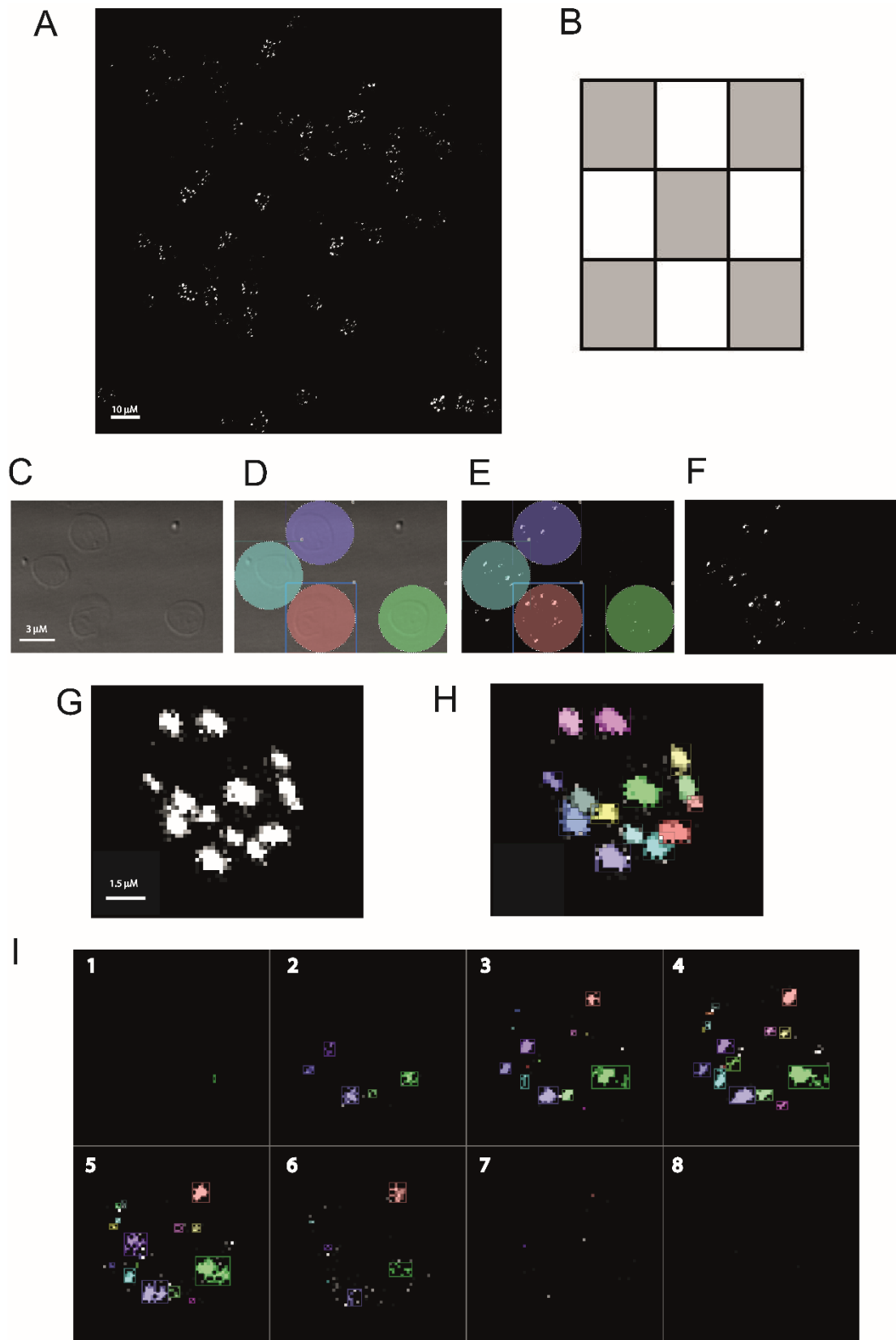


Figure 3-3. Immunofluorescent staining of erythrocyte CR1 clusters and image analysis.
 (Legend continued overleaf)

A) Erythrocyte CR1 clusters were visualised by staining with 5 µg/ml of CR1 monoclonal antibody J3D3, followed by 4 µg/ml of Alexa Fluor 488 goat anti-mouse IgG. See methods for full details. B) For each donor, five confocal microscopy images were taken from the central area of the microscope slide as indicated by the grey shaded areas. Each image was a z-stack comprising 8-10 steps. C-F) To illustrate the image analysis process, a section containing 4 erythrocytes from one of the 5 images from a single donor is shown. Overall, at least 200 erythrocytes were examined per donor. C) For each image, the bright-field view was used to identify the positions of erythrocytes. D) Non-touching cells were then stamped. E) The stamped region was then applied to the fluorescent image. F) Cluster numbers and volumes within the stamped regions were assessed by an automated protocol using Volocity software as described in the methods. G) An example of the clusters identified in a single erythrocyte. H) The same erythrocyte as shown in G, with distinct clusters being shown in different colours. I) A different erythrocyte with each of the 8 steps that comprise the z-stack shown separately (1 to 8).

3.6.6 Confocal microscopy

Slides were imaged with a Leica SP5 confocal microscope using the glycerol x 63 objective, argon laser and differential interference contrast settings (now referred to as “bright field”). Five images per slide (Figure 3-3 A shows a representative image) were taken from predefined areas (Figure 3-3 B). To prevent bias for stained cells, each slide was navigated using the bright field image, ensuring that only erythrocyte outlines, rather than CR1 clusters, were visible. To minimise photo-bleaching, a z-stack of images was taken at 0.8 µm intervals and between eight to ten steps were acquired per stack (an example of the 8 steps comprising a z-stack are shown in Figure 3-3 I. The images in the z-stack were then merged into one 3D image using Volocity 3D Image Analysis Software version 6.3 (PerkinElmer, Massachusetts, USA). Slides were imaged blind to donor information.

3.6.7 Image Analysis

Using the bright field image (to obscure CR1 clusters and increase objectivity) (Figure 3-3 C), a region of interest stamp 9 µm in diameter (area 63.6 µm², slightly larger than an erythrocyte) was used to identify individual erythrocytes that were not touching other cells (Figure 3-3 D). Approximately 40 erythrocytes per image were stamped. Image analysis was then carried out within the stamped areas in the fluorescent channel (Figure 3-3 E-F). An automated software protocol was developed using the “Find objects” task in the “Measurements” module in Volocity

version 6.3 (Perkin Elmer), and was used to determine the number of CR1 clusters per erythrocyte (Figure 3-3 G-H), and to calculate the volume of each cluster. The protocol identified objects within the stamped area based on a minimum size threshold and subsequently separated touching objects using an object size guide. To establish the protocol settings, five cells from five separate donors (total cell number = 25) were reviewed. Settings over a range from 0.01 to 2.56 μm^3 were examined for both minimum size and object size guide. A minimum size threshold of 0.06 μm^3 and object size guide of 0.06 μm^3 gave the optimal correlation with number of clusters identified by eye (Pearson's correlation coefficient of 0.927 and r^2 of 0.859), therefore these settings were used throughout. To account for background fluorescence, 30 maximum fluorescent intensity (MFI) readings were taken from areas of cells without visible CR1 clusters for each donor. The median of these readings was calculated for each individual to give the background MFI. The median of all donor medians was then calculated, giving a universal background correction factor (median = 554, IQR = 554-693) that was subtracted from all samples before running the Volocity protocol.

In order to determine the optimal number of cells to image from each donor, 400 erythrocytes were imaged from a single donor. The standard error of the mean (SEM) of the number of CR1 clusters per erythrocyte was plotted against the number of erythrocytes imaged (Figure 3-4). It was decided to image 200 erythrocytes for each donor, as gains in SEM beyond this point were small.

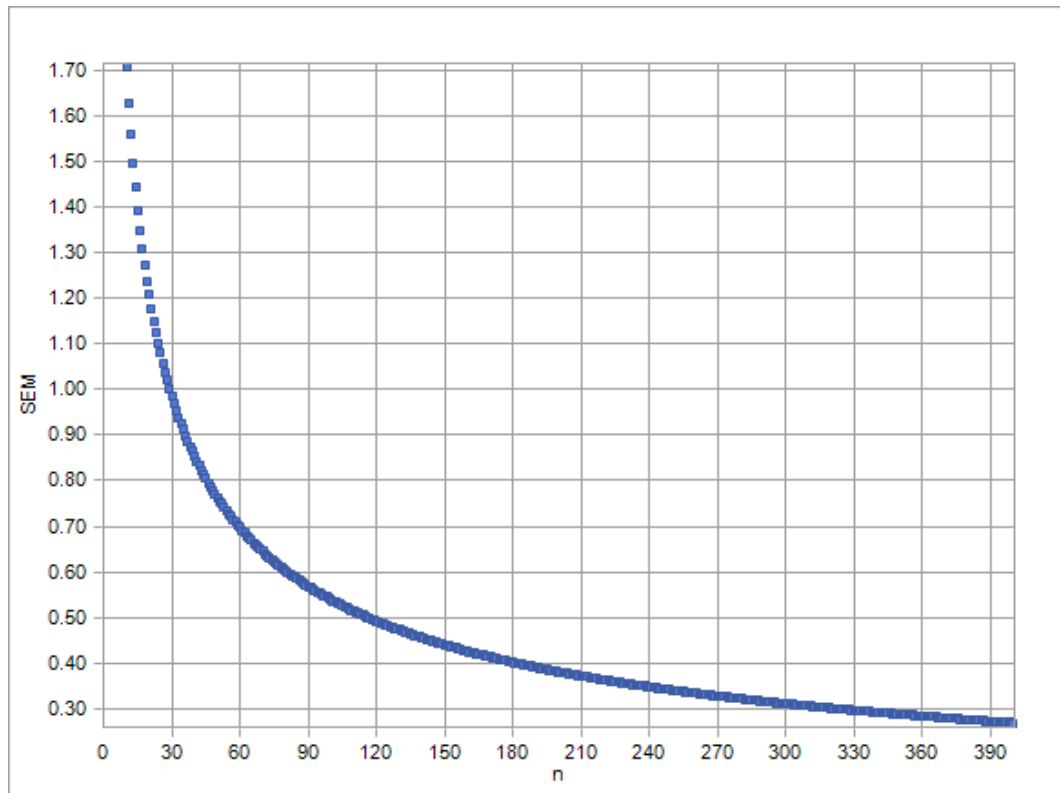


Figure 3-4. Determining the optimal number of erythrocytes to image.

The plot illustrates how the standard error of the mean (SEM) of the number of CR1 clusters per erythrocyte alters with increasing number of erythrocytes imaged (n) from a single donor. Based on these data, it was decided to image 200 erythrocytes for each sample, as reductions in SEM beyond this point were small.

The reproducibility of the assay was assessed by imaging a blood sample taken from a single donor at the same time each day for three consecutive days. Neither the median number of CR1 clusters per cell, nor the mean CR1 cluster volume was significantly different across the three days (Kruskal-Wallis test $p = 0.337$ and 0.054 respectively, Figure 3-5).

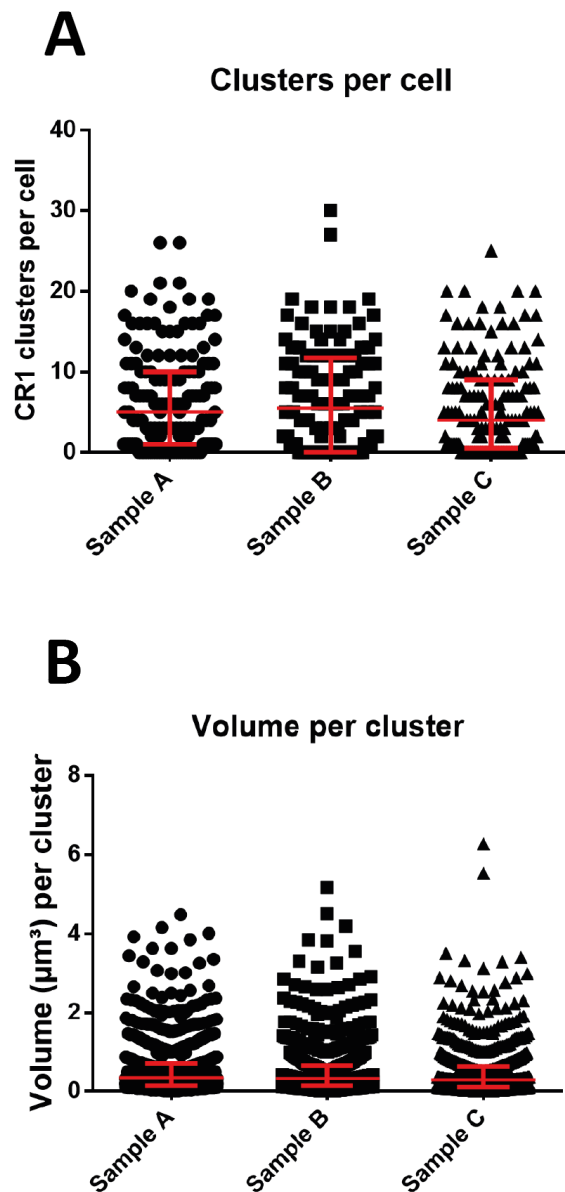


Figure 3-5. CR1 cluster number and volume for three samples taken over consecutive days from one donor.

A) CR1 cluster number per cell. Each data point represents one of the 200 cells imaged. The median and interquartile range are shown as red bars. There were no significant differences between the sample medians (Kruskal-Wallis test $p=0.337$). **B)** Volume per CR1 cluster. The median and interquartile range are shown as red bars. The difference between the median cluster volumes was of borderline significance (Kruskal-Wallis test $p=0.054$), but the absolute difference between the medians was extremely small.

3.6.8 Statistical analyses

Our experiments generated data on individual CR1 clusters from at least 200 erythrocytes per donor. These data were then summarised at three levels: 1) at the level of each individual cluster (to allow for detailed analysis of cluster volume); 2) at the level of each individual cell (to allow for detailed analyses of cluster number per cell) and 3) at the level of each individual donor (to provide a single data point for each participant which represented their median CR1 cluster number or mean cluster volume).

Initial exploratory analyses used the data at the level of the individual donor to examine the influence of donor variables on CR1 copy number, CR1 cluster number and cluster volume. The donor variables explored in our analyses were basic demographic data (age and gender), other variables reported to influence CR1 copy number (α^+ thalassaemia genotype and sickle cell genotype (Cockburn et al., 2004; Opi et al., 2016; Otenio et al., 2013)), ABO blood group (repeatedly associated with malaria in this population) (Fry et al., 2008; Rowe et al., 2007) and Knops genotype (1a, 2a and 2b). Correlation between continuous variables was analysed by linear regression, and differences between means were analysed by one-way ANOVA or t tests.

To examine factors potentially influencing CR1 cluster number, the data were then analysed at the level of the individual cells. To permit inclusion of all the data collected and account for the intra-donor individual variation in the number of clusters per cell, a two-level hierarchical mixed effects Poisson regression model was used. Donor identifier and date the experiment was performed were included as random effects. Each donor variable (as above) was then examined in turn as a fixed effect. In view of the well documented relationship between CR1 cluster number and CR1 copy number (Cosio et al., 1990; Paccaud et al., 1988; Taylor et al., 1991), each variable was examined both with and without CR1 copy number in the model.

Finally, to examine factors potentially influencing CR1 cluster volume and account for both intra-individual and intra-cell variation in volume of clusters, a three-level hierarchical mixed effects linear regression model was used with both donor identifier and cell identifier included as random effects. Each donor variable was then examined as a fixed effect with and without CR1 copy number in the model. Where t values were significant, bootstrapping with 1000 iterations was performed to provide an equivalent p value for ease of interpretation.

Analyses were performed using R statistical software (R Foundation for Statistical Computing, Vienna, Austria) (R Development Core Team, 2010) using the packages “plyr”, “ggplot2”, “boot” and “lme4” (Bates et al., 2013; Wickham, 2009, 2011). Graphs were drawn using GraphPad Prism 7 (GraphPad Software, Inc., La Jolla, CA, USA).

3.7 Results

Erythrocyte CR1 clustering was assessed in blood samples from 125 Kenyan children with the homozygous Knops genotypes *SI1/SI1 McC^a/McC^a*, *SI2/SI2 McC^a/McC^a* or *SI2/SI2 McC^b/McC^b*. These genotypes are hereafter referred to as 1a, 2a and 2b respectively. Only homozygous genotypes were studied in order to examine the associations of the “pure forms” of the polymorphisms on CR1 clustering. The characteristics of the children are summarised in Table 3-1; no significant differences were seen between the 1a, 2a or 2b genotype groups in terms of gender, age, ABO blood group, α^+ thalassaemia genotype or sickle cell genotype.

Characteristic	Total (n)	Genotype [‡]			p value
		1a (n = 29) (%)	2a (n = 88) (%)	2b (n = 8) (%)	
Gender					
Male	73	17 (59)	51 (58)	5 (62.5)	1*
Female	52	12 (41)	37 (42)	3 (37.5)	
Age (months)					
Mean (SD)	NA	130 (34)	119 (32)	138 (36)	0.124 [§]
ABO blood group					
O	68	16 (55)	47 (53)	5 (62.5)	0.930*
A	29	8 (28)	19 (22)	2 (25)	
B	23	5 (17)	17 (19)	1 (12.5)	
AB	5	0 (0)	5 (6)	0 (0)	
α +thalassaemia genotype [‡]					
$\alpha\alpha/\alpha\alpha$	49	12 (41)	33 (38)	4 (50)	0.857*
$-\alpha/\alpha\alpha$	51	13 (45)	35 (40)	3 (37.5)	
$-\alpha/-\alpha$	25	4 (14)	20 (22)	1 (12.5)	
Sickle cell (HbS) genotype [‡]					
AA	108	25 (86)	77 (88)	6 (75)	0.547*
AS	17	4 (14)	11 (12)	2 (25)	
CR1 copy number					
Mean (SD)	NA	495 (204)	478 (221)	658 (305)	0.098 [§]

Table 3-1. Characteristics of individuals studied.

#1a = S11/S11, McC^a/McC^a genotype, 2a = S12/S12, McC^a/McC^a genotype, 2b = S12/S12, McC^b/McC^b genotype. *Fisher's exact test, §One-way ANOVA. ‡ α +thalassaemia and sickle cell genotype were included in the study as both have previously been reported to influence CR1 copy number (Cockburn et al., 2004; Opi et al., 2016; Otenio et al., 2013). SD, standard deviation. NA, not applicable.

In order to examine CR1 clusters, we carried out immunofluorescent staining of unfixed erythrocytes with a monoclonal antibody to CR1 (Figure 3-3 A), and analysed confocal microscopy images with an automated protocol developed using Volocity Image Analysis software (version 6.3, Perkin Elmer) to determine CR1 erythrocyte cluster number and volume (Figure 3-3 B-H).

3.7.1 Increased CR1 copy number in individuals with the *McC^b/McC^b* genotype.

CR1 copy number (mean number of CR1 molecules per erythrocyte) positively correlates with number of CR1 clusters (Cosio et al., 1990; Paccaud et al., 1988; Taylor et al., 1991) and was therefore measured in all individuals. We first examined the association of CR1 copy number and donor variables in univariate analyses. We observed that individuals with the 2b genotype had a higher CR1 copy number when compared to individuals with 1a and 2a genotypes (Table 3-1 and Figure 3-6 A, $p=0.098$ by ANOVA). This was driven by the *McC* component of the genotype, as individuals with the *McC^b/McC^b* genotype had a significantly higher CR1 copy number than *McC^a/McC^a* (mean 658 copies per cell versus 483 copies per cell, $p=0.033$, t-test, Figure 3-6 B). The *Sl* component of the genotype was not significantly associated with CR1 copy number ($p=0.978$, t-test, Figure 3-6 C). Age, gender, ABO blood group and sickle cell trait showed no significant association with CR1 copy number in this study. Individuals who were homozygotes for α^+ thalassaemia had a lower CR1 copy number (441) than those who were heterozygotes (495) or who had normal α globin (520), however this was not significant ($p=0.366$, ANOVA, Figure 3-7).

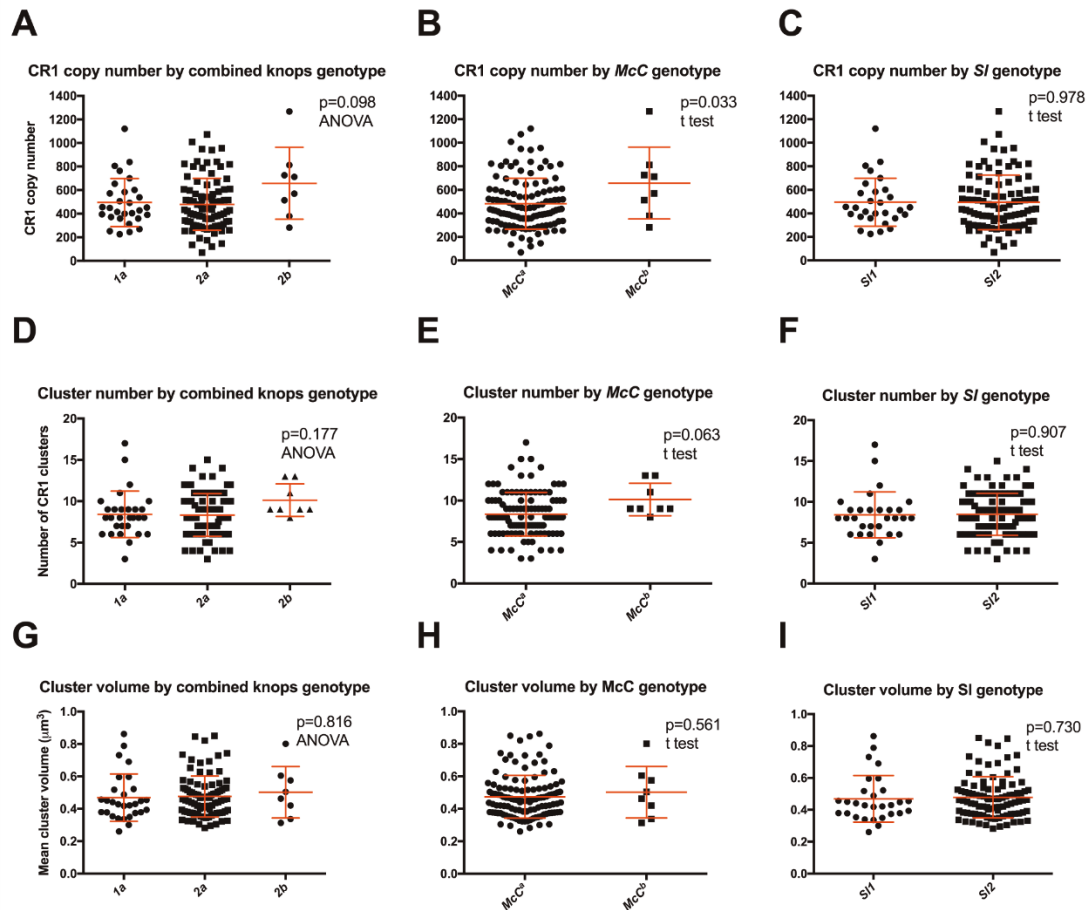


Figure 3-6. The *McC^b* genotype is associated with CR1 copy number and cluster number. Preliminary exploration of the association of Swain Langley (*SI*) and McCoy (*McC*) genotypes with CR1 copy number (mean number of CR1 molecules per erythrocyte), median CR1 cluster number per cell and mean cluster volume. **Panels A-C:** Relationship between CR1 copy number and (A) combined *SI* and *McC* genotype (1a = *SI1/SI1 McC^a/McC^a*, 2a = *SI2/SI2 McC^a/McC^a* and 2b = *SI2/SI2 McC^b/McC^b*), (B) *McC* genotype and (C) *SI* genotype. **Panels D-F:** Relationship between median number of CR1 clusters per cell and (D) combined *SI* and *McC* genotype, (E) *McC* genotype and (F) *SI* genotype. **Panels G-I:** Relationship between mean CR1 cluster volume per cell and (G) combined *SI* and *McC* genotype, (H) *McC* genotype and (I) *SI* genotype. Red bars indicate mean and standard deviation, with statistical testing by t test or ANOVA as indicated. Individuals with the *McC^b* genotype had higher CR1 copy numbers than *McC^a* individuals, with higher CR1 cluster numbers (although not statistically significant).

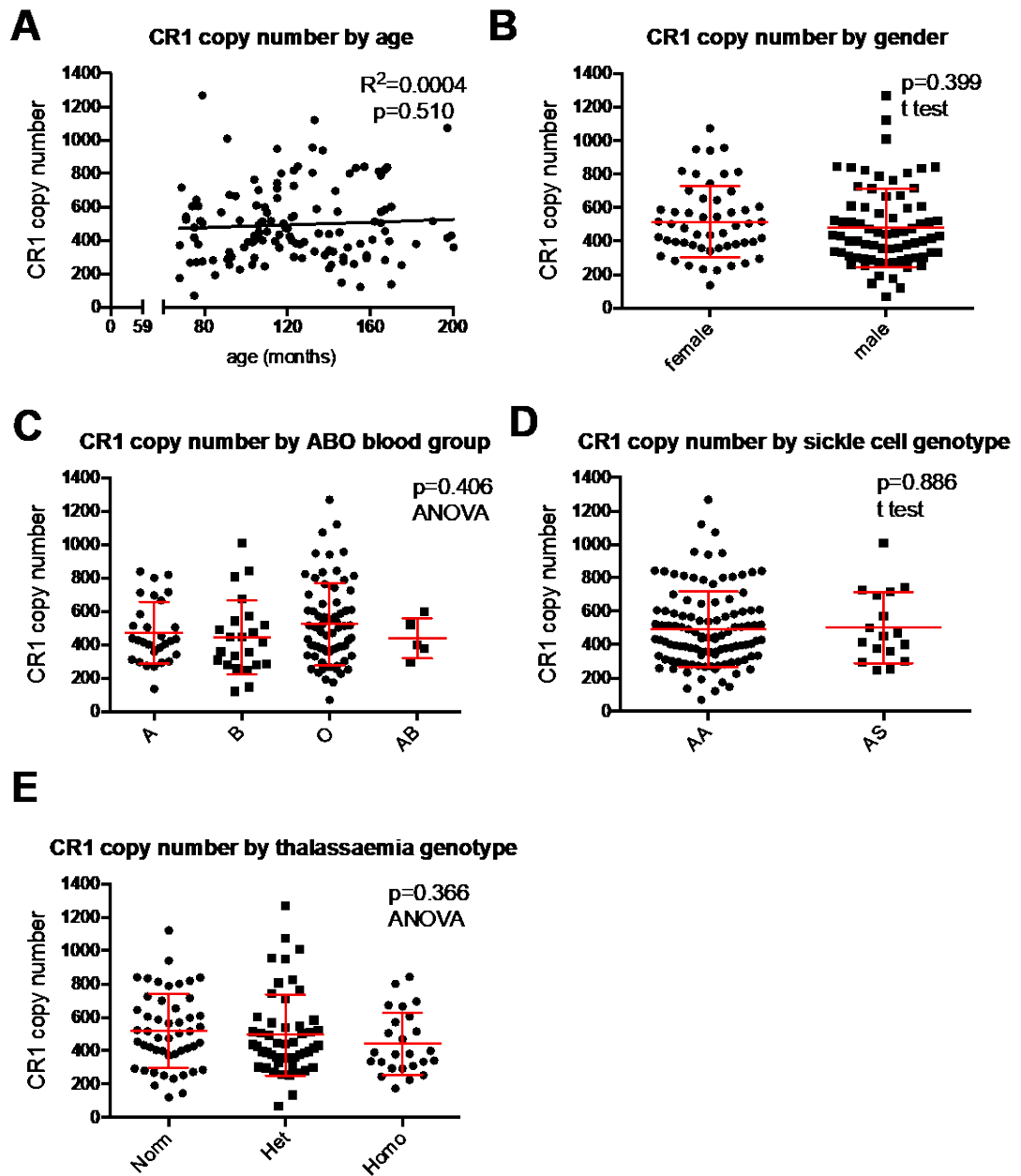


Figure 3-7. Preliminary exploration of the association of donor variables and erythrocyte CR1 copy number (mean number of CR1 molecules per cell).
 A) host age B) gender C) ABO blood group D) sickle cell genotype E) α^+ thalassaemia genotype (Norm, normal α globin; Het, heterozygote; Homo, homozygote). Red bars represent mean and standard deviation. Correlation was analysed by linear regression, and differences between means were analysed by one-way ANOVA or t test as shown above.

3.7.2 Increased CR1 cluster number in individuals with the *McC^b/McC^b* genotype.

As previously reported (Chevalier and Kazatchkine, 1989; Cosio et al., 1990; Glodek et al., 2010), the number of CR1 clusters per cell varied widely within each individual. Overall, the number of clusters per cell ranged from 0 to 43, with the maximum number of clusters per cell ranging from 15 to 43 amongst different individuals (Figure 3-8). The volume of CR1 clusters also varied within individuals, with the largest clusters being $>3\mu\text{m}^3$ (Figure 3-9).

Preliminary analysis of the relationship between Knops genotype and erythrocyte CR1 cluster number was conducted by ANOVA, with data summarised at the level of the individual donor (i.e. using a single data point per donor, representing the median cluster number for that donor). These data were suggestive of a higher cluster number in 2b individuals, driven by the *McC^b* genotype, although this was not statistically significant (Figure 3-6 D-F). Similar analysis by ANOVA of the relationship between Knops genotype and mean CR1 cluster volume revealed no significant associations (Figure 3-6 G-I). There were also no significant associations between CR1 cluster number (Figure 3-7) or cluster volume (Figure 3-10) and age, gender, ABO blood group, sickle cell genotype and α^+ thalassaemia genotype.

In agreement with previous findings (Cosio et al., 1990; Taylor et al., 1991), a strong positive linear correlation was observed between CR1 cluster number and CR1 copy number ($R^2 = 0.530$, $p < 0.001$, Figure 3-11 A), and a positive correlation was also observed between CR1 cluster volume and CR1 copy number ($R^2 = 0.398$, $p < 0.001$, Figure 3-11 B). Cluster number and cluster volume were also strongly positively correlated ($R^2 = 0.573$, $p < 0.001$, Figure 3-11 C). Because of the potential confounding effect of CR1 copy number on the relationship between Knops genotype and CR1 cluster number and volume, more detailed statistical analyses were carried out.

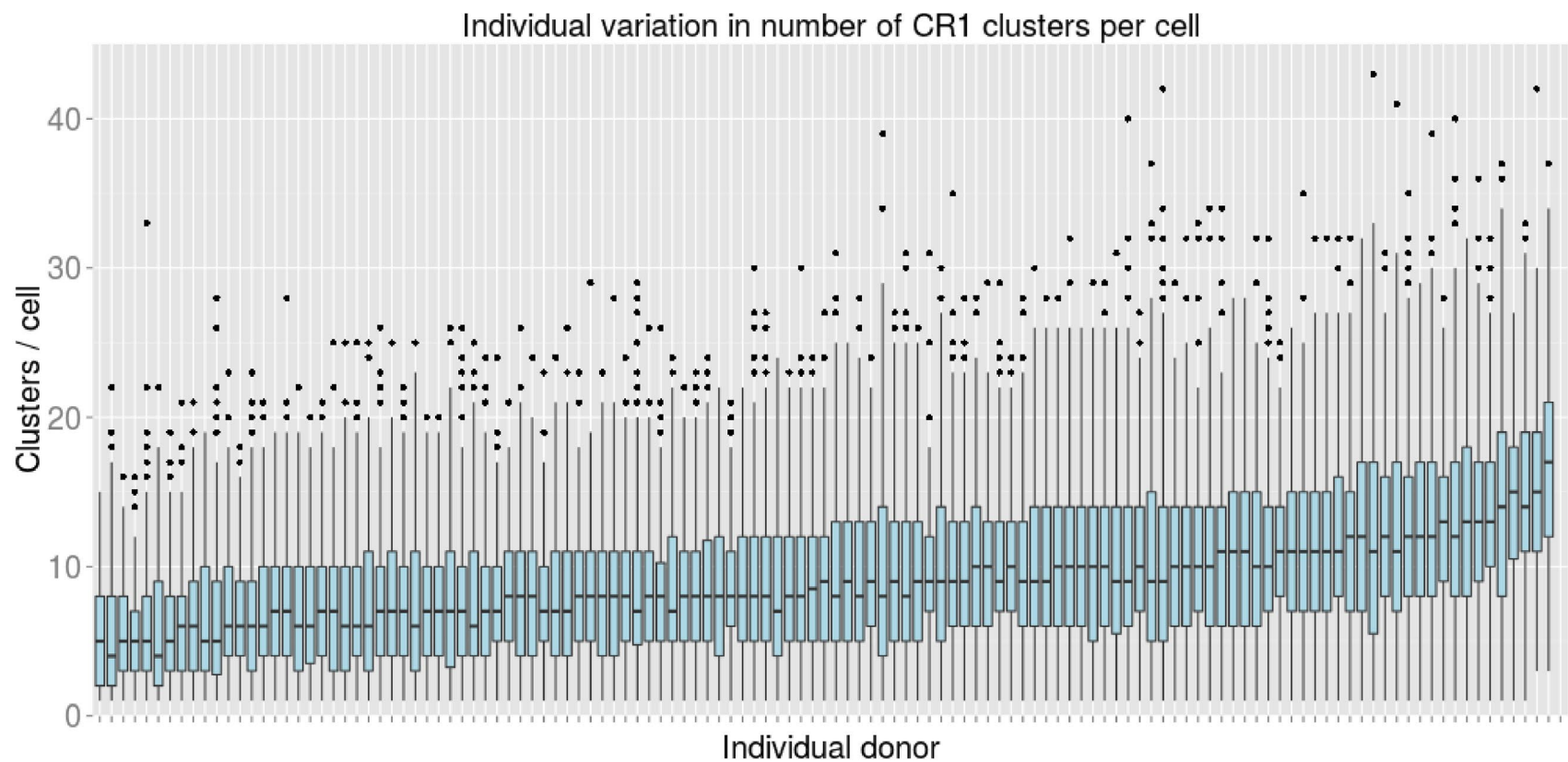


*Figure 3-8. Box plot to illustrate within individual variation in number of CR1 clusters per cell. Line = median, box = IQR, whiskers = data within 1.5 *IQR of lower/upper quartiles. Each box represents an individual donor, ordered by increasing CR1 copy number.*

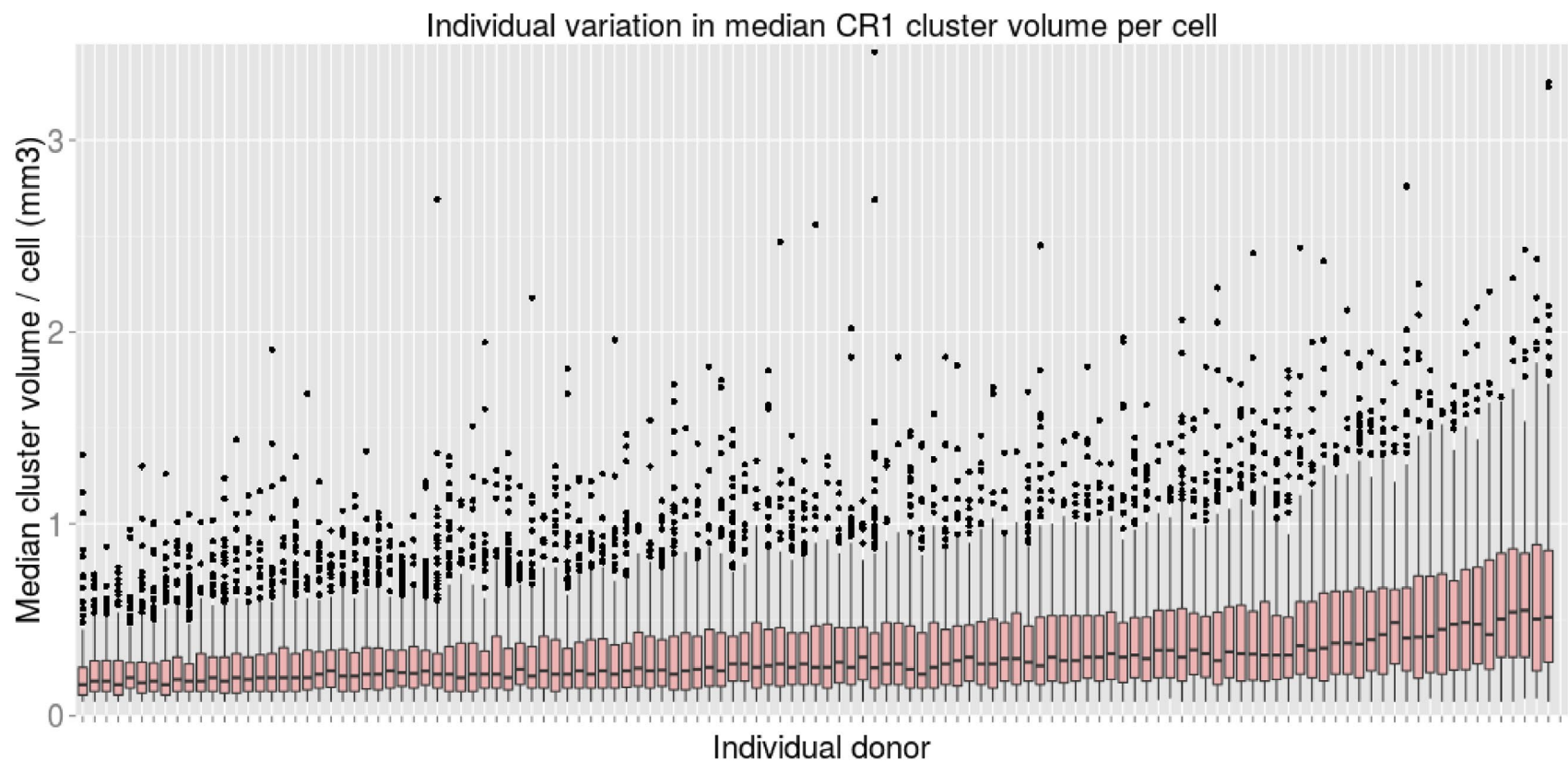


Figure 3-9. Box plot to illustrate within individual variation in median cluster volume per cell.
 Line = median, box = IQR, whiskers = data within 1.5 *IQR of lower/upper quartiles. Each box represents an individual donor, ordered by increasing CR1 copy number

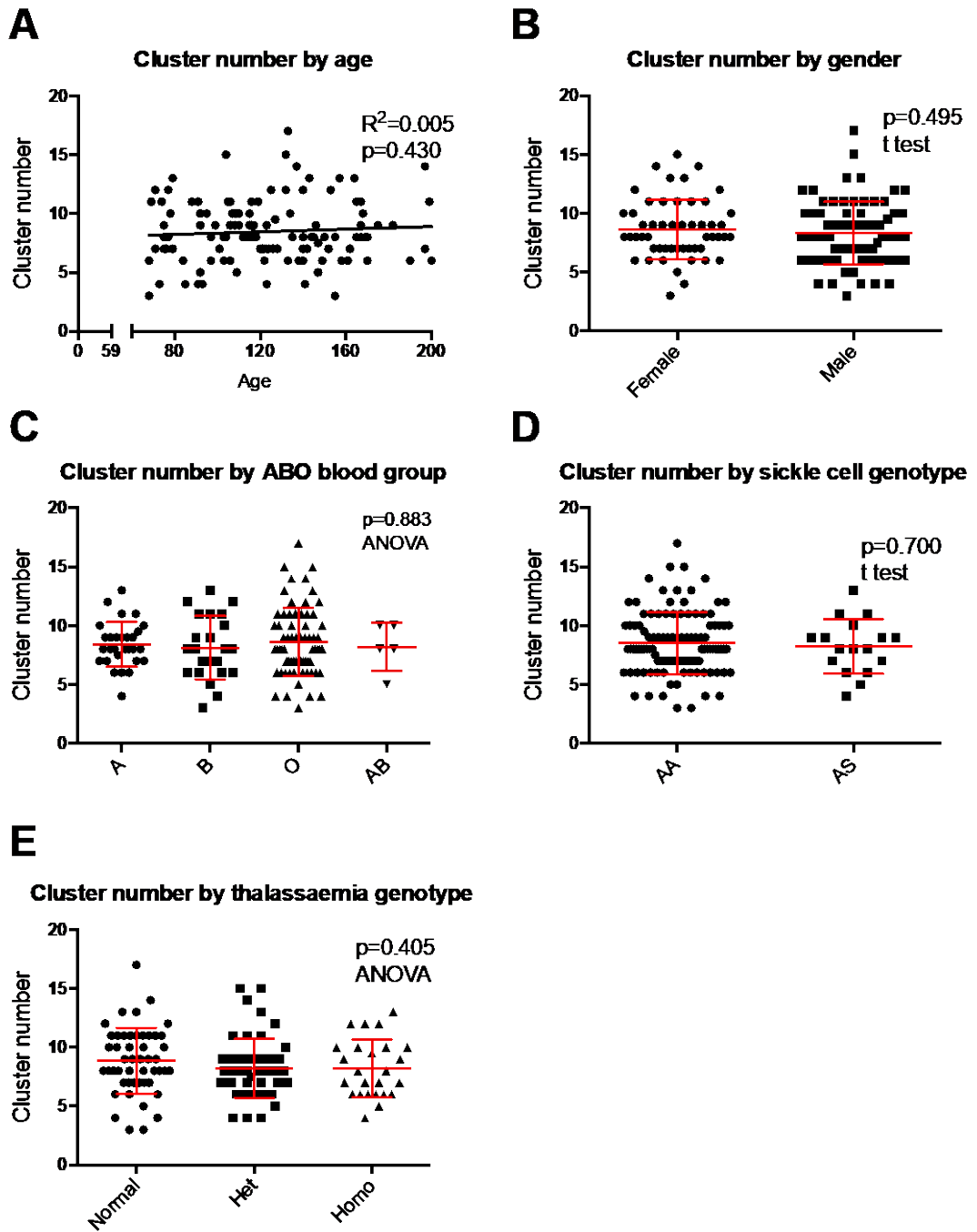


Figure 3-10. Preliminary exploration of the association of donor variables and mean erythrocyte cluster volume.

Red bars represent mean and standard deviation. **A)** host age **B)** gender **C)** ABO blood group **D)** sickle cell genotype **E)** α -thalassaemia genotype (Norm, normal α globin; Het, heterozygote; Homo, homozygote). Red bars represent mean and standard deviation. Correlation was analysed by linear regression, and differences between means were analysed by one-way ANOVA or t test as shown above.

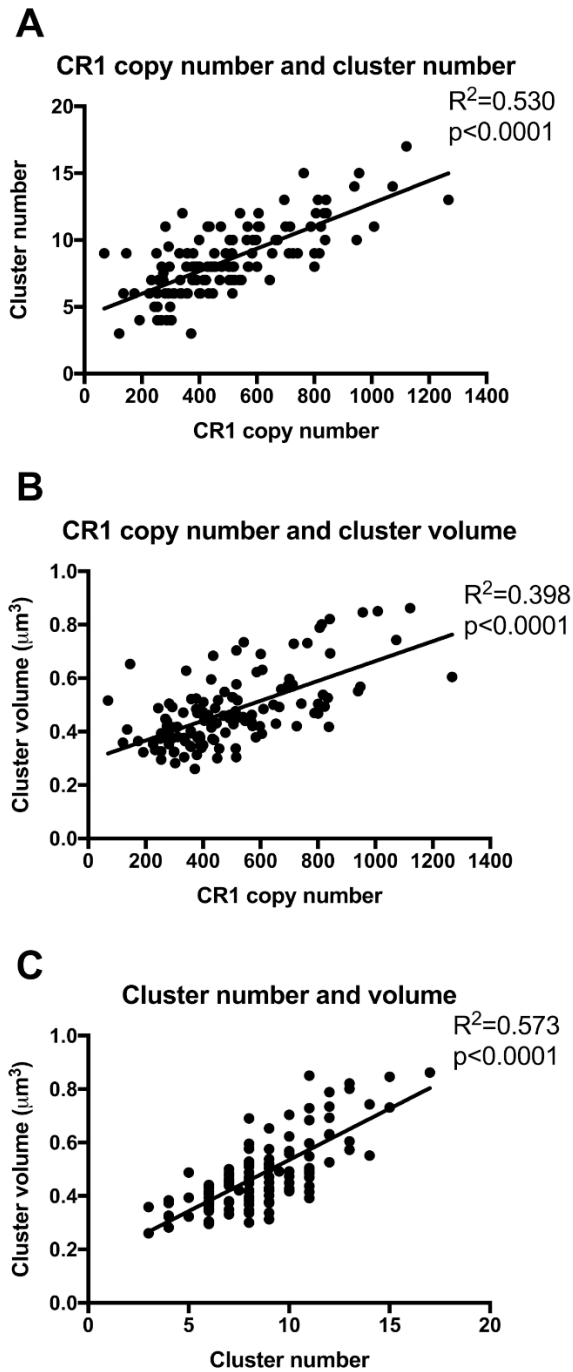


Figure 3-11. Positive correlation between CR1 copy number, cluster number and cluster volume. **A)** Scatter plot of median CR1 cluster number per cell by CR1 copy number (mean number of CR1 molecules per cell) with linear regression. Each dot represents an individual donor. **B)** Scatter plot of median CR1 cluster volume per cell by CR1 copy number with linear regression. Each dot represents an individual donor. **C)** Scatter plot of median CR1 cluster volume per cell by CR1 cluster number with linear regression. Each dot represents an individual donor. There were significant positive correlations between all three variables studied.

3.7.3 No evidence of an association between Knops genotype and CR1 cluster number after adjustment for CR1 copy number.

A hierarchical mixed effects Poisson regression analysis was constructed to include all available data at the level of the cell (using at least 200 data points per individual donor, representing the CR1 cluster number for each cell imaged) and to allow for adjustment for CR1 copy number. The analysis examined each donor variable (combined *Sl* and *McC* genotype, *Sl* genotype alone, *McC* genotype alone, gender, age, ABO blood group, α^+ thalassaemia genotype or sickle cell genotype) in turn. Each donor variable was specified as a fixed effect and donor identifier and date of assay were specified as random effects. The relationship between each donor variable and the number of CR1 clusters per cell was reviewed both before and after adjustment for CR1 copy number.

Prior to inclusion of CR1 copy number in the model, the 2b genotype was associated with a higher number of clusters per cell than the 1a genotype (multiplicative increase of 1.200 (95% CI 0.997-1.443, $p=0.053$, Table 3-2)). When broken down by component genotypes, this association was driven by the *McC* component rather than the *Sl* component, with the *McC^b/McC^b* genotype associated with a significantly higher number of clusters per cell than the *McC^a/McC^a* genotype (multiplicative increase = 1.216, 95% CI 1.027-1.439, $p=0.023$, Table 3-2). No significant associations were seen for gender, age, ABO blood group, α^+ thalassaemia genotype or sickle cell genotype.

The correlation between CR1 copy number and number of clusters per cell was strong, with each increase in CR1 copy number of 100 being associated with a multiplicative increase in CR1 cluster number of 1.084 ($p < 0.001$). Adjustment for CR1 copy number obscured any association between cluster number and *McC* genotype (Table 3-2). This suggests that the original association was likely to be driven by a difference in CR1 copy number, rather than any unique effect of the *McC* genotype itself.

Cluster number			Without adjustment for CR1 copy number			With adjustment for CR1 copy number		
Variable	Median	IQR	Rate Ratio	95% CI	p value	Rate Ratio	95% CI	p value
Combined <i>SI/McC</i> genotype [#]								
<i>1a</i>	8	7-9	Reference	NA	NA	Reference	NA	NA
<i>2a</i>	8	7-10	0.982	0.888-1.085	0.717	0.992	0.920-1.069	0.831
<i>2b</i>	9	9-11.5	1.200	0.997-1.443	0.053	1.043	0.906-1.201	0.557
Swain-Langley component alone								
<i>SI1/SI1</i>	8	7-9	Reference	NA	NA	Reference	NA	NA
<i>SI2/SI2</i>	8	7-10	1.000	0.904-1.106	0.998	0.997	0.925-1.073	0.926
McCoy component alone								
<i>McC^a/McC^a</i>	8	7-10	Reference	NA	NA	Reference	NA	NA
<i>McC^b/McC^b</i>	9	9-10.5	1.216	1.027-1.439	0.023	1.049	0.921-1.195	0.470
Gender								
Female	8	7-10	Reference	NA	NA	Reference	NA	NA
Male	8	6-10	0.970	0.891-1.056	0.488	1.014	0.952-1.081	0.669
ABO blood group								
O	8	7-10.25	Reference	NA	NA	Reference	NA	NA
A	8	7-9	1.030	0.926-1.146	0.587	1.044	0.966-1.129	0.277
B	8	6-10.5	0.970	0.864-1.089	0.604	1.019	0.936-1.109	0.669
AB	8	8-10	0.979	0.784-1.222	0.851	1.053	0.895-1.241	0.532
α +thalassaemia genotype								
$\alpha\alpha/\alpha\alpha$	9	7-11	Reference	NA	NA	Reference	NA	NA
$-\alpha/\alpha\alpha$	8	7-9	0.934	0.846-1.031	0.176	0.982	0.911-1.058	0.631
$-\alpha/-\alpha$	8	6-10	0.926	0.824-1.040	0.194	1.011	0.926-1.104	0.808
Sickle cell (HbS) genotype								
AA	8	7-10	Reference	NA	NA	Reference	NA	NA
AS	8	7-9	0.965	0.855-1.089	0.562	0.989	0.904-1.081	0.800
Age (years) Change in CR1 cluster number with each additional year of age			1.006	0.991-1.021	0.461	1.001	0.990-1.013	0.822
CR1 copy number Change in CR1 cluster number with each additional 100 CR1 copies per cell			NA	NA	NA	1.084	1.067-1.101	<0.001

Table 3-2. Effect of donor variables on cluster number from mixed effects Poisson regression.

The rate ratio is the multiplicative change from the reference group.

#*1a* = *SI1/SI1*, *McC^a/McC^a* genotype, *2a* = *SI2/SI2*, *McC^a/McC^a* genotype, *2b* = *SI2/SI2*, *McC^b/McC^b*.

IQR = inter-quartile range, CI = confidence interval by Wald. NA, not applicable.

3.7.4 No evidence of an association between Knops genotype and erythrocyte CR1 cluster volume after adjustment for CR1 copy number.

Similarly, a more detailed hierarchical mixed effects linear regression analysis was constructed to include all available data at the level of the individual clusters, and to allow for adjustment for CR1 copy number. Donor variables (combined *SI* and *McC* genotype, *SI* genotype alone, *McC* genotype alone, gender, age, ABO blood group, α^+ thalassaemia genotype or sickle cell genotype) were examined individually as fixed effects, while cell identifier and donor identifier were specified as random effects (Table 3-3). The relationship between each donor variable and CR1 cluster volume was reviewed both before and after adjustment for CR1 copy number.

No donor variables were found to have a significant association with cluster volume before adjustment for CR1 copy number (i.e. t values were all <1.96 or > -1.96). The correlation between CR1 copy number and cluster volume was extremely strong, with each increase in CR1 copy number of 100 being associated with an absolute increase in CR1 cluster volume of $0.039 \mu\text{m}^3$ (t value = 9.446, Table 3-3.

Bootstrapped p value <0.001). Adjustment for CR1 copy number had no impact on the non-significant relationships between cluster volume and combined *SI* and *McC* genotype, *SI* genotype alone, *McC* genotype alone, gender, age, α^+ thalassaemia genotype or sickle cell genotype (Table 3-3). However, in models adjusting for CR1 copy number, the B blood group was associated with an absolute increase in cluster volume of $0.057 \mu\text{m}^3$ when compared to the reference O blood group (t value = 2.305, Table 3-3. Bootstrapped p value = 0.028).

Variable	Mean cluster volume (μm^3)	SD	Without adjustment for CR1 copy number			With adjustment for CR1 copy number		
			Coefficient	Standard error	t value	Coefficient	Standard error	t value
Combined genotype [#]								
1a	0.468	0.146	Reference	NA	NA	Reference	NA	NA
2a	0.476	0.127	0.012	0.029	0.400	0.016	0.022	0.717
2b	0.502	0.160	0.035	0.054	0.658	-0.029	0.042	-0.708
SI component alone								
SI1/SI1	0.468	0.146	Reference	NA	NA	Reference	NA	NA
SI2/SI2	0.478	0.130	0.014	0.029	0.475	0.012	0.022	0.552
McC component alone								
McC ^a /McC ^a	0.474	0.131	Reference	NA	NA	Reference	NA	NA
McC ^b /McC ^b	0.502	0.160	0.027	0.049	0.545	-0.041	0.038	-1.08
Gender								
Female	0.486	0.126	Reference	NA	NA	Reference	NA	NA
Male	0.468	0.137	-0.022	0.024	-0.895	-0.011	0.019	-0.584
ABO blood group								
O	0.469	0.137	Reference	NA	NA	Reference	NA	NA
A	0.476	0.100	0.008	0.030	0.264	0.029	0.023	1.275
B	0.502	0.164	0.032	0.033	0.994	0.057	0.025	2.305
AB	0.451	0.083	-0.022	0.063	-0.355	0.012	0.047	0.262
α +thalassaemia genotype								
$\alpha\alpha/\alpha\alpha$	0.493	0.139	Reference	NA	NA	Reference	NA	NA
$-\alpha/\alpha\alpha$	0.475	0.136	-0.022	0.027	-0.805	-0.008	0.021	-0.401
$-\alpha/-\alpha$	0.444	0.109	-0.051	0.033	-1.54	-0.017	0.026	-0.654
Sickle cell (Hbs) genotype								
AA	0.472	0.133	Reference	NA	NA	Reference	NA	NA
AS	0.500	0.133	0.031	0.035	0.880	0.029	0.027	1.089
Age (years)	Change in cluster volume with each additional year of age		-0.002	0.004	-0.560	-0.005	0.003	-1.411
CR1 copy number	Change in cluster volume with each additional 100 CR1 copies per cell		NA	NA	NA	0.039	0.004	9.446

Table 3-3. Effect of donor variables on cluster volume from mixed effects linear regression.

The coefficient is the absolute change from the reference group.

#1a = SI1/SI1, McC^a/McC^a genotype, 2a = SI2/SI2, McC^a/McC^a genotype, 2b = SI2/SI2, McC^b/McC^b.
SD, standard deviation. NA, not applicable.

3.8 Discussion

In agreement with existing literature, we report that both the number of CR1 clusters per erythrocyte and CR1 cluster volume are highly correlated with an individual's erythrocyte CR1 copy number (Cosio et al., 1990; Paccaud et al., 1988; Taylor et al., 1991). The strength of association between CR1 copy number and cluster number was such that the inclusion of CR1 copy number in the statistical model obscured any other associations. However, on review of individual explanatory variables (without CR1 copy number in the model), the McC^b/McC^b genotype was associated with significantly higher cluster number than the McC^a/McC^a genotype. Individuals of the McC^b/McC^b genotype were found to have a significantly higher CR1 copy number than McC^a/McC^a , which is in agreement with a larger analysis of Kenyan children (Opi et al., 2016). As such, it is likely that the association of the McC^b/McC^b genotype with increased CR1 cluster number was due to the higher CR1 copy numbers in McC^b/McC^b individuals, rather than being a distinct biological effect of the variant itself. Exactly how the McC^b polymorphism influences erythrocyte CR1 copy number is unknown, but could be due to resistance to cleavage by tryptic proteases resulting from the lysine to glutamic acid (K1590E) mutation, as discussed previously (Opi et al., 2016).

In contrast to existing literature (Opi et al., 2016; Waitumbi et al., 2004), we found no evidence of an association between age and CR1 copy number. However, the previous studies included children between birth and 13 years (Opi et al., 2016) or birth and 32 years (Waitumbi et al., 2004), with the major changes occurring during the first four years of life. The narrower age range of our study (5.7 years – 12.7 years) may explain why no association between age and CR1 copy number was detected. We also found no significant effect of α^+ thalassaemia genotype on CR1 copy number, unlike other studies which showed lower CR1 copy number in α^+ thalassaemia homozygotes compared to normal individuals in Papua New Guinea (Cockburn et al., 2004) and Kenya (Opi et al., 2016). Whilst we also observed a lower CR1 copy number in α^+ thalassaemia homozygote individuals, the small

sample size in our study may have prevented this from reaching statistical significance.

One unexpected finding from this study was that blood group B was associated with significantly larger CR1 clusters than the reference blood group O. There is no known link between ABO blood group and CR1 function, and further work will be required to determine if this is a reproducible finding, and if so, to determine its biological significance.

Owing to the high level of within and between donor variation, this was a challenging assay to develop and interpret. The sample size of this study was small, in particular for the 2b genotype, which is a limitation of this study. However, given the logistics of sampling (see methods), it was not possible to recruit more individuals prospectively. Another consideration is that although all children positive for malaria on a thick film were excluded, information on other infective or inflammatory conditions that might influence CR1 copy number was not available. Therefore, it is possible that the CR1 copy number of some children may have been transiently altered by concurrent conditions. However, all children were sampled in the community and were not inpatients in health centres, therefore were in broadly good health.

The use of field samples also conferred other limitations on our study. When carrying out the confocal imaging in Edinburgh, we used conservative imaging settings to avoid photo-bleaching the slides during image acquisition. This was done in case repeat imaging was needed, as the slides themselves could not be replaced. Therefore, it is possible that we may have under-sampled the immunofluorescent slides, resulting in missing very small clusters. As temperature has been reported to affect cluster size in some studies (Chen et al., 2007), the use of physiological temperature during the assay (rather than 4°C as used here) may have increased the relevance of the findings, as may the use of a physiological ligand to induce clustering (e.g. C3b covered beads or immune complexes). Furthermore, the J3D3 monoclonal antibody used here recognises multiple epitopes in LHRs A, B and C

(Nickells et al., 1998), and results could therefore be influenced by CR1 size polymorphisms (allotype), which was not accounted for here. An antibody with a single epitope on CR1 that would not be affected by CR1 allotype (Chen et al., 2007) could be used in future studies. Other technical aspects of the assay may have affected the results shown here. For example, the mounting medium used after staining and preparing the thin blood films can cause lysis of the erythrocytes, potentially bringing the top and bottom membranes closer together. This could cause overlap of some clusters making them appear fewer or larger than in vivo. Despite these limitations, our methods were consistent throughout all samples, thus allowing for direct comparison between the different genotypes.

The functional effects of the *Sl* and *McC* polymorphisms remain elusive. Laboratory evidence suggests that *Sl2* may affect rosetting (the binding of *Plasmodium falciparum* IEs to uninfected erythrocytes) (Rowe et al., 1997), a parasite virulence factor associated with severe malaria in African children (Rowe et al., 1995). Rosetting occurs when *P. falciparum* Erythrocyte Membrane Protein 1 (PfEMP1) expressed on the surface of IEs binds to uninfected erythrocyte receptors, and is thought to involve site 2 on CR1 (the C3b binding site) in LHR-B and LHR-C (Rowe et al., 2000). Erythrocytes from *Sl2/Sl2* donors rosette less well than erythrocytes from *Sl1/Sl1* donors when PfEMP1 is expressed heterologously on the surface of COS-7 cells (Rowe et al., 1997). However, a study using short recombinant proteins of the *Sl* and *McC* variants found no difference in their abilities to disrupt rosettes (Tetteh-Quarcoo et al., 2012). Further investigation of the effects of the Knops polymorphisms on *P. falciparum* rosetting is required.

In addition to its role in rosetting, CR1 has also been identified as a sialic acid-independent invasion receptor for *P. falciparum* (Spadafora et al., 2010), via the reticulocyte-binding-like homolog 4 (PfRh4) (Tham et al., 2010). The binding of PfRh4 has been mapped to site 1 in LHR-A (Lim et al., 2015; Park et al., 2013; Tham et al., 2011). Immunofluorescent staining of freshly released invasive merozoites showed CR1 on erythrocytes to be more intense around the merozoite, referred to

by the authors as “capping,” suggesting CR1 clustering may have a role in invasion (Spadafora et al., 2010). However, the previously cited study using short recombinant proteins of the *SI* and *McC* variants also found no difference in their abilities to inhibit erythrocyte invasion by *P. falciparum* (Tetteh-Quarcoo et al., 2012).

Interestingly, the binding site for mannose binding lectin (MBL) has been mapped to CCP 24-25, in close proximity to the *SI* and *McC* polymorphisms (Jacquet et al., 2013). MBL may influence malaria in Ghanaian children, with alleles responsible for low levels of MBL associated with increased parasite load, lower blood glucose levels and increased odds of severe malarial anaemia (Garred et al., 2003; Holmberg et al., 2008). It has also been suggested that MBL may opsonize *P. falciparum* IEs (Garred et al., 2003) or merozoites (Korir et al., 2014). However, whether the *SI* or *McC* polymorphisms have functional effects on MBL interactions with CR1 has not yet been explored.

In summary, after accounting for the effect of CR1 copy number, there was no significant association between *SI* or *McC* genotypes (separately or in combination) and erythrocyte CR1 cluster number or cluster volume in Kenyan children. The effects of the *SI* and *McC* Knops blood group polymorphisms on CR1 function remain unknown.

3.9 Additional discussion to this manuscript

Whilst the investigation of whether *SI* and *McC* polymorphisms affected CR1 clustering appears to be a simple question, as discussed above, this assay was more challenging than anticipated. In addition, whilst no association was found between the *SI* and *McC* polymorphisms and CR1 cluster number or volume, it is possible that such differences do exist, but that this assay was insufficiently sensitive to detect them. A previous report used scanning near-field optical microscopy to quantify CR1 cluster number on erythrocyte ghosts which reported a far higher number of clusters per erythrocyte (mean = 92 clusters per erythrocyte, range = 61–124, (Lapin et al., 2012)) than in my investigation (mean = 9 clusters per erythrocyte, range = 0–43). The near-field optical microscopy approach also identified many more clusters per erythrocyte than previous studies on CR1 clustering (8–20 clusters per erythrocyte reported in two donors by electron microscopy (Chevalier and Kazatchkine, 1989), 8 ± 4 and 15 ± 6 clusters per erythrocyte (low and high CR1 donors respectively) by fluorescence microscopy (Ghiran et al., 2008) and between 1 - 40 clusters per erythrocyte in three donors by fluorescence microscopy (Paccaud et al., 1988)). As such, it is possible that near-field optical microscopy might have identified more clusters than using my methodology. However near-field optical microscopy required wet preparations of erythrocytes labelled with α -CR1 monoclonal antibodies (which would have prohibited shipping of the samples out of Kenya) and an investigator-built scanning near-field optical microscope, neither of which were practical for field work studies. In addition, the report only describes the CR1 clusters on erythrocytes from a single donor and number of erythrocytes imaged is not described. Thus, while using the near-field optical microscopy approach may have identified more clusters in my study, this may have introduced other problems with validity, reproducibility and artefact.

Another possibility is that the *SI* or *McC* polymorphisms might affect the distribution of the CR1 molecules in the resting (i.e. un-clustered) form rather than bound to a ligand. A previous study reported diffuse small CR1 clusters on erythrocytes fixed

with dimethylsuberimidate in a sodium borate buffer and 0.05% glutaraldehyde and fewer larger clusters after incubation with an α -CR1 monoclonal antibody, suggesting that CR1 is un-clustered in its resting state on the erythrocyte membrane (Glodek et al., 2010). Although this was explored during assay development, attempts to recreate this fixation method were unsuccessful and the fixed timing of the Immunology Cohort annual venepuncture precluded using this approach.

A further possibility is that *S//McC* might affect CR1 clustering, but on cells other than erythrocytes. CR1 also clusters on the membranes of polymorphonuclear leucocytes (PMNs) but to a lesser extent than on erythrocytes (Paccaud et al., 1990). In addition, a separate study describes CR1 clustering on neutrophils using electron microscopy but also the internalisation of the receptor on stimulation with formyl methionyl leucyl phenylalanine (fMLP) (Carpentier et al., 1991). In addition, PMNs are able to quickly upregulate the amount of CR1 on their membranes in response to a number of stimuli (including temperature change and local C3b concentration) (Berger et al., 1989; Fearon and Collins, 1983; Porteu et al., 1987). These issues potentially introduce a large number of confounding variables into the study of CR1 clustering on PMNs and it was felt this question could not be addressed satisfactorily using a field study. As such, erythrocytes with stable levels of CR1 were investigated in the first instance.

In summary, this chapter found no evidence to support the hypothesis that the *S/* or *McC^b* polymorphisms influenced CR1 cluster number or volume on erythrocytes. As such, this seems unlikely to be the functional mechanism behind the polymorphisms' association with CM. For the next line of enquiry, the focus of investigation was turned back to the specificity of the polymorphisms' relationship with CM by considering whether human brain endothelial cells might express CR1.

4 Do human brain endothelial cells express CR1?

4.1 Abstract

Expression of complement receptor 1 (CR1) by endothelial cells has been reported, but there are no reports on brain endothelium. It was hypothesised that the association between the *S12* and *McC^b* polymorphisms in CR1 and cerebral malaria could be due to human brain endothelial cells (HBECs) expressing CR1.

The immortalised cell line HBEC-5i was investigated for expression of CR1 using immunofluorescence assays (IFA), flow cytometry, western blotting, functional C3b degradation assays, mass spectrometry, immunoprecipitation and siRNA knockdown experiments.

A pool of α -CR1 monoclonal antibodies weakly stained unpermeabilised HBEC-5i cells. Staining was increased on permeabilisation of the cells, whereby a large intracellular pool of antigen was recognised. Western blotting of HBEC-5i lysate revealed a band recognised by the pool of α -CR1 monoclonal antibodies of a similar molecular weight to CR1. However, when the α -CR1 monoclonal antibodies were tested individually, only E11 recognised an HBEC-5i protein on western blot and IFA.

HBEC-5i lysate was resolved by gel electrophoresis and the band of interest was submitted for mass spectrometry, but no CR1 was detected. HBEC-5i + factor I could degrade C3b to C3dg, but this was not inhibited by the α -CR1 monoclonal 3D9, suggesting a cofactor other than CR1. Immunoprecipitation with E11 failed to produce CR1 from an HBEC-5i lysate. CR1 siRNA knockdown did not alter E11 staining of HBEC-5i, implying E11 is not specific for CR1. The E11-staining was found to co-localize to the Golgi apparatus in HBEC-5i.

In conclusion, these data indicate that HBEC-5i cells do not express CR1. In addition, the data suggest that the widely used α -CR1 monoclonal E11 is not entirely specific for CR1, as it cross-reacts with a protein present in the Golgi apparatus of HBEC-5i cells.

4.2 Introduction

4.2.1 The blood-brain barrier

In the cerebral vasculature, the blood-brain barrier (BBB) is predominantly formed by brain endothelial cells and provides a highly selective semi-permeable membrane which divides the circulating blood from brain tissue. Cerebral microvessels are continuous and nonfenestrated allowing the movement of molecules, ions, and cells between the blood and the CNS to be tightly regulated (reviewed in (Daneman, 2012)). The endothelial cells are incompletely surrounded by a layer of vascular smooth muscle cells and pericytes which are involved in angiogenesis, vascular tone and remodelling as well as the function of the BBB (Armulik et al., 2011; Winkler et al., 2011). These, in turn, are enclosed by a basal lamina consisting of collagens, laminins and heparan sulfate proteoglycans (Tilling et al., 2002) which provides a structural matrix for the cells (Daneman, 2012). Astrocyte (glial cell) endfeet then encircle the blood vessels and can regulate the transport properties of the BBB (Janzer and Raff, 1987). Immune cells interacting with the BBB include perivascular macrophages and microglia which are involved in CNS innate immunity, antigen presentation and regulation of immune cell passage across the BBB (Hudson et al., 2005; Streit et al., 2005). Together with neurons, these cells comprise the neurovascular unit (Figure 4-1).

Endothelial cells in the CNS differ from those in non-neuronal tissues as they are highly polarised and linked by tight junctions which regulate the paracellular movement of molecules and ions (reviewed by (Daneman, 2012)). Transcellular movement of molecules and ions is limited by the lack of fenestra and low rates of pinocytosis of the brain endothelial cells (Brightman and Reese, 1969; Reese and Karnovsky, 1967). Together, these mechanisms impede the transfer of large and hydrophilic molecules.

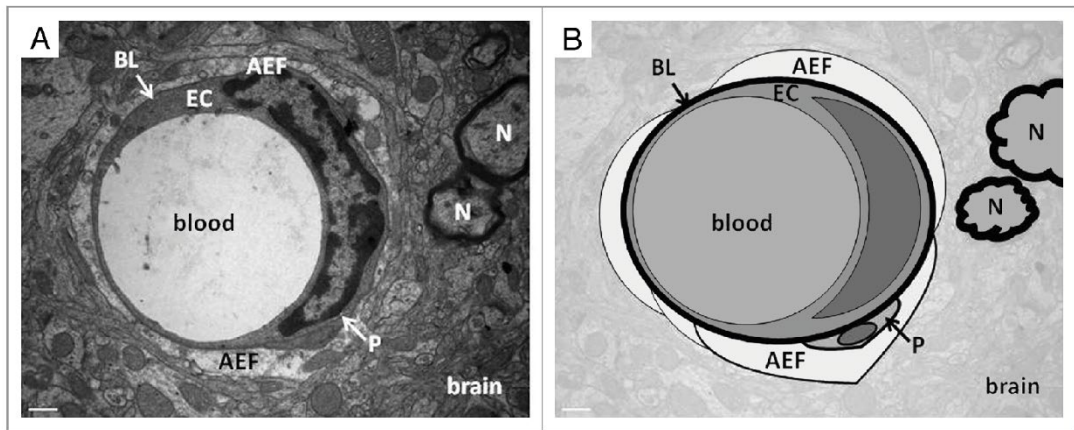


Figure 4-1. Example of a neurovascular unit in a rat brain.

Panel A - Electron microscopy. Panel B – schematic representation.

The relationship between the endothelial cell, basal lamina and astrocyte can be seen. EC = endothelial cell, BL = basal lamina, AEF = astrocyte end-feet, N = neurons, P = pericyte.

Scale bar = 0.5 μ m. (Figure from (Miller et al., 2012).

A critical function of any endothelium is to provide an antithrombotic surface to prevent blood clots. Heparan sulfate in the basal lamina together with the expression of thrombomodulin and production of tissue-type plasminogen activator are key for thrombostasis (Bernfield et al., 1999; Esmon, 1989; Levin et al., 1989). In addition, the endothelium is key in the regulation of cerebral microvascular tone through the release of vasodilators (including nitric oxide and prostaglandin PGI₂) and vasoconstrictors (including endothelin-1 and platelet activating factor (Cines et al., 1998; Palmer et al., 1987)).

4.2.2 Complement and the endothelium

The endothelium plays a dynamic role in the equilibrium between complement activation and regulation. Constant exposure to circulating complement components leaves the endothelium at risk of complement activation. To minimise this, endothelial cells are able to locally produce many of the regulators of complement. Resting HUVECS are reported to express soluble complement regulators; C1-inhibitor, factor H and factor I (Brooimans et al., 1990; Gulati et al., 1993; Julen et al., 1992) in addition to the membrane bound regulators; decay-

accelerating factor (CD55), membrane inhibitor of reactive lysis (CD59) and membrane cofactor protein (CD46) (Collard et al., 1997; Hamilton et al., 1990).

Damaged endothelium can activate complement, for example endothelial cells which have undergone hypoxia-reoxygenation can activate complement via the LP (Collard et al., 2000, 2001). Apoptotic endothelial cells can also activate the complement system via the CP, either through the globular heads of C1q recognising surface blebs on these apoptotic cells or by the exposure of phosphatidylserine on their surface (Navratil et al., 2001). The effects on the endothelium of activation by C1q, C5a and MAC culminate in the increased expression of endothelial adhesion molecules (including ICAM-1, vWF and P-selectin (Albrecht et al., 2004; Foreman et al., 1994)), increased production of cytokines and chemokines (including IL-1, IL-6 and TNF- α (Kilgore et al., 1996, 1997), as well as an increase in PMN adhesion to endothelial cells (Foreman et al., 1994), leucocyte extravasation (Casarsa et al., 2003; Dobrina et al., 2002) and the creation of a pro-coagulopathic state (reviewed in (Roumenina et al., 2016; Wiegner et al., 2016)).

Endothelial cells themselves are also sources of complement components.

Quiescent HUVECs have been reported to produce the components C1r, C1s, C2, C3, C5, C6, C7, C8 and C9 (Gulati et al., 1993; Johnson and Hetland, 1991; Langeeggen et al., 2000, 2001; Warren et al., 1987), with production being upregulated by pro-inflammatory cytokines (Berge et al., 1996; Brooimans et al., 1990; Dauchel et al., 1990; Langeeggen et al., 2000).

4.2.2.1 Complement and the human brain endothelium

Most of the above evidence derives from HUVECs, which are cells from medium sized umbilical vessels. As such, parallels cannot always be drawn with microvascular endothelium, particularly brain microvascular endothelium. Such specific studies are lacking with information being particularly scarce regarding HBEC complement receptors and membrane regulatory proteins. However, cultured human brain endothelial cells have been reported to produce factor H, C1-inhibitor, and C4 in the resting state with factor B being produced by stimulation with

interferon γ (Vastag et al., 1998). A separate study reported the synthesis of factor H, factor B and C4 synthesis by cultured human brain endothelial cells, increasing in response to TNF- α and IL-1 α stimulation (Nagy et al., 1996). A further study examined complement mRNA expression in primary human brain endothelial cells for the CP and reported the expression of mRNAs for C1qB, C1r, C1s, C2, C3, C4, C5, C7, C8 γ and C9 (Klegeris et al., 2000).

Human brain endothelial cells have also been reported to express the complement regulatory proteins CD55 (Visser et al., 2002), CD46 (Andres et al., 2003) and CD59 (Vedeler et al., 1994), suggesting that these proteins are important in protecting the brain endothelium from complement attack. Taken together, these studies present the brain endothelium as a dynamic player in local CP and AP activation and support a role for HBECs as a significant source of complement proteins and regulatory proteins.

4.2.3 CR1 expression on endothelial cells

A table summarising the evidence for CR1 expression on endothelial cells is presented below (Table 4-1). CR1 expression has been reported by hypoxic HUVECs, with expression determined by ELISA, western blotting of HUVEC lysates and RT-PCR for human CR1 (Collard et al., 1999). The same study reported hypoxic HUVECs were able to bind immune complexes, which was inhibited by the addition of sCR1. Confocal microscopy of the cells found the majority of the CR1 was intracellular and colocalised with von Willebrand factor (vWF). Finally, the authors used a western blot-based method to illustrate that CR1 on HUVECs was functional and able to cleave C3b to C3dg (method detailed in 4.4.14). Human bone marrow microvascular endothelial cells have also been reported to express CR1 when exposed to shear stress and tobacco smoke extract (Yin et al., 2008).

After these reports of CR1 on activated endothelium, expression of CR1 on unstimulated HUVECs was described (Langeeggen et al., 2002). In contrast to the predominantly intracellular expression reported by Collard et al., Langeeggen et al. reported CR1 expression on the surface of HUVECs based on flow cytometry

experiments which was supplemented by RT-PCR for human CR1. The authors repeated their experiments after stimulation of the cells with TNF α , lipopolysaccharide (LPS) and C5a, but in contrast to earlier studies, found no increase in CR1 expression. The same group later reported that HUVECs were able to uptake opsonised zymogen particles and postulated that this may be through CR1, but evidence presented was not definitive (Langeeggen et al., 2003). A recent investigation into HUVECs and microfilariae reported surface CR1 expression determined by flow cytometry which was not altered by stimulation with IFN- γ (Schroeder et al., 2017).

However, multiple studies have been unable to demonstrate the presence of CR1 on HUVECs. Tsuji *et al.* detected no CR1 expression by flow cytometry on either quiescent or apoptotic HUVECs (Tsuji et al., 1994). Similarly, other groups could not detect CR1 by flow cytometry on quiescent HUVECs (Oroszlán et al., 2007; Roumenina et al., 2009) or on LPS/TNF α stimulation (Oroszlán et al., 2007).

No studies to date have closely investigated the presence of CR1 on HBECs. The supplementary information of one paper suggested that α -CR1 antibodies (E11, J3D3, H-300 and rabbit polyclonal α -CR1 antibodies) might recognise brain vessel endothelial cells on immunohistochemical staining of cortical and hippocampal sections (Fonseca et al., 2016). However, the paper presented no data to support this and also included the caveat these antibodies may have been recognising RBCs within the vasculature instead.

CR1 is a well-defined host receptor on erythrocytes for *P. falciparum*, both for rosetting via the N-terminal domain of PfEMP1 (DBL α) and as the host receptor for the sialic acid-independent invasion via the ligand PfRh4 (Cockburn et al., 2004; Rowe et al., 1997, 2000; Spadafora et al., 2010; Tham et al., 2010) (see sections 1.7.1 and 1.7.2). However, there have been no reports of *P. falciparum* interacting directly with CR1 on HBEC.

Study (date)	Cells/tissue studied	Methods used	α -CR1 antibodies used	CR1 detected?	Comments
Tsuji et al. (1994)	HUVECs	FC	31R	No (live or apoptotic HUVECs)	No positive control
Collard et al. (1999)	HUVECs	ELISA, IFA, WB, RT-PCR, FISH C3b breakdown assay (with factor I) IC binding assay	Rabbit polyclonal + 3C6.D11 (ELISA) YZ-1 (IFA + WB)	Yes (hypoxic HUVECs and after stimulation with LPS and TNF- α)	CR1 predominantly intracellular Inappropriate isotype controls used for ELISA No isotype control used for IFA No negative control used for WB
Langeeggen et al (2002)	HUVECs	FC WB RT-PCR	E11	Yes (unstimulated HUVECs, no change with LPS/ C5a/TNF- α stimulation)	CR1 predominantly extracellular Data from WB described but not shown
Oroszlán et al. (2007)	HUVECs	FC	Rabbit polyclonal (produced in the Laboratory of Nephrology, Leiden, The Netherlands)	No (unstimulated or stimulated with LPS or TNF- α)	No positive control
Yin et al. (2008)	HBMMVECs	ELISA	E11	Yes (HBMVECs stimulated with tobacco smoke and shear stress)	No negative or positive controls
Roumenina et al. (2009)	HUVECs	FC	E11	No (unstimulated HUVECs)	Data described but not shown
Schroeder et al. (2017)	HUVECs	FC	3D9	Yes (no change with IFN- γ)	No negative or positive controls used

Table 4-1. Summary of published data investigating CR1 expression by human endothelial cells.

HUVECs= Human umbilical vein endothelial cells, HBMMVECs = human bone marrow microvascular endothelial cells, FC= flow cytometry, ELISA = enzyme-linked immunosorbent assay, IFA – immunofluorescence assay, WB = western blotting, RT-PCR = reverse transcription polymerase chain reaction, FISH = fluorescent in-situ hybridisation

4.3 Aims

As human brain endothelial cells have been reported to express both complement components and complement regulatory proteins (see 4.2.2.1), I postulated that human brain endothelial cells might also be able to produce CR1. If true, IEs might therefore use CR1 as a cytoadherence receptor via PfEMP1 on their surfaces, contributing to sequestration of IEs in the brain. Alternatively, if HBECs expressed CR1, this might modulate local complement activation in the cerebral microenvironment and control a potentially damaging complement response to *P. falciparum*. In addition, if CR1 was present on HBECs, it might bind malarial immune complexes limiting their ability to activate the cerebral endothelium. Finally, if CR1 was present on HBECs, this could explain why the protective association with *SL2/SL2* is specific to cerebral malaria. In this chapter, I aim to establish whether HBECs can express CR1 protein using antibody-based approaches.

4.4 Methods

4.4.1 Antibodies used

4.4.1.1 α -CR1 antibodies

CR1 is a large and complex protein, thus α -CR1 antibodies have various epitopes. Table 4-2 and Figure 4-2 summarise the α -CR1 antibodies used in these studies.

4.4.1.2 Other antibodies and cellular markers

Antibodies used for isotype controls, characterisation of cell lines, colocalisation experiments and detection of complement components are summarised in Table 4-3. In addition, low density lipoprotein acetylated Dil complex (Dil-AcLDL, Thermo Fisher Scientific, L3484) which is taken up by endocytosis by endothelial cells was used as a cellular marker (Voyta et al., 1984). Secondary antibodies used in these experiments are detailed in Table 4-4 and were made up to contain 1 μ g/ml of the DNA stain DAPI (4,6-diamidino-2-phenylindole, Molekula, M70277046) to visualise cell nuclei.

Antibody	Host	Clonality	Class/subclass	Source (Cat #)	Probable CR1 CCP epitope(s)	Comment
J3D3	Mouse	Monoclonal	IgG1	GeneTex (44217)	5-7, 12-14, 19-21 [§]	These antibodies make up the “commercial pool”
To5	Mouse	Monoclonal	IgG1	Santa Cruz (20055)	5-7, 12-14, 19-21 [§]	
E11	Mouse	Monoclonal	IgG1	Abcam (76520)	5-7, 12-14, 19-21, 26-27 [§]	
HB8592	Mouse	Monoclonal	IgG1	Gift – Ron Taylor	5-7, 12-14, 19-21, 26-27 [§]	These antibodies added to the “commercial pool” → “extended pool”
9H3	Mouse	Monoclonal	IgG1	Gift – Ron Taylor	5-7, 12-14, 19-21 [§]	
57F	Mouse	Monoclonal	IgG1	Gift – Ron Taylor	8-10, 15-17 [*]	
YZ-1	Mouse	Monoclonal	IgG1	Gift - Ionita Ghiran	5-7, 12-14, 19-21 [§]	
Ber-Mac-DRC	Mouse	Monoclonal	IgG1	Santa Cruz (19662)	5-7, 12-14, 19-21 [§]	
3D9	Mouse	Monoclonal	IgG1	Gift – Ron Taylor	3, 10,17 [§]	
1B4	Mouse	Monoclonal	IgG1	Gift – Ron Taylor	3, 10,17 [§]	
J3B11	Mouse	Monoclonal	IgG1	Gift – Jacques Cohen	8,15 [§]	
EPR6602	Rabbit	Monoclonal	IgG	Abcam (126737)	Amino acid residues at C terminus [¥]	
H300	Rabbit	Polyclonal	IgG	Santa Cruz (20924)	Amino acids 1740-2039 at C terminus [¥]	
Rabbit polyclonal	Rabbit	Polyclonal	IgG	Gift - John Atkinson	“Rabbits immunised with purified sCR1” [†]	

Table 4-2. Summary of α -CR1 antibodies used in this chapter.

Affiliations of collaborators: **Prof Jacques Cohen** - Hospital Robert Debré, Reims, France, **Prof Ron Taylor** - University of Virginia, USA, **Prof Ionita Ghiran** - Beth Israel Deaconess Medical Center, USA, **Prof John Atkinson** - Washington University, USA. References for antibody epitopes; [§](Nickells et al. 1998), ^{*}(Iida et al., 1982)

[¥]information provided by supplier, [†](Makrides et al., 1992).

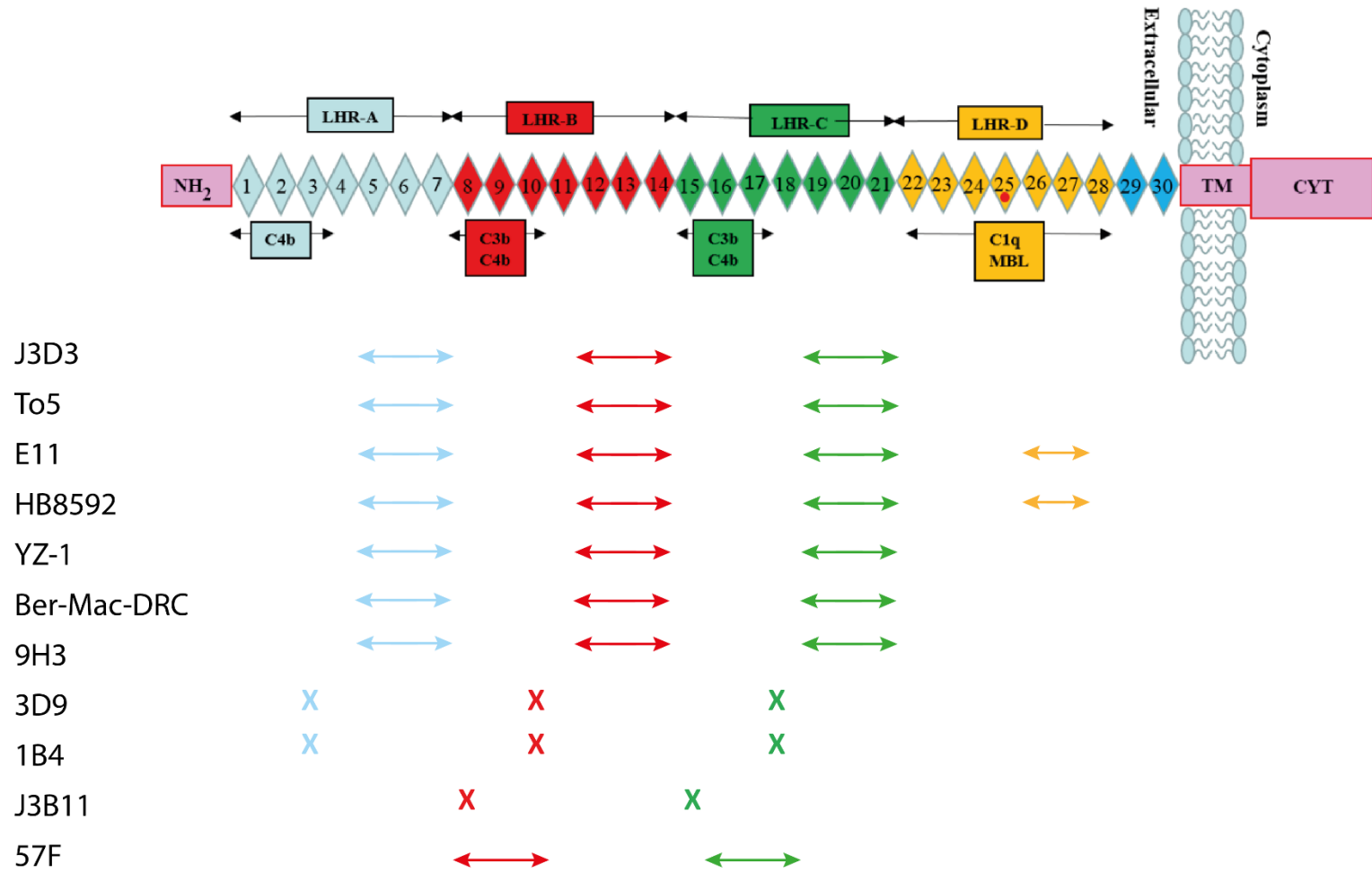


Figure 4-2. Epitopes of α -CR1 mouse monoclonal antibodies used in this chapter.

Image adapted from (Fonseca et al., 2016) with information from (Iida et al., 1982; Nickells et al., 1998). Red dot = site of SI and McC antigens

Antibody	Host	Clonality	(Sub) Class	Source (Cat #)	Comment
Isotype controls					
MOPC-21	Mouse	Monoclonal	IgG1	Abcam (18443)	
Rabbit polyclonal IgG	Rabbit	Polyclonal	IgG	Rowe laboratory	From non-immunised rabbits
Goat polyclonal IgG	Goat	Polyclonal	IgG	R&D Systems (AB-108-C)	
HBEC-5i characterisation					
Intercellular adhesion molecule 1	Mouse	Monoclonal	IgG1	Bio-Rad (1615)	Clone 15:2
Smooth muscle actin	Mouse	Monoclonal	IgG1	Santa Cruz (53142)	Not present on endothelial cells
von Willebrand factor	Rabbit	Polyclonal	IgG	Abcam (6994)	
Zona occludens 1	Rabbit	Polyclonal	IgG	Abcam (59720)	Tight junction marker
Endothelial protein C receptor	Goat	Polyclonal	IgG	R&D Systems (AF2245)	
Intracellular co-localisation					
Apoptosis-inducing factor	Rabbit	Monoclonal	IgG	These antibodies comprise the Organelle Localization IF Antibody Sampler Kit (Cell Signalling Technology, 8653)	Mitochondrial marker
Early endosome antigen 1	Rabbit	Monoclonal	IgG		Endosome marker
Lysosome-associated membrane protein 1	Rabbit	Monoclonal	IgG		Lysosome marker
Protein disulfide isomerase	Rabbit	Monoclonal	IgG		Endoplasmic reticulum marker
Receptor binding cancer antigen expressed on SiSo cells	Rabbit	Monoclonal	IgG		Golgi apparatus marker
Complement components					
C3d	Rabbit	Polyclonal	IgG	DAKO (0063)	

Table 4-3. Primary antibodies used for HBEC-5i experiments.

Antibody	Host	Target species	Fluorophore	Source (Cat #)
Goat α -mouse IgG (H+L) 488	Goat	Mouse IgG	Green	Thermo Fisher Scientific, A11029
Goat α -mouse IgG (H+L) 594	Goat	Rabbit IgG	Red	Thermo Fisher Scientific, A11032
Goat α -rabbit IgG (H+L) 488	Goat	Rabbit IgG	Green	Thermo Fisher Scientific, A11034
Goat α -rabbit IgG (H+L) 594	Goat	Rabbit IgG	Red	Thermo Fisher Scientific, R37117
Goat α -rabbit IgG (H+L) 647	Goat	Rabbit IgG	Far red	Thermo Fisher Scientific, A32733
Donkey α -goat IgG (H+L) 488	Donkey	Goat IgG	Green	Thermo Fisher Scientific, A11055
Goat α -rabbit IgG (H+L) 680RD	Goat	Rabbit IgG	Near infrared	Li-cor Biosciences UK, 925-68071
Goat α -mouse IgG (H+L) 800CW	Goat	Mouse IgG	Infrared	Li-cor Biosciences UK, 925-32210
Rat α -mouse IgG1 phycoerythrin (PE) conjugated	Rat	Mouse IgG1	Red-orange	BD Biosciences, 550083

Table 4-4. Secondary antibodies used for HBEC-5i experiments.

4.4.2 Human Brain Endothelial cell line (HBEC-5i)

Commercially available primary HBEC cells have been found to have batch-to-batch differences due to multidonor origins (reviewed in (Bouïs et al., 2001)) with immortalised HBEC lines being more stable in their endothelial traits. The immortalised human brain endothelial cell line HBEC-5i was established from the microvessels of cortical fragments of human brains (Dorovini-Zis et al., 1991; Wassmer et al., 2006) and provided by Francisco Candal (Centers for Disease Control and Prevention, Atlanta, USA).

Primary cell lines were established using multiple cortical fragments, with 19 from temporal lobe biopsies and 11 from autopsies, with patients ranging from 19 to 75 years old (Dorovini-Zis et al., 1991). Following this, primary HBEC cells (single donor) in their fifth passage were transfected with a plasmid containing the large T transforming protein of simian virus 40 (SV40) and Rous sarcoma virus long terminal repeat sequences to produce an immortalised cell line (Wassmer et al., 2006). In culture, HBEC-5i cells form monolayers with tight junctions as seen in the blood brain barrier (confirmed by the ability to exclude horseradish peroxidase from penetrating inter-endothelial spaces), showed cytoplasmic staining for von Willebrand factor (vWF) antigen and have lectin binding sites for *Ulex europaeus* agglutination, properties which support the endothelial nature of these cells (Dorovini-Zis et al., 1991). HBEC-5i do not express the receptors CD36 or CD31 either at rest or on stimulation (Wassmer et al., 2006). The cell line is a key tool in the investigation of cerebral malaria pathogenesis (Adams et al., 2014; Claessens and Rowe, 2012; Claessens et al., 2012; Jambou et al., 2010; Wassmer et al., 2005, 2006).

4.4.3 HBEC-5i culture media

All work using HBEC-5i cells was performed in a Class II biological safety cabinet under sterile conditions. All culturing solutions were sterile and pre-warmed to 37°C before use.

Dulbecco's Modified Eagle's Medium/Nutrient Mixture F-12 Ham (DMEM, Sigma-Aldrich, D6421) was used in the culture process as either complete DMEM or incomplete DMEM.

Incomplete DMEM - DMEM supplemented with 2mM L-glutamine (Thermo Fisher Scientific, 25030) and 100 U/ml penicillin/0.1mg/ml streptomycin (Gibco, 15140) with the pH adjusted to 7.4 with 1M NaOH.

Complete DMEM - incomplete DMEM plus 10% v/v heat-inactivated foetal bovine serum (HI-FBS, Thermo Fisher Scientific, 10500064), 1% v/v endothelial cell growth supplement (ScienCell, 1052) with the pH adjusted to 7.4 with 1M NaOH.

4.4.4 HBEC-5i thawing

HBEC-5i cells were grown on Corning® tissue flasks (Sigma-Aldrich, CLS430639) coated with gelatin. In preparation for seeding cells into a 25cm² flask, 3 ml of 0.1% v/v sterile gelatin (Sigma-Aldrich, G1393) in dH₂O was added to the flask. This was lain flat for 30 minutes at 37°C before excess gelatin was aspirated, leaving an optimal coating for cell growth.

HBEC-5i were maintained in liquid nitrogen for long term storage. For thawing, a 1 ml aliquot of HBEC-5i cells was placed in a water bath at 37°C and then gently resuspended in 10 ml complete DMEM in a 15 ml Falcon tube. The tube was spun at 800g for 4 minutes and the supernatant removed. The cell pellet was thoroughly resuspended with 10 ml of fresh complete DMEM until no clumps remained and seeded onto gelatin-coated 25 cm² tissue culture flask with a filter cap and incubated at 37°C with 5% CO₂/air. The medium was replaced with fresh complete DMEM on the following day.

4.4.5 General HBEC-5i culture and passage

Before reaching 100% confluency, cells were passaged and diluted into a new flask. Cell medium was changed every 48 hours or earlier if the medium changed from red/orange to yellow, implying acidity and nutrient depletion. For the passage of cells in a 75cm² flask (Sigma-Aldrich, CLS430641U), spent medium was aspirated and cells washed twice with 10 ml incomplete DMEM. Two ml of 0.25% trypsin-EDTA (Thermo Fisher Scientific, 25200) was added and the flask was incubated at 37°C for 2-3 minutes until the cells had detached. Nine ml of complete DMEM was added to terminate protease activity. Cells were resuspended, transferred to a 15 ml tube and centrifuged at 800g for 4 minutes. The supernatant was aspirated and cells diluted 1 in 10 in complete DMEM into a new gelatin-coated flask.

CR1 is extremely sensitive to cleavage by trypsin (Pascual et al., 1994b; Sugita et al., 1986) making trypsin-based cell lifting unsuitable for downstream assays investigating CR1 expression. Instead, cells were lifted using lignocaine hydrochloride, an approach used for cells including macrophages and fibroblasts (Fleit et al., 1984; Rabinovitch and DeStefano, 1975). For a 75 cm² flask, cells were washed twice with 10 ml of calcium and magnesium-free PBS x 1 (Sigma Aldrich, P4417) which had been warmed to 37°C, following which 5 ml of pre-warmed lignocaine hydrochloride 4 mg/ml (AppliChem, A2870) made up in calcium and magnesium-free PBS x 1) was added and the flask was incubated at room temperature for 20 minutes. The flask was tapped to release the cells and 5 ml of calcium and magnesium-free PBS was added to aid detachment. The cell suspension was then used for various CR1 assays as described below.

4.4.6 HBEC-5i freezing

HBEC-5i at 80 – 100% confluency were lifted using the trypsin-EDTA method and washed in complete DMEM. Cell density was estimated using a haemocytometer and cells diluted in Cell Freezing Medium (ScienCell, 0133) at ~ 1 x 10⁶ cells / ml. Aliquots were frozen overnight at -70°C and transferred to liquid nitrogen.

4.4.7 CHO cell culture

Chinese hamster ovary (CHO) cells are a commonly used epithelial cell line and are well adapted to culture and to protein expression. Two stably transfected CHO cell lines were used in these experiments; CR1-CHO (CHO cells expressing ~ 200,000 copies of CR1 per cell, positive control) and RCHO (CHO cells transfected with CR1 cDNA in the reverse orientation, negative control), both kind gifts from John Atkinson (St Louis, USA) (Gunning et al., 1987; Java et al., 2015). Untransfected CHO cells do not have any membrane regulatory proteins with activity for human complement components, thus this system allows for the investigation of CR1 alone (Barilla-LaBarca et al., 2002).

CHO cells were cultured in complete Ham's F-12 media with 10% HI-FBS, 100 U/ml penicillin/0.1mg/ml streptomycin, 2mM L-glutamine, geneticin 250 µg/ml (Thermo Fisher Scientific, 10131019), Incomplete Ham's F-12 media was made as above without HI-FBS and used for washes. Cells were routinely passaged using trypsin-EDTA and with lignocaine hydrochloride if being used for a downstream CR1 assay (as described in 4.4.5). Freezing and thawing techniques were as described in 4.4.4 and 4.4.6, using Ham's F-12 media rather than DMEM.

4.4.8 Mycoplasma surveillance

Mycoplasma are common bacteria that can contaminate laboratory cultures, affecting cell physiology and metabolism which may influence experimental findings (reviewed in (Rottem and Naot, 1998)). Cell cultures were regularly checked for mycoplasma contamination using a commercial PCR detection kit (Venor™ GeM Mycoplasma Detection Kit (Minerva Biolabs, 11-1025)). An aliquot (100 µl) of cell medium was removed and heated to 100°C for 5 minutes. In a new tube, a 25 µl reaction was prepared consisting of 2 µl of heat-treated medium, 15.3 µl dH₂O, 2.5 µl primer-nucleotide mix, 2.5 µl 10x buffer (100 mM Tris-HCl pH 8.5, 500 nM KCl, 30 mM MgCl₂), 2.5 µl internal control and 0.2 µl of GoTaq® G2 DNA Polymerase (Promega, M7841). Separate tubes containing 2 µl of mycoplasma DNA (positive

control) or 2 µl of dH₂O (negative control) were run alongside the sample. The PCR programme is shown in Figure 4-3.

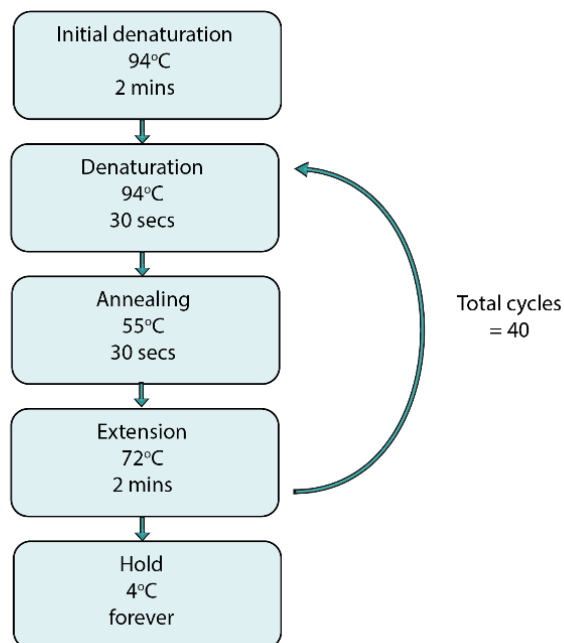


Figure 4-3. PCR programme for mycoplasma surveillance.

PCR products were run on a 1.5 % agarose gel (see section 5.4.5), with a band at 350 bp indicating a successful PCR and a second band at 280 bp indicating mycoplasma contamination. Contaminated cultures were discarded.

4.4.9 Preparation of cell lysates

Cell lysates of HBEC-5i, CR1-CHO and RCHO cells were made for SDS-PAGE / western blot analysis for CR1. A cell lysis buffer was prepared containing 2mM of the protease inhibitor phenylmethylsulfonyl fluoride (PMSF) (Sigma-Aldrich, P7626), 1% v/v Nonidet™ P-40 (Sigma-Aldrich, 18896) and 0.05% SDS in PBS. For some experiments, PMSF was substituted for cOmplete™ Mini EDTA-free Protease Inhibitor Cocktail (PIC, Sigma, 11836170001) with one tablet made up in 10 ml of the above cell lysis buffer.

A 90-100% confluent flask of cells was washed twice in warm calcium and magnesium-free PBS and lifted with lignocaine hydrochloride as described in 4.4.5.

Ten μl of the sample was removed and cell concentration calculated using a haemocytometer. The remaining recovered cells were centrifuged at 800g for 5 minutes. The supernatant was removed and the cells resuspended in ice cold lysis buffer to adjust the concentration to 2×10^7 cells/ml. The cell suspensions were incubated on ice for 20 minutes with resuspension every 5 minutes. They were then centrifuged at 11942g at 4°C for 10 minutes, 100 μl aliquots prepared and used immediately or frozen at -70°C until required. Whilst lysates were produced from the same number of cells, it should be remembered that HBEC-5i cells are considerably larger than CHO cells.

4.4.10 Immunofluorescence assays

To enable visualisation of immunofluorescence assays (IFAs), it was necessary to grow HBEC-5i on glass coverslips. This was performed using a Corning® 24-well plate (Sigma-Aldrich, CLS3527) with one 10 mm diameter glass coverslip (Thermo Fisher Scientific, 12392108) placed at the bottom of each well. The coverslips were coated with 0.1 % gelatin prior to the experiment (as outlined in 4.4.4). Confluent HBEC-5i cells were lifted with lignocaine (as described in 4.4.5) and plated onto the gelatin coated coverslips and cultured until they were ~ 80% confluent (with higher confluences resulting in the cells lifting off the glass). The media was aspirated and cells washed with 500 μl of pre-warmed calcium and magnesium-free PBS added to each well, gently swirled and aspirated off. The cells were fixed by adding 500 μl of 1% v/v methanol-free formaldehyde (Thermo Fisher Scientific, 28906) in calcium and magnesium-free PBS to each well. The cells were fixed for 15 minutes at room temperature, following which the formaldehyde solution was removed and the cells washed with 500 μl of calcium and magnesium-free PBS.

For experiments requiring permeabilised cells, an extra step was included at this point by adding 500 μl 0.1% v/v Triton™ X-100 (Sigma-Aldrich, T9284) in PBS to the wells with incubation at room temperature for 5 minutes. This was then aspirated and the cells washed twice with 500 μl PBS. Each well was then blocked with 500 μl 1 % bovine serum albumin (BSA, Sigma-Aldrich, A0336) or 5% goat serum (Sigma-

Aldrich, G9023) in PBS for 15 minutes before this was aspirated. 120 µl of the primary antibody was then carefully added to each coverslip and the 24 well plate was incubated in a humid chamber at room temperature for 60 minutes. The wells were then washed twice with 500 µl PBS and then incubated with 120 µl of the secondary antibody and incubated in a humid chamber at room temperature for 45 minutes. Antibody concentrations varied with experiments. The coverslips were then washed twice in PBS and carefully removed with curved tweezers before being mounted upside down on a glass slide with a drop of Fluoromount (SouthernBioTech 0100-01). Slides were stored at 4°C overnight before being imaged the next morning.

For staining with ZO-1, HBEC-5i were grown on polylysine coated glass coverslips (VWR, 631-0683) which had been coated with human fibronectin (50 µg/ml,) Merck Millipore, FC1010) in PBS for 20 minutes prior to seeding the cells. For staining with vWF antibody, the marker was most clearly visualised by growing the HBEC-5i on 8 well Nunc Lab-Tek II CC2 Chamber slides (Thermo Fisher Scientific, 154941) as described in (Dmitrieva and Burg, 2014).

On occasion, staining with two primary antibodies was necessary. When this was the case, primary antibodies produced in different species were used (i.e. mouse and rabbit) and secondary antibodies with different excitation wavelengths were used for detection to allow discrimination between the staining.

To assess the ability of HBEC-5i to take up Dil-Ac-LDL, HBEC-5i grown on glass coverslips were incubated with 25 µg/ml of Dil-Ac-LDL in complete DMEM and incubated at 37°C in 5% CO₂/air for 4 hours. After this they were washed three times in PBS and fixed with 1% v/v formaldehyde in PBS, blocked for 15 minutes with 1% BSA in PBS and the nuclei stained with 1 µg/ml DAPI before visualisation.

The stained HBEC-5i were imaged using standard fluorescent microscopy or confocal fluorescent microscopy. For fluorescent microscopy, a Leica DMLB2 microscope was used with x20, x40 or x100 objective. Pictures were taken using a DFC300FX digital camera with the same exposure used for negative controls,

positive controls and samples. Separate images were obtained for nuclear and cytoplasmic/membrane staining, which were overlain to produce a composite using the open source imaging processing software, ImageJ (version 1.51j8, National Institutes of Health, USA, <https://imagej.nih.gov/ij/index.html>). For confocal images, slides were imaged with a Leica SP5 confocal microscope using the glycerol x 63 objective. A z-stack of images was taken at 0.8 μm intervals, with number of images taken depending on the thickness of the slide. A composite image was created using Volocity 3D Image Analysis Software version 6.3 (PerkinElmer, Massachusetts, USA).

4.4.11 Flow cytometry

HBEC-5i at 80 – 100% confluency were lifted using lignocaine hydrochloride as described in 4.4.5, placed in a polypropylene tube (Greiner Bio-One International, 115201) and centrifuged at 400g for 5 minutes at 4°C. Most experiments were performed on live (unfixed) cells, however some experiments required a fixation +/- permeabilisation step, which was performed at this point. (NB – subsequent steps were performed at 4°C for live cells or at room temperature for fixed cells). For fixation, the supernatant was removed and 1 ml of 1% v/v formaldehyde in PBS was added to each sample tube, resuspended with a pipette and incubated at room temperature for 10 minutes. Following this, 2 ml of FACS buffer (0.1% v/v BSA and 0.1% v/v azide in PBS) was added to the sample which was centrifuged at 400g for 5 minutes at room temperature. The supernatant was removed and 1 ml 0.1% v/v Triton™ X-100 in PBS was added and incubated for 5 minutes at room temperature. Following this, 2 ml of fluorescent activated cell sorting (FACS) buffer was added and the sample centrifuged at 400g for 5 minutes at room temperature.

The supernatant was removed and 100 μl of 100 $\mu\text{g}/\text{ml}$ α -CR1 monoclonal antibody pool (commercial or extended) made up in PBS/1% BSA containing 1.25 $\mu\text{g}/\text{ml}$ Hoechst (Thermo Fisher Scientific: H3570) was added. The commercial pool contained the antibodies J3D3, To5 and E11, each at a concentration of 33.3 $\mu\text{g}/\text{ml}$. The extended pool contained the antibodies J3D3, To5, E11, HB8592, 9H3 and 57F, each at a concentration of 16.7 $\mu\text{g}/\text{ml}$.

The sample was incubated at 4°C for one hour with resuspension every 10 minutes. Three ml of ice cold FACS buffer was added and the tube was centrifuged at 400g for 5 minutes at 4°C. The supernatant was removed and 100 µl of 0.07 µg/ml phycoerythrin (PE)-conjugated rat α-mouse IgG1 (BD Biosciences, 550083) made up in 1% BSA in PBS containing 1.25 µg/ml Hoechst.

Samples were protected from light and incubated at 4°C for 30 minutes with resuspension every 10 minutes. Three ml of ice cold FACS buffer was added and the tube was centrifuged at 400g for 5 minutes at 4°C. The supernatant was removed and the sample resuspended in 250 µl of ice cold FACS buffer and analysed immediately. Approximately 60,000 events per sample were analysed on an LSR II flow cytometer (Beckton Dickinson Biosciences). Flow cytometry data were analysed using FlowJo v10 software (Tree Star Inc., Ashland USA).

4.4.12 Sodium dodecyl sulfate polyacrylamide gel electrophoresis (SDS-PAGE)

Sodium dodecyl sulfate polyacrylamide gel electrophoresis (SDS-PAGE) gels were cast to run samples prior to western blotting and for mass spectrometry. Separating gels generally contained 10% polyacrylamide. The separating solution was prepared by combining 7.9 ml dH₂O, 6.7 ml 30% w/v bis-acrylamide (Sigma-Aldrich, L3771), 5.0 ml 1.5M Tris (ThermoFisher Scientific, 17926) (pH 8.8), 0.2 ml 10% w/v SDS (Sigma-Aldrich, L3771), 0.2 ml 10% w/v ammonium persulfate (APS, Sigma-Aldrich, A3678) and 8 µl N,N,N',N'-tetramethylethylenediamine (TEMED, Sigma-Aldrich, T9821) and swirling gently. The separating solution was pipetted between two glass plates in the casting frame and allowed to gelate for 30 minutes. A small amount of isopropanol (ThermoFisher Scientific, 10315720) was pipetted over the separating gel to remove bubbles and protect from oxidation. Once set, the isopropanol was poured off. Five ml of stacking solution was made by combining 3.4 ml dH₂O, 0.83 ml 30% w/v bis-acrylamide, 0.63 ml 1.0 M Tris (pH 6.8), 50 µl 10% w/v SDS, 50 µl 10% w/v APS and 5 µl TEMED which was swirled gently. The stacking solution was pipetted on top of the separating solution until it overflowed and a comb was

inserted ensuring no air was trapped beneath the teeth. The solution was allowed to gelate for at least 30 minutes before the gel was loaded.

The samples to be run were mixed with loading buffer (0.375 M Tris pH 6.8, 12% w/v SDS, 60% v/v glycerol and 0.06 % w/v bromophenol blue (Electra, 44305) for non-reducing loading buffer (or the same buffer with the addition of 30% 2-mercaptoethanol (Sigma-Aldrich, M3148) for reducing loading buffer) in a ratio of 5 parts sample, 1 part loading buffer. The comb was removed from the SDS gel and it was clipped into the electrophoresis apparatus. SDS PAGE running buffer (25 mM Tris-HCl, pH 8.3, 192 mM Glycine, 0.1% SDS) was poured into the inner chamber until it overflowed. Eight μl of Novex Sharp pre-stained protein standard (Thermo Fisher Scientific, LC5800) were loaded into the first well of the gel and $\sim 15 \mu\text{l}$ of sample (depending on the experiment) loaded into the subsequent wells. The gel was run at 125V until the protein marker was seen at the foot of the glass plate.

4.4.13 Western blotting

Western blotting was used to probe cell lysates with α -CR1 monoclonal antibodies, as part of immunoprecipitation process (see 4.4.16) and to visualise C3b breakdown products (see 4.4.14). SDS-PAGE gels were transferred to a polyvinylidene fluoride (PVDF, Merk Millipore, IPVH00010) or nitrocellulose membrane (Sigma-Aldrich, GE10600003). PVDF was activated with methanol for 1 minute before use. Filter paper and sponges were soaked in transfer buffer (25 mM Tris, 192 mM glycine, 20% v/v methanol) for 10 minutes prior to the assembling the transfer stack. The blotting stack was prepared as shown in Figure 4-4.



Figure 4-4. Representation of western blot transfer stack.

An ice block was placed in the tank which was then filled with transfer buffer and run at 15V overnight at 4°C (or 80 V for 1 hour for the C3b degradation assay). The next morning the membrane was incubated with Ponceau S (Sigma-Aldrich, P7170) for 2 mins to allow visualisation of the transferred proteins and removal of extraneous membrane. The membrane was washed in 0.1% Tween®20 in PBS (Sigma-Aldrich, P9416) and blocked in in 5% non-fat milk (instant dried skimmed milk, Tesco) in 0.1% Tween®20 in PBS for two hours on a rocker. The membrane was washed three times in 0.1% Tween®20 in PBS for 10 minutes and incubated with the primary antibody (made up in 1% v/v IgG-free BSA and 0.05% v/v Tween®20 in PBS) overnight at 4°C.

The membrane was washed three times in 0.1% Tween®20 in PBS for 10 minutes and secondary antibody added (Goat anti-Rabbit IgG (H + L), IRDye® 680RD, Li-Cor Biosciences UK, 925-68071 or IRDye® 800CW Goat anti-Mouse IgG (H + L) Li-Cor Biosciences UK, 925-32210) at a dilution of 1:5000 – 1:8000 (made up in 0.05% v/v Tween®20 and 50% v/v Odyssey Blocking Buffer (Li-Cor Biosciences UK, 927-40010) in PBS) and incubated in the dark at room temperature for an hour and washed a final three times in 0.1% Tween®20 in PBS for 10 minutes. Stained membranes were imaged directly on a Li-COR Odyssey® scanner using the 700 nm and 800 nm channels. Images were imported using Image Studio Lite software v5.2 and contrast adjusted to allow visualisation of the bands without changing the raw data. (https://www.licor.com/bio/products/software/image_studio_lite/).

4.4.14 C3b degradation assay

4.4.14.1 Role of CR1 in C3b breakdown

C3 is an essential component of the complement system consisting of an α -chain (~110 kDa) and a β -chain (~75 kDa) connected by cysteine bridges. In its native form, C3 is inactive, requiring activation through cleavage by one of three forms of C3 convertase; C3(H₂O)Bb and C3bBb in the alternative pathway (Fearon et al., 1973; Nilsson and Nilsson Ekdahl, 2012), and C4b2a in the classical and lectin complement pathways (Müller-Eberhard et al., 1967). Cleavage of C3 with one of

these C3-convertases produce C3a and C3b. On host cells, C3b subsequently undergoes successive proteolytic cleavages which produce inactive C3 products, thus protecting the cell from opsonisation and complement attack. The first cleavage of C3b to iC3b (+ C3f) is performed by factor I, together with another cofactor which can be factor H, MCP or CR1 (reviewed in (Foley et al., 2015)) and is thus not CR1-dependent. The degradation of iC3b to C3dg (+ C3c) is performed by factor I with CR1 as a cofactor. The presence of C3dg thus suggests that CR1 is present and acting as a cofactor for iC3b breakdown (Ross et al., 1982). Identification of C3dg in this instance has been used as a method to determine whether functional CR1 is present (Collard et al., 1997). CR1 has the capacity to bind C3b, iC3b, and C3c but not to C3d (Becherer and Lambris 1988).

The C3b breakdown pathway is detailed in Figure 4-5.

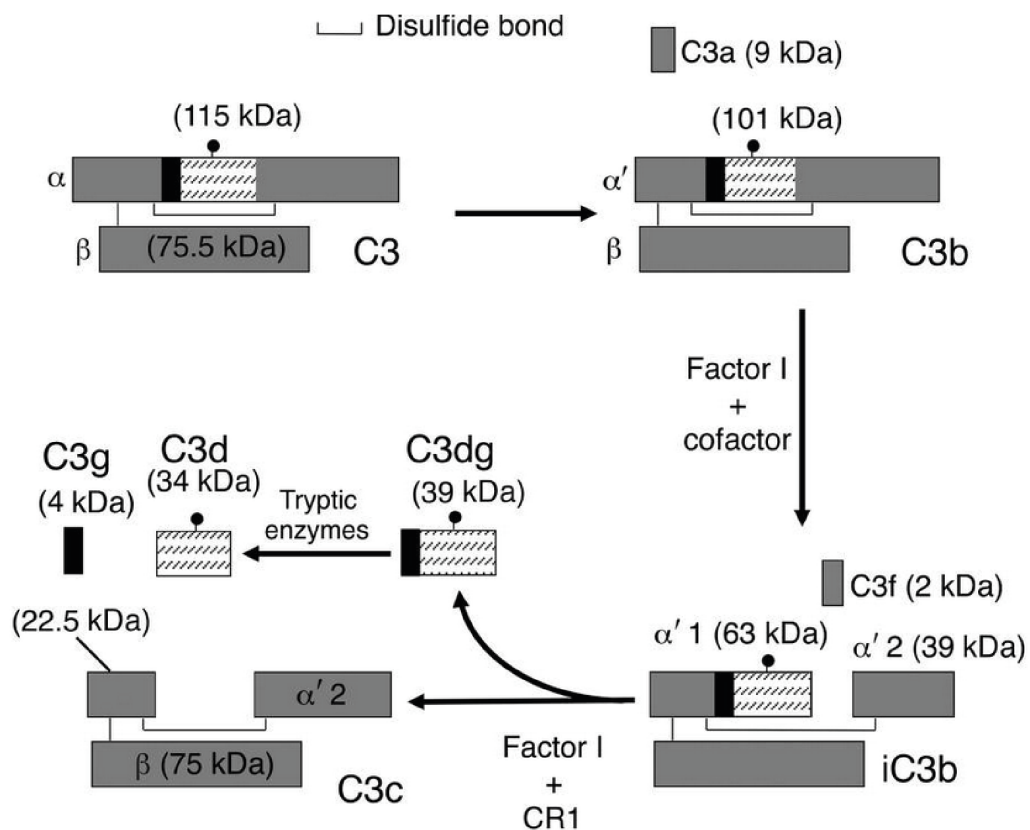


Figure 4-5. The C3 degradation pathway.

Degradation of C3b to iC3b requires factor I and a cofactor (either factor H, MCP or CR1). The C3d domain present within the C3, C3b and iC3b molecules is shown by a hashed area. Image taken directly from (Thurman et al., 2013).

4.4.14.2 Western blot to detect C3dg in supernatant

A modified version of the assay described by Collard *et al.* was used (Collard *et al.*, 1999). As complement components C3b, iC3b, C3dg and C3d all contain the C3d region (see Figure 4-5), an α -C3d antibody would be anticipated to detect all complement components which include this region, (depending on conformational changes of the C3d epitope during cleavage). An assay was therefore designed to detect the presence of C3dg after incubation of confluent cells (HBEC-5i, CR1-CHO or RCHO) with C3b and factor I as an indicator of the presence of functional CR1. The α -CR1 monoclonal antibody 3D9 (which abrogates the binding of C3b to CR1 was used to inhibit C3b binding and breakdown (Madi *et al.*, 1991; Nickells *et al.*, 1998; O'Shea *et al.*, 1985)) was used to determine specificity of the process to CR1.

Approximately 2×10^4 HBEC-5i, CR1-CHO or RCHO cells were added to each well of a flat bottomed 96-well plate (Sigma-Aldrich, CLS3799, which had been coated with gelatin) and grown to a confluent monolayer. The spent media was removed and cells were washed twice with incomplete DMEM. Fifty μ l of incomplete DMEM (non-permeabilised experiments) or 50 μ l of incomplete DMEM with 0.1% v/v Triton[®] X-100 (permeabilised experiments) was added to each well. To examine each cell line's ability to cleave C3b, wells were incubated with either:

- C3b alone
- Factor I alone
- C3b + factor I
- C3b + factor I + mouse IgG1 isotype control antibody MOPC-21
- C3b + factor I + α -CR1 monoclonal antibody 3D9

C3b was sourced from Merk Milipore (204860), factor I from Sigma (C5938) and recombinant CR1 from R and D systems (5748). Antibody sources for this section are detailed in Table 4-3. C3b was used at 27.5 μ g/ml, factor I at 22 μ g/ml, mouse IgG1 isotype antibody at 10 μ g/ml and 3D9 at 10 μ g/ml.

Cells were incubated in incomplete DMEM with the complement components/antibodies as described for 7 hours at 37°C in 5% CO₂. The supernatants were then removed. 15 μ l of each supernatant was added to 3 μ l of

reducing loading buffer and heated for 7 minutes at 95°C. The samples were then resolved by SDS-PAGE on a 10% SDS gel run at 125 V for 60 minutes. The gel was transferred to an activated PVDF membrane by western blotting at 80 V for 60 minutes. The membrane was blocked with 0.1% Tween[®]20 in PBS with 5% milk for two hours, then probed with α -C3d rabbit polyclonal antibody (Dako, A0063) at 15.5 μ g/ μ l (made up in 1% v/v IgG-free BSA and 0.05% v/v Tween[®]20 in PBS). The reaction was left overnight at 4°C on a rocker. The membrane was then washed three times in 0.1% Tween[®]20 in PBS and incubated with 1:8000 goat α -rabbit IgG (H + L), IRDye[®] 680RD (made up in 0.05% Tween[®]20 in PBS and 50% v/v Odyssey Blocking Buffer) and developed as described in 4.4.13.

4.4.15 Transfection of HBEC-5i with CR1 siRNA

α -CR1 antibody staining of HBEC-5i after treatment with CR1 siRNA (Santa Cruz, sc-29994) was investigated. Transfection with EPCR siRNA (Santa Cruz, sc-39932) was used as a positive control for transfection, and two negative controls were included; transfection with control A siRNA (“control KD”, scrambled sequence with no known target, Santa Cruz, sc-37007) and incubation with transfection agent alone (“vehicle only”).

CR1 siRNA, EPCR siRNA or control A siRNA (10 μ M) was diluted in Opti-MEM reduced serum medium (Thermo Fisher Scientific, 31985062) at a ratio of 3:50. Separately, Lipofectamine RNAiMAX transfection reagent (Thermo Fisher Scientific, 13778030) was diluted in Opti-MEM reduced serum medium at a ratio of 3:30. Following this, an equal volume of the diluted CR1 siRNA, EPCR siRNA or control A siRNA was added to the diluted Lipofectamine RNAiMAX and incubated at room temperature for 5 minutes to allow the formation of each respective siRNA-lipid complex. For “vehicle only” experiments, one-part Lipofectamine/Opti-MEM solution was diluted with one part Opti-MEM (i.e. no siRNA).

HBEC-5i were seeded onto gelatin-coated coverslips in 24 well plates on the day before the experiment to allow them to reach 60-80% confluency. Old medium was aspirated and 500 μ l of fresh complete DMEM was added to each well. 100 μ l of the

siRNA-lipid complex of interest was then added to each relevant well. CR1 siRNA, EPCR siRNA or control A wells each contained a final amount of 30 pmol siRNA.

The cells were incubated at 37°C for 24 or 48 hours in 5% CO₂ in air. Following this, an IFA was performed as per 4.4.10 to determine the effect of the transfection process. E11, and its respective mouse IgG1 isotype control MOPC-21, were used at 15 µg/ml and polyclonal α-EPCR (R&D Systems, AF2245), and its respective goat IgG isotype control (R&D Systems, AB-108-C) were used at 10 µg/ml. As EPCR is a surface receptor, cells stained with α-EPCR and goat isotype control were not permeabilised, whereas cells stained for E11 and mouse isotype control were permeabilised with 0.1% Triton® X-100.

4.4.16 Immunoprecipitation

Immunoprecipitation with the α-CR1 monoclonal antibody E11 was performed to determine whether CR1 could be isolated from the lysates of HBEC-5i, CR1-CHO and RCHO cells. For each cell line to be examined, 100 µl of protein G coated Dynabeads (Novex, 10003D) were washed in tissue-grade pre-prepared PBS (Sigma, D8537), for one minute, after which the beads were separated using a magnet and the supernatant discarded (“magnetic wash”). The bead pellet was made up to 100 µl with PBS and divided into two aliquots. Fifty µl of beads was incubated with 5 µg of E11 antibody in 200 µl of PBS while the other 50 µl of beads was incubated with 5 µg of mouse IgG1 isotype control MOPC-21. The antibody-bead mixtures were incubated for 30 minutes at room temperature with resuspension. Three magnetic washes in 1 ml PBS were performed and beads made up to 50 µl volume with PBS.

Lysates from the three cell lines; HBEC-5i, CR1-CHO and RCHO had previously been prepared as described in 4.4.9, at a cell density of 2 x 10⁷ cells /ml. 100 µl of each lysate was added to the E11 or isotype control bead mixture and made up to 1 ml with ice cold tissue grade PBS. The lysate-bead mixture was incubated overnight at 4°C with continuous agitation on a rotating mixer. The next day, the mixtures underwent 3 magnetic washes in 0.05% Tween®20 in PBS followed by 2 magnetic washes with PBS. The antibodies were then eluted from the beads by the addition

of 50 μ l 0.1 M glycine (ThermoFisher Scientific, BP381-500) pH 2.7 to the bead pellet with gentle agitation by hand for 5 minutes at room temperature. The beads were then pelleted using a magnet and the supernatant removed. The mixture was neutralised with 5 μ l of 1M Tris pH9 to prevent hydrolysis of the protein.

The immunoprecipitates were immediately run on a non-reducing 8% polyacrylamide gel. Duplicate gels were run for each experiment at 125 V for 80 minutes. One gel was stained with InstantBlue Protein Stain (Expedeon, UK, ISB1L) for one hour on a rocker while the other was transferred onto a nitrocellulose membrane overnight at 15 V at 4°C.

While the proteins were transferring, the detection antibody was prepared. It was necessary to use E11 as both the capture and detection antibody in this experiment. As such, the E11 to be used for detection on the western blot was conjugated to a fluorescent dye to differentiate it from the capture E11. The Lightning-Link Rapid Dylight 800 antibody and protein labelling kit (Innova Biosciences, 329-0030) was used to label E11 at 1 μ g/ μ l as per the kit instructions.

After transfer, the nitrocellulose membrane was blocked in 0.1% Tween[®]20 and 5% milk in PBS for 2 hours, then washed with 0.1% Tween[®]20 in PBS and then incubated with 1:10,000 conjugated-E11 (made up in 0.05% Tween[®]20 and 50% v/v Odyssey Blocking Buffer in PBS) in the dark at 4°C for 24 hours. The membrane was washed 3 times in 0.1% Tween[®]20 in PBS and imaged using the Li-COR Odyssey[®] scanner and Image Studio Lite software as described in section 4.4.13.

4.4.17 Mass Spectrometry

Cell lysates were prepared for HBEC-5i and CR1-CHO (positive control) as outlined in 4.4.9. Twenty μ l of lysate was mixed with 4 μ l of non-reducing loading buffer and resolved by SDS-PAGE on a non-reducing 8% polyacrylamide gel at 80 V for 100 minutes. Duplicate gels were run to allow one to be stained for protein detection and one for western blotting and probing with the α -CR1 antibody pool. The first gel was stained with InstantBlue Protein Stain on a rocker for one hour at room

temperature and then stored at 4°C until ready to be cut. The second gel was transferred onto a nitrocellulose membrane over night at 15 V at 4°C. The membrane was then blocked with 5% milk and 0.1% Tween®20 in PBS for one hour and incubated with E11, J3D3 and To5 α-CR1 antibodies. Each antibody was used at 0.33 µg/µl concentration with a final concentration of 1 µg/µl. The membrane was incubated overnight on a rocker at 4°C then washed 3 times in 0.1% Tween®20 in PBS before incubation with 1:8000 IRDye® 800CW Goat anti-Mouse IgG (H + L) antibody (made up in made up in 0.05% Tween®20 and 50% v/v Odyssey Blocking Buffer in PBS) for 1 hour on a rocker. The membrane was washed three times in 0.1% Tween®20 in PBS and imaged using the Li-COR Odyssey® scanner and Image Studio Lite software as described in section 4.4.13.

The western blot was used to determine the position of the band of interest on the corresponding stained gel. A scalpel was used to cut gel bands from the HBEC-5i lysate and the CR1-CHO lysate lanes, which were destained in 40 % v/v methanol (ThermoFisher Scientific, 10284580) and 10 % v/v acetic acid (ThermoFisher Scientific, 10394970) in dH₂O for 20 minutes at room temperature followed by a wash with dH₂O.

Samples were sent for processing to the Mass Spectrometry and Proteomics Facility at the University of St Andrews (<http://mass-spec.wp.st-andrews.ac.uk/>) which performs nano-scale liquid chromatographic electrospray ionisation tandem mass spectrometry (nLC-ESI-MS/MS). Downstream reduction, alkylation and trypsin digestion of the gel bands was performed by the facility. Trypsin cleaves the proteins at arginine and lysine residues into peptides, which are acid-extracted and injected into the liquid chromatography mass spectrometer. The resultant spectra are searched against NCBI, Swissprot and the facility's internal database, Mascot (<https://bsrcmascot.st-andrews.ac.uk/mascot/>) for potential peptide matches. The Mascot search algorithm is based on probability scoring (Perkins et al., 1999).

4.5 Results

4.5.1 HBEC-5i cell line expresses expected cellular markers

HBEC-5i cells were grown to ~ 80% confluence on glass coverslips and IFAs carried out as detailed in 4.4.10. Non-permeabilised HBEC-5i were stained for ICAM-1 (intercellular adhesion molecule 1, 50 $\mu\text{g/ml}$), zona-occludens-1 (ZO-1, 50 $\mu\text{g/ml}$) and α -SMA (20 $\mu\text{g/ml}$) and permeabilised cells were stained for intracellular von Willebrand factor (vWF, 62 $\mu\text{g/ml}$).

HBEC-5i were found to take up Dil-Ac-LDL (Figure 4-6) and expressed ICAM-1 and ZO-1 (tight junction marker) on the membrane as anticipated (Figure 4-7).

Permeabilised HBEC-5i were confirmed to contain intracellular stores of the endothelial marker vWF as well as having ultra-long fibres of vWF coating their surfaces (Figure 4-8). As anticipated, HBEC-5i did not express the fibroblast marker α -SMA (Figure 4-8).

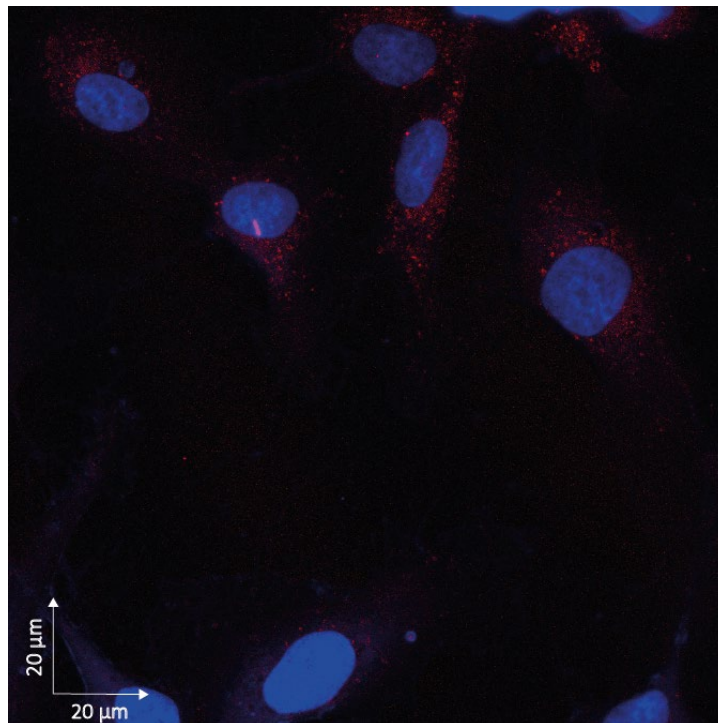


Figure 4-6. HBEC-5i can take up Dil-Ac-LDL.

Blue = DAPI nuclear staining. **Red** = Dil-Ac-LDL. x63 magnification.
Live HBEC-5i co-incubated with Dil-Ac-LDL 25 $\mu\text{g/ml}$ for four hours at 37°C

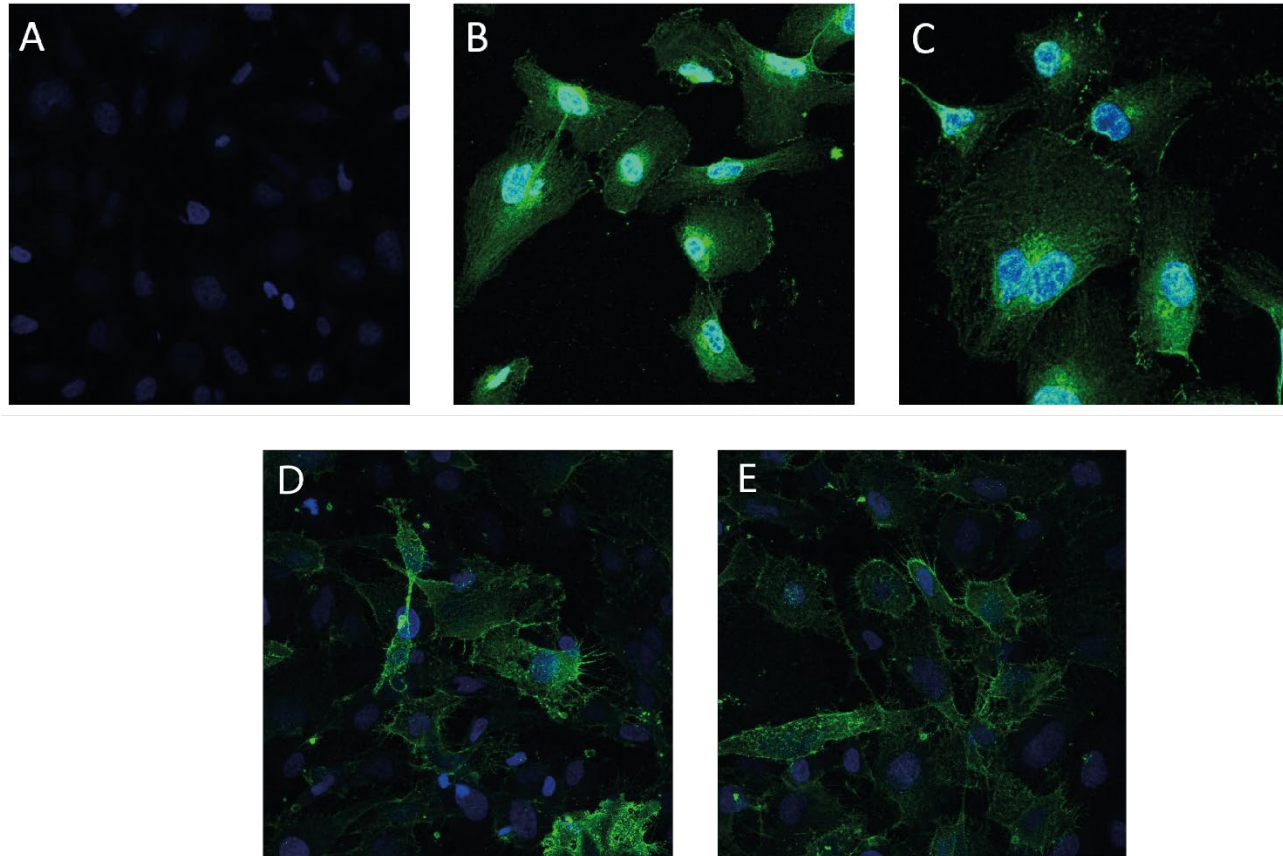


Figure 4-7. HBEC-5i form tight junctions and express intercellular adhesion molecule 1 (ICAM-1).

Panel A: **Green** = Mouse IgG1 isotype control (50 $\mu\text{g}/\text{ml}$). **Blue** = DAPI nuclear staining. Panels B and C: **Green** = Zona occludens-1 (50 $\mu\text{g}/\text{ml}$). **Blue** = DAPI nuclear staining.

Panels D and E: **Green** = ICAM-1 (50 $\mu\text{g}/\text{ml}$). **Blue** = DAPI nuclear staining.

Fixed non-permeabilised HBEC-5i. Panel A, B, D and E x63 magnification. Panel C x100 magnification.

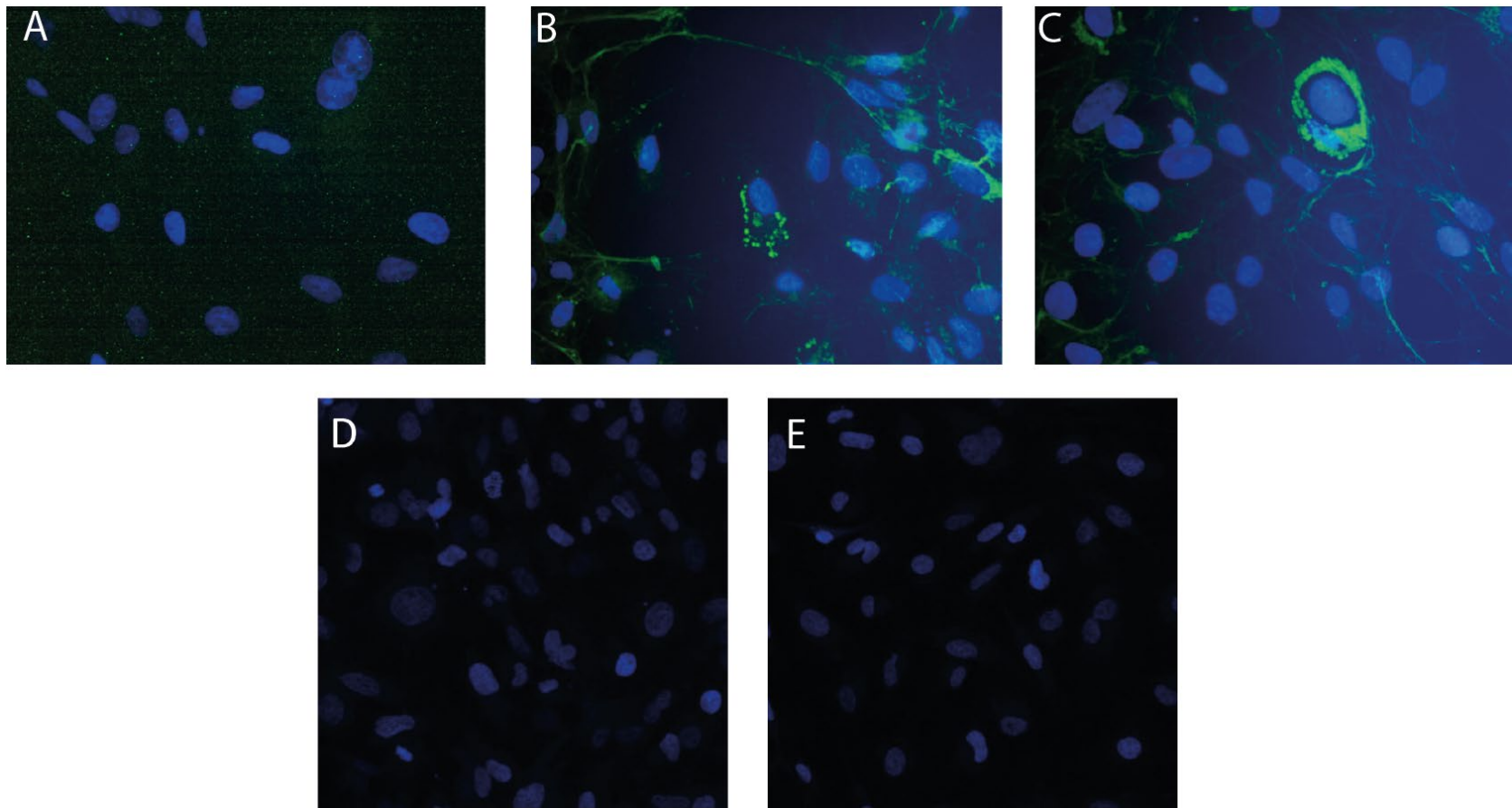


Figure 4-8. HBEC-5i contain intracellular von Willebrand factor (vWF) and do not express α -smooth muscle actin (α -SMA).
Panel A: **Green** = Rabbit IgG isotype control (62 μ g/ml). **Blue** = DAPI nuclear staining. Panels B and C: **Green** = vWF (62 μ g/ml). **Blue** = DAPI nuclear staining.
Panel D: **Green** = Mouse IgG1 isotype control (20 μ g/ml). **Blue** = DAPI nuclear staining. Panel E: **Green** = α -SMA (20 μ g/ml). **Blue** = DAPI nuclear staining.
Panels A-C: Fixed permeabilised HBEC-5i. Panels D and E: Fixed non-permeabilised HBEC-5i. x40 magnification.

4.5.2 α -CR1 monoclonal antibodies recognise an epitope on HBEC-5i

After characterising the HBEC-5i line, IFAs using a pool of α -CR1 monoclonal antibodies were performed. Two pools of IgG1 mouse monoclonal antibodies were used; the “commercial α -CR1 pool,” which included three commercially available antibodies J3D3, To5 and E11 and the “extended α -CR1 pool” containing the commercial antibodies plus 57F, 9H3 and HB95G2 (kind gifts detailed in Table 4-2).

IFAs were performed on unpermeabilised HBEC-5i with the extended α -CR1 pool suggested low levels of staining on the surface of some HBEC-5i (representative images in Figure 4-9). It had previously been reported that the expression of CR1 by HUVEC was increased under hypoxic conditions (Collard et al., 1999). As such, the experiment was repeated comparing the antibody staining of HBEC-5i cultured in normal growing conditions of 5% CO₂/air (“normoxic”) with those grown in 1% O₂, 3% CO₂ and 96% N₂ (“hypoxic”) for 48 hours. HBEC-5i grown under hypoxic conditions were seen to stain more brightly and more uniformly with the extended α -CR1 pool than those grown under normal culture conditions (representative images in Figure 4-10). Fewer hypoxic cells were available for staining as they detached from the glass coverslip under these conditions.

Collard et al. also reported the majority of CR1 identified in HUVECs was intracellular (Collard et al., 1999). The IFA was repeated using permeabilised HBEC-5i and the commercial α -CR1 pool. Large intracellular stores of the antigen were seen in all cells with prominent peri-nuclear vesicles (Figure 4-11). Staining was particularly marked in dividing cells (Figure 4-12).

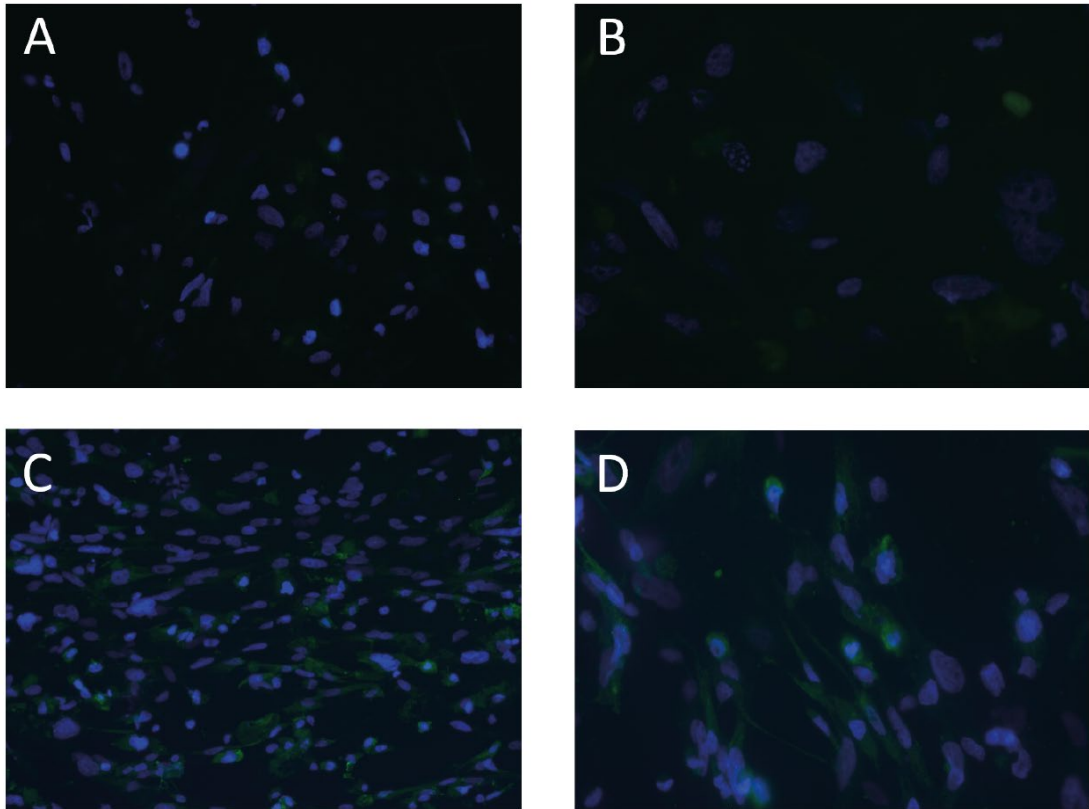


Figure 4-9. Extended pool of α -CR1 monoclonal antibodies recognises an antigen on the surface of HBEC-5i cells.

Panels A+B: **Green** = Mouse IgG1 isotype control (100 μ g/ml). **Blue** = DAPI nuclear staining.
Panels C+D: **Green** = Extended α -CR1 monoclonal pool (100 μ g/ml). **Blue** = DAPI nuclear staining.
Fixed non-permeabilised HBEC-5i. Panels A+C x20 magnification. Panels B+D x 40 magnification.

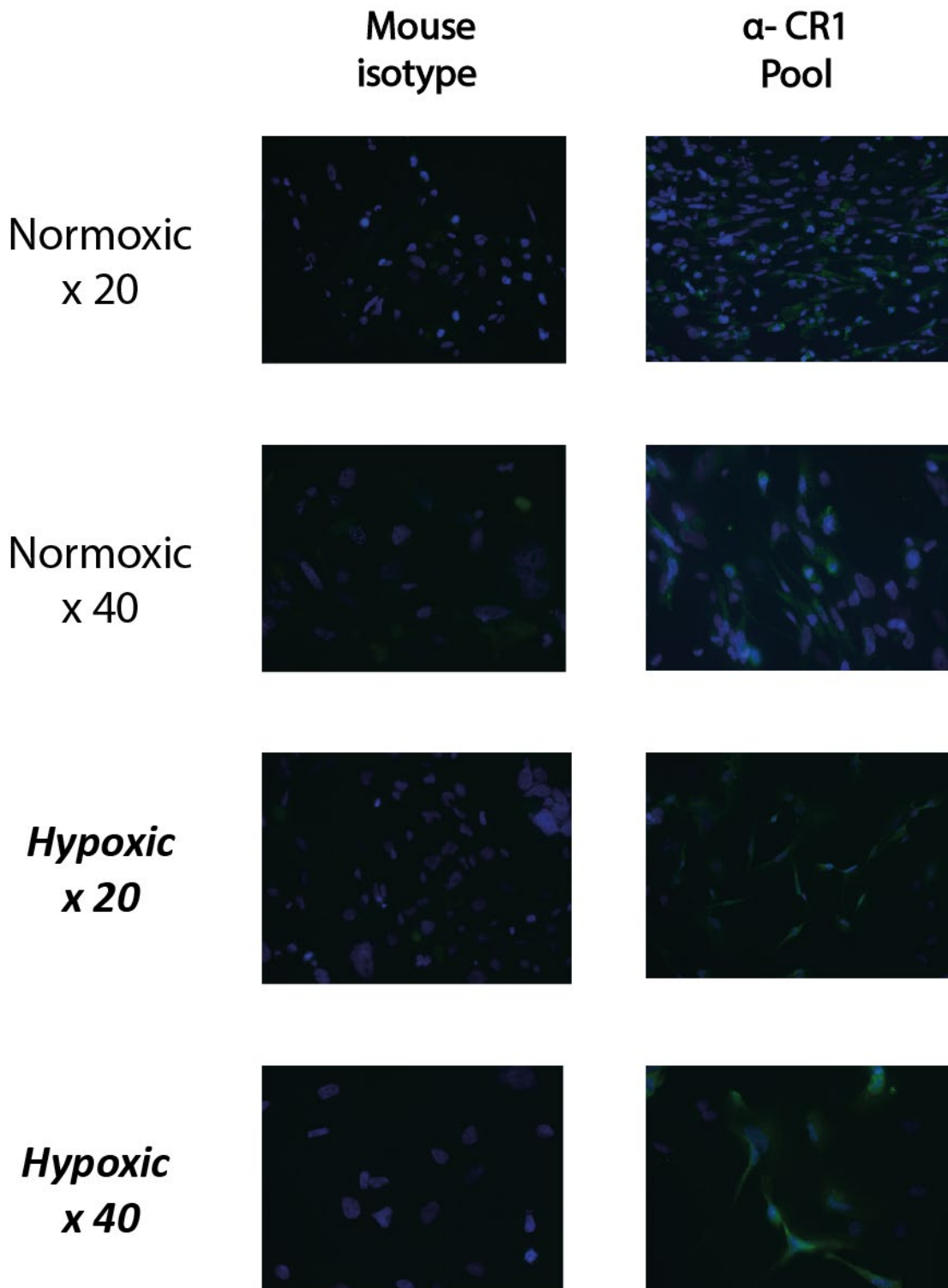


Figure 4-10. Staining of HBEC-5i by extended pool of α -CR1 antibodies is increased under hypoxic conditions.

Green = extended α -CR1 monoclonal pool (100 μ g/ml) or mouse isotype control (100 μ g/ml) respectively.

Blue = DAPI nuclear staining. HBEC-5i fixed and not permeabilised.

HBEC-5i incubated in 5% CO₂/air ("normoxic") or in 1% O₂, 3% CO₂ and 96% N₂ ("hypoxic").

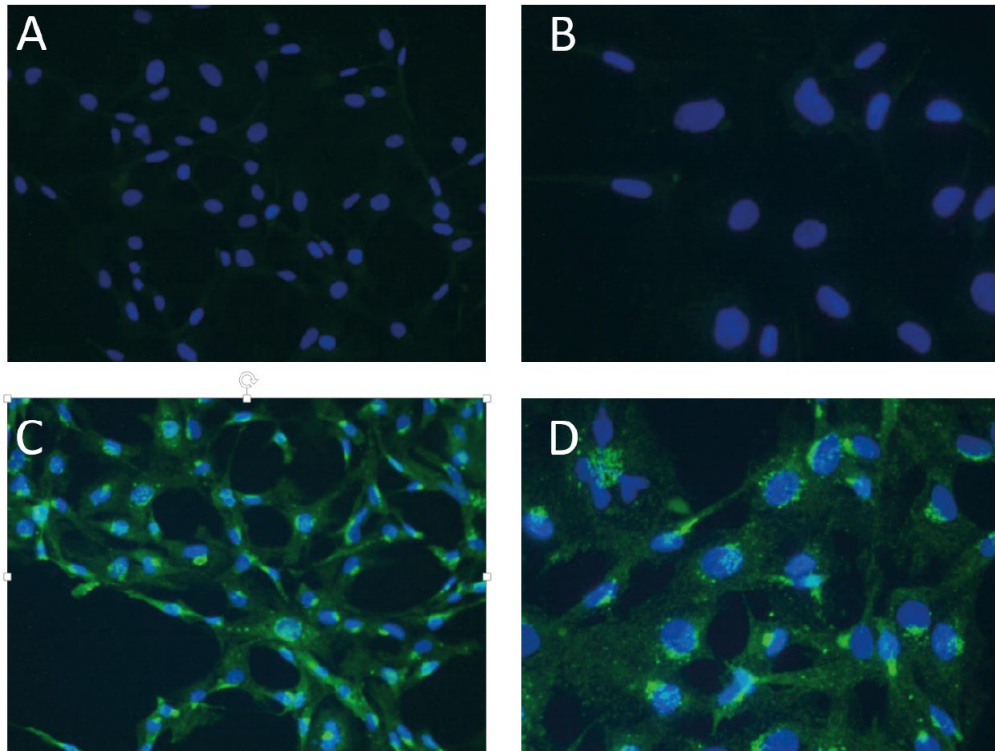


Figure 4-11. α -CR1 monoclonal pool detects intracellular pool of antigen in permeabilised HBEC-5i. Panels A+B: **Green** = Mouse IgG1 isotype control (100 μ g/ml). **Blue** = DAPI nuclear staining. Panels C+D: **Green** = Commercial α -CR1 monoclonal pool (100 μ g/ml). **Blue** = DAPI nuclear staining. Fixed permeabilised HBEC-5i. Panels A+C x20 magnification. Panels B+D x 40 magnification.

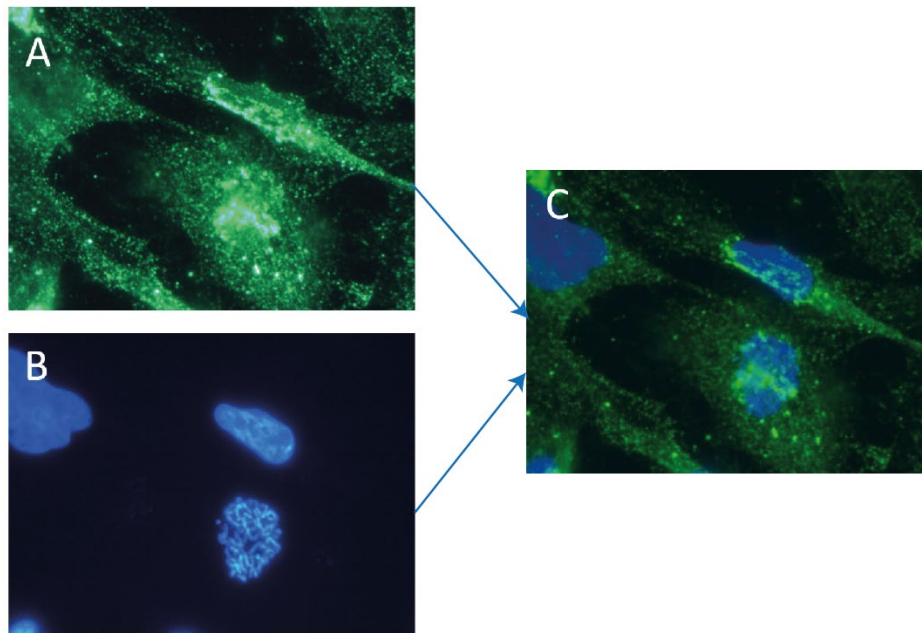


Figure 4-12. α -CR1 monoclonal pool stains dividing HBEC-5i. **Green** = commercial α -CR1 monoclonal pool (100 μ g/ml). **Blue** = DAPI nuclear staining. **Panel A** = α -CR1 monoclonal pool staining. **Panel B** = DAPI DNA staining identifies dividing cell. **Panel C**: composite of A and B. Fixed permeabilised HBEC-5i. x100 magnification.

To quantify the staining of HBEC-5i by α -CR1 monoclonal antibodies, flow cytometry was performed using live HBEC-5i cells as outlined in 4.4.11.

The gating was performed as follows. Firstly, cells that lay at the boundaries of visualisation were excluded using the gate "Visible." The amount of Hoechst detected in these visible cells was then used to assign them to where they were in the cell cycle (G0-G1, S and G2-M phases) allowing exclusion of apoptotic cells and debris. Cells in cycle were then gated on PE fluorescence to categorise them into "CR1 positive" or "CR1 negative." Figure 4-13 shows an example of the gating strategy used.

Lignocaine-lifted non-permeabilised HBEC-5i stained with the α -CR1 monoclonal pool showed a modest increase in MFI over those stained with an isotype control (Figure 4-14 Panel A), which was greatly increased by permeabilisation with Triton™ X-100 (Figure 4-14 Panel B). MFI was also increased when HBEC-5i were lifted, cooled and then rewarmed to 37°C (Figure 4-14 Panel C). However, MFI was reduced when cells were lifted with trypsin rather than lignocaine, suggesting that antigen recognised was trypsin-sensitive (Figure 4-14 Panel D).

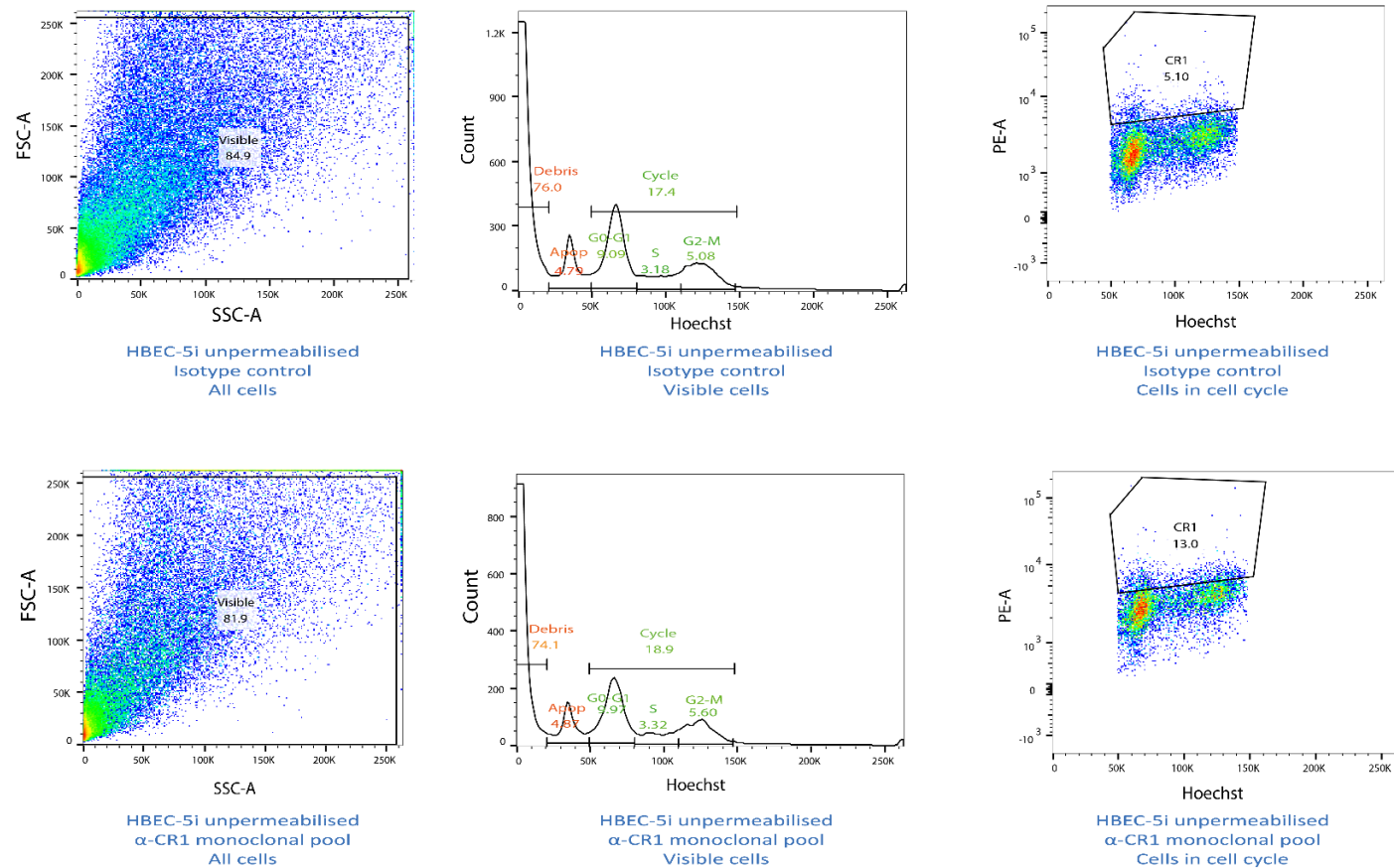


Figure 4-13. Example of gating strategy used for HBEC-5i flow cytometry experiments.

Unpermeabilised HBEC-5i stained with 100 μ g/ml isotype control (top row) or α -CR1 antibody pool (bottom row) with 0.07 μ g/ml PE-conjugated rat α -mouse IgG as secondary antibody. Only visible cells determined to be in cycle were included in the analysis. CR1 gate = cells determined to be CR1 positive by flow cytometry.

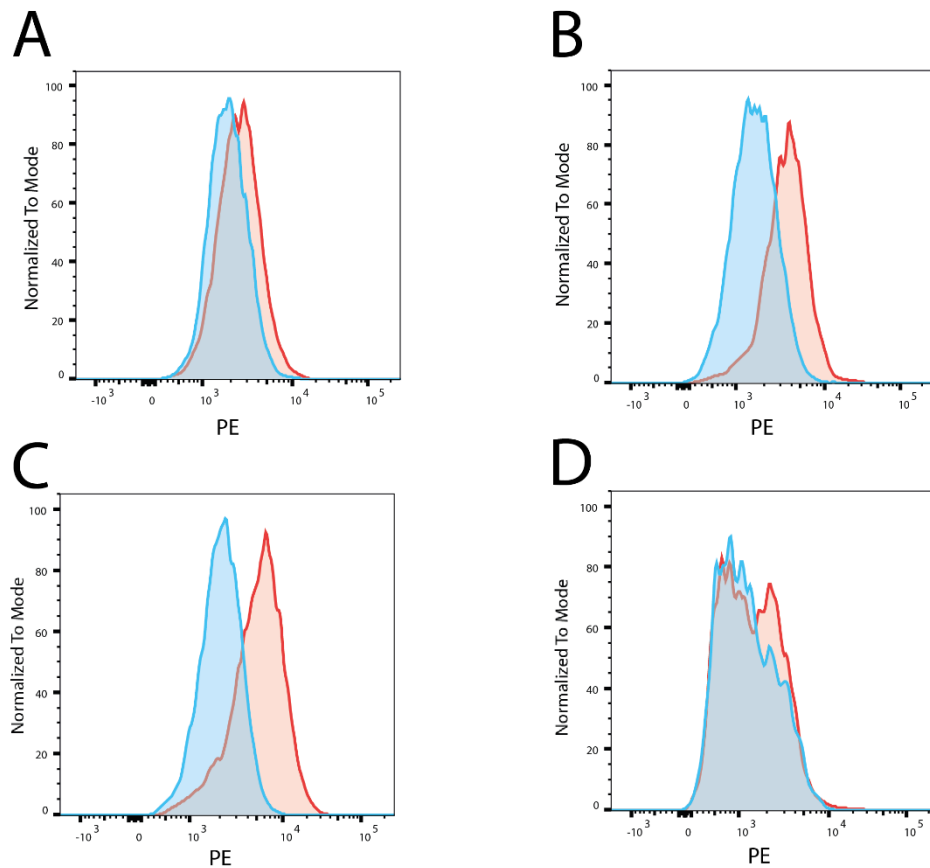


Figure 4-14. Staining of HBEC-5i by an α -CR1 antibody pool is increased with permeabilisation and heat treatment but decreased by treatment with trypsin.

Red histograms - α -CR1 antibody pool (J3D3, To5, E11, 57F, 9H3, HB85G2), 100 μ g/ml.

Blue histograms – mouse IgG1 isotype control (MOPC-21, 100 μ g/ml).

Panel A – Unpermeabilised HBEC-5i. **Panel B** – HBEC-5i cells permeabilised with Triton™ X-100.

Panel C – Unpermeabilised HBEC-5i cooled to 4°C then heated to 37°C for 5 minutes

Panel D – Unpermeabilised HBEC-5i cells treated with trypsin EDTA for 5 minutes.

All cells lignocaine-lifted and then treated as described. Data shown is from all cells in cell cycle.

4.5.2.1 Epitope on HBEC-5i recognised by α -CR1 monoclonal antibodies is the same molecular weight as CR1

Western blotting was then undertaken to ascertain the molecular weight of the antigen being detected by the pool of α -CR1 monoclonal antibodies. Twenty μ l of HBEC-5i lysate, RCHO lysate (negative control), CR1-CHO lysate (positive control) and 100 ng of recombinant CR1 were resolved by SDS-PAGE on a non-reducing 8% polyacrylamide gel at 125 V for 100 minutes followed by overnight transfer to a nitrocellulose membrane at 15 V at 4°C. The membrane was stained with the commercial α -CR1 monoclonal antibody pool (J3D3, To5 and E11), each used at a concentration of 0.1 μ g/ml with a final concentration of 0.3 μ g/ml. The membrane was incubated overnight at 4°C, followed by detection with 1:8000 IRDye 800CW (green) goat anti-Mouse IgG (H + L) antibody and developed using the Odyssey imaging system (see 4.4.13).

A specific band was seen in the positive control (CR1-CHO lysate) at \sim 250 kDa. A band migrating at a slightly lower apparent molecular weight was also seen in the HBEC-5i lysate lane, suggesting that the presence of CR1. CR1 is known to vary slightly in molecular weight in different cell types as a result of glycosylation differences (Dykman et al., 1983a; Lublin et al., 1986). In addition, a strong lower band was seen in the HBEC-5i lysate lane at \sim 170 kDa at a similar molecular weight to a band in both the CR1-CHO and RCHO lysate lanes. Variations on this experiment were conducted on four occasions. A representative blot is shown in Figure 4-15.

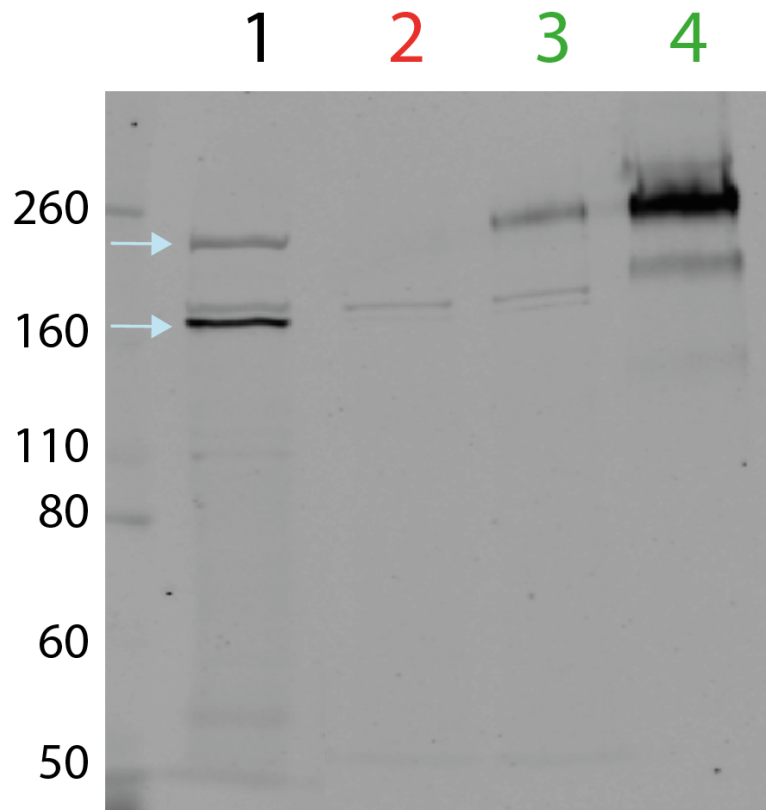


Figure 4-15. Western blot of HBEC-5i lysate reveals a band of the same molecular weight as CR1. Western blot probed with commercial α -CR1 pool (E11, J3D3 and To5) concentration 1 μ g/ml 16 hours at 4°C. Blue arrows indicate bands of interest (see text).

Non-reducing 8% polyacrylamide gel.

Lane 1 = HBEC-5i lysate.

Lane 2 = negative control (RCHO lysate).

Lane 3 = positive control (CR1-CHO lysate).

Lane 4 = positive control (recombinant CR1 100 ng).

4.5.3 HBEC-5i together with factor I can cleave C3b to C3dg, but this is not inhibited by the α -CR1 monoclonal antibody 3D9

The next step of the investigation was to determine whether the putative CR1 expressed by HBEC-5i was functional. One of the functions of CR1 is to act as a cofactor with factor I in the breakdown of iC3b (reviewed in section 4.4.14.1). In the presence of CR1, factor I will act as a cofactor with it to breakdown iC3b to C3dg. Therefore, the detection of C3dg in such an assay acts as a proxy for the presence of functional CR1.

An assay to assess C3b degradation was performed as described in 4.4.14.2. To investigate the possibility of membrane-bound or intracellular CR1 in HBEC-5i cells having different cofactor abilities, the experiment was performed in parallel with both permeabilised and unpermeabilised cells. To further examine whether the breakdown of C3b was CR1-specific, experiments were also performed with HBEC-5i incubated with α -CR1 monoclonal antibody 3D9 (which blocks the C3b binding site on CR1) or relevant mouse IgG1 isotype control (final concentration 10 μ g/ml). CR1-CHO cells were used as a positive control and RCHO as a negative control. Variations on this experiment were performed four times and representative western blots are shown in Figure 4-16.

CR1-CHO cells were able to breakdown C3b to C3dg when coincubated with factor I (positive control). The 3D9 antibody inhibited this breakdown (green circled bands), but the isotype control had no blocking effect, implying the breakdown of iC3b to C3dg by CR1-CHO cells was specifically performed by CR1. In contrast, HBEC-5i cells were able to breakdown C3b to C3dg in the presence of factor I, but this was not affected by the presence of 3D9 antibody (blue circled bands), suggesting this process may not be CR1 specific on HBEC-5i cells. Negative control RCHO cells were unable to degrade C3b to C3dg in the presence of factor I.

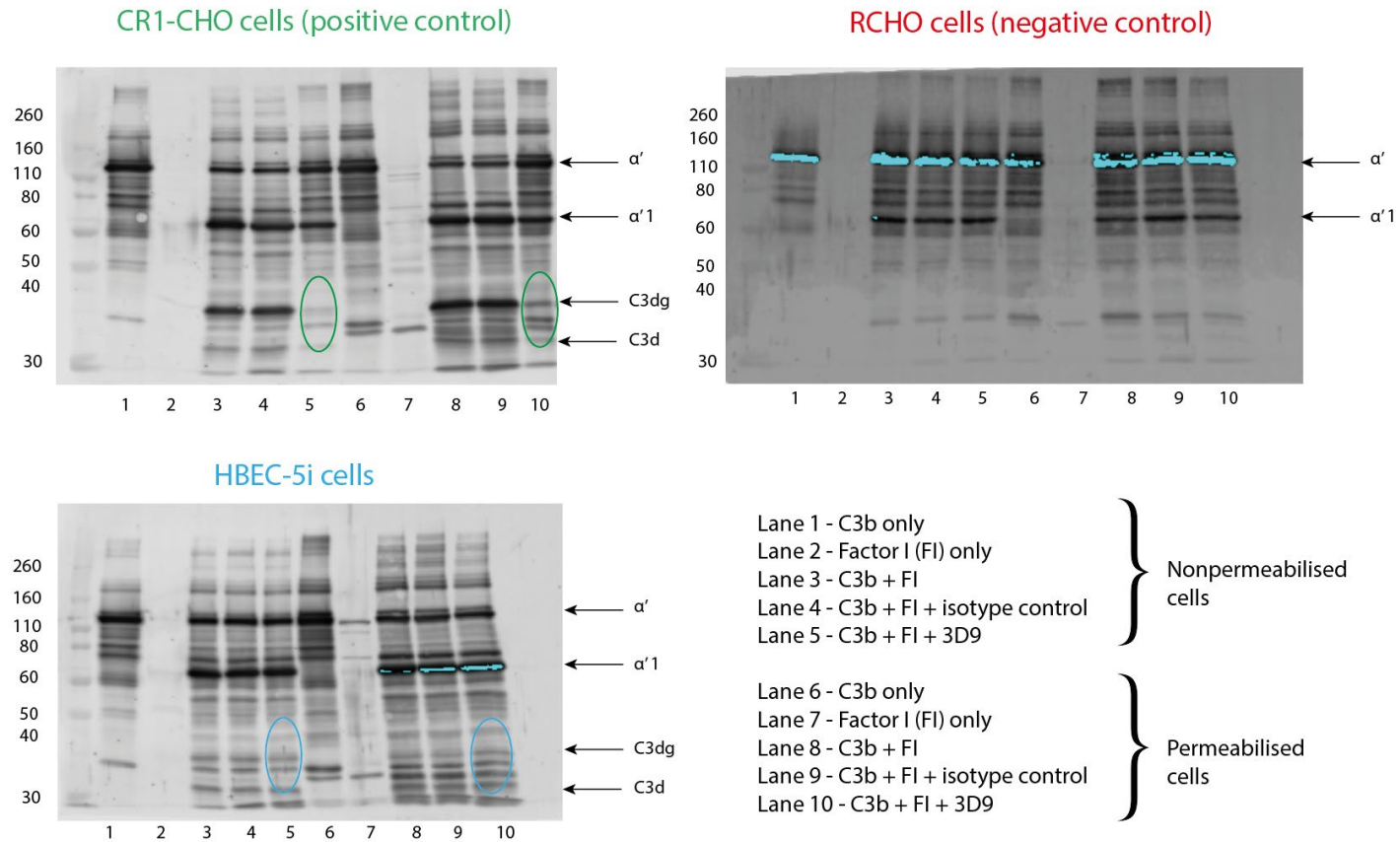


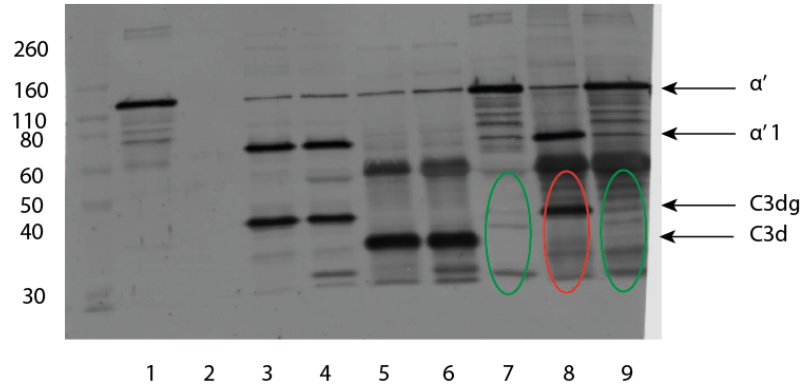
Figure 4-16. HBEC-5i can breakdown C3b to C3dg with factor I, but this is not inhibited by the α -CR1 monoclonal antibody 3D9. CR1-CHO (positive control) and HBEC-5i cells are both able to cleave C3b to C3dg but 3D9 only inhibits this process in CR1-CHO cells (green circles), not in HBEC-5i (blue circles). As expected, RCHO cells (negative control) are unable to cleave C3b to C3dg. Concentrations: C3b - 27.5 μ g/ml, factor I - 22 μ g/ml, mouse IgG1 isotype - 10 μ g/ml and 3D9 α -CR1 monoclonal antibody 10 μ g/ml. Components/antibodies incubated with cells for 7 hours at 37°C. Reducing 10% polyacrylamide gels. Western blot of supernatants probed with 11.5 μ g/ml α -C3d rabbit polyclonal antibody overnight.

One possibility for the inability of 3D9 to block iC3b breakdown by HBEC-5i together with factor I is the presence of an alternative cofactor for this degradation process. Factor H has been reported to act as a cofactor with factor I to breakdown iC3b to C3dg, but only in low ionic strength conditions (Ross et al., 1982), which were not used in this assay. More recent work has also identified von Willebrand factor (vWF) as a cofactor with Factor I to degrade iC3b to C3dg (Feng et al., 2015). HBEC-5i cells produce vWF (see Figure 4-8) making this a potential alternative to CR1 in the cleavage process.

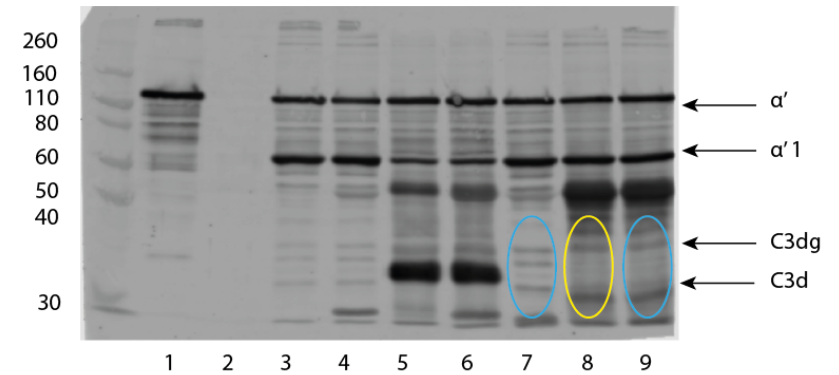
An extension to the C3b degradation assay was performed to block vWF cofactor activity by incubating cells with α -vWF antibody. As the portion of the vWF molecule involved in cofactor activity has not been identified, a polyclonal α -vWF antibody was chosen to block as many sites as possible. Recombinant CR1 was used as a positive control at 1 μ g/ml with C3b and FI concentrations unaltered. The effects of 3D9 and its isotype control were compared to that of the polyclonal α -vWF antibody and its rabbit IgG control. All antibodies were used at 100 μ g/ml.

Western blots are shown in Figure 4-17. As anticipated, the 3D9 antibody was able to block C3dg production when recombinant CR1 was used as a cofactor (green circled bands) but no effect was seen on C3dg production when the reaction was incubation with α -vWF (red circled band). The 3D9 antibody (even at a higher concentration than previously) had no effect on C3dg production by non-permeabilised HBEC-5i (blue circled bands). No effect on C3dg production was seen in non-permeabilised HBEC-5i incubated with α -vWF antibody (yellow circled band), implying that vWF is unlikely to be acting as a cofactor for factor I for HBEC-5i, leaving this cofactor unidentified. (NB - Results for permeabilised HBEC-5i mirror those for non-permeabilised HBEC-5i, data not shown).

Recombinant CR1 (positive control)



HBEC-5i cells - nonpermeabilised



- Lane 1 - C3b only
- Lane 2 - Factor I (FI) only
- Lane 3 - C3b + FI
- Lane 4 - C3b + FI + mouse isotype control
- Lane 5 - C3b + FI + rabbit isotype control
- Lane 6 - C3b + FI + mouse + rabbit isotype controls
- Lane 7 - C3b + FI + 3D9
- Lane 8 - C3b + FI + α -vWF
- Lane 9 - C3b + FI + 3D9 + α -vWF

Figure 4-17. Polyclonal α -vWF antibody is unable to inhibit the breakdown of C3b \rightarrow C3dg by HBEC-5i.

No effect on C3dg production was seen when α -vWF polyclonal antibody was incubated with recombinant CR1 (red circle) or HBEC-5i (yellow circle).

α -CR1 monoclonal antibody 3D9 was able to inhibit the breakdown of C3b \rightarrow C3dg for recombinant CR1 (green circles) but not for HBEC-5i cells (blue circles).

Concentrations: C3b - 27.5 μ g/ml, factor I - 22 μ g/ml, 3D9 α -CR1 monoclonal antibody, α -vWF polyclonal antibody, mouse IgG1 isotype and rabbit IgG isotype, all used at 100 μ g/ml. Components/antibodies incubated with cells for 7 hours at 37°C. Reducing 10% polyacrylamide gels.

Western blot of supernatants probed with 11.5 μ g/ml α -C3d rabbit polyclonal antibody overnight

4.5.4 Mass spectrometry of HBEC-5i lysate fails to detect CR1

Mass spectrometry was performed to identify the HBEC-5i antigen being detected by the commercial pool of α -CR1 antibodies. Hypoxic lignocaine-lifted HBEC-5i lysates were resolved in duplicate on non-reducing 8% polyacrylamide gels, with one gel subsequently transferred onto nitrocellulose and probed with the commercial α -CR1 pool (1 μ g/ml for 18 hours) and the other gel stained with InstantBlue (as detailed in 4.4.17). CR1-CHO cell and RCHO cell lysates served as positive and negative controls respectively. The western blot and the stained gel were compared and gel sections corresponding to the bands were excised and sent for mass spectrometry analysis.

Figure 4-18 shows the corresponding western blot of the cell lysates and the gel slices excised. Three slices were taken from the HBEC-5i lane gel; one spanning \sim 220-260kDa (slice A, corresponding to the upper band recognised by α -CR1 antibodies at \sim 250 kDa), one spanning \sim 160-190 kDa (slice C, corresponding to the lower band detected by α -CR1 antibodies at \sim 170 kDa) and the gel slice in between these spanning \sim 190-220 kDa (slice B). As a positive control, the gel slice corresponding to the upper band on the CR1-CHO lane was also sent (slice D, spanning \sim 220-260 kDa).

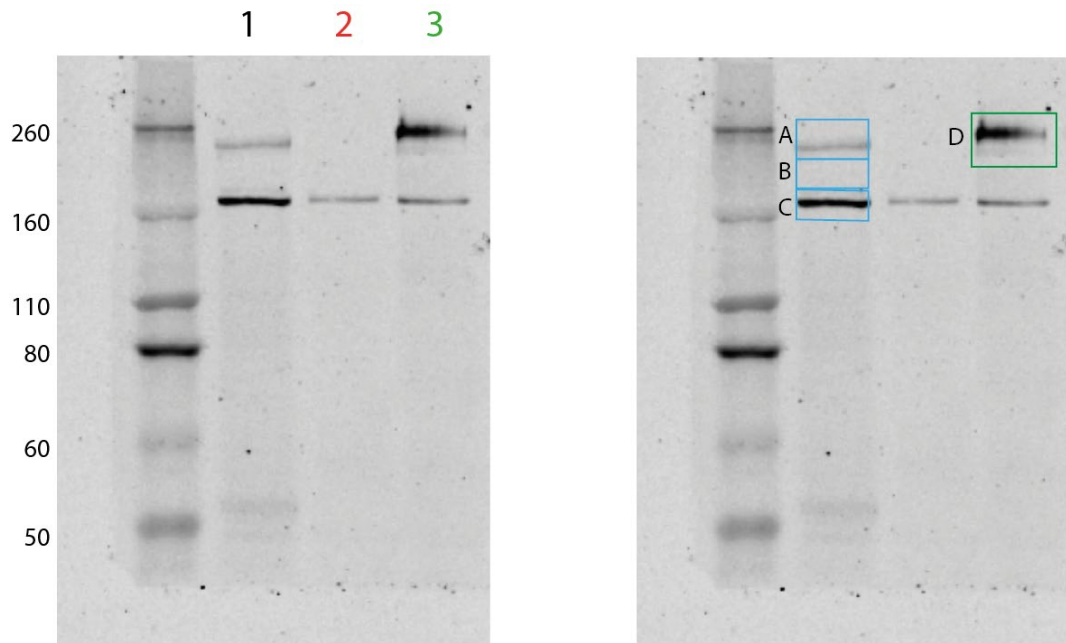


Figure 4-18. Western blot of HBEC-5i and CR1-CHO lysates illustrating gel slices sent for mass spectrometry

Lane 1 = HBEC-5i lysate, **Lane 2** = RCHO lysate (negative control),
Lane 3 = CR1-CHO lysate (positive control).

Duplicate SDS gels of cell lysates were run. One gel subsequently underwent western blotting and staining with E11, J3D3 and To5 α -CR1 antibodies 1 μ g/ μ l overnight.

The corresponding gel bands of interest (bands A, B and C) were then excised from the HBEC-5i lane of the untransferred gel and sent for mass spectrometry. The upper band in the CR1-CHO lane (band D) was sent as a positive control. Non-reducing 8% polyacrylamide gel.

Primary mass spectrometry analysis revealed a very complex, high molecular weight mixture in all four slices. The peptide fragment masses were searched against all human proteins in the NCBIprot database. CR1 was not detected in any of the three HBEC-5i samples. However, CR1 was also not detected in the positive control CR1-CHO sample by this approach. Tables of human protein matches for each of the gel slices are detailed in Appendix 8.1.

In a complex, high molecular weight mixture, the detection of a protein with relatively low abundance can be challenging. To increase the chance of detection, the CR1 amino acid sequence from NCBI (<http://www.ncbi.nlm.nih.gov/nucleotide/767908442>) was added to an internal database of \sim 4800 human peptides curated by the BSRC Mass Spectrometry Facility and acquisition data files for the samples reanalysed. Comparison of sample

peptides against this smaller database is reserved for the detection of low quantities of protein in a sample, as database size will affect probability scoring. This method resulted in the detection of CR1 in the CR1-CHO positive control sample, ranking 12th in this smaller database. Four peptides corresponding to CR1 were identified, as shown below Table 4-5. However, scores for these peptides were extremely low. The location of these peptides in the CR1 amino acid sequence is shown in Figure 4-19. Even using this more restrictive analysis, no peptides matching CR1 were identified in any of the HBEC-5i samples. Matched proteins for this reanalysis are detailed in Appendix 8.1.

Observed m/z	Mr (expt)	Mr (calc)	Score	Peptide
608.2754	1214.5362	1214.5390	41	K.VSFVCDEGFR.L
639.9083	1277.8020	1277.8071	72	R.VLLPLNLQLGAK.V
656.9000	1311.7854	1311.7914	48	R.VLFPLNLQLGAK.V
720.3756	1438.7367	1438.7456	97	R.SLFSLNEVVEFR.C

Table 4-5. CR1 peptides detected in the CR1-CHO positive control by mass spectrometry. m/z = mass to charge ratio. Mr (expt) = expected molecular weight, Mr (calc) = calculated molecular weight.

As a final approach, the HBEC-5i samples were reanalysed using a product ion scan. This method restricted the apparatus to only fragment peptides of the same mass as those four previously identified in the CR1-CHO control. The anticipated fragmentation pattern for each of the peptides was retrieved from the Mascot server. Peptide elution times were determined by running a product ion scan on the CR1-CHO positive control and noting when each peptide eluted. The same restricted product ion scan was run on the HBEC-5i samples and ion chromatograms were examined from the elution times of interest and compared against the expected Mascot predicted fragmentation. None of the 4 CR1 peptides were identified in any of the HBEC-5i samples. As such, despite extensive efforts, no CR1 peptides could be detected by mass spectrometry of HBEC-5i lysates. An example peptide ion scan analysis is shown in Figure 4-20 for the peptide K.VSFVCDEGFR.L.

1	MCLGRMGASS	FRSPEFVGPP	APGLPFCCGG	SL LAVVVLLA	LPVANGQCNA
51	FEWLFFARPT	NLTDEFEFPI	GYLNYECRP	GYSGRPFSII	CLKNSVWTGA
101	KDRCRRKSCR	NPPDFVNGMV	HVIRGIQFGS	QIKYSCTRGY	RLIGSSSATC
151	IISGDTVIND	NETPICDRIP	CGLPPTITNG	DFISTNRENF	HYGSVVTYRC
201	NPGSGGRKVF	ELVGEPsiYC	TSNDDQVGW	SGPAPQCIIP	NKCTPPNVEN
251	GILVSDNRS L FSLNEVVEFR	CQPGFVMKGP	RRVKQALNK	WEPELPSCSR	
301	VCQPPFDVLH	AERTQRDKDN	FSPGQEVFYS	CEPGYDLRGA	ASMRCTPQGD
351	WSPAAPTCEV	KSCDDFMGQL	LNGRVLFVFN	LQLGAKVDFV	CDEGFQLKGS
401	SASYCVLAGM	ESLWNSVFPV	CEQIFCPSP	VIPNGRHTGK	FLEVFPFGKI
451	VNYTCDFPHD	RGTSFDLIGE	STIRCTSDPQ	GNGVWSSPAP	RCGILGHCQA
501	PDHFLFAKLK	TQTNASDFPI	GTSLKYECP	EYGRPFSIT	CLDNLVWSSP
551	KDVCKRKSK	TPPDFVNGMV	HVIDIQVGS	RINYSCTTGH	RLIGHSSAEC
601	ILSGNAAHWS	TKPPICQRIP	CGLPPTIANG	DFISTNRENF	HYGSVVTYRC
651	NPGSGGRKVF	ELVGEPsiYC	TSNDDQVGW	SGPAPQCIIP	NKCTPPNVEN
701	GILVSDNRS L FSLNEVVEFR	CQPGFVMKGP	RRVKQALNK	WEPELPSCSR	
751	VCQPPFDVLH	AERTQRDKDN	FSPGQEVFYS	CEPGYDLRGA	ASMRCTPQGD
801	WSPAAPTCEV	KSCDDFMGQL	LNGRVLFVFN	LQLGAKVDFV	CDEGFQLKGS
851	SASYCVLAGM	ESLWNSVFPV	CEQIFCPSP	VIPNGRHTGK	FLEVFPFGKI
901	VNYTCDFPHD	RGTSFDLIGE	STIRCTSDPQ	GNGVWSSPAP	RCGILGHCQA
951	PDHFLFAKLK	TQTNASDFPI	GTSLKYECP	EYGRPFSIT	CLDNLVWSSP
1001	KDVCKRKSK	TPPDFVNGMV	HVIDIQVGS	RINYSCTTGH	RLIGHSSAEC
1051	ILSGNAAHWS	TKPPICQRIP	CGLPPTIANG	DFISTNRENF	HYGSVVTYRC
1101	NPGSGGRKVF	ELVGEPsiYC	TSNDDQVGW	SGPAPQCIIP	NKCTPPNVEN
1151	GILVSDNRS L FSLNEVVEFR	CQPGFVMKGP	RRVKQALNK	WEPELPSCSR	
1201	VCQPPFDVLH	AERTQRDKDN	FSPGQEVFYS	CEPGYDLRGA	ASMRCTPQGD
1251	WSPAAPTCEV	KSCDDFMGQL	LNGRVLFVFN	LQLGAKVDFV	CDEGFQLKGS
1301	SASYCVLAGM	ESLWNSVFPV	CEQIFCPSP	VIPNGRHTGK	FLEVFPFGKA
1351	VNYTCDFPHD	RGTSFDLIGE	STIRCTSDPQ	GNGVWSSPAP	RCGILGHCQA
1401	PDHFLFAKLK	TQTNASDFPI	GTSLKYECP	EYGRPFSIT	CLDNLVWSSP
1451	KDVCKRKSK	TPPDFVNGMV	HVIDIQVGS	RINYSCTTGH	RLIGHSSAEC
1501	ILSGNTAHWS	TKPPICQRIP	CGLPPTIANG	DFISTNRENF	HYGSVVTYRC
1551	NLGSRGKRVF	ELVGEPsiYC	TSNDDQVGW	SGPAPQCIIP	NKCTPPNVEN
1601	GILVSDNRS L FSLNEVVEFR	CQPGFVMKGP	RRVKQALNK	WEPELPSCSR	
1651	VCQPPFEILH	GEHTPSHQDN	FSPGQEVFYS	CEPGYDLRGA	ASLHCTPQGD
1701	WSPAAPCAV	KSCDDFLGQL	PHGRV LFPLN	LQLGAKVSFV	CDEGFRLKGS
1751	SVSHCVLVGM	ESLWNSVFPV	CEHIFCPNPP	AILNGRHTGT	PSGDIPIYKKE
1801	ISYTCDFPHD	RGMTFNLI	STIRCTSDPH	GNGVWSSPAP	RCELSVRAGH
1851	CKTPEQFFFA	SFTIPINDFE	FFVGTSLN	CRPGYFGRMF	SISCLENLVW
1901	SSVEDNCRK	SCGPPPEFPN	GMVHINTDTQ	FGSTVNYSCN	EGFRLIGSPS
1951	TTCLVSGMNV	TWDRKAPICE	IISCEPPPTI	SNGDFYSNMR	TSFHNGTVVT
2001	YQCHTGPDGE	QLFELVGER	IYCTSKDDQV	GVWSSPPPRC	ISTNKCTAPE
2051	VENAIRVPGN	RSFPTLTEII	RFRQPGFVM	VGSHTVQCQT	NGRWGPKLPH
2101	CSRVCQPPPE	ILHGEHTLSH	QDNFSPGQEV	FYSCEPSYDL	RGAASLHCTP
2151	QGDWSPEAPR	CTVKSDDFL	GQLPHGR VLL	PLNLQLGAKV	SFVCEGFRL
2201	KGRSASHCVL	AGMRALWNS	VPVCEQIFCP	NPPAILNGRH	TGTPFGDIPY
2251	GKEISYACDT	HPDRGMTFNL	IGESSIRCTS	DPQNGVWSS	PAPRCELSVP
2301	AACPHPPRIQ	NGHYIGGHVS	LYLPGMTISY	ICDPGYLLVG	KGFIFCTDQG
2351	IWSQLDHYCK	EVNCSFPLFM	NGISKELEMK	KVYHYGDYVT	LKCEDGYTLE
2401	GSPWSQCQAD	DRWDFPLAKC	TSRTHDALIV	GTLSGTIFFI	LLIIFLSWII
2451	LKHRKGVLP				

Figure 4-19. Peptides matching the CR1 amino acid sequence identified in the positive control by mass spectrometry.

Matched peptides are shown in **bold red**.

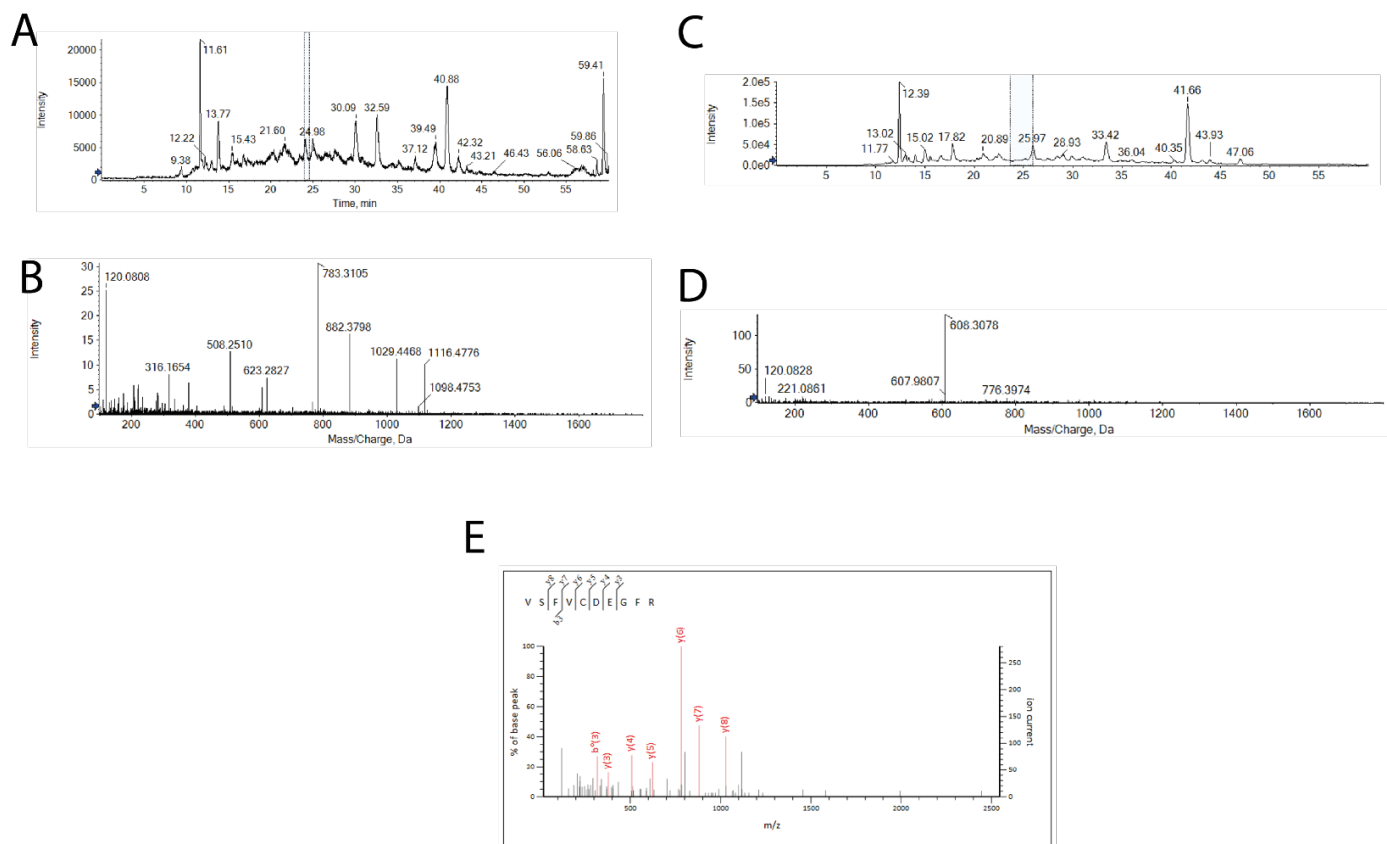


Figure 4-20. CR1 peptide fragments can be identified in CR1-CHO sample but not in HBEC-5i. Peptide ion scans of CR1-CHO and HBEC-5i sample A for peptide fragment 608 m/z (see Table 4-5).

Panel A – Peptide ion scan shows peptide 608 m/z eluting at 24 minutes for CR1-CHO positive control (dotted rectangle). **Panel B** – Tandem mass spectrometry fragmentation pattern from 24 minutes for CR1-CHO. **Panel C** – Peptide ion scan for HBEC-5i sample A, 24 minutes marked by blue shaded area. **Panel D** – Tandem mass spectrometry fragmentation pattern for 24 minutes for HBEC-5i sample A. **Panel E** – Expected tandem mass spectrometry fragmentation pattern for 680 m/z peptide (from Mascot). **Panel B matches Panel E**, (i.e. detection of a CR1 peptide in the CR1-CHO sample). **Panel D does not match Panel E** (i.e. this CR1 peptide cannot be detected in HBEC-5i sample A).

4.5.5 E11 is the only α -CR1 monoclonal antibody to recognise an HBEC-5i antigen

Given the failure to detect CR1 in functional assays and mass spectrometry, I returned to the antibody-based assays to investigate the possibility that artefactual results had been obtained. To investigate whether all three of the α -CR1 monoclonal antibodies within the commercial pool were able to recognise HBEC-5i, staining was carried out with individual antibodies (J3D3, To5 and E11). The α -CR1 antibody 3D9 was also examined. In addition to the separate antibodies, the pooled α -CR1 monoclonal antibody staining pattern was compared to the staining of a pool of isotype controls, to ascertain whether the use of multiple antibodies might contribute to the staining pattern of the α -CR1 pool. Two mouse IgG1 monoclonal antibodies to PfEMP1 epitopes (KE6 and TC7, which would not be expected to recognise human antigens) were included in this pool of isotype controls.

HBEC-5i on coverslips were separately stained with J3D3, To5, E11, 3D9 and MOPC-21 mouse IgG1 isotype control at 16.7 μ g/ml. In parallel, HBEC-5i were stained with either the α -CR1 monoclonal pool (J3D3, To5 and E11) at a final concentration of 50 μ g/ml, MOPC-21 mouse IgG1 isotype control at 50 μ g/ml, or an isotype control pool (consisting of MOPC-21 mouse IgG1 isotype control, KE6 and TC7) at a final concentration of 50 μ g/ml. Representative images are shown in Figure 4-21.

Of the three α -CR1 antibodies comprising the pool, only E11 recognised an antigen on permeabilised HBEC-5i cells (Figure 4-21). J3D3, To5 and 3D9 did not stain above the level of the isotype control. The E11 staining pattern was identical to that of the α -CR1 pool, suggesting that all the signal from experiments using this pool may be coming from a single antibody. The pooled isotype control did give higher background staining than the MOPC-21 isotype control alone (Figure 4-22), suggesting the use of a single isotype control may have underestimated the background staining that would be expected from a pool of antibodies.

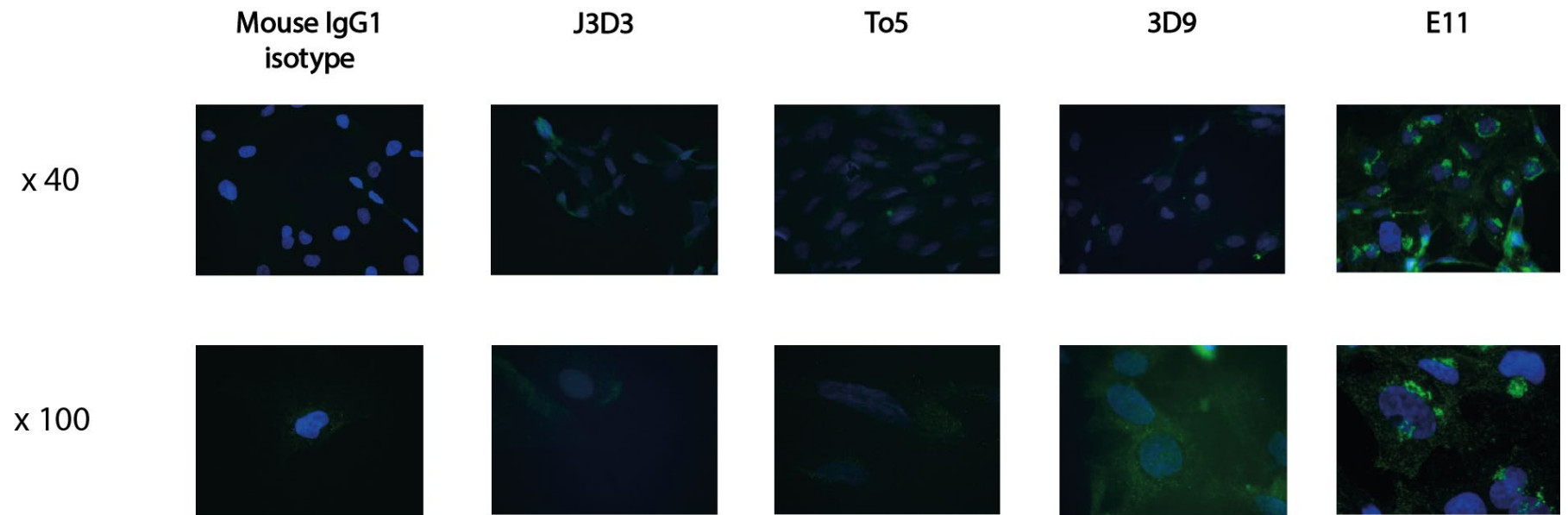


Figure 4-21. Only E11 recognises an antigen on HBEC-5i when staining is performed with individual α -CR1 monoclonal antibodies.

Mouse IgG1 isotype control, J3D3, To5, 3D9 and E11 all used at 16.7 μ g/ml.

Fixed permeabilised HBEC-5i.

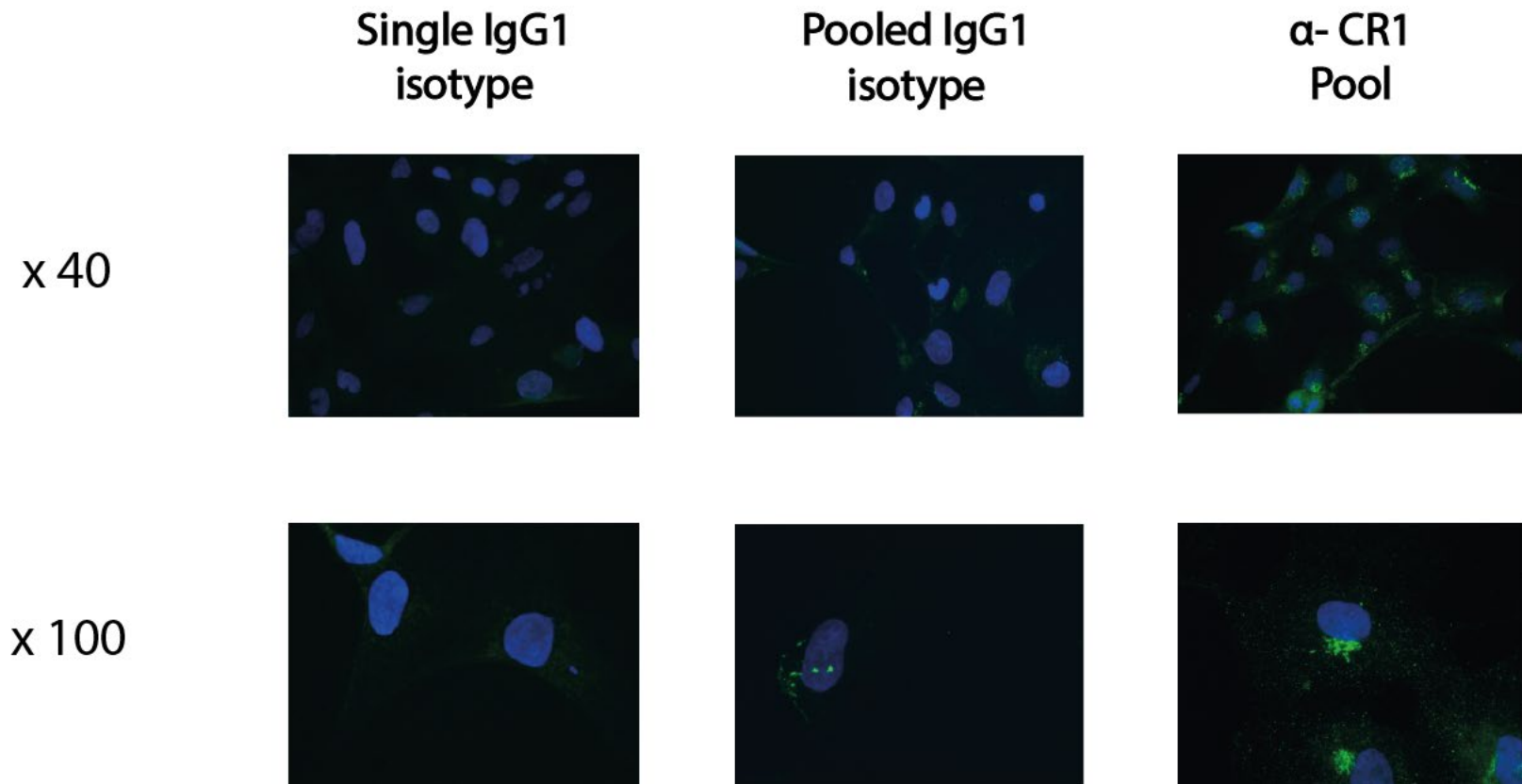


Figure 4-22. A pool of isotype control antibodies increases background staining of HBEC-5i compared to a single isotype control antibody. Single isotype control = MOPC-21 mouse IgG1 isotype control. Pooled isotype control contains MOPC-21 plus KE6 and TC7 mouse IgG1 monoclonal antibodies against PfEMP1 epitopes (should not recognise human antigens). α -CR1 monoclonal pool contains J3D3, To5 and E11 monoclonal antibodies. Final concentrations for each experiment = 50 μ g/ml. Fixed permeabilised HBEC-5i.

IFA data suggested that only E11 was recognising an epitope on HBEC-5i cells. To investigate the possibility that the fixation process was influencing HBEC-5i epitopes (or changing their availability to antibodies), a series of western blots was performed using HBEC-5i lysates probed with individual antibodies.

As initial experiments had suggested that α -CR1 antibodies stained hypoxic HBEC-5i more strongly (Figure 4-10) lysates were made from HBEC-5i as described in 4.4.9) which had been cultured for 24 hours in hypoxic conditions (1% O₂, 3% CO₂ and 96% N₂). Hypoxic HBEC-5i lysates that had been lifted with lignocaine or with trypsin were compared. RCHO lysate was used as a negative control and CR1-CHO lysate as a positive control. Lysates were resolved by SDS-PAGE on non-reducing 10% polyacrylamide gels, transferred overnight onto a nitrocellulose membrane and probed with individual α -CR1 antibodies (as described in 4.4.13). Antibodies were used at concentrations between 0.3 and 1.9 μ g/ml and the membrane incubated 18 to 48 hours depending on the experiment. Some experiments examined whether the composition of the cell lysis buffer (PMSF or PIC) affected antibody binding.

Cell lifting conditions, lysis buffers, antibody concentrations and incubation times are detailed for each experiment in the respective figure legends.

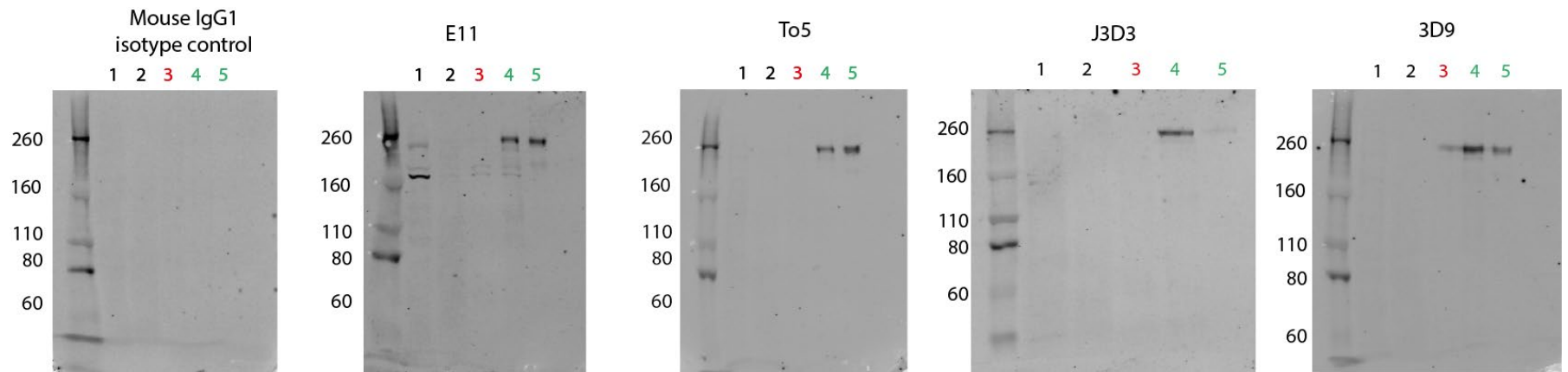


Figure 4-23. Only E11 recognises an antigen in HBEC-5i lysates when western blotting is performed with individual α -CR1 monoclonal antibodies.

HBEC-5i lysates probed with monoclonal α -CR1 antibodies E11, To5, J3D3 and 3D9.

Lane 1 Hypoxic HBEC-5i lysate (lignocaine lifted)

Lane 2 Hypoxic HBEC-5i lysate (trypsin lifted)

Lane 3 RCHO lysate (negative control)

Lane 4 CR1-CHO lysate (positive control)

Lane 5 Recombinant CR1 - 10 ng (positive control)

Non-reducing 10% polyacrylamide gels. Antibodies used at 0.3 μ g/ml with 48 hour incubation.

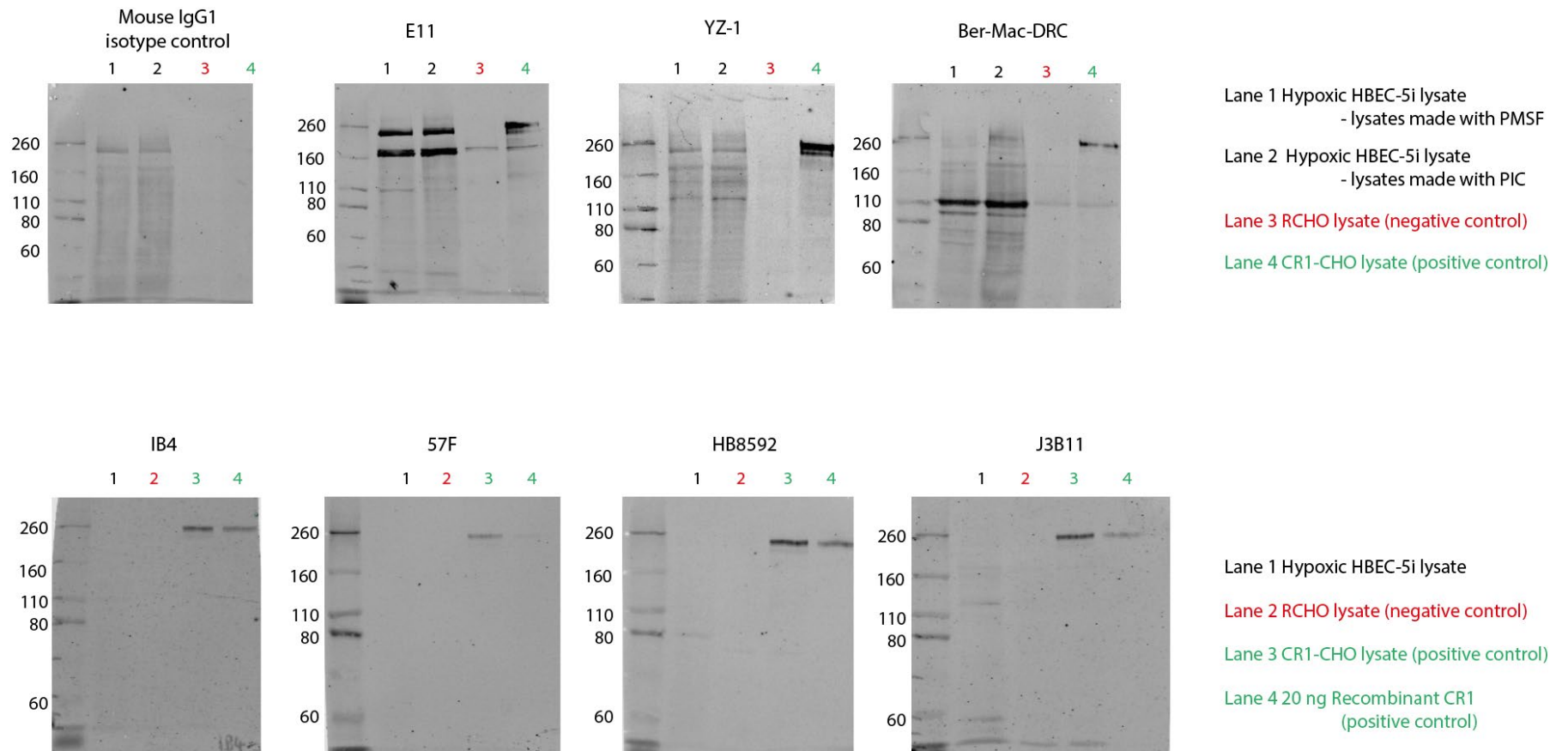


Figure 4-24. Only E11 recognises an antigen in HBEC-5i lysates when western blotting is performed with individual α -CR1 monoclonal antibodies HBEC-5i lysates probed with monoclonal α -CR1 antibodies E11, YZ-1, Ber-Mac-DRC, IB4, 57F, HB8592 and J3B11. All cells lifted with lignocaine. Non-reducing 10% polyacrylamide gels. Antibodies used at 1 μ g/ml with 48 hour incubation. Please note, the top four panels were developed using enhanced chemiluminescent method (ECL) prior to being developed using the Odyssey system which has increased background staining. PMSF = phenylmethylsulfonyl fluoride (protease inhibitor), PIC = protease inhibitor cocktail.

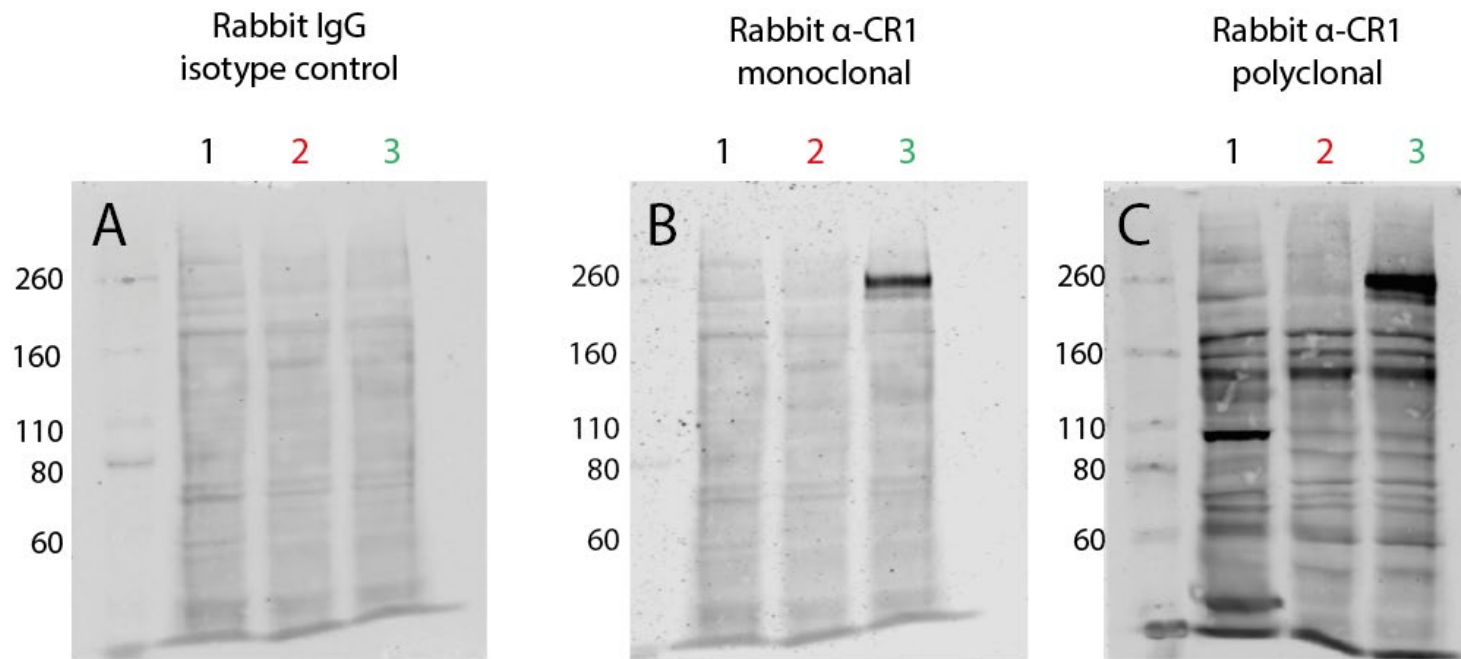


Figure 4-25. Rabbit α -CR1 antibodies do not recognise antigens of a similar molecular weight to CR1 in HBEC-5i lysate.

Lane 1 Hypoxic HBEC-5i lysate

Lane 2 RCHO lysate (negative control)

Lane 3 CR1-CHO lysate (positive control)

All cells lifted with lignocaine. Non-reducing 10% polyacrylamide gels.

Non-immunised rabbit IgG was used as an isotype control. All antibodies were used at a concentration of 1.9 μ g/ml with 18 hour incubation.

NB. Panel B is the same membrane as Panel A (isotype control) which was subsequently reprobed with rabbit monoclonal antibody.

E11 was the only mouse monoclonal α -CR1 antibody to recognise a band at ~250 kDa in lignocaine-lifted hypoxic HBEC-5i lysate of a similar molecule weight to that in the CR1-CHO positive control (Figure 4-23 and Figure 4-24). E11 did not recognise this band in the trypsin-lifted hypoxic HBEC-5i lysate, suggesting that the antigen is trypsin sensitive. However, no other mouse monoclonal α -CR1 antibodies (To5, J3D3, 3D9, YZ-1, Ber-Mac-DRC, IB4, 57F, HB8592 or J3B11) identified any proteins of a similar molecular weight to CR1 (Figure 4-23 and Figure 4-24). It appears that, as with the IFAs, all the signal from the α -CR1 commercial pool of antibodies is coming from monoclonal antibody E11.

Hypoxic HBEC-5i lysate probed with monoclonal rabbit α -CR1 antibody showed no difference to the isotype control (Figure 4-25). Probing with polyclonal rabbit α -CR1 antibody identified a band just below 260 kDa, but a band at this molecular weight was also seen in a fainter form on the isotype control membrane.

To further explore whether the antigen recognised by E11 was the same on HBEC-5i cells as on CR1-CHO cells, the effect of heat on the sample was examined.

Lignocaine-lifted HBEC-5i, CR1-CHO and RCHO lysates were either heated at 95°C for 7 minutes (in non-reducing loading buffer) or not heated prior to resolution on by SDS-PAGE on a non-reducing 8% polyacrylamide gel. Samples were transferred overnight and then stained for 48 hours with E11 or mouse IgG1 isotype control at 1 μ g/ml.

E11 could not recognise an antigen in hypoxic lignocaine-lifted HBEC-5i lysates after they had been heat-treated, but continued to recognise the CR1 antigen in heat-treated CR1-CHO cell lysate, suggesting the antigens on the two cell lines recognised by E11 are not identical (Figure 4-26).

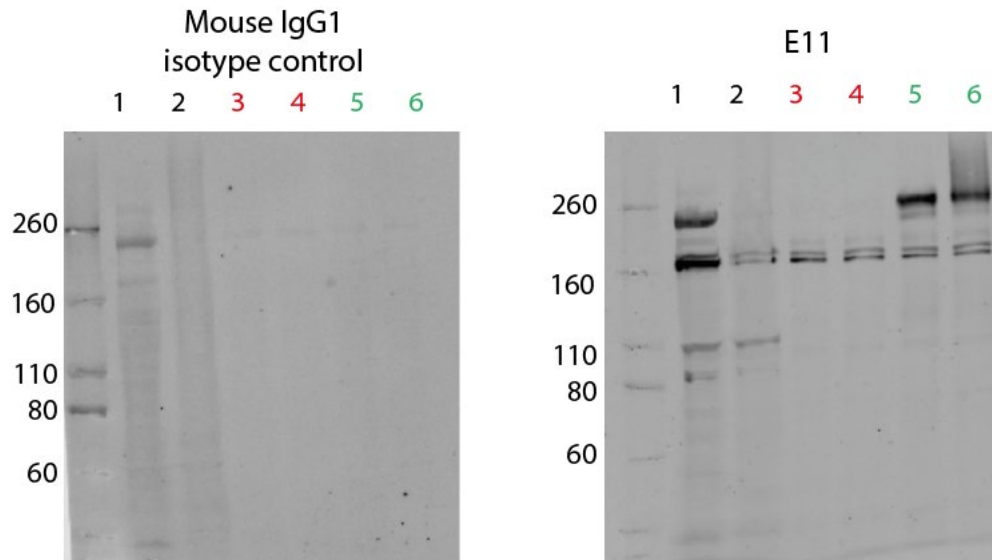


Figure 4-26. E11 does not recognise HBEC-5i antigen after heat treatment.

Lane 1 Hypoxic HBEC-5i lysate - **not boiled**. Lane 2 Hypoxic HBEC-5i lysate – **boiled**.

Lane 3 RCHO lysate (negative control) – **not boiled**. Lane 4 RCHO lysate (negative control) –**boiled**.

Lane 5 CR1-CHO lysate (positive control) – **not boiled**. Lane 6 CR1-CHO lysate (positive control) – **boiled**.

Boiled samples = 7 minutes at 95°C in non-reducing loading buffer.

Non-reducing 10% polyacrylamide gels.

E11 and mouse isotype control used at 1 µg/ml with 48-hour incubation.

All cells lignocaine-lifted.

4.5.6 CR1 siRNA knockdown does not alter E11 staining of HBEC-5i

To further examine the specificity of E11 for CR1, an experiment to silence any expression of CR1 by HBEC-5i with CR1 siRNA was performed. EPCR was chosen as a positive control, as previous successful knockdowns using EPCR siRNA have been performed in this cell line with the same method (Azasi et al., 2018). In addition to incubation of the cells with CR1/EPCR siRNA, two negative transfection controls were performed: incubation with Lipofectamine RNAiMAX transfection agent without any siRNA (to examine the effect this reagent on protein expression (“vehicle only”)) and incubation of the cells with the Lipofectamine RNAiMAX plus control A siRNA (scrambled sequence, control for the transfection process).

Transfections were performed as described in 4.4.15.

IFAs were performed at 24 and 48 hours post-transfection, with cells stained with E11 (and mouse IgG1 isotype control) and α -EPCR (and goat IgG isotype control). The experiment was performed twice. Representative immunofluorescent images from 48 hours after transfection are shown in Figure 4-27 (at x 40 magnification) and in Figure 4-28 (at x100 magnification).

Incubation with the vehicle only had no effect on the subsequent staining patterns of E11 or α -EPCR on their respective knockdowns. Incubation with control A siRNA resulted in a moderate reduction of the α -EPCR staining (suggesting potential broader effects on protein expression by the transfection method), but α -EPCR staining was greatly reduced by incubation with EPCR siRNA. In contrast, incubation with control A siRNA had little effect on E11 staining and incubation with CR1 siRNA had no effect on subsequent staining with E11, supporting the conclusion that E11 is not specific for CR1 in HBEC-5i cells.

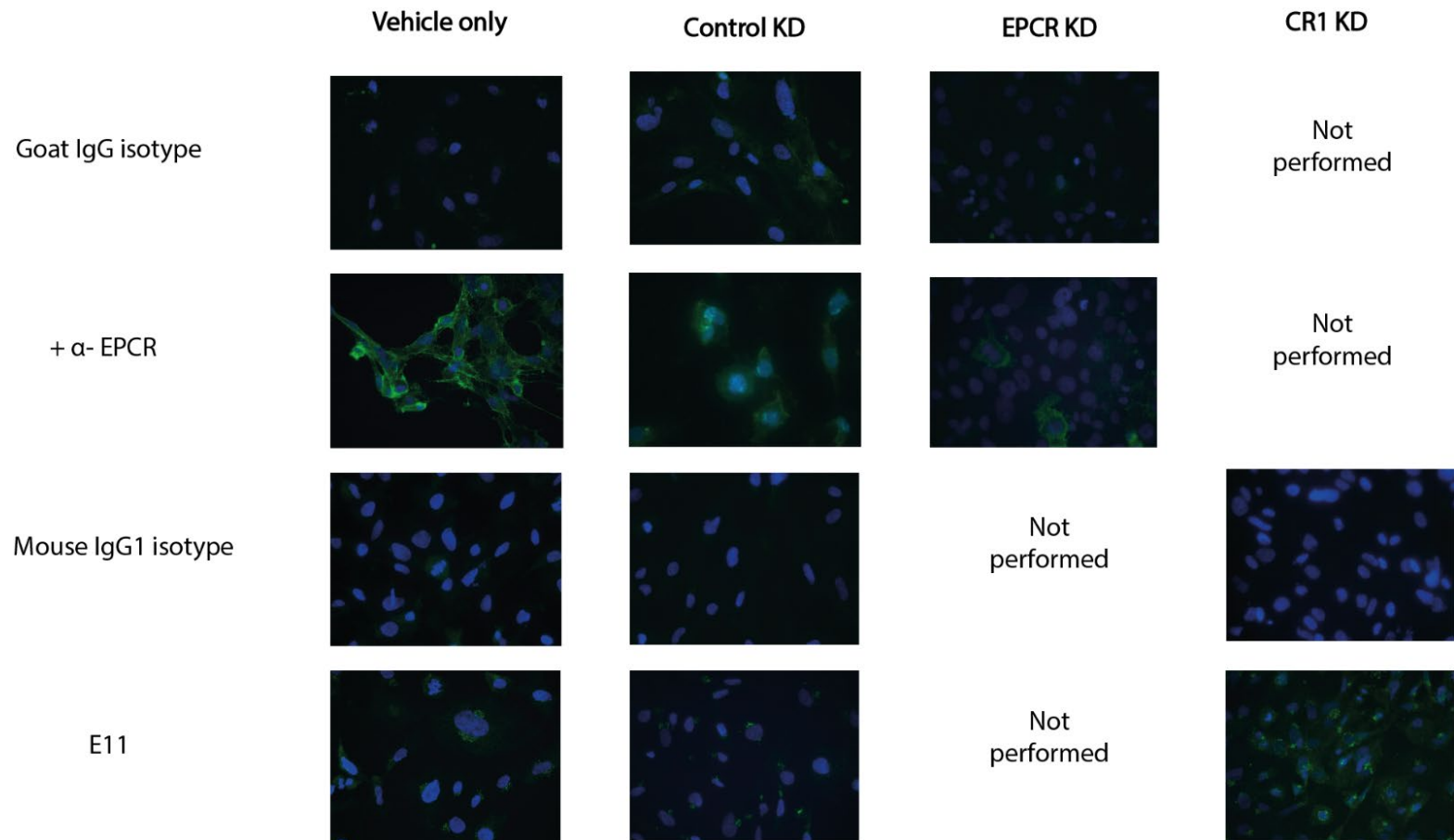


Figure 4-27. CR1 siRNA knockdown of HBEC-5i does not alter E11 staining (lower magnification).
 EPCR KD = positive control. Vehicle only = no siRNA. Control KD = control A (scrambled) siRNA. α -EPCR and goat isotype control = 10 μ g/ml. E11 and mouse isotype control = 15 μ g/ml. Cells stained with α -EPCR and goat isotype control are fixed but not permeabilised. Cells stained for E11 and mouse isotype control are fixed and permeabilised. X 40 magnification.

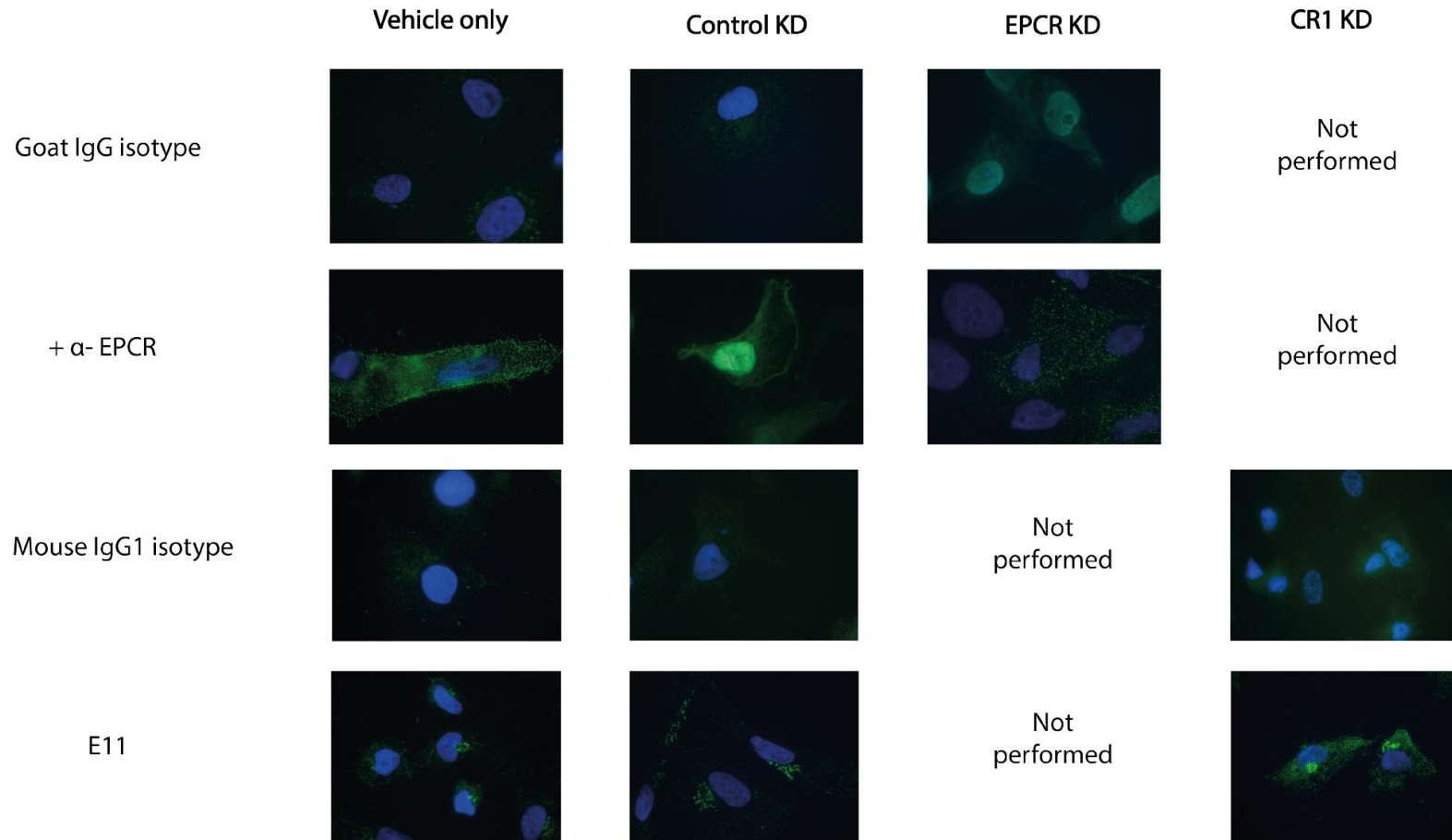


Figure 4-28. CR1 siRNA knockdown of HBEC-5i does not alter E11 staining (higher magnification).
 EPCR KD = positive control. Vehicle only = no siRNA. Control KD = control A (scrambled) siRNA. α -EPCR and goat isotype control = 10 μ g/ml. E11 and mouse isotype control = 15 μ g/ml. Cells stained with α -EPCR and goat isotype control are fixed but not permeabilised. Cells stained for E11 and mouse isotype control are fixed and permeabilised. x100 magnification.

4.5.7 Immunoprecipitation of HBEC-5i lysate fails to produce CR1

Immunoprecipitation with E11 or mouse IgG1 isotype control of hypoxic lignocaine-lifted HBEC-5i lysates was performed, with CR1-CHO cell lysate as a positive control and RCHO lysate and PBS as negative controls (as detailed in 4.4.16).

As E11 was the only antibody to recognise the HBEC-5i antigen, it was necessary to use this both as the capture and the detection antibody for this assay. To differentiate these roles, after “capture” E11 had bound the antigen and the lysates were resolved on SDS-PAGE (non-reducing 8% polyacrylamide gel) and transferred to nitrocellulose membrane, “detection” E11 was conjugated to a fluorescent marker (DyLight 680 fluorophore) before incubation with the membrane (antibody concentration for 24 hours). As such, only “detection” E11 was seen when the membrane was developed using the Li-Cor system.

The assay successfully immunoprecipitated CR1 from the CR1-CHO cell lysate, but no signal was detected in the HBEC-5i lane (Figure 4-29). It was considered possible that all E11 binding sites on the HBEC-5i antigen were saturated with “capture” E11, preventing the “detection” E11 from binding to them. Rabbit polyclonal α -CR1 antibody had previously detected a possible faint band on HBEC-5i lysate of similar size to CR1 (Figure 4-25). The membrane was washed three times in 0.1 % Tween[®]20 in PBS for 10 minutes and re-probed with polyclonal rabbit α -CR1 antibody at 1.9 μ g/ml for 18 hours. No signal was detected in the HBEC-5i lane (data not shown).

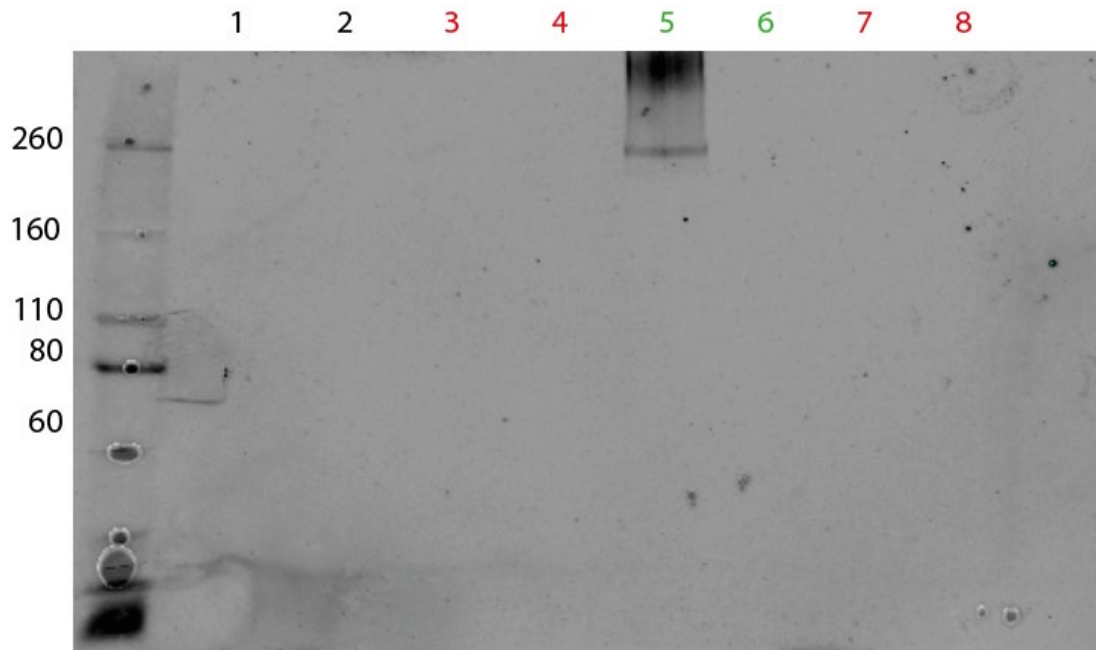


Figure 4-29. E11 can immunoprecipitate CR1 from CR1-CHO lysate but not from HBEC-5i lysate. Immunoprecipitates (IP) of E11 or isotype control antibody from HBEC-5i, CR1-CHO and RCHO lysates.

Lane 1 – E11 IP of HBEC-5i. **Lane 2** – Isotype control IP of HBEC-5i.

Lane 3 – E11 IP of RCHO. **Lane 4** – Isotype control IP of RCHO.

Lane 5 – E11 IP of CR1-CHO. **Lane 6** – Isotype control IP of CR1-CHO isotype control.

Lane 7 - E11 IP of PBS. **Lane 8** – Isotype control IP of PBS.

Non-reducing 8% polyacrylamide gel.

Membrane probed with 0.1 $\mu\text{g/ml}$ Dylight-conjugated E11 for 24 hours.

4.5.8 Intracellular HBEC-5i antigen recognised by E11 α -CR1 monoclonal antibody colocalises to the Golgi apparatus.

(Please note – the experiments in this section were designed, supervised and analysed by myself but performed by Mr Alexandros Constaninou whilst a summer student in the Rowe laboratory.)

To ascertain which intracellular compartment the epitope recognised by E11 was located in, a series of colocalisation experiments were carried out by dual-staining HBEC-5i with E11 antibody (20 μ g/ml) together with markers for mitochondria (apoptosis-inducing factor, AIF, 0.5 μ g/ml), endosomes (early endosome antigen 1, EEA-1, 0.5 μ g/ml), lysosomes (lysosome-associated membrane protein 1, LAMP-1, 1 μ g/ml), endoplasmic reticulum (protein disulphide isomerase, PDI, 1 μ g/ml) and the Golgi apparatus (receptor binding cancer antigen expressed on SiSo cells, RCAS, 1 μ g/ml). Mouse monoclonal IgG1 MOPC-21 (20 μ g/ml) was used as an isotype control for E11 and non-immunised rabbit IgG (7 μ g/ml) was used as an isotype control for the intracellular markers.

E11 was found to colocalise with RCAS, a marker for the Golgi apparatus, but not with any of the other organelle markers (Figure 4-30, Figure 4-31 and Figure 4-32).

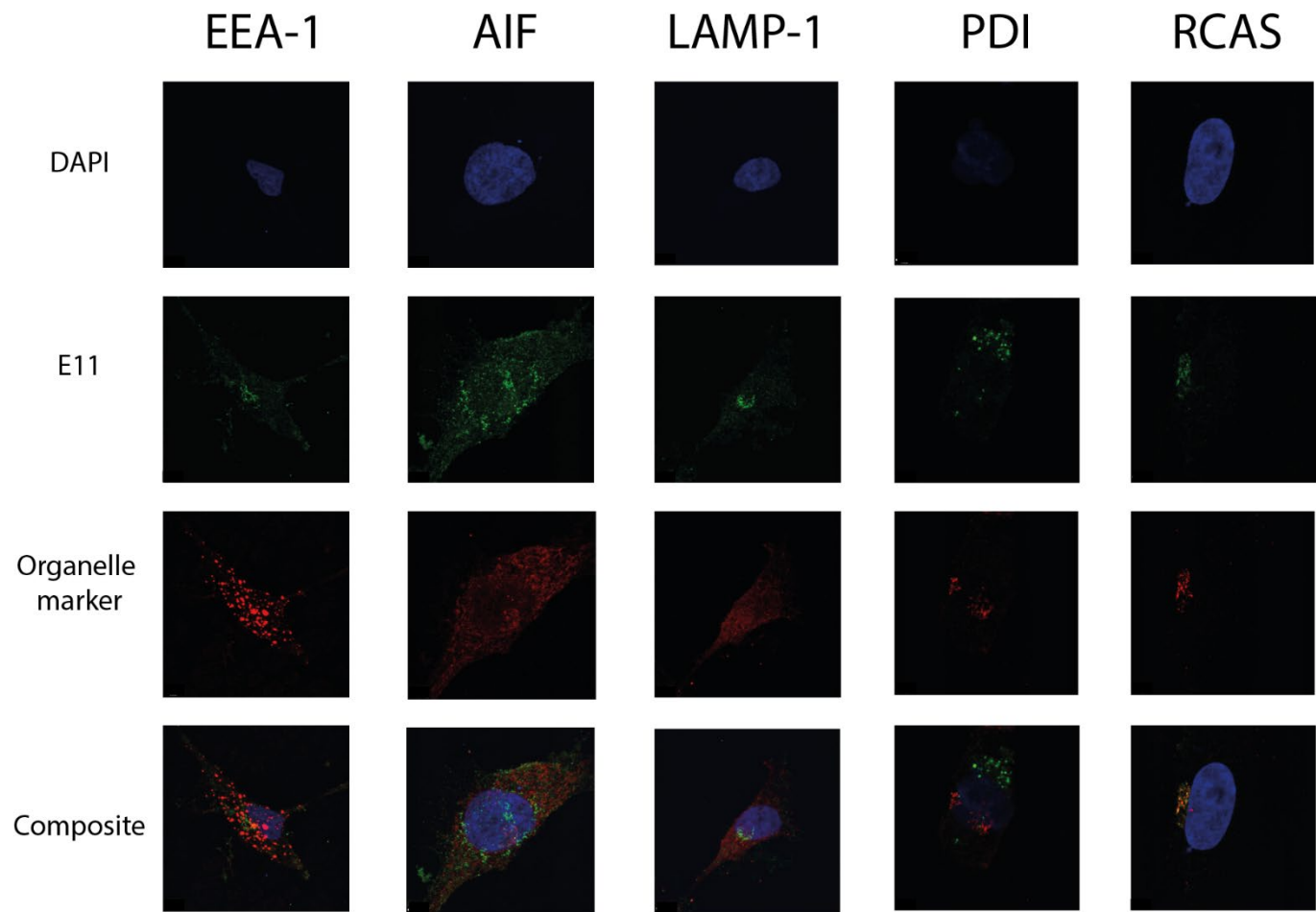


Figure 4-30. E11 staining of HBEC-5i cells colocalises with staining for the Golgi marker RCAS (part 1). EEA-1 - endosomal marker (0.5 $\mu\text{g} / \text{ml}$), AIF - mitochondrial marker (0.5 $\mu\text{g} / \text{ml}$), LAMP-1 – lysosomal marker (1 $\mu\text{g} / \text{ml}$), PDI – endoplasmic reticulum marker (1 $\mu\text{g} / \text{ml}$), RCAS – Golgi apparatus marker (1 $\mu\text{g} / \text{ml}$). E11 – $\alpha\text{-CR1}$ antibody (20 $\mu\text{g} / \text{ml}$). Fixed permeabilised HBEC-5i. $\sim\text{x}100$ magnification.

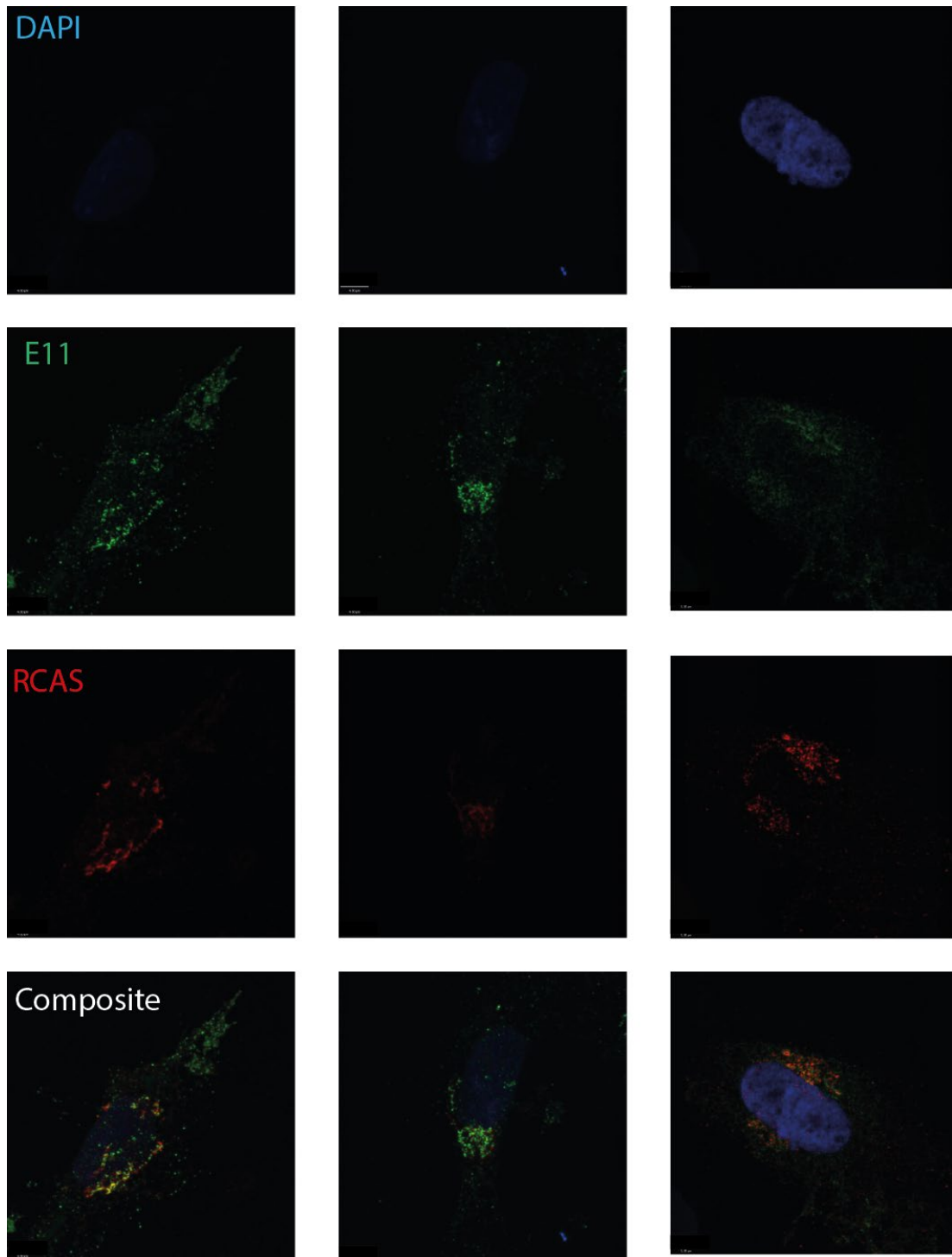


Figure 4-31. E11 staining of HBEC-5i cells colocalises with staining for the Golgi marker RCAS (part 2).
Further examples of RCAS (1 $\mu\text{g}/\text{ml}$) / E11 (20 $\mu\text{g}/\text{ml}$) colocalisation.
Fixed and permeabilised HBEC-5i \sim x100 magnification.

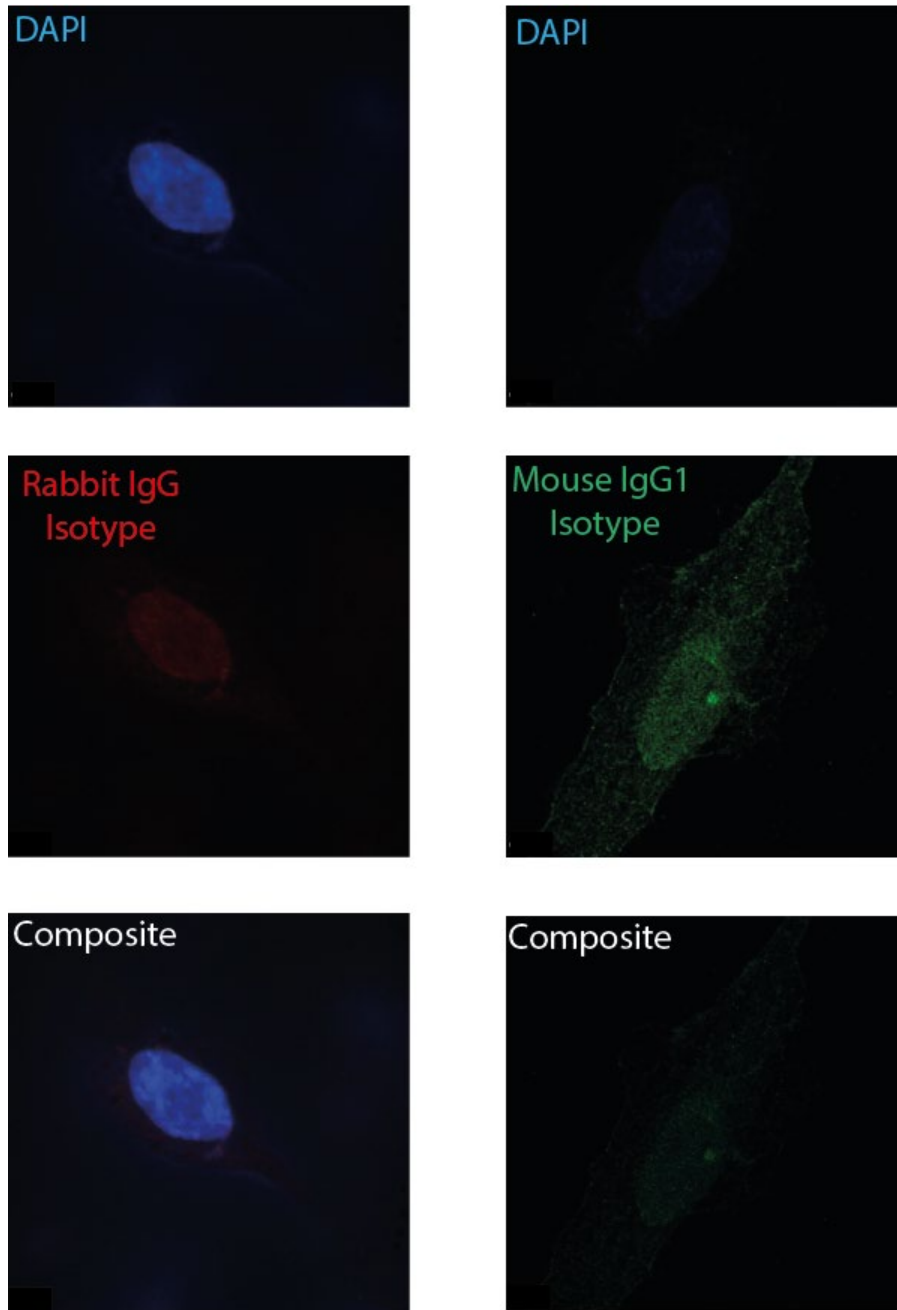


Figure 4-32. Isotype controls for colocalisation experiment.

Right hand panels: Non-immunised rabbit IgG (7 $\mu\text{g}/\text{ml}$) – isotype control for intracellular organelle staining.

*Left hand panels: MOPC-21 mouse IgG1 isotype control (20 $\mu\text{g}/\text{ml}$) – isotype control for E11 staining.
Fixed permeabilised HBEC-5i. \sim x100 magnification.*

In light of the finding that E11 colocalises with a marker for the Golgi apparatus, the original mass spectrometry data was revisited to see if any Golgi-specific proteins had been detected in the upper and lower gel bands of HBEC-5i lysate. Several candidate Golgi proteins with mass spectrometry scores over 300 were identified (Table 4-6).

Golgi protein	Mass spectrometry score	Molecular weight	Comments
Upper gel band			
Golgi-specific brefeldin A-resistance guanine nucleotide exchange factor 1 isoform 1	2955	206 kDa	Similar IFA staining pattern to E11 in HBEC-5i when used to stain HeLa cells (Quilty et al., 2018)
Golgi alpha-mannosidase II	1284	132 kDa	
Golgin subfamily A member 4	629	261 kDa	Similar IFA staining pattern to E11 in HBEC-5i when used to stain HeLa cells (Shin et al., 2017)
Golgi-associated microtubule-binding protein	438	228 kDa	
Golgi membrane protein GP73	240	45 kDa	
Lower band			
Golgin subfamily A member 3	1771	168 kDa	Similar IFA staining pattern to E11 in HBEC-5i when used to stain HeLa cells (Maag et al., 2005)

Table 4-6. Golgi proteins identified by mass spectrometry of HBEC-5i lysate

The Golgin subfamily A member 3 protein was considered to be a potential match for the lower band seen on E11 staining of HBEC-5i lysate and is of a similar molecular weight to that seen. However, there appear to be multiple Golgi-specific possibilities for the upper band. A preliminary exploration of the protein sequence homology between CR1, Golgin subfamily A member 3 and each of the five potential upper band proteins in turn was explored using Protein BLAST

(<https://blast.ncbi.nlm.nih.gov/Blast.cgi?PAGE=Proteins&PROGRAM=blastp&BLAST>)

[PROGRAMS=blastp&PAGE_TYPE=BlastSearch&BLAST_SPEC=blast2seq](#), National Center for Biotechnology Information, USA). A small area of low homology was identified between CR1, Golgin subfamily A member 3 and Golgi-specific brefeldin A-resistance guanine nucleotide exchange factor 1 isoform 1 (Figure 4-33), which might represent an overlapping epitope between the three proteins.

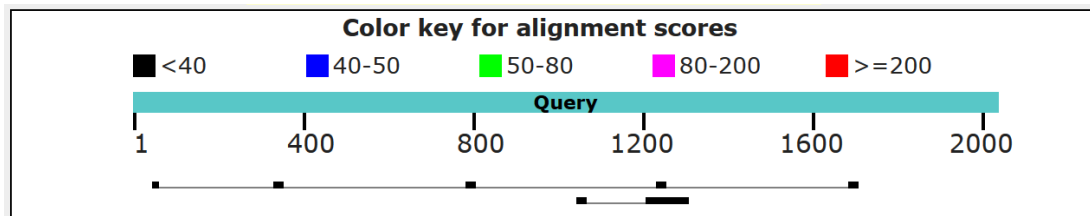


Figure 4-33. Small area of homology between CR1 and two Golgi-specific proteins sequences. Ref sequence (green) = CR1, middle protein sequence = Golgin subfamily A member 3, lower protein sequence = Golgi-specific brefeldin A-resistance guanine nucleotide exchange factor 1 isoform 1.

4.6 Discussion

4.6.1 Summary and interpretation of results

The finding that *Sl* and *Mc* polymorphisms in CR1 are specifically associated with cerebral malaria but not with other clinical sub-phenotypes of the disease (Chapter 2) raised the hypothesis that this association might be due to the expression of CR1 by brain endothelial cells. This chapter examined whether CR1 protein was expressed by the immortalised brain endothelial cell line HBEC-5i. The overall experimental design included antibody-based assays (IFA, flow cytometry, western blotting and immunoprecipitation) complimented by siRNA knock down experiments, functional complement assays and mass spectrometry studies to ensure the question was investigated by a variety of approaches.

Initial experiments found that a pool of α -CR1 monoclonal antibodies (including J3D3, To5 and E11) detected low levels of an antigen on the surface of unpermeabilised HBEC-5i cells (IFA and flow cytometry data). Commensurate with the antigen being CR1, treatment with trypsin reduced the signal seen in unpermeabilised HBEC-5i cells (flow cytometry data). When HBEC-5i were

permeabilised, the pool of α -CR1 monoclonal antibodies recognised intracellular antigen in all cells (IFA and flow cytometry data). An intracellular pool of CR1 has been described in neutrophils (Berger et al., 1988; Kumar et al., 1997; O'Shea et al., 1985) with surface CR1 expression stimulated by cooling and reheating neutrophils to 37°C (Fearon and Collins, 1983). A similar increase in signal was seen when HBEC-5i cells were cooled to room temperature and reheated to 37°C (flow cytometry data). Western blot experiments using HBEC-5i lysate probed with a pool of α -CR1 monoclonal antibodies identified a band of a similar molecular weight to that seen in CR1-CHO lysate (positive control). Together with factor I, HBEC-5i were capable of cleaving C3b to C3dg, with the final step of this process classically performed by CR1. Findings to this point supported the presence of functional CR1 on HBEC-5i.

However, an extension of the functional iC3b breakdown assay found that the breakdown of iC3b to C3dg in the presence of factor I and HBEC-5i cells was not inhibited by the α -CR1 monoclonal 3D9 (which blocks the C3b binding site (Madi et al., 1991; Nickells et al., 1998; O'Shea et al., 1985)). This suggested a cofactor other than CR1 was responsible for this breakdown on HBEC-5i cells. HBECs can produce factor H (Vastag et al., 1998) which has been reported to act as a cofactor with factor I to breakdown iC3b to C3dg (Ross et al., 1982). However, this was only reported under low ionic strength conditions, which were not used in this assay. Another cofactor (vWF (Feng et al., 2015)) was explored, but polyclonal α -vWF antibody was also unable to block iC3b breakdown. However, as the vWF epitope involved in iC3b to C3dg breakdown is unknown, it may not have been covered by the polyclonal antibody. In addition, the cofactor activity of vWF was only reported in experiments using a non-physiological pH of 8.5.

Another alternative degrading enzyme is plasmin (Foley et al., 2015; Lachmann et al., 1982). It has been reported that "*Plasmin cleavage of iC3b provides a complement regulatory pathway that is as efficient as FI/CR1 but does not require a cellular cofactor*" (Foley et al., 2015). A potential source of plasmin in the HBEC-5i setting is unclear. To date, endothelial cells have not been reported to produce

plasmin, however HBEC-5i were grown in complete DMEM containing foetal bovine serum (potentially containing plasmin) before being washed with incomplete DMEM for the C3b degradation assay. However, the foetal bovine serum had been heat treated at 56°C for 30 minutes inactivating any residual plasmin (Metwalli et al., 1998). As such, it appears that the iC3b to C3dg breakdown is being performed by an as yet unidentified cofactor on HBEC-5i cells.

Following the inability of 3D9 to block C3dg production, the identity of the antigen recognised by α -CR1 antibodies was brought into doubt. The next step was to establish whether CR1 could be identified in HBEC-5i lysate by mass spectrometry. The high molecular weight and complexity of the cell lysate made this very difficult, as shown by the inability to detect CR1 in the CR1-CHO cell lysate (positive control) on the first analysis. Only once the spectra were compared directly against a smaller dataset containing the CR1 amino acid sequence were four CR1 peptides detected in the positive control. Proton ion scanning based on the elution times of these four peptides in the positive control was unable to detect them in the HBEC-5i sample. Thus, there was no evidence from mass spectrometry that HBEC-5i express CR1. An attempt to reduce the complexity of the sample by immunoprecipitation was unsuccessful. It should be noted that the detection of a high molecular weight protein in a complex mixture by mass spectrometry can be challenging (Angel et al., 2012). As an example of this, despite many attempts, another group was recently unable to detect CR1 in erythrocyte lysates by mass spectrometry (personal communication, Prof Tom Williams, Kilifi, Kenya).

The question was then raised as to the specificity of the α -CR1 monoclonal antibody pool used, namely J3D3, To5 and E11. The antibodies were examined individually by IFA of fixed HBEC-5i cells and western blotting of HBEC-5i lysates. It transpired that the IFA signal was coming from only one of the three antibodies (E11) and that the other two (J3D3 and To5) did not stain above the level of the isotype control. E11 was also the only antibody to recognise a trypsin-sensitive antigen in HBEC-5i lysate of a similar weight to CR1 on western blotting. Seven other α -CR1 monoclonal

antibodies (3D9, YZ-1, Ber-Mac-DRC, IB4, 57F, HB8592 or J3B11) failed to detect a band of similar molecular weight to CR1 on western blotting.

The molecular weight of CR1 is variable with four allotypes of 160 kDa (CR1*3/CR1-C), 190 kDa (CR1*1/CR1-A), 220 kDa (CR1*2/CR1-B) and 250 kDa (CR1*4/CR1-D) under non-reducing conditions (Dykman et al., 1983b, 1984, 1985). The 30 kDa size differences between these variants corresponds to the deletion or duplication of a LHR (Wong and Farrell, 1991; Wong et al., 1989). The relative molecular weights of these alleles are further altered under reducing conditions, whereby they increase by ~ 30 kDa (Birmingham and Hebert, 2001). Experimental conditions have also been found to influence the molecular weight of CR1 reported (Dykman et al., 1985; Wong et al., 1983, 1986). sCR1 was used as a positive control for some western blots, with the manufacturers (R&D Systems) stating it produces a band of 200-220 kDa on SDS-PAGE under reducing conditions (R&D Systems, 2018). Western blotting experiments in this chapter were performed under non-reducing conditions so the sCR1 would be expected to produce a band at ~190 kDa. However, a band was seen at ~250 kDa for sCR1, regardless of which α -CR1 antibody was used. This was seen across three different batches of recombinant sCR1 protein. A band of the same size was also seen for the CR1-CHO lysates throughout the experiments. As such, it is likely that the experimental conditions or the protein ladder used may have influenced apparent size of the CR1 protein detected. It thus seems likely that the sCR1 and CR1-CHO CR1 are CR1*1 variants. The band recognised by E11 in HBEC-5i lysate was slightly lower than this, but not 30 kDa lower (i.e. not the size of a whole LHR). It has been reported that CR1 from different cells varies slightly in size – for example CR1 isolated from urinary vesicles (from glomerular podocytes) was reported to be 15 kDa larger than CR1 isolated from erythrocytes (Pascual et al., 1994a). However, if HBEC-5i were truly producing a cell-specific form of CR1, it is extremely hard to explain why this was not detected by any of the other α -CR1 monoclonal antibodies. The antibody with the most similarity to E11 is HB8592, which was reported to have the same reactivity pattern to sCR1 and its truncated forms by dot blotting, recognising full length sCR1 and CCP repeats 15-21 (LHR C)

and 22-30 (LHR D+) (Nickells et al., 1998). In the current experiments, HB8592 did not show the same pattern as E11 on western blotting of HBEC-5i lysates.

The next set of experiments examined whether siRNA CR1 knockdown altered the E11 intracellular staining HBEC-5i. The siRNA knockdown worked well for the positive control (EPCR) but had no effect on the E11 signal from permeabilised HBEC-5i. It is plausible that the length of the experiment (48 hours) was insufficient to deplete the cells of their intracellular stores of CR1, but this seems unlikely. This appears to be strong evidence that the antigen recognised by E11 is not CR1.

Following this, an attempt was made to immunoprecipitate the HBEC-5i antigen recognised by E11 prior to further mass spectrometry. As only one antibody recognised an HBEC-5i antigen, it was necessary to use E11 as both “capture” and “detection” antibody. E11 has been used in multiple reports to immunoprecipitate CR1 (Fonseca et al., 2016; Hogg et al., 1984; Mathew et al., 1995) and the protocol used in this chapter successfully immunoprecipitated CR1 from CR1-CHO lysate. However, no band was seen for the HBEC-5i lysate. It is possible that the level of antigen was too low for immunoprecipitation, but also possible that all available E11 binding sites on the antigen were occupied with “capture” E11, preventing “detection” E11 from binding. To see if this was the case the western blot membrane was reprobed with polyclonal rabbit anti-CR1 (which had weakly recognised a band of the anticipated size on HBEC-5i lysate), but no signal was seen. These experiments further suggest the antigen recognised by E11 was not CR1.

4.6.2 E11 and the Golgi apparatus

The question of what E11 was recognising was examined from another direction by performing colocalisation IFAs alongside organelle markers. Using this approach, E11 was found to be recognising an antigen that colocalised with receptor binding cancer antigen expressed on SiSo cells, (RCAS) which is used as a marker to identify the Golgi apparatus. CR1 is first synthesised as pro-CR1, a pre-Golgi precursor molecule, ~ 23 kDa smaller than mature CR1 (Atkinson and Jones, 1984; Lublin et al., 1986). The pro-CR1 molecule has high mannose N-linked oligosaccharide chains

which are thought to be trimmed in the *cis* and *medial*-Golgi cisternae before entering vesicles for incorporation into the cell membrane (Danielsson et al., 1994; Hamer et al., 1998). In some circumstances, CR1 is cleaved (from cell membrane or secretory vesicles) at a site within the transmembrane domain, releasing soluble CR1 (sCR1) (Hamer et al., 1998). As such, it is possible that CR1 could be detected in the Golgi apparatus of a permeabilised cell. However, evidence from mass spectrometry, C3b breakdown assay and siRNA knockdown of CR1 already strongly suggested that E11 was recognising an antigen other than CR1.

Interrogation of the mass spectrometry data from HBEC-5i lysate revealed potential matches for Golgi-specific proteins in both the upper and lower bands recognised by E11. Protein sequence alignment suggested a small area of sequence homology between CR1, Golgin subfamily A member 3 (168 kDa) and Golgi-specific brefeldin A-resistance guanine nucleotide exchange factor 1 isoform 1 (206 kDa), which might represent an overlapping epitope between these proteins. Further experiments are planned to determine whether these Golgi antigens are being detected by E11. Experiments will include dual staining IFA of HBEC-5i using E11 and antibodies against each Golgi protein in turn to see if there is colocalisation. If successful, a western blot of HBEC-5i lysate will be undertaken using E11 and Golgi protein antibodies conjugated to different fluorophores to see what size bands are being detected. Finally, an siRNA knockdown of the Golgi proteins in question and IFA with E11 would confirm whether they are responsible for the cross reactivity.

E11 is a widely used α -CR1 antibody and it will be essential to communicate to the scientific community that it may give false positive results in some situations. The likelihood of E11 not being specific for CR1 also calls into question some previous reports. For example, Langeggen et al.'s report of CR1 on HUVEC used E11 as the only antibody for flow cytometry and western blotting (confirmed by personal communication with Sanquin, formerly CLB, Amsterdam, Netherlands who supplied the antibody) (Langeggen et al., 2002). In addition, the study by Yin et al. where the presence of CR1 was reported on bone marrow microvascular endothelial cells also

appears to have relied entirely on data from ELISAs using E11 (methods section states “*Murine monoclonal anti-CD35 (...) obtained from Ancell Corporation (Bayport, MN).*” E11 is the only α -CR1 clone supplied by this company) (Yin et al., 2008). As such, the antibody-based evidence for CR1 protein in HUVECs is limited to two papers; Collard et al., who used the monoclonal antibody 3C6.D11 and rabbit polyclonal antibodies for detection of CR1 by ELISA, and used YZ-1 for IFAs and western blots of the cell lysates (Collard et al., 1999) and Schroeder et al. who used 3D9 to detect CR1 on HUVECs during an experiment to examine microfilariae binding (Schroeder et al., 2017). Collard et al. also used inappropriate isotype controls for their ELISAs (i.e. an IgG2a isotype control used for 3C6.D11, which is an IgG1 antibody and the use of a polyclonal rabbit α -horse antibody as an isotype for a polyclonal rabbit α -CR1 antibody, which is human) and did not use isotype controls for their IFA experiments, making interpretation more difficult. The evidence from Schroeder et al. also did not include any negative or positive controls when reporting for CR1 expression by flow cytometry in that study.

It is important to remember that HBEC-5i is an immortalised cell line and may not perfectly reflect primary HBEC. For example, comparison of the transcriptional profiles of primary HBEC and the immortalised cell line hCMEC/D3 revealed differences in immune response genes which were related to the immortalisation procedure (Urich et al., 2012). As such, it is possible that primary HBEC might express CR1, the ability of which has been lost as a quirk of the immortalisation process. Parallel investigation of primary HBECs was initially attempted in this chapter, but abandoned over concerns that the cells were not exhibiting the usual growth characteristics of primary cells (extremely fast growth) and did not show a classic cobblestone appearance with the majority staining positive for the fibroblast marker SMA (data not shown). It will be important to repeat some of these experiments with an authenticated primary HBEC line before publication of these data.

4.6.3 Findings in context

The data presented in this chapter do not support the expression of CR1 by HBEC-5i cells. As previously discussed, the expression of CR1 on HUVECs remains controversial and there are no detailed reports investigating CR1 protein expression on HBECs. However, a study of the proteome of primary HBEC under oxidative stress did not identify CR1 amongst the proteins reported (Ning et al., 2011). Although transcription does not always equate with the expression of a protein, recent transcriptomic studies have not provided evidence for CR1 transcription by HBECs. Two microarray-based studies, the first examining the transcriptional profiles of primary HBEC and the immortalised HBEC line hCMEC/D3 with and without co-culture with astrocytes and the second study of unstimulated commercially available primary HBEC found no evidence of CR1 transcription (Aung et al., 2014; Urich et al., 2012).

In conclusion, the data from this chapter does not provide clear evidence for the expression of functional CR1 protein by HBEC-5i cells, which corresponds to the transcriptional data available from other studies. This finding cannot be directly extrapolated to primary HBECs and experiments will be necessary in these cells too. In addition, the α -CR1 monoclonal antibody E11 does not appear to be specific for CR1 and further experiments will be necessary to elucidate the antigen it is recognising. These investigations suggest that the production of CR1 by HBECs is unlikely to help explain the association between *S12/McC^b* and CM. As such, attention was turned back to the polymorphisms themselves with the aim of producing recombinant proteins containing the mutations to directly characterise their binding properties.

5 Do the *SI* and *McC* polymorphisms affect the binding of complement components to CR1?

5.1 Abstract

The work from this thesis has suggested that the *SI* and *McC^b* polymorphisms in CR1 have opposing associations with cerebral malaria. These associations do not appear to be due to the polymorphisms influencing CR1 clustering on erythrocyte membranes, or to human brain endothelium expressing CR1. The LHR-D region containing these polymorphisms has been reported as the binding site for the complement components mannose binding lectin (MBL), C1q and L-ficolin, all associated with malaria to varying degrees. This chapter aimed to generate the reagents needed to test the hypothesis that the *SI* and *McC^b* polymorphisms affect the binding of these complement components to the LHR-D region.

A region of CR1 cDNA corresponding to LHR-D plus CCP 29-30 (i.e. CCP 22-30) was amplified and cloned into pCRII vector. Site-directed mutagenesis was undertaken on the insert to create three mutant plasmids; pCRII CCP 22-30 *SI*, pCRII CCP 22-30 *McC^b* and pCRII CCP 22-30 *SI/McC^b*. The successful mutations were confirmed by sequencing. An *Age*I restriction site was introduced at the 3' end of these mutant amplicons in preparation for sub-cloning.

The expression plasmid pcDNA3.1 (-) CCP 22-30 His was obtained, which contains the unmutated CCP 22-30 region of CR1 with an additional 5' CR1 signal peptide and 3' His tag. The restriction enzymes *Age*I and *Pas*I were used to digest the expression plasmid and remove the region containing the *SI* and *McC* sites but preserve the signal peptide and His tag. The *SI*, *McC^b* and *SI/McC^b* mutant amplicons were also digested using *Age*I and *Pas*I to produce corresponding ends. Unfortunately, due to problems with restriction digestion, subcloning of the mutant amplicons into the expression vector was unsuccessful.

5.2 Introduction

The association between the *SI/McC* polymorphisms and cerebral malaria does not appear to be due to differences in the clustering of CR1 on erythrocyte membranes (Chapter 3) or to an ability of human brain endothelial cells to express CR1 (Chapter 4). Another possibility is that the polymorphisms might alter CR1 binding to complement components and hence influence complement activation or regulation.

5.2.1 Function of the LHR-D region and relevance to malaria.

The *SI* and *McC* polymorphisms are located in CCP 25 of LHR-D on the CR1 molecule (Moulds et al., 2001). Unlike the rest of the CR1 molecule, the function of the LHR-D region is unclear, but has been reported as a binding site for the complement components mannose binding lectin (MBL), C1q and ficolins.

5.2.1.1 *LHR-D as a binding site for mannose binding lectin*

Mannose binding lectin (MBL) is a C-type lectin belonging to the collectin protein family. MBL consists of a collagen-like domain and carbohydrate-recognition domain with high affinity for N-acetylglucosamine and mannose (prominent in many micro-organisms) but does not recognise galactose or sialic acid (prominent in mammalian glycoproteins) (Drickamer, 1992). A review of MBL in the lectin pathway is provided in section 1.4.1 and Figure 1-7. MBL was first reported to bind to immobilised whole length sCR1 and was inhibited by C1q (Ghiran et al., 2000). As C1q had been reported to bind to LHR-D (Klickstein et al., 1997), MBL was deduced to bind in the same site. A later study used recombinant CR1 proteins spanning CCP 22-30 (i.e. LHR-D plus CCP 29-30) and found a binding site for MBL in CCP 24/25 using SPR (Jacquet et al., 2013). By aligning the amino acid sequences of the 30 CCP modules, Glu¹⁵⁵⁵ was suggested as a potential MBL-binding site. This residue is surrounded by a patch of negative charge, with two acidic residues in CCP 24 (Asp¹⁵⁵³ and Glu¹⁵⁵⁹) and two glutamic acid residues in CCP 25 (Glu¹⁵⁹⁵ and Glu¹⁵⁹⁷). This area is shown in Figure 5-1 with the *SI* and *McC* polymorphism sites added for comparison.

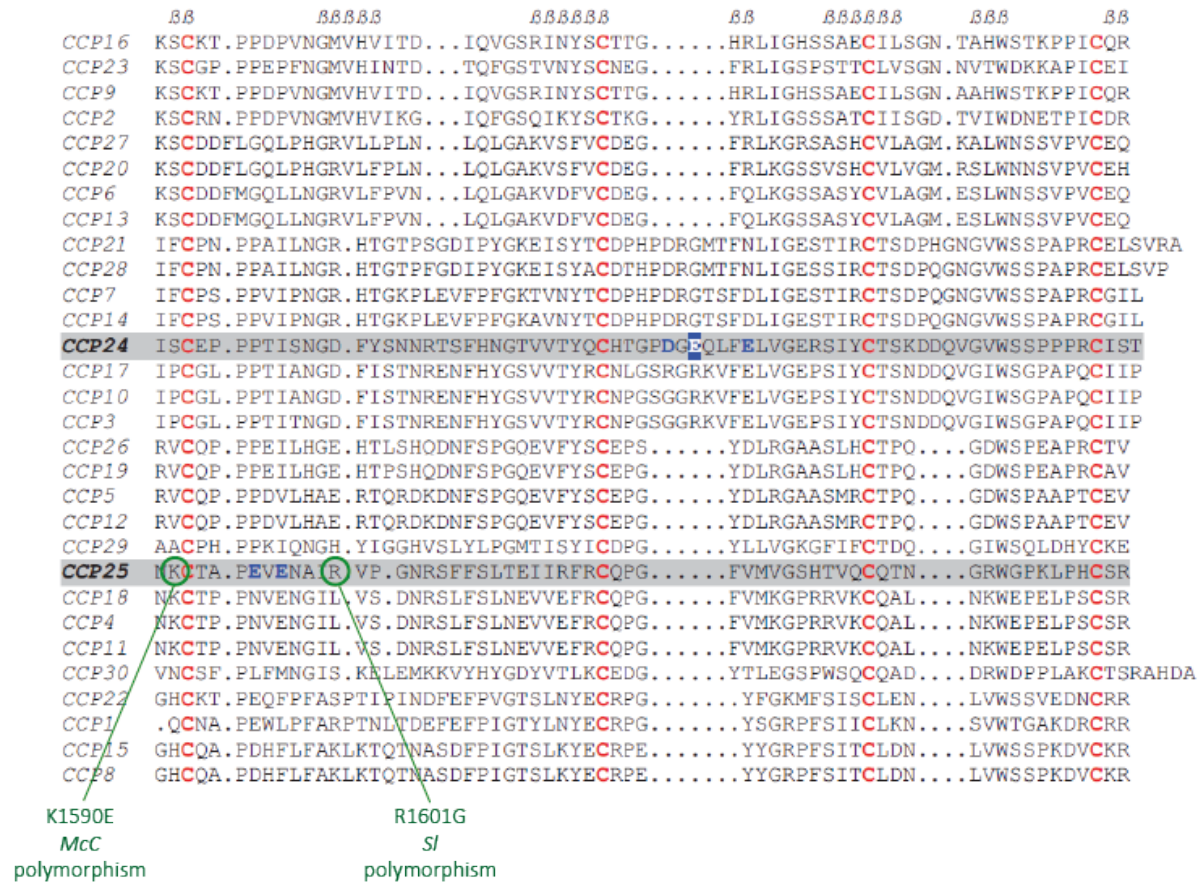


Figure 5-1. Putative binding site for MBL on CR1.

Amino acid sequences of the 30 CCPs comprising CR1 are aligned and CCP 24 and 25 are highlighted in grey. Conserved Cys residues are shown in red. The putative binding residue for MBL is shown in white lettering in a blue box (Glu1555). Negatively charged residues surrounding this are highlighted in blue. The sites of the McC and SI polymorphisms are identified with green circles. Image adapted from (Jacquet et al., 2013).

5.2.1.2 *The role of MBL in malaria*

The role of MBL in malaria is unclear. Alleles responsible for low levels of functional MBL are common in sub-Saharan Africa (Garred et al., 2003; Holmberg et al., 2008; Lipscombe et al., 1992) and have been associated with increased parasite load, lower blood glucose levels and increased odds of severe malarial anaemia in Ghanaian children (Garred et al., 2003; Holmberg et al., 2008). A small study of Gabonese children also reported lower MBL levels on admission with severe malaria than with UM (Luty et al., 1998).

It has also been suggested that MBL may opsonize *P. falciparum* IEs (Garred et al., 2003; Klabunde et al., 2002) and merozoites (Korir et al., 2014). Downstream MBL-mediated phagocytosis may be important as it attenuates the inflammatory response resulting in decreased production of IL-6, IL-1 β , and TNF- α by monocytes (Bajtay et al., 2000; Jack et al., 2001). Indeed, a Gabonese study found malaria patients who had high MBL levels had lower levels of IL-1 β , TNF- α and other pro-inflammatory cytokines than those with low MBL levels (Boldt et al., 2006).

Whether the *S1* or *McC* polymorphisms have functional effects on MBL interactions with CR1 has not yet been explored. As both *S1* and *McC* have been associated with infectious diseases other than malaria (Fitness et al., 2004a; Noumsi et al., 2011), any impact they may have on CR1 function is likely to be broad and not malaria-specific. As such, the hypothesis that they might affect MBL binding to CR1 and the subsequent opsonisation or phagocytosis of malarial matter is plausible.

5.2.1.3 *LHR-D as a binding site for C1q*

C1q is the recognition molecule of the classical pathway and is composed of collagen-like stalks and globular heads, with the latter able to recognise and opsonise over 100 foreign and modified self-antigens (reviewed in (Kishore and Reid, 2000)). C1q also binds avidly to IgG and IgM-containing immune complexes, enabling the complement pathway to be activated in both an immune complex-dependant and independent manner (reviewed in section 1.4.1 and Figure 1-7). The first report of C1q binding to LHR-D compared the binding of radio-labelled C1q to

recombinant LHR-D and full length CR1 (Klickstein et al., 1997). However, this study did not examine the binding of C1q to LHR-A, B or C separately and used low ionic strength buffers, potentially affecting the relevance of the finding. The same group later reported that C1q and C4b bound to different sites on recombinant sCR1, but offered no further data to support LHR-D as the C1q binding site (Tas et al., 1999).

There is some evidence that the C1q binding site may not be localised in LHR-D. In a experiments using short recombinant proteins, Tetteh-Quarcoo et al. reported C1q to bind most efficiently to CCP 15-17 (Tetteh-Quarcoo et al., 2012). However, these proteins were deglycosylated and the authors did not examine CCPs 26-28, and as such could have missed a C1q binding site there. In summary, the binding of C1q to the LHR-D region of CR1, whilst an oft accepted fact in textbooks, is actually based on a single paper (Klickstein et al., 1997).

5.2.1.4 *The role of C1q in malaria*

The role of C1q in malaria is unclear, but may interact with malaria-specific antibodies. A recent study examining malaria-exposed individuals from Papua New Guinea reported that their IgG was able to inhibit the invasion of erythrocytes by *P. falciparum* only when the assay was supplemented with C1q, but not when it was depleted of C1q (Boyle et al., 2015). The authors also reported that the antibodies of older children had higher C1q-fixing ability than younger children. Children with high C1q fixation ability were subsequently found to be less likely to develop clinical malaria and high density parasitaemia. The antigens underlying this antibody-mediated complement-dependant protection included the merozoite surface proteins MSP-1 and MSP-2. The authors postulated that C1q-fixation may be inhibiting invasion through steric hindrance by blocking parasite proteins binding to cellular receptors. IgM is also a potent activator of C1q, with antibody pentamer binding to the cell surface, leaving the C1q binding sites on the Fc component accessible (Czajkowsky and Shao, 2009). PfEMP1 binds to natural IgM and may block its C1q binding sites, thus evading complement-mediated lysis of the parasitised erythrocyte (Akhouri et al., 2016; Barfod et al., 2011).

5.2.1.5 LHR-D as a binding site for L-ficolin

The ficolins are a group of lectins containing collagen-like and fibrinogen-like domains, which have structural and functional similarities to MBL. Three ficolins have been identified in humans; L-ficolin, H-ficolin and M-ficolin, each with different tissue distributions which act as pattern recognition molecules to recognise pathogens and activate complement via the LP. L-ficolin has been reported to bind to CCP 24/25, but CCP 27-30 may also be involved (Jacquet et al., 2013).

5.2.1.6 The role of ficolins in malaria

Data for an association between ficolins and malaria is scarce. A small study conducted in Gabon reported that levels of L-ficolin (also known as ficolin-2, FCN-2) were significantly raised in severe malaria when compared to mild malaria but found no association between any of three promoter SNPs in the FCN-2 gene and severe malaria (Faik et al., 2011). The same study reported “(...) *we were unable to show a direct binding of ficolin-2 to parasitized erythrocytes, although suitable sugar moieties are found in plasmodial proteins (...).*”

5.2.2 Previous investigations into *SI/McC* polymorphisms and complement function

Considering the above evidence, it is plausible that the *SI/McC* polymorphisms might affect the nearby binding of MBL, C1q or L-ficolin to LHR-D, with a subsequent influence on malarial infection and clinical outcome. The first step in testing any of these hypotheses is to examine the binding of MBL, C1q and L-ficolin to CR1 bearing the *SI2* and/or *McC^b* mutations.

One previous study has tried to elucidate the function of the *SI2* and *McC^b* polymorphisms using four short recombinant proteins spanning CCP 15-25 which corresponded to the *SI1/McC^a*, *SI1/McC^b*, *SI2/McC^a* and *SI2/McC^b* haplotypes (Tetteh-Quarcoo et al., 2012). Recombinant proteins were expressed in *Pichia pastoris* yeast and underwent enzymatic deglycosylation. Binding of the four variants to C1q, C3b and C4b was determined using surface plasmon resonance and ELISAs. Investigation of the ability of each variant to act as a cofactor for C3b and

C4b cleavage with factor I was investigated using a fluid-phase assay and western blotting. In addition, the ability of the four variants to disrupt *P. falciparum* rosettes and block RBC invasion was examined. No differences were found in the proteins' ability to bind C1q, C3b and C4b, or act as cofactors (with factor I) for the breakdown of C3b and C4b. The mutations were not found to affect inhibition of erythrocyte invasion by *P. falciparum* (3D7 parasite strain) or disruption of rosettes (R29 parasite strain). The authors concluded that "*Neither differences in complement-regulatory functionality, nor interactions with P. falciparum proteins tested here, appear to have driven the non-uniform geographic distribution of these alleles* (Tetteh-Quarcoo et al., 2012)."

5.2.3 Choice of protein expression system and CR1 glycosylation

The four potential protein expression systems (bacterial, yeast, insect and mammalian) differ in their ability to fold and glycosylate proteins. The glycosylation repertoire of mammalian expression systems most closely resembles that seen in human cells (particularly N-glycosylation, reviewed in (Brooks, 2004)). It has been predicted that sCR1 has 25 N-linked glycosylation sites (Klickstein et al., 1988), of which 14 are occupied (Furtado et al., 2008). Eight of the glycosylation sites are located in CCP 22-30 (Figure 5-2 and (Morley and Walport, 2000)). N-linked glycosylation comprises ~25,000 Da of the mature form of CR1 and also accounts for the ~5,000 Da difference seen between PMN and erythrocyte CR1 (Dykman et al., 1983a; Lublin et al., 1986). High-mannose N-linked oligosaccharide chains in pro-CR1 are converted to complex-type chains in mature CR1 (Atkinson and Jones, 1984). N-linked glycosylation also appears to be key to CR1 function, with deglycosylated CR1 having ~50% half-life and 41% of the iC3 binding efficiency of the glycosylated form (Lublin et al., 1986).

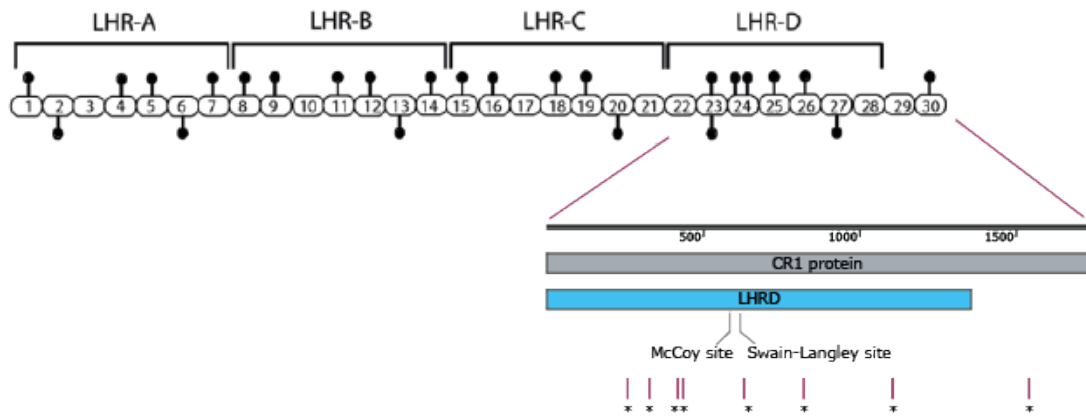


Figure 5-2. Glycosylation sites in CR1.

Insert shows the potential glycosylation sites in LHR-D in relation to *SI* and *McC* mutation sites. Image adapted from (Furtado et al., 2008), with additional information from (Klickstein et al., 1988).

Previous investigation into the functional effects of the *SI2* and *McC^b* mutations used a yeast-based protein expression system (*Pichia pastoris*) and then deglycosylated using the endoglycosidase EndoH_f (Tetteh-Quarcoo et al., 2012). Indeed, the first author's thesis states: "... a limitation of the present work is that it effectively ignores any effects of glycosylation on structure and function of CR1 (Tetteh-Quarcoo, 2011)." As such, the study's findings may not represent naturally glycosylated CR1. Another study reported the LHR-D region as the binding site for MBL and the ficolins using proteins expressed using a baculovirus-insect cell expression system (Jacquet et al., 2013).¹ This system produces more simple N-glycans in comparison to mammalian cells (Harrison and Jarvis, 2006).

Given the importance of N-glycosylation in CR1, it is possible the reliance of these two studies on yeast and baculovirus-insect systems may have affected the conclusions drawn. As four of the eight potential N-glycosylation sites in CCP 22-30 are very close to the *SI* and *McC* polymorphism sites (Figure 5-2), I decided to produce constructs for the *SI2*, *McC^b* and *SI2/McC^b* recombinant proteins for expression in mammalian cells in order to maximise the natural N-glycosylation pattern.

¹ It should be clarified that the expression plasmid pcDNA 3.1 (-) CCP 22-30 His used in this chapter was a kind gift from this group.

5.3 Aim

The aim of this chapter was to generate constructs in order to express recombinant, His-tagged proteins representing the LHR-D region of CR1 containing the *SI2*, *McC^b* and the *SI2/McC^b* double mutation, to enable future work examining their interactions with MBL, C1q and L-ficolin.

5.4 Methods

5.4.1 Overview of cloning strategy

A section of CR1 cDNA spanning CCP 22-30 was amplified by PCR and ligated into the cloning vector pCRII. The resultant plasmid was transformed into *Escherichia coli* and selected on antibiotic-containing agar using blue/white screening. Colonies were subsequently screened by PCR to determine whether they contained an insert of the anticipated size. Promising colonies were picked and grown in broth containing ampicillin, following which the plasmid DNA was purified and sequenced.

The *SI2*, *McC^b* and *SI2/McC^b* mutations were introduced by site-directed mutagenesis and confirmed by sequencing. Restriction enzyme sites were then added to the ends of the mutant inserts. The resulting PCR amplicon was double-digested by the appropriate restriction enzymes. The digested insert was ligated into a (previously double-digested) expression vector (pcDNA3.1 (-)) bearing a CR1 signal peptide and a His-tag. The final plasmid was transformed into *E. coli*, expanded and the insert confirmed by sequencing.

5.4.2 Primer sequences

Amplifying, sequencing and restriction enzyme site primers were designed using SnapGene molecular biology software version 4.1 (GSL Biotech). Site-directed mutagenesis primers were designed using PrimerX (<http://www.bioinformatics.org/primerx/>). Primers were supplied by Sigma (Sigma-Aldrich, St. Louis, MO, USA) desalted and in solution at 100 µM concentration.

Table 5-1 outlines the primers used in these experiments.

Primer name	Sequence (5'-3')	T _m (°C)
Amplifying primers		
LHRD_F	CACTGTAAAACCCAGAGCAGTT	67.5
LHRD_R	ATGTGCACGAGAGGTACATTTGG	69.9
Site-directed mutagenesis primers		
SL2_F	AGTTGAAAATGCAATTGGAGTACCAGGAAACAGG	75.3
SL2_R	CCTGTTTCCTGGTACTCCAATTGCATTTTCAACT	75.3
MCCB_F	GGTGTATTTCTACTAATGAATGCACAGCTCCAGA	72.3
MCCB_R	TCTGGAGCTGTGCATTATTAGTAGAAATACACC	72.3
Sequencing primers		
LHRD_SP1_F	AACTTACCAGTGCCCACTG	60.3
LHRD_SP2_R	CTTGTGCAGCGGATGGAG	65.9
LHRD_SP4_R	CAGGATTTCTGGAGGCGG	65.8
SP6_PROM	ATTTAGGTGACTATAGAA	50.9
T7_PROM	TAATACGACTCACTATAGGG	47.7
Restriction enzyme site primers		
AGE1_PRIMER	CAGCTGACCGGTCACTGTAAAACCCAGAGCAG	80.7
PAS1_PRIMER	AGTCTCCTGGGCGTG	66.7

Table 5-1: Primer sequences.

For site-directed mutagenesis primers, the mutated nucleotide is indicated in **red**. For restriction enzyme site primers, restriction sites are indicated in **green** letters. SP6_PROM and T7_PROM were kind gifts from Dr Mathieu Cayla.

T_m = melting temperature.

5.4.3 PCR amplification of CR1 CCP 22-30

The nucleotide sequence of human mRNA for CR1 was sourced from GenBank (<https://www.ncbi.nlm.nih.gov/nuccore/Y00816>) and imported into SnapGene. The mature peptide sequence corresponding to CCP 22-30 was identified (nucleotides 4210-5937, amino acids 1404-1979). This sequence encompasses LHR-D (CCP 22-28) and CCP 29-30. Primers were designed to amplify this segment of cDNA (termed LHRD_F and LHRD_R, see Table 5-1). Full length CR1 cDNA was a kind gift from Lloyd Klickstein (Boston, USA). To minimise introduction of unwanted errors, the CCP 22-30 fragment was amplified using Platinum™ Taq DNA Polymerase High Fidelity

(Thermo Fisher Scientific 11304011) using the PCR buffer and MgSO₄ supplied with this enzyme. Deoxynucleotide triphosphate (DNTP) mix was sourced from Takara (4030). The reaction was made up as follows:

50 ng/μl CR1 template cDNA	1 μl
10x High fidelity PCR buffer	2.5 μl
50 mM MgSO ₄	1 μl
10 μM DNTP mix	0.5 μl
10 μM LHRD_F primer	0.5 μl
10 μM LHRD_R primer	0.5 μl
Sterilised dH ₂ O	18.9 μl
Platinum™ Taq DNA Polymerase High Fidelity (5 units/μl)	0.1 μl

The reaction was run on the PCR cycle parameters in Figure 5-3. Melting temperature was calculated using the New England Biolabs tool (<https://tmcalsculator.neb.com/>). Extension time was adjusted to allow approximately one minute per thousand base pairs of DNA as per the Platinum™ Taq DNA Polymerase High Fidelity protocol.

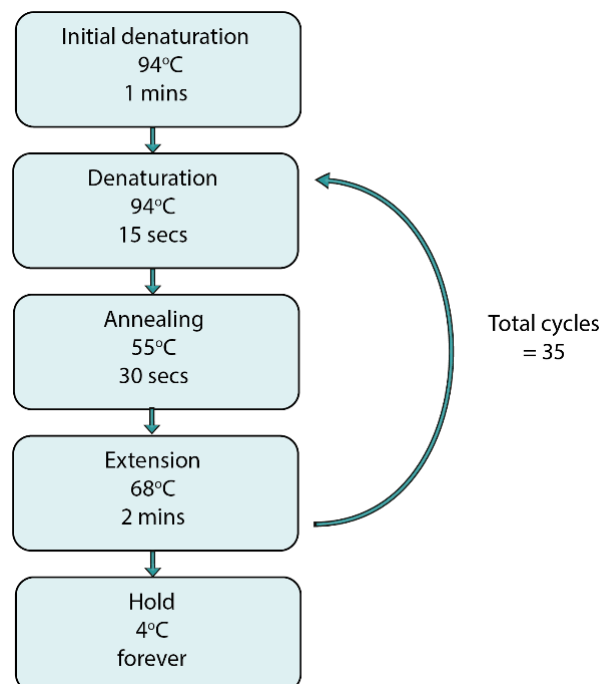


Figure 5-3: PCR programme for amplification of CCP 22-30 from CR1 cDNA.

5.4.4 Adding 3' adenine overhangs

As a highfidelity enzyme had been used to amplify the cDNA, the purified PCR product did not possess adenine (A) overhangs, which are necessary for TA cloning. As such, an extra step was included to replace these A overhangs prior to ligation. The following products were sourced from Promega; dATP (U120A), GoTaq G2 DNA Polymerase (M7841) and 5x Green GoTaq Reaction Buffer (M791A).

The reaction was set up as follows:

Purified PCR product	20 μ l
dATP (100 mM)	0.1 μ l
5x Green GoTaq Reaction Buffer	10 μ l
Sterilised dH ₂ O	19.7 μ l
GoTaq G2 DNA Polymerase	0.2 μ l

The reaction was incubated at 72°C for 20 minutes and then purified using the Nucleospin® Gel and PCR Clean-up kit (Macherey-Nagel, 74060950) according to the manufacturer's instructions. DNA quantity was determined by spectrophotometry.

5.4.5 Agarose gels

100 ml of 1x tris-acetate EDTA (TAE) buffer was made by diluting 50x tris acetate EDTA (TAE, ThermoFisher Scientific, BP1332-1) in dH₂O. To cast 1% agarose gels, 0.5g UltraPure™ agarose (ThermoFisher Scientific, 16500500) was dissolved in 50 ml of 1x TAE and heated at 800W in a microwave for 90 seconds with agitation until completely dissolved (for 0.75% gels 0.375 g of agarose was used). The melted agarose was poured into a cast, a well-comb inserted and set for 30 minutes. The comb was removed and the remaining 50 ml of 1x TAE buffer poured over the gel.

5 μ l of the molecular marker Quick-Load® 1 kb DNA Ladder (New England Biolabs, N0468S) was added to estimate the molecular weight of the DNA samples. To allow visualisation and increase the density, samples were mixed with 6x gel loading dye

(New England Biolabs, B7420S) at a ratio of five parts sample to one-part loading dye. The gel was run at 80V for 40-60 minutes. The gel was protected from light and incubated on a rocker with either 0.5 µg/ml ethidium bromide (Sigma-Aldrich, 46067) in 1x TAE for 15 minutes or 1:10,000 SYBR Safe[®] DNA Gel Stain (Thermo Fisher Scientific, S33102) in 1x TAE for 30 minutes. DNA was visualised under ultra-violet (UV) light using a G:Box gel system and GeneSnap software (Syngene, India).

5.4.6 Gel fragment isolation and purification

Gel extraction was used to purify the amplified portion of CR1, and was also used following restriction digests when more than one gel band was generated. In addition to the sample to be purified, a guide sample was also run on an agarose gel and stained with ethidium bromide. The gel was divided and the guide sample visualised under UV light. The band of interest was then excised under direct vision. The gel was reassembled away from the UV source and the cut band used as a guide for excision of the sample band whilst avoiding exposure to mutagenic UV radiation. The final cut band was purified using the Nucleospin[®] Gel and PCR Clean-up kit (Macherey-Nagel, 74060950) according to the manufacturer's instructions. The process is illustrated in Figure 5-4.

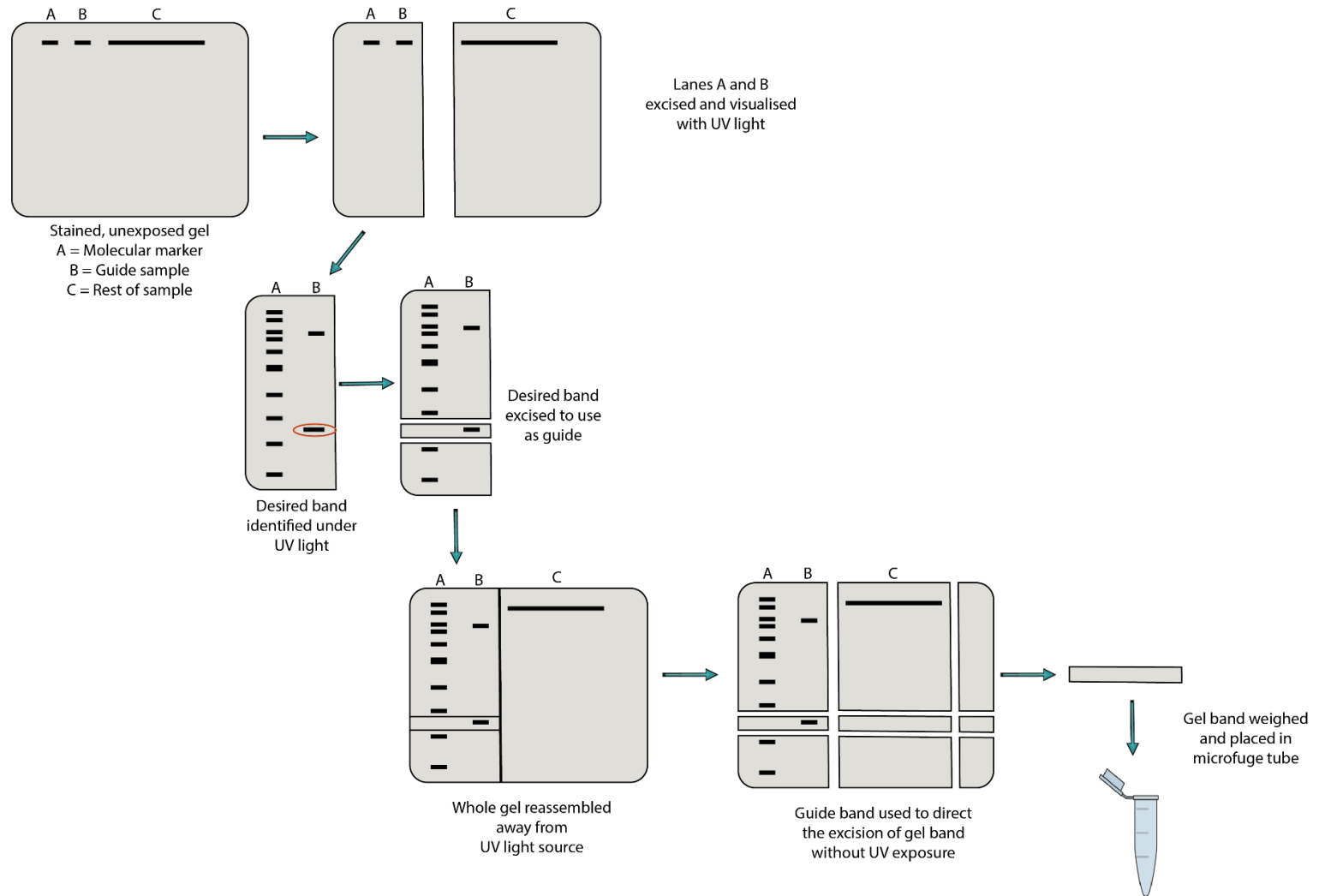


Figure 5-4. Isolation of agarose gel band to minimise exposure of sample to UV light.

5.4.7 Preparation of growth media

In preparation for ligation and transformation, antibiotic-supplemented growth medium was prepared. Luria-Bertani (LB) agar plates were prepared by adding 17.5 g LB broth with agar (Lennox, Sigma L2897) to 500 of dH₂O (final concentration 15 g/L agar, 10 g/L, tryptone, 5 g/L yeast extract and 5 g/L NaCl). The solution was autoclaved for 15 minutes at 121 °C and left until cool to touch. 0.5ml of 100 mg/ml ampicillin was added to give a final concentration of 100 µg/ml. While still molten, the sterile LB agar was poured into 100 mm x 15 mm petri dishes next to a Bunsen burner on a blue flame. 25 ml of LB agar was added to each dish and left to cool for 30 minutes at room temperature. Agar plates were stored at 4°C for up to five weeks and checked for contamination before use.

For work with plasmids containing a multiple cloning site (MCS) within a *lacZα* sequence, isopropyl-β-d-thiogalactopyranoside (IPTG) and X-gal were added to the plate. 40 µl each of 20 mg/ml X-gal (Melford, B71800) and 100 mM IPTG (Promega, V3951) were spread onto the plate and incubated at 37°C for 30 minutes prior to plating out the transformed *E. coli*. LB broth was prepared by adding 20 g of LB-broth powder (Sigma-Aldrich, L3022) to 1L dH₂O and autoclaving for 15 minutes at 121 °C. LB-broth was kept at 4°C and ampicillin added to small aliquots as necessary (to minimise antibiotic degradation) to give a final concentration of 100 µg/ml.

5.4.8 Ligation into the pCRII cloning vector

The purified PCR product with A overhangs was ligated into the cloning vector pCRII using the TA Cloning® Dual Promoter pCRII kit (which contains the ExpressLink™ T4 DNA ligase and buffer, Thermo Fisher Scientific, K2070). The linearised pCRII vector has single thymidine (T) residues at the 3' ends which are complimentary to the single A added to the 3' ends of PCR products by the Taq polymerase step (described in section 5.4.3), enabling efficient ligation (Figure 5-5).

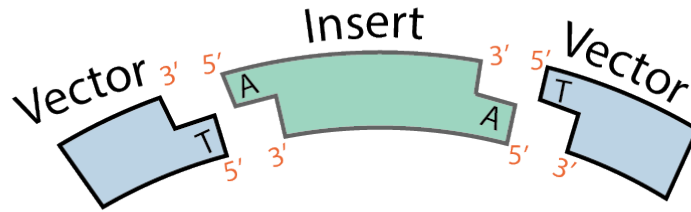


Figure 5-5: Cartoon of TA cloning.

“T” ends of pCRII vector and “A” ends of the PCR product (insert) are complimentary, allowing efficient ligation.

Image adapted from TA Cloning® Dual Promoter pCRII kit manual, Thermo Fisher Scientific.

Fresh PCR products were used for ligation to ensure A-overhangs were maintained. Ratios of the cDNA inserts and linearised vector were calculated using New England Biolabs Ligation Calculator (<http://nebiocalculator.neb.com/#!/ligation>), with an insert DNA length of 1.79 kb, vector DNA length of 3.9 kb and vector mass of 50 ng. A ratio of 3 (insert): 1 (vector) was used, which resulted in using 68.85 ng of insert and 50 ng of pCRII vector. The reaction was set up as follows:

Purified PCR product with A overhangs (48.6 ng/μl)	1.42 μl
5x ExpressLink™ T4 DNA ligase buffer	2 μl
pCRII vector (25 ng/μl)	2 μl
Sterilised dH ₂ O	3.6 μl
ExpressLink™ T4 DNA ligase (5 units/μl)	1 μl

The ligation reaction was mixed and incubated at room temperature for one hour.

5.4.9 Transformation into *E. coli*

Four μl of the ligation reaction was added to 50 μl of One Shot™ TOP10F' chemically competent *E. coli* cells (Thermo Fisher Scientific, C303003) and swirled gently. The reaction was placed on ice for 30 minutes following which cells were heat shocked in a water bath at 42°C for 30 seconds then returned immediately to ice for a further two minutes. 250 μl of room temperature Super Optimal broth with Catabolite repression (SOC medium, Thermo Fisher Scientific, 15544034) was added and the reaction incubated at 37°C on an orbital shaker at 225 rpm for one hour.

100 µl of the reaction was spread evenly onto a 100 mm LB agar plate containing ampicillin, IPTG and X-gal and incubated overnight at 37°C. Plates were inspected the following morning and colonies selected for expansion either by blue/white screening or colony PCR (see below). If colony PCR was not being performed, isolated colonies were selected for expansion and added to 3 ml of LB broth (with 100 µg/ml of ampicillin) in a 14 ml vented round-bottom polypropylene tube (Falcon 352059). These “mini-broths” were incubated at 37°C at 225 rpm on an orbital shaker overnight.

5.4.10 Colony PCR

To minimise the number of colonies expanded and sequenced, colony PCR was performed to screen colonies and determine whether they contained an insert of the anticipated size. Primers spanning the MCS of the pCRII vector were used to amplify any inserted DNA sequence (T7_PROM SP6_PROM primer pair, see Table 5-1). For each colony to be screened, a PCR tube was made up containing:

Sterilised dH ₂ O	33.75 µl
5 x GoTaq green buffer	10 µl
T7_PROM (10 µM)	2.5 µl
SP6_PROM (10 µM)	2.5 µl
DNTP (10 µM)	1 µl

Single isolated white colonies were lightly touched with a sterile 200 µl pipette tip and the tip then swirled in the respective PCR tube. The rest of the colony was then picked and placed into 3 ml of LB broth with 100 µg/ml of ampicillin in a labelled 14 ml polypropylene tube with snap cap (Falcon 352059). These cultures were stored at 4°C until the screening PCR was complete. As the final step, 0.25 µl of GoTaq DNA polymerase was added to the PCR mixture and run on the following programme:

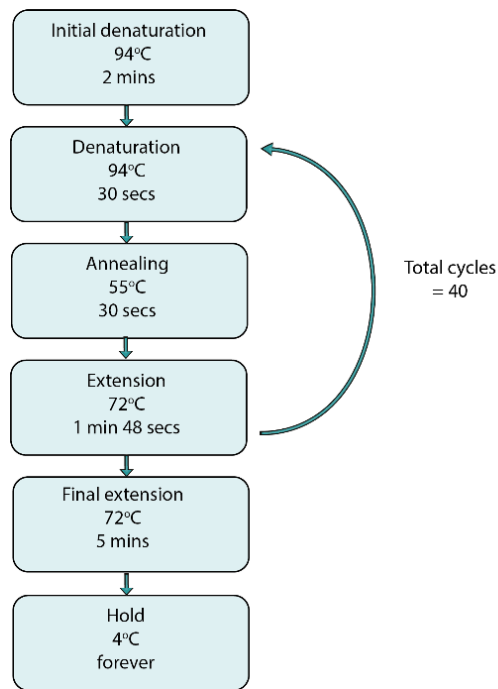


Figure 5-6. PCR programme for screening of colonies.

The PCR products were then run on a 1% agarose gel in 1 x TAE buffer at 80 V for 40 minutes followed by staining in 0.5 µg/ml ethidium bromide for 15 minutes. Colonies containing inserts of the expected molecular weight were selected for expansion +/- sequencing. These promising colonies were expanded in 3 ml of LB broth with 100 µg/ml ampicillin and the “mini-broth” culture was incubated overnight at 37°C on an orbital shaker at 225 rpm.

5.4.11 Miniprep

Plasmids were extracted from the “mini-broth” culture using the GeneJET Plasmid Miniprep Kit (Thermo Fisher Scientific, K0502) as per the manufacturer’s instructions. DNA quantity and purity was determined using a spectrophotometer.

5.4.12 Diagnostic restriction digestion

To confirm that the plasmids contained inserts of the expected size, a diagnostic digest was undertaken using the restriction enzyme EcoRI – High Fidelity (New England Biolabs, R3101S) which has restriction sites flanking the TA cloning site in the pCRII plasmid. The following reaction was set up:

Miniprep elute	3 μ l
CutSmart buffer x 10	2.5 μ l
Sterilised dH ₂ O	19.5 μ l
EcoRI – HF	1 μ l

The reaction was incubated at 37°C for one hour followed by an inactivation step at 65°C for 20 minutes. The digestion products were visualised on a 1% agarose gel.

5.4.13 Sequencing

Three unique sequencing primers were designed for the CCP 22-30 insert (SP1, SP2 and SP4, see Table 5-1). Two further sequencing primers (T7_PROM and SP6_PROM) flanking the TA cloning site were also used. Following colony PCR screening and diagnostic restriction digestion, clones were selected for Sanger sequencing. One reaction was prepared per primer as follows:

Miniprep eluate (~ 500 ng/ μ l)	1 μ l
Sequencing primer (6.4 μ M)	1 μ l
Sterilised dH ₂ O	4 μ l

Samples were submitted for BigDye reaction and Sanger sequencing using an ABI 3730XL capillary sequencing instrument (Edinburgh Genomics, The University of Edinburgh, <http://genomics.ed.ac.uk/>). Sequences were aligned using SnapGene molecular biology software version 4.1 (GSL Biotech). Where mismatches occurred, the quality of the base calls was visually inspected and calls updated as necessary.

5.4.14 Glycerol stocks

After sequencing had confirmed that a plasmid contained the desired insert without unwanted mutations, glycerol stocks of the respective transformed *E. coli* were made. 10 μ l of the original mini-broth was used to inoculate 3ml of LB broth containing 100 μ g/ml of ampicillin. The mixture was incubated at 37°C on an orbital shaker at 225 rpm for six hours, to ensure the bacteria were still in the exponential

growth phase. Next to a Bunsen burner, the 3 ml culture was divided into 500 µl aliquots in Nunc™ cryogenic tubes (ThermoFisher Scientific, 366656) to which 500 µl of 50% sterile glycerol (Applied Biosystems, 4392215) was added and the tube inverted until no layers could be seen. Glycerol stocks were stored at -70°C.

When new colonies were required, the tube was placed on dry ice and the surface of the glycerol stock was scratched with a colony picker, streaked onto a new LB agar plate (with ampicillin) and incubated overnight at 37°C.

5.4.15 Site-directed mutagenesis

Once the expected CR1 CCP 22-30 DNA sequence was confirmed without unwanted errors, site-directed mutagenesis was performed to introduce the *SI2* and *McC^b* mutations. Coordinates are given as per the human mRNA sequence for CR1 (GenBank, <https://www.ncbi.nlm.nih.gov/nucore/Y00816>).

SI1 → *SI2*

- Nucleotide change A4828G
- Amino acid change R1610G
- Primers used SL2_F and SL2_R

McC^a → *McC^b*

- Nucleotide change A4795G
- Amino acid change K1595E
- Primers used MCCB_F and MCCB_R

The *McC^b* mutation has not been reported as a single mutation and only occurs on the background of *SI2*. However, the decision was taken to also produce the *McC^b* mutation on its own (i.e. on an *SI1* background) in order to allow detailed examination of any influence the *McC^b* mutation might have on CR1 function.

The following three mutants were made using site-directed mutagenesis.

- *SI2/MCC^a*
- *SI1/MCC^b*
- *SI2/MCC^b*

In the case of the double mutant *SL2/McCb*, mutations were introduced one at a time. CloneAmp HiFi PCR Premix (Takara, 639298) which contains the enzyme CloneAmp HiFi Polymerase was used for site-directed mutagenesis. For each mutation, the following reaction was set up:

SL2_F or MCCB_F (10 μ M)	0.5 μ l
SL2_R or MCCB_R (10 μ)	0.5 μ l
Plasmid template (100 ng/ μ l)	1 μ l
Sterilised dH ₂ O	11.5 μ l
CloneAmp HiFi PCR Premix	12.5 μ l

Extension time was adjusted to 5 seconds per thousand base pairs of DNA as per CloneAmp HiFi Polymerase protocol. As the plasmid was \sim 6 kb, this was set to 30 seconds. To reduce the risk of unwanted mutations in the process, number of cycles performed was kept to a minimum (18 cycles). The site-directed mutagenesis reaction was run on the following programme:

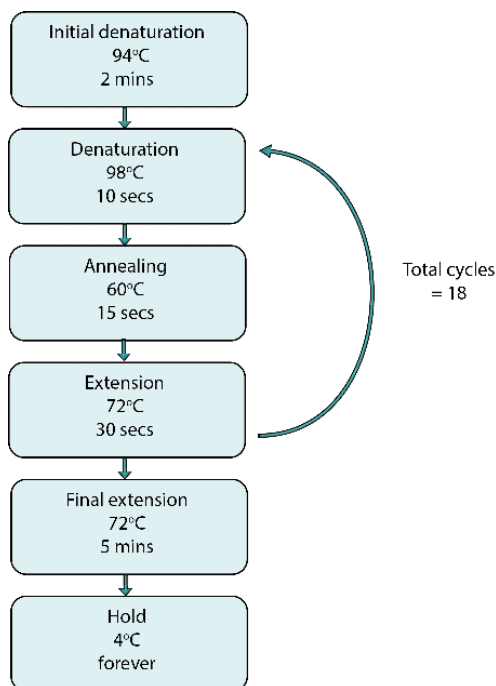


Figure 5-7: PCR programme for site-directed mutagenesis

Five μ l of the reaction was removed to visualise on an agarose gel. The remaining reaction was treated with DpnI restriction enzyme to remove the methylated DNA

of the template plasmid. The mutation product was added to 5 µl of 10x CutSmart buffer (New England Biolabs, B7204S) with 0.5 µl DpnI (New England Biolabs, R0176S). The reaction was incubated at 37°C for one hour followed by an inactivation step of 80°C for 20 minutes.

After DpnI treatment, the mutated plasmid was purified (described in 5.4.6) and eluted with a final volume of 15 µl to concentrate the DNA. Five µl of the eluate was transformed into One Shot™ TOP10F' *E. coli* (outlined in 5.4.9). As this step only involved mutation, not ligation, blue/white screening was not necessary. The transformed *E. coli* were plated onto LB agar with ampicillin and incubated overnight at 37°C. Colonies were selected, plasmids purified by miniprep and sequenced as previously described. Glycerol stocks were made of successful mutants.

After the single *SI2* and *McC^b* clones were made, the *SI2/McC^b* double mutant was produced. The *McC^b* mutation was introduced onto the back of the *SI2* clone using the primers MCCB_F and MCCB_R and the procedure described above.

5.4.16 Expression plasmid

The expression plasmid pcDNA 3.1 (-) CCP22-30 His was a kind gift from Dr Nicole Thielens, Grenoble, France. The group had previously produced the plasmid which contains the mammalian expression vector pcDNA 3.1 (-) with a 1804 bp insert corresponding to the CCP 22-30 fragment (nucleotides 4210-5926, amino acids 1404-1976, with no *SI/McC* mutations) (Jacquet et al., 2013). CCP 22-30 is in frame with part of the native CR1 signal peptide (nucleotides 100-147, amino acids 34-49, inserted using site-directed mutagenesis) cloned into the BamHI – KpnI sites of the pcDNA 3.1 (-) vector. The plasmid also has a fusion 6x His-tag at the C-terminal end of CCP 22-30 (introduced using site-directed mutagenesis) (Jacquet et al., 2013). Like the pCRII vector, the pcDNA 3.1 vector also contains an ampicillin resistance gene. The effect of the His tag has previously been examined and found not to influence the binding of MBL or L-ficolin to the CCP 22-30 recombinant fragment (Jacquet et al., 2013).

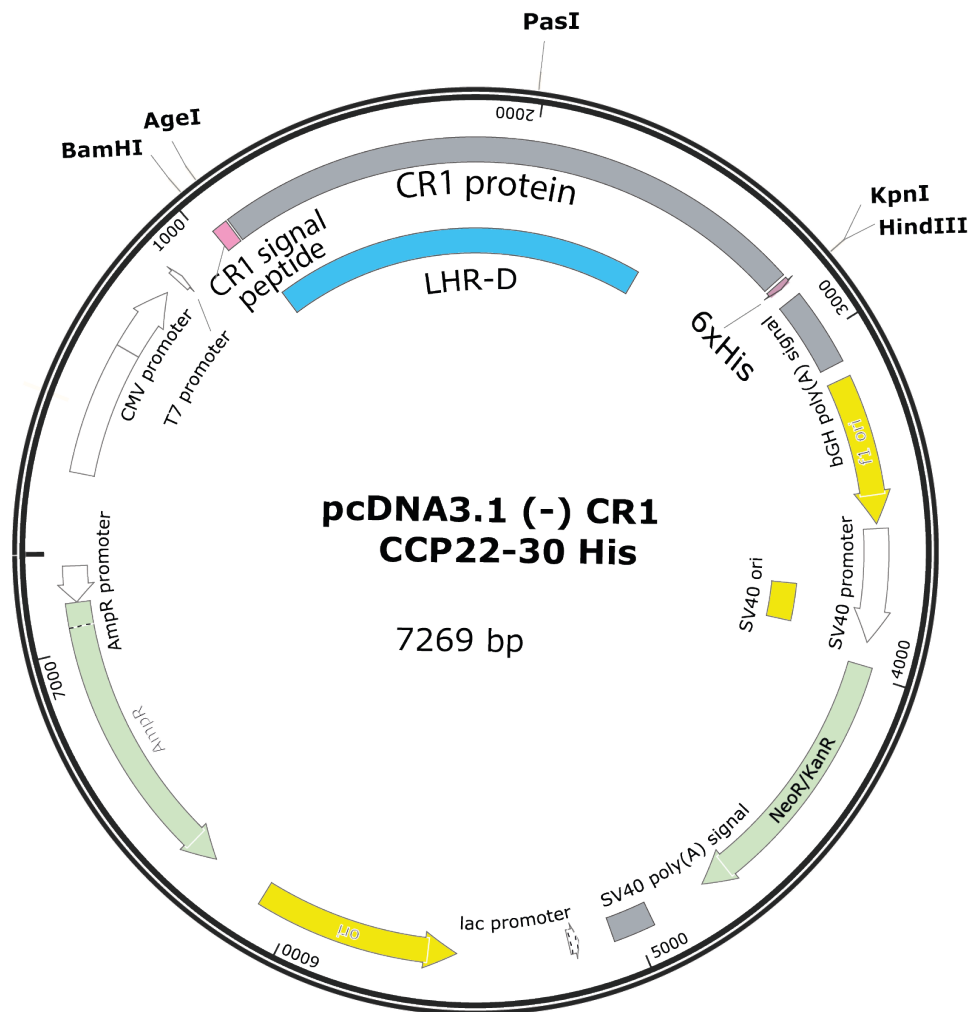


Figure 5-8: Original expression plasmid *pcDNA3.1 (-) CCP 22-30 His*. CR1 signal peptide, LHR-D region, His-tag and AgeI, PasI, BamHI, KpnI and HindIII restriction sites are shown.

To allow cloning in of the mutant sequences, unique restriction enzyme sites within the expression plasmid's insert were explored and AgeI and PasI were selected. Digestion at these points preserves the CR1 signal peptide and the His-tag, allowing insertion of the mutant insert.

5.4.17 Maxi prep

In preparation for digestion of the *pcDNA3.1 (-) CCP 22-30 His* plasmid, transformation, expansion and purification of the plasmid was performed by Maxi-prep (EndoFree Plasmid Maxi Kit, Qiagen, 12362) as per the manufacturer's instructions.

5.4.18 Adding restriction sites to mutant inserts

To facilitate sub-cloning, the *SI2*, *McC^b* and *SI2/McC^b* mutant inserts were amplified by PCR with an *AgeI* added to the 5' primer and the *PasI* site included in the 3' primer (Table 5-1). A separate reaction was set up of for each of the mutants as follows:

10x High fidelity PCR buffer	2.5 µl
50 mM MgSO ₄	1 µl
10 µM DNTP mix	0.5 µl
10 µM <i>AgeI</i> primer	0.5 µl
10 µM <i>PasI</i> primer	0.5 µl
50 ng/µl Mutant plasmid	1 µl
Sterilised dH ₂ O	18.9 µl
Platinum™ Taq DNA Polymerase High Fidelity (5 units/µl)	0.1 µl

The PCR reaction was run on the following programme.

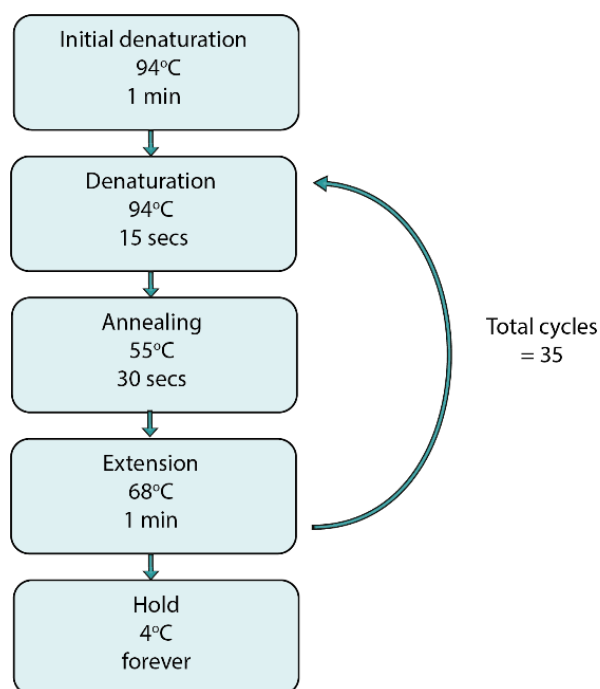


Figure 5-9: PCR programme to add *AgeI* and *PasI* restriction sites to mutant inserts

Once finished, 2.5 µl of the PCR reaction was visualised on an agarose gel.

5.4.19 Double digestion

Digestion of mutant inserts

The *SI2*, *McC^b* and *SI2/McC^b* PCR products from above were digested with *AgeI* (Thermo Fisher Scientific, ER1461) and *PasI* (Thermo Fisher Scientific, ER1861) to produce “sticky ends.” Sequential digests were performed, both using the *PasI* buffer due to incompatibility of this enzyme in other buffers. The following reaction was set up:

Mutant PCR products with restriction enzyme sites	20 μ l
Sterilised dH ₂ O	36 μ l
10x <i>PasI</i> buffer	4 μ l
<i>PasI</i> (10 units/ μ l)	2.5 μ l
<i>AgeI</i> (10 units/ μ l)	2.5 μ l

The reaction was incubated at 37°C for 3 hours followed by 55°C for a further 3 hours. The products were run on a 1% agarose gel and the expected band gel-purified as previously outlined.

Expression vector digestion

Double digestion of the expression plasmid pcDNA3.1 (-) CCP 22-30 His using the above did not yield the expected band sizes, hence an alternative method was used. Alternative sources of *PasI* (*PasI* Optizyme™, Thermo Fisher Scientific, BP8073-1) and *AgeI* (*AgeI*-HF New England Biolabs, R3552S) were used and digestions performed sequentially. Ten parallel reactions were set up:

Expression plasmid (250 ng/ μ l)	2 μ l
Sterilised dH ₂ O	15.9 μ l
10x <i>PasI</i> buffer	2 μ l
<i>PasI</i> (10 units/ μ l)	0.15 μ l

The reaction was incubated at 55°C for 2 hours followed by 20 minutes at 80°C to heat inactivate *PasI*. The resultant digest was purified using a Nucleospin column (see “Gel fragment isolation and purification”) to remove the restriction enzyme

and eluted into 30 μ l of elution buffer. Twelve reactions were then set up in parallel each containing:

PasI digest product	2 μ l
Sterilised dH ₂ O	19.5 μ l
CutSmart buffer x10	2.5 μ l
Agel-HF (20 units/ μ l)	1 μ l

The digestion reaction was incubated for 15 minutes at 37°C. The size of digestion products was subsequently confirmed using agarose gel electrophoresis. The gel band of the expected size was excised and purified as detailed in 5.4.6.

5.4.20 Ligation into expression vector

Following digestion, the inserts and the expression vector had compatible ends.

Three separate reactions were set up; *SI2* mutant insert + expression vector, *McC^b* mutant insert + expression vector and *SI2/McC^b* mutant insert + expression vector.

A 3 (insert): 1 (vector) molar ratio was calculated using New England Biolabs Ligation Calculator (<http://nebiocalculator.neb.com/#!/ligation>), with an insert DNA length of 906 bp, vector DNA length of 6391 bp and a vector mass of 50 ng, which resulted in using 21.26 ng of insert. The concentration of the three purified inserts ranged from 44.4-60.7 ng/ μ l). The reaction was set up as follows:

Gel purified insert (44.4-60.7 ng/ μ l)	0.35-0.48 μ l
5x ExpressLink™ T4 DNA ligase buffer	2 μ l
Gel purified expression vector (30 ng/ μ l)	1.67 μ l
Sterilised dH ₂ O	4.85-4.98 μ l
ExpressLink™ T4 DNA ligase (5 units/ μ l)	1 μ l

As a negative control, a further reaction was set up which contained the digested expression vector only without an insert. The volume of sterilised dH₂O was increased accordingly.

The four ligation reactions were incubated at room temperature for 15 minutes followed by 2 hours at 4°C. Following this, 5 μ l of each ligation reaction was

transformed into 50 µl of One Shot™ TOP10F' chemically competent *E. coli* cells (Thermo Fisher Scientific, C303003) as described in section 5.4.9. Blue/white screening was not possible as the expression vector did not contain a *lacZα* sequence.

The next morning, four colonies were selected from each plate and expanded in LB broth with ampicillin as described in 5.4.9. Plasmid DNA was isolated by miniprep as described in 5.4.11. A diagnostic restriction digestion was performed using the restriction enzymes BamHI-HF (New England Biolabs, R3136S) and HindIII-HF (New England Biolabs, R3104S), which cleave either side of the full insert (CR1 signal peptide + CCP 22-30 + His tag), as shown in Figure 5-8. The reaction was set up as follows:

Miniprep eluate (approx. 350 ng/µl)	1 µl
10x CutSmart buffer	2.5 µl
BamHI-HF (20 units/µl)	1 µl
HindIII-HF 20 (units/µl)	1 µl
Sterilised dH ₂ O	19.5 µl

As a positive control, 250 ng of original expression plasmid DNA (prior to digestion or ligation) was used as this contains an insert of the identical size, but without any mutations. The samples were incubated at 37°C for 15 minutes, run on a 1% agarose gel at 70V for 45 minutes and visualised after staining with ethidium bromide.

5.5 Results

5.5.1 Creation of the pCRII plasmid with CCP 22-30 insert

A delay in the arrival of the expression plasmid meant it was necessary to produce a pCRII plasmid containing the CCP 22-30 insert, perform site-directed mutagenesis and then ligate the mutated insert into the expression plasmid.

Full length human CR1 cDNA was used as a template for amplification of the region of interest. The sequence corresponding to CCP 22-30 was selected (nucleotides 4210-5937, amino acids 1404-1979), which encompasses LHR-D (CCP 22-28) and CCP 29-30. The intended amplicon was 1729 bp and is shown in Figure 5-10.

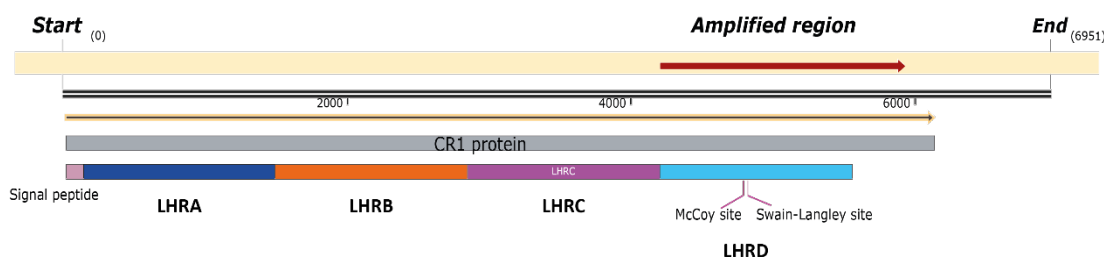


Figure 5-10: Amplified region of CR1 cDNA

CR1 cDNA sequence (double black line) is shown with the region corresponding to the mature CR1 peptide (below in grey). CR1 signal peptide is shown in pink and the functional regions of CR1 are outlined (annotated colour blocks). The CCP 22-30 amplified is shown at the top of the figure (red arrow).

The primer pair LHRD_F and LHRD_R were used to amplify the region of interest by PCR. To permit TA cloning, the PCR product was incubated with dATP and GoTaq G2 DNA polymerase to add adenine overhangs to the 3' ends of the amplicon. The resultant product was run on a 1% agarose gel at 80V for 40 minutes and stained with ethidium bromide for 15 minutes. The expected band at ~1.7 kb was excised while protecting it from UV light (Figure 5-11, Gel A). DNA was purified from the gel slice, eluted with 30 μ l of elution buffer and quantified as 168.9 ng/ μ l on spectrophotometry. The purified amplicon was ligated into the commercial vector pCRII at a ratio of 3:1 (amplicon:vector) and transformed into One Shot™ TOP10F' *E. coli* chemically competent cells. 100 μ l of the reaction was spread on an LB agar plate (with ampicillin, X-gal and IPTG) and incubated overnight at 37°C.

Thirteen white colonies were selected from the LB agar plate and screened for the presence of the desired insert using colony PCR with the primer pair T7_PROM (T7 promoter region) and SP6_PROM (SP6 promoter region). These regions flank the MCS of the cloning vector, therefore amplifying any insert contained. PCR products were visualised on a 1 % agarose gel (Figure 5-11, Gel B).

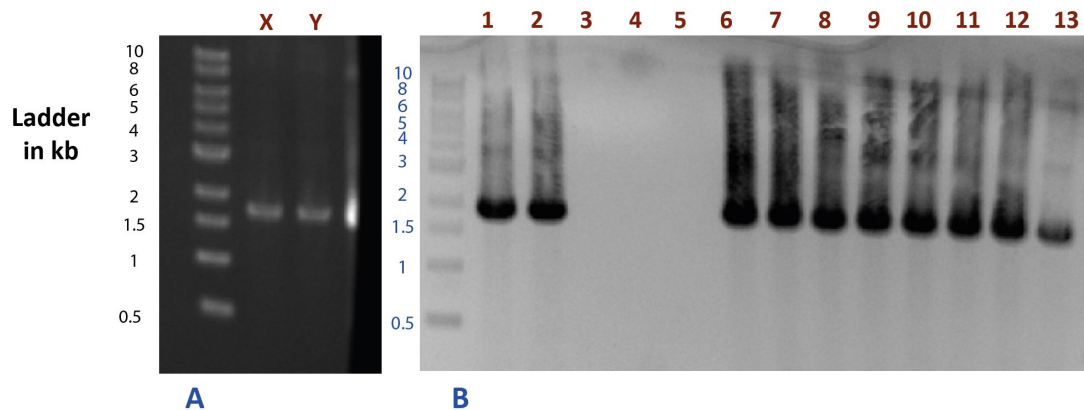


Figure 5-11: Amplification and cloning of CCP 22-30 fragment.

Gel A: Amplification of CCP 22-30 from CR1 cDNA using primer pair LHRD_F and LHRD_R produces a PCR product of expected molecular weight (~1.7kb). Lanes X and Y are both samples of the same PCR reaction.

Gel B: Following ligation and transformation of above amplicon, colonies were screened by colony PCR.

Primers spanning the multiple cloning site (MCS) were used. Each lane represents a unique colony.

Lanes 1, 2, and 6-13 show bands at the expected molecular weight (~1.7 kb)

PCR products were run on 1% agarose gels with 5 μ l Quick-Load® 1 kb DNA ladder and stained with ethidium bromide.

Ten colonies produced bands at the expected molecular weight (~ 1.7 kb) when amplified with T7_PROM and SP6_PROM primers. Eight “positive” colonies (1, 2 and 7-12) and two “negative” colonies (3 and 4), serving as negative controls, were expanded overnight in LB broth with ampicillin. Minipreps were performed the next morning to purify the plasmid. A diagnostic restriction digest was performed using EcoRI to digest the insert from the vector. The digested plasmids were then run on 1% agarose gels to confirm the size of the insert, as shown in Figure 5-12.

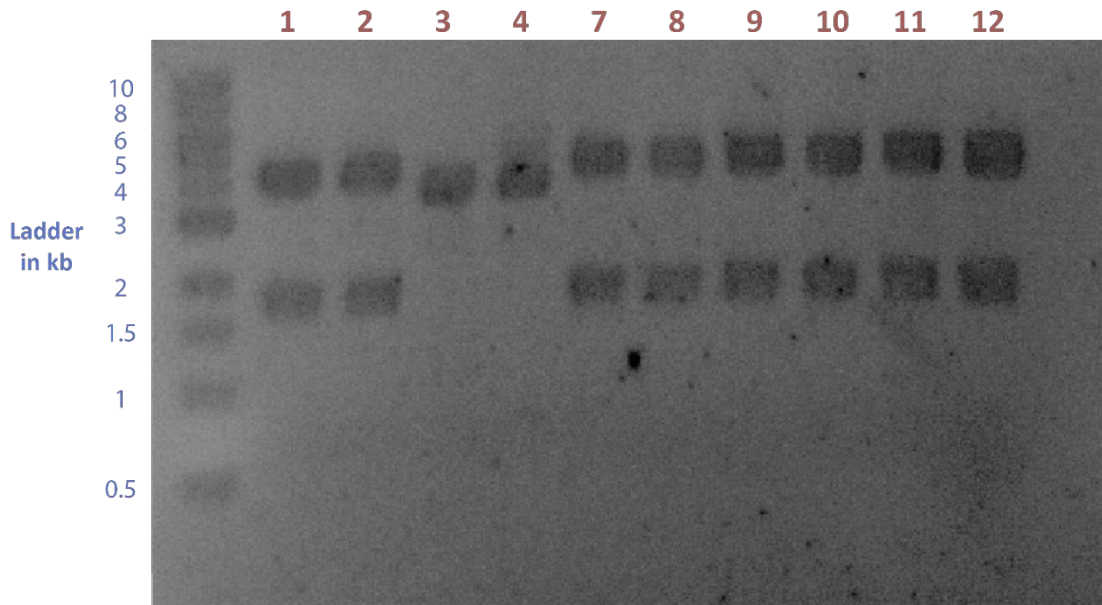


Figure 5-12: *EcoRI* restriction digestion of miniprep eluates.

Lanes 1, 2 and 5-10 contain the two expected bands; vector at ~4kb and insert at ~1.7 kb. Lanes 3 and 4 are negative controls identified through colony PCR (see above), which did not contain the insert.

NB - Lanes correspond with those samples in Figure 5-11.

PCR products were run on a 1% agarose gel with 5 μ l Quick-Load® 1 kb DNA ladder and stained with ethidium bromide.

5.5.2 Sequencing of the inserts

Clone 1 was selected for Sanger sequencing of the CCP 22-30 insert. Spacing and direction of the sequencing primers is shown below:

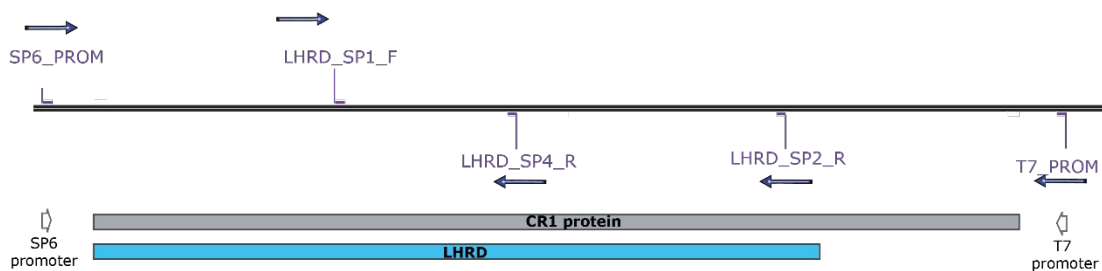


Figure 5-13: Spacing and direction of primers for sequencing of the insert.

The region of the cloning vector (pCRII) immediately surrounding the insert is also shown to illustrate where the SP6_PROM and T7_PROM primers bind.

Sequences were aligned against the nucleotide sequence of human mRNA for CR1 (GenBank , <https://www.ncbi.nlm.nih.gov/nuccore/Y00816>), see Figure 5-14.

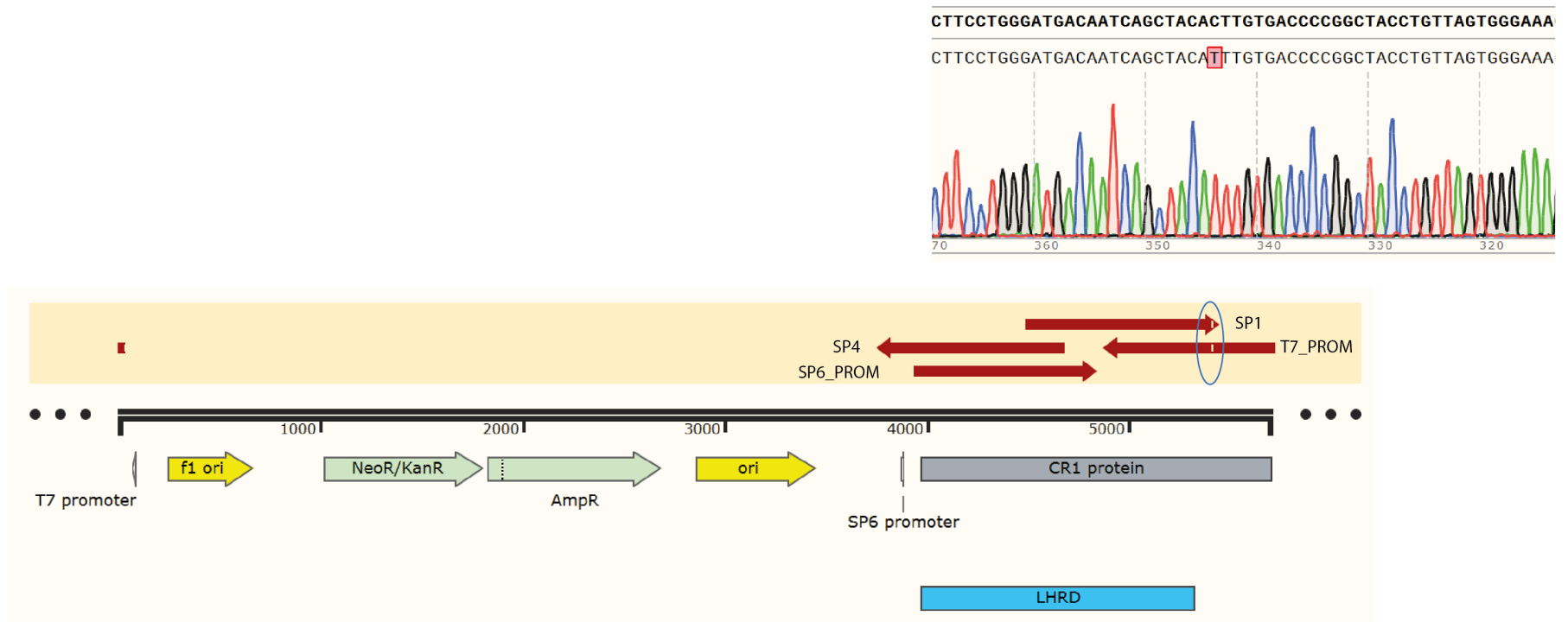


Figure 5-14: Sanger sequencing of CCP 22-30 insert (Clone 1)

Reads from insert-specific sequencing primers SP1 and SP4 (NB – sequencing with SP2 failed in this experiment) and vector-specific sequencing primers (T7_PROM and SP6_PROM) are shown. Filled red arrows indicate perfect alignment with the reference sequence. White bars within the red arrows indicate a mismatch (highlighted by blue circle). The insert shows the section of the chromatogram from SP1 corresponding to the mismatch at position 5416 on the plasmid with the reference sequence along the top in bold.

Although the sequencing primer SP2 failed to provide a read, overall sequencing coverage was adequate. All regions of the insert aligned with the CR1 reference sequence (<https://www.ncbi.nlm.nih.gov/nuccore/Y00816>), but a C→T mismatch was detected at plasmid nucleotide position 5416 by the SP1 and T7_PROM primer. This mutation on the insert corresponds to nucleotide 5654 and amino acid 1885 on the CR1 reference sequence, resulting in a non-synonymous codon change from ACT → ATT which represents an amino acid change of threonine (T) to isoleucine (I).

Six further clones were selected to investigate this potential mismatch further to undergo targeted sequencing using just the T7_PROM sequencing primer (which provided the best coverage of the region in question). All six clones showed the same mutation, suggesting this was either in the template cDNA or introduced very early in the amplification PCR process (data not shown).

Alternative online reference sequences of mRNA from this region of the CR1 gene were interrogated to ascertain whether the accepted amino acid in the human genome sequence at this codon represents a threonine or an isoleucine.

Alternative sequences were retrieved from the National Center for Biotechnology Information (NCBI) GenBank and dbSNP databases were used. Gorilla (*Gorilla gorilla*) and chimpanzee (*Pan troglodytes*) sequences were also reviewed to investigate the evolutionary history at this site (Table 5-2).

Reference genome Source	Sequence ID	Species	Reported amino acid
NCBI GenBank	Y00816.1	<i>Homo sapiens</i>	T
NCBI GenBank	X05309.1	<i>Homo sapiens</i>	T
NCBI GenBank	XM_011509205.1	<i>Homo sapiens</i>	I
NCBI GenBank	XM_006711166.2	<i>Homo sapiens</i>	I
NCBI GenBank	NM_000651.4	<i>Homo sapiens</i>	I
NCBI GenBank	NM_000573.3	<i>Homo sapiens</i>	I
NCBI dbSNP	rs=200990657	<i>Homo sapiens</i>	I
NCBI GenBank	XM_019035938.1	<i>Gorilla gorilla</i>	I
NCBI GenBank	XM_016949043.1	<i>Pan troglodytes</i>	I

Table 5-2: Comparison of published amino acids at the site of interest.
T = threonine, I = isoleucine. *Gorilla gorilla* = Gorilla. *Pan troglodytes* = chimpanzee.

Five of the seven human mRNA sources reported an isoleucine at this site. On further examination, both of the sequences reporting a threonine at this site were published by the same group (Klickstein et al., 1987, 1988). Both gorilla and chimpanzee mRNA also contained an isoleucine at this site, suggesting that this was the ancestral amino acid. As such, it was determined that the C nucleotide at position 5416 change in our plasmid was unlikely to be a mutation and the observed mismatch was more likely to be due to a SNP or by a sequencing error in the reference sequence used.

As such, Clone 1 was selected for further work and glycerol stocks made of the plasmid prior to site-directed mutagenesis.

Of note, the expression plasmid pcDNA3.1 (-) CCP 22-30 His was sequenced and also found to contain an isoleucine instead of a threonine at the corresponding CR1 amino acid site.

5.5.3 Creation of *SI2* and *McC^b* mutations

The CCP 22-30 insert successfully ligated into the Clone 1 plasmid contains an LHR-D region corresponding to the Caucasian or “wild type” genotype of Swain-Langley and McCoy polymorphisms, *i.e.* bearing the *SI1* and *McC^a* alleles. Table 5-3 summarises the nucleotide, amino acid and charge changes of the wild type and planned mutant inserts. Coordinates are given as per the human mRNA sequence for CR1 (GenBank, <https://www.ncbi.nlm.nih.gov/nucore/Y00816>).

Insert	Nucleotide 4795 (<i>McC</i>)	Nucleotide 4828 (<i>SI</i>)	Amino acid 1595 and charge (<i>McC</i>)	Amino acid 1610 and charge (<i>SI</i>)
<i>Wild type</i>	A	A	K (+)	R (+)
<i>SI2/McC^a</i>	A	G	K (+)	G (-)
<i>SI2/McC^b</i>	G	G	E (neutral)	G (-)
<i>SI1/McC^b</i>	G	A	E (neutral)	R (+)

Table 5-3 Mutations and their respective nucleotide, amino acid and charge. Co-ordinates are given as per the complete ligated plasmid.

Site-directed mutagenesis was performed using the enzyme CloneAmp HiFi Polymerase as detailed in section 5.4.15. The primer pairs SL2_F/SL2_R and MCCB_F/MCCB_R (see Table 5-1) were used to introduce the *SI2* and *McC^b* mutations respectively in separate PCR reactions. To reduce the chance of introducing unwanted mutations, PCR cycles were kept to a minimum (18 in total).

Five µl of the resultant PCR product was run on a 1% agarose gel at 80V for 40 minutes and stained with ethidium bromide to visualise the size of the product. This revealed a strong band at the expected size of ~6 kb (plasmid = 5699 bp) for both PCR reactions (Figure 5-15).

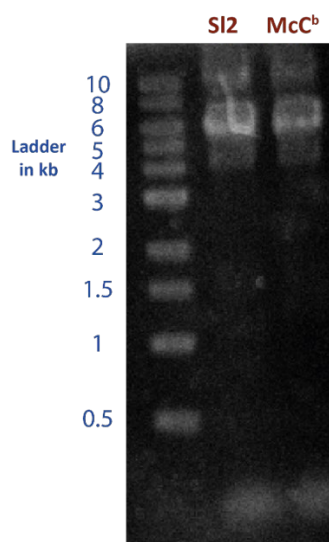


Figure 5-15. Site-directed mutagenesis PCR products for *SI2* and *McCb* mutants
 A band at ~6 kb is seen as expected. PCR products were run on a 1% agarose gel with 5 μ l Quick-Load[®] 1 kb DNA ladder and stained with ethidium bromide.

The PCR product was treated with Dpn1 to remove the methylated DNA of the original template plasmid and purified. As only 18 PCR cycles had been performed, it was anticipated that a small amount of DNA would have been produced. As such, the sample was eluted twice using 15 μ l of elution buffer to concentrate the DNA prior to ligation and transformation. The *SI2* and *McCb* PCR products had concentrations of 115 ng/ μ l and 67.7 ng/ μ l respectively. Five μ l of each were transformed into *E. coli* as per section 5.4.9. 100 μ l of each transformation reaction was plated onto LB agar plates and incubated at 37°C overnight. Six colonies from each plate were expanded into “mini-broths” and plasmid DNA extracted by miniprep. One μ l of each miniprep eluate was sent for Sanger sequencing using the sequencing primer SP1 (which provided the best coverage of the *SI2/McCb* mutation site region; Table 5-1, Figure 5-13 and section 5.4.13).

Clones were numbered sequentially and originated from Clone 1. Clones 1-1 to 1-6 were from the experiment to introduce the *SI2* mutation (sequencing results Figure 5-16) and Clones 1-7 to 1-12 from the *McCb* experiment (sequencing results Figure 5-17). Clones 1-5 (*SI2*) and 1-9 (*McCb*) were taken forward for full sequencing, which did not identify any unwanted mutations (Figure 5-18).

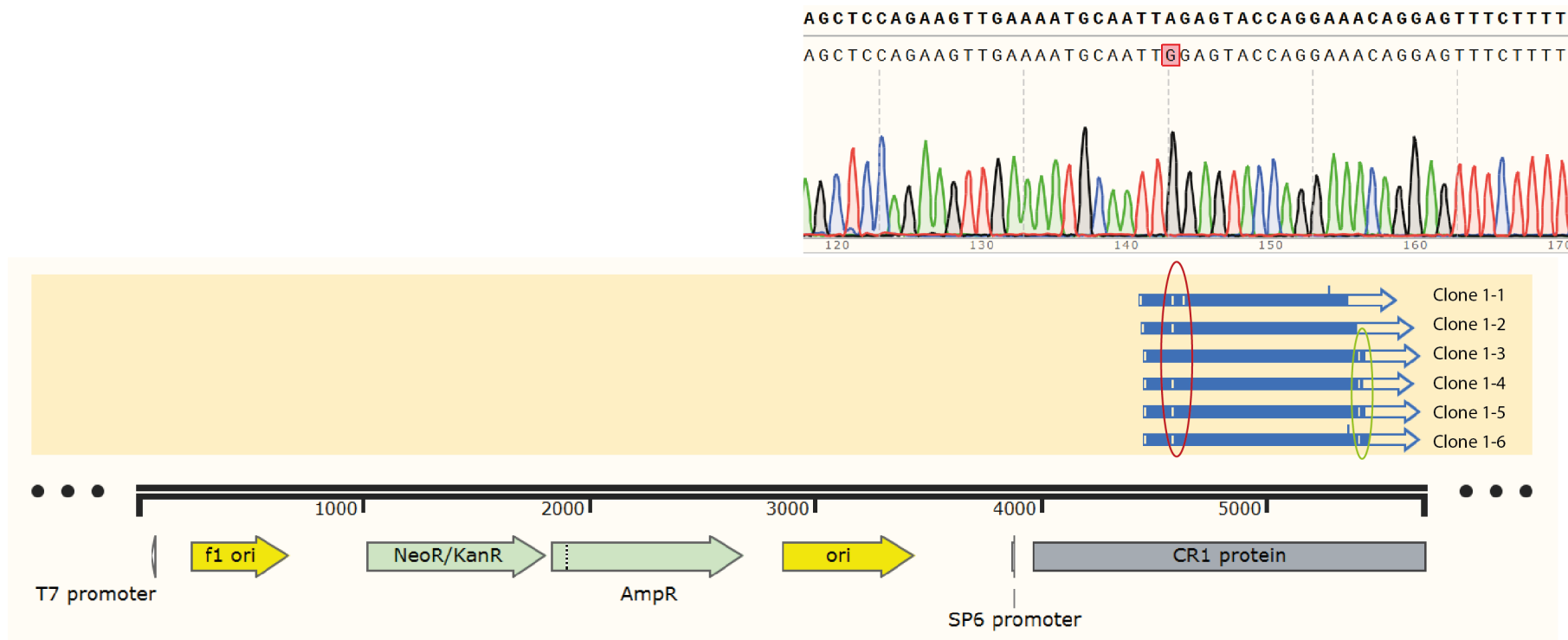


Figure 5-16. Preliminary sequencing of SI2 mutation site-directed mutagenesis.

Clones were sequenced with the SP1 sequencing primer. The SI2 mutation region is circled in red. The chromatogram insert shows the SI2 mutation region from Clone 1-5, with the clone sequence on the bottom and the reference sequence along the top in bold. The C5416T "mutation" is circled in green.

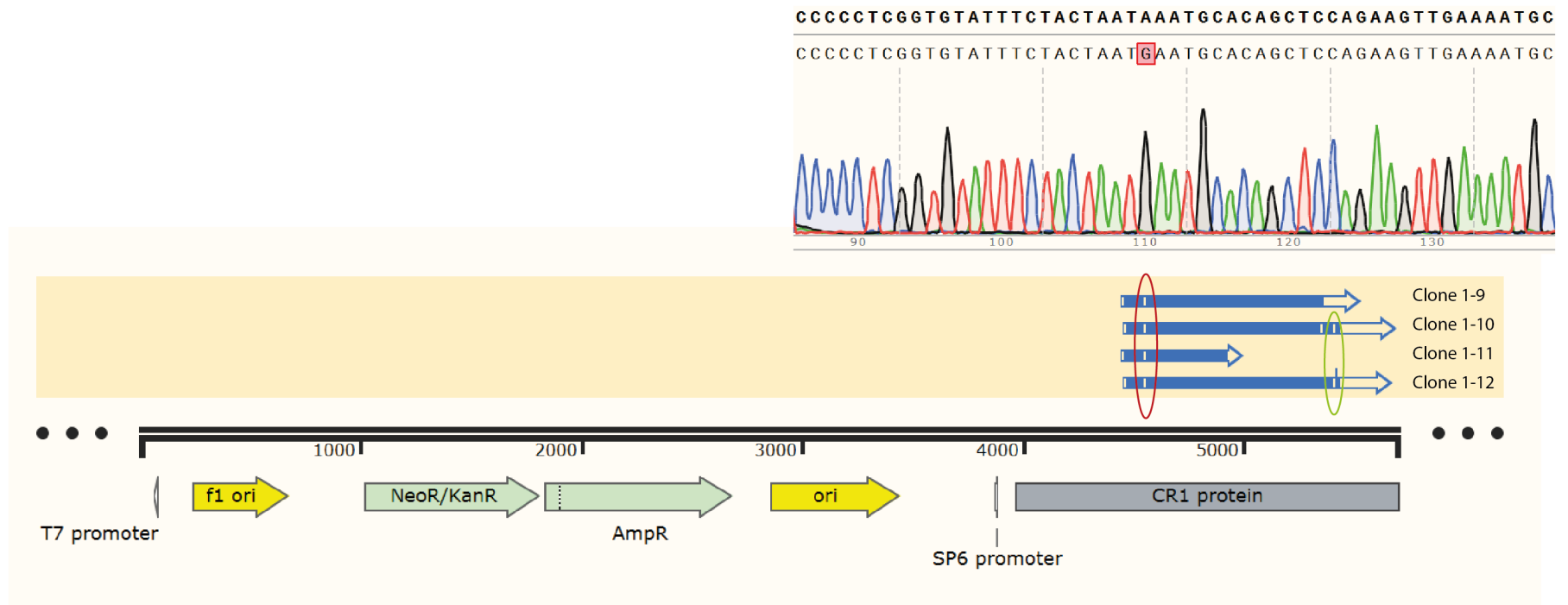


Figure 5-17. Preliminary sequencing of McC^b mutation site-directed mutagenesis.

Clones were sequenced with the SP1 sequencing primer. The McC^b mutation region is circled in red. The chromatogram insert shows the McC^b mutation region from Clone 1-9, with the clone sequence on the bottom and the reference sequence along the top in bold. The C5416T “mutation” is circled in green. Sequencing failed for Clones 1-7 and 1-8.

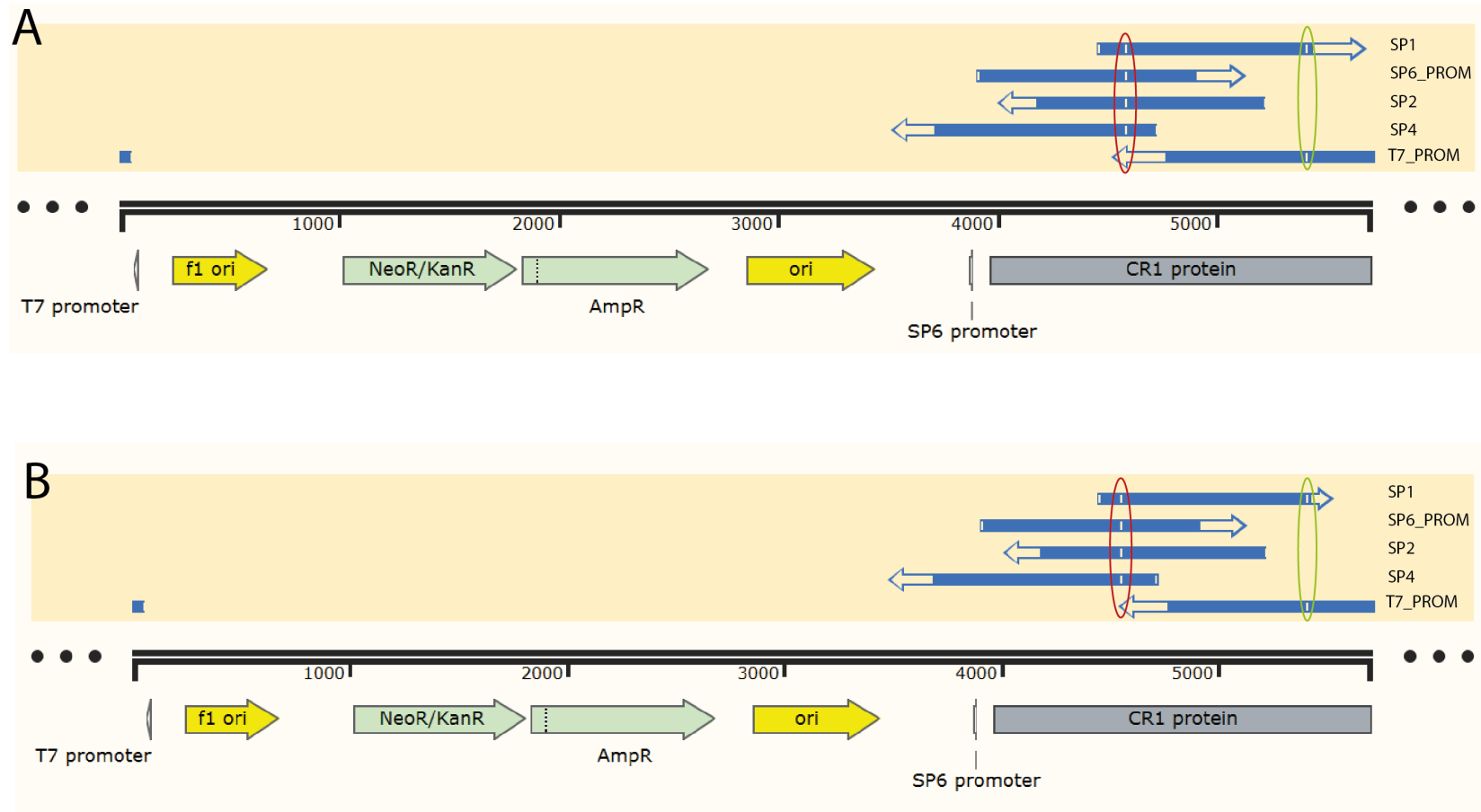


Figure 5-18. Full sequencing of SI2 and McC^b mutant constructs.

Panel A = SI2 experiment. **Panel B** = McC^b experiment. Sequencing primers used are adjacent to the read given. The mutation regions are circled in red. The C5416T area is circled in green.

5.5.4 Creation of the double mutant *SI2/McC^b*

To produce the double mutant, *SI2/McC^b*, the plasmid containing the *SI2* mutation (Clone 1-5) was selected, the primer pair MCCB_F/MCCB_R (Table 5-1) were used to introduce the *McC^b* mutation (section 5.4.15) and the PCR product was run on a 1% agarose gel at 80V for 40 minutes.

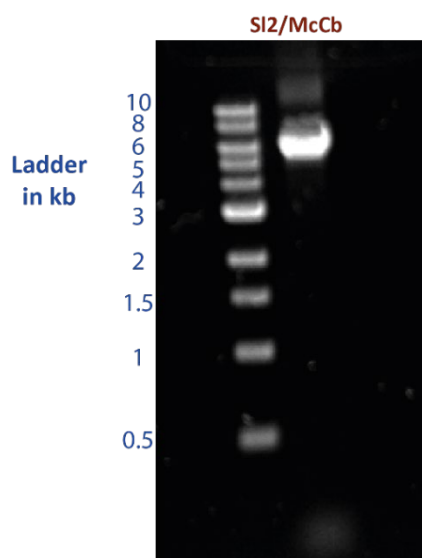


Figure 5-19. PCR product of *McC^b* mutant on background of *SI2* shows a band of expected size (~6 kb). PCR products were run on a 1% agarose gel with 5 μ l Quick-Load[®] 1 kb DNA ladder and stained with ethidium bromide.

A clear band was seen at the expected size (~6 kb). The PCR product was treated with Dpn1 and purified (detailed in 5.4.6) and eluted into 15 μ l of elution buffer. The eluate concentration was determined by Nanodrop to be 82.5 ng/ μ l. Five μ l of this was subsequently transformed into One Shot[™] TOP10F' *E. coli* chemically competent cells (described in 5.4.9). 100 μ l of the transformation reaction was plated onto an LB agar plate containing ampicillin and incubated overnight at 37°C. Six colonies were selected for expansion and miniprep (5.4.11). Preliminary sequencing was performed using the SP1 primer only (Figure 5-20). Clone 1-5-3 contained the double *SI2/McC^b* mutation and was selected for complete sequencing, which confirmed no unwanted mutations (Figure 5-21).

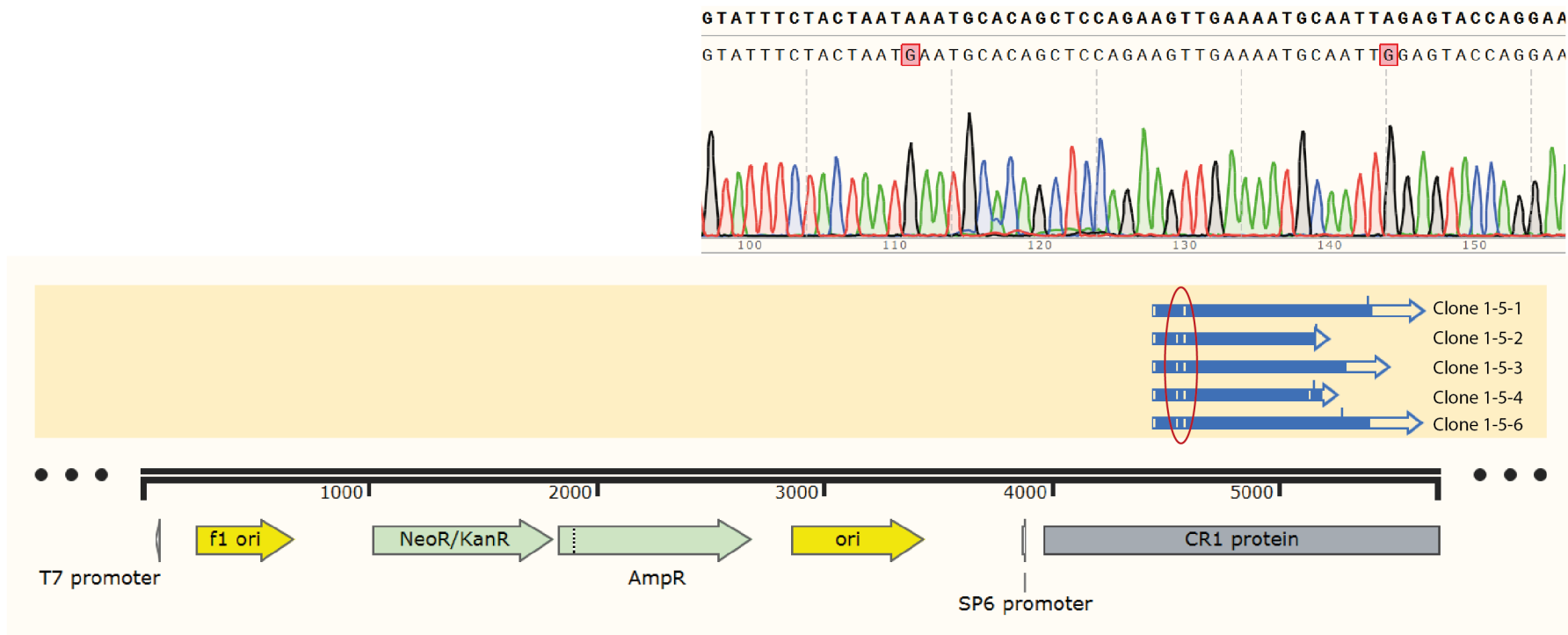


Figure 5-20. Preliminary sequencing of Mcc^b mutation on back of SI2. Clones were sequenced with the SP1 sequencing primer. The SI2/ Mcc^b mutation region is circled in red. The chromatogram insert shows the SI2/ Mcc^b mutation region from Clone 1-5-3, with the clone sequence on the bottom and the reference sequence along the top in bold.

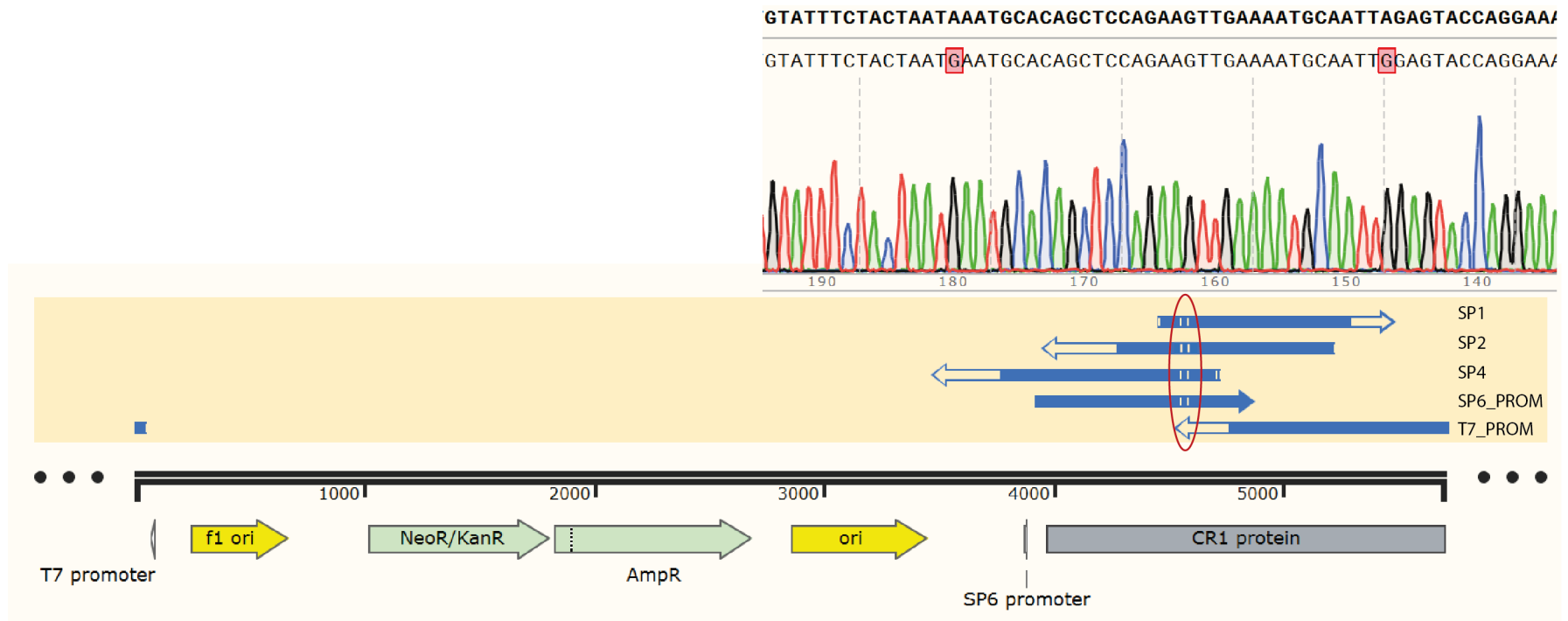
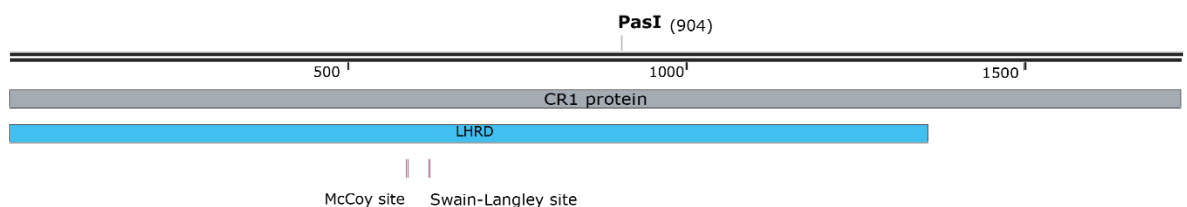


Figure 5-21. Full sequencing of the McC^b mutation on back of SI2. Sequencing primers used are adjacent to the read given. The mutation region is circled in red. The chromatogram insert shows the SI2/ McC^b mutation region from the SP4 read, with the clone sequence on the bottom and the reference sequence along the top in bold.

Please note, clone 1-5-3 was made before it was determined that the T seen at position 5416 was the ancestral allele and not a mutation (Table 5-2). An extra site-directed mutagenesis step had previously been undertaken to change this nucleotide to a C using primer pair CAATCAGCTACACTTGTGACCCCGGC and GCCGGGGTCACAAGTGTAGCTGATTG. As such, the sequencing results for the *SI2/McC^b* double mutant in Figure 5-20 and Figure 5-21 show no deviation from the CR1 reference sequence at position 5416 on the plasmid. As the *PasI* restriction site was chosen for ligation into the expression plasmid (Figure 5-22), the 5416 area of the insert was not included in the final construct, rendering this extra site-directed mutagenesis step irrelevant to subsequent experiments.

5.5.5 Sub-cloning of the CCP 22-30 mutants into the expression plasmid

The *AgeI* and *PasI* restriction sites on the expression plasmid were chosen for sub-cloning (shown on Figure 5-8). On the expression plasmid, the *AgeI* site is immediately prior to the CR1 signal peptide and the *PasI* restriction site is midway along the CCP-22-30 insert. This strategy therefore preserves the signal peptide and the His tag on the expression plasmid, but allows for the removal of the most of the existing CCP 22-30 region to allow replacement with the new mutant inserts, which already contain a *PasI* restriction site as shown below.



*Figure 5-22. PasI restriction site in CCP 22-30 insert.
The position of the restriction site is shown with respect to the *SI2* and *McC^b* sites.
The grey box represents the mature CR1 protein and the blue box the LHR-D region of CR1.*

The *AgeI* restriction site was added to the 5' end of the *SI2*, *McC^b* and *SI2/McC^b* mutant inserts using the *AGEI_primer* as described in 5.4.18 and was combined with the *PASI_primer* (see Table 5-1). This was expected to produce a DNA sequence 925 bp in length. Three separate reactions were carried out to modify the *SI2*, *McC^b*

and *SI2/McC^b* mutant inserts. 2.5 μ l of the product from each PCR reaction was then run on a 1% agarose gel at 80V for 40 minutes and stained with Syber Safe. Clear bands were seen at \sim 1 kb.

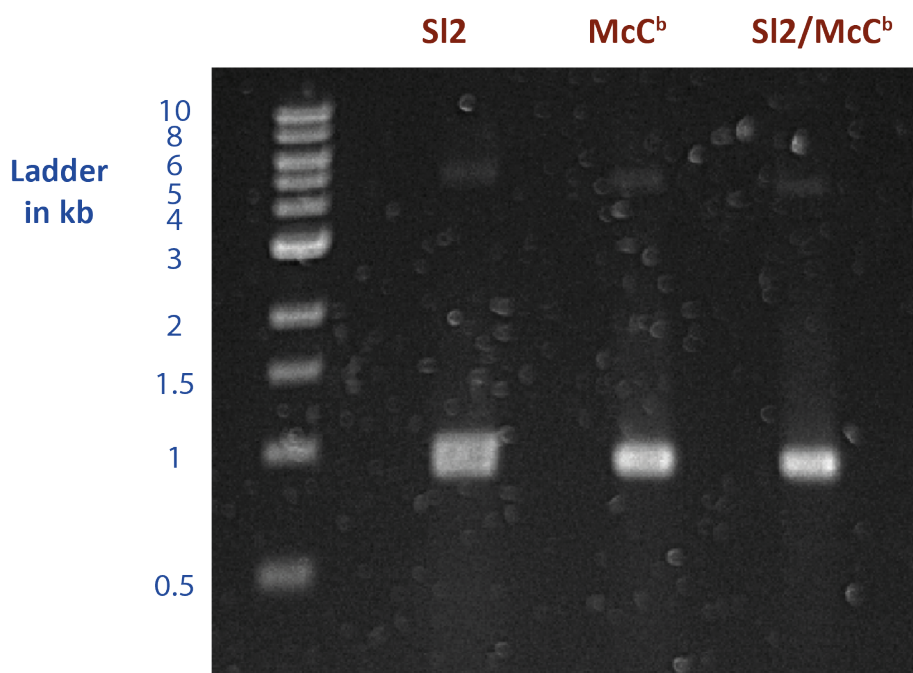


Figure 5-23. Mutant inserts after amplification using AGEI_PRIMER and Pasi_PRIMER. Bands seen of the expected size (\sim 1 kb). PCR products were run on a 1% agarose gel with 5 μ l Quick-Load[®] 1 kb DNA ladder and stained with Syber Safe.

A double digest of the mutant inserts was subsequently undertaken using the restriction enzymes AgeI and Pasi. Owing to the specificity of the Pasi enzyme, both steps were performed in the Pasi buffer as described in 5.4.19. The digestion products were then run on a 1% agarose gel and the digested DNA purified by gel extraction of the \sim 1 kb band.

High quality maxiprep DNA of the expression vector pcDNA 3.1 (-) CCP 22-30 His was digested separately (detailed in 5.4.17). The double digestion of the expression vector was simulated using the SnapGene software and predicted to create two fragments of 908 bp and 6361 bp, with the larger fragment representing the desired vector for further subcloning. Unfortunately, double digestion of the vector using the same approach as for the mutant inserts did not yield bands of the anticipated size. As such, alternate approaches were explored with a different source of the

PasI enzyme, a lower concentration of PasI (in PasI buffer) and a shorter incubation time with PasI. A method was found (5.4.19) which produced a band of the expected size (~7.3 kb) on an 0.75% agarose gel. (Figure 5-24). Five µg of the expression vector was subsequently digested with PasI using this approach.

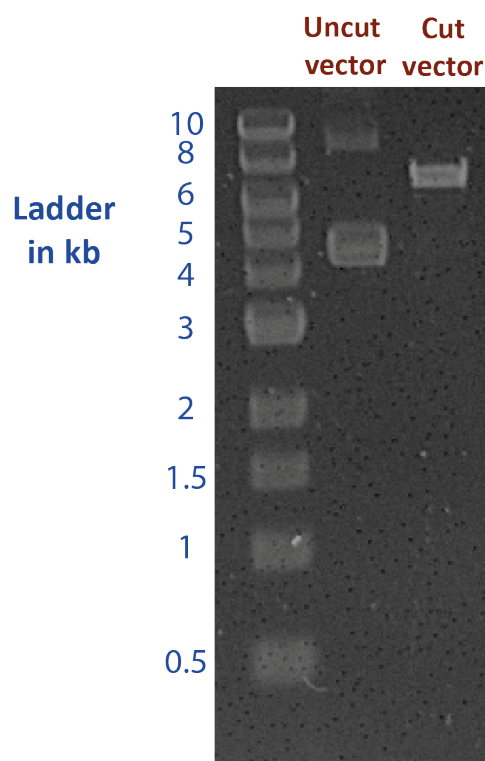


Figure 5-24. Expression vector pcDNA 3.1 (-) CCP 22-30 His before and after digestion with PasI. Cut (uncoiled) and uncut (supercoiled) vector are seen to run at different sizes as expected. PCR products were run on a 0.75% agarose gel with 5 µl Quick-Load® 1 kb DNA ladder and stained with Syber Safe.

The resultant PasI digest was purified using a Nucleospin® column (see section 5.4.4) and the eluate further digested with Agel-HF in CutSmart buffer (5.4.19). This double digest was run on a 0.75% agarose gel and the gel band corresponding to the expected size of the cut vector was excised and purified as detailed in 5.4.6. This process is shown in Figure 5-25. The double digestion produced a band of the expected size (~6.9 kb) representing the cut vector (lane 3). As the samples were run on a 0.75% gel, smaller bands were harder to visualise. A very faint band was seen at ~ 900 bp (seen as a diffuse haze in lane 3) representing the excised insert from the original expression vector.

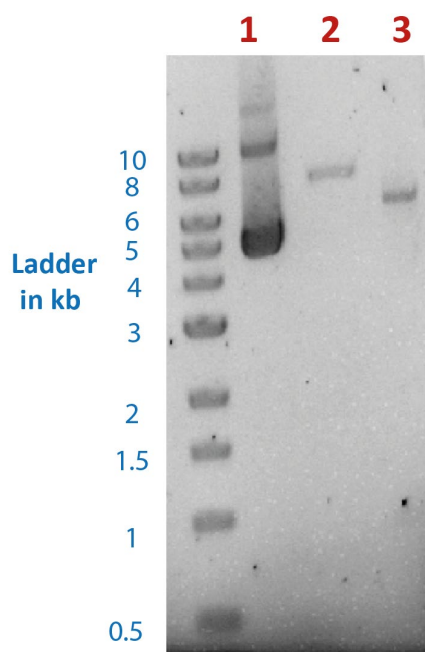


Figure 5-25. Double digest of expression vector with PstI and AgeI.

Lane 1 = uncut vector. **Lane 2** = vector digested with PstI only. **Lane 3** = vector digested with PstI and AgeI produces a band at ~6.9 kb as expected.

PCR products run on a 0.75% agarose gel with 5 μ l Quick-Load[®] 1 kb DNA ladder and stained with Syber Safe.

With the inserts and the vector now having compatible ends, ligation was performed. A 3:1 insert:vector ratio was set up of each of the three ligation reactions (*SI2* mutant insert + expression vector, *McC^b* mutant insert + expression vector and *SI2/McC^b* + expression vector) and a negative control comprising the vector without an insert. Ligations were set up as detailed in 5.4.20 and incubated at room temperature for 15 minutes followed by 2 hours at 4°C. Five μ l of each ligation reaction was then transformed into a separate vial One Shot™ TOP10F' *E. coli* cells and subsequently plated onto LB agar plates containing ampicillin. Blue / white screening was not possible with this plasmid. Plates were incubated overnight at 37°C. The plates from the *SI2*, *McC^b* and *SI2/McC^b* reactions showed good growth (35 colonies, >200 colonies and >200 colonies respectively) in comparison to the plate from the vector only reaction (12 colonies).

Four colonies were selected from each plate, expanded in LB broth with ampicillin and plasmid DNA purified by miniprep. A diagnostic restriction digestion was then

performed using restriction enzymes BamHI-HF and HindIII-HF, which cleave either side of the full insert, (i.e. section containing the CR1 signal peptide + CCP 22-30 + His tag). These restriction sites are shown in Figure 5-8. The undigested expression plasmid (containing the CR1 signal peptide + CCP 22-30 + His tag) was used as a positive control.

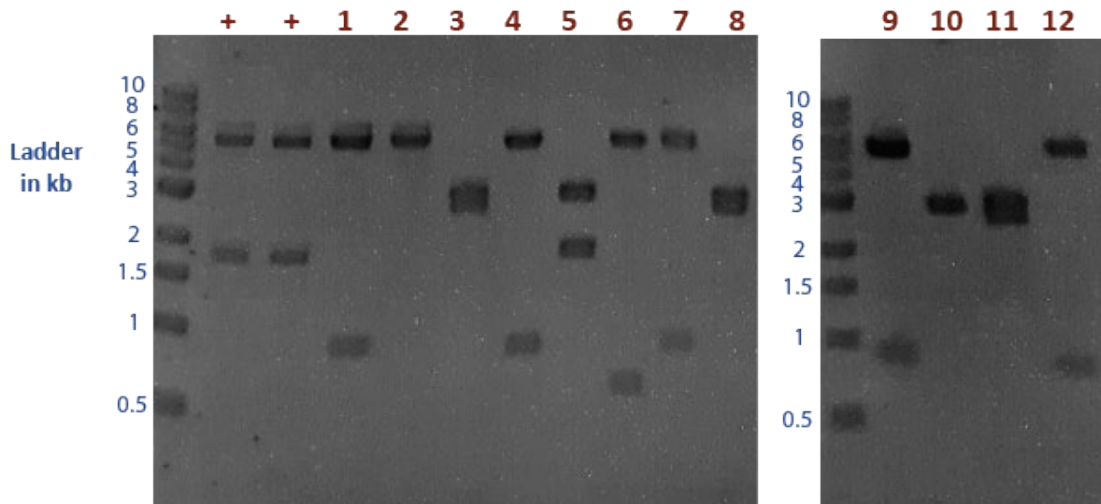


Figure 5-26. Diagnostic restriction digest of final mutant constructs using BamHI-HF and HindIII-HF. The first two lanes (positive control, labelled with "+") are the original undigested expression plasmid which contains the CR1 signal peptide, CCP 22-30 and His tag but no mutations. Lanes 1-4 are from the ligation of the SI2 insert + digested expression vector, lanes 5-8 from McCb + digested expression vector and lanes 9-12 from SI2/McCb double mutant insert + digested expression vector. No constructs contain inserts of the expected size. PCR products were run on a 1% agarose gel with 5 μ l Quick-Load[®] 1 kb DNA ladder and stained with ethidium bromide.

As expected, digestion of the positive control provided a band representing the vector at ~ 6 kb and one representing the insert at ~ 1.7 kb. However, the pattern of the other restriction digests suggested none of the constructs contained inserts of the expected size. To try and understand where the process had failed, the minipreps corresponding to lanes 1 + 2 (SI2), 5 + 6 (McCb) and 9 and 10 (SI2/McCb) were sequenced using the SP1, SP2, SP4 and T7_PROM primers. None of the plasmids contained CR1 inserts.

Unfortunately, time did not permit the continuation of this project. I intend to complete the mutant constructs and examine their binding properties as part of my early post-doctoral work.

5.6 Discussion

5.6.1 Generation of Knops blood group mutant inserts

The aim of this chapter was to generate expression constructs of three short proteins containing the Knops blood group mutations *S12*, *McC^b* and the double mutant *S12/McC^b*, in order to examine whether these mutations might influence MBL and C1q binding to the region. Time constraints did not permit this. However, amplification of the relevant CCP 22-30 region of CR1 cDNA and ligation into the cloning vector pCRII with subsequent site-directed mutagenesis to introduce the nucleotide changes for the *S12*, *McC^b* and *S12/McC^b* polymorphisms were successful.

5.6.2 Inability to ligate mutant inserts into digested expression vector

Attempts to subclone the mutant inserts into the expression vector pcDNA 3.1 (-) CCP 22-30 His were unsuccessful. Double digestion of the vector was challenging and it is possible that neither the inserts nor the vector were correctly digested. The unique restriction sites *AgeI* and *PasI* were chosen for subcloning as they would allow for insertion of the CR1 mutants whilst preserving the CR1 signal peptide and His tag. The *AgeI* restriction site was added to the mutant inserts using a specifically designed primer and amplified by PCR. The *PasI* site was naturally occurring in the CCP 22-30 insert (see Figure 5-22). Following introduction of the *AgeI* site, the expected PCR product size was verified by gel electrophoresis, but sequencing was not performed. Gel electrophoresis would not have been sufficiently sensitive to confirm whether the *AgeI* site had been incorporated as planned. As such, it may be that the inserts did not have *AgeI* sites.

It is also possible that the use of the *PasI* enzyme contributed to the failure of ligation. Whilst commercially available, this is not a common restriction enzyme and only two suppliers provide it. This enzyme is only functional in its own specific buffer and is acknowledged to be prone to star activity (Restriction Enzymes Buffer Activity Chart, Thermo Scientific, 2014). For future work, an alternative subcloning strategy may be necessary.

5.6.3 Troubleshooting for future experiments

PasI was selected as it represented a unique cutter in the expression vector which allowed the preservation of the CR1 cDNA sequence beyond it and the His tag. However, it is clear from the data presented that the enzyme has been suboptimal for this task. There are no other unique cutters within the original insert of the expression vector pcDNA 3.1 (-) CCP 22-30 His that would preserve the His tag. Alternative subcloning strategies were considered using the “dual cutters” function on SnapGene. This identified BsmBI as a possible candidate (Figure 5-27).

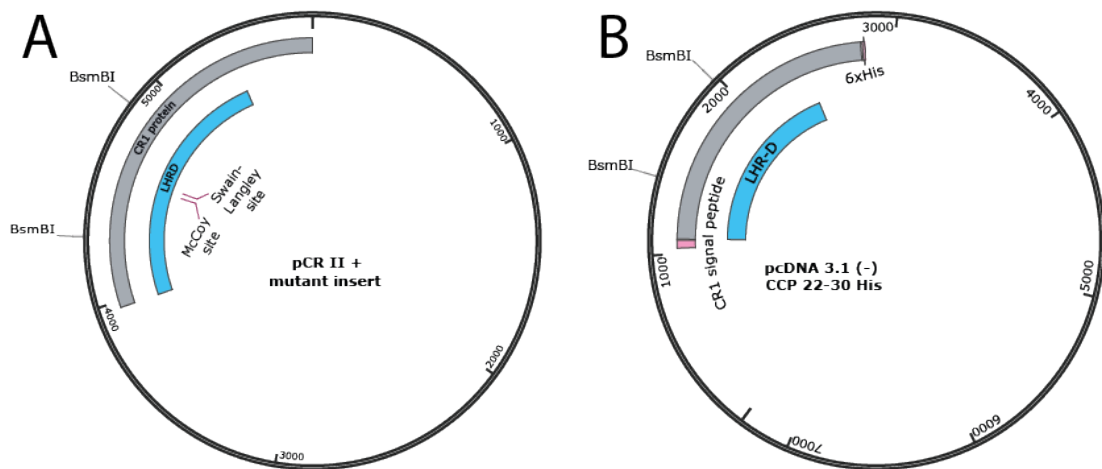


Figure 5-27. New cloning strategy using *BsmBI* restriction sites on the cloning and expression plasmids.

BsmBI should excise a 569 bp region containing the desired mutations when digesting the pCRII-based plasmid and also preserve the CR1 signal peptide and His tag when digesting the pcDNA 3.1 (-) CCP 22-30 His expression plasmid (Figure 5-27). Potential colonies will be sequenced to select those with the desired orientation of the insert. This approach will be explored as soon as time permits.

5.6.4 The Thr1885Ile substitution

cDNA for this project was kindly supplied by Lloyd Klickstein (Boston, USA) with the CR1 mRNA sequence which was used for reference (<https://www.ncbi.nlm.nih.gov/nuccore/Y00816>) also published by the Klickstein group. After sequencing the initial, non-mutated inserts, a discrepancy was found

between the reference sequence and that obtained by Sanger sequencing. This corresponded to a C5654T nucleotide substitution and Thr1885Ile amino acid substitution (or C5416T if using the cloning plasmid coordinates). The substitution results in the neutral, nonpolar amino acid isoleucine instead of the polar amino acid threonine.

Interestingly, this substitution was also present in the expression plasmid pcDNA 3.1 (-) CCP 22-30 His, which cited a different source of CR1 cDNA (Prof. J. Cohen Université de Reims Champagne-Ardennes, Reims, France) (Jacquet et al., 2013). After reviewing published CR1 cDNA sequences, it was determined that instead of being a substitution, the isoleucine was likely to represent the ancestral amino acid (Table 5-2) and experiments were continued. Two previous reports have also noted this substitution and concluded that it is unlikely to affect CR1 function (Furtado et al., 2008; Vik and Wong, 1993).

5.6.5 Future intended experiments

Once the mutant inserts have been efficiently ligated into the expression vector, the aim will be to produce the wild-type and mutant CCP 22-30 proteins using the Freestyle™ 293 expression system (Thermo Fisher Scientific, K900001). The final plasmid (pcDNA 3.1 (-) CCP 22-30 *mutant* His) containing the mutant inserts *SI2*, *MCC^b* or *SI2/MCC^b*, the CR1 signal protein and His tag will be transiently transfected into the HEK 293-F cells, and after 72 hours the his-tagged recombinant protein in the culture supernatant will be purified on a nickel-nitrilotriacetic acid (Ni-NTA) column. The intended method is as described by the authors of the original plasmid (Jacquet et al., 2013). Surface plasmon resonance (SPR) will then be used to examine whether the mutations alter how the CR1 fragments bind to MBL, C1q and L-ficolin as described in (Jacquet et al., 2013). Results from these experiments will help to shape the future direction of this research project. Potential directions are further discussed in Chapter 6.

6 General Discussion and Conclusion

6.1 Summary of findings

The aim of this thesis was to investigate the relationship between malaria and the *SI* and *McC* polymorphisms in CR1 and examine potential hypotheses for the results found. In Chapter 2 using the power of a large case-control study in Kenya, I identified a protective association between *SI2* homozygosity and both cerebral malaria (CM) and death from malaria. The associations were most clearly seen in children who had normal α -globin, suggesting that previous studies which did not include α -thalassaemia in their models may have obfuscated this important association. In contrast, the *McC^b* polymorphism was associated with increased odds of cerebral malaria and may be under selection pressure from diseases other than malaria.

The specificity of these associations to cerebral malaria alone, and not other sub-phenotypes of the disease, lead to investigation of the potential functions of these polymorphisms. In Chapter 3, using an IFA with confocal microscopy and fresh blood samples from children prospectively genotyped for the polymorphisms, I found no evidence that *SI2* or *McC^b* influenced the number or volume of CR1 clusters formed on erythrocyte membranes. Subsequently in Chapter 4, using a variety of methods I could find no compelling evidence that an immortalised human brain endothelial cell line (HBEC-5i) expressed CR1. Finally, whilst the work in Chapter 5 made significant headway towards expressing the LHR-D regions containing the *SI* and *McC* mutations for examining their binding affinities with the complement components MBL, C1q and L-ficolin, there was insufficient time to complete this project.

My hope is that this thesis will reignite discussion into the role of the *SI* and *McC* polymorphisms in malaria and provide a firm foundation for future research into their function. I hope also that my work will prompt other groups to reanalyse their case control studies in the light of α -thalassaemia genotyping.

6.2 Limitations of these findings

6.2.1 Limitations of genetic association study

No scientific work is without its limitations. One potential weakness in this work is in the hypothesis that the *SI* and *McC* polymorphisms are the drivers behind the altered odds of cerebral malaria and death. Association is not causation and the possibility persists that these polymorphisms are not causal but actually signposts for another as yet unidentified mutation. As discussed in 2.7, we cannot be sure of this, but GWAS studies have not identified other potential SNPs associated with severe malaria in this region (Jallow et al., 2009; Malaria Genomic Epidemiology Network, 2015). In addition, there is strong biological plausibility to these blood group antigens being causative, as malaria has strongly influenced the frequencies of other blood groups. The best characterised of these is the Duffy blood group antigen (reviewed in (Langhi and Bordin, 2006)), which plays an essential role as the invasion receptor for *P. vivax* on reticulocytes (Chitnis and Miller, 1994; Miller et al., 1976). Individuals with the *Fy(a-b-)* mutation in the promoter region of the *DARC* gene do not express Duffy antigen on erythrocytes (Tournamille et al., 1995) and the polymorphism has reached fixation in much of west and central Africa, areas where *P. vivax* is now rare (Culleton et al., 2008; Miller et al., 1976). Another example is the ABO blood group which has been repeatedly associated with severe malaria in epidemiological studies (Fry et al., 2008; Jallow et al., 2009; Rowe et al., 2007; Timmann et al., 2012; Toure et al., 2012). Laboratory studies have demonstrated that *P. falciparum* strains cultured in blood group O form fewer weaker rosettes than those in A, B or AB blood (Carlson and Wahlgren, 1992; Rowe et al., 2007; Udomsangpetch et al., 1993). A further example is the Gerbich-negative blood group (Ge-) which occurs at high frequency in malaria-endemic regions of Papua New Guinea (Booth and McLoughlin, 1972) and results from the deletion of exon 3 in the Glycophorin C gene (Maier et al., 2003). Glycophorin C is an invasion receptor on erythrocytes for *P. falciparum* (Maier et al., 2003; Mayer et al., 2006). With these roles for blood group in the protection against malaria, it seems

reasonable to pursue the hypothesis that the *SI* and *McC* polymorphisms of the Knops blood group are causative in the respective protection against/susceptibility to against CM and death. However, as in all research, we must be mindful of alternative possibilities and be prepared to re-examine this if new evidence becomes available.

Another limitation of this work may be in the construction of the genetic model. When developing models for genetic association studies, there is always a balance to be struck between ensuring important confounders are not excluded and taking care that the model is not over-fitted to the data (i.e., producing an analysis that corresponds too closely to the idiosyncrasies in a particular dataset, which is not able to fit subsequent datasets). The latter is a possibility in the analysis presented in Chapter 2 as the final model used in the case control study is quite complex. In particular, the novel finding of the *SI*/ α +thalassaemia interaction will require replication before it can be substantiated. Whilst the interaction was seen in both the case control and cohort studies, these were both performed on children residing in the same area of Kenya. Investigating this interaction in a separate population will therefore be paramount. This could be performed through collaboration with another of the large severe malaria case control studies comprising the MalariaGEN consortium (Achidi et al., 2008). Existing samples could be genotyped for α +thalassaemia by PCR (Chong et al., 2000) although this method is labour-intensive and may be off-putting for potential collaborators. An alternative might be the development of an algorithm to impute the α +thalassaemia genotype; as the α +thalassaemia polymorphism results in a 3.7 kb deletion in the α -globin gene it may be possible to identify a pattern of “missing” SNP calls beyond the start of the mutation. However, this to date, this approach has not been successful (personal communication with Dr Gavin Band, Wellcome Trust Centre for Human Genetics, Oxford, UK).

However, it should be recalled that the *SI*/ α +thalassaemia interaction is also biologically plausible and there are multiple examples of interactions between

malaria protective polymorphisms. Of these, α +thalassaemia features prominently, with evidence of an epistatic interaction between α +thalassaemia and both sickle cell (Williams et al., 2005c) and haptoglobin (Atkinson et al., 2014). It is likely such interactions may not only explain the complex global distribution of haemoglobinopathies (Penman et al., 2009) but also underpin why the same polymorphisms have different impacts on susceptibility to malaria when examined in different populations (Taylor et al., 2012). As noted by Williams; *“Interactions of this sort are unpredictable and, if common, could make the hunt for both protective alleles and their mechanisms even more difficult (Williams, 2006).”* This is an important point when considering the findings of multi-centre case control studies of severe malaria; whilst it might be presumed their size would increase their power to detect new susceptibility loci, in truth it may obfuscate them if population-specific interactions are not considered. This might explain why the *SI* polymorphism was not identified in the recent multi-centre MalariaGEN study (Rockett et al., 2014), even though the study included the same Kilifi data that I analysed in Chapter 2. Indeed, the authors of this study state *“(...) it is undoubtedly also the case that authentic genetic associations might be missed by multi-centre studies if the effect is weak and there is heterogeneity of effect across different study sites.”*

6.2.2 Limitations of laboratory-based studies

In addition to the limitations of the genetic association analysis, there are important limitations to the laboratory work carried out in this thesis. As noted in Chapter 3, the immunofluorescent assay for measuring clusters on erythrocytes of different *SI* and *McC* genotypes could be argued not to be physiologically relevant as it was performed at 4°C and used the α -CR1 antibody J3D3 rather than physiological ligands such as immune complexes. Another criticism of this work might be that the distances between the z-stacks on confocal imaging were too large to sufficiently image the size of the clusters. Both of these criticisms are valid and may potentially have altered the findings. Whilst it is conceivable that findings might have been

different if conditions were altered, some concessions must be made to practicality when designing experiments with field samples.

Two limitations stand out clearly from the investigation of CR1 expression on HBEC-5i in Chapter 4. Firstly, whilst an immortalised cell line is a good representation of human brain endothelium, is it not the same and findings should automatically not be extrapolated from one to the other. Examination of a reliable source of primary HBEC will be very important for clarification of these findings. It would also be valuable to use the same methods to examine the expression of CR1 on HUVECs and compare this to the published findings (Collard et al., 1999; Langeeggen et al., 2002). The other obvious limitation of the work in this chapter was the confusion caused by using pool of multiple α -CR1 antibodies. The error here was to presume that the signal seen was coming from all antibodies equally and not examining their individual staining patterns earlier in the course of these experiments. It also became clear that a single isotype control was not a suitable comparison to a pool of antibodies, but that the control should have comprised the same number of separate antibodies as the α -CR1 pool. These errors were costly in terms of the time, but have been valuable on a personal level. Undertaking a PhD is as much about understanding what constitutes robust methodology as contributing to new knowledge. These errors will influence my future approaches to research questions.

Time did not permit completion of the work in Chapter 5 and I was unable to express the mutant LHR-D regions in HEK 293-F cells as hoped. Progress was hampered by problems with restriction digests, which prevented effective digestion of the mutated inserts and subsequent subcloning into the expression vector. The fact that the PstI enzyme was hard to source may have hinted at its unpopularity due to technical difficulties. Again, whilst this problem was time-consuming, it was instructive in how to problem-shoot sub-cloning strategies, a skill that will be useful for future molecular biology work.

6.3 Questions remaining and future work

6.3.1 What are the functional effects of the *SI* and *McC* polymorphisms?

Although the *SI* and *McC* polymorphisms are sufficient to alter blood group, their function remains undefined. Production of the CCP 22-30 region of CR1 containing the mutations will permit detailed investigation into whether they alter the binding of MBL, C1q or ficolins. Experiments will be performed as outlined in section 5.6.5, with initial characterisation of the mutants by SDS-PAGE and circular dichromism and binding to the ligands assessed by SPR. Limitations of the previous work using short recombinant proteins spanning CCP 15-25 with the *SI* and *McC* polymorphisms has been discussed in section 5.2.3 (primarily concerns regarding correct glycosylation of the proteins in a *P. pastoris* system) (Tetteh-Quarcoo et al., 2012). As such, it may also be prudent to repeat experiments from this study using recombinant proteins expressed in a mammalian system, including investigation of the recombinant mutant proteins' ability to inhibit invasion by *P. falciparum* or rosetting of infected cells.

If initial investigations suggest differences in binding to complement components, further parallel experiments could be performed to assess the complement activation. Precise experiments would be guided by the findings, but may include assays to determine the mutant effects on activation of the classical and lectin pathways. Such approaches might include wells pre-coated with immune complexes (for C1q investigation) or mannan (for MBL investigation) and incubation with normal human serum and transfected 293-F cells expressing different CCP 22-30 mutants, with the subsequent deposition of C3b and the MAC on cell surfaces measured by measured by α -C3 and α -C5-9 antibodies respectively and flow cytometry (Palarasah et al., 2011). Experiments should be performed in factor B depleted serum to restrict the influence of the alternative pathway on the findings (Java et al., 2015).

6.3.2 Why are the *SI* and *McC* associations specific to cerebral malaria?

The protective association between the *SI2/SI2* genotype and severe malaria described in Chapter 2 is specific to the cerebral form of the disease and not associated with severe malarial anaemia or respiratory distress. This finding replicates that of Thathy et al. who described a CM-specific protective association for the *SI2/SI2* genotype in a smaller study in Western Kenya in 2005 (Thathy et al., 2005). This CM-specificity may provide a crucial route of investigation into the pathogenesis of the disease. The findings of Chapters 3 and 4 suggest that this is not due to a difference in clustering of CR1 on erythrocytes or to the expression of functional CR1 by human brain endothelial cells. While there is evidence that the *SI2/SI2* genotype is associated with reduced rosetting (analysis of ex-vivo parasite samples from Mali in Chapter 2 and (Rowe et al., 1997)), further investigation is needed.

If experiments outlined in 6.3.1 do suggest differences in MBL or C1q binding between the mutants, this could direct further investigation into rosetting. The *SI2* mutation site is distant from the CR1 site involved in rosetting (CCPs 15-17) (Rowe et al., 2000) making it unlikely that it could directly influence rosetting. However, it is possible that MBL could act as a mediator of rosetting. Both natural IgM and α_2 -macroglobulin have been identified as serum rosetting factors for subsets of *P. falciparum* parasites (Akhouri et al., 2016; Rowe et al., 2002a; Stevenson et al., 2015b). MBL can bind to both the glycosylated fraction of natural IgM and to α_2 -macroglobulin (Arnold et al., 2005, 2006a, 2006b). As such, MBL bound to CR1 on erythrocytes could be important in stabilising rosette formation. Individuals with different MBL-CR1 binding affinities (owing to different *SI/McC* genotypes) could therefore produce stronger or weaker rosettes during malaria infection, potentially affecting disease severity. This possibility could be examined by performing rosetting assays with the ITvar60 rosetting strain of *P. falciparum* which binds IgM (Ghumra et al., 2012). Experiments could be repeated using primary erythrocytes of different *SI/McC* genotypes in normal human serum and MBL-depleted serum.

Alternatively, immune complexes may provide another important route of enquiry. As discussed in section 5.2, high levels of ICs have been reported in children with CM in a small Kenyan study (Mibei et al., 2008). The class and subclass of immunoglobulins making up these ICs differed significantly between CM and SMA, with children with CM displaying higher levels of IgG ICs than those with SMA. However, it is worth noting that IC-quantification in this study was performed using a C1q-based ELISA, which could bias against detecting ICs opsonised by MBL. In addition, the ability of this C1q-based assay to detect ICs containing IgM has been questioned. IgM has a high C1q affinity, potentially blocking further binding of C1q in the ELISA and leading to misleadingly low levels of identification of IgM-ICs (Pleass, 2009). As such, whilst these data linking severe malaria to IC subtypes are interesting, these findings require further investigation.

MBL binds to human immunoglobulins; agalactosylated IgG (which comprise 35% of the IgG pool (Butler et al., 2003)), IgA and IgM (Malhotra et al., 1995; McMullen et al., 2006; Roos et al., 2001). Evidence suggests that MBL plays a role in clearing these ICs (Saevarsdottir et al., 2004, 2007) with the avidity of the MBL-immunoglobulin interaction increased in immune complexes containing multiple immunoglobulin molecules (Arnold et al., 2006c). If, for example, CR1 with the *S/2* polymorphism was found to bind MBL more strongly, it might help clear MBL-opsonised IgG ICs more readily, potentially reducing IC deposition in the cerebral endothelium, lowering the production of pro-inflammatory cytokines.

Experiments examining the effect of *S/* and *McC* polymorphisms on IC binding and transfer to macrophages/monocytes could help investigate this possibility.

Erythrocytes and PBMCs collected from the Immunology Cohort annual venepuncture in Kilifi, Kenya would represent a source of primary cells with the *S/* and *Mc* genotypes of interest (collected in children with normal α -globin) and the capacity of erythrocytes of each genotype to transfer ICs to monocytes investigated. Erythrocytes carrying MBL-opsonised fluorescently-labelled ICs could be co-incubated with monocytes from the same donor and IC-transfer efficiency

quantified by flow cytometry (Emlen et al., 1992). The experiment could be performed with ICs of different classes. Influence of *Sf/McC* genotype on MBL-IC opsonophagocytosis could be also be studied by quantifying fluorescent ICs taken up by the monocytes using flow cytometry and cytokine multiplex assays (MacMullin et al., 2012).

A number of other human red blood cell polymorphisms have been associated specifically with protection against CM and review of these may prompt alternative explanations for the association seen with *Sf* and *McC*. Example include Southeast Asian ovalocytosis (SAO), HbC and G6PD have been discussed previously (section 1.3.3) and may provide other potential CM-specific mechanisms to investigate. However, it should be recalled that associations between the *Sf* and *McC* polymorphisms were also seen for UM and other common childhood infections. As such, they may have broader effects, potentially affecting complement pathways as hypothesised above.

6.3.3 What is the underlying mechanism of the *Sf*/ α +thalassaemia interaction?

The third outstanding question focuses on the mechanism of the *Sf*/ α +thalassaemia interaction. It is worth reiterating that the novel interaction between *Sf* and α +thalassaemia reported in this chapter will need to be replicated in a separate population. If this is the possible, attempting to understand the mechanism underpinning it may help clarify the functional effects of both the *Sf* polymorphism and α +thalassaemia in CM.

One point from the analysis in Chapter 2 that may be important is that the negative epistasis between α +thalassaemia/sickle cell trait was confined to cases **without** CM, whereas the *Sf*/ α +thalassaemia interaction was only significant in cases **with** CM (section 2.7.4). This pair of interactions appear to have mutually exclusive effects and it may be possible to exploit this to further unpick the functions of these polymorphisms.

Potential protective mechanisms for sickle cell and α +thalassaemia have been described in section 1.3. The geographical distribution of the two variants overlap and as such, they are often inherited together (Flint et al., 1998). However, the protective effects are not additive, instead coinherence of HbAS and α +thalassaemia appears to cancel out their malaria-protective traits (negative epistasis) (Crompton et al., 2008; May et al., 2007; Williams et al., 2005c). Biological mechanisms for this unexpected interaction appear to be due to the properties of reduced rosetting, cytoadherence and PfEMP1 expression levels which are enjoyed by HbAS-IEs being nullified by co-inheritance with α +thalassaemia (Opi et al., 2014). Indeed, erythrocytes with both variants were indistinguishable from normal erythrocytes in terms of the above properties.

The studies reporting negative epistasis between α +thalassaemia and HbAS did not examine the interaction by clinical outcome, instead considering all cases of severe malaria together (Crompton et al., 2008; May et al., 2007; Williams et al., 2005c). In Chapter 2, this interaction was examined by clinical outcome and found to only be pertinent to cases of severe malaria without CM. This was in contrast to the *S*/ α +thalassaemia interaction which was only seen in cases with CM. We can read important points into these contrasting findings; firstly that the *S*/ α +thalassaemia interaction is very unlikely to be attributable to the HbAS/ α +thalassaemia interaction as the groups affected are mutually exclusive. Secondly, it would appear that these interactions have distinct biological effects as they affect different clinical outcomes.

In contrast to the HbAS/ α +thalassaemia negative epistasis, where addition of the two variants results in loss of malaria protection, the *S*/ α +thalassaemia interaction is not simply additive. This might suggest that whilst the effects of HbAS and α +thalassaemia are biologically different (and not complimentary), the effects of *S*/ α +thalassaemia are biologically similar, but not additive as a “saturation point” of the effect is reached with either variant alone. An important consideration of this may be the functional number of CR1 molecules on the surface of the erythrocyte.

Erythrocytes with α -thalassaemia have fewer CR1 molecules on their membranes (Cockburn et al., 2004; Opi et al., 2016). Erythrocytes with low CR1 copy numbers (<100) show greatly reduced rosetting when infected with *P. falciparum* (Rowe et al., 1997), which may be one of the protective mechanisms of α -thalassaemia. As such, it might be proposed that the *S/2* polymorphism has a similar effect on CR1 copy number. However, the *S/2/S/2* is actually associated with a very modest increase in CR1 copy number when compared with *S/1/S/1* genotype (303 CR1 copies, 95% CI 294–313 vs 256 CR1 copies; 95% CI 236–276 $p<0.001$) (Opi et al., 2016), suggesting the effect is not due to absolute CR1 copy number.

Instead, it is possible that the *S/2* polymorphism reduces one of the functions of CR1, thus while the absolute number of CR1 copies on the erythrocyte is static, the functional ability of CR1 on the erythrocyte is reduced to that of a cell with a lower CR1 copy number. If this were the case, co-inheritance with α -thalassaemia would further lower the absolute number of CR1 molecules on an erythrocyte, but with no additive protection, as a functional threshold had already been reached.

Importantly, as with *S/2*, α -thalassaemia has been reported to be associated with protection out-with malaria (respiratory infection, gastroenteritis and meningitis) (Allen et al., 1997; Wambua et al., 2006). As such, *S/2* and α -thalassaemia appear to mirror each other in both associated with protection against severe malaria and other childhood infections but not affecting parasite density. Further investigation into the function of the *S/2* polymorphism might in turn shed light on the protective mechanism of α -thalassaemia.

6.4 Conclusion

This thesis presents evidence that *S12*, a common African polymorphism in complement receptor 1, is strongly associated with protection against CM and death. This association was made apparent by considering an interaction with α -thalassaemia. Previous studies have been contradictory in terms of associations between *S1/McC* and severe malaria, but they did not consider the *S12*/ α -thalassaemia interaction. The work in this thesis suggests that far from being inconsistent in their findings, previous studies may have simply been incomplete.

The mechanism of how *S12* might protect against CM has yet to be solved. This relationship does not appear to be explained by the expression of CR1 on human brain endothelium or through *S1/McC* altering how CR1 clusters on the surface of erythrocytes. However, there are many possible threads to follow to determine the function of these polymorphisms and their influence on the malarial infection. In addition, determining the biological basis of the interaction between *S12* and α -thalassaemia may also help explain how the latter confers protection against severe malaria.

The work in this thesis also serves as a reminder that no gene acts alone, and that conflicting studies may be trying to tell you something important. Interactions with other biologically relevant genes should always be considered.

We shall not cease from exploration

And the end of all our exploring

Will be to arrive where we started

And know the place for the first time.

T.S. Eliot 1943

7 References

- Abdalla, S.H. (1988). Peripheral blood and bone marrow leucocytes in Gambian children with malaria: numerical changes and evaluation of phagocytosis. *Ann. Trop. Paediatr.* *8*, 250–258.
- Abugri, J., Tetteh, J.K.A., Oseni, L.A., Mensah-Brown, H.E., Delimini, R.K., Obuobi, D.O., and Akanmori, B.D. (2014). Age-related pattern and monocyte-acquired haemozoin associated production of erythropoietin in children with severe malarial anaemia in Ghana. *BMC Res. Notes* *7*, 551.
- Achidi, E.A., Agbenyega, T., Allen, S., Amodu, O., Bojang, K., Conway, D., Corran, P., Deloukas, P., Djimde, A., Dolo, A., et al. (2008). A global network for investigating the genomic epidemiology of malaria. *Nature* *456*, 732–737.
- Adam, C., Géniteau, M., Gougerot-Pocidallo, M., Verroust, P., Lebras, J., Gibert, C., and Morel-Maroger, L. (1981). Cryoglobulins, circulating immune complexes, and complement activation in cerebral malaria. *Infect. Immun.* *31*, 530–535.
- Adams, Y., Kuhnrae, P., Higgins, M.K., Ghumra, A., and Rowe, J.A. (2014). Rosetting *Plasmodium falciparum*-infected erythrocytes bind to human brain microvascular endothelial cells in vitro, demonstrating a dual adhesion phenotype mediated by distinct *P. falciparum* erythrocyte membrane protein 1 domains. *Infect. Immun.* *82*, 949–959.
- Ade-Serrano, M.A., Ejezie, G.C., and Kassim, O.O. (1981). Correlation of *Plasmodium falciparum* gametocytemia with complement component titers in rural Nigerian school children. *J. Clin. Microbiol.* *13*, 195–198.
- Agarwal, A., Guindo, A., Cissoko, Y., Taylor, J.G., Coulibaly, D., Koné, A., Kayentao, K., Djimde, A., Plowe, C.V., Doumbo, O., et al. (2000). Hemoglobin C associated with protection from severe malaria in the Dogon of Mali, a West African population with a low prevalence of hemoglobin S. *Blood* *96*, 2358–2363.
- Aird, W.C. (2012). Endothelial cell heterogeneity. *Cold Spring Harb. Perspect. Med.* *2*, a006429.
- Akhouri, R.R., Goel, S., Furusho, H., Skoglund, U., and Wahlgren, M. (2016). Architecture of Human IgM in Complex with *P. falciparum* Erythrocyte Membrane Protein 1. *Cell Rep.* *14*, 723–736.
- Albrecht, E.A., Chinnaiyan, A.M., Varambally, S., Kumar-Sinha, C., Barrette, T.R., Sarma, J.V., and Ward, P.A. (2004). C5a-induced gene expression in human umbilical vein endothelial cells. *Am. J. Pathol.* *164*, 849–859.

- Allen, S.J., O'Donnell, A., Alexander, N.D., and Clegg, J.B. (1996). Severe malaria in children in Papua New Guinea. *QJM Mon. J. Assoc. Physicians* 89, 779–788.
- Allen, S.J., O'Donnell, A., Alexander, N.D.E., Alpers, M.P., Peto, T.E.A., Clegg, J.B., and Weatherall, D.J. (1997). α -Thalassemia protects children against disease caused by other infections as well as malaria. *Proc. Natl. Acad. Sci. U. S. A.* 94, 14736–14741.
- Allen, S.J., O'Donnell, A., Alexander, N.D., Mgone, C.S., Peto, T.E., Clegg, J.B., Alpers, M.P., and Weatherall, D.J. (1999). Prevention of cerebral malaria in children in Papua New Guinea by southeast Asian ovalocytosis band 3. *Am. J. Trop. Med. Hyg.* 60, 1056–1060.
- Allison, A.C. (1964). Polymorphism and Natural Selection in Human Populations. *Cold Spring Harb. Symp. Quant. Biol.* 29, 137–149.
- Amara, U., Flierl, M.A., Rittirsch, D., Klos, A., Chen, H., Acker, B., Brückner, U.B., Nilsson, B., Gebhard, F., Lambris, J.D., et al. (2010). Molecular intercommunication between the complement and coagulation systems. *J. Immunol. Baltim. Md 1950* 185, 5628–5636.
- Andres, O., Obojes, K., Kim, K.S., ter Meulen, V., and Schneider-Schaulies, J. (2003). CD46- and CD150-independent endothelial cell infection with wild-type measles viruses. *J. Gen. Virol.* 84, 1189–1197.
- Angel, T.E., Aryal, U.K., Hengel, S.M., Baker, E.S., Kelly, R.T., Robinson, E.W., and Smith, R.D. (2012). Mass spectrometry based proteomics: existing capabilities and future directions. *Chem. Soc. Rev.* 41, 3912–3928.
- Angkasekwinai, P., Looareesuwan, S., and Chaiyaroj, S.C. (1998). Lack of significant association between rosette formation and parasitized erythrocyte adherence to purified CD36. *Southeast Asian J. Trop. Med. Public Health* 29, 41–45.
- Arman, M., Raza, A., Tempest, L.J., Lyke, K.E., Thera, M.A., Koné, A., Plowe, C.V., Doumbo, O.K., and Rowe, J.A. (2007). Platelet-mediated clumping of *Plasmodium falciparum* infected erythrocytes is associated with high parasitemia but not severe clinical manifestations of malaria in African children. *Am. J. Trop. Med. Hyg.* 77, 943–946.
- Armulik, A., Genové, G., and Betsholtz, C. (2011). Pericytes: developmental, physiological, and pathological perspectives, problems, and promises. *Dev. Cell* 21, 193–215.
- Arnold, J.N., Wormald, M.R., Suter, D.M., Radcliffe, C.M., Harvey, D.J., Dwek, R.A., Rudd, P.M., and Sim, R.B. (2005). Human serum IgM glycosylation: identification of glycoforms that can bind to mannan-binding lectin. *J. Biol. Chem.* 280, 29080–29087.

Arnold, J.N., Wallis, R., Willis, A.C., Harvey, D.J., Royle, L., Dwek, R.A., Rudd, P.M., and Sim, R.B. (2006a). Interaction of Mannan Binding Lectin with α 2 Macroglobulin via Exposed Oligomannose Glycans, a Conserved Feature of the Thiol Ester Protein Family? *J. Biol. Chem.* *281*, 6955–6963.

Arnold, J.N., Dwek, R.A., Rudd, P.M., and Sim, R.B. (2006b). Mannan binding lectin and its interaction with immunoglobulins in health and in disease. *Immunol. Lett.* *106*, 103–110.

Arnold, J.N., Dwek, R.A., Rudd, P.M., and Sim, R.B. (2006c). Mannan binding lectin and its interaction with immunoglobulins in health and in disease. *Immunol. Lett.* *106*, 103–110.

Ashley, E.A., Dhorda, M., Fairhurst, R.M., Amaratunga, C., Lim, P., Suon, S., Sreng, S., Anderson, J.M., Mao, S., Sam, B., et al. (2014). Spread of Artemisinin Resistance in *Plasmodium falciparum* Malaria. *N. Engl. J. Med.* *371*, 411–423.

Atkinson, J.P., and Jones, E.A. (1984). Biosynthesis of the human C3b/C4b receptor during differentiation of the HL-60 cell line. Identification and characterization of a precursor molecule. *J. Clin. Invest.* *74*, 1649–1657.

Atkinson, S.H., Uyoga, S.M., Nyatichi, E., Macharia, A.W., Nyutu, G., Ndila, C., Kwiatkowski, D.P., Rockett, K.A., and Williams, T.N. (2014). Epistasis between the haptoglobin common variant and α -thalassemia influences risk of severe malaria in Kenyan children. *Blood* *123*, 2008–2016.

Aung, H.H., Tsoukalas, A., Rutledge, J.C., and Tagkopoulos, I. (2014). A systems biology analysis of brain microvascular endothelial cell lipotoxicity. *BMC Syst. Biol.* *8*, 80.

Avril, M., Tripathi, A.K., Brazier, A.J., Andisi, C., Janes, J.H., Soma, V.L., Sullivan, D.J., Bull, P.C., Stins, M.F., and Smith, J.D. (2012). A restricted subset of var genes mediates adherence of *Plasmodium falciparum*-infected erythrocytes to brain endothelial cells. *Proc. Natl. Acad. Sci. U. S. A.* *109*, E1782-1790.

Avril, M., Brazier, A.J., Melcher, M., Sampath, S., and Smith, J.D. (2013). DC8 and DC13 var Genes Associated with Severe Malaria Bind Avidly to Diverse Endothelial Cells. *PLOS Pathog.* *9*, e1003430.

Avril, M., Bernabeu, M., Benjamin, M., Brazier, A.J., and Smith, J.D. (2016). Interaction between Endothelial Protein C Receptor and Intercellular Adhesion Molecule 1 to Mediate Binding of *Plasmodium falciparum*-Infected Erythrocytes to Endothelial Cells. *MBio* *7*.

Awandare, G.A., Spadafora, C., Moch, J.K., Dutta, S., Haynes, J.D., and Stoute, J.A. (2011). *Plasmodium falciparum* field isolates use complement receptor 1 (CR1) as a receptor for invasion of erythrocytes. *Mol. Biochem. Parasitol.* *177*, 57–60.

- Ayi, K., Turrini, F., Piga, A., and Arese, P. (2004). Enhanced phagocytosis of ring-parasitized mutant erythrocytes: a common mechanism that may explain protection against falciparum malaria in sickle trait and beta-thalassemia trait. *Blood* *104*, 3364–3371.
- Azasi, Y., Lindergard, G., Ghumra, A., Mu, J., Miller, L.H., and Rowe, J.A. (2018). Infected erythrocytes expressing DC13 PfEMP1 differ from recombinant proteins in EPCR-binding function. *Proc. Natl. Acad. Sci. U. S. A.* *115*, 1063–1068.
- Bajtay, Z., Józsi, M., Bánki, Z., Thiel, S., Thielens, N., and Erdei, A. (2000). Mannan-binding lectin and C1q bind to distinct structures and exert differential effects on macrophages. *Eur. J. Immunol.* *30*, 1706–1713.
- Band, G., Le, Q.S., Jostins, L., Pirinen, M., Kivinen, K., Jallow, M., Sisay-Joof, F., Bojang, K., Pinder, M., Sirugo, G., et al. (2013). Imputation-Based Meta-Analysis of Severe Malaria in Three African Populations. *PLOS Genet.* *9*, e1003509.
- Barfod, L., Dalgaard, M.B., Pleman, S.T., Ofori, M.F., Pleass, R.J., and Hviid, L. (2011). Evasion of immunity to Plasmodium falciparum malaria by IgM masking of protective IgG epitopes in infected erythrocyte surface-exposed PfEMP1. *Proc. Natl. Acad. Sci. U. S. A.* *108*, 12485–12490.
- Barilla-LaBarca, M.L., Liszewski, M.K., Lambris, J.D., Hourcade, D., and Atkinson, J.P. (2002). Role of membrane cofactor protein (CD46) in regulation of C4b and C3b deposited on cells. *J. Immunol. Baltim. Md 1950* *168*, 6298–6304.
- Barrera, V., MacCormick, I.J., Czanner, G., Hiscott, P.S., White, V.A., Craig, A.G., Beare, N.A.V., Culshaw, L.H., Zheng, Y., Biddolph, S.C., et al. (2018). Neurovascular sequestration in paediatric P.falciparum malaria is visible clinically in the retina. *ELife* *7*.
- Baruch, D.I., Pasloske, B.L., Singh, H.B., Bi, X., Ma, X.C., Feldman, M., Taraschi, T.F., and Howard, R.J. (1995). Cloning the P. falciparum gene encoding PfEMP1, a malarial variant antigen and adherence receptor on the surface of parasitized human erythrocytes. *Cell* *82*, 77–87.
- Bates, D., Maechler, M., Bolker, B., and Walker, S. (2013). lme4: Linear mixed-effects models using Eigen and S4.
- Baum, J., Maier, A.G., Good, R.T., Simpson, K.M., and Cowman, A.F. (2005). Invasion by P. falciparum Merozoites Suggests a Hierarchy of Molecular Interactions. *PLOS Pathog.* *1*, e37.
- Beare, N.A.V., Taylor, T.E., Harding, S.P., Lewallen, S., and Molyneux, M.E. (2006). Malarial retinopathy: a newly established diagnostic sign in severe malaria. *Am. J. Trop. Med. Hyg.* *75*, 790–797.

- Bellamy, R., Kwiatkowski, D., and Hill, A.V. (1998). Absence of an association between intercellular adhesion molecule 1, complement receptor 1 and interleukin 1 receptor antagonist gene polymorphisms and severe malaria in a West African population. *Trans. R. Soc. Trop. Med. Hyg.* *92*, 312–316.
- Berendt, A.R., Simmons, D.L., Tansey, J., Newbold, C.I., and Marsh, K. (1989). Intercellular adhesion molecule-1 is an endothelial cell adhesion receptor for *Plasmodium falciparum*. *Nature* *341*, 57–59.
- Berg, A., Otterdal, K., Patel, S., Gonca, M., David, C., Dalen, I., Nymo, S., Nilsson, M., Nordling, S., Magnusson, P.U., et al. (2015). Complement activation correlates to disease severity and contribute to cytokine response in falciparum malaria. *J. Infect. Dis.* *jiv283*.
- Berge, V., Johnson, E., and Berge, K.E. (1996). Interleukin-1 alpha, interleukin 6 and tumor necrosis factor alpha increase the synthesis and expression of the functional alternative and terminal complement pathways by human umbilical vein endothelial cells in vitro. *APMIS Acta Pathol. Microbiol. Immunol. Scand.* *104*, 213–219.
- Berger, M., Wetzler, E.M., and Wallis, R.S. (1988). Tumor necrosis factor is the major monocyte product that increases complement receptor expression on mature human neutrophils. *Blood* *71*, 151–158.
- Berger, M., Sorensen, R.U., Tosi, M.F., Dearborn, D.G., and Döring, G. (1989). Complement receptor expression on neutrophils at an inflammatory site, the *Pseudomonas*-infected lung in cystic fibrosis. *J. Clin. Invest.* *84*, 1302–1313.
- Bernfield, M., Götte, M., Park, P.W., Reizes, O., Fitzgerald, M.L., Lincecum, J., and Zako, M. (1999). Functions of cell surface heparan sulfate proteoglycans. *Annu. Rev. Biochem.* *68*, 729–777.
- Bertin, G.I., Lavstsen, T., Guillonneau, F., Doritchamou, J., Wang, C.W., Jespersen, J.S., Ezimegnon, S., Fievet, N., Alao, M.J., Lalya, F., et al. (2013). Expression of the Domain Cassette 8 *Plasmodium falciparum* Erythrocyte Membrane Protein 1 Is Associated with Cerebral Malaria in Benin. *PLoS ONE* *8*.
- Beynon, H.L., Davies, K.A., Haskard, D.O., and Walport, M.J. (1994). Erythrocyte complement receptor type 1 and interactions between immune complexes, neutrophils, and endothelium. *J. Immunol. Baltim. Md 1950* *153*, 3160–3167.
- Biagini, M., Spinsanti, M., Angelis, G.D., Tomei, S., Ferlenghi, I., Scarselli, M., Rigat, F., Messuti, N., Biolchi, A., Muzzi, A., et al. (2016). Expression of factor H binding protein in meningococcal strains can vary at least 15-fold and is genetically determined. *Proc. Natl. Acad. Sci.* *113*, 2714–2719.

- Birmingham, D.J., and Hebert, L.A. (2001). CR1 and CR1-like: the primate immune adherence receptors. *Immunol. Rev.* *180*, 100–111.
- Biryukov, S., and Stoute, J.A. (2014). Complement activation in malaria: friend or foe? *Trends Mol. Med.* *20*, 293–301.
- Biryukov, S., Angov, E., Landmesser, M.E., Spring, M.D., Ockenhouse, C.F., and Stoute, J.A. (2016). Complement and Antibody-mediated Enhancement of Red Blood Cell Invasion and Growth of Malaria Parasites. *EBioMedicine* *9*, 207–216.
- Boldt, A.B.W., Luty, A., Grobusch, M.P., Dietz, K., Dzeing, A., Kombila, M., Kremsner, P.G., and Kun, J.F.J. (2006). Association of a new mannose-binding lectin variant with severe malaria in Gabonese children. *Genes Immun.* *7*, 393–400.
- Booth, P.B., and McLoughlin, K. (1972). The Gerbich Blood Group System, Especially in Melanesians. *Vox Sang.* *22*, 73–84.
- Bouïs, D., Hospers, G.A., Meijer, C., Molema, G., and Mulder, N.H. (2001). Endothelium in vitro: a review of human vascular endothelial cell lines for blood vessel-related research. *Angiogenesis* *4*, 91–102.
- Boyle, M.J., Reiling, L., Feng, G., Langer, C., Osier, F.H., Aspeling-Jones, H., Cheng, Y.S., Stubbs, J., Tetteh, K.K.A., Conway, D.J., et al. (2015). Human antibodies fix complement to inhibit *Plasmodium falciparum* invasion of erythrocytes and are associated with protection against malaria. *Immunity* *42*, 580–590.
- Brightman, M.W., and Reese, T.S. (1969). Junctions between intimately apposed cell membranes in the vertebrate brain. *J. Cell Biol.* *40*, 648–677.
- Brooimans, R.A., Ark, A.A. van der, Buurman, W.A., Es, L.A. van, and Daha, M.R. (1990). Differential regulation of complement factor H and C3 production in human umbilical vein endothelial cells by IFN-gamma and IL-1. *J. Immunol.* *144*, 3835–3840.
- Brooks, S.A. (2004). Appropriate glycosylation of recombinant proteins for human use: implications of choice of expression system. *Mol. Biotechnol.* *28*, 241–255.
- Brown, H., Rogerson, S., Taylor, T., Tembo, M., Mwenechanya, J., Molyneux, M., and Turner, G. (2001). Blood-brain barrier function in cerebral malaria in Malawian children. *Am. J. Trop. Med. Hyg.* *64*, 207–213.
- Bull, P.C., and Abdi, A.I. (2016). The role of PfEMP1 as targets of naturally acquired immunity to childhood malaria: prospects for a vaccine. *Parasitology* *143*, 171–186.
- Bull, P.C., Berriman, M., Kyes, S., Quail, M.A., Hall, N., Kortok, M.M., Marsh, K., and Newbold, C.I. (2005). *Plasmodium falciparum* variant surface antigen expression patterns during malaria. *PLoS Pathog.* *1*, e26.

Busby, G.B., Band, G., Le, Q.S., Jallow, M., Bougama, E., Mangano, V.D., Amenga-Etego, L.N., Enimil, A., Apinjoh, T., Ndila, C.M., et al. (2016). Admixture into and within sub-Saharan Africa. *ELife* 5, e15266.

Butler, M., Quelhas, D., Critchley, A.J., Carchon, H., Hebestreit, H.F., Hibbert, R.G., Vilarinho, L., Teles, E., Matthijs, G., Schollen, E., et al. (2003). Detailed glycan analysis of serum glycoproteins of patients with congenital disorders of glycosylation indicates the specific defective glycan processing step and provides an insight into pathogenesis. *Glycobiology* 13, 601–622.

Butthep, P., Wanram, S., Pattanapanyasat, K., Vattanaviboon, P., Fucharoen, S., and Wilairat, P. (2006). Cytoadherence between endothelial cells and *P. falciparum* infected and noninfected normal and thalassemic red blood cells. *Cytometry B Clin. Cytom.* 70, 432–442.

Cabrales, P., Zanini, G.M., Meays, D., Frangos, J.A., and Carvalho, L.J.M. (2010). Murine cerebral malaria is associated with a vasospasm-like microcirculatory dysfunction, and survival upon rescue treatment is markedly increased by nimodipine. *Am. J. Pathol.* 176, 1306–1315.

Calis, J.C.J., Phiri, K.S., Faragher, E.B., Brabin, B.J., Bates, I., Cuevas, L.E., de Haan, R.J., Phiri, A.I., Malange, P., Khoka, M., et al. (2008). Severe anemia in Malawian children. *N. Engl. J. Med.* 358, 888–899.

Cappadoro, M., Giribaldi, G., O'Brien, E., Turrini, F., Mannu, F., Ulliers, D., Simula, G., Luzzatto, L., and Arese, P. (1998). Early phagocytosis of glucose-6-phosphate dehydrogenase (G6PD)-deficient erythrocytes parasitized by *Plasmodium falciparum* may explain malaria protection in G6PD deficiency. *Blood* 92, 2527–2534.

Carlson, J., and Wahlgren, M. (1992). *Plasmodium falciparum* erythrocyte rosetting is mediated by promiscuous lectin-like interactions. *J. Exp. Med.* 176, 1311–1317.

Carlson, J., Nash, G.B., Gabutti, V., al-Yaman, F., and Wahlgren, M. (1994). Natural protection against severe *Plasmodium falciparum* malaria due to impaired rosette formation. *Blood* 84, 3909–3914.

Carneiro, I., Roca-Feltrer, A., Griffin, J.T., Smith, L., Tanner, M., Schellenberg, J.A., Greenwood, B., and Schellenberg, D. (2010). Age-Patterns of Malaria Vary with Severity, Transmission Intensity and Seasonality in Sub-Saharan Africa: A Systematic Review and Pooled Analysis. *PLOS ONE* 5, e8988.

Carpentier, J.L., Lew, D.P., Paccaud, J.P., Gil, R., Iacopetta, B., Kazatchkine, M., Stendahl, O., and Pozzan, T. (1991). Internalization pathway of C3b receptors in human neutrophils and its transmodulation by chemoattractant receptors stimulation. *Cell Regul.* 2, 41–55.

- Casarsa, C., De Luigi, A., Pausa, M., De Simoni, M.G., and Tedesco, F. (2003). Intracerebroventricular injection of the terminal complement complex causes inflammatory reaction in the rat brain. *Eur. J. Immunol.* *33*, 1260–1270.
- Chen, C.-H., Ghiran, I., Beurskens, F.J.M., Weaver, G., Vincent, J.A., Nicholson-Weller, A., and Klickstein, L.B. (2007). Antibody CR1-2B11 recognizes a non-polymorphic epitope of human CR1 (CD35). *Clin. Exp. Immunol.* *148*, 546–554.
- Chen, Q., Fernandez, V., Sundström, A., Schlichtherle, M., Datta, S., Hagblom, P., and Wahlgren, M. (1998). Developmental selection of var gene expression in *Plasmodium falciparum*. *Nature* *394*, 392–395.
- Cheng, Q., Cloonan, N., Fischer, K., Thompson, J., Waine, G., Lanzer, M., and Saul, A. (1998). *stevor* and *rif* are *Plasmodium falciparum* multicopy gene families which potentially encode variant antigens. *Mol. Biochem. Parasitol.* *97*, 161–176.
- Chevalier, J., and Kazatchkine, M.D. (1989). Distribution in clusters of complement receptor type one (CR1) on human erythrocytes. *J. Immunol. Baltim. Md 1950* *142*, 2031–2036.
- Chitnis, C.E., and Miller, L.H. (1994). Identification of the erythrocyte binding domains of *Plasmodium vivax* and *Plasmodium knowlesi* proteins involved in erythrocyte invasion. *J. Exp. Med.* *180*, 497–506.
- Cholera, R., Brittain, N.J., Gillrie, M.R., Lopera-Mesa, T.M., Diakité, S.A.S., Arie, T., Krause, M.A., Guindo, A., Tubman, A., Fujioka, H., et al. (2008). Impaired cytoadherence of *Plasmodium falciparum*-infected erythrocytes containing sickle hemoglobin. *Proc. Natl. Acad. Sci. U. S. A.* *105*, 991–996.
- Chong, S.S., Boehm, C.D., Higgs, D.R., and Cutting, G.R. (2000). Single-tube multiplex-PCR screen for common deletional determinants of alpha-thalassemia. *Blood* *95*, 360–362.
- Chou, Y.K., Sherwood, T., and Virella, G. (1985). Erythrocyte-bound immune complexes trigger the release of interleukin-1 from human monocytes. *Cell. Immunol.* *91*, 308–314.
- Cines, D.B., Pollak, E.S., Buck, C.A., Loscalzo, J., Zimmerman, G.A., McEver, R.P., Pober, J.S., Wick, T.M., Konkle, B.A., Schwartz, B.S., et al. (1998). Endothelial cells in physiology and in the pathophysiology of vascular disorders. *Blood* *91*, 3527–3561.
- Claessens, A., and Rowe, J.A. (2012). Selection of *Plasmodium falciparum* parasites for cytoadhesion to human brain endothelial cells. *J. Vis. Exp. JoVE* e3122.
- Claessens, A., Adams, Y., Ghumra, A., Lindergard, G., Buchan, C.C., Andisi, C., Bull, P.C., Mok, S., Gupta, A.P., Wang, C.W., et al. (2012). A subset of group A-like var

genes encodes the malaria parasite ligands for binding to human brain endothelial cells. *Proc. Natl. Acad. Sci. U. S. A.* *109*, E1772-1781.

Clarke, G.M., Rockett, K., Kivinen, K., Hubbard, C., Jeffreys, A.E., Rowlands, K., Jallow, M., Conway, D.J., Bojang, K.A., Pinder, M., et al. (2017). Characterisation of the opposing effects of G6PD deficiency on cerebral malaria and severe malarial anaemia. *ELife* *6*, e15085.

Cockburn, I.A., Donvito, B., Cohen, J.H.M., and Rowe, J.A. (2002). A simple method for accurate quantification of complement receptor 1 on erythrocytes preserved by fixing or freezing. *J. Immunol. Methods* *271*, 59–64.

Cockburn, I.A., Mackinnon, M.J., O'Donnell, A., Allen, S.J., Moulds, J.M., Baisor, M., Bockarie, M., Reeder, J.C., and Rowe, J.A. (2004). A human complement receptor 1 polymorphism that reduces *Plasmodium falciparum* rosetting confers protection against severe malaria. *Proc. Natl. Acad. Sci. U. S. A.* *101*, 272–277.

Collard, C.D., Väkevä, A., Büküsoglu, C., Zünd, G., Sperati, C.J., Colgan, S.P., and Stahl, G.L. (1997). Reoxygenation of Hypoxic Human Umbilical Vein Endothelial Cells Activates the Classic Complement Pathway. *Circulation* *96*, 326–333.

Collard, C.D., Bukusoglu, C., Agah, A., Colgan, S.P., Reenstra, W.R., Morgan, B.P., and Stahl, G.L. (1999). Hypoxia-induced expression of complement receptor type 1 (CR1, CD35) in human vascular endothelial cells. *Am. J. Physiol.* *276*, C450-458.

Collard, C.D., Vakeva, A., Morrissey, M.A., Agah, A., Rollins, S.A., Reenstra, W.R., Buras, J.A., Meri, S., and Stahl, G.L. (2000). Complement Activation after Oxidative Stress. *Am. J. Pathol.* *156*, 1549–1556.

Collard, C.D., Montalto, M.C., Reenstra, W.R., Buras, J.A., and Stahl, G.L. (2001). Endothelial Oxidative Stress Activates the Lectin Complement Pathway. *Am. J. Pathol.* *159*, 1045–1054.

Conroy, A.L., Hawkes, M., Elphinstone, R.E., Morgan, C., Hermann, L., Barker, K.R., Namasopo, S., Opoka, R.O., John, C.C., Liles, W.C., et al. (2016). Acute Kidney Injury Is Common in Pediatric Severe Malaria and Is Associated With Increased Mortality. *Open Forum Infect. Dis.* *3*, ofw046.

Conroy, A.L., Hawkes, M.T., Elphinstone, R., Opoka, R.O., Namasopo, S., Miller, C., John, C.C., and Kain, K.C. (2018). Chitinase-3-like 1 is a biomarker of acute kidney injury and mortality in paediatric severe malaria. *Malar. J.* *17*, 82.

Cortés, A., Mellombo, M., Mgone, C.S., Beck, H.-P., Reeder, J.C., and Cooke, B.M. (2005). Adhesion of *Plasmodium falciparum*-infected red blood cells to CD36 under flow is enhanced by the cerebral malaria-protective trait South-East Asian ovalocytosis. *Mol. Biochem. Parasitol.* *142*, 252–257.

- Cosio, F.G., Shen, X.P., and Hebert, L.A. (1990). Immune complexes bind preferentially to specific subpopulations of human erythrocytes. *Clin. Immunol. Immunopathol.* *55*, 337–354.
- Covas, D.T., de Oliveira, F.S., Rodrigues, E.S., Abe-Sandes, K., Silva, W.A., and Fontes, A.M. (2007). Knops blood group haplotypes among distinct Brazilian populations. *Transfusion (Paris)* *47*, 147–153.
- Cowman, A.F., Berry, D., and Baum, J. (2012). The cellular and molecular basis for malaria parasite invasion of the human red blood cell. *J. Cell Biol.* *198*, 961–971.
- Craig, A.G., Grau, G.E., Janse, C., Kazura, J.W., Milner, D., Barnwell, J.W., Turner, G., and Langhorne, J. (2012). The role of animal models for research on severe malaria. *PLoS Pathog.* *8*, e1002401.
- Crompton, P.D., Traore, B., Kayentao, K., Doumbo, S., Ongoiba, A., Diakite, S.A.S., Krause, M.A., Doumtabe, D., Kone, Y., Weiss, G., et al. (2008). Sick cell trait is associated with a delayed onset of malaria: implications for time-to-event analysis in clinical studies of malaria. *J. Infect. Dis.* *198*, 1265–1275.
- Culleton, R.L., Mita, T., Ndounga, M., Unger, H., Cravo, P.V.L., Paganotti, G.M., Takahashi, N., Kaneko, A., Eto, H., Tinto, H., et al. (2008). Failure to detect *Plasmodium vivax* in West and Central Africa by PCR species typing. *Malar. J.* *7*, 174.
- Czajkowsky, D.M., and Shao, Z. (2009). The human IgM pentamer is a mushroom-shaped molecule with a flexural bias. *Proc. Natl. Acad. Sci. U. S. A.* *106*, 14960–14965.
- Da Silva, R.P., Hall, B.F., Joiner, K.A., and Sacks, D.L. (1989). CR1, the C3b receptor, mediates binding of infective *Leishmania major* metacyclic promastigotes to human macrophages. *J. Immunol. Baltim. Md 1950* *143*, 617–622.
- Daneman, R. (2012). The blood-brain barrier in health and disease. *Ann. Neurol.* *72*, 648–672.
- Danielsson, C., Pascual, M., French, L., Steiger, G., and Schifferli, J.A. (1994). Soluble complement receptor type 1 (CD35) is released from leukocytes by surface cleavage. *Eur. J. Immunol.* *24*, 2725–2731.
- Dasari, P., Heber, S.D., Beisele, M., Torzewski, M., Reifenberg, K., Orning, C., Fries, A., Zapf, A.-L., Baumeister, S., Lingelbach, K., et al. (2012). Digestive vacuole of *Plasmodium falciparum* released during erythrocyte rupture dually activates complement and coagulation. *Blood* *119*, 4301–4310.
- Dasari, P., Fries, A., Heber, S.D., Salama, A., Blau, I.-W., Lingelbach, K., Bhakdi, S.C., Udomsangpetch, R., Torzewski, M., Reiss, K., et al. (2014). Malarial anemia: digestive vacuole of *Plasmodium falciparum* mediates complement deposition on

bystander cells to provoke hemophagocytosis. *Med. Microbiol. Immunol. (Berl.)* 203, 383–393.

Dauchel, H., Julen, N., Lemercier, C., Daveau, M., Ozanne, D., Fontaine, M., and Ripoche, J. (1990). Expression of complement alternative pathway proteins by endothelial cells. Differential regulation by interleukin 1 and glucocorticoids. *Eur. J. Immunol.* 20, 1669–1675.

Day, N.P., Hien, T.T., Schollaardt, T., Loc, P.P., Chuong, L.V., Chau, T.T., Mai, N.T., Phu, N.H., Sinh, D.X., White, N.J., et al. (1999). The prognostic and pathophysiologic role of pro- and antiinflammatory cytokines in severe malaria. *J. Infect. Dis.* 180, 1288–1297.

Debets, J.M., Van der Linden, C.J., Dieteren, I.E., Leeuwenberg, J.F., and Buurman, W.A. (1988). Fc-receptor cross-linking induces rapid secretion of tumor necrosis factor (cachectin) by human peripheral blood monocytes. *J. Immunol. Baltim. Md* 1950 141, 1197–1201.

Dempsey, P.W., Allison, M.E., Akkaraju, S., Goodnow, C.C., and Fearon, D.T. (1996). C3d of complement as a molecular adjuvant: bridging innate and acquired immunity. *Science* 271, 348–350.

Dmitrieva, N.I., and Burg, M.B. (2014). Secretion of von Willebrand factor by endothelial cells links sodium to hypercoagulability and thrombosis. *Proc. Natl. Acad. Sci. U. S. A.* 111, 6485–6490.

Dobrina, A., Pausa, M., Fischetti, F., Bulla, R., Vecile, E., Ferrero, E., Mantovani, A., and Tedesco, F. (2002). Cytolytically inactive terminal complement complex causes transendothelial migration of polymorphonuclear leukocytes in vitro and in vivo. *Blood* 99, 185–192.

Dondorp, A.M., Angus, B.J., Hardeman, M.R., Chotivanich, K.T., Silamut, K., Ruangveerayuth, R., Kager, P.A., White, N.J., and Vreeken, J. (1997). Prognostic significance of reduced red blood cell deformability in severe falciparum malaria. *Am. J. Trop. Med. Hyg.* 57, 507–511.

Dondorp, A.M., Pongponratn, E., and White, N.J. (2004). Reduced microcirculatory flow in severe falciparum malaria: pathophysiology and electron-microscopic pathology. *Acta Trop.* 89, 309–317.

Dondorp, A.M., Lee, S.J., Faiz, M.A., Mishra, S., Price, R., Tjitra, E., Than, M., Htut, Y., Mohanty, S., Yunus, E.B., et al. (2008a). The Relationship between Age and the Manifestations of and Mortality Associated with Severe Malaria. *Clin. Infect. Dis.* 47, 151–157.

Dondorp, A.M., Ince, C., Charunwatthana, P., Hanson, J., van Kuijen, A., Faiz, M.A., Rahman, M.R., Hasan, M., Bin Yunus, E., Ghose, A., et al. (2008b). Direct in vivo

assessment of microcirculatory dysfunction in severe falciparum malaria. *J. Infect. Dis.* *197*, 79–84.

Dondorp, A.M., Fanello, C.I., Hendriksen, I.C.E., Gomes, E., Seni, A., Chhaganlal, K.D., Bojang, K., Olaosebikan, R., Anunobi, N., Maitland, K., et al. (2010). Artesunate versus quinine in the treatment of severe falciparum malaria in African children (AQUAMAT): an open-label, randomised trial. *Lancet Lond. Engl.* *376*, 1647–1657.

Doolan, D.L., Dobaño, C., and Baird, J.K. (2009). Acquired immunity to malaria. *Clin. Microbiol. Rev.* *22*, 13–36, Table of Contents.

Dörmer, P., Dietrich, M., Kern, P., and Horstmann, R.D. (1983). Ineffective erythropoiesis in acute human *P. falciparum* malaria. *Blut* *46*, 279–288.

Dorovini-Zis, K., Prameya, R., and Bowman, P.D. (1991). Culture and characterization of microvascular endothelial cells derived from human brain. *Lab. Investig. J. Tech. Methods Pathol.* *64*, 425–436.

Dorovini-Zis, K., Schmidt, K., Huynh, H., Fu, W., Whitten, R.O., Milner, D., Kamiza, S., Molyneux, M., and Taylor, T.E. (2011). The Neuropathology of Fatal Cerebral Malaria in Malawian Children. *Am. J. Pathol.* *178*, 2146–2158.

Dumbo, O.K., Thera, M.A., Koné, A.K., Raza, A., Tempest, L.J., Lyke, K.E., Plowe, C.V., and Rowe, J.A. (2009). High levels of *Plasmodium falciparum* rosetting in all clinical forms of severe malaria in African children. *Am. J. Trop. Med. Hyg.* *81*, 987–993.

Drickamer, K. (1992). Engineering galactose-binding activity into a C-type mannose-binding protein. *Nature* *360*, 183–186.

Dykman, T., Cole, J., Iida, K., and Atkinson, J.P. (1983a). Structural heterogeneity of the C3b/C4b receptor (Cr 1) on human peripheral blood cells. *J. Exp. Med.* *157*, 2160–2165.

Dykman, T.R., Cole, J.L., Iida, K., and Atkinson, J.P. (1983b). Polymorphism of human erythrocyte C3b/C4b receptor. *Proc. Natl. Acad. Sci. U. S. A.* *80*, 1698–1702.

Dykman, T.R., Hatch, J.A., and Atkinson, J.P. (1984). Polymorphism of the human C3b/C4b receptor. Identification of a third allele and analysis of receptor phenotypes in families and patients with systemic lupus erythematosus. *J. Exp. Med.* *159*, 691–703.

Dykman, T.R., Hatch, J.A., Aqua, M.S., and Atkinson, J.P. (1985). Polymorphism of the C3b/C4b receptor (CR1): characterization of a fourth allele. *J. Immunol. Baltim. Md* *1950* *134*, 1787–1789.

Egan, T.J. (2002). Physico-chemical aspects of hemozoin (malaria pigment) structure and formation. *J. Inorg. Biochem.* *91*, 19–26.

Ehrnthaller, C., Ignatius, A., Gebhard, F., and Huber-Lang, M. (2011). New insights of an old defense system: structure, function, and clinical relevance of the complement system. *Mol. Med. Camb. Mass* *17*, 317–329.

Eid, N.A., Hussein, A.A., Elzein, A.M., Mohamed, H.S., Rockett, K.A., Kwiatkowski, D.P., and Ibrahim, M.E. (2010). Candidate malaria susceptibility/protective SNPs in hospital and population-based studies: the effect of sub-structuring. *Malar. J.* *9*, 119.

Elphinstone, R.E., Conroy, A.L., Hawkes, M., Hermann, L., Namasopo, S., Warren, H.S., John, C.C., Liles, W.C., and Kain, K.C. (2016). Alterations in Systemic Extracellular Heme and Hemopexin Are Associated With Adverse Clinical Outcomes in Ugandan Children With Severe Malaria. *J. Infect. Dis.* *214*, 1268–1275.

Elvington, M., Liszewski, M.K., and Atkinson, J.P. (2016). Evolution of the complement system: from defense of the single cell to guardian of the intravascular space. *Immunol. Rev.* *274*, 9–15.

Emlen, W., Carl, V., and Burdick, G. (1992). Mechanism of transfer of immune complexes from red blood cell CR1 to monocytes. *Clin. Exp. Immunol.* *89*, 8–17.

Esmon, C.T. (1989). The roles of protein C and thrombomodulin in the regulation of blood coagulation. *J. Biol. Chem.* *264*, 4743–4746.

Faik, I., Oyedeji, S.I., Idris, Z., de Messias-Reason, I.J., Lell, B., Kremsner, P.G., and Kun, J.F.J. (2011). Ficolin-2 levels and genetic polymorphisms of FCN2 in malaria. *Hum. Immunol.* *72*, 74–79.

Fairhurst, R.M., Baruch, D.I., Brittain, N.J., Ostera, G.R., Wallach, J.S., Hoang, H.L., Hayton, K., Guindo, A., Makobongo, M.O., Schwartz, O.M., et al. (2005). Abnormal display of PfEMP-1 on erythrocytes carrying haemoglobin C may protect against malaria. *Nature* *435*, 1117–1121.

Fearon, D.T. (1980). Identification of the membrane glycoprotein that is the C3b receptor of the human erythrocyte, polymorphonuclear leukocyte, B lymphocyte, and monocyte. *J. Exp. Med.* *152*, 20–30.

Fearon, D.T. (1985). Human Complement Receptors for C3b (CR1) and C3d (CR2). *J. Invest. Dermatol.* *85*, 53s-57s.

Fearon, D.T., and Collins, L.A. (1983). Increased expression of C3b receptors on polymorphonuclear leukocytes induced by chemotactic factors and by purification procedures. *J. Immunol. Baltim. Md 1950* *130*, 370–375.

Fearon, D.T., Austen, K.F., and Ruddy, S. (1973). Formation of a Hemolytically Active Cellular Intermediate by the Interaction Between Properdin Factors B and D and the Activated Third Component of Complement. *J. Exp. Med.* *138*, 1305–1313.

Feng, S., Liang, X., Kroll, M.H., Chung, D.W., and Afshar-Kharghan, V. (2015). von Willebrand factor is a cofactor in complement regulation. *Blood* *125*, 1034–1037.

Fernandez, V., Hommel, M., Chen, Q., Hagblom, P., and Wahlgren, M. (1999). Small, clonally variant antigens expressed on the surface of the Plasmodium falciparum-infected erythrocyte are encoded by the rif gene family and are the target of human immune responses. *J. Exp. Med.* *190*, 1393–1404.

Fett, A.L., Hermann, M.M., Muether, P.S., Kirchhof, B., and Fauser, S. (2012). Immunohistochemical localization of complement regulatory proteins in the human retina. *Histol. Histopathol.* *27*, 357–364.

Fiedler, K., Kutzner, F., and Krueger, J.I. (2012). The Long Way From α -Error Control to Validity Proper: Problems With a Short-Sighted False-Positive Debate. *Perspect. Psychol. Sci. J. Assoc. Psychol. Sci.* *7*, 661–669.

Fischer, E., Appay, M.D., Cook, J., and Kazatchkine, M.D. (1986). Characterization of the human glomerular C3 receptor as the C3b/C4b complement type one (CR1) receptor. *J. Immunol. Baltim. Md 1950* *136*, 1373–1377.

Fitness, J., Floyd, S., Warndorff, D.K., Sichali, L., Mwaungulu, L., Crampin, A.C., Fine, P.E.M., and Hill, A.V.S. (2004a). Large-scale candidate gene study of leprosy susceptibility in the Karonga district of northern Malawi. *Am. J. Trop. Med. Hyg.* *71*, 330–340.

Fitness, J., Floyd, S., Warndorff, D.K., Sichali, L., Malema, S., Crampin, A.C., Fine, P.E.M., and Hill, A.V.S. (2004b). Large-scale candidate gene study of tuberculosis susceptibility in the Karonga district of northern Malawi. *Am. J. Trop. Med. Hyg.* *71*, 341–349.

Fleit, S.A., Fleit, H.B., and Zolla-Pazner, S. (1984). Culture and recovery of macrophages and cell lines from tissue culture-treated and -untreated plastic dishes. *J. Immunol. Methods* *68*, 119–129.

Flint, J., Harding, R.M., Boyce, A.J., and Clegg, J.B. (1998). The population genetics of the haemoglobinopathies. *Baillieres Clin. Haematol.* *11*, 1–51.

Foley, J.H., Peterson, E.A., Lei, V., Wan, L.W., Krisinger, M.J., and Conway, E.M. (2015). Interplay between fibrinolysis and complement: plasmin cleavage of iC3b modulates immune responses. *J. Thromb. Haemost.* n/a-n/a.

Fonseca, M.I., Chu, S., Pierce, A.L., Brubaker, W.D., Hauhart, R.E., Mastroeni, D., Clarke, E.V., Rogers, J., Atkinson, J.P., and Tenner, A.J. (2016). Analysis of the

Putative Role of CR1 in Alzheimer's Disease: Genetic Association, Expression and Function. *PLOS ONE* *11*, e0149792.

Foreman, K.E., Vaporciyan, A.A., Bonish, B.K., Jones, M.L., Johnson, K.J., Glovsky, M.M., Eddy, S.M., and Ward, P.A. (1994). C5a-induced expression of P-selectin in endothelial cells. *J. Clin. Invest.* *94*, 1147–1155.

Fowkes, F.J.I., Allen, S.J., Allen, A., Alpers, M.P., Weatherall, D.J., and Day, K.P. (2008). Increased microerythrocyte count in homozygous alpha(+)-thalassaemia contributes to protection against severe malarial anaemia. *PLoS Med.* *5*, e56.

Franke-Fayard, B., Janse, C.J., Cunha-Rodrigues, M., Ramesar, J., Büscher, P., Que, I., Löwik, C., Voshol, P.J., Boer, M.A.M. den, Duinen, S.G. van, et al. (2005). Murine malaria parasite sequestration: CD36 is the major receptor, but cerebral pathology is unlinked to sequestration. *Proc. Natl. Acad. Sci.* *102*, 11468–11473.

Fry, A.E., Griffiths, M.J., Auburn, S., Diakite, M., Forton, J.T., Green, A., Richardson, A., Wilson, J., Jallow, M., Sisay-Joof, F., et al. (2008). Common variation in the ABO glycosyltransferase is associated with susceptibility to severe *Plasmodium falciparum* malaria. *Hum. Mol. Genet.* *17*, 567–576.

Furtado, P.B., Huang, C.Y., Ihyembe, D., Hammond, R.A., Marsh, H.C., and Perkins, S.J. (2008). The partly folded back solution structure arrangement of the 30 SCR domains in human complement receptor type 1 (CR1) permits access to its C3b and C4b ligands. *J. Mol. Biol.* *375*, 102–118.

Gandhi, M., Singh, A., Dev, V., Adak, T., Dashd, A.P., and Joshi, H. (2009). Role of CR1 Knops polymorphism in the pathophysiology of malaria: Indian scenario. *J. Vector Borne Dis.* *46*, 288–294.

Garg, S., Agarwal, S., Dabral, S., Kumar, N., Sehrawat, S., and Singh, S. (2015). Visualization and quantification of *Plasmodium falciparum* intraerythrocytic merozoites. *Syst. Synth. Biol.* *9*, 23–26.

Garred, P., Nielsen, M.A., Kurtzhals, J.A.L., Malhotra, R., Madsen, H.O., Goka, B.Q., Akanmori, B.D., Sim, R.B., and Hviid, L. (2003). Mannose-binding lectin is a disease modifier in clinical malaria and may function as opsonin for *Plasmodium falciparum*-infected erythrocytes. *Infect. Immun.* *71*, 5245–5253.

Garred, P., Genster, N., Pilely, K., Bayarri-Olmos, R., Rosbjerg, A., Ma, Y.J., and Skjoedt, M.-O. (2016). A journey through the lectin pathway of complement—MBL and beyond. *Immunol. Rev.* *274*, 74–97.

Gazzinelli, R.T., and Denkers, E.Y. (2006). Protozoan encounters with Toll-like receptor signalling pathways: implications for host parasitism. *Nat. Rev. Immunol.* *6*, 895–906.

Genton, B., al-Yaman, F., Mgone, C.S., Alexander, N., Paniu, M.M., Alpers, M.P., and Mokela, D. (1995). Ovalocytosis and cerebral malaria. *Nature* 378, 564–565.

Ghiran, I., Barbashov, S.F., Klickstein, L.B., Tas, S.W., Jensenius, J.C., and Nicholson-Weller, A. (2000). Complement Receptor 1/Cd35 Is a Receptor for Mannan-Binding Lectin. *J. Exp. Med.* 192, 1797–1808.

Ghiran, I., Glodek, A.M., Weaver, G., Klickstein, L.B., and Nicholson-Weller, A. (2008). Ligation of erythrocyte CR1 induces its clustering in complex with scaffolding protein FAP-1. *Blood* 112, 3465–3473.

Ghumra, A., Semblat, J.-P., McIntosh, R.S., Raza, A., Rasmussen, I.B., Braathen, R., Johansen, F.-E., Sandlie, I., Mongini, P.K., Rowe, J.A., et al. (2008). Identification of residues in the Cmu4 domain of polymeric IgM essential for interaction with Plasmodium falciparum erythrocyte membrane protein 1 (PfEMP1). *J. Immunol. Baltim. Md 1950* 181, 1988–2000.

Ghumra, A., Semblat, J.-P., Ataide, R., Kifude, C., Adams, Y., Claessens, A., Anong, D.N., Bull, P.C., Fennell, C., Arman, M., et al. (2012). Induction of Strain-Transcending Antibodies Against Group A PfEMP1 Surface Antigens from Virulent Malaria Parasites. *PLoS Pathog* 8, e1002665.

Glodek, A.M., Mirchev, R., Golan, D.E., Khoory, J.A., Burns, J.M., Shevkoplyas, S.S., Nicholson-Weller, A., and Ghiran, I.C. (2010). Ligation of complement receptor 1 increases erythrocyte membrane deformability. *Blood* 116, 6063–6071.

Golgi, C. (1886). Sull'infezione malarica. *Arch Sci Med Torino* 10, 109–135.

Gonçalves, B.P., Huang, C.-Y., Morrison, R., Holte, S., Kabyemela, E., Prevots, D.R., Fried, M., and Duffy, P.E. (2014). Parasite Burden and Severity of Malaria in Tanzanian Children. *N. Engl. J. Med.* 370, 1799–1808.

Goodfellow, R.M., Williams, A.S., Levin, J.L., Williams, B.D., and Morgan, B.P. (2000). Soluble complement receptor one (sCR1) inhibits the development and progression of rat collagen-induced arthritis. *Clin. Exp. Immunol.* 119, 210–216.

Graffelman, J., and Camarena, J.M. (2008). Graphical tests for Hardy-Weinberg equilibrium based on the ternary plot. *Hum. Hered.* 65, 77–84.

Greenland, S., Mansournia, M.A., and Altman, D.G. (2016). Sparse data bias: a problem hiding in plain sight. *BMJ* 352, i1981.

Greenwood, B.M., and Brueton, M.J. (1974). Complement activation in children with acute malaria. *Clin. Exp. Immunol.* 18, 267–272.

Gulati, P., Lemerrier, C., Guc, D., Lappin, D., and Whaley, K. (1993). Regulation of the synthesis of C1 subcomponents and C1-inhibitor. *Behring Inst. Mitt.* 196–203.

- Gunning, P., Leavitt, J., Muscat, G., Ng, S.Y., and Kedes, L. (1987). A human beta-actin expression vector system directs high-level accumulation of antisense transcripts. *Proc. Natl. Acad. Sci. U. S. A.* *84*, 4831–4835.
- Haldane, J.B.S. (1949). The Rate of Mutation of Human Genes. *Hereditas* *35*, 267–273.
- Hamer, I., Paccaud, J.P., Belin, D., Maeder, C., and Carpentier, J.L. (1998). Soluble form of complement C3b/C4b receptor (CR1) results from a proteolytic cleavage in the C-terminal region of CR1 transmembrane domain. *Biochem. J.* *329*, 183–190.
- Hamilton, K.K., Ji, Z., Rollins, S., Stewart, B.H., and Sims, P.J. (1990). Regulatory control of the terminal complement proteins at the surface of human endothelial cells: neutralization of a C5b-9 inhibitor by antibody to CD59. *Blood* *76*, 2572–2577.
- Hannan, J.P. (2016). The Structure-Function Relationships of Complement Receptor Type 2 (CR2; CD21). *Curr. Protein Pept. Sci.* *17*, 463–487.
- Hanson, J., Lam, S.W.K., Mahanta, K.C., Pattnaik, R., Alam, S., Mohanty, S., Hasan, M.U., Hossain, A., Charunwatthana, P., Chotivanich, K., et al. (2012). Relative contributions of macrovascular and microvascular dysfunction to disease severity in falciparum malaria. *J. Infect. Dis.* *206*, 571–579.
- Hanson, J., Lee, S.J., Hossain, M.A., Anstey, N.M., Charunwatthana, P., Maude, R.J., Kingston, H.W.F., Mishra, S.K., Mohanty, S., Plewes, K., et al. (2015). Microvascular obstruction and endothelial activation are independently associated with the clinical manifestations of severe falciparum malaria in adults: an observational study. *BMC Med.* *13*, 122.
- Hansson, H.H., Kurtzhals, J.A., Goka, B.Q., Rodriques, O.P., Nkrumah, F.N., Theander, T.G., Bygbjerg, I.C., and Alifrangis, M. (2013). Human genetic polymorphisms in the Knops blood group are not associated with a protective advantage against *Plasmodium falciparum* malaria in Southern Ghana. *Malar. J.* *12*, 400.
- Harrison, R.L., and Jarvis, D.L. (2006). Protein N-glycosylation in the baculovirus-insect cell expression system and engineering of insect cells to produce “mammalianized” recombinant glycoproteins. *Adv. Virus Res.* *68*, 159–191.
- Helegbe, G., Goka, B., Kurtzhals, J., Addae, M., Ollaga, E., Tetteh, J., Dodoo, D., Ofori, M., Obeng-Adjei, G., Hirayama, K., et al. (2007). Complement activation in Ghanaian children with severe *Plasmodium falciparum* malaria. *Malar. J.* *6*, 165.
- Henson, P.M. (1969). The adherence of leucocytes and platelets induced by fixed IgG antibody or complement. *Immunology* *16*, 107–121.

- Herrera, A.H., Xiang, L., Martin, S.G., Lewis, J., and Wilson, J.G. (1998). Analysis of complement receptor type 1 (CR1) expression on erythrocytes and of CR1 allelic markers in Caucasian and African American populations. *Clin. Immunol. Immunopathol.* *87*, 176–183.
- van der Heyde, H.C., Nolan, J., Combes, V., Gramaglia, I., and Grau, G.E. (2006). A unified hypothesis for the genesis of cerebral malaria: sequestration, inflammation and hemostasis leading to microcirculatory dysfunction. *Trends Parasitol.* *22*, 503–508.
- Hirsch, C.S., Ellner, J.J., Russell, D.G., and Rich, E.A. (1994). Complement receptor-mediated uptake and tumor necrosis factor-alpha-mediated growth inhibition of *Mycobacterium tuberculosis* by human alveolar macrophages. *J. Immunol. Baltim. Md 1950* *152*, 743–753.
- Ho, M., Davis, T.M., Silamut, K., Bunnag, D., and White, N.J. (1991). Rosette formation of *Plasmodium falciparum*-infected erythrocytes from patients with acute malaria. *Infect. Immun.* *59*, 2135–2139.
- Hochman, S.E., Madaline, T.F., Wassmer, S.C., Mbale, E., Choi, N., Seydel, K.B., Whitten, R.O., Varughese, J., Grau, G.E.R., Kamiza, S., et al. (2015). Fatal Pediatric Cerebral Malaria Is Associated with Intravascular Monocytes and Platelets That Are Increased with HIV Coinfection. *MBio* *6*, e01390-01315.
- Hogg, N., Ross, G.D., Jones, D.B., Slusarenko, M., Walport, M.J., and Lachmann, P.J. (1984). Identification of an anti-monocyte monoclonal antibody that is specific for membrane complement receptor type one (CR1). *Eur. J. Immunol.* *14*, 236–243.
- Holmberg, V., Schuster, F., Dietz, E., Sagarriga Visconti, J.C., Anemana, S.D., Bienzle, U., and Mockenhaupt, F.P. (2008). Mannose-binding lectin variant associated with severe malaria in young African children. *Microbes Infect. Inst. Pasteur* *10*, 342–348.
- Hourcade, D., Holers, V.M., and Atkinson, J.P. (1989). The regulators of complement activation (RCA) gene cluster. *Adv. Immunol.* *45*, 381–416.
- Hudson, L.C., Bragg, D.C., Tompkins, M.B., and Meeker, R.B. (2005). Astrocytes and microglia differentially regulate trafficking of lymphocyte subsets across brain endothelial cells. *Brain Res.* *1058*, 148–160.
- Hugli, T.E. (1981). The structural basis for anaphylatoxin and chemotactic functions of C3a, C4a, and C5a. *Crit. Rev. Immunol.* *1*, 321–366.
- Hviid, L. (2005). Naturally acquired immunity to *Plasmodium falciparum* malaria in Africa. *Acta Trop.* *95*, 270–275.
- Iida, K., and Nussenzweig, V. (1981). Complement receptor is an inhibitor of the complement cascade. *J. Exp. Med.* *153*, 1138–1150.

- lida, K., Mornaghi, R., and Nussenzweig, V. (1982). Complement receptor (CR1) deficiency in erythrocytes from patients with systemic lupus erythematosus. *J. Exp. Med.* *155*, 1427–1438.
- Jack, D.L., Read, R.C., Tenner, A.J., Frosch, M., Turner, M.W., and Klein, N.J. (2001). Mannose-binding lectin regulates the inflammatory response of human professional phagocytes to *Neisseria meningitidis* serogroup B. *J. Infect. Dis.* *184*, 1152–1162.
- Jacquet, M., Lacroix, M., Ancelet, S., Gout, E., Gaboriaud, C., Thielens, N.M., and Rossi, V. (2013). Deciphering Complement Receptor Type 1 Interactions with Recognition Proteins of the Lectin Complement Pathway. *J. Immunol.* *190*, 3721–3731.
- Jajosky, R.P., Jajosky, A.N., and Jajosky, P.G. (2017). Can exchange transfusions using red blood cells from donors with Southeast Asian ovalocytosis prevent or ameliorate cerebral malaria in patients with multi-drug resistant *Plasmodium falciparum*? *Transfus. Apher. Sci.* *56*, 865–866.
- Jallow, M., Teo, Y.Y., Small, K.S., Rockett, K.A., Deloukas, P., Clark, T.G., Kivinen, K., Bojang, K.A., Conway, D.J., Pinder, M., et al. (2009). Genome-wide and fine-resolution association analysis of malaria in West Africa. *Nat. Genet.* *41*, 657–665.
- Jambou, R., Combes, V., Jambou, M.-J., Weksler, B.B., Couraud, P.-O., and Grau, G.E. (2010). *Plasmodium falciparum* Adhesion on Human Brain Microvascular Endothelial Cells Involves Transmigration-Like Cup Formation and Induces Opening of Intercellular Junctions. *PLoS Pathog* *6*, e1001021.
- Jancar, S., and Sánchez Crespo, M. (2005). Immune complex-mediated tissue injury: a multistep paradigm. *Trends Immunol.* *26*, 48–55.
- Janzer, R.C., and Raff, M.C. (1987). Astrocytes induce blood-brain barrier properties in endothelial cells. *Nature* *325*, 253–257.
- Java, A., Liszewski, M.K., Hourcade, D.E., Zhang, F., and Atkinson, J.P. (2015). Role of complement receptor 1 (CR1; CD35) on epithelial cells: A model for understanding complement-mediated damage in the kidney. *Mol. Immunol.* *67*, 584–595.
- Jensen, A.T.R., Magistrado, P., Sharp, S., Joergensen, L., Lavstsen, T., Chiucchiuini, A., Salanti, A., Vestergaard, L.S., Lusingu, J.P., Hermsen, R., et al. (2004). *Plasmodium falciparum* associated with severe childhood malaria preferentially expresses PfEMP1 encoded by group A var genes. *J. Exp. Med.* *199*, 1179–1190.
- Johnson, E., and Hetland, G. (1991). Human umbilical vein endothelial cells synthesize functional C3, C5, C6, C8 and C9 in vitro. *Scand. J. Immunol.* *33*, 667–671.

- Julen, N., Dauchel, H., Lemerrier, C., Sim, R.B., Fontaine, M., and Ripoche, J. (1992). In vitro biosynthesis of complement factor I by human endothelial cells. *Eur. J. Immunol.* *22*, 213–217.
- Kalli, K.R., Hsu, P.H., Bartow, T.J., Ahearn, J.M., Matsumoto, A.K., Klickstein, L.B., and Fearon, D.T. (1991). Mapping of the C3b-binding site of CR1 and construction of a (CR1)2-F(ab')2 chimeric complement inhibitor. *J. Exp. Med.* *174*, 1451–1460.
- Kariuki, S.M., Rockett, K., Clark, T.G., Reyburn, H., Agbenyega, T., Taylor, T.E., Birbeck, G.L., Williams, T.N., and Newton, C.R.J.C. (2013). The genetic risk of acute seizures in African children with falciparum malaria. *Epilepsia* *54*, 990–1001.
- Kaul, D.K., Roth, E.F., Nagel, R.L., Howard, R.J., and Handunnetti, S.M. (1991). Rosetting of Plasmodium falciparum-infected red blood cells with uninfected red blood cells enhances microvascular obstruction under flow conditions. *Blood* *78*, 812–819.
- Kaviratne, M., Khan, S.M., Jarra, W., and Preiser, P.R. (2002). Small variant STEVOR antigen is uniquely located within Maurer's clefts in Plasmodium falciparum-infected red blood cells. *Eukaryot. Cell* *1*, 926–935.
- Keshavjee, S., Davis, R.D., Zamora, M.R., de Perrot, M., and Patterson, G.A. (2005). A randomized, placebo-controlled trial of complement inhibition in ischemia-reperfusion injury after lung transplantation in human beings. *J. Thorac. Cardiovasc. Surg.* *129*, 423–428.
- Khaw, L.T., Ball, H.J., Golenser, J., Combes, V., Grau, G.E., Wheway, J., Mitchell, A.J., and Hunt, N.H. (2013). Endothelial Cells Potentiate Interferon- γ Production in a Novel Tripartite Culture Model of Human Cerebral Malaria. *PLOS ONE* *8*, e69521.
- Khera, R., and Das, N. (2009). Complement Receptor 1: Disease associations and therapeutic implications. *Mol. Immunol.* *46*, 761–772.
- Kilgore, K.S., Shen, J.P., Miller, B.F., Ward, P.A., and Warren, J.S. (1995). Enhancement by the complement membrane attack complex of tumor necrosis factor-alpha-induced endothelial cell expression of E-selectin and ICAM-1. *J. Immunol. Baltim. Md 1950* *155*, 1434–1441.
- Kilgore, K.S., Flory, C.M., Miller, B.F., Evans, V.M., and Warren, J.S. (1996). The membrane attack complex of complement induces interleukin-8 and monocyte chemoattractant protein-1 secretion from human umbilical vein endothelial cells. *Am. J. Pathol.* *149*, 953–961.
- Kilgore, K.S., Schmid, E., Shanley, T.P., Flory, C.M., Maheswari, V., Tramontini, N.L., Cohen, H., Ward, P.A., Friedl, H.P., and Warren, J.S. (1997). Sublytic concentrations of the membrane attack complex of complement induce endothelial interleukin-8

and monocyte chemoattractant protein-1 through nuclear factor-kappa B activation. *Am. J. Pathol.* *150*, 2019–2031.

Kim, H., Erdman, L.K., Lu, Z., Serghides, L., Zhong, K., Dhabangi, A., Musoke, C., Gerard, C., Cserti-Gazdewich, C., Liles, W.C., et al. (2014). Functional Roles for C5a and C5aR but Not C5L2 in the Pathogenesis of Human and Experimental Cerebral Malaria. *Infect. Immun.* *82*, 371–379.

Kirkitadze, M.D., and Barlow, P.N. (2001). Structure and flexibility of the multiple domain proteins that regulate complement activation. *Immunol. Rev.* *180*, 146–161.

Kishore, U., and Reid, K.B. (2000). C1q: structure, function, and receptors. *Immunopharmacology* *49*, 159–170.

Klabunde, J., Uhlemann, A.-C., Tebo, A.E., Kimmel, J., Schwarz, R.T., Kremsner, P.G., and Kun, J.F.J. (2002). Recognition of plasmodium falciparum proteins by mannan-binding lectin, a component of the human innate immune system. *Parasitol. Res.* *88*, 113–117.

Klegeris, A., Bissonnette, C.J., Dorovini-Zis, K., and McGeer, P.L. (2000). Expression of complement messenger RNAs by human endothelial cells. *Brain Res.* *871*, 1–6.

Klickstein, L.B., Wong, W.W., Smith, J.A., Weis, J.H., Wilson, J.G., and Fearon, D.T. (1987). Human C3b/C4b receptor (CR1). Demonstration of long homologous repeating domains that are composed of the short consensus repeats characteristics of C3/C4 binding proteins. *J. Exp. Med.* *165*, 1095–1112.

Klickstein, L.B., Bartow, T.J., Miletic, V., Rabson, L.D., Smith, J.A., and Fearon, D.T. (1988). Identification of distinct C3b and C4b recognition sites in the human C3b/C4b receptor (CR1, CD35) by deletion mutagenesis. *J. Exp. Med.* *168*, 1699–1717.

Klickstein, L.B., Barbashov, S.F., Liu, T., Jack, R.M., and Nicholson-Weller, A. (1997). Complement receptor type 1 (CR1, CD35) is a receptor for C1q. *Immunity* *7*, 345–355.

Korir, J.C., Nyakoe, N.K., Awinda, G., and Waitumbi, J.N. (2014). Complement Activation by Merozoite Antigens of Plasmodium falciparum. *PLoS ONE* *9*.

Krause, M.A., Diakite, S.A.S., Lopera-Mesa, T.M., Amaratunga, C., Arie, T., Traore, K., Doumbia, S., Konate, D., Keefer, J.R., Diakite, M., et al. (2012). α -Thalassemia impairs the cytoadherence of Plasmodium falciparum-infected erythrocytes. *PLoS One* *7*, e37214.

Krych, M., Hourcade, D., and Atkinson, J.P. (1991). Sites within the complement C3b/C4b receptor important for the specificity of ligand binding. *Proc. Natl. Acad. Sci. U. S. A.* *88*, 4353–4357.

Krych-Goldberg, M., and Atkinson, J.P. (2001). Structure-function relationships of complement receptor type 1. *Immunol. Rev.* *180*, 112–122.

Krych-Goldberg, M., Hauhart, R.E., Subramanian, V.B., Yurcisin, B.M., Crimmins, D.L., Hourcade, D.E., and Atkinson, J.P. (1999). Decay accelerating activity of complement receptor type 1 (CD35). Two active sites are required for dissociating C5 convertases. *J. Biol. Chem.* *274*, 31160–31168.

Krych-Goldberg, M., Moulds, J.M., and Atkinson, J.P. (2002). Human complement receptor type 1 (CR1) binds to a major malarial adhesin. *Trends Mol. Med.* *8*, 531–537.

Kuehn, A., and Pradel, G. (2010). The Coming-Out of Malaria Gametocytes. *J. Biomed. Biotechnol.* *2010*.

Kumar, A., Wetzler, E., and Berger, M. (1997). Isolation and characterization of complement receptor type 1 (CR1) storage vesicles from human neutrophils using antibodies to the cytoplasmic tail of CR1. *Blood* *89*, 4555–4565.

Kun, J.F., Schmidt-Ott, R.J., Lehman, L.G., Lell, B., Luckner, D., Greve, B., Matousek, P., and Kremsner, P.G. (1998). Merozoite surface antigen 1 and 2 genotypes and rosetting of *Plasmodium falciparum* in severe and mild malaria in Lambaréné, Gabon. *Trans. R. Soc. Trop. Med. Hyg.* *92*, 110–114.

Kwiatkowski, D., Hill, A.V., Sambou, I., Twumasi, P., Castracane, J., Manogue, K.R., Cerami, A., Brewster, D.R., and Greenwood, B.M. (1990). TNF concentration in fatal cerebral, non-fatal cerebral, and uncomplicated *Plasmodium falciparum* malaria. *Lancet Lond. Engl.* *336*, 1201–1204.

Kyes, S.A., Rowe, J.A., Kriek, N., and Newbold, C.I. (1999). Rifins: a second family of clonally variant proteins expressed on the surface of red cells infected with *Plasmodium falciparum*. *Proc. Natl. Acad. Sci. U. S. A.* *96*, 9333–9338.

Kyriacou, H.M., Stone, G.N., Challis, R.J., Raza, A., Lyke, K.E., Thera, M.A., Koné, A.K., Doumbo, O.K., Plowe, C.V., and Rowe, J.A. (2006). Differential var gene transcription in *Plasmodium falciparum* isolates from patients with cerebral malaria compared to hyperparasitaemia. *Mol. Biochem. Parasitol.* *150*, 211–218.

Lachmann, P.J., Pangburn, M.K., and Oldroyd, R.G. (1982). Breakdown of C3 after complement activation. Identification of a new fragment C3g, using monoclonal antibodies. *J. Exp. Med.* *156*, 205–216.

Lambris, J.D., Ricklin, D., and Geisbrecht, B.V. (2008). Complement evasion by human pathogens. *Nat. Rev. Microbiol.* *6*, 132.

- Langeeggen, H., Pausa, M., Johnson, E., Casarsa, C., and Tedesco, F. (2000). The endothelium is an extrahepatic site of synthesis of the seventh component of the complement system. *Clin. Exp. Immunol.* *121*, 69–76.
- Langeeggen, H., Berge, K.E., Macor, P., Fischetti, F., Tedesco, F., Hetland, G., Berg, K., and Johnson, E. (2001). Detection of mRNA for the terminal complement components C5, C6, C8 and C9 in human umbilical vein endothelial cells in vitro. *APMIS Acta Pathol. Microbiol. Immunol. Scand.* *109*, 73–78.
- Langeeggen, H., Berge, K., Johnson, E., and Hetland, G. (2002). Human Umbilical Vein Endothelial Cells Express Complement Receptor 1 (CD35) and Complement Receptor 4 (CD11c/CD18) in vitro. *Inflammation* *26*, 103–110.
- Langeeggen, H., Namork, E., Johnson, E., and Hetland, G. (2003). HUVEC take up opsonized zymosan particles and secrete cytokines IL-6 and IL-8 in vitro. *FEMS Immunol. Med. Microbiol.* *36*, 55–61.
- Langhi, D.M., and Bordin, J.O. (2006). Duffy blood group and malaria. *Hematol. Amst. Neth.* *11*, 389–398.
- Lapin, Z.J., Höppener, C., Gelbard, H.A., and Novotny, L. (2012). Near-field quantification of complement receptor 1 (CR1/CD35) protein clustering in human erythrocytes. *J. Neuroimmune Pharmacol. Off. J. Soc. NeuroImmune Pharmacol.* *7*, 539–543.
- Lau, C.K.Y., Turner, L., Jespersen, J.S., Lowe, E.D., Petersen, B., Wang, C.W., Petersen, J.E.V., Lusingu, J., Theander, T.G., Lavstsen, T., et al. (2015). Structural conservation despite huge sequence diversity allows EPCR binding by the PfEMP1 family implicated in severe childhood malaria. *Cell Host Microbe* *17*, 118–129.
- Lavstsen, T., Turner, L., Saguti, F., Magistrado, P., Rask, T.S., Jespersen, J.S., Wang, C.W., Berger, S.S., Baraka, V., Marquard, A.M., et al. (2012). Plasmodium falciparum erythrocyte membrane protein 1 domain cassettes 8 and 13 are associated with severe malaria in children. *Proc. Natl. Acad. Sci. U. S. A.* *109*, E1791-1800.
- Lazar, H.L., Keilani, T., Fitzgerald, C.A., Shapira, O.M., Hunter, C.T., Shemin, R.J., Marsh, H.C., Ryan, U.S., and TP10 Cardiac Surgery Study Group (2007). Beneficial effects of complement inhibition with soluble complement receptor 1 (TP10) during cardiac surgery: is there a gender difference? *Circulation* *116*, 183-88.
- Levin, E.G., Marotti, K.R., and Santell, L. (1989). Protein kinase C and the stimulation of tissue plasminogen activator release from human endothelial cells. Dependence on the elevation of messenger RNA. *J. Biol. Chem.* *264*, 16030–16036.
- Lewis, C., Hill, M., Arthurs, O.J., Hutchinson, C., Chitty, L.S., and Sebire, N.J. (2018). Factors affecting uptake of postmortem examination in the prenatal, perinatal and paediatric setting. *BJOG Int. J. Obstet. Gynaecol.* *125*, 172–181.

Li, L.M., Li, J.B., Zhu, Y., and Fan, G.Y. (2010). Soluble complement receptor type 1 inhibits complement system activation and improves motor function in acute spinal cord injury. *Spinal Cord* 48, 105–111.

Lim, N.T.Y., Harder, M.J., Kennedy, A.T., Lin, C.S., Weir, C., Cowman, A.F., Call, M.J., Schmidt, C.Q., and Tham, W.-H. (2015). Characterization of Inhibitors and Monoclonal Antibodies That Modulate the Interaction between Plasmodium falciparum Adhesin PfRh4 with Its Erythrocyte Receptor Complement Receptor 1. *J. Biol. Chem.* 290, 25307–25321.

Lin, E., Tavul, L., Michon, P., Richards, J.S., Dabod, E., Beeson, J.G., King, C.L., Zimmerman, P.A., and Mueller, I. (2010). Minimal association of common red blood cell polymorphisms with Plasmodium falciparum infection and uncomplicated malaria in Papua New Guinean school children. *Am. J. Trop. Med. Hyg.* 83, 828–833.

Lipscombe, R.J., Sumiya, M., Hill, A.V., Lau, Y.L., Levinsky, R.J., Summerfield, J.A., and Turner, M.W. (1992). High frequencies in African and non-African populations of independent mutations in the mannose binding protein gene. *Hum. Mol. Genet.* 1, 709–715.

Lishimpi, K., Chintu, C., Lucas, S., Mudenda, V., Kaluwaji, J., Story, A., Maswahu, D., Bhat, G., Nunn, A.J., and Zumla, A. (2001). Necropsies in African children: consent dilemmas for parents and guardians. *Arch. Dis. Child.* 84, 463–467.

Liu, W., Li, Y., Learn, G.H., Rudicell, R.S., Robertson, J.D., Keele, B.F., Ndjango, J.-B.N., Sanz, C.M., Morgan, D.B., Locatelli, S., et al. (2010). Origin of the human malaria parasite Plasmodium falciparum in gorillas. *Nature* 467, 420–425.

Looareesuwan, S., Laothamatas, J., Brown, T.R., and Brittenham, G.M. (2009). Cerebral malaria: a new way forward with magnetic resonance imaging (MRI). *Am. J. Trop. Med. Hyg.* 81, 545–547.

Lou, J., Lucas, R., and Grau, G.E. (2001). Pathogenesis of Cerebral Malaria: Recent Experimental Data and Possible Applications for Humans. *Clin. Microbiol. Rev.* 14, 810–820.

Lublin, D.M., Griffith, R.C., and Atkinson, J.P. (1986). Influence of glycosylation on allelic and cell-specific Mr variation, receptor processing, and ligand binding of the human complement C3b/C4b receptor. *J. Biol. Chem.* 261, 5736–5744.

Luty, A.J., Kun, J.F., and Kremsner, P.G. (1998). Mannose-binding lectin plasma levels and gene polymorphisms in Plasmodium falciparum malaria. *J. Infect. Dis.* 178, 1221–1224.

Lyke, K.E., Diallo, D.A., Dicko, A., Kone, A., Coulibaly, D., Guindo, A., Cissoko, Y., Sangare, L., Coulibaly, S., Dakouo, B., et al. (2003). Association of intraleukocytic Plasmodium falciparum malaria pigment with disease severity, clinical

manifestations, and prognosis in severe malaria. *Am. J. Trop. Med. Hyg.* 69, 253–259.

Lyke, K.E., Burges, R., Cissoko, Y., Sangare, L., Dao, M., Diarra, I., Kone, A., Harley, R., Plowe, C.V., Doumbo, O.K., et al. (2004). Serum Levels of the Proinflammatory Cytokines Interleukin-1 Beta (IL-1 β), IL-6, IL-8, IL-10, Tumor Necrosis Factor Alpha, and IL-12(p70) in Malian Children with Severe *Plasmodium falciparum* Malaria and Matched Uncomplicated Malaria or Healthy Controls. *Infect. Immun.* 72, 5630–5637.

Maag, R.S., Mancini, M., Rosen, A., and Machamer, C.E. (2005). Caspase-resistant Golgin-160 disrupts apoptosis induced by secretory pathway stress and ligation of death receptors. *Mol. Biol. Cell* 16, 3019–3027.

Mackinnon, M.J., Mwangi, T.W., Snow, R.W., Marsh, K., and Williams, T.N. (2005). Heritability of Malaria in Africa. *PLOS Med.* 2, e340.

MacMullin, G., Mackenzie, R., Lau, R., Khang, J., Zhang, H., Rajwans, N., Liles, W.C., and Pillai, D.R. (2012). Host immune response in returning travellers infected with malaria. *Malar. J.* 11, 148.

MacPherson, G.G., Warrell, M.J., White, N.J., Looareesuwan, S., and Warrell, D.A. (1985). Human cerebral malaria. A quantitative ultrastructural analysis of parasitized erythrocyte sequestration. *Am. J. Pathol.* 119, 385–401.

Madi, N., Paccaud, J.P., Steiger, G., and Schifferli, J.A. (1991). Immune complex binding efficiency of erythrocyte complement receptor 1 (CR1). *Clin. Exp. Immunol.* 84, 9–15.

Maeno, Y., Perlmann, P., Perlmann, H., Kusuhara, Y., Taniguchi, K., Nakabayashi, T., Win, K., Looareesuwan, S., and Aikawa, M. (2000). IgE deposition in brain microvessels and on parasitized erythrocytes from cerebral malaria patients. *Am. J. Trop. Med. Hyg.* 63, 128–132.

Maier, A.G., Duraisingh, M.T., Reeder, J.C., Patel, S.S., Kazura, J.W., Zimmerman, P.A., and Cowman, A.F. (2003). *Plasmodium falciparum* erythrocyte invasion through glycophorin C and selection for Gerbich negativity in human populations. *Nat. Med.* 9, 87–92.

Maitland, K., Kiguli, S., Opoka, R.O., Engoru, C., Olupot-Olupot, P., Akech, S.O., Nyeko, R., Mtove, G., Reyburn, H., Lang, T., et al. (2011). Mortality after fluid bolus in African children with severe infection. *N. Engl. J. Med.* 364, 2483–2495.

Makrides, S.C., Scesney, S.M., Ford, P.J., Evans, K.S., Carson, G.R., and Marsh, H.C. (1992). Cell surface expression of the C3b/C4b receptor (CR1) protects Chinese hamster ovary cells from lysis by human complement. *J. Biol. Chem.* 267, 24754–24761.

- Malaria Genomic Epidemiology Network (2015). A novel locus of resistance to severe malaria in a region of ancient balancing selection. *Nature* 526, 253–257.
- Malhotra, R., Wormald, M.R., Rudd, P.M., Fischer, P.B., Dwek, R.A., and Sim, R.B. (1995). Glycosylation changes of IgG associated with rheumatoid arthritis can activate complement via the mannose-binding protein. *Nat. Med.* 1, 237–243.
- Manjurano, A., Clark, T.G., Nadjm, B., Mtove, G., Wangai, H., Sepulveda, N., Campino, S.G., Maxwell, C., Olomi, R., Rockett, K.R., et al. (2012). Candidate Human Genetic Polymorphisms and Severe Malaria in a Tanzanian Population. *PLoS ONE* 7, e47463.
- Marsh, K., and Kinyanjui, S. (2006). Immune effector mechanisms in malaria. *Parasite Immunol.* 28, 51–60.
- Marsh, K., Forster, D., Waruiru, C., Mwangi, I., Winstanley, M., Marsh, V., Newton, C., Winstanley, P., Warn, P., and Peshu, N. (1995). Indicators of life-threatening malaria in African children. *N. Engl. J. Med.* 332, 1399–1404.
- Mathew, J.M., Naziruddin, B., Duffy, B., Krych, M., and Mohanakumar, T. (1995). Functional analysis of complement receptor 1 using a new monoclonal antibody, KuN241. *Hybridoma* 14, 29–35.
- May, J., Evans, J.A., Timmann, C., Ehmen, C., Busch, W., Thye, T., Agbenyega, T., and Horstmann, R.D. (2007). Hemoglobin variants and disease manifestations in severe falciparum malaria. *JAMA* 297, 2220–2226.
- Mayer, D.C.G., Jiang, L., Achur, R.N., Kakizaki, I., Gowda, D.C., and Miller, L.H. (2006). The glycophorin C N-linked glycan is a critical component of the ligand for the Plasmodium falciparum erythrocyte receptor BAEFL. *Proc. Natl. Acad. Sci. U. S. A.* 103, 2358–2362.
- Mayor, A., Bir, N., Sawhney, R., Singh, S., Pattnaik, P., Singh, S.K., Sharma, A., and Chitnis, C.E. (2005). Receptor-binding residues lie in central regions of Duffy-binding-like domains involved in red cell invasion and cytoadherence by malaria parasites. *Blood* 105, 2557–2563.
- Mayor, A., Hafiz, A., Bassat, Q., Rovira-Vallbona, E., Sanz, S., Machevo, S., Aguilar, R., Cisteró, P., Sigaúque, B., Menéndez, C., et al. (2011). Association of severe malaria outcomes with platelet-mediated clumping and adhesion to a novel host receptor. *PloS One* 6, e19422.
- Mbogo, C.M., Mwangangi, J.M., Nzovu, J., Gu, W., Yan, G., Gunter, J.T., Swalm, C., Keating, J., Regens, J.L., Shililu, J.I., et al. (2003). Spatial and temporal heterogeneity of Anopheles mosquitoes and Plasmodium falciparum transmission along the Kenyan coast. *Am. J. Trop. Med. Hyg.* 68, 734–742.

- McMullen, M.E., Hart, M.L., Walsh, M.C., Buras, J., Takahashi, K., and Stahl, G.L. (2006). Mannose-binding lectin binds IgM to activate the lectin complement pathway in vitro and in vivo. *Immunobiology* 211, 759–766.
- Mebius, R.E., and Kraal, G. (2005). Structure and function of the spleen. *Nat. Rev. Immunol.* 5, 606–616.
- Medana, I.M., and Turner, G.D.H. (2006). Human cerebral malaria and the blood-brain barrier. *Int. J. Parasitol.* 36, 555–568.
- Medof, M.E., and Nussenzweig, V. (1984). Control of the function of substrate-bound C4b-C3b by the complement receptor Cr1. *J. Exp. Med.* 159, 1669–1685.
- Medof, M.E., Iida, K., Mold, C., and Nussenzweig, V. (1982). Unique role of the complement receptor CR1 in the degradation of C3b associated with immune complexes. *J. Exp. Med.* 156, 1739–1754.
- Melhorn, M.I., Brodsky, A.S., Estanislau, J., Khoory, J.A., Illigens, B., Hamachi, I., Kurishita, Y., Fraser, A.D., Nicholson-Weller, A., Dolmatova, E., et al. (2013). CR1-mediated ATP Release by Human Red Blood Cells Promotes CR1 Clustering and Modulates the Immune Transfer Process. *J. Biol. Chem.* 288, 31139–31153.
- Mensah-Brown, H.E., Amoako, N., Abugri, J., Stewart, L.B., Agongo, G., Dickson, E.K., Ofori, M.F., Stoute, J.A., Conway, D.J., and Awandare, G.A. (2015). Analysis of Erythrocyte Invasion Mechanisms of Plasmodium falciparum Clinical Isolates Across 3 Malaria-Endemic Areas in Ghana. *J. Infect. Dis.* 212, 1288–1297.
- Metwalli, A.A.M., de Jongh, H.H.J., and van Boekel, M.A.J.S. (1998). Heat inactivation of bovine plasmin. *Int. Dairy J.* 8, 47–56.
- Mibei, E.K., Otieno, W.O., Orago, A.S.S., and Stoute, J.A. (2008). Distinct pattern of class and subclass antibodies in immune complexes of children with cerebral malaria and severe malarial anaemia. *Parasite Immunol.* 30, 334–341.
- Miller, F., Afonso, P.V., Gessain, A., and Ceccaldi, P.-E. (2012). Blood-brain barrier and retroviral infections. *Virulence* 3, 222–229.
- Miller, L.H., Mason, S.J., Clyde, D.F., and McGinniss, M.H. (1976). The resistance factor to Plasmodium vivax in blacks. The Duffy-blood-group genotype, FyFy. *N. Engl. J. Med.* 295, 302–304.
- Miller, L.H., Baruch, D.I., Marsh, K., and Doumbo, O.K. (2002). The pathogenic basis of malaria. *Nature* 415, 673–679.
- Milner, D.A. (2010). Rethinking cerebral malaria pathology. *Curr. Opin. Infect. Dis.* 23, 456–463.

Milner, D.A., Montgomery, J., Seydel, K.B., and Rogerson, S.J. (2008). Severe malaria in children and pregnancy: an update and perspective. *Trends Parasitol.* 24, 590–595.

Milner, D.A., Whitten, R.O., Kamiza, S., Carr, R., Liomba, G., Dзамalala, C., Seydel, K.B., Molyneux, M.E., and Taylor, T.E. (2014). The systemic pathology of cerebral malaria in African children. *Front. Cell. Infect. Microbiol.* 4, 104.

Milner, D.A., Lee, J.J., Frantzreb, C., Whitten, R.O., Kamiza, S., Carr, R.A., Pradham, A., Factor, R.E., Playforth, K., Liomba, G., et al. (2015). Quantitative Assessment of Multiorgan Sequestration of Parasites in Fatal Pediatric Cerebral Malaria. *J. Infect. Dis.* 212, 1317–1321.

Mishra, S.K., and Das, B.S. (2008). Malaria and acute kidney injury. *Semin. Nephrol.* 28, 395–408.

Mockenhaupt, F.P., Ehrhardt, S., Cramer, J.P., Otchwemah, R.N., Anemana, S.D., Goltz, K., Mylius, F., Dietz, E., Eggelte, T.A., and Bienzle, U. (2004). Hemoglobin C and resistance to severe malaria in Ghanaian children. *J. Infect. Dis.* 190, 1006–1009.

Modiano, D., Sirima, B.S., Sawadogo, A., Sanou, I., Paré, J., Konaté, A., and Pagnoni, F. (1998). Severe malaria in Burkina Faso: influence of age and transmission level on clinical presentation. *Am. J. Trop. Med. Hyg.* 59, 539–542.

Mohanty, S., Mishra, S.K., Patnaik, R., Dutt, A.K., Pradhan, S., Das, B., Patnaik, J., Mohanty, A.K., Lee, S.J., and Dondorp, A.M. (2011). Brain swelling and mannitol therapy in adult cerebral malaria: a randomized trial. *Clin. Infect. Dis. Off. Publ. Infect. Dis. Soc. Am.* 53, 349–355.

Mohanty, S., Taylor, T.E., Kampondeni, S., Potchen, M.J., Panda, P., Majhi, M., Mishra, S.K., and Wassmer, S.C. (2014). Magnetic resonance imaging during life: the key to unlock cerebral malaria pathogenesis? *Malar. J.* 13, 276.

Mohanty, S., Benjamin, L.A., Majhi, M., Panda, P., Kampondeni, S., Sahu, P.K., Mohanty, A., Mahanta, K.C., Pattnaik, R., Mohanty, R.R., et al. (2017). Magnetic Resonance Imaging of Cerebral Malaria Patients Reveals Distinct Pathogenetic Processes in Different Parts of the Brain. *MSphere* 2.

Molyneux, M.E., Taylor, T.E., Wirima, J.J., and Borgstein, A. (1989). Clinical features and prognostic indicators in paediatric cerebral malaria: a study of 131 comatose Malawian children. *Q. J. Med.* 71, 441–459.

Molyneux, M.E., Engelmann, H., Taylor, T.E., Wirima, J.J., Aderka, D., Wallach, D., and Grau, G.E. (1993). Circulating plasma receptors for tumour necrosis factor in Malawian children with severe falciparum malaria. *Cytokine* 5, 604–609.

- Morgan, B.P. (1999). Regulation of the complement membrane attack pathway. *Crit. Rev. Immunol.* *19*, 173–198.
- Morley, B.J., and Walport, M. (2000). *The complement facts book* (San Diego, CA: Academic Press).
- Moulds, J.M. (2010). The Knops blood-group system: a review. *Immunohematol. Am. Red Cross* *26*, 2–7.
- Moulds, J.M., Nickells, M.W., Moulds, J.J., Brown, M.C., and Atkinson, J.P. (1991). The C3b/C4b receptor is recognized by the Knops, McCoy, Swain-Langley, and York blood group antisera. *J. Exp. Med.* *173*, 1159–1163.
- Moulds, J.M., Moulds, J.J., Brown, M., and Atkinson, J.P. (1992). Antiglobulin testing for CR1-related (Knops/McCoy/Swain-Langley/York) blood group antigens: negative and weak reactions are caused by variable expression of CR1. *Vox Sang.* *62*, 230–235.
- Moulds, J.M., Kassambara, L., Middleton, J.J., Baby, M., Sagara, I., Guindo, A., Coulibaly, S., Yalcouye, D., Diallo, D.A., Miller, L., et al. (2000). Identification of complement receptor one (CR1) polymorphisms in west Africa. *Genes Immun.* *1*, 325–329.
- Moulds, J.M., Zimmerman, P.A., Doumbo, O.K., Kassambara, L., Sagara, I., Diallo, D.A., Atkinson, J.P., Krych-Goldberg, M., Hauhart, R.E., Hourcade, D.E., et al. (2001). Molecular identification of Knops blood group polymorphisms found in long homologous region D of complement receptor 1. *Blood* *97*, 2879–2885.
- Moulds, J.M., Zimmerman, P.A., Doumbo, O.K., Diallo, D.A., Atkinson, J.P., Krych-Goldberg, M., Hourcade, D.E., and Moulds, J.J. (2002). Expansion of the Knops blood group system and subdivision of Sl(a). *Transfusion (Paris)* *42*, 251–256.
- Moulds, J.M., Thomas, B.J., Doumbo, O., Diallo, D.A., Lyke, K.E., Plowe, C.V., Rowe, J.A., and Birmingham, D.J. (2004). Identification of the Kna/Knb polymorphism and a method for Knops genotyping. *Transfusion (Paris)* *44*, 164–169.
- Moulds, J.M., Pierce, S., Peck, K.B., Tulley, M.L., Doumbo, O., and Moulds, J.J. (2005). KAM; A new allele in the Knops blood group system. *Transfusion (Paris)* *45*, S82-040F.
- Müller-Eberhard, H.J., Polley, M.J., and Calcott, M.A. (1967). Formation and functional significance of a molecular complex derived from the second and the fourth component of human complement. *J. Exp. Med.* *125*, 359–380.
- Murray, C.J.L., Ortblad, K.F., Guinovart, C., Lim, S.S., Wolock, T.M., Roberts, D.A., Dansereau, E.A., Graetz, N., Barber, R.M., Brown, J.C., et al. (2014). Global, regional, and national incidence and mortality for HIV, tuberculosis, and malaria during 1990-

2013: a systematic analysis for the Global Burden of Disease Study 2013. *Lancet Lond. Engl.* *384*, 1005–1070.

Nagayasu, E., Ito, M., Akaki, M., Nakano, Y., Kimura, M., Looareesuwan, S., and Aikawa, M. (2001). CR1 density polymorphism on erythrocytes of falciparum malaria patients in Thailand. *Am. J. Trop. Med. Hyg.* *64*, 1–5.

Nagy, Z., Vastag, M., Skopál, J., Kolev, K., Machovich, R., Krámer, J., Karádi, I., and Tóth, M. (1996). Human brain microvessel endothelial cell culture as a model system to study vascular factors of ischemic brain. *Keio J. Med.* *45*, 200–206.

Nakagawa, S. (2004). A farewell to Bonferroni: the problems of low statistical power and publication bias. *Behav. Ecol.* *15*, 1044–1045.

Nash, G.B., Cooke, B.M., Marsh, K., Berendt, A., Newbold, C., and Stuart, J. (1992). Rheological analysis of the adhesive interactions of red blood cells parasitized by *Plasmodium falciparum*. *Blood* *79*, 798–807.

National Malaria Control Programme, University of Health and Allied Sciences, AGA Malaria Control Programme, World Health Organization, and INFORM Project (2013). An Epidemiological Profile of Malaria and its Control in Ghana. A report prepared for the Ministry of Health, Ghana, the Roll Back Malaria Partnership and the Department for International Development, UK.

Nauta, A.J., Daha, M.R., van Kooten, C., and Roos, A. (2003). Recognition and clearance of apoptotic cells: a role for complement and pentraxins. *Trends Immunol.* *24*, 148–154.

Navratil, J.S., Watkins, S.C., Wisnieski, J.J., and Ahearn, J.M. (2001). The globular heads of C1q specifically recognize surface blebs of apoptotic vascular endothelial cells. *J. Immunol. Baltim. Md 1950* *166*, 3231–3239.

Neva, F.A., Howard, W.A., Glew, R.H., Krotoski, W.A., Gam, A.A., Collins, W.E., Atkinson, J.P., and Frank, M.M. (1974). Relationship of serum complement levels to events of the malarial paroxysm. *J. Clin. Invest.* *54*, 451–460.

Newton, C.R., Peshu, N., Kendall, B., Kirkham, F.J., Sowunmi, A., Waruiru, C., Mwangi, I., Murphy, S.A., and Marsh, K. (1994). Brain swelling and ischaemia in Kenyans with cerebral malaria. *Arch. Dis. Child.* *70*, 281–287.

Nguansangiam, S., Day, N.P.J., Hien, T.T., Mai, N.T.H., Chaisri, U., Riganti, M., Dondorp, A.M., Lee, S.J., Phu, N.H., Turner, G.D.H., et al. (2007). A quantitative ultrastructural study of renal pathology in fatal *Plasmodium falciparum* malaria. *Trop. Med. Int. Health* *12*, 1037–1050.

- Nickells, M., Hauhart, R., Krych, M., Subramanian, V.B., Geoghegan-Barek, K., Marsh, H.C., Jr, and Atkinson, J.P. (1998). Mapping epitopes for 20 monoclonal antibodies to CR1. *Clin. Exp. Immunol.* *112*, 27–33.
- Nilsson, B., and Nilsson Ekdahl, K. (2012). The tick-over theory revisited: Is C3 a contact-activated protein? *Immunobiology* *217*, 1106–1110.
- Ning, M., Sarracino, D.A., Kho, A.T., Guo, S., Lee, S.-R., Krastins, B., Buonanno, F.S., Vizcaíno, J.A., Orchard, S., McMullin, D., et al. (2011). Proteomic Temporal Profile of Human Brain Endothelium After Oxidative Stress. *Stroke J. Cereb. Circ.* *42*, 37–43.
- Noris, M., and Remuzzi, G. (2013). Overview of Complement Activation and Regulation. *Semin. Nephrol.* *33*, 479–492.
- Noumsi, G.T., Tounkara, A., Diallo, H., Billingsley, K., Moulds, J.J., and Moulds, J.M. (2011). Knops blood group polymorphism and susceptibility to Mycobacterium tuberculosis infection. *Transfusion (Paris)* *51*, 2462–2469.
- Nwaneshiudu, A., Kuschal, C., Sakamoto, F.H., Rox Anderson, R., Schwarzenberger, K., and Young, R.C. (2012). Introduction to Confocal Microscopy. *J. Invest. Dermatol.* *132*, 1–5.
- Nyakeriga, A.M., Troye-Blomberg, M., Chemtai, A.K., Marsh, K., and Williams, T.N. (2004). Malaria and nutritional status in children living on the coast of Kenya. *Am. J. Clin. Nutr.* *80*, 1604–1610.
- Nyakoe, N.K., Taylor, R.P., Makumi, J.N., and Waitumbi, J.N. (2009). Complement consumption in children with Plasmodium falciparum malaria. *Malar. J.* *8*, 7.
- Odera, M., Otieno, W., Adhiambo, C., and Stoute, J.A. (2011). Dual role of erythrocyte complement receptor type 1 in immune complex-mediated macrophage stimulation: implications for the pathogenesis of Plasmodium falciparum malaria. *Clin. Exp. Immunol.* *166*, 201–207.
- Odhiambo, C.O., Otieno, W., Adhiambo, C., Odera, M.M., and Stoute, J.A. (2008). Increased deposition of C3b on red cells with low CR1 and CD55 in a malaria-endemic region of western Kenya: Implications for the development of severe anemia. *BMC Med.* *6*, 23.
- Okpere, A.N., Anochie, I.C., and Eke, F.U. (2017). Acute kidney injury in children with severe malaria. *Afr. J. Paediatr. Nephrol.* *4*, 28–33.
- Oluwayemi, I.O., Brown, B.J., Oyedeji, O.A., and Oluwayemi, M.A. (2013). Neurological sequelae in survivors of cerebral malaria. *Pan Afr. Med. J.* *15*, 88.

- O'Meara, W.P., Bejon, P., Mwangi, T.W., Okiro, E.A., Peshu, N., Snow, R.W., Newton, C.R.J.C., and Marsh, K. (2008). Effect of a fall in malaria transmission on morbidity and mortality in Kilifi, Kenya. *Lancet* 372, 1555–1562.
- Opi, D.H. (2013). Red Blood Cell Polymorphisms And Their Associations With Malaria And Other Non-malaria Related Diseases In Kilifi, Kenya (Edinburgh, UK: University of Edinburgh).
- Opi, D.H., Ochola, L.B., Tendwa, M., Siddondo, B.R., Ocholla, H., Fanjo, H., Ghumra, A., Ferguson, D.J.P., Alexandra Rowe, J., and Williams, T.N. (2014). Mechanistic Studies of the Negative Epistatic Malaria-protective Interaction Between Sickle Cell Trait and α +thalassemia. *EBioMedicine* 1, 29–36.
- Opi, D.H., Uyoga, S., Orori, E.N., Williams, T.N., and Rowe, J.A. (2016). Red blood cell complement receptor one level varies with Knops blood group, α (+)thalassaemia and age among Kenyan children. *Genes Immun.* 17, 171–178.
- Opi D. Herbert, S.O., Macharia, A., Uyoga, S., Band, G., Ndila, C.M., Harrison, E.M., Thera, M.A., Kone, A.K., Diallo, D.A., Doumbo, O.K., et al. (2018). Two complement receptor one alleles have opposing associations with cerebral malaria and interact with α +thalassaemia. *ELife* 7.
- Oroszlán, M., Daha, M.R., Cervenak, L., Prohászka, Z., Füst, G., and Roos, A. (2007). MBL and C1q compete for interaction with human endothelial cells. *Mol. Immunol.* 44, 1150–1158.
- Orsini, F., De Blasio, D., Zangari, R., Zanier, E.R., and De Simoni, M.-G. (2014). Versatility of the complement system in neuroinflammation, neurodegeneration and brain homeostasis. *Front. Cell. Neurosci.* 8, 380.
- O'Shea, J.J., Brown, E.J., Seligmann, B.E., Metcalf, J.A., Frank, M.M., and Gallin, J.I. (1985). Evidence for distinct intracellular pools of receptors for C3b and C3bi in human neutrophils. *J. Immunol. Baltim. Md 1950* 134, 2580–2587.
- Otenio, W., Estamble, B., Odera, M., Aluoch, J., Gondi, S., and Stoute, J. (2013). Sickle Cell Trait (HbAS) is Associated with Increased Expression of Erythrocyte Complement Regulatory Proteins CR1 and CD55 Levels in Children. *Int. J. Trop. Dis.* 3, 133–147.
- Owuor, B.O., Odhiambo, C.O., Otieno, W.O., Adhiambo, C., Makawiti, D.W., and Stoute, J.A. (2008). Reduced Immune Complex Binding Capacity and Increased Complement Susceptibility of Red Cells from Children with Severe Malaria-Associated Anemia. *Mol. Med.* 14, 89–97.
- Paccaud, J.P., Carpentier, J.L., and Schifferli, J.A. (1988). Direct evidence for the clustered nature of complement receptors type 1 on the erythrocyte membrane. *J. Immunol. Baltim. Md 1950* 141, 3889–3894.

Paccaud, J.P., Carpentier, J.L., and Schifferli, J.A. (1990). Difference in the clustering of complement receptor type 1 (CR1) on polymorphonuclear leukocytes and erythrocytes: effect on immune adherence. *Eur. J. Immunol.* *20*, 283–289.

Pain, A., Ferguson, D.J., Kai, O., Urban, B.C., Lowe, B., Marsh, K., and Roberts, D.J. (2001). Platelet-mediated clumping of *Plasmodium falciparum*-infected erythrocytes is a common adhesive phenotype and is associated with severe malaria. *Proc. Natl. Acad. Sci. U. S. A.* *98*, 1805–1810.

Palarasah, Y., Nielsen, C., Sprogøe, U., Christensen, M.L., Lillevang, S., Madsen, H.O., Bygum, A., Koch, C., Skjodt, K., and Skjoedt, M.-O. (2011). Novel assays to assess the functional capacity of the classical, the alternative and the lectin pathways of the complement system. *Clin. Exp. Immunol.* *164*, 388–395.

Palmer, R.M., Ferrige, A.G., and Moncada, S. (1987). Nitric oxide release accounts for the biological activity of endothelium-derived relaxing factor. *Nature* *327*, 524–526.

Panda, A.K., Panda, M., Tripathy, R., Pattanaik, S.S., Ravindran, B., and Das, B.K. (2012). Complement receptor 1 variants confer protection from severe malaria in Odisha, India. *PLoS One* *7*, e49420.

Park, H.J., Guariento, M., Maciejewski, M., Hauhart, R., Tham, W.-H., Cowman, A.F., Schmidt, C.Q., Mertens, H.D.T., Liszewski, M.K., Hourcade, D.E., et al. (2013). Using mutagenesis and structural biology to map the binding site for the *Plasmodium falciparum* merozoite protein PfRh4 on the human immune adherence receptor. *J. Biol. Chem.*

Pascual, M., Lutz, H.U., Steiger, G., Stammli, P., and Schifferli, J.A. (1993). Release of vesicles enriched in complement receptor 1 from human erythrocytes. *J. Immunol.* *151*, 397–404.

Pascual, M., Steiger, G., Sadallah, S., Paccaud, J.P., Carpentier, J.L., James, R., and Schifferli, J.A. (1994a). Identification of membrane-bound CR1 (CD35) in human urine: evidence for its release by glomerular podocytes. *J. Exp. Med.* *179*, 889–899.

Pascual, M., Danielsson, C., Steiger, G., and Schifferli, J.A. (1994b). Proteolytic cleavage of CR1 on human erythrocytes in vivo: evidence for enhanced cleavage in AIDS. *Eur. J. Immunol.* *24*, 702–708.

Patankar, T.F., Karnad, D.R., Shetty, P.G., Desai, A.P., and Prasad, S.R. (2002). Adult cerebral malaria: prognostic importance of imaging findings and correlation with postmortem findings. *Radiology* *224*, 811–816.

Patel, S.N., Berghout, J., Lovegrove, F.E., Ayi, K., Conroy, A., Serghides, L., Min-oo, G., Gowda, D.C., Sarma, J.V., Rittirsch, D., et al. (2008). C5 deficiency and C5a or C5aR blockade protects against cerebral malaria. *J. Exp. Med.* *205*, 1133–1143.

- Pawluczkwycz, A.W., Lindorfer, M.A., Waitumbi, J.N., and Taylor, R.P. (2007). Hematin Promotes Complement Alternative Pathway-Mediated Deposition of C3 Activation Fragments on Human Erythrocytes: Potential Implications for the Pathogenesis of Anemia in Malaria. *J. Immunol.* *179*, 5543–5552.
- Payne, N.R., and Horwitz, M.A. (1987). Phagocytosis of *Legionella pneumophila* is mediated by human monocyte complement receptors. *J. Exp. Med.* *166*, 1377–1389.
- Penman, B.S., Pybus, O.G., Weatherall, D.J., and Gupta, S. (2009). Epistatic interactions between genetic disorders of hemoglobin can explain why the sickle-cell gene is uncommon in the Mediterranean. *Proc. Natl. Acad. Sci.* *106*, 21242–21246.
- Perkins, D.N., Pappin, D.J.C., Creasy, D.M., and Cottrell, J.S. (1999). Probability-based protein identification by searching sequence databases using mass spectrometry data. *ELECTROPHORESIS* *20*, 3551–3567.
- Perneger, T.V. (1998). What's wrong with Bonferroni adjustments. *BMJ* *316*, 1236–1238.
- Phanuphak, P., Hanvanich, M., Sakulramrung, R., Moollaor, P., Sitprija, V., and Phanthumkosol, D. (1985). Complement changes in falciparum malaria infection. *Clin. Exp. Immunol.* *59*, 571–576.
- Piddlesden, S.J., Jiang, S., Levin, J.L., Vincent, A., and Morgan, B.P. (1996). Soluble complement receptor 1 (sCR1) protects against experimental autoimmune myasthenia gravis. *J. Neuroimmunol.* *71*, 173–177.
- Piel, F.B., Patil, A.P., Howes, R.E., Nyangiri, O.A., Gething, P.W., Williams, T.N., Weatherall, D.J., and Hay, S.I. (2010). Global distribution of the sickle cell gene and geographical confirmation of the malaria hypothesis. *Nat. Commun.* *1*, 104.
- Planche, T., and Krishna, S. (2006). Severe malaria: metabolic complications. *Curr. Mol. Med.* *6*, 141–153.
- Pleass, R.J. (2009). When is a malaria immune complex not an immune complex? *Parasite Immunol.* *31*, 61–63.
- Pongponratn, E., Riganti, M., Punpoowong, B., and Aikawa, M. (1991). Microvascular sequestration of parasitized erythrocytes in human falciparum malaria: a pathological study. *Am. J. Trop. Med. Hyg.* *44*, 168–175.
- Pongponratn, E., Turner, G.D.H., Day, N.P.J., Phu, N.H., Simpson, J.A., Stepniewska, K., Mai, N.T.H., Viriyavejakul, P., Looareesuwan, S., Hien, T.T., et al. (2003). An ultrastructural study of the brain in fatal *Plasmodium falciparum* malaria. *Am. J. Trop. Med. Hyg.* *69*, 345–359.

- Porteu, F., Mir, A., and Halbwachs-Mecarelli, L. (1987). Modulation of neutrophil expression of C3b receptors (CR1) by soluble monomeric human C3b. *Eur. J. Immunol.* *17*, 629–635.
- Potchen, M.J., Kampondeni, S.D., Seydel, K.B., Haacke, E.M., Sinyangwe, S.S., Mwenechanya, M., Glover, S.J., Milner, D.A., Zeli, E., Hammond, C.A., et al. (2018). 1.5 Tesla Magnetic Resonance Imaging to Investigate Potential Etiologies of Brain Swelling in Pediatric Cerebral Malaria. *Am. J. Trop. Med. Hyg.* *98*, 497–504.
- Prudêncio, M., Rodriguez, A., and Mota, M.M. (2006). The silent path to thousands of merozoites: the Plasmodium liver stage. *Nat. Rev. Microbiol.* *4*, 849–856.
- Quilty, D., Chan, C.J., Yurkiw, K., Bain, A., Babolmorad, G., and Melançon, P. (2018). The Arf-GDP-regulated recruitment of GBF1 to Golgi membranes requires domains HDS1 and HDS2 and a Golgi-localized protein receptor. *J. Cell Sci.* *132*.
- R Development Core Team (2010). R: A language and environment for statistical computing. (Vienna, Austria: R Foundation for Statistical Computing), p.
- Rabinovitch, M., and DeStefano, M.J. (1975). Use of the Local Anesthetic Lidocaine for Cell Harvesting and Subcultivation. *In Vitro* *11*, 379–381.
- Radfar, A., Méndez, D., Moneriz, C., Linares, M., Marín-García, P., Puyet, A., Diez, A., and Bautista, J.M. (2009). Synchronous culture of Plasmodium falciparum at high parasitemia levels. *Nat. Protoc.* *4*, 1899–1915.
- Ramos, T.N., Darley, M.M., Hu, X., Billker, O., Rayner, J.C., Ahras, M., Wohler, J.E., and Barnum, S.R. (2011). Cutting edge: the membrane attack complex of complement is required for the development of murine experimental cerebral malaria. *J. Immunol. Baltim. Md 1950* *186*, 6657–6660.
- R&D Systems (2018). Recombinant Human CD35. Catalog Number 5748-D.
- Reese, T.S., and Karnovsky, M.J. (1967). Fine structural localization of a blood-brain barrier to exogenous peroxidase. *J. Cell Biol.* *34*, 207–217.
- Reiling, L., Richards, J.S., Fowkes, F.J.I., Wilson, D.W., Chocejindachai, W., Barry, A.E., Tham, W.-H., Stubbs, J., Langer, C., Donelson, J., et al. (2012). The Plasmodium falciparum Erythrocyte Invasion Ligand Pfrh4 as a Target of Functional and Protective Human Antibodies against Malaria. *PLOS ONE* *7*, e45253.
- Reynes, M., Aubert, J.P., Cohen, J.H., Audouin, J., Tricottet, V., Diebold, J., and Kazatchkine, M.D. (1985). Human follicular dendritic cells express CR1, CR2, and CR3 complement receptor antigens. *J. Immunol. Baltim. Md 1950* *135*, 2687–2694.

- Riley, E.M., Couper, K.N., Helmbly, H., Hafalla, J.C.R., Souza, J.B. de, Langhorne, J., Jarra, W., and Zavala, F. (2010). Neuropathogenesis of human and murine malaria. *Trends Parasitol.* *26*, 277–278.
- Roberts, D.J., Craig, A.G., Berendt, A.R., Pinches, R., Nash, G., Marsh, K., and Newbold, C.I. (1992). Rapid switching to multiple antigenic and adhesive phenotypes in malaria. *Nature* *357*, 689–692.
- Rockett, K.A., Clarke, G.M., Fitzpatrick, K., Hubbart, C., Jeffreys, A.E., Rowlands, K., Craik, R., Jallow, M., Conway, D.J., Bojang, K.A., et al. (2014). Reappraisal of known malaria resistance loci in a large multicenter study. *Nat. Genet.* *46*, 1197–1204.
- Roestenberg, M., McCall, M., Mollnes, T.E., van Deuren, M., Sprong, T., Klasen, I., Hermsen, C.C., Sauerwein, R.W., and van der Ven, A. (2007). Complement activation in experimental human malaria infection. *Trans. R. Soc. Trop. Med. Hyg.* *101*, 643–649.
- Roos, A., Bouwman, L.H., Gijlswijk-Janssen, D.J. van, Faber-Krol, M.C., Stahl, G.L., and Daha, M.R. (2001). Human IgA Activates the Complement System Via the Mannan-Binding Lectin Pathway. *J. Immunol.* *167*, 2861–2868.
- Ross, G.D., Lambris, J.D., Cain, J.A., and Newman, S.L. (1982). Generation of three different fragments of bound C3 with purified factor I or serum. I. Requirements for factor H vs CR1 cofactor activity. *J. Immunol. Baltim. Md 1950* *129*, 2051–2060.
- Roth, E.F., Raventos-Suarez, C., Rinaldi, A., and Nagel, R.L. (1983). Glucose-6-phosphate dehydrogenase deficiency inhibits in vitro growth of *Plasmodium falciparum*. *Proc. Natl. Acad. Sci. U. S. A.* *80*, 298–299.
- Rothman, K.J. (1990). No adjustments are needed for multiple comparisons. *Epidemiol. Camb. Mass* *1*, 43–46.
- Rothman, K.J. (2014). Six Persistent Research Misconceptions. *J. Gen. Intern. Med.* *29*, 1060–1064.
- Rottem, S., and Naot, Y. (1998). Subversion and exploitation of host cells by mycoplasmas. *Trends Microbiol.* *6*, 436–440.
- Roumenina, L.T., Jablonski, M., Hue, C., Blouin, J., Dimitrov, J.D., Dragon-Durey, M.-A., Cayla, M., Fridman, W.H., Macher, M.-A., Ribes, D., et al. (2009). Hyperfunctional C3 convertase leads to complement deposition on endothelial cells and contributes to atypical hemolytic uremic syndrome. *Blood* *114*, 2837–2845.
- Roumenina, L.T., Rayes, J., Frimat, M., and Fremeaux-Bacchi, V. (2016). Endothelial cells: source, barrier, and target of defensive mediators. *Immunol. Rev.* *274*, 307–329.

Rout, R., Dhangadamajhi, G., Mohapatra, B.N., Kar, S.K., and Ranjit, M. (2011). High CR1 level and related polymorphic variants are associated with cerebral malaria in eastern-India. *Infect. Genet. Evol.* *11*, 139–144.

Rowe, J.A., Obeiro, J., Newbold, C.I., and Marsh, K. (1995). *Plasmodium falciparum* rosetting is associated with malaria severity in Kenya. *Infect. Immun.* *63*, 2323–2326.

Rowe, J.A., Moulds, J.M., Newbold, C.I., and Miller, L.H. (1997). *P. falciparum* rosetting mediated by a parasite-variant erythrocyte membrane protein and complement-receptor 1. *Nature* *388*, 292–295.

Rowe, J.A., Rogerson, S.J., Raza, A., Moulds, J.M., Kazatchkine, M.D., Marsh, K., Newbold, C.I., Atkinson, J.P., and Miller, L.H. (2000). Mapping of the region of complement receptor (CR) 1 required for *Plasmodium falciparum* rosetting and demonstration of the importance of CR1 in rosetting in field isolates. *J. Immunol. Baltim. Md 1950* *165*, 6341–6346.

Rowe, J.A., Shafi, J., Kai, O.K., Marsh, K., and Raza, A. (2002a). Nonimmune IgM, but not IgG binds to the surface of *Plasmodium falciparum*-infected erythrocytes and correlates with rosetting and severe malaria. *Am. J. Trop. Med. Hyg.* *66*, 692–699.

Rowe, J.A., Raza, A., Diallo, D.A., Baby, M., Poudiougou, B., Coulibaly, D., Cockburn, I.A., Middleton, J., Lyke, K.E., Plowe, C.V., et al. (2002b). Erythrocyte CR1 expression level does not correlate with a HindIII restriction fragment length polymorphism in Africans; implications for studies on malaria susceptibility. *Genes Immun.* *3*, 497–500.

Rowe, J.A., Handel, I.G., Thera, M.A., Deans, A.-M., Lyke, K.E., Koné, A., Diallo, D.A., Raza, A., Kai, O., Marsh, K., et al. (2007). Blood group O protects against severe *Plasmodium falciparum* malaria through the mechanism of reduced rosetting. *Proc. Natl. Acad. Sci. U. S. A.* *104*, 17471–17476.

Rowe, J.A., Claessens, A., Corrigan, R.A., and Arman, M. (2009). Adhesion of *Plasmodium falciparum*-infected erythrocytes to human cells: molecular mechanisms and therapeutic implications. *Expert Rev. Mol. Med.* *11*.

Saevarsdottir, S., Vikingsdottir, T., and Valdimarsson, H. (2004). The potential role of mannan-binding lectin in the clearance of self-components including immune complexes. *Scand. J. Immunol.* *60*, 23–29.

Saevarsdottir, S., Steinsson, K., Ludviksson, B.R., Grondal, G., and Valdimarsson, H. (2007). Mannan-binding lectin may facilitate the clearance of circulating immune complexes - implications from a study on C2-deficient individuals. *Clin. Exp. Immunol.* *148*, 248–253.

- Sasi, P., Burns, S.P., Waruiru, C., English, M., Hobson, C.L., King, C.G., Mosobo, M., Beech, J.S., Iles, R.A., Boucher, B.J., et al. (2007). Metabolic Acidosis and Other Determinants of Hemoglobin-Oxygen Dissociation in Severe Childhood Plasmodium falciparum Malaria. *Am. J. Trop. Med. Hyg.* 77, 256–260.
- Scherf, A., Lopez-Rubio, J.J., and Riviere, L. (2008). Antigenic variation in Plasmodium falciparum. *Annu. Rev. Microbiol.* 62, 445–470.
- Schifferli, J.A., and Taylor, R.P. (1989). Physiological and pathological aspects of circulating immune complexes. *Kidney Int.* 35, 993–1003.
- Schifferli, J.A., Ng, Y.C., Paccaud, J.P., and Walport, M.J. (1989). The role of hypocomplementaemia and low erythrocyte complement receptor type 1 numbers in determining abnormal immune complex clearance in humans. *Clin. Exp. Immunol.* 75, 329–335.
- Schlesinger, L.S., and Horwitz, M.A. (1990). Phagocytosis of leprosy bacilli is mediated by complement receptors CR1 and CR3 on human monocytes and complement component C3 in serum. *J. Clin. Invest.* 85, 1304–1314.
- Schlesinger, L.S., Bellinger-Kawahara, C.G., Payne, N.R., and Horwitz, M.A. (1990). Phagocytosis of Mycobacterium tuberculosis is mediated by human monocyte complement receptors and complement component C3. *J. Immunol. Baltim. Md* 1950 144, 2771–2780.
- Schmidt, C.Q., Kennedy, A.T., and Tham, W.-H. (2015). More than just immune evasion: Hijacking complement by Plasmodium falciparum. *Mol. Immunol.*
- Schmidtchen, A., Holst, E., Tapper, H., and Björck, L. (2003). Elastase-producing Pseudomonas aeruginosa degrade plasma proteins and extracellular products of human skin and fibroblasts, and inhibit fibroblast growth. *Microb. Pathog.* 34, 47–55.
- Schneider, M.C., Prosser, B.E., Caesar, J.J.E., Kugelberg, E., Li, S., Zhang, Q., Quoraishi, S., Lovett, J.E., Deane, J.E., Sim, R.B., et al. (2009). Neisseria meningitidis recruits factor H using protein mimicry of host carbohydrates. *Nature* 458, 890–893.
- Schofield, L. (2007). Intravascular infiltrates and organ-specific inflammation in malaria pathogenesis. *Immunol. Cell Biol.* 85, 130–137.
- Schroeder, J.-H., McCarthy, D., Szeszak, T., Cook, D.A., Taylor, M.J., Craig, A.G., Lawson, C., and Lawrence, R.A. (2017). Brugia malayi microfilariae adhere to human vascular endothelial cells in a C3-dependent manner. *PLoS Negl. Trop. Dis.* 11, e0005592.

Scott, J.A.G., Bauni, E., Moisi, J.C., Ojal, J., Gatakaa, H., Nyundo, C., Molyneux, C.S., Kombe, F., Tsofa, B., Marsh, K., et al. (2012). Profile: The Kilifi Health and Demographic Surveillance System (KHDSS). *Int. J. Epidemiol.* *41*, 650–657.

von Seidlein, L., Olaosebikan, R., Hendriksen, I.C.E., Lee, S.J., Adedoyin, O.T., Agbenyega, T., Nguah, S.B., Bojang, K., Deen, J.L., Evans, J., et al. (2012). Predicting the Clinical Outcome of Severe Falciparum Malaria in African Children: Findings From a Large Randomized Trial. *Clin. Infect. Dis. Off. Publ. Infect. Dis. Soc. Am.* *54*, 1080–1090.

Serjeant, G.R., and Serjeant, B.E. (2001). *Sickle cell disease* (Oxford : New York: Oxford University Press).

Seydel, K.B., Milner, D.A., Kamiza, S.B., Molyneux, M.E., and Taylor, T.E. (2006). The distribution and intensity of parasite sequestration in comatose Malawian children. *J. Infect. Dis.* *194*, 208–205.

Seydel, K.B., Kampondeni, S.D., Valim, C., Potchen, M.J., Milner, D.A., Muwalo, F.W., Birbeck, G.L., Bradley, W.G., Fox, L.L., Glover, S.J., et al. (2015). Brain swelling and death in children with cerebral malaria. *N. Engl. J. Med.* *372*, 1126–1137.

Shin, J.J.H., Gillingham, A.K., Begum, F., Chadwick, J., and Munro, S. (2017). TBC1D23 is a bridging factor for endosomal vesicle capture by golgins at the trans-Golgi. *Nat. Cell Biol.* *19*, 1424–1432.

Silvestrini, F., Alano, P., and Williams, J.L. (2000). Commitment to the production of male and female gametocytes in the human malaria parasite *Plasmodium falciparum*. *Parasitology* *121 Pt 5*, 465–471.

Sinha, S., Jha, G.N., Anand, P., Qidwai, T., Pati, S.S., Mohanty, S., Mishra, S.K., Tyagi, P.K., Sharma, S.K., Venkatesh, V., et al. (2009). CR1 levels and gene polymorphisms exhibit differential association with falciparum malaria in regions of varying disease endemicity. *Hum. Immunol.* *70*, 244–250.

Slutsker, L., Taylor, T.E., Wirima, J.J., and Steketee, R.W. (1994). In-hospital morbidity and mortality due to malaria-associated severe anaemia in two areas of Malawi with different patterns of malaria infection. *Trans. R. Soc. Trop. Med. Hyg.* *88*, 548–551.

Smith, R.A. (2002). Targeting anticomplement agents. *Biochem. Soc. Trans.* *30*, 1037–1041.

Smith, J.D., Chitnis, C.E., Craig, A.G., Roberts, D.J., Hudson-Taylor, D.E., Peterson, D.S., Pinches, R., Newbold, C.I., and Miller, L.H. (1995). Switches in expression of *Plasmodium falciparum* var genes correlate with changes in antigenic and cytoadherent phenotypes of infected erythrocytes. *Cell* *82*, 101–110.

- Snow, R.W., Bastos de Azevedo, I., Lowe, B.S., Kabiru, E.W., Nevill, C.G., Mwangusye, S., Kassiga, G., Marsh, K., and Teuscher, T. (1994). Severe childhood malaria in two areas of markedly different falciparum transmission in east Africa. *Acta Trop.* *57*, 289–300.
- Snow, R.W., Omumbo, J.A., Lowe, B., Molyneux, C.S., Obiero, J.O., Palmer, A., Weber, M.W., Pinder, M., Nahlen, B., Obonyo, C., et al. (1997). Relation between severe malaria morbidity in children and level of *Plasmodium falciparum* transmission in Africa. *Lancet Lond. Engl.* *349*, 1650–1654.
- Soares, S.C., Abé-Sandes, K., Nascimento Filho, V.B., Nunes, F.M.F., and Silva, W.A. (2008). Genetic polymorphisms in TLR4, CR1 and Duffy genes are not associated with malaria resistance in patients from Baixo Amazonas region, Brazil. *Genet. Mol. Res. GMR* *7*, 1011–1019.
- Sokhna, C., Ndiath, M.O., and Rogier, C. (2013). The changes in mosquito vector behaviour and the emerging resistance to insecticides will challenge the decline of malaria. *Clin. Microbiol. Infect. Off. Publ. Eur. Soc. Clin. Microbiol. Infect. Dis.* *19*, 902–907.
- Somner, E.A., Black, J., and Pasvol, G. (2000). Multiple human serum components act as bridging molecules in rosette formation by *Plasmodium falciparum*-infected erythrocytes. *Blood* *95*, 674–682.
- Spadafora, C., Awandare, G.A., Kopydlowski, K.M., Czege, J., Moch, J.K., Finberg, R.W., Tsokos, G.C., and Stoute, J.A. (2010). Complement receptor 1 is a sialic acid-independent erythrocyte receptor of *Plasmodium falciparum*. *PLoS Pathog.* *6*, e1000968.
- Srichaikul, T., Puwasatien, P., Karnjanajetanee, J., Bokisch, V.A., and Pawasatien, P. (1975). Complement changes and disseminated intravascular coagulation in *Plasmodium falciparum* malaria. *Lancet Lond. Engl.* *1*, 770–772.
- Stevenson, L., Huda, P., Jeppesen, A., Laursen, E., Rowe, J.A., Craig, A., Streicher, W., Barfod, L., and Hviid, L. (2015a). Investigating the function of Fc-specific binding of IgM to *Plasmodium falciparum* erythrocyte membrane protein 1 mediating erythrocyte rosetting. *Cell. Microbiol.* *17*, 819–831.
- Stevenson, L., Laursen, E., Cowan, G.J., Bando, B., Barfod, L., Cavanagh, D.R., Andersen, G.R., and Hviid, L. (2015b). α 2-Macroglobulin Can Crosslink Multiple *Plasmodium falciparum* Erythrocyte Membrane Protein 1 (PfEMP1) Molecules and May Facilitate Adhesion of Parasitized Erythrocytes. *PLoS Pathog.* *11*, e1005022.
- Stoute, J.A., Odindo, A.O., Owuor, B.O., Mibei, E.K., Opollo, M.O., and Waitumbi, J.N. (2003). Loss of Red Blood Cell–Complement Regulatory Proteins and Increased

Levels of Circulating Immune Complexes Are Associated with Severe Malarial Anemia. *J. Infect. Dis.* *187*, 522–525.

Streit, W.J., Conde, J.R., Fendrick, S.E., Flanary, B.E., and Mariani, C.L. (2005). Role of microglia in the central nervous system's immune response. *Neurol. Res.* *27*, 685–691.

Sturm, A., Amino, R., van de Sand, C., Regen, T., Retzlaff, S., Rennenberg, A., Krueger, A., Pollok, J.-M., Menard, R., and Heussler, V.T. (2006). Manipulation of host hepatocytes by the malaria parasite for delivery into liver sinusoids. *Science* *313*, 1287–1290.

Su, X.Z., Heatwole, V.M., Wertheimer, S.P., Guinet, F., Herrfeldt, J.A., Peterson, D.S., Ravetch, J.A., and Wellems, T.E. (1995). The large diverse gene family var encodes proteins involved in cytoadherence and antigenic variation of *Plasmodium falciparum*-infected erythrocytes. *Cell* *82*, 89–100.

Sugita, Y., Nakano, Y., and Tomita, M. (1986). Solubilization of Active Complement Receptor Type 1 (CR1) from Human Erythrocyte Stroma with Trypsin and Its Purification. *J. Biochem. (Tokyo)* *100*, 1193–1200.

Suwanarusk, R., Cooke, B.M., Dondorp, A.M., Silamut, K., Sattabongkot, J., White, N.J., and Udomsangpetch, R. (2004). The deformability of red blood cells parasitized by *Plasmodium falciparum* and *P. vivax*. *J. Infect. Dis.* *189*, 190–194.

Swann, O.V., Harrison, E.M., Opi, D.H., Nyatichi, E., Macharia, A., Uyoga, S., Williams, T.N., and Rowe, J.A. (2017). No Evidence that Knops Blood Group Polymorphisms Affect Complement Receptor 1 Clustering on Erythrocytes. *Sci. Rep.* *7*, 17825.

Takahashi, K., and Ezekowitz, R.A.B. (2005). The Role of the Mannose-Binding Lectin in Innate Immunity. *Clin. Infect. Dis.* *41*, S440–S444.

Tas, S.W., Klickstein, L.B., Barbashov, S.F., and Nicholson-Weller, A. (1999). C1q and C4b bind simultaneously to CR1 and additively support erythrocyte adhesion. *J. Immunol. Baltim. Md 1950* *163*, 5056–5063.

Taylor, R.P., Kujala, G., Wilson, K., Wright, E., and Harbin, A. (1985). In vivo and in vitro studies of the binding of antibody/dsDNA immune complexes to rabbit and guinea pig platelets. *J. Immunol. Baltim. Md 1950* *134*, 2550–2558.

Taylor, R.P., Pocanic, F., Reist, C., and Wright, E.L. (1991). Complement-opsonized IgG antibody/dsDNA immune complexes bind to CR1 clusters on isolated human erythrocytes. *Clin. Immunol. Immunopathol.* *61*, 143–160.

Taylor, S.M., Parobek, C.M., and Fairhurst, R.M. (2012). Haemoglobinopathies and the clinical epidemiology of malaria: a systematic review and meta-analysis. *Lancet Infect. Dis.* *12*, 457–468.

Taylor, T.E., Fu, W.J., Carr, R.A., Whitten, R.O., Mueller, J.S., Fosiko, N.G., Lewallen, S., Liomba, N.G., Molyneux, M.E., and Mueller, J.G. (2004). Differentiating the pathologies of cerebral malaria by postmortem parasite counts. *Nat. Med.* *10*, 143–145.

Tedder, T.F., Fearon, D.T., Gartland, G.L., and Cooper, M.D. (1983). Expression of C3b receptors on human be cells and myelomonocytic cells but not natural killer cells. *J. Immunol. Baltim. Md 1950* *130*, 1668–1673.

Teeranaipong, P., Ohashi, J., Patarapotikul, J., Kimura, R., Nuchnoi, P., Hananantachai, H., Naka, I., Putaporntip, C., Jongwutiwes, S., and Tokunaga, K. (2008). A functional single-nucleotide polymorphism in the CR1 promoter region contributes to protection against cerebral malaria. *J. Infect. Dis.* *198*, 1880–1891.

Tetteh-Quarcoo, P.B. (2011). Investigations into polymorphisms within complement receptor type 1 (CD35) thought to protect against severe malaria. (Edinburgh, UK: University of Edinburgh).

Tetteh-Quarcoo, P.B., Schmidt, C.Q., Tham, W.-H., Hauhart, R., Mertens, H.D.T., Rowe, A., Atkinson, J.P., Cowman, A.F., Rowe, J.A., and Barlow, P.N. (2012). Lack of Evidence from Studies of Soluble Protein Fragments that Knops Blood Group Polymorphisms in Complement Receptor-Type 1 Are Driven by Malaria. *PLoS ONE* *7*, e34820.

Tettey, R., Ayeh-Kumi, P., Tettey, P., Adjei, G.O., Asmah, R.H., and Dodoo, D. (2015). Severity of malaria in relation to a complement receptor 1 polymorphism: a case-control study. *Pathog. Glob. Health* *109*, 247–252.

Tham, W.-H., Wilson, D.W., Lopaticki, S., Schmidt, C.Q., Tetteh-Quarcoo, P.B., Barlow, P.N., Richard, D., Corbin, J.E., Beeson, J.G., and Cowman, A.F. (2010). Complement receptor 1 is the host erythrocyte receptor for *Plasmodium falciparum* PfRh4 invasion ligand. *Proc. Natl. Acad. Sci. U. S. A.* *107*, 17327–17332.

Tham, W.-H., Schmidt, C.Q., Hauhart, R.E., Guariento, M., Tetteh-Quarcoo, P.B., Lopaticki, S., Atkinson, J.P., Barlow, P.N., and Cowman, A.F. (2011). *Plasmodium falciparum* uses a key functional site in complement receptor type-1 for invasion of human erythrocytes. *Blood* *118*, 1923–1933.

Thathy, V., Moulds, J., Guyah, B., Otieno, W., and Stoute, J. (2005). Complement receptor 1 polymorphisms associated with resistance to severe malaria in Kenya. *Malar. J.* *4*, 54.

Thomson, J.G. (1918). Preliminary Note on the Complement Deviation in Cases of Malaria: A New Aid to Diagnosis. *Br. Med. J.* 2, 628–629.

Thurman, J.M., Kulik, L., Orth, H., Wong, M., Renner, B., Sargsyan, S.A., Mitchell, L.M., Hourcade, D.E., Hannan, J.P., Kovacs, J.M., et al. (2013). Detection of complement activation using monoclonal antibodies against C3d. *J. Clin. Invest.* 123, 2218–2230.

Tilling, T., Engelbertz, C., Decker, S., Korte, D., Hüwel, S., and Galla, H.-J. (2002). Expression and adhesive properties of basement membrane proteins in cerebral capillary endothelial cell cultures. *Cell Tissue Res.* 310, 19–29.

Timmann, C., Thye, T., Vens, M., Evans, J., May, J., Ehmen, C., Sievertsen, J., Muntau, B., Ruge, G., Loag, W., et al. (2012). Genome-wide association study indicates two novel resistance loci for severe malaria. *Nature* 489, 443–446.

Toure, O., Konate, S., Sissoko, S., Niangaly, A., Barry, A., Sall, A.H., Diarra, E., Poudiougou, B., Sepulveda, N., Campino, S., et al. (2012). Candidate Polymorphisms and Severe Malaria in a Malian Population. *PLoS ONE* 7, e43987.

Tournamille, C., Colin, Y., Cartron, J.P., and Le Van Kim, C. (1995). Disruption of a GATA motif in the Duffy gene promoter abolishes erythroid gene expression in Duffy-negative individuals. *Nat. Genet.* 10, 224–228.

Treutiger, C.J., Hedlund, I., Helmbj, H., Carlson, J., Jepson, A., Twumasi, P., Kwiatkowski, D., Greenwood, B.M., and Wahlgren, M. (1992). Rosette formation in *Plasmodium falciparum* isolates and anti-rosette activity of sera from Gambians with cerebral or uncomplicated malaria. *Am. J. Trop. Med. Hyg.* 46, 503–510.

Tsuji, S., Kaji, K., and Nagasawa, S. (1994). Activation of the alternative pathway of human complement by apoptotic human umbilical vein endothelial cells. *J. Biochem. (Tokyo)* 116, 794–800.

Turner, G.D., Morrison, H., Jones, M., Davis, T.M., Looareesuwan, S., Buley, I.D., Gatter, K.C., Newbold, C.I., Pukritayakamee, S., and Nagachinta, B. (1994). An immunohistochemical study of the pathology of fatal malaria. Evidence for widespread endothelial activation and a potential role for intercellular adhesion molecule-1 in cerebral sequestration. *Am. J. Pathol.* 145, 1057–1069.

Turner, L., Lavstsen, T., Berger, S.S., Wang, C.W., Petersen, J.E.V., Avril, M., Brazier, A.J., Freeth, J., Jespersen, J.S., Nielsen, M.A., et al. (2013). Severe malaria is associated with parasite binding to endothelial protein C receptor. *Nature* 498, 502–505.

Udeinya, I.J., Schmidt, J.A., Aikawa, M., Miller, L.H., and Green, I. (1981). *Falciparum* malaria-infected erythrocytes specifically bind to cultured human endothelial cells. *Science* 213, 555–557.

Udomsangpetch, R., Wåhlin, B., Carlson, J., Berzins, K., Torii, M., Aikawa, M., Perlmann, P., and Wahlgren, M. (1989). Plasmodium falciparum-infected erythrocytes form spontaneous erythrocyte rosettes. *J. Exp. Med.* *169*, 1835–1840.

Udomsangpetch, R., Todd, J., Carlson, J., and Greenwood, B.M. (1993). The effects of hemoglobin genotype and ABO blood group on the formation of rosettes by Plasmodium falciparum-infected red blood cells. *Am. J. Trop. Med. Hyg.* *48*, 149–153.

Urich, E., Lazic, S.E., Molnos, J., Wells, I., and Freskgård, P.-O. (2012). Transcriptional Profiling of Human Brain Endothelial Cells Reveals Key Properties Crucial for Predictive In Vitro Blood-Brain Barrier Models. *PLoS ONE* *7*, e38149.

Uyoga, S., Ndila, C.M., Macharia, A.W., Nyutu, G., Shah, S., Peshu, N., Clarke, G.M., Kwiatkowski, D.P., Rockett, K.A., Williams, T.N., et al. (2015). Glucose-6-phosphate dehydrogenase deficiency and the risk of malaria and other diseases in children in Kenya: a case-control and a cohort study. *Lancet Haematol.* *2*, e437-444.

Van Dyne, S., Holers, V.M., Lublin, D.M., and Atkinson, J.P. (1987). The polymorphism of the C3b/C4b receptor in the normal population and in patients with systemic lupus erythematosus. *Clin. Exp. Immunol.* *68*, 570–579.

Vastag, M., Skopál, J., Kramer, J., Kolev, K., Vokó, Z., Csonka, É., Machovich, R., and Nagy, Z. (1998). Endothelial Cells Cultured from Human Brain Microvessels Produce Complement Proteins Factor H, Factor B, C1 Inhibitor, and C4. *Immunobiology* *199*, 5–13.

Vedeler, C., Ulvestad, E., Bjørge, L., Conti, G., Williams, K., Mørk, S., and Matre, R. (1994). The expression of CD59 in normal human nervous tissue. *Immunology* *82*, 542–547.

Veldhuisen, B., Ligthart, P.C., Vidarsson, G., Roels, I., Folman, C.C., van der Schoot, C.E., and de Haas, M. (2011). Molecular analysis of the York antigen of the Knops blood group system. *Transfusion (Paris)* *51*, 1389–1396.

Vik, D.P., and Wong, W.W. (1993). Structure of the gene for the F allele of complement receptor type 1 and sequence of the coding region unique to the S allele. *J. Immunol. Baltim. Md* *151*, 6214–6224.

Visser, L., de Vos, A.F., Hamann, J., Melief, M.-J., van Meurs, M., van Lier, R.A.W., Laman, J.D., and Hintzen, R.Q. (2002). Expression of the EGF-TM7 receptor CD97 and its ligand CD55 (DAF) in multiple sclerosis. *J. Neuroimmunol.* *132*, 156–163.

Vorup-Jensen, T., Petersen, S.V., Hansen, A.G., Poulsen, K., Schwaeble, W., Sim, R.B., Reid, K.B., Davis, S.J., Thiel, S., and Jensenius, J.C. (2000). Distinct pathways of mannan-binding lectin (MBL)- and C1-complex autoactivation revealed by

reconstitution of MBL with recombinant MBL-associated serine protease-2. *J. Immunol. Baltim. Md* 1950 *165*, 2093–2100.

Voyta, J.C., Via, D.P., Butterfield, C.E., and Zetter, B.R. (1984). Identification and isolation of endothelial cells based on their increased uptake of acetylated-low density lipoprotein. *J. Cell Biol.* *99*, 2034–2040.

Wahlgren, M., Goel, S., and Akhouri, R.R. (2017). Variant surface antigens of *Plasmodium falciparum* and their roles in severe malaria. *Nat. Rev. Microbiol.* *15*, 479–491.

Waitumbi, J.N., Opollo, M.O., Muga, R.O., Misore, A.O., and Stoute, J.A. (2000). Red cell surface changes and erythrophagocytosis in children with severe plasmodium falciparum anemia. *Blood* *95*, 1481–1486.

Waitumbi, J.N., Donvito, B., Kisserli, A., Cohen, J.H.M., and Stoute, J.A. (2004). Age-related changes in red blood cell complement regulatory proteins and susceptibility to severe malaria. *J. Infect. Dis.* *190*, 1183–1191.

Walker, O., Salako, L.A., Sowunmi, A., Thomas, J.O., Sodeine, O., and Bondi, F.S. (1992). Prognostic risk factors and post mortem findings in cerebral malaria in children. *Trans. R. Soc. Trop. Med. Hyg.* *86*, 491–493.

Waller, D., Krishna, S., Crawley, J., Miller, K., Nosten, F., Chapman, D., ter Kuile, F.O., Craddock, C., Berry, C., and Holloway, P.A. (1995). Clinical features and outcome of severe malaria in Gambian children. *Clin. Infect. Dis. Off. Publ. Infect. Dis. Soc. Am.* *21*, 577–587.

Wambua, S., Mwangi, T.W., Kortok, M., Uyoga, S.M., Macharia, A.W., Mwacharo, J.K., Weatherall, D.J., Snow, R.W., Marsh, K., and Williams, T.N. (2006). The Effect of α -Thalassaemia on the Incidence of Malaria and Other Diseases in Children Living on the Coast of Kenya. *PLoS Med.* *3*.

Warimwe, G.M., Fegan, G., Musyoki, J.N., Newton, C.R.J.C., Opiyo, M., Githinji, G., Andisi, C., Menza, F., Kitsao, B., Marsh, K., et al. (2012). Prognostic Indicators of Life-Threatening Malaria Are Associated with Distinct Parasite Variant Antigen Profiles. *Sci. Transl. Med.* *4*, 129ra45-129ra45.

Warrell, D.A., Looareesuwan, S., Phillips, R.E., White, N.J., Warrell, M.J., Chapel, H.M., Areekul, S., and Tharavanij, S. (1986). Function of the Blood-Cerebrospinal Fluid Barrier in Human Cerebral Malaria: Rejection of the Permeability Hypothesis. *Am. J. Trop. Med. Hyg.* *35*, 882–889.

Warren, H.B., Pantazis, P., and Davies, P.F. (1987). The third component of complement is transcribed and secreted by cultured human endothelial cells. *Am. J. Pathol.* *129*, 9–13.

- Wassmer, S.C., Lépolard, C., Traoré, B., Pouvelle, B., Gysin, J., and Grau, G.E. (2004). Platelets reorient Plasmodium falciparum-infected erythrocyte cytoadhesion to activated endothelial cells. *J. Infect. Dis.* *189*, 180–189.
- Wassmer, S.C., Cianciolo, G.J., Combes, V., and Grau, G.E. (2005). Inhibition of endothelial activation: a new way to treat cerebral malaria? *PLoS Med.* *2*, e245.
- Wassmer, S.C., Combes, V., Candal, F.J., Juhan-Vague, I., and Grau, G.E. (2006). Platelets Potentiate Brain Endothelial Alterations Induced by Plasmodium falciparum. *Infect. Immun.* *74*, 645–653.
- Wassmer, S.C., Taylor, T., Maclennan, C.A., Kanjala, M., Mukaka, M., Molyneux, M.E., and Grau, G.E. (2008). Platelet-induced clumping of Plasmodium falciparum-infected erythrocytes from Malawian patients with cerebral malaria-possible modulation in vivo by thrombocytopenia. *J. Infect. Dis.* *197*, 72–78.
- Wassmer, S.C., Moxon, C.A., Taylor, T., Grau, G.E., Molyneux, M.E., and Craig, A.G. (2011). Vascular endothelial cells cultured from patients with cerebral or uncomplicated malaria exhibit differential reactivity to TNF. *Cell. Microbiol.* *13*, 198–209.
- Waterfall, C.M., and Cobb, B.D. (2001). Single tube genotyping of sickle cell anaemia using PCR-based SNP analysis. *Nucleic Acids Res.* *29*, E119.
- Weatherall, D.J., and Clegg, J.B. (2001). Inherited haemoglobin disorders: an increasing global health problem. *Bull. World Health Organ.* *79*, 704–712.
- Weber, M.W., Zimmermann, U., van Hensbroek, M.B., Frenkel, J., Palmer, A., Ehrich, J.H., and Greenwood, B.M. (1999). Renal involvement in Gambian children with cerebral or mild malaria. *Trop. Med. Int. Health TM IH* *4*, 390–394.
- Weis, J.J., Tedder, T.F., and Fearon, D.T. (1984). Identification of a 145,000 Mr membrane protein as the C3d receptor (CR2) of human B lymphocytes. *Proc. Natl. Acad. Sci. U. S. A.* *81*, 881–885.
- Weksler, B., Romero, I.A., and Couraud, P.-O. (2013). The hCMEC/D3 cell line as a model of the human blood brain barrier. *Fluids Barriers CNS* *10*, 16.
- Wellems, T.E., and Fairhurst, R.M. (2005). Malaria-protective traits at odds in Africa? *Nat. Genet.* *37*, 1160–1162.
- Wenisch, C., Spitzauer, S., Florris-Linau, K., Rumpold, H., Vannaphan, S., Parschalk, B., Graninger, W., and Loareesuwan, S. (1997). Complement activation in severe Plasmodium falciparum malaria. *Clin. Immunol. Immunopathol.* *85*, 166–171.
- White, N.J. (1987). Clinical and pathological aspects of severe malaria. *Acta Leiden.* *56*, 27–46.

- White, N.J., Pukrittayakamee, S., Hien, T.T., Faiz, M.A., Mokuolu, O.A., and Dondorp, A.M. (2014). Malaria. *Lancet Lond. Engl.* *383*, 723–735.
- WHO (2014). Severe Malaria. *Trop. Med. Int. Health* *19*, 7–131.
- WHO (2017). World Malaria Report 2017 - World Health Organization (WHO).
- Wickham, H. (2009). *Ggplot2: elegant graphics for data analysis* (New York: Springer).
- Wickham, H. (2011). The Split-Apply-Combine Strategy for Data Analysis. *J. Stat. Softw.* *40*.
- Wiegner, R., Chakraborty, S., and Huber-Lang, M. (2016). Complement-coagulation crosstalk on cellular and artificial surfaces. *Immunobiology* *221*, 1073–1079.
- Williams, T.N. (2006). Human red blood cell polymorphisms and malaria. *Curr. Opin. Microbiol.* *9*, 388–394.
- Williams, T.N., Maitland, K., Bennett, S., Ganczakowski, M., Peto, T.E., Newbold, C.I., Bowden, D.K., Weatherall, D.J., and Clegg, J.B. (1996). High incidence of malaria in alpha-thalassaemic children. *Nature* *383*, 522–525.
- Williams, T.N., Mwangi, T.W., Wambua, S., Alexander, N.D., Kortok, M., Snow, R.W., and Marsh, K. (2005a). Sickle cell trait and the risk of *Plasmodium falciparum* malaria and other childhood diseases. *J. Infect. Dis.* *192*, 178–186.
- Williams, T.N., Wambua, S., Uyoga, S., Macharia, A., Mwacharo, J.K., Newton, C.R.J.C., and Maitland, K. (2005b). Both heterozygous and homozygous α + thalassaemias protect against severe and fatal *Plasmodium falciparum* malaria on the coast of Kenya. *Blood* *106*, 368–371.
- Williams, T.N., Mwangi, T.W., Wambua, S., Peto, T.E.A., Weatherall, D.J., Gupta, S., Recker, M., Penman, B.S., Uyoga, S., Macharia, A., et al. (2005c). Negative epistasis between the malaria-protective effects of alpha+-thalassemia and the sickle cell trait. *Nat. Genet.* *37*, 1253–1257.
- Williams, T.N., Uyoga, S., Macharia, A., Ndila, C., McAuley, C.F., Opi, D.H., Mwarumba, S., Makani, J., Komba, A., Ndiritu, M.N., et al. (2009). Bacteraemia in Kenyan children with sickle-cell anaemia: a retrospective cohort and case-control study. *Lancet Lond. Engl.* *374*, 1364–1370.
- Wilson, J.G., Murphy, E.E., Wong, W.W., Klickstein, L.B., Weis, J.H., and Fearon, D.T. (1986). Identification of a restriction fragment length polymorphism by a CR1 cDNA that correlates with the number of CR1 on erythrocytes. *J. Exp. Med.* *164*, 50–59.

Winkler, E.A., Bell, R.D., and Zlokovic, B.V. (2011). Central nervous system pericytes in health and disease. *Nat. Neurosci.* *14*, 1398–1405.

Wong, W.W. (1990). Structural and Functional Correlation of the Human Complement Receptor Type 1. *J. Invest. Dermatol.* *94*, 64s-67s.

Wong, W.W., and Farrell, S.A. (1991). Proposed structure of the F' allotype of human CR1. Loss of a C3b binding site may be associated with altered function. *J. Immunol. Baltim. Md 1950* *146*, 656–662.

Wong, W.W., Wilson, J.G., and Fearon, D.T. (1983). Genetic regulation of a structural polymorphism of human C3b receptor. *J. Clin. Invest.* *72*, 685–693.

Wong, W.W., Kennedy, C.A., Bonaccio, E.T., Wilson, J.G., Klickstein, L.B., Weis, J.H., and Fearon, D.T. (1986). Analysis of multiple restriction fragment length polymorphisms of the gene for the human complement receptor type I. Duplication of genomic sequences occurs in association with a high molecular mass receptor allotype. *J. Exp. Med.* *164*, 1531–1546.

Wong, W.W., Cahill, J.M., Rosen, M.D., Kennedy, C.A., Bonaccio, E.T., Morris, M.J., Wilson, J.G., Klickstein, L.B., and Fearon, D.T. (1989). Structure of the human CR1 gene. Molecular basis of the structural and quantitative polymorphisms and identification of a new CR1-like allele. *J. Exp. Med.* *169*, 847–863.

World Health Organization, and Global Malaria Programme (2015). Guidelines for the treatment of malaria.

Xiang, L., Rundles, J.R., Hamilton, D.R., and Wilson, J.G. (1999). Quantitative Alleles of CR1: Coding Sequence Analysis and Comparison of Haplotypes in Two Ethnic Groups. *J. Immunol.* *163*, 4939–4945.

Yin, W., Ghebrehiwet, B., Weksler, B., and Peerschke, E.I.B. (2008). Regulated complement deposition on the surface of human endothelial cells: effect of tobacco smoke and shear stress. *Thromb. Res.* *122*, 221–228.

Yoon, J.H., Oh, S., Shin, S., Park, J.S., Roh, E.Y., Song, E.Y., Park, M.H., Han, K.S., and Chang, J.Y. (2013). The polymorphism of Knops blood group system in Korean population and their relationship with HLA system. *Hum. Immunol.* *74*, 196–198.

Zimmerman, P.A., Fitness, J., Moulds, J.M., McNamara, D.T., Kasehagen, L.J., Rowe, J.A., and Hill, A.V.S. (2003). CR1 Knops blood group alleles are not associated with severe malaria in the Gambia. *Genes Immun.* *4*, 368–373.

8 Appendices

8.1 Mass spectrometry data

Mass spectrometry data for HBEC-5i lysate gel slices can be accessed here:

<https://bsrcmascot.st-andrews.ac.uk/mascot/>

User: Olivia_Swann

Password: swann

Then “Home” → “Search Log” under the heading “Mascot Utilities”.

With reference to Figure 4-18

Human matched proteins (matched against NCBIprot database)

Job # 14467 = Band A (upper HBEC-5i lysate gel band)

Job # 14468 = Band B (middle HBEC-5i lysate gel band)

Job # 14470 = Band C (lower HBEC-5i lysate gel band)

Job # 14483 = Band D (CR1-CHO lysate gel band)

Restricted matching (matched against small internal database including CR1)

Job # 14554 = Band A (upper HBEC-5i lysate gel band)

Job # 14555 = Band B (middle HBEC-5i lysate gel band)

Job # 14556 = Band C (lower HBEC-5i lysate gel band)

Job # 14553 = Band D (CR1-CHO lysate gel band)

8.2 University of Edinburgh regulations: Including Publications in Postgraduate Research Theses

Including Publications in Postgraduate Research Theses



Purpose of Guidance

To provide guidance on including publications within a thesis for students matriculated on a programme of doctoral study. It supports the Postgraduate Assessment Regulations for Research Degrees. This guidance does not relate to the PhD by Research Publications. There is no requirement in the assessment regulations for publications to be included in PhD thesis and this guidance is aimed at student who wish to include publications as a part of their thesis.

Scope: Guidance is not Mandatory

Doctoral students (except those matriculated for PhD by Research Publications), postgraduate research supervisors and professional support staff involved in doctoral thesis submission.

Contact Officer Academic Policy Officer

Document control

Dates	Approved: 23.04.2015	Starts: 15.09.2015	Equality impact assessment: 10.06.2015	Amendments:	Next Review: 2015/2016
Approving authority	Curriculum and Student Progression Committee				
Consultation undertaken	Colleges via Task Group of Researcher Experience Committee				
Section responsible for guidance maintenance & review	Academic Services				
Related policies, procedures, guidelines & regulations	Postgraduate Assessment Regulations for Research Degrees Postgraduate Degree Regulations (www.drps.ed.ac.uk) Guidance on Signed Declaration in Thesis				
UK Quality Code	UK Quality Code Chapter B11 Research Degrees				
Guidance superseded by this guidance	None				
Alternative format	If you require this document in an alternative format please email Academic.Services@ed.ac.uk or telephone 0131 650 2138.				
Keywords	PhD thesis, publications in PhD, publications in thesis, journal articles in thesis, journal articles in PhD thesis				

Including Publications in Postgraduate Research Theses




THE UNIVERSITY
of EDINBURGH

- 1.1 It is acknowledged that publishing journal articles is increasingly important for PhD students, particularly for career development in some disciplines. The tension between the need to write a traditional monograph thesis in addition to publishing journal articles is recognised.
- 1.2 This guidance relates to students matriculated on a programme of doctoral study, producing a traditional thesis with publications included. It should not be confused with the PhD by Research Publications award for which there are separate regulations and guidance.
- 1.3 All PhD theses must form a coherent body of interrelated work that shows ability for critical analysis. The importance of the expectation of coherence for PhD theses including publications is emphasised and the inclusion of publications must present a similar body of work to that expected in a monograph style thesis. Where publications are to be included they should include an introduction and conclusion, in effect forming a thesis chapter and placing the publication within the structure of the thesis. Assessment of the standard of the thesis will remain with the examiners thus ensuring that discipline specific standards are met. PhD theses containing publications are subject to the University's degree and assessment regulations.
- 1.4 Published journal articles cannot be expected to be subject to correction. However, corrections indicated by the thesis examiners can be dealt with in the introduction or conclusion of the chapter containing the publication.
- 1.5 Articles included in the thesis which have been submitted for publication but which have not been published, or which are in proof, will be included in a format comparable to monograph thesis content. The complete body of work submitted, including published articles should be equivalent to that expected of a monograph thesis and adhere to similar word lengths, as laid out within University regulations and local discipline specific guidance.
- 1.6 It should be emphasised that whilst peer reviewing of publications is a good measure of progress, it does not guarantee success at examination.
- 1.7 Responsibility for the quality of the submitted thesis lies with the student and the assessment of the standard of the submitted thesis rests with the examiners. Examiners will assess the standard and appropriateness of papers and publications included within a thesis.
- 1.8 Articles may not be included in the thesis for which students do not retain copyright. As students are responsible for the quality of the submitted thesis, it is therefore also the student's responsibility to ensure that the thesis complies with copyright law and advice should be sought in relation to copyright implications. Supervisors
- 1.9 The signed declaration in the thesis must include a statement that any included publications are the student's own work, except where indicated throughout the thesis and summarised and clearly identified on the declarations page of the thesis.
- 1.10 The inclusion of journal articles is also permissible for other postgraduate research degrees which are exit routes for the PhD, for example MPhil and MSc by Research.

15 May 2015

8.3 Open Access Licence for Chapter 2



ABOUT COMMUNITY [SUBMIT MY RESEARCH](#) [LOG IN/REGISTER](#)

HOME MAGAZINE INNOVATION

EPIDEMIOLOGY AND GLOBAL HEALTH, MICROBIOLOGY AND INFECTIOUS DISEASE

Two complement receptor one alleles have opposing associations with cerebral malaria and interact with α^+ thalassaemia

[f](#) [t](#) [e](#) [v](#)

D Herbert Opi, Olivia Swann [✉], Alexander Macharia, Sophie Uyoga, Gavin Band, Carolyne M Ndila, Ewen M Harrison, Mahamadou A Thera, Abdoulaye K Kone [see all »](#)

Kenya Medical Research Institute-Wellcome Trust Research Programme, Kenya; University of Edinburgh, United Kingdom; University of Oxford, United Kingdom; Usher Institute of Population Health Sciences and Informatics, University of Edinburgh, United Kingdom; University of Bamako, Mali; University of Maryland School of Medicine, United States; Lifeshare Blood Centers, United States; Imperial College, United Kingdom; Wellcome Trust Sanger Institute, United Kingdom

RESEARCH ARTICLE Apr 25, 2018

CITED 0 VIEWS 700 ANNOTATIONS [4](#) CITE AS: eLife 2018;7:e31579 DOI: 10.7554/eLife.31579

Welcome and Consent to Terms

eLife Sciences Publications, Ltd. ("eLife") is a 501(c)(3) nonprofit initiative for the very best in science and science communication. In furtherance of our mission, eLife operates websites, including the websites at elifesciences.org, submit.elifesciences.org, payments.elifesciences.org and other eLife websites (the "eLife Sites"). We offer use of the eLife journal content free of charge to the public through the eLife Sites. Access to and use of the eLife Sites is provided by eLife subject to the following Terms and Conditions, which are a contract between eLife and you. Use of the eLife Sites constitutes your acceptance of these Terms and Conditions. If you do not accept these Terms and Conditions in full, you do not have permission to access and use the eLife Sites and should cease doing so immediately.

Ownership

The eLife Sites, the software ("eLife Software"), application programming interfaces ("eLife APIs"), content and trademarks used on or in connection with the eLife Sites are owned by eLife or its licensors, and are subject to US and international intellectual property rights and laws. Nothing contained herein shall be construed as conferring by implication, or otherwise any license or right under any trademark, copyright or patent of eLife or any other third party and all rights are reserved, except as explicitly stated in these Terms and Conditions.

License to Use Journal Articles and Related Content

Unless otherwise indicated, the articles and journal content published by eLife on the eLife Sites are licensed under a [Creative Commons Attribution license](#) (also known as a CC-BY license). This means that you are free to use, reproduce and distribute the articles and related content (unless otherwise noted), for commercial and noncommercial purposes, subject to citation of the original source in accordance with the CC-BY license.

8.4 Open Access Licence for Chapter 3

nature.com

Licence to publish

Manuscript id:	SREP-17-09869A
Proposed title:	No Evidence that Knops Blood Group Polymorphisms Affect Complement Receptor 1 Clustering on Erythrocytes
The "Author(s)":	Olivia Swann, Ewen Harrison, D. Herbert Opi, Emily Nyatichi, Alex Macharia, Sophie Uyoga, Tom Williams, J. Alexandra Rowe
The "Article":	All content of the article, with the Proposed title listed above, including but not limited to all text, supplementary information, tables, graphs and images.
The "Journal":	Scientific Reports

Purpose

NPG will consider publishing the Contribution pursuant to the terms set forth herein, including granting readers rights to use the Contribution on an open access basis identified below.

Open access licence

CC BY*: This licence allows readers to copy, distribute and transmit the Contribution as long as it is attributed back to the author. Readers are permitted to alter, transform or build upon the Contribution, and to use the article for commercial purposes. Please read the full licence for further details at - <http://creativecommons.org/licenses/by/4.0>.

* The Creative Commons Attribution (CC BY) Licence is preferred by many research funding bodies. We support use of this licence as it is recommended for maximum dissemination and use of open access materials.

8.5 Publications arising from this thesis

Swann, O. V., E. M. Harrison, D. H. Opi, E. Nyatichi, A. Macharia, S. Uyoga, T. N. Williams, and J. A. Rowe. 2017.

No Evidence That Knops Blood Group Polymorphisms Affect Complement Receptor 1 Clustering on Erythrocytes.

Scientific Reports 7 (1): 17825. <https://doi.org/10.1038/s41598-017-17664-9>.

D Herbert Opi§, **Swann O§**, Band G, Ndila C, Thera AT, Kone A, Diallo DA, Doumbo OK, Raza A, Williams TN and Rowe JA. (§ Denotes joint first author)

Complement receptor one (CR1) Knops blood group polymorphisms are associated with contrasting effects on susceptibility to severe malaria and other common childhood diseases.

Elife. 2018 Apr 25;7. pii: e31579. <https://www.elifesciences.org/articles/31579>

8.6 Presentations arising from this thesis

Oral Presentations

International Presentations

2017 **Swann O**, D Herbert Opi, Band G, Ndila C, Thera AT, Kone A, Diallo DA, Doumbo OK, Raza A, Williams TN and Rowe JA.

Complement receptor one (CR1) Knops blood group polymorphisms are associated with contrasting effects on susceptibility to severe malaria and other common childhood diseases.

Gordon Research Seminar on Malaria. Les Diablerets, Switzerland.

2014 **Swann O**, Williams TN, Rowe JA.

No evidence that Knops blood group polymorphisms affect complement receptor 1 (CR1) clustering on erythrocytes.

British Society of Parasitology Spring Meeting. Cambridge.

2013 **Swann. O.**

Clustering of complement receptor one (CR1) on erythrocytes.

Kenya Medical Research Institute (KEMRI) – Wellcome Trust Research Unit Immunology Group Meeting. Kilifi, Kenya.

Local Presentations

- 2014 **Swann O.**
Cerebral malaria and complement receptor 1.
Invited to present to Prof Jeremy Farrar, Director of the Wellcome Trust, during his visit to Edinburgh.
- 2014 **Swann O.**
Cerebral malaria & complement receptor 1.
ECATRIP (Edinburgh Clinical Academic Training Research in Progress Meeting, Edinburgh

Poster Presentations

International

- 2017 **Swann O**, D Herbert Opi, Band G, Ndila C, Thera AT, Kone A, Diallo DA, Doumbo OK, Raza A, Williams TN and Rowe JA.
Neighbouring polymorphisms in Complement Receptor 1 have opposing associations with cerebral malaria in two discrete African case-control studies
Gordon Research Conference on Malaria. Les Diablerets, Switzerland.
- 2017 **Swann O**, Constantinou A, D Herbert Opi, Band G, Ndila C, Thera AT, Kone A, Diallo DA, Doumbo OK, Raza A, Williams TN and Rowe JA.
Complement receptor 1 polymorphism is associated with cerebral malaria, but no evidence that human brain endothelial cells express the molecule.
European Meeting on Complement in Human Disease. Copenhagen, Denmark.
- 2013 **Swann O**, Opi DH, Nyatichi E, Tendwa M, Macharia A, Uyoga S, Williams TN and Rowe JA.
Do polymorphisms in complement receptor 1 affect how it clusters on red blood cells?
Gordon Research Conference on Malaria. Tuscany, Italy.

8.7 Grants arising from this thesis

2016 **Vacation Scholarship for Mr Alexandros Constaninou (£2000)** – Medical Research Scotland (for work outlined in Chapter 4).

8.8 Public engagement projects arising from this thesis

2017 **Meet the Researcher Day for sixth form students.** Presentation of work funded by Medical Research Scotland at the Science Centre, Glasgow.

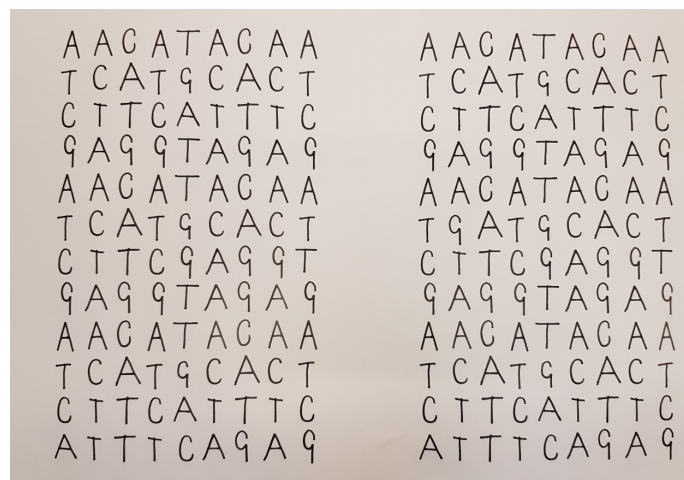
2018 **Edinburgh International Science Festival.** Designing, producing and running an exhibit about rosetting and sequestration in severe malaria for primary and secondary school students. Plush toy erythrocytes and Velcro were used to explain the process. This project was carried out together with colleagues from the Edinburgh College of Art.



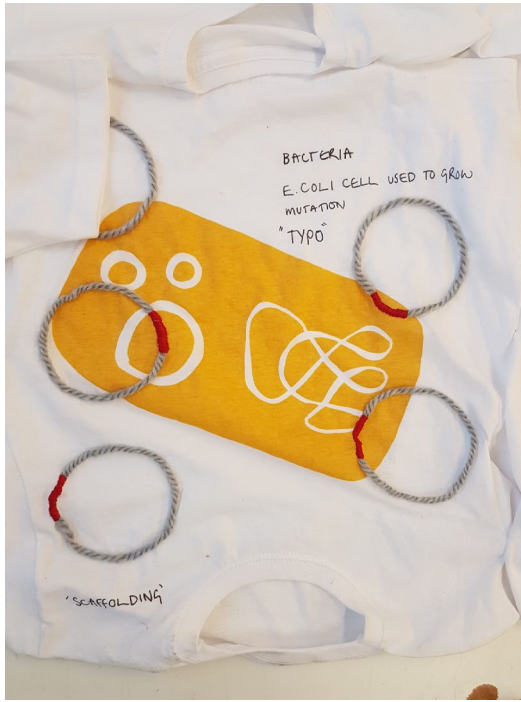
2017 “Visualising the Unseen” with Edinburgh College of Art. Working with undergraduate art students and ECAT scientists to create visual responses to scientists’ work. Conception, planning and execution.



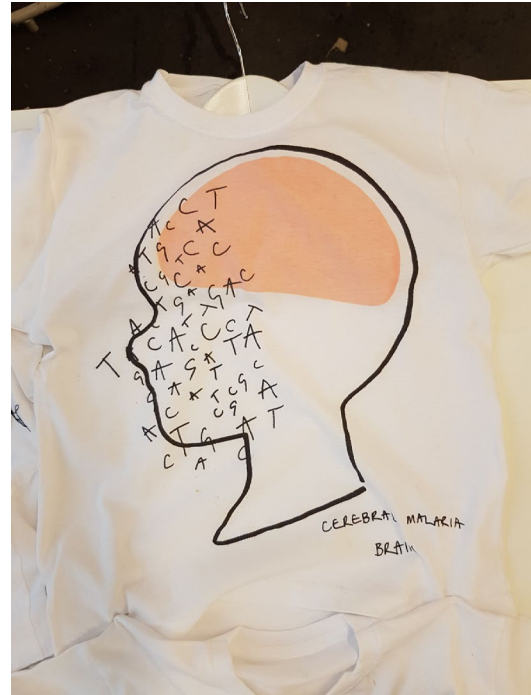
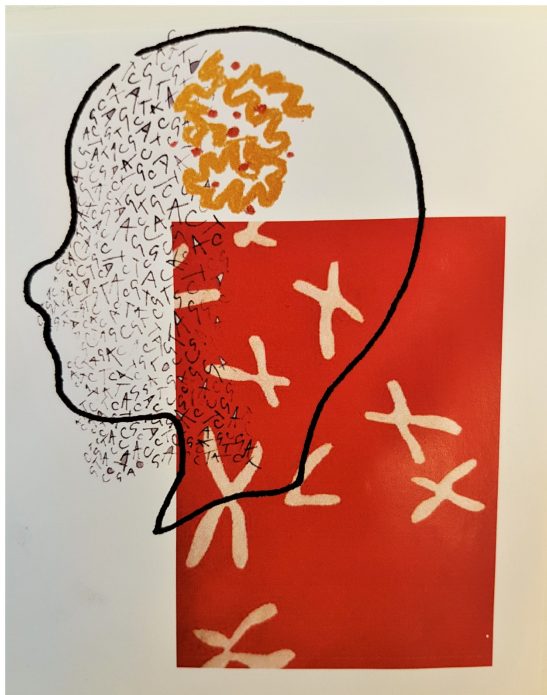
Themes from my thesis depicted on children’s T-shirts



Genetic mutations “spot the difference”



Artistic representations of cloning (left panel) and rosetting (right panel)



Artistic representations of genetic mutations influencing the risk of cerebral malaria

(Artists: Claudia Carreras, Vivian Chen, Katie Forrest-Smith and Rebecca Raper)